PROCEEDINGS ISSUE

International Symposium on Physical Separation Methods in Chemical Analysis, Amsterdam, April 10–14, 1967

Associate Editor: J. F. K. HUBER

ANALYTICA CHIMICA ACTA

International monthly devoted to all branches of analytical chemistry
Revue mensuelle internationale consacrée à tous les domaines de la chimie analytique
Internationale Monatsschrift für alle Gebiete der analytischen Chemie

ELSEVIER PUBLISHING COMPANY
AMSTERDAM

Anal. Chim. Acta, Vol. 38, No. 1/2, 1–314, May–June 1967

GENERAL INFORMATION

Languages

Papers will be published in English, French or German.

Submission of papers

Papers should be sent to: Prof. PHILIP W. WEST, Coates Chemical Laboratories, College of Chemistry and Physics, Louisiana State University, Baton Rouge 3, La. 70803 (U.S.A.) or to

DR. A. M. G. MACDONALD, Department of Chemistry, The University, P.O. Box 363, Birmingham 15 (Great Britain)

Manuscripts

Authors should submit two copies in double-spaced type with adequate margins on pages of uniform size. Acknowledgements, summary and references should be placed at the end of the paper.

Tables should be typed on separate pages and numbered in Roman numerals in the order in which they are mentioned in the text. All Tables should have descriptive titles. The use of chemical formulae and conventional abbreviations is encouraged in Tables and Figures but chemical formulae should not be used in the text unless they are necessary for clarity. Units of weight, volume, etc., when used with numerals should be abbreviated and unpunctuated (*e.g.*, 2%, 2 ml, 2 g, 2 μl, 2 μg, 2 ng, 2 cm, 200 mμ).

Figures should be drawn in Indian ink on drawing or tracing paper with all lettering in **thin** pencil. Standard symbols should be used in line drawings; the following are available to the printers:

Photographs should be submitted as clear black and white glossy prints. Figures and photographs should be of the same size as the typed pages. Legends for figures should be **typed on a separate page.** Figures should be numbered in Arabic numerals in the order in which they are mentioned in the text.

References should be given at the end of the paper and should be numbered in the order of their appearance in the text (**not** arranged alphabetically). Abbreviations of journal titles should conform to those adopted by the *Chemical Abstracts List of Periodicals*, 1961 Edition and supplements. The recommended form for references to journal papers and books is as follows:

1. J. J. LINGANE AND A. M. HARTLEY, *Anal. Chim. Acta*, 11 (1954) 475.
2. F. FEIGL, *Spot Tests in Organic Analysis*, 7th Ed., Elsevier, Amsterdam, 1966, p. 516.

For multi-author references, **all** authors must be named, and initials given, in the reference list, although the use of, for example, SMITH *et al.*, is desirable in the text.

Summaries are published in English, French and German; authors must always provide a summary in the language of the paper, and are encouraged to supply translations where convenient. No summaries are needed for Short Communications.

Reprints

Fifty reprints will be supplied free of charge. Additional reprints (minimum 100) can be ordered at quoted prices. They must be ordered on order forms which are sent together with the proofs.

Publication

Analytica Chimica Acta has four issues to the volume, and three volumes appear per year. Subscription prices: $ 17.50 or £ 6.6.— or Dfl. 63.— per volume; $ 52.50 or £ 18.18.— or Dfl. 189.— per year, plus postage. Additional cost for copies by airmail available on request. For advertising rates apply to the publishers.

Subscriptions

Subscriptions should be sent to:

ELSEVIER PUBLISHING COMPANY, P.O. Box 211, Amsterdam, The Netherlands

Burette électrique

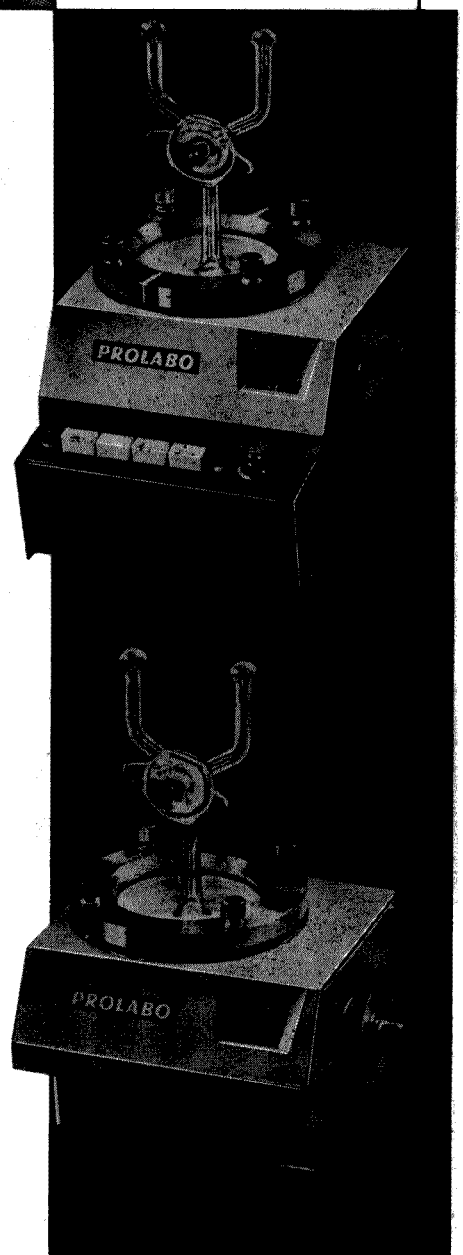

■ Ces burettes sont destinées à délivrer progressivement un réactif ou une liqueur titrée. Le volume de liquide écoulé est engendré par le déplacement d'un piston calibré, commandé par rotation à l'aide d'une vis micrométrique. La quantité de liquide écoulée est lue directement sur un cadran numérique.

Le piston des burettes PROLABO, pièce dont la qualité détermine la précision de l'instrument, est en invar, métal dont le coefficient de dilatation est pratiquement nul. Il est usiné, rectifié avec une précision impossible à obtenir avec un piston en verre.

Le piston se déplace dans un réservoir à huile, séparé de la chambre à réactif par une membrane souple en « SOREFLON ».
Les réactifs ne sont au contact que de la membrane en « SOREFLON » et d'une pièce en verre « PYREX ».

■ La capacité des burettes à piston PROLABO est de 12,5 cm^3. Les lectures sont faites en centièmes de cm^3 sur un cadran numérique à quatre chiffres. La burette à *commande manuelle* n° 1030.00 est manœuvrée en tournant un seul bouton qui détermine le remplissage ou le vidage. La burette *électrique* n° 1031.02 est mise en œuvre par le jeu de plusieurs interrupteurs électriques qui commandent les opérations suivantes : remplissage, suivi d'une remise au zéro automatique ; vidage rapide ; vidage lent ; vidage « coup par coup », par dixièmes de cm^3. Les moteurs électriques sont tous synchrones, et le réactif toujours délivré à vitesse constante. La burette électrique peut évidemment être commandée à distance, soit à l'aide d'un interrupteur manuel, soit par le signal de sortie d'un titrimètre automatique.

■ Ces burettes sont exemptes des erreurs classiques de mouillage ou de lecture. Elles offrent les plus larges possibilités d'emploi dans des montages automatiques, avec ou sans enregistrement. Les circuits de réactifs sont construits, en dehors de la burette, à l'aide de tubes en verre à rodages sphériques de 2/12. Un grand nombre d'éléments de construction à rodages sphériques a été prévu : flacon-réservoir de réactif, récipients de titrage, tubes droits ou coudés de diverses dimensions.

Burette à commande manuelle

PROLABO 12, RUE PELÉE * 75 PARIS 11e - TÉL. : 797-41-59

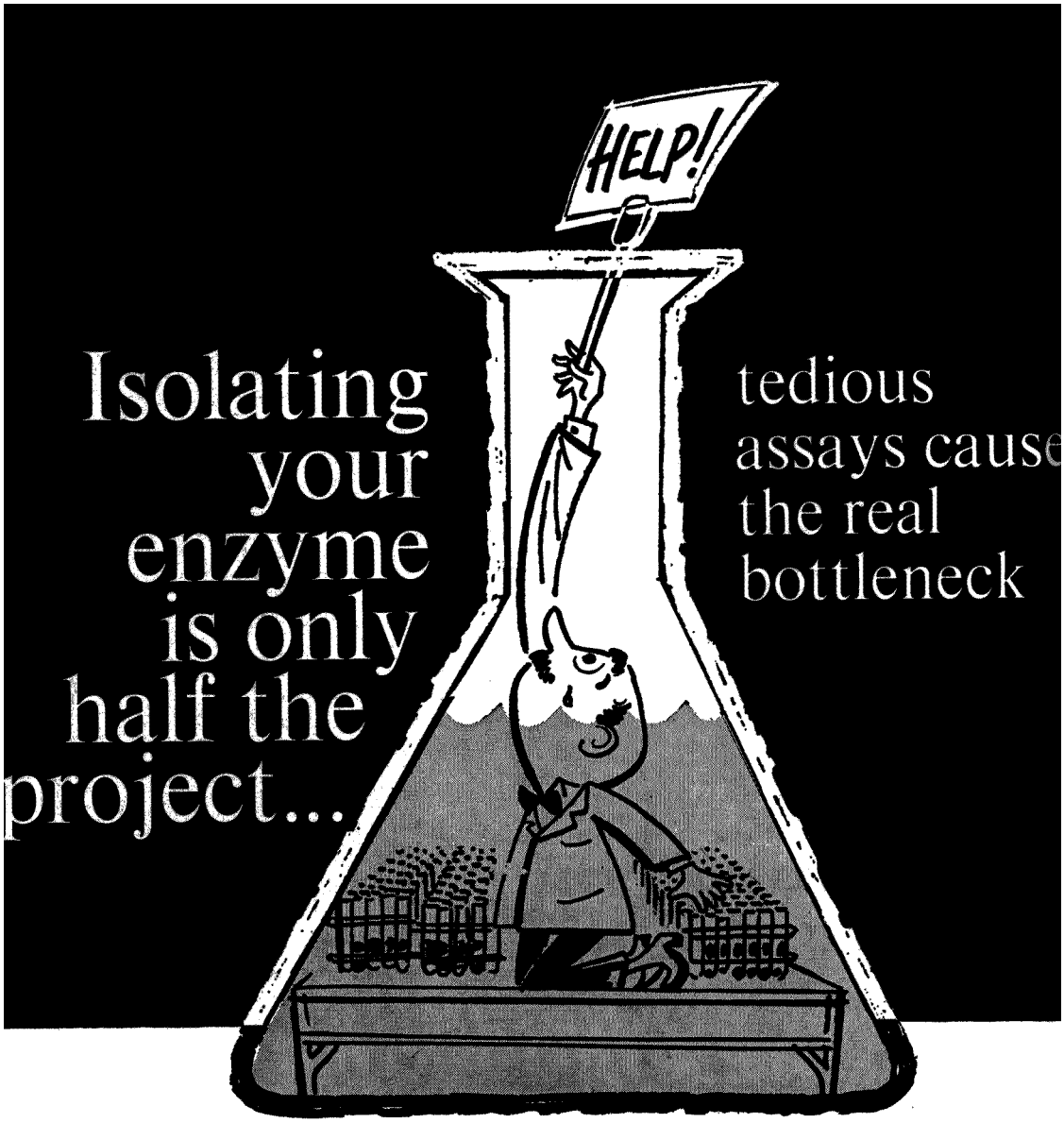

But they needn't. The frustrations of manually assaying enzymes can be broken with the Technicon® AutoAnalyzer.® The following procedures have been automated at rates up to 60 samples per hour or by continuous monitoring of column effluents:

amylase	6-phosphogluconate-1, dehydrogenase
cholinesterase	hydrolytic enzymes
cytochrome oxidase	lysolytic enzymes
amino acid decarboxylases	NAD-NADH systems
dehydrase	peptidase
alcohol dehydrogenase	phosphohexose isomerase
lactic dehydrogenase	phosphorylase
glucokinase	acid phosphatase
glucose oxidase	alkaline phosphatase
glucuronidase	proteolytic enzymes
hexokinase	sulfatase
histidase	glutamic oxalacetic transaminase
urease	glutamic pyruvic transaminase
glutamine synthetase	ornithine carbamoyl transferase
ornithine transaminase	and others

Reaction rates...quantitation...
assay...chromatography

It is quite likely that we can automate the assay for the enzyme system you have under investigation.

Contact us... we may already have done so.

In any case, we will be happy to furnish a selection of reprints which report the methods and equipment employed to effect significant savings in time labor and material.

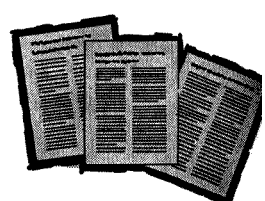

TECHNICON
INSTRUMENTS CORPORATION
Ardsley (Chauncey), New York 10502

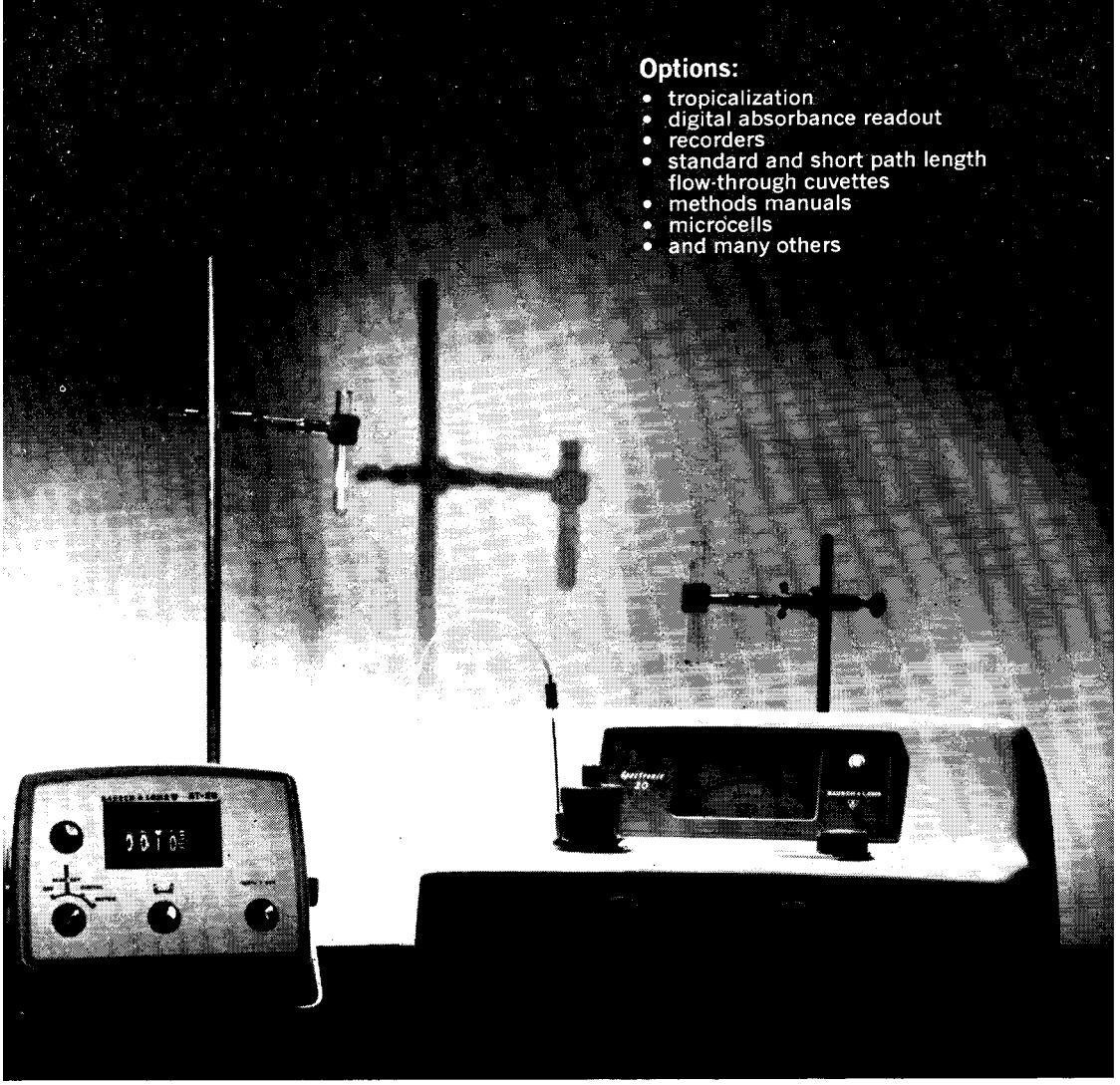

This is the Spectronic 20. No other spectrophotometer gives you so much for so little.

Wavelength range . . . from 340 to 950 nm and anywhere between.

Speed and precision . . . better than ±0.5 percent T with optional semi-automatic cuvette, four times a minute.

Stability . . . always within 1 percent T—no matter how severe the changes in line voltage and frequency.

To learn more about the Spectronic 20 spectrophotometer, ask one of 35,000 owners or write Bausch & Lomb, International Division, 12041 Bausch Street, Rochester, New York 14602, U.S.A.

438 A

BAUSCH & LOMB

TECHNIQUES IN PROTEIN CHEMISTRY

by **J. LEGGETT BAILEY**
Twyford Laboratories, London, Great Britain

Second revised and expanded edition

6 × 9″, xiv + 406 pages, 54 tables, 120 illustrations, 1023 lit. refs., 1966, £5.10.0, $20.00, Dfl. 55.00

There has been no diminution of activity among protein and peptide chemists in the years that have elapsed since the first edition of this book in 1962. On the contrary, advances made in separational methods have already become established in many laboratories and applied routinely. The first edition of this very successful book was sold out in short order, and a reprint was similarly sold out. It has proven particularly valuable to biochemists with limited practical experience in the chemistry of proteins. Dr. Leggett Bailey has compiled a handbook which discusses in detail the established analytical methods, as well as promising techniques too recently developed to fit into such a definition.

In this second edition considerable expansion of the text has resulted from the revision. A careful selection process has been applied to the vast array of material which constitutes the stock-in-trade of protein and peptide chemists all over the world.

Besides being of immediate interest to biochemists, this volume will be an invaluable laboratory handbook to non-specialists and advanced workers in protein chemistry, as well as scientists in related fields.

CONTENTS:

ELSEVIER PUBLISHING COMPANY
AMSTERDAM LONDON NEW YORK

Where in the world are EASTMAN Organic Chemicals and EASTMAN CHROMAGRAM System available?

Here:

EASTMAN Organic Chemicals and CHROMAGRAM products are sold in the U.S.A. by Distillation Products Industries and local laboratory supply houses, and throughout the world by the following:

AUSTRALIA
H. B. Selby & Co. Pty. Ltd.
Sydney—Melbourne
Brisbane—Perth
Adelaide—Hobart

BELGIUM
s. a. Belgolabo
Overijse

BRAZIL
Atlantida Representacoes e Importacoes Ltda.
Rio de Janeiro

CANADA
Fisher Scientific Co. Ltd.
Edmonton—Don Mills
Vancouver—Montreal

DENMARK
H. Struers Chemiske Laboratorium
Copenhagen

FINLAND
Havulinna Oy
Helsinki

FRANCE
*Kodak-Pathé
Paris
**Touzart & Matignon
Paris

GERMANY
SERVA-Entwicklungslabor
Heidelberg

GREECE
*P. Bacacos
Chemical and Pharmaceutical Products Co., Ltd.
Athens

ISRAEL
Landseas (Israel) Ltd.
Tel Aviv

ITALY
Prodotti Gianni s.r.l.
Milan

JAPAN
Muromachi Kagaku Kogyo Kaisha, Ltd.
Tokyo
Mitsumi Scientific Industry Co., Ltd.
Tokyo

MEXICO
Hoffmann-Pinther & Bosworth, S. A.
Mexico 1, D. F.

NETHERLANDS
N. V. Holland-Indie Agenturen Mij, HIAM
Amsterdam C

NEW ZEALAND
Kempthorne, Prosser & Co's.
New Zealand Drug Co., Ltd.
Wellington—Dunedin

NORWAY
Nerliens Kemisk Tekniske Aktieselskap
Oslo

PORTUGAL
Soquimica, Sociedade de Representacoes de Quimica, Lda.
Lisbon

REPUBLIC OF SOUTH AFRICA
Baird & Tatlock (S.A.) (Pty.) Limited
Johannesburg

SPAIN
CEPA, Sociedad Anonima
Barcelona

SWEDEN
*Rudolph Grave A/B
Solna
**KEBO AB
Stockholm 6

SWITZERLAND
Dr. Bender & Dr. Hobein AG
Zurich 6

UNITED KINGDOM
Kodak Limited
Kirkby, Liverpool

* For CHROMAGRAM products only

** For EASTMAN Organic Chemicals only

Of the thousands of EASTMAN Organic Chemicals distributed by these firms, some are uncommon and some are uncommonly pure. You will probably find it more economical to buy them than to make them yourself.

The EASTMAN CHROMAGRAM System for thin-layer chromatography consists of flexible EASTMAN CHROMAGRAM Sheet and the simple EASTMAN CHROMAGRAM Developing Apparatus. The advantages of TLC are preserved without the nuisance of coating one's own plates. The distributors listed here can supply detailed information, including separation procedures. Get in touch with the firm best located to serve you.

Distillation Products Industries
Rochester, N.Y. 14603, U.S.A. (Division of Eastman Kodak Company)

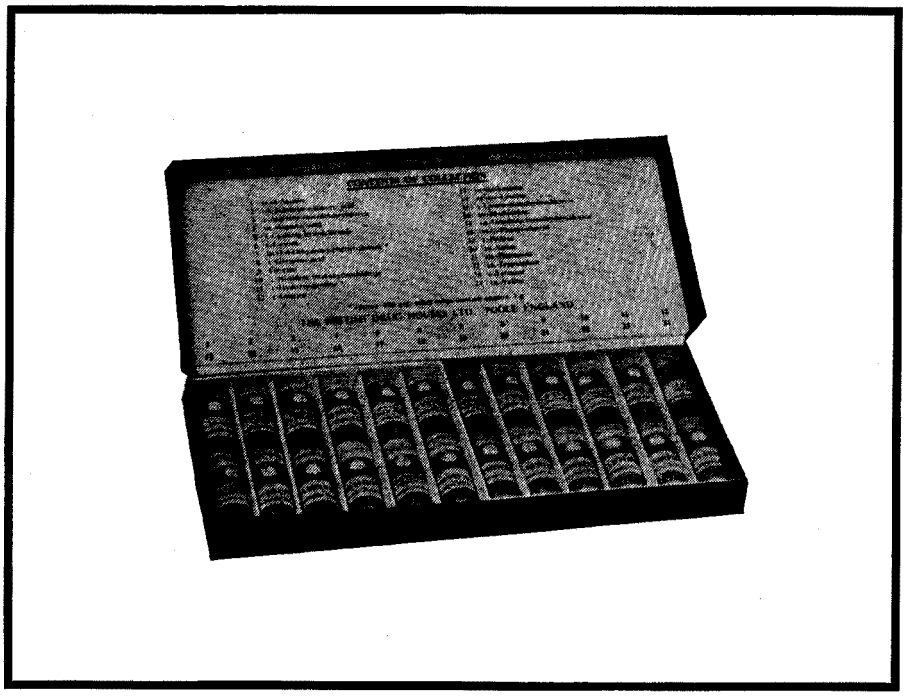

BDH Amino Acids and Amino Acid Derivatives

The 200 items in the BDH range of amino acids, peptides and derivatives, most of them chromatographically homogeneous, include acetyl, benzoyl, benzyl-oxy-carbonyl (CBZ), dansyl and DNP (dinitro-phenyl) amino acids.
Collections of 24 amino acids or 24 DNP derivatives, separately boxed and labelled, are also available:

AMINO ACID REFERENCE COLLECTION
The BDH Amino Acid Reference Collection contains a representative selection of 24 chromatographically homogeneous amino acids in kit form. These pure amino acids, for use as chromatographic standards, are also available singly.

DNP-AMINO ACID REFERENCE COLLECTION for Chromatography
The preparation of 2:4-dinitro-phenyl derivatives of amino acids is an important aspect of many biochemical studies, e.g. in identifying protein fragments and in determining amino acid sequences. The isolation and chromatographic identification of DNP-amino acids is much facilitated by the use of pure DNP acids as reference compounds.
The BDH DNP-Amino Acid Reference Collection consists of 24 chromatographically homogeneous DNP-amino acids, 100 mg of each. Individual items are also supplied separately.

BDH (International) Ltd.,
Laboratory Chemicals Division,
POOLE ENGLAND

AAIb

SUMMARIES OF PAPERS PUBLISHED IN ANALYTICA CHIMICA ACTA

Vol. 38, No. 1/2, May–June 1967

BAND-BROADENING IN PACKED CHROMATOGRAPHIC COLUMNS

In the past few years some problems have arisen as to the interpretation of experimental plate height data of packed chromatographic columns by means of the theory of VAN DEEMTER *et al.* These difficulties concern the "eddy diffusion" and "mass transfer" terms in particular. Light may be thrown on this matter by the recognition of unevenness of flow throughout the column cross-section as a major source of band-broadening. By considering the contribution to plate height resulting from the interaction between such flow profiles and various mechanisms of lateral transport of material it proved possible to solve the above-mentioned difficulties.

S. T. SIE AND G. W. A. RIJNDERS,
Anal. Chim. Acta, 38 (1967) 3–16

LIQUID-CRYSTALLINE MELTS AS STATIONARY PHASES IN GAS CHROMATOGRAPHY

(in German)

Nematic melts can be very efficient phases for the separation of positional isomers. In order to develop liquid-crystalline phases for working temperatures below 100° and above 200°, various nematic substances were synthesized and tested for stability and solvent properties under gas-chromatographic conditions. Substances with liquid-crystalline phases persisting over wide temperature ranges proved especially suitable for separation work. Retention volumes for various isomers are reported for stationary phases consisting of a eutectic mixture of 4,4′-azoxyanisole and -phenetole, 4-methoxybenzylidine-4′-cyanoaniline and -4′-acetoxyaniline.

Of the several substances with melting points above 200° examined, the most suitable for gas chromatography were 4,4′-benzylidinebenzidine, 4,4′-bis(*p*-methoxybenzylidine)-4,4′-diaminostilbene, and bis-phenetidineterephthalaldehyde. Specific retention volumes for substituted aromatics and optimal working temperatures are reported. The bisphenetidine derivative, which is easily synthesized, is suitable for various industrial analytical separations. Separations of α- and β-naphthols, benzenedicarboxylic acid esters, condensed aromatics, isomeric benzylpyridines and chlorotoluenes, *etc.* are readily done.

H. KELKER, B. SCHEURLE AND H. WINTERSCHEIDT,
Anal. Chim. Acta, 38 (1967) 17–30

CHROMATOGRAPHY WITH SUPERCRITICAL FLUIDS

Molecular interactions in the gas phase may be utilized for enhancing the volatility of substances in gas chromatography. A study of the effect of pressure on equilibria in GLC revealed that at higher pressures these interactions are quite appreciable, especially near the critical point. Measurements of plate heights show that with suitable adaptation of columns to the specific properties of high-pressure, dense fluids, the separating efficiency can be high and the speed of analysis fast. Experiments conducted with n-pentane and isopropanol as mobile fluids under supercritical conditions demonstrate that the volatility of heavy compounds may be enhanced by a factor of as much as 10^4. With either a liquid or a solid adsorbent as a stationary phase, chromatography with supercritical fluids proves to be very suitable for the rapid analysis of heavy compounds. The effect of various operational parameters on the separation is discussed. Certain features of the technique are illustrated with several examples.

S. T. SIE AND G. W. A. RIJNDERS,
Anal. Chim. Acta, 38 (1967) 31–44

THE STRUCTURE AND RETENTION PROPERTIES OF OPEN-CHAIN AND CYCLIC HYDROCARBONS AND THEIR SIMPLE SUBSTITUTION PRODUCTS

(in German)

Modern hydrocarbon and especially olefin chemistry is concerned with the stereospecifity of catalytic reactions. Mixtures resulting from these reactions must be analyzed for all possible isomers. Only gas chromatography with high resolution and mainly open tubular columns is able to separate the different isomers of unsaturated hydrocarbons present in such mixtures. The identification of the separated species is difficult, as the modern combination of mass spectroscopy with capillary columns supplies spectra which are not characteristic enough for identification of such unsaturated hydrocarbons. However, the interpretation of retention data of hydrocarbons may be successful, because small structural variations correspond to definite differences of retention data. The chemical history of the analyzed products and in the case of methyl-substituted isomers, data on the methylene insertion reaction, makes it possible to obtain a relative correlation of separated species.

G. SCHOMBURG,
Anal. Chim. Acta, 38 (1967) 45–64

TWO-STAGE CAPILLARY GAS CHROMATOGRAPHY

A two-stage capillary gas-chromatographic method has been developed with the aim of obtaining a better separation of the saturated hydrocarbons from petroleum in the C_{10}–C_{18} molecular weight range. The method should also be applicable to other hydrocarbon fractions and to compounds other than hydrocarbons. Two capillary gas-chromatographic columns of different kinds and two flame-ionisation detectors were used. A four-way valve after the first column and before the first flame detector made it possible to force a fraction indicated by one peak of the chromatogram from the first column directly into the second one. Application of an immobile phase of different kind in the second column makes separations possible on this column that cannot be obtained by use of a single capillary column. The use of a second column which separates, say, according to molecular weight allows resolution of a mixture of compounds that have identical retention times when analysed over a "boiling-point" column.

P. A. SCHENCK AND C. H. HALL,
Anal. Chim. Acta, 38 (1967) 65–71

STUDIES ON THE PREPARATION AND PERFORMANCE OF PREPARATIVE GAS-CHROMATOGRAPHIC COLUMNS

(in French)

The dependence of the efficiency and productivity of preparative-scale gas-chromatographic columns on various parameters is discussed. The minimum HETP is experimentally shown to increase almost proportionally to the column diameter in the range 1–5 cm. The HETP also increases with a power of the sample amount which depends on the quality of the column packing and can be as low as 1.2. High-diffusivity carrier gases (H_2 and He) are shown to allow a three-fold increase of column productivity. The productivity (amount of sample separated/unit time) increases with the column diameter. Given a fixed volume of stationary phase and a known mixture, the column diameter which will accept the largest sample can be calculated. The performance of a preparative unit is limited more by the loadability of columns than by loss of efficiency with increasing diameters. The performances of preparative columns can be improved by putting rods parallel to the column axis regularly spaced in the packing. The column can be heated internally either for programmed temperature separations or to allow thermal equilibrium to be reached rapidly.

M.-B. DIXMIER, B. ROZ ET G. GUIOCHON,
Anal. Chim. Acta, 38 (1967) 73–88

MOLECULAR SIEVE EFFECTS IN CHROMATOGRAPHY

The utilization of molecular sieve effects is reviewed. Applications to biochemical separations and the determination of molecular weights are discussed, as well as the properties of the different gels and the theory underlying their use.

P. FLODIN,
Anal. Chim. Acta, 38 (1967) 89–96

CHROMATO-POLAROGRAPHIC ANALYSIS OF MONONITROETHYLBENZENE MIXTURES

A method of partition and determination of *o*-, *m*- and *p*-nitroethylbenzenes with clathrates as fillers of the chromatographic column is described. The clathrate used was of composition Ni(γ-picoline)$_4$(SCN)$_2$·γ-picoline. The degree of filling of clathrate used was 0.4–0.7. The aqueous moving phase contained 2 *M* NH_4SCN, 0.3 *M* γ-picoline and 40–60 vol.% organic solvent. The applicability of the solvents: acetone, acetonitrile, ethanol, methanol, formamide and dimethylformamide, was checked; acetone and dimethylformamide were found best. Quantitative partition and evaluation of all three isomers was achieved on a 2.5-cm column. The recovery of the eluted individuals was complete. The samples used weighed only 0.05–0.3 mg. The relative error of evaluated components was not greater than $\pm$ 5%. The clathrate filler can be used many times.

W. KEMULA AND D. SYBILSKA,
Anal. Chim. Acta, 38 (1967) 97–104

THE USE OF A MOVING WIRE DETECTOR SYSTEM FOR THE STUDY OF LIQUID CHROMATOGRAPHIC COLUMNS

A detector system for liquid columns which employs a moving wire system and a gas–liquid chromatographic detector, is described. The performance of silicic acid columns was studied by investigating the effect of particle size, sample size and flow rate of the mobile phase on the HETP of squalane for coiled and straight columns. The effect of sample size on the resolution of methyl oleate and olive oil on coiled and straight columns was also studied.

T. E. YOUNG AND R. J. MAGGS,
Anal. Chim. Acta, 38 (1967) 105–112

HEATS OF PREFERENTIAL ADSORPTION OF CHELATES

A method employing a flow calorimeter for determining heats of preferential adsorption of certain organic chelates of metals from organic solutions is described. Experimental heats of adsorption are correlated with the chromatographic behaviour of the chelates and it is shown that irreversible retention on a column occurs when the heat is greater than 6 kcal mole^{-1} for the first stage of the two-stage adsorption process. The special case of the 2-methyl-8-quinoline chelate of copper(II) and its elution with solutions of the reagent is examined in more detail: heats of preferential adsorption decrease with increasing concentrations of reagent and the optimum experimental concentration can be predicted from the heat results.

M. P. T. BRADLEY AND D. A. PANTONY,
Anal. Chim. Acta, 38 (1967) 113–118

THE DETERMINATION OF NORMAL PARAFFINS IN PETROLEUM PRODUCTS

A normal paraffin, outside the carbon number range of the sample, is quantitatively added to the sample as an internal standard, and 10–100 μl of the mixture are injected into a small absorber unit which contains 400 mg of activated molecular sieve. The temperature of the absorber unit is raised from ambient to 300° at about 15°/min while nitrogen is passed. This elutes the non-linear hydrocarbons but leaves the normal paraffins absorbed. The sieve is removed from the absorber unit and the paraffins are released by destroying the sieve structure with hydrofluoric acid. A pellet of potassium hydroxide is then added to neutralise the excess acid and the released normal paraffins are extracted in 0.3 ml of isooctane. This isooctane solution is examined on a programmed-temperature chromatograph; the chromatogram obtained consists of a solvent peak followed by well-resolved peaks representing the normal paraffins. These are easily measured and the concentrations of the normal paraffins in the original sample are calculated against the internal standard.

J. V. MORTIMER AND L. A. LUKE,
Anal. Chim. Acta, 38 (1967) 119–126

CORRELATIONS IN THE PARTITION THIN-LAYER CHROMATOGRAPHY OF ALKALI METALS

The behavior of the alkali group in thin-layer chromatography on silica gel in the polyiodide–nitroaromatic system is described. R_M values are correlated with ionic radii, free energies of hydration, and the dielectric constant of solvent mixtures. The chromatographic distribution ratios on plates were measured as a function of the phase ratio and compared to bulk distribution ratios. Differences of orders of magnitudes between bulk and chromatographic distribution ratios are attributed to the peculiar nature of the water on the gel.

G. E. JANAUER, R. C. JOHNSTON, A. J. OLIVERI AND J. CARRANO,
Anal. Chim. Acta, 38 (1967) 127–135

PROCESSING ULTRACENTRIFUGE DATA WITH AN "ON-LINE" DIGITAL COMPUTER

A system is described for coupling the photoelectric scanner of an analytical ultracentrifuge to a high-speed digital computer. Following from a definition of the problem, use is made of the theory of radar pulse reception to show how the uncertainty in the measured pulse amplitudes can be improved. A two-way information exchange between the ultracentrifuge and the processor is involved.

S. P. SPRAGG,
Anal. Chim. Acta, 38 (1967) 137–142

PARTICLE SIZE ANALYSIS OF INORGANIC PIGMENTS

A disc-type centrifuge has been found satisfactory for the fractionation of several inorganic pigments including titania and calcium carbonate. It is particularly useful for pigments of less than 10 μ.

M. H. JONES AND T. R. MANLEY,
Anal. Chim. Acta, 38 (1967) 143–146

THE DETERMINATION OF MOLECULAR WEIGHTS, SEDIMENTATION COEFFICIENTS AND BUOYANT DENSITIES, USING THE ABSORPTION OPTICS OF AN ANALYTICAL ULTRACENTRIFUGE WITH AN ELECTRONIC SCANNING SYSTEM

A double-beam scanning system, developed for use with an analytical ultracentrifuge and equipped with absorption optics, is described. For the study of proteins and nucleic acids with this system, light filters for 260 mμ and 280 mμ proved to be completely satisfactory. The possibilities of the apparatus were illustrated with the following examples: (1) band sedimentation velocity; (2) density gradient centrifugation with CsCl; (3) determination of molecular weights from the sedimentation diffusion equilibrium. The possibility of applying Archibald's method with this system is discussed.

W. S. BONT AND W. L. VAN ES,
Anal. Chim. Acta, 38 (1967) 147–156

CONTINUOUS PREPARATIVE THIN-LAYER CHROMATOGRAPHY

A short survey of preparative chromatographic methods is given. An apparatus for general use in continuous preparative thin-layer chromatography is described, and its performance compared with some related preparative techniques.

R. VISSER,
Anal. Chim. Acta, 38 (1967) 157–162

ION-EXCHANGE CHROMATOGRAPHY

A review is given of variables which affect the separation factors in ion-exchange chromatography. In favorable cases the influence of complex formation, pH, and eluant concentration can be predicted by simple calculations, whereas the interaction forces inside the resin phase are still largely unexplored.

O. SAMUELSON,
Anal. Chim. Acta, 38 (1967) 163–168

THE EFFECT OF THE MEDIUM ON ELECTROPHORETIC SEPARATIONS

Various electrophoretic techniques are discussed with bovine lens crystallins as test substance. Moving boundary, paper, starch-block, starch-gel and polyacrylamide gel procedures are compared.

H. BLOEMENDAL,
Anal. Chim. Acta, 38 (1967) 169–177

SEPARATION OF NOBLE METALS FROM BASE METALS BY MEANS OF A NEW CHELATING RESIN

A new type of chelating resin, which is highly selective for gold and the platinum metals, is described. Its properties and applications are indicated. The reaction mechanism between this resin and the noble metal ions was investigated with the aid of some monomer analogues.

G. KOSTER AND G. SCHMUCKLER,
Anal. Chim. Acta, 38 (1967) 179–184

ADSORPTION OF THE RARE-EARTH ELEMENTS ON AN ANION-EXCHANGE RESIN FROM NITRIC ACID–ACETONE MIXTURES

The distribution coefficients on Dowex 1-X8 anion-exchange resin were determined for all the rare earths at various proportions of concentrated nitric acid and acetone, using radioactive tracers of the metallic ions. In the range 4–40% nitric acid, the distribution coefficients decrease with increasing content of nitric acid, and at a given ratio of acid to acetone, they decrease with increasing atomic number in the lanthanum series. The value for yttrium is close to that of thulium; scandium is much less adsorbed. Literature data for aqueous systems and other mixed solvent systems are discussed. The distribution of scandium between Dowex 1-X8 and conc. nitric acid–methanol, ethanol or acetone systems is described. The separation power of the nitric acid–acetone system at different acid concentrations is analysed. Dowex 1-X8 resin with a nitric acid–acetone solvent is shown to be sufficient for separation of the rare earth elements by ion-exchange chromatography.

J. ALSTAD AND A. O. BRUNFELT,
Anal. Chim. Acta, 38 (1967) 185–192

MACRORETICULAR ION-EXCHANGE RESINS; SOME ANALYTICAL APPLICATIONS TO PETROLEUM PRODUCTS

Extraction and subsequent recovery, in four separate fractions, of naphthenic acids, alkylphenols, pyrrollic compounds and nitrogen bases can be made from petroleum products using macroporous ion-exchange resins. Distinctive features of the technique are the use of dissolved gases in polar solvents as eluants and the application of the carbonate form of anion-exchange resins. The transition metal form of a macroreticular cation exchanger is shown to extract ligands from non-aqueous systems and a specific application to petroleum analysis is given.

P. V. WEBSTER, J. N. WILSON AND M. C. FRANKS,
Anal. Chim. Acta, 38 (1967) 193–200

THE SEPARATION OF TRACE METALS BY ION EXCHANGE ON SILICA GEL

(in German)

The mechanism of sorption of cationic metal complexes on silica gel and the utilization of this process for separation of trace concentrations of metals are discussed. Some practical examples are given.

F. VYDRA,
Anal. Chim. Acta, 38 (1967) 201–205

THE USE OF ION-EXCHANGE CHROMATOGRAPHY IN ACTIVATION ANALYSIS FOR SODIUM AND POTASSIUM IN MOLYBDENUM AND TUNGSTEN

(in German)

A method for the determination of traces of sodium and potassium in molybdenum or tungsten by activation analysis is described. Radiochemically pure sodium-24 and potassium-42 are separated from other radionuclides by anion- and cation-exchange chromatography. The limits of detection are 5 p.p.b. of sodium and 50 p.p.b. of potassium.

H.-G. DÖGE,
Anal. Chim. Acta, 38 (1967) 207–211

APPLICATION OF RADIOISOTOPES IN COLUMN CHROMATOGRAPHY ON SUBSTITUTED CELLULOSES
PART V. THE SEPARATION OF ARSENIC FROM COPPER AND OTHER METALS

The chromatographic behaviour of arsenic and copper was studied with radioisotopes on natural cellulose, cellobiose and seven substituted celluloses in ethyl ether. Arsenic was not adsorbed; copper was retained and eluted quantitatively. For preparative purposes, one gram of arsenic trioxide was purified from nanograms of copper on natural and diethylaminoethyl celluloses. The possibility of purifying arsenic from several other metals, and gold and mercury from copper is indicated.

R. A. A. MUZZARELLI AND G. MARCOTRIGIANO,
Anal. Chim. Acta, 38 (1967) 213–218

CRITERIA FOR SUCCESSFUL SEPARATION BY CONTINUOUS ELECTROPHORESIS AND ELECTROCHROMATOGRAPHY IN BLOCKS AND COLUMNS

By analysis of some important process variables, criteria for successful separation by continuous electrophoresis and electrochromatography in packed beds are derived. A general theory correlating power input, residence time and temperature rise in cylindrical and rectangular geometries is presented. The limitation of the separating capacity by transverse diffusion effects is shown to be predictable in terms of other operational conditions. These separation criteria appear to be in agreement with experimental evidence, and may find analytical as well as preparative application.

E. RAVOO, P. J. GELLINGS AND T. VERMEULEN,
Anal. Chim. Acta, 38 (1967) 219–232

DISPLACEMENT ELECTROPHORESIS

The displacement method of electrophoresis has been studied for strong anions, electropherograms being given as integral and/or differential temperature recordings. The theory and utility of the method are discussed.

A. J. P. MARTIN AND F. M. EVERAERTS,
Anal. Chim. Acta, 38 (1967) 233–237

MOBILITY DETERMINATIONS BY ELECTROPHORESIS IN AGAR GELS

(in German)

Agar-gel electrophoresis allows a simple rapid determination of the mobility of a protein in relation to a reference protein (*e.g.* human serum albumin). The electro-osmotic transport is determined by means of an uncharged substance, usually dextran. The dextran zone can be located more exactly by chemical than mechanical means. However, chemical marking makes the correct choice of the dextran concentration important; 2% dextran seems to be optimal. The mobility of transferrin is significantly higher with 0.5% dextran than with higher concentrations.

Replacement of agar bridges with foam plastic was studied for 5 migration times of 55–95 min. With agar the mobilities for transferrin were significantly higher and their fluctuations lower. Also, a dependence on migration time was found with foam but not with agar. A more exact parameter for the product field-strength · time proved desirable: *viz.* the distance between the dextran zone and the point of application ($\overline{DO}$). The distances dextran–transferrin and dextran–albumin plotted against $\overline{DO}$ showed perfect straight lines, which could be extrapolated to the origin.

H. J. HOENDERS, W. DE BOER AND P. A. J. DE BOER,
Anal. Chim. Acta, 38 (1967) 239–248

ELECTROPHORETIC SEPARATION OF INORGANIC CATIONS ON CELLULOSE ACETATE

The electrophoretic separation of mixtures of rare earths was investigated. All rare-earth elements could be separated using α-hydroxyisobutyric acid and acetylated cellulose films; the separation times were 14–20 min. This method is very suitable for the separation of small amounts of radioactive samples. Separation of radioactive rare earths, alkaline earths, fission products, transuranium elements, natural radioactive elements and their decay products, etc., are feasible.

Small amounts of carrier-free radioactive daughter products produced by β-decay of neutron-irradiated rare-earth elements could be separated from a considerable excess of starting material. A method for using activation analysis for the detection of cations after the electrophoretic separation on acetylcellulose strips is discussed.

K. AITZETMÜLLER, K. BUCHTELA AND F. GRASS,
Anal. Chim. Acta, 38 (1967) 249–254

A NEW APPARATUS FOR CONTINUOUS SEPARATION BY COUNTERCURRENT ELECTROPHORESIS

A new apparatus is described for separation by countercurrent carrier-free electrophoresis. Chemically very similar ions can be separated because of the freely variable sojourn time. It is possible to separate continually mixed ligand complexes of the type $[MCl_xBr_{6-x}]^{2-}$ (M = Ir, Os; $x = 0, 1, \ldots, 6$); the differences in mobilities are below 2%. The separated zones are pure aqueous salt solutions of definite concentrations, which are not contaminated by base electrolyte.

W. PREETZ AND H. L. PFEIFER,
Anal. Chim. Acta, 38 (1967) 255–260

ZONE MELTING AND COLUMN CRYSTALLIZATION AS ANALYTICAL TOOLS

The techniques of normal freezing, zone melting and column crystallization are discussed; special attention is given to micro zone melting. The preparation of absolutely pure benzene by column crystallization is shown to be possible. Many examples of the utilization of these techniques are given, including work on isomeric compounds, plant and animal products and meteorite samples.

H. SCHILDKNECHT,
Anal. Chim. Acta, 38 (1967) 261–273

EFFECT OF INTERACTION OF MACROMOLECULES IN GEL PERMEATION, ELECTROPHORESIS AND ULTRACENTRIFUGATION

The recognition of interaction in solution, when macromolecules are studied by transport methods, is usefully followed by model building and the comparison of model and experiments. An example is given to show how models can be used to improve the effectiveness of experiments.

G. A. GILBERT,
Anal. Chim. Acta, 38 (1967) 275–278

A FAST METHOD OF ZONE MELTING AS AN AID IN ANALYTICAL CHEMISTRY

A new zone-melting apparatus is described which allows relatively high zone speeds up to 60 cm/h. The time required for effective separations is only a few hours so that the apparatus can be used for analytical purposes. The difference between the theoretical and actual distribution coefficients obtained is small; the distribution coefficients of unknown substances in mixtures can thus be derived from the result of zone melting, which offers a means of identification. The apparatus is fully automated and normal freezing is incorporated as a first step. A means of preventing the breakage of the glass tube containers is described. The principles of operation and possible applications are discussed.

N. J. G. BOLLEN, M. J. VAN ESSEN AND W. M. SMIT,
Anal. Chim. Acta, 38 (1967) 279–284

ZONE MELTING AS AN AID TO IMPURITY DETERMINATION BY THERMAL ANALYSIS

The determination of the impurity content of a sample by means of the melting-curve method (calorimetric analysis) is often seriously hampered when solid soluble contaminants are present. Solid solutions often occur in substances purified by crystallization or extraction. A simple test on mixed crystals is described. When three or more impurities are present the relations obtainable from a melting curve are insufficiently accurate for computing the unknown concentrations and distribution coefficients to an acceptable extent. Only melting curves obtained from samples containing one or two impurities permit an exact, simple interpretation. A complex of impurities may be analysed when the sample is subjected to zone melting and a set of melting curves is obtained for parts of the ingot.

H. F. VAN WIJK, P. F. J. VAN DER MOST AND W. M. SMIT,
Anal. Chim. Acta, 38 (1967) 287–290

PURIFICATION OF LIQUID AROMATIC AMINES BY ZONE MELTING AND COLUMN CRYSTALLIZATION

(in French)

Purification by zone melting of seven aromatic amines was studied; 400 g of substance could be purified at one time between $+15°$ and $-35°$. Criteria of purity and some physical constants of purified amines are given. A related method—column crystallization—was also studied for the same starting materials and the results are compared. The two methods of purification give comparable results. Column crystallisation does not give such good purification as zone melting, but has the advantages that it can be operated with continuous throughput, much less time is needed, and rather impure starting materials can be employed.

B. POUYET,
Anal. Chim. Acta, 38 (1967) 291–297

ULTRAMICRQ ZONE MELTING

A systematic classification of zone melting is discussed with respect to the volume, *i.e.* weight, of the ingot. A new apparatus and technique of "ultra-micro zone melting" are described for amounts less than 500 μg. The plates of the heating and cooling blocks are placed into one another like two combs; an iron–nickel alloy with a very low coefficient of expansion permits "zone melting units" between 1.7 mm and 2.5 mm in size.Because of the close packing of the 30 "units" and a steep temperature gradient, separation effects can be achieved after a few hours. For work at low temperatures and under inert gas, the apparatus can be enclosed in an air-tight plastic cylinder. The sample capillaries are prepared by capillary action followed by centrifuging. Ultra-micro zone melting finds application in natural product chemistry and radiochemistry.

K. MAAS AND H. SCHILDKNECHT,
Anal. Chim. Acta, 38 (1967) 299–303

A STUDY OF LIQUID CHROMATOGRAPHY IN COLUMNS. THE TIME OF SEPARATION

The factors affecting the time in which a given resolution can be obtained are investigated. It is concluded that for columns of the same bed geometry, the minimum separation time is much longer in liquid chromatography than in gas chromatography. However, the separation time in liquid chromatography can be reduced considerably if a higher pressure drop is acceptable. The expected improvement is restricted by the difficulty of obtaining regular packings from very small particles.

J. F. K. HUBER AND J. A. R. J. HULSMAN,
Anal. Chim. Acta, 38 (1967) 305–314

ANALYTICA CHIMICA ACTA

Vol. 38 (1967)

ANALYTICA CHIMICA ACTA

International monthly devoted to all branches of analytical chemistry
Revue mensuelle internationale consacrée à tous les domaines de la chimie analytique
Internationale Monatsschrift für alle Gebiete der analytischen Chemie

ELSEVIER PUBLISHING COMPANY
AMSTERDAM

PRINTED IN THE NETHERLANDS

International Symposium on Physical Separation Methods in Chemical Analysis, organized under the auspices of the Koninklijke Nederlandse Chemische Vereniging
April 10th—14th, 1967, Amsterdam

INTRODUCTION

Since the last war the development of physical separation methods for chemical analysis has been very spectacular. Specialists have explored the possibilities of the various techniques and have deepened our insight into the physical nature of the processes. The application of the valuable theories thus developed makes it possible to choose the best technique and the optimum working conditions to solve a particular problem.

The diversity and rapid development of the processes, however, has made it very difficult for analytical chemists to keep abreast of all the new developments and of the most important points of dispute. What the organizers of this symposium had in mind was to provide an opportunity to fill this gap. How far this aim has been achieved can be judged from the contents of these Proceedings and the ensuing discussions. The papers presented at this symposium comprise invited papers of a general nature, each of which deals with the technique and theory of an important separation process and discusses some special aspect more thoroughly, and contributed papers, most of which deal with new developments and applications to specific cases.

The organizing committee consisting of E. A. M. F. DAHMEN (president), C. L. DE LIGNY (secretary), G. DEN BOEF, Mrs. L. FREESE-WOUDENBERG and J. F. K. HUBER received much support from the Section for Analytical Chemistry of the Koninklijke Nederlandse Chemische Vereniging and from the Koninklijke Nederlandse Chemische Vereniging itself. The scientific committee consisted of G. W. A. RIJNDERS (president), C. L. DE LIGNY (secretary), H. BENOIT (France), H. BLOEMENDAL, E. A. M. F. DAHMEN, G. DIJKSTRA, G. A. GILBERT (Great Britain), J. F. K. HUBER and H. SCHILDKNECHT (Germany).

In view of the fact that proceedings of symposia must very often be ordered separately and so are not easily obtained in libraries, the organizers preferred to publish them in a special volume of a current analytical journal. To our satisfaction, suitable arrangements were made with the Editors of *Analytica Chimica Acta* and the Elsevier Publishing Company. The papers presented at the Symposium are published in this issue of *Analytica Chimica Acta*. The discussions together with any additional information from the authors will be published shortly after the symposium in a separate booklet (Editor: J. F. K. HUBER) by the Elsevier Publishing Company. This booklet will automatically be sent to all participants; others interested can obtain copies from the Analytical Section of the K.N.C.V. (c/o Burnierstraat 1, Den Haag, The Netherlands, price D.fl. 5.—).

We hope that this symposium will prove successful and will stimulate further activities in the field of physical separations in chemical analysis.

E. A. M. F. DAHMEN,
President, Organizing Committee

Analytica Chimica Acta
Elsevier Publishing Company, Amsterdam
Printed in the Netherlands.

BAND-BROADENING IN PACKED CHROMATOGRAPHIC COLUMNS

S. T. SIE AND G. W. A. RIJNDERS
Koninklijke/Shell-Laboratorium Amsterdam (Shell Research N.V.), (The Netherlands)

(Received November 1st, 1966)

One of the main themes in the theory of chromatography concerns the broadening of a solute band moving through a chromatographic column. A measure of this band-broadening is the plate number n, defined by $n = (\mu/\sigma)^2$ where μ is the mean, and σ the standard deviation of the concentration profile. The quality of the packing is judged by the plate height H, which is found by $H = L/n$, L being the column length.

Among the theories describing plate height as a function of operational parameters the theory of VAN DEEMTER, ZUIDERWEG AND KLINKENBERG[1] has become very well known. H is regarded as being built up from various contributions which can be classed into two types: (1) axial diffusion and (2) slowness of mass transfer between the phases. The first-named effect comprises two mechanisms of spreading, a molecular one (molecular diffusion in axial direction) and a hydrodynamic one ("eddy diffusion"), *i.e.* the spreading resulting from statistical variations of the fluid velocity in different channels of the packed bed. In a simplified form the van Deemter equation is written as:

$$H = A + B/\bar{v} + C\bar{v},$$

where $\bar{v}$ is the interstitial fluid velocity; A, B and C are constants pertaining to the "eddy diffusion", molecular diffusion and mass transfer resistance, respectively. In GLC these constants are given as

$$A = 2\lambda d_p; \qquad B = 2\gamma D_g;$$

$$C = \frac{2}{3}\frac{k'}{(1+k')^2}\frac{d_l^2}{D_l} + 0.01\frac{(k')^2}{(1+k')^2}\frac{d_p^2}{D_g}$$

Here λ and γ are dimensionless constants depending upon packing geometry, D_g and D_l are the diffusivities in the gas and the liquid phase, respectively, and d_p and d_l represent the mean particle diameter and the effective liquid film thickness. k' is the capacity ratio, *i.e.* the ratio of the amount of solute in the liquid over the amount in the gas phase at equilibrium. C is seen to be composed of two terms, which are contributions of mass transfer resistances in the stationary liquid and the mobile gas phase, respectively.

Objections raised against the van Deemter equation

Although in the early days of GLC the original van Deemter equation proved very useful, many data—especially newer ones—have accumulated which resist inter-

pretation by this theory alone. The difficulties concern the terms representing "eddy diffusion" (A) and mass transfer (C).

Term A. The "eddy diffusion" term in GLC is sometimes present, sometimes absent and occasionally even negative. In analytical GLC it is at any rate small and cannot therefore be determined with certainty. This is somewhat at variance with results from liquid chromatography, where the contribution of packing irregularity is usually much more pronounced, notwithstanding the fact that liquid chromatography columns are often packed with much more care.

For reasons just mentioned the existence of an "eddy diffusivity" contribution has come to be doubted in GLC. GIDDINGS[2] rejects the idea of an additive contribution of "eddy diffusivity" and suggests that "eddy diffusivity" and "mass transfer" should be "coupled" in a non-additive way as follows.

$$\frac{1}{1/2\lambda d_p + 1/C_g\bar{v}}$$

This "coupling theory" is referred to again later.

Term C. According to the van Deemter equation the contribution of mass transfer resistance in the gas-filled channels should be negligible in comparison with the stationary-phase contribution*. However, many results obtained in GLC work point to a gas-phase contribution which is considerably larger (say, by two orders of magnitude) than the above-mentioned "intergranular mass transfer" contribution. It proved impossible to explain the discrepancy by also taking into account an "intragranular mass transfer" contribution (*i.e.* the contribution caused by the slowness of diffusion in the gas-filled pores), since this contribution is also too small.

The role of flow profiles in packed chromatographic columns

The gap between theory and experiment can be filled by extending the van Deemter theory to incorporate the contribution of flow profiles *i.e.* unevenness of flow throughout the column cross-section. Such profiles have been shown to exist in preparative GLC columns[3]. Our starting point will, however, be that such unevenness of flow is present to a greater or lesser extent in all columns, whether operated with liquid or gaseous eluents and whether of analytical or preparative size.

An idea of the kind of profiles involved can be obtained from Fig. 1, showing the distortion of a coloured band in gel-permeation chromatography. Although the profile is very pronounced, the column is not a particularly bad one (judged by normal standards), as evidenced by a plate number of 1250 m^{-1}. Nevertheless, the consequences of the unevenness of flow are quite important: without the profile the bandwidth as seen by the detector would have been only half the actual one. Plate numbers of 5000 m^{-1} should therefore be attainable if the flow were even.

Such unevenness of flow can result even from differences in packing density and mean particle size (caused by segregation) too small to be detected by, *e.g.*, microscopic examination of the packing.

Expression for the profile contribution to plate height

For a fluid flowing through an empty cylindrical tube the velocity is zero near

* The numerical constant in the gas-phase term, 0.01, is approximate only. Its magnitude follows from mass transfer data as well as from capillary models.

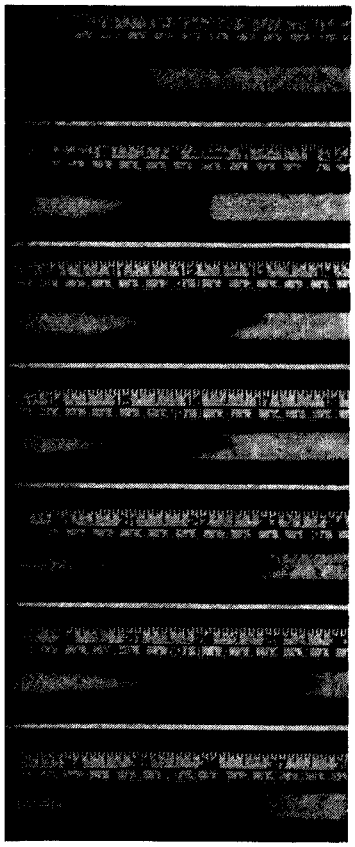

Fig. 1. Flow profile in a gel-permeation chromatography column. Column: 10 mm ID × 100 cm. Filling: styrene–divinylbenzene copolymer beads, approx. 50 μ. Eluant: tetrahydrofuran. Flow rate, 1 ml/min. T, 20°. Sample: 350 μl of a dilute solution of Sudan Blue in THF.

the wall and large in the centre (*e.g.* parabolical in the case of laminar flow through a tube of circular cross section). This velocity profile causes a spread in residence time of fluid elements, which is, however, lessened if appreciable exchange of material occurs in a lateral direction. This problem has been dealt with by TAYLOR[4] and, more generally, by ARIS[5].

By applying their theory to the analogous case of flow profiles in a packed chromatographic column we arrive at the following expression for the profile contribution to plate height

$$h = \frac{2\kappa R^2}{D}\bar{v}$$

where κ is a dimensionless constant depending on the flow profile (1/48 for the parabolic profile); R is a dimension characteristic for the profile (*e.g.* the tube radius), while D is the diffusivity in a lateral direction.

The above equation is valid for any flow profile and any cross-section, provided that the tube is of sufficient length to permit appreciable exchange in a lateral direc-

tion. Two different mechanisms can cause such lateral transport of material, viz., molecular diffusion and a "convective" diffusion. The latter results from the repeated division and combination of fluid streams in the three-dimensional network formed by the interstitial channels.

The effect of lateral diffusion counteracting the profile can be seen from Fig. 1. In the later stages of elution the band is straighter but more diffuse.

Magnitude of the convective diffusivity in packed beds

From a simple two-dimensional model it can be seen that the convective lateral transport can be treated as a "diffusion". Such a model is depicted in Fig. 2. The distri-

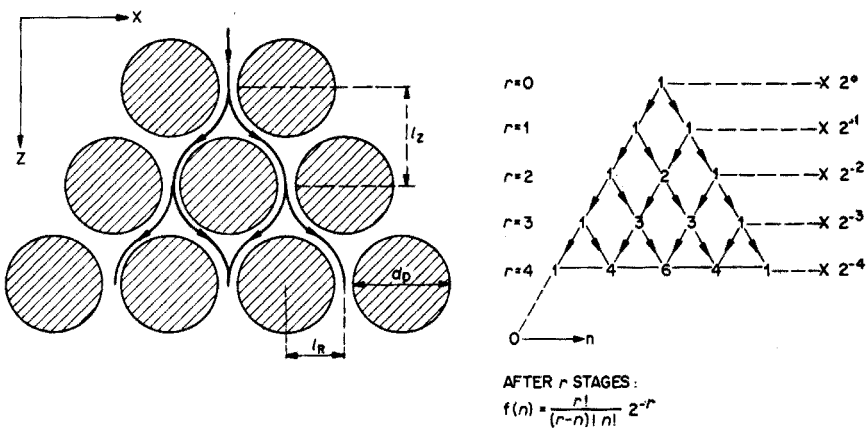

Fig. 2. Lateral spreading in a simple two-dimensional packing.

bution for this model is completely analogous to that of falling balls with the Galton board. It is a binomial distribution

$$f(n) = \frac{r!}{(r-n)!n!}\,2^{-r}\ (0 < n < r),$$

where $f(n)$ is the fraction of the original amount of material present at location n after r stages.

It can be shown that this distribution approaches a Gaussian distribution (if r is large), which is identical with the one resulting from a diffusion with a diffusivity constant D_R given by

$$D_R = \lambda_R d_p \bar{v},$$

where λ_R is a dimensionless constant depending on bed geometry. An analogous treatment of three-dimensional beds yields the same equation. In this case λ_R is given by

$$\lambda_R = \tfrac{1}{4}\frac{(l_R/d_p)^2}{l_z/d_p}.$$

By simply assuming that l_R and l_z (the lateral and axial displacements per step) are $\frac{1}{2}d_p$ and d_p, respectively (*cf.* Fig. 2), we obtain a value of 1/16 for λ_R. How-

TABLE I

VALUES OF λ_R ESTIMATED FOR MODELS OF A RANDOMLY PACKED BED OF SPHERES

Model	*Description*	$1/\lambda_R$
Random close packing	Mixture of a hexagonal and cubic close packing	$\frac{32}{3}\sqrt{6} \simeq 26$
Random packing acc. to SMITH *et al.*[8]	Mixture of a simple cubical packing and a rhombic close packing	$16\,(1 + \frac{1}{2}\sqrt{2}) \simeq 27$
Random packing acc. to HRUBIŠEK[9]	Simple cubical packing with alternate layers shifted by half a sphere diameter in directions of cube edges	$16\sqrt{3} \simeq 28$
Chaotic	No regularity, stream paths with lateral deviations from 0 to d_p all equally probable. Tendency of stream to follow a path with deviation l_R proportional to $(d_p - l_R)$	24

ever, closer examination of various random bed models makes it probable that λ_R is somewhat smaller, viz. about 1/30 (*cf.* Table I). This value is in very good agreement with the experimental results of HARTMAN *et al.*[6] from which it can be deduced that $1/\lambda_R = 27 \pm 4$.

Relative magnitude of convective and molecular diffusion

If we consider convective and molecular diffusion as statistically independent processes, the profile contribution becomes

$$h = \frac{2\kappa R^2}{\lambda_R d_p \bar{v} + \gamma_R D}\,\bar{v}$$

The tortuosity factor γ_R is the same as the one in the second term of the van Deemter equation in the case of isotropic beds. Its value will generally be of the order of 0.7.

Under typical GLC conditions ($d_p = 0.2$ mm, $\bar{v} = 5$ cm sec^{-1}) we find for the convective diffusivity $3 \cdot 10^{-3}$ cm^2 sec^{-1}, which is a considerably smaller value than the molecular diffusivities (*e.g.* 0.2 cm^2 sec^{-1} in H_2 or He and 0.05 cm^2 sec^{-1} in N_2). Hence, in normal GLC lateral transport is predominantly due to molecular diffusion, so that the profile contribution is first order in velocity. The effect of packing irregularity does not therefore come within the scope of a velocity-independent term, but under the C term. This explains why the C term is so much larger than the theoretical "mass-transfer" contribution, a possibility which has also been suggested by LITTLEWOOD[7].

Only at unusually high velocities does the convective diffusivity come into play. It becomes equal to the molecular diffusivity at velocities of a few metres per second. At higher pressures molecular diffusion in gases diminishes and convective transport becomes more important.

In a typical case of liquid chromatography ($d_p = 0.1$ mm, $\bar{v} = 0.01$ cm sec^{-1}) the convective diffusivity will be about $3 \cdot 10^{-6}$ cm^2 sec^{-1}. This value is not too different from that for molecular diffusivity. If the latter is 10^{-5} cm^2 sec^{-1}, the two processes become equivalent at a fluid velocity of 0.03 cm sec^{-1}.

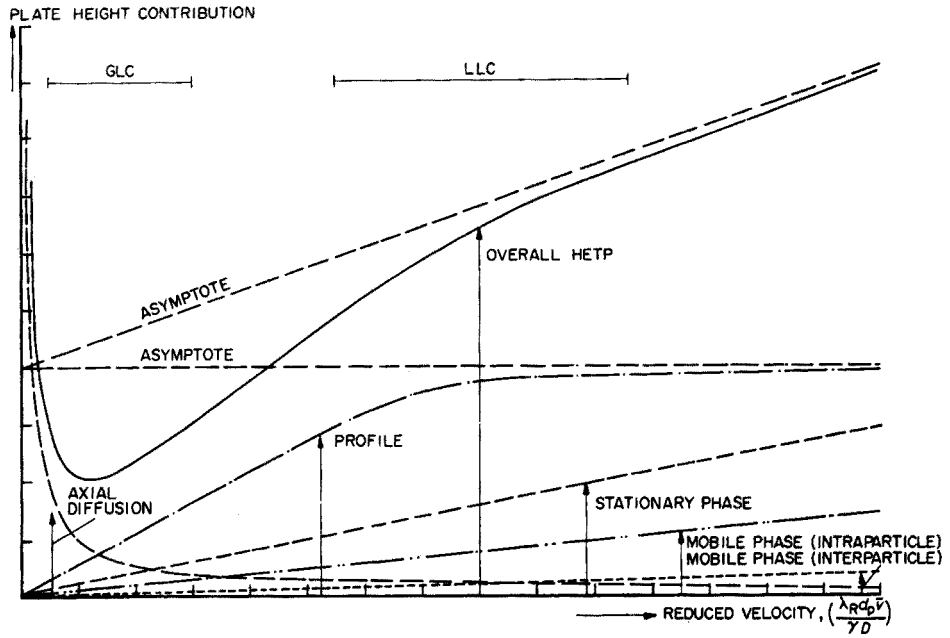

Fig. 3. Schematic representation of various plate height contributions as a function of mobile fluid velocity.

When the convective diffusivity dominates completely, the profile contribution is independent of velocity. In this case the band-broadening by velocity differences is determined entirely by the hydrodynamics of the packed bed. It is under such conditions that the classical concept of "eddy diffusivity" has its meaning.

Figure 3 schematically illustrates the contribution of different band-broadening processes to the overall plate height for laminar flow.

The magnitude of κ

The more irregular the packing, the larger κ. Columns used in GLC mostly have κ values of about 10^{-3}. Very evenly packed columns in GLC may have κ values as low as 10^{-5}.

We found that κ depends not only upon the packing material and the packing technique, but also on the ratio of column radius to particle diameter. Figure 4, pertaining to GLC columns, shows the tendency of κ to increase as this ratio diminishes. This trend does not seem illogical, since the effect of the wall becomes more important the narrower the column. At very low values of R/d_p a homogeneous packing is not possible at all. It is seen that if R/d_p becomes of the order of unity κ attains values of the same magnitude as in empty capillaries (1/48). At larger values of R/d_p the spread between κ values becomes larger. In other words, we may then have good and bad columns while at low R/d_p columns are always badly packed.

Relative magnitude of C_g *and* C_l *terms in analytical GLC*

Opinions differ as to the relative magnitude of C_g and C_l, the coefficients of the

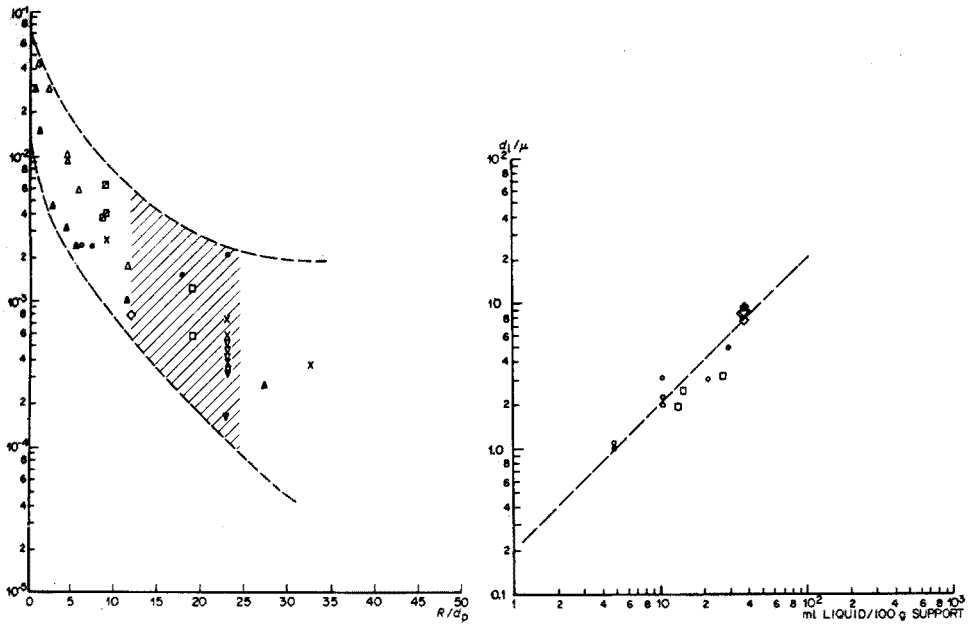

Fig. 4. Effect of the ratio of column radius to particle diameter on packing irregularity for gas chromatographic columns packed in the conventional way. ●, ○, NOREM[17]; ×, KIESELBACH[18]; ▼, ▽, KIESELBACH[16]; ⊖, LITTLEWOOD[7]; □, PERRETT AND PURNELL[19]; □, DEFORD, LLOYD AND AYERS[20]; ◇, our work; ▲, STERNBERG AND POULSON[18]. Open points, porous packing; filled points, glass beads. Hatched area, region of usual analytical-scale GLC columns.

Fig. 5. Relationship between liquid loading and effective liquid film thickness for Sil-O-Cel (Chromosorb P). $\bar{d}_p$ = 0.09–0.34 mm. ○, KIESELBACH[18]; □, PERRETT AND PURNELL[19]; ●, DEFORD *et al.*[20]; ◇, our work.

velocity-proportional contributions pertaining to gas and liquid-phase effects. Some people believe the liquid contribution to dominate (*cf.* the van Deemter equation). Others hold the opposite view, while some take C_g and C_l to be equal. Since the major cause of C_g is now known, this issue can be clarified.

TABLE II

RELATIVE MAGNITUDE OF C_g AND C_l IN TWO HYPOTHETICAL CASES OF ANALYTICAL GLC

	Case 1	*Case 2*
Column diameter (mm)	6	6
Liquid loading (% wt)	40	5
Liquid density (g/ml)	0.9	1.0
d_l (μ)	15	1
D_l (cm^2 sec^{-1})	10^{-6}	10^{-5}
D_g (cm^2 sec^{-1})	0.5	0.05
γ	0.7	0.7
κ	10^{-4}	$5 \cdot 10^{-3}$
k'	1	100
C_l (sec)	0.4	0.000008
C_g (sec)	0.00005	0.03

Figure 5 shows the dependence of the effective film thickness on the liquid loading, as calculated from results with various solutes, stationary liquids and particle sizes. Taking these values into account and also considering the magnitudes of κ as discussed in the preceding section, we may calculate C_g and C_l for two hypothetical cases, specified in Table II.

In one case C_l and in the other C_g dominates completely. The ratios of C_g to C_l differ by about 10^7. It is therefore completely impossible to generalize. Even in one and the same chromatogram we may observe that for some components C_g dominates, while for others C_l is more important. The above explains why some authors found the van Deemter theory satisfactory (*e.g.* KEULEMANS AND KWANTES[10]), whereas others did not.

The effect of various operational parameters on the profile contribution in GLC

The effect of particle size in analytical GLC columns. Under conditions where C_g dominates, variations of d_p at constant R will affect C for a given packing technique. As R/d_p becomes larger with finer particles there will be a tendency towards a more even packing. If we assume that for the usual technique of packing the most probable values of κ are between the boundary lines in Fig. 4, we may calculate C_g as a function of particle size for a given case. Using Fig. 5 to determine d_l, we may also calculate C_l.

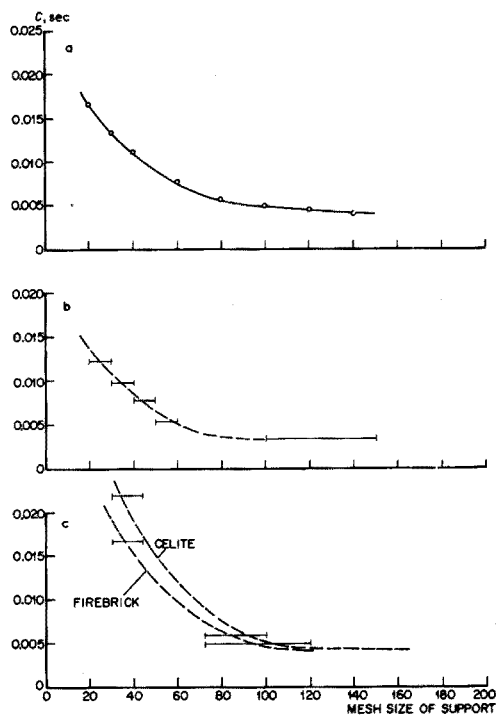

Fig. 6. Dependence of C on particle size for analytical GLC columns. (a), predicted trend; (b–c), actual trends. a. Set of hypothetical columns. ID, 4 mm; d_l, 5 μ; D_l, $2 \cdot 10^{-6}$ cm^2 sec^{-1}; k', 25; D_g, 0.1 cm^2 sec^{-1}. b. Actual columns (BOHEMEN AND PURNELL). ID, 4–4.5 mm; 20%-wt PEG on Sil-O-Cel. Solute, benzene. Carrier gas, N_2. T, 47°. c. Actual columns (DESTY *et al.*). ID, ~ 4.5 mm; 20%-wt paraffin wax. Solutes, C_{11}–C_{14} paraffins. Carrier gas, N_2. T, 134°.

Figure 6 shows the sum of the two as a function of mesh size and compares the predicted trend with the actual experiments of BOHEMEN AND PURNELL[11] and of DESTY *et al.*[12]. Not only is the predicted trend fully confirmed, but the calculated values of C are of the right order of magnitude.

BOHEMEN AND PURNELL have also carried out measurements on columns packed with mixtures of two mesh fractions. Their results are shown in Table III.

TABLE III

EFFECT OF UNIFORMITY OF PARTICLE SIZE ON COLUMN EFFICIENCY

Experiments of BOHEMEN AND PURNELL (Benzene as solute on 4–4.5 mm ID columns with 20%-wt PEG 400 on Sil-O-Cel. Nitrogen carrier at 20°).

Packing composition		C
%-wt 30/40 mesh	*%-wt 50/60 mesh*	*(10^{-4} sec)*
100	0	66
75	25	94
50	50	72
25	75	49
0	100	31

It is to be expected that a regular packing is more difficult to obtain with materials more heterogeneous as regards particle size, or in other words, we may expect κ to increase. This is borne out by the fact that C_g and therefore also C, is a maximum with mixed packing, a result which cannot be satisfactorily explained by classical theory.

The effect of diminishing column diameter in GLC (semi-micro columns and packed capillaries). The effect of reducing column diameter becomes noticeable if C_g dominates. A reduction of R/d_p will increase κ (*cf.* Fig. 4), but the reduction of R^2 in the profile term will more than off-set the increase of κ. Accordingly, C_g will be smaller for narrower columns. This explains the better performance of semi-micro columns with low liquid loadings as compared with conventional GLC columns of, say, 6-mm ID. The former can attain high efficiencies at high speeds.

The foregoing conclusions apply *a fortiori* to the so-called packed capillaries in which R/d_p is of the order of unity. The fact that such columns can attain high efficiencies at high speeds and can have plate heights even lower than d_p has aroused some astonishment[13]. These features of packed capillaries may, however, be made plausible by simple calculation.

If plate height is written as

$$H = B/\bar{v} + C\bar{v}$$

the minimum plate height and the corresponding velocity are given by

$$H_{min} = 2\sqrt{BC},$$

and

$$\bar{v}_{opt} = \sqrt{B/C}.$$

If the liquid mass transfer contribution is zero (air peak) or negligible, $B = 2\gamma D_g$ and $C = 2\kappa R^2/\gamma D_g$, whence

$$H_{min} = 4R\kappa^{\frac{1}{2}}$$

and

$$\bar{v}_{opt} = \gamma D_g / R\kappa^{\frac{1}{2}}.$$

We have seen that in a "packed capillary" the packing is far from regular, κ being of the same order as in an empty capillary ($\sim$1/48). For a column of 0.991 mm ID filled with particles of 0.42 mm diameter, STERNBERG AND POULSON[13] found for methane in He:

$$H_{min} = 0.24 \text{ mm } (\sim 0.6 d_p)$$
$$\bar{v}_{opt} = 80 \text{ cm sec}^{-1},$$

whereas with $\kappa = 1/48$ and $\gamma D_g = 0.5$ cm^2 sec^{-1} we may arrive at values of 0.28 mm and 70 cm sec^{-1} for H_{min} and $\bar{v}_{opt}$, respectively.

Effect of increasing column diameter in GLC (preparative columns). The equation for the profile contribution shows that with increasing diameter plate height should increase, if other conditions are kept unaltered. In preparative work relatively high liquid loadings are usual, *e.g.* 30%-wt. Under such conditions C_l will be of the order of 10^{-2} sec. The effect of increasing diameter becomes noticeable if C_g becomes of the same order. With $D_g = 0.1$ cm^2 sec^{-1} (N_2 carrier), $\kappa = 10^{-3}$ and $\gamma_R = 0.7$ it is calculated that this situation corresponds with $R = 0.6$ cm. Thus, it is expected that the increase in plate height will be noticeable for tube diameters in the range of 1–2 cm. This conclusion is in agreement with experimental findings. Examination of published

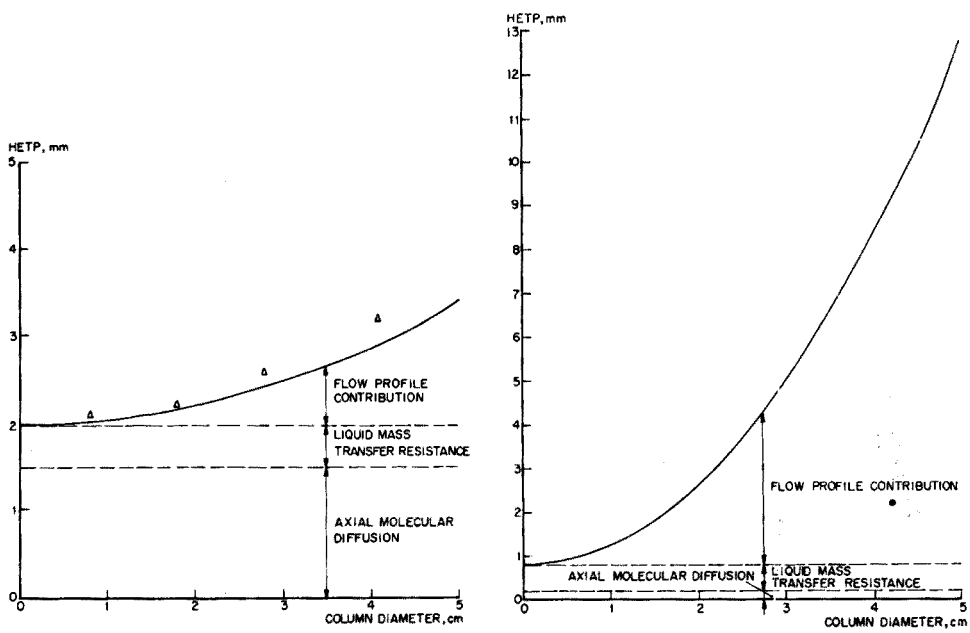

Figs. 7–8. Predicted trend of HETP with increasing column diameter. 20%-wt dinonyl phthalate on diatomaceous support. T, 24°. Solute, n-C_6. (7) Carrier gas, H_2. $\bar{v}$, 2 cm sec^{-1}. △, actual experiments of BAYER AND WITSCH. (8) Carrier gas, N_2. $\bar{v}$, 5 cm sec^{-1}.

H–$\bar{v}$ data on columns of larger diameter than 1 cm (*e.g.* from HIGGINS AND SMITH[14]) indeed shows that increase of plate height is mainly caused by an increase in the C-term, whilst variations in the A-term, if present, are insignificant, considering the experimental accuracy.

Figure 7 shows the predicted trend of the plate height with increasing diameter for a series of columns with $\kappa = 10^{-3}$. The conditions chosen for these hypothetical columns are close to the experimental ones of BAYER AND WITSCH[15], whose results are indicated by triangles. The breakdown of plate height into its various contributors shows that in this case the profile contribution is less important than the axial-diffusion term. If nitrogen were used instead of hydrogen and if the carrier gas velocity were somewhat higher, the increase of plate height with increasing diameter would have been much more pronounced (Fig. 8).

Experiments at high velocities and with large particles. In the cases considered so far convective diffusion is negligible compared with molecular diffusion. Such is no longer the case in GLC at unusually high velocities. Experiments at such velocities have been conducted by KIESELBACH[16] and by STERNBERG AND POULSON[13]. From their results it can be concluded that at higher velocities H–$\bar{v}$ curves tend to become concave relative to the velocity axis. This cannot be explained by classical theory, but follows logically from the equation of the profile term (see also Fig. 3).

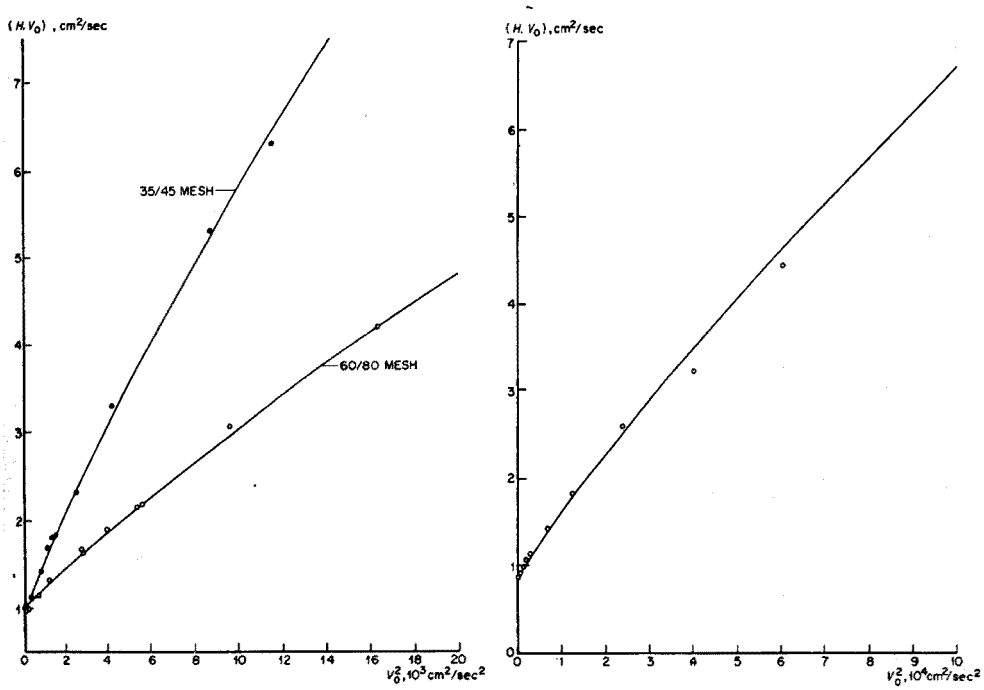

Fig. 9. Experiments of STERNBERG AND POULSON interpreted by the present theory. v_0, velocity at the column outlet.

Fig. 10. Measurements of KIESELBACH interpreted by the present theory. v_0, velocity at the column outlet. 100–200 mesh microbeads; 6 mm ID columns; T, 25°. Solute, air. Carrier gas, He.

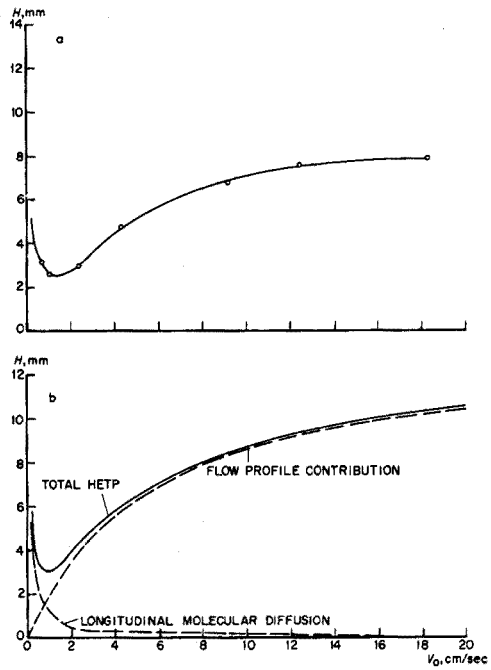

Fig. 11. H–v_0 curve for columns packed with uncoated large-diameter beads. (a) experimental curve; (b) curve calculated for laminar flow. 5 cm ID column filled with 3 mm glass beads. Carrier gas, N_2. Solute, n-C_8. (a) room temperature; ε, 0.364. (b) 24°; κ, 10^{-3} F.

Figures 9 and 10 show that the experimental points closely follow the predicted curvature.

Since the convective diffusivity is proportional to d_p, with larger particle diameters convective diffusivity must come into play at lower velocities. Figure 11 shows the results of some experiments with 3-mm glass beads. The shape of the experimental curve is well explained by the profile contribution.

Comparison of the present treatment with the eddy diffusivity concept and the coupling theory

The eddy diffusivity concept considers the packing irregularity to be of a statistical nature and assumes that this irregularity contributes as a velocity-independent term to plate height. As we have seen, the latter conclusion is not always true and certainly does not hold for GLC. Only at very high velocities does the profile contribution become independent of velocity, *viz.*

$$\lim_{v \to \infty} h = \frac{2\kappa R^2}{\lambda_R d_p}$$

Considering the profile contribution at low velocities where molecular diffusion dominates, we may write

$$\lim_{v \to \infty} h = \frac{2\kappa R^2}{\gamma_R D_g} \bar{v}$$

By representing the profile contribution as

$$h = \frac{1}{\lambda_R d_p / 2\kappa R^2 + \gamma_R D_g / 2\kappa R^2 \bar{v}},$$

we see that the two terms below the bar are the reciprocals of the two limiting values of the profile contribution. Setting these limiting values equal to A and $C_g\bar{v}$, respectively, we may write

$$h = \frac{1}{1/A + 1/C_g\bar{v}},$$

which is, in fact a coupling of the A and C_g terms in the way suggested by GIDDINGS[2]. Thus, the present treatment goes some way towards explaining his coupling theory although it remains uncertain whether the generalizations in this theory are correct.

The profile contribution in liquid and high-pressure gas chromatography

The examples discussed so far all pertain to GLC. Since the role of flow profiles is even more pronounced in liquid chromatography and chromatography with high-pressure gases or supercritical fluids and since in these techniques both molecular diffusion and convective diffusion take part in lateral transport, it would be very tempting to discuss the band-broadening in these forms of chromatography. Such a discussion would take us too far, however. Suffice it to say that the present extension of the classical theory has aided very much in our understanding of the band-spreading in these techniques and has provided clear explanations for experimental effects hitherto insufficiently understood.

SUMMARY

In the past few years some problems have arisen as to the interpretation of experimental plate height data of packed chromatographic columns by means of the theory of VAN DEEMTER *et al.* These difficulties concern the "eddy diffusion" and "mass transfer" terms in particular. Light may be thrown on this matter by the recognition of unevenness of flow throughout the column cross-section as a major source of band-broadening. By considering the contribution to plate height resulting from the interaction between such flow profiles and various mechanisms of lateral transport of material it proved possible to solve the above-mentioned difficulties.

REFERENCES

1 J. J. VAN DEEMTER, F. ZUIDERWEG AND A. KLINKENBERG, *Chem. Eng. Sci.*, 5 (1956) 271. See also D. H. DESTY, A. GOLDUP AND B. H. F. WHYMAN, *J. Inst. Petroleum*, 45 (1959) 295.
2 J. C. GIDDINGS, *Nature*, 184 (1959) 357; J. C. GIDDINGS, *Anal. Chem.*, 34 (1962) 1186.
3 F. H. HUYTEN, W. VAN BEERSUM AND G. W. A. RIJNDERS, in R. P. W. SCOTT (Ed.), *Gas chromatography*, Butterworths, London, 1960.
4 G. TAYLOR, *Proc. Roy. Soc.*, A 219 (1953) 186; A 223 (1954) 446; A 225 (1954) 473.
5 R. ARIS, *Proc. Roy. Soc.*, A 235 (1956) 67.
6 M. E. HARTMAN, C. J. H. WEVERS AND H. KRAMERS, *Chem. Eng. Sci.*, 9 (1958) 80.
7 A. B. LITTLEWOOD, *Proc. 5th Intern. Symp. Gas Chromatography, Brighton, 1964*, Institute of Petroleum, London, 1965; A. B. LITTLEWOOD, *Anal. Chem.*, 38 (1966) 2.
8 W. O. SMITH, P. D. FOOTE AND P. F. BUSANG, *Phys. Rev.*, 34 (1929) 1271.
9 J. HRUBIŠEK, *Kolloid Beihefte*, 53 (1941) 385.
10 A. I. M. KEULEMANS AND A. KWANTES, in D. H. DESTY (Ed.), *Vapour phase chromatography*, Butterworths, London, 1956, p. 15.
11 J. BOHEMEN AND J. H. PURNELL, in D. H. DESTY (Ed.), *Gas chromatography*, Butterworths, London, 1958), p. 6.
12 D. H. DESTY, F. M. GODFREY AND C. L. A. HARBOURN, in D. H. DESTY (Ed.), *Gas chromatography*, Butterworths, London, 1958, p. 200.

13 J. C. STERNBERG AND R. E. POULSON, *Anal. Chem.*, 36 (1964) 1492.
14 G. M. C. HIGGINS AND J. F. SMITH, *Proc. 5th Intern. Symp. Gas Chromatography, Brighton, 1964*, Institute of Petroleum, London, 1965.
15 E. BAYER AND H. G. WITSCH, *Z. Anal. Chem.*, 170 (1959) 278; E. BAYER, in R. P. W. SCOTT (Ed.), *Gas chromatography*, Butterworths, London, 1960, p. 236.
16 R. KIESELBACH, *Anal. Chem.*, 35 (1963) 1342.
17 S. D. NOREM, *Anal. Chem.*, 34 (1962) 40.
18 R. KIESELBACH, *Anal. Chem.*, 33 (1961) 23.
19 R. H. PERRETT AND J. H. PURNELL, *Anal. Chem.*, 35 (1963) 430.
20 D. D. DEFORD, R. J. LLOYD AND B. O. AYERS, *Anal. Chem.*, 35 (1963) 426.

Analytica Chimica Acta
Elsevier Publishing Company, Amsterdam
Printed in the Netherlands.

FLÜSSIG-KRISTALLINE SCHMELZEN BEI TEMPERATUREN UNTERHALB 100° UND OBERHALB 200° ALS STATIONÄRE PHASEN IN DER GASCHROMATOGRAPHIE

H. KELKER, B. SCHEURLE UND H. WINTERSCHEIDT
Farbwerke Hoechst A.G. (vormals Meister Lucius & Brüning), Frankfurt-Höchst (Deutschland)

(Eingegangen den 1. November, 1966)

Da mit flüssig-kristallinen Schmelzen als stationäre Phasen Trenneffekte erzielt werden, die offenkundig sehr eng mit der molekularen Nahordnung (Schwarmbildung) solcher Flüssigkeiten zusammenhängen[1–6], besteht der Wunsch, Anhaltspunkte für eine Relation zwischen möglichst leicht bestimmbaren, wohldefinierten Stoffeigenschaften und dem Löseverhalten aufzufinden.

Das Lösevermögen kann auch bei flüssig-kristallinen Schmelzen wie üblich und mit einem geringstmöglichen Grad an prinzipiell unerwünschter Relativierung der Messwerte als spezifisches Retentionsvolumen ($V_g^{(T)}$ bzw. $V_g^{(N)}$) angegeben werden. Es muss jedoch darauf hingewiesen werden, dass es nicht in jedem Fall unbeeinflusst von der Oberfläche des Trägers und der Vorgeschichte der stationären Phase ist, wie es für normale Flüssigkeiten in relativ weiten Grenzen der Fall ist. Trotz einer Reihe positiver Ergebnisse, die die Invarianz von V_g (z.B. gegenüber Strömungsgeschwindigkeit und Beladungsmenge) bestätigen[3] und die inzwischen durch weitere Beispiele erhärtet wurden, sei darauf hingewiesen, dass ein und dieselbe flüssig-kristalline Substanz unter gleichen Bedingungen bezüglich Druck und Temperatur verschiedenartige Texturen auszubilden vermag. Es hängt dies insbesondere von der Art der Trägeroberfläche und von der thermischen Vorbehandlung ab. Neben der bekannten Fadenstruktur der nematischen Phase ist unter den Bedingungen der gepackten Säule auch mit der Bildung homöotroper oder homogener Texturen zu rechnen. Näheres über die Textur von flüssig-kristallinen Phasen ist z.B. bei ORNSTEIN[7] und bei GRAY[8] zu finden. Wir würden es jedoch für verfehlt halten, auf die Mitteilung von spezifischen Retentionsvolumina wegen dieser Gefahr ganz zu verzichten. Bisher liessen sich bei Einhaltung zusätzlicher Bedingungen insbesondere bei nematischen Substanzen nach vorhergehendem Erhitzen über den Klärpunkt hinaus reproduzierbare V_g-Werte erhalten; die auch für flüssig-kristalline Phasen charakteristische "Selektivität", hier besonders interessant gegenüber Stellungsisomeren, wird für praktische Zwecke durch das Verhältnis $V_g^{(T)}(i)/V_g^{(T)}(j) = r_{ij} = a_j/a_i = f_j p_j^0/f_i p_i^0$ beschrieben. Wo im folgenden $V_g^{(T)}$-Werte allein angegeben worden sind, lassen sich selbstverständlich die r_{ij}-Werte leicht ermitteln, und für die theoretische Betrachtung ist die Eliminierung von p_i^0 jederzeit möglich, sofern der Anschluss an das Modell der idealen Mischung im Sinne des verallgemeinerten Raoult–Henry'schen Gesetzes gesucht wird.

In dem Bestreben, das eigenartige Lösevermögen flüssig-kristalliner Phasen besser zu verstehen, und bezüglich der praktischen Analyse organischer Zwischen-

produkte, wo oft in erster Linie die Trennung von verschieden substituierten Aromaten gefordert wird, interessierten folgende beiden Fragen:

1. Besteht ein direkter Zusammenhang zwischen Lösungsmittel-Spezifität, insbesondere gegenüber *meta–para*-Isomeren, und vergleichbaren Substitutionstypen und Persistenzbereich? Mit anderen Worten: Gelten die von VORLÄNDER[9] ausgesprochenen Gesetzmässigkeiten, die das Ausmass des "liquokristallinen Charakters" ausmachen, im übertragenen Sinne auch bezüglich der Selektivität? Wir gehen von der naheliegenden Hypothese aus, dass diejenigen zwischenmolekularen Kräfte und diejenigen konstitutionellen Eigenschaften, welche Voraussetzungen für die Existenz der flüssig-kristallinen Phase sind, auch entscheidend zur Lösewirkung gegenüber konstitutionell vergleichbaren Partnern beitragen. Es liegt nahe, solche Untersuchungen an möglichst niedrig schmelzenden Substanzen auszuführen, da bei niedrigen Temperaturen bekanntermassen der durch Dampfdruckunterschiede verursachte Anteil der Trennwirkung am grössten ist.

2. Welche kristallin-schmelzbaren Substanzen sind thermisch und chemisch soweit stabil, dass sie für den höheren Temperaturbereich, d.h. etwa oberhalb ca. 200°, eingesetzt werden können und dabei nicht nur aufgrund ihrer flüssig-kristallinen Textur eine sterische Wirkung entfalten, sondern zugleich polare Molekeln von wohldefinierter Zusammensetzung und Grösse sind? Solche stationären Phasen verdienen auch deshalb Interesse, weil viele der heute oberhalb 200° benutzten Phasen Verbindungen von relativ geringer Polarität und wenig stark ausgeprägter Anisotropie der molekularen Eigenschaften sind. Zudem ist meist kein "Molekulargewicht" dieser Verbindungen, das für die Berechnung von f^0-Werten benötigt wird, angegeben. Meist handelt es sich um Mischungen, die oft nicht einmal aus Polymerhomologen bestehen.

Die ersten gaschromatographischen Untersuchungen mit flüssig-kristallinen Phasen wurden mit dem in jeder Hinsicht am eingehendsten untersuchten 4,4'-Methoxy-azoxy-benzol ("Azoxyanisol") und seinem nächsthöheren Homologen, dem 4,4'-Äthoxy-azoxy-benzol, ausgeführt[1,2]. Nur die letzte Substanz erwies sich als für die Praxis geeignet, indem sie bei 140°, d.h. wenig oberhalb ihres Schmelzpunktes, als nematische Phase ein Verhältnis der Grenzaktivitätskoeffizienten für *p*- und *m*-Xylol von 0.9 ergab[2]. Für Azoxyanisol erhielt man trotz der Möglichkeit, wegen des niedrigen Schmelzpunktes bereits bei etwas 118° arbeiten zu können, günstigstenfalls ein Verhältnis f_p/f_m von 0.9[6]. DEWAR UND SCHRÖDER[4,5] haben dann gezeigt, dass auch die von WEYGAND[10] erstmalig dargestellten und systematisch untersuchten höheren Homologen der Azoxyäther, vor allem auch deren smektische Phasen, generell die *para*-Isomeren besser als die *meta*-Isomeren lösen. Doch zeigte sich, dass Azoxyphenetol mit dem 30° breiten Persistenzbereich seiner nematischen Schmelze die bisher wirksamste reine Phase zur Trennung von *m–p*-Xylol ist. Unter den von DEWAR UND SCHRÖDER[5] zur Isomerentrennung benutzten Hydrochinonestern *p*-substituierter Alkoxycarbonsäuren war es die Verbindung

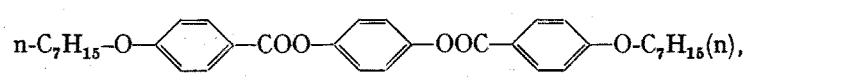

welche im unterkühlten Zustand ihrer smektischen Schmelze (Fp., 83°) bei 68° die Trennwirkung des 4,4'-Azoxyphenetols für *m–p*-Xylol erreicht.

Zur Fortsetzung unserer Versuche mit den ersten beiden Verbindungen aus der

TABELLE I

RELATIVE RETENTIONSVOLUMINA (*r*) FÜR EIN EUTEKTISCHES GEMISCH AUS 4,4'-AZOXYANISOL UND 4,4'-AZOXYPHENETOL (1)

Bezugssubstanz: *o*-Xylol ($r = 1.00$; $V_g^{(T)} = 116\ cm^3/g$). $T = 99°$.

Xylol	*o*-, 1.0	*p*-, 0.77	*m*-, 0.70
Äthyltoluol	*o*-, 1.30	*p*-, 1.30	*m*-, 1.10
Chlortoluol	*o*-, 1.47	*p*-, 2.01	*m*-, 1.68

Reihe der Azoxyäther und im Hinblick auf möglichst niedrige Arbeitstemperaturen bei breitem Persistenzbereich zeigte sich, dass die Verwendung eines eutektischen flüssig-kristallinen Systems Vorteile hat, was z.B. ZADO UND JUVET an einem Beispiel aus dem anorganischen Bereich ($NaClO_3$–NaCl) mitteilten[12].

Wir trennen z.B. *m*–*p*-Xylol und die Chlortoluole an einer (eutektischen) Mischung von Azoxyanisol und Azoxyphenetol bei der in jeder Hinsicht günstigen, relativ niedrigen Temperatur von 99°. Unter diesen Bedingungen erhielt man die $V_g^{(T)}$-Werte der Tabelle I. Das Phasendiagramm dieses Zweistoffsystems wurde von PRINS[29] und in letzter Zeit von SACKMANN UND ARNOLD[11,14] aufgenommen und diskutiert. Für unsere Betrachtung mag die Feststellung genügen, dass der Schmelzpunkt des eutektischen Gemisches bei 97° liegt und einem Mol-verhältnis von 60 Teilen 4,4'-Azoxyanisol zu 40 Teilen 4,4'-Azoxyphenetol entspricht. Für diese Zusammensetzung beträgt der Persistenzbereich 49 Grad (der Klärpunkt liegt bei 146°).

In diesem Zusammenhang sei an die Tatsache erinnert, dass auch durch Mischung nematogener Substanzen mit konstitutionell verwandten, für sich allein jedoch nicht zur Ausbildung flüssig-kristalliner Schmelzen befähigten Substanzen noch flüssig-kristalline Phasen mit wesentlich niedrigeren Erstarrungspunkten hergestellt werden können[13]. Es gibt dagegen kaum chemisch einheitliche Substanzen, die eine enantiotrope flüssig-kristalline Schmelze wesentlich unterhalb von etwa 80° zu bilden vermögen, die für die analytische Gaschromatographie bei tiefen Temperaturen geeignet erscheint. Eine Übersicht über die hier zur Zeit bestehenden Möglichkeiten vermittelt eine Arbeit von BILLARD UND CERNE[15].

Im folgenden wird über Versuche mit relativ niedrig schmelzenden Verbindungen berichtet, womit ein Vergleich zwischen Schmelzpunkt, Persistenzbereich und speziellem Trennvermögen gegenüber Xylolen als Testsubstanzen möglich wird. Unter den hier in Betracht kommenden Substanzen wählten wir das 1910 von FRÖHLICH[16] erstmalig hergestellte 4-Methoxybenzyliden-4'-cyananilin, das nach Angabe des Autors bei 103° eine nematische Schmelze bildet. Der Klärpunkt liegt nach FRÖHLICH bei 113.5°. Wir fanden 106° bzw. 117–118° mit Hilfe des Heiztisch-(Kofler)-Mikroskops. Der Verlauf der Retentionsvolumina mit der Temperatur zeigte allerdings ein Maximum bei 113–114°. Diese Diskrepanz konnte noch nicht geklärt werden.

Tabelle II zeigt Retentionsvolumina an 4-Methoxybenzyliden-4'-cyananilin. Die Selektivität gegenüber *m*–*p*-Xylol ist sehr gering, und die Umkehr der Elutionsfolge für *m*- und *p*-Xylol am Klärpunkt entspricht früheren Beobachtungen am Azoxyanisol. Man gewinnt auch hier den Eindruck, dass ein enger Existenzbereich der nematischen Phase geringe Selektivität zur Folge hat, und auch Azoxyanisol verhält sich in diesem Sinne ungünstiger als das Azoxyphenetol[1,2].

TABELLE II

RELATIVE (KORRIGIERTE) RETENTIONSVOLUMINA *(r)* FÜR 4-METHOXYBENZYLIDEN-4'-CYANANILIN (2)

Bezugssubstanz: *o*-Xylol (r = 1.00; $V_g^{(T)}$ in Spalte 6).

T	*m-Xylol*	*p-Xylol*	*n-Octan*	*n-Decan*	$V_g^{(T)}$ (cm³/g)
105	0.78	0.80	0.10	0.36	162
108	0.79	0.80	0.10	0.35	160
111	0.79	0.80	0.10	0.34	162
114[a]	0.79	0.78	0.11	0.36	168
117	0.80	0.79	0.11	0.37	161
120	0.80	0.78_5	0.11	0.37	148
125	0.80	0.78_5	0.12	0.37	134
130	0.81	0.79	0.12	0.37	119

[a] Klärpunkt.

Als weitere Substanz wurde das 4-Methoxybenzyliden-4'-acetoxyanilin mit dem schon bemerkenswert niedrigen Schmelzpunkt von 83° und einem Klärpunkt der nematischen Phase bei 107° hergestellt (siehe Anhang) und für entsprechende, beim 4-Methoxybenzyliden-4'-cyananilin beschriebene Versuche eingesetzt. Man erhielt, vorausgesetzt, dass zunächst die stationäre Phase einmal über den Klärpunkt hinaus erhitzt worden war, reproduzierbare Retentionsvolumina für die Xylol-Isomeren und einige n-Alkane. Tabelle III zeigt eine Zusammenstellung der Retentionswerte.

TABELLE III

RELATIVE (KORRIGIERTE) RETENTIONSVOLUMINA FÜR 4-METHOXYBENZYLIDEN-4'-ACETOXYANILIN (3)

Bezugssubstanz: *o*-Xylol (r = 1.00; $V_g^{(T)}$ in Spalte 6).

T	*m-Xylol*	*p-Xylol*	*n-Octan*	*n-Decan*	$V_g^{(T)}$ (cm³/g)
84.5	0.79_6	0.83	0.10	0.40	257
97.0	0.79_8	0.82	0.11	0.40	199
108.4	0.80	0.79	0.12	0.41	192
120	0.81	0.79	0.13	0.42	145

Die Werte der Tabelle III zeigen wiederum die für eine nematische Phase typische Selektivität gegenüber den Xylol-Isomeren, die sich nach Überschreitung des Klärpunktes beim *m*–*p*-Xylol umkehrt. Die Normalparaffine n-Octan und n-Decan ergaben ähnliche Werte wie an 4-Methoxybenzyliden-4'-cyananilin. Das Flüchtigkeitsverhältnis *m*-Xylol zu *p*-Xylol ist auch an dieser Phase nicht sehr hoch; es beträgt günstigstenfalls 1.05.

In Tabelle IV wurden zu einem Vergleich zwischen Schmelzpunkt, Klärpunkt, Persistenzbereich ΔT und maximalen Flüchtigkeitsverhältnis *m*-Xylol zu *p*-Xylol diese Werte für alle bisher von uns gemessenen Systeme zusammengestellt.

TABELLE IV

RELATIVE FLÜCHTIGKEIT VON *p*-XYLOL GEGENÜBER *m*-XYLOL AN VERSCHIEDENEN NEMATISCHEN PHASEN

(Maximalwerte, untere Temperaturgrenze der Mesophase).

	Klärpunkt	*ΔT (Grad)*	*Schmelzpunkt*	*Maximales Flüchtigkeitsverhältnis m-Xylol–p-Xylol*
4-Methoxybenzyliden-4′-cyananilin	117°	11	106°	1.03
4,4′-Azoxyanisol	134.5°	17.5	117°	1.04
4-Methoxybenzyliden-4′-acetoxyanilin[24]	107°	24	83°	1.05
4,4′-Azoxyphenetol	168°	30	138°	1.09
Eutektikum (siehe Tab. I)	146°	49	97°	1.10

Es zeigt sich deutlich, dass die relative Flüchtigkeit der beiden Xylol-Isomeren symbath zur Breite des Persistenzbereichs verläuft. Wenn also VORLÄNDER ein Mass für den "liquokristallinen Charakter" einer Substanz in der Breite dieses Temperaturbereichs sieht, so kann man dem hinzufügen, dass auch die "Selektivität" — selbstverständlich beschränkt auf ein sicherlich besonders typisches, weil von polaren, zusätzlich wirksamen Gruppen weitgehend freies Isomerenpaar — unter dem gleichen Aspekt zu betrachten ist. Inwieweit das auch für smektische Phasen gilt, lässt sich nicht entscheiden. Sicherlich ist auch die absolute Lage der Umwandlungspunkte von Bedeutung.

Bestimmt man für den Bereich zwischen Schmelzpunkt bis wenige Grade unterhalb des Klärpunktes die dem Lösungsvorgang zugeordnete Wärmesumme, so erhält man für alle bisher untersuchten reinen Phasen im anisotropen Bereich einen im Vergleich zur isotropen Schmelze höheren (positiven) Anteil an Mischungswärme[1,2,17] (vgl. die Neigung der in Abb. 1 eingezeichneten Geraden). Bei Mischphasen erhielt man stets geringere Unterschiede in den Mischungswärmen (vgl. Abb. 1a und b).

Wenige Grade vor Erreichen des Klärpunktes wird der Beitrag, den die Mischungswärme zur gesamten Lösungswärme liefert, immer stärker positiv, je weiter man sich dem Klärpunkt nähert*. Man bemerkt, dass hier der seltene Fall eintritt,

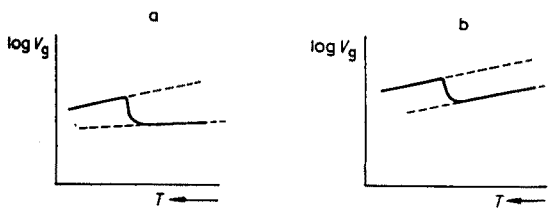

Abb. 1. Temperaturabhängigkeit des spezifischen Retentionsvolumens an nematischen Schmelzen beim Überschreiten des Klärpunktes (schematisch). Bezugssubstanz: *o*-Xylol. (a) reine Phasen; (b) Mischphasen.

* Vgl. Abb. 1 unserer Mitteilung über cholesterinartige Mischphasen, die ein analoges Verhalten zeigten[17].

TABELLE V

RELATIVE (r) UND SPEZIFISCHE RETENTIONSVOLUMINA ($V_g^{(T)}$) AN DEN BEI HOHEN ARBEITSTEMPERATUREN VERWENDETEN SCHIFF'SCHEN BASEN

Die relativen Werte sind auf *o*-Phthalsäuredimethylester bezogen.

Substanz	*4,4'-Bis-benzyliden-benzidin* ($T = 240°$)		*Bis-(p-methoxy-benzyliden)-4,4'-diaminostilben (trans)* ($T = 270°$)		*Bis-phenetidyl-terephthalaldehyd* ($T = 206°$)	
	r	$V_g^{(T)}$ (cm^3/g)	r	$V_g^{(T)}$ (cm^3/g)	r	$V_g^{(T)}$ (cm^3/g)
o-Xylol	0.06	8	0.06	2	0.05_4	9 meta: 7 para: 8
n-Hexadecan	0.22	30	0.13	4.4	0.21	33
Naphthalin	0.38	52	0.45	15	0.37	59
Diphenyl	0.70	95	0.76	26	0.74	118
Diphenylmethan	0.69	94	0.61	21	0.60	96
Acenaphthen	1.28	174	1.37	46.5	1.3_1	208
trans-Stilben	2.85	388	2.75	93.5	4.0	640
Phenanthren	5.32	724	5.6_8	193	7.0	1100
Anthracen	6.00	816	6.7_4	229	9.6	1530
o-Kresol	0.21_3	29	0.19_4	6.6	0.22_5	36
m-Kresol	0.26	35.4	0.36	12	0.28	44.5
p-Kresol	0.25_4	34.5	0.36	12	0.29	46
o-Dimethoxybenzol	0.22_8	31.0	0.25	8.5	0.20	32
m-Dimethoxybenzol	0.26_7	36.3	0.31	10.5	0.25	40
p-Dimethoxybenzol	0.27_5	37.4	0.37	12.5	0.30	48
Laurinsäuremethylester	0.35	48	0.19	6.5	0.33_5	53
Sebacinsäuredimethylester	0.98	133	0.72	25	1.0_1	161
o-Phthalsäuredimethylester	1.00	136	1.00	34	1.00	159
m-Phthalsäuredimethylester	1.2_4	169	1.2_5	42.5	1.4_2	226
p-Phthalsäuredimethylester	1.2_7	173	1.5_3	52	1.8_4	293
o-Phenylphenol	1.5_7	214	1.6_2	55	1.7_1	272
p-Phenylphenol	—	—	—	—	7.8	1240
α-Naphthol	—	—	—	—	3.04	484
β-Naphthol	—	—	—	—	3.9_2	625
Pyridin	0.05	7	0.07	2.5	—	—
Anilin	0.17	23	—	—	—	—
Chinolin	0.60	82	0.80	27	—	—
α-Benzylpyridin	1.00	136	1.0_1	34	0.90	143
γ-Benzylpyridin	1.5_2	207	1.5_8	54	1.26	200
Carbazol	9.8	1330	11.6	39	16.4	2550
4-Methylacetidinon-2	0.22	30	0.38	13	—	—
2,3-Dichlortoluol	0.25	34	0.30	10	0.22	35
2,4-Dichlortoluol	0.20	27	0.22	7.5	0.18	29
2,5-Dichlortoluol	0.21	28.3	0.22	7.5	0.19	30
2,6-Dichlortoluol	0.20	27	0.23	8	0.18	29
3,4-Dichlortoluol	0.26	35	0.29	10	0.23	37
3,5-Dichlortoluol	0.19_5	26.5	0.21	7	0.16	25

Substanz	*4,4'-Bis-benzyliden-benzidin (T = 240°)*		*Bis-(p-methoxy-benzyliden)-4,4'-diaminostilben (trans) (T = 270°)*		*Bis-phenetidyl-terephthalaldehyd (T = 206°)*	
	r	$V_g^{(T)}$ *(cm³/g)*	*r*	$V_g^{(T)}$ *(cm³/g)*	*r*	$V_g^{(T)}$ *(cm³/g)*
1,2-Dibrombenzol	0.43	58	0.45	15	—	—
1,3-Dibrombenzol	0.35	48	0.38	13	—	—
1,4-Dibrombenzol	0.37	50	0.37	12.5	—	—
1,2-Dimethyl-3-nitrobenzol	0.60	82	0.65	22	0.56	89
1,2-Dimethyl-4-nitrobenzol	0.91	124	1.03	35	0.93	148
1,3-Dimethyl-2-nitrobenzol	0.60	82	0.67	23	0.59	94
1,3-Dimethyl-4-nitrobenzol	0.32	44.5	0.29	10	0.27	43
1,4-Dimethyl-2-nitrobenzol	0.52	71	0.55	19	0.50	79.5
1-Nitro-2-äthylbenzol	0.39	53	0.40	13.5	0.34	54
1-Chlornaphthalin	0.86	117	1.0_4	35.5	0.83	132
2-Chlornaphthalin	0.87	118	1.0_7	36.5	0.96	153

dass die Affinität des Lösungsmittels zum Gelösten in diesem dem Klärpunkt vorgelagerten Temperaturbereich mit steigender Temperatur grösser wird. Dies besagt, dass in immer stärker zunehmendem Masse der Mischungsvorgang Energie erfordert, die schliesslich dem Betrage nach scheinbar sogar den der Verdampfungsenthalpie der reinen Phase des Gelösten übersteigt. Näheres über dieses Verhalten flüssig-kristalliner Schmelzen in dieser Vorperiode des Klärpunktes sei einer weiteren Mitteilung vorbehalten. Unterhalb des Schmelzpunktes werden, von höheren Temperaturen her kommend, infolge teilweiser Unterkühlung der Schmelze öfters streuende Werte für $V_g^{(T)}$ erhalten. Dass an (nematogenen) organischen Substanzen unterhalb des Schmelzpunktes auch Adsorptionschromatographie möglich ist, wurde bereits erwähnt[1]. Für 4-Methoxybenzyliden-4'-cyananilin gilt das gleiche, und auch die weiter unten beschriebenen höher schmelzenden Substanzen zeigen unterhalb des Schmelzpunktes eine bemerkenswerte Selektivität gegenüber flüchtigen Komponenten; sie lassen sich u. U. also auch als stationäre Phasen für die Adsorptions-Gaschromatographie verwenden*. In Anbetracht vordringlicher praktischer Probleme der Isomerentrennung wurden solche Untersuchungen vorerst zurückgestellt und das Hauptaugenmerk auf Versuche mit temperaturbeständigen nematischen Schmelzen gerichtet, die u.a. die Trennung und Bestimmung praktisch beliebiger Mengenverhältnisse von *o*-, *m*- und *p*-Phthalsäuredimethylestern einiger kondensierter Aromaten und die des *α*- und *β*-Naphthols zum Ziel hatten. Mit einer gewissen Willkür den früheren Veröffentlichungen Vorländers folgend und im Hinblick auf vorhandene Ausgangssubstanzen wurden für die weiteren Versuche folgende Bis-azomethin-Verbindungen synthetisiert (Näheres über Darstellung und Eigenschaften dieser Substanzen im Anhang).

* Wie Versuche zeigten, ist diese Eigenschaft keineswegs auf nematogene Substanzen beschränkt.

4,4'-Bis-benzyliden-benzidin[27,30] (4) *und Bis-(4-methoxy-benzyliden)-benzidin*[23,24] (4a)

Wie viele der nematogenen Substanzen, fällt auch das Benzyliden-benzidin in schwer pulverisierbaren Kristallplättchen an, die in allen gängigen Lösungsmitteln nur wenig löslich sind. Es empfiehlt sich daher, die Beladung des Trägermaterials mit der feinkristallinen Substanz durch Vermischen in festem Zustand vorzunehmen. Mit der durch Gummihandschuh geschützten Hand vermischt man ohne Anwendung von Druck die feinst pulverförmige, kristalline Phase mit dem Träger in einer Kasserolle, bis die heterogene Mischung einen einheitlichen Farbton zeigt (Beladungsstärke durchweg 15 Gew.-% auf HDMS-behandeltem Chromosorb W). Die stationäre Phase haftet gut auf dem Träger. Auch aus heissem Dioxan liess sich die Substanz aufbringen, was jedoch keinerlei Vorteile ergibt. Wir benutzten für die im folgenden beschriebenen Versuche — soweit nicht anders vermerkt — Säulen aus Kupferrohr, Länge ca. 5 m, aussen 6 und innen 4 mm Durchmesser. In einem F & M-Gerät Modell 720 wurden die mit stationärer Phase beladenen, gefüllten Säulen einige Grad oberhalb des Schmelzpunktes während 30 Min bei abgestelltem Gasstrom konditioniert, dann auf die gewählte Arbeitstemperatur (für 4,4'-Bis-benzyliden-benzidin: 240°) eingestellt. Bei angestelltem Gasstrom (Helium) wurde während des Betriebes anfangs noch ein Anflug von gelbem Sublimat im Säulenausgang wahrgenommen. Die spezifischen Retentionsvolumina blieben indessen während mehrtägiger Versuchsreihen konstant. Die Temperatur im Säulenraum wurde mit Hilfe eines durch den Deckel des Thermostaten eingeführten geeichten Quecksilberthermometers gemessen. Zur Messung des Säulenvordrucks war ein Feinmessmanometer (Bereich 0–1.6 atü) zusätzlich eingebaut. Tabelle V zeigt in den Spalten 1 und 2 die relativen bzw. spezifischen Retentionsvolumina einiger typischer Testsubstanzen. Hervorgehoben seien folgende Trennungen, die von Interesse sind.

Für α-Benzylpyridin–γ-Benzylpyridin (Zwischenprodukte für Arzneimittelsynthesen) beträgt die relative Flüchtigkeit ca. 1.5. Somit lässt sich jedes, auch das extremste Isomerenverhältnis dieser Komponenten einwandfrei bestimmen. Für das schwierige Paar Anthracen–Phenanthren* beträgt die relative Flüchtigkeit ca. 1.15. Diese Trennung ist schon recht gut und lässt eine quantitative Analyse auch im Bereich weit unter 1% zu. Carbazol ist vom Phenanthren–Anthracen völlig getrennt. Noch besser sind die nematischen Phasen 5) und 6) geeignet (siehe Tabelle V). Besonders interessiert waren wir an einer möglichst weitgehenden Trennung der drei isomeren Phthalsäuredimethylester, die mit einem Verhältnis von *o*:*m*:*p* wie 1:1.24:1.27 an dieser Phase jedoch nicht gelungen ist. Die später untersuchten Substanzen 5) und 6) zeigen höhere Flüchtigkeitsunterschiede, und eine sehr gute Trennung wurde mit der Schiff'schen Base aus Terephthalaldehyd und *p*-Phenetidin 6) erzielt. Nachdem diese Versuche gezeigt hatten, dass die Verwendung nematischer Schmelzen auch bei relativ hohen Temperaturen erfolgversprechend für gewisse Isomerentrennungen ist, wurden die Verbindungen 4a)–6) entsprechend untersucht. Die Ergebnisse mit dem in *p*-Stellung beiderseits durch Methoxyl substituierten Benzyliden-benzidin 4a) werden im einzelnen nicht näher beschrieben, da die Säulen aus bisher nicht vollkommen geklärten Gründen wenig stabil waren.

* Vergleiche hierzu die Ergebnisse von SAUERLAND an geschmolzenem Calciumchlorid als stationärer Phase[18]. Auch in diesem Fall ist die Elutionsfolge: Phenanthren–Anthracen–Carbazol. Die Analogie im Elutionsverhalten ist in Anbetracht der ausserordentlich verschiedenartigen stationären Phasen interessant.

Bis-(p-methoxy-benzyliden)-4,4'-diaminostilben (trans)[25] (5)

Von Interesse dürften auch die Ergebnisse mit Bis-(*p*-methoxy-benzyliden)-4,4'-diaminostilben (*trans*) sein. In Tabelle V, Spalte 4 und 5, sind die Retentionswerte aufgeführt. Die Säule wurde, wie oben beschrieben, in trockenem Zustand beladen (15 Gew.-% auf HMDS-behandeltem Chromosorb W, 45–60 mesh, Länge 5 m, Säulenmaterial hier V4A-Stahl). Bei der Arbeitstemperatur von 270° traten zwar auch bei der Konditionierung der Säule (siehe oben) geringfügige Zersetzungserscheinungen auf. Ein Nachlassen der Säulenwirkung (spezifisches Retentionsvolumen, Auflösungsvermögen) wurde jedoch in nennenswertem Umfange nicht beobachtet, so dass diese Phase als geeignet zur Verwendung bei sehr hohen Arbeitstemperaturen (270°) empfohlen werden kann. Hervorgehoben sei die gute Trennung der drei isomeren Phthalsäureester, möglicherweise eine spezielle Wirkung der Methoxyl-Endgruppen. Die spezifischen Retentionsvolumina für das Stilbenderivat liegen — auch in Anbetracht der relativ hohen Arbeitstemperatur — wesentlich niedriger als beim Benzyliden-benzidin. So werden für die Elution des *o*-Phthalsäuredimethylesters an der 5-m-Säule bei einer Strömung von 0.62 ml/sec nur 2½ Min benötigt (Vordruck 1.5 kg/cm²; Helium). Als Apparatur ist u.a. das Modell F & M 720, konstant auf 270±2° einstellbar, geeignet. Für hochsiedende Komponenten muss naturgemäss die Temperatur des Einspritzblocks und der Wärmeleitfähigkeitsmesszelle entsprechend hoch gewählt werden. Für den Dauerbetrieb zulässig und für die Analyse von hochsiedenden Komponenten erforderlich sind Temperaturen von 380° im Einspritz- und im Detektorblock. Für die quantitative Analyse einer typischen Kohlenwasserstoffmischung (Anthracen–Phenanthren–Carbazol) kann folgende Arbeitsweise vorgeschlagen werden: Substanzgemisch in Pyridin unter Erwärmen lösen (etwa 8%ige Lösungen). Als inneren Standard verwendeten wir beispielsweise (*trans*)-Stilben. Die Auswertung

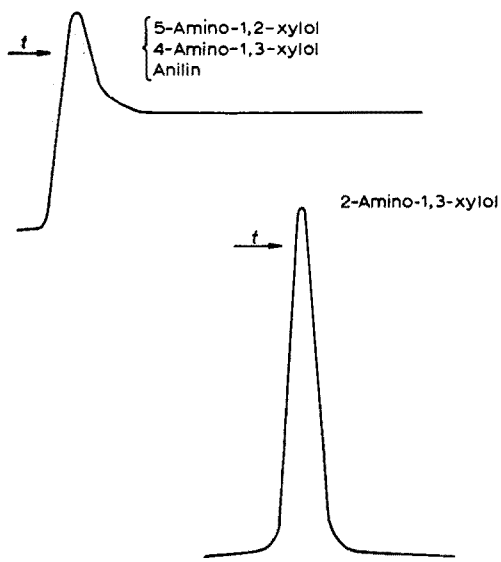

Abb. 2. Signalform, wie sie infolge Zersetzung primärer Amine an Schiff'schen Basen resultiert. Nur das sterisch geschützte 2-Amino-1,3-xylol zeigt keinen für die Umsetzung typischen Schwanz. Stationäre Phase: Bis-(*p*-methoxy-benzyliden)-4,4'-diaminostilben. $T = 270°$. Beladung: 15% auf R Chromosorb W (HMDS-behandelt).

erfolgt in bekannter Weise durch Flächenvergleich mit spezifischen Signalfaktoren. Die Erfassungsgrenze bei Verwendung der Wärmeleitfähigkeitsmesszelle ist besser als 0.3 Gew.-% für jede Komponente bei praktisch beliebigen Mischungsverhältnissen.

Bei der Verwendung Schiff'scher Basen als stationäre Phasen ist auf deren chemische Natur Rücksicht zu nehmen. Die Verbindungen sind empfindlich gegen Säuren, stabil gegen die meisten Basen. Primäre aromatische Basen jedoch, Anilinhomologe z.B., unterliegen einem recht gut reproduzierbaren Zersetzungsprozess, der aus einer typischen Form des Peaks zu erkennen ist (Abb. 2). Das Ausmass der Umsetzung hängt in charakteristischer Weise von den ausser der primären Aminogruppe vorhandenen Substituenten ab. 2,5-Dimethylanilin z.B. zeigte infolge Abschirmung der NH_2-Gruppe durch die benachbarten Gruppen kaum Neigung zur Umsetzung, während die Amine mit freiliegender NH_2-Gruppe den typischen, auf Umsetzung hindeutenden Schwanz zeigten. Es erscheint zunächst mit normalem Peakanstieg die eluierte Komponente, deren Konzentration aber nicht auf Null zurückgeht, sondern erst konstant bleibt und schliesslich langsam abklingt. Da die Erscheinung für die primären Amine typisch ist, nehmen wir an, dass ein Basenaustausch stattfindet. Das unsymmetrische Signal deutet auf Zersetzungsprodukte, deren Retentionsvolumina grösser oder allenfalls gleich dem des primär eingesetzten Amins sind. Es ist bekannt (vgl. der Lit. 28), dass die Schiff'schen Basen um so instabiler sind, je schwächer basisch die Aminkomponente ist. Wahrscheinlich findet folgende Reaktion statt:

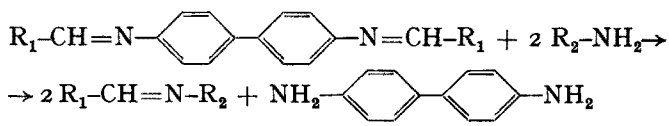

(oder einseitige Umsetzung).

Ein ähnliches Verhalten wurde von DU PLESSIS UND SPONG beobachtet, wenn sich infolge Reaktion mit der stationären Phase Komplexe auf der Säule bilden[19]. Über ähnliche typische Zersetzungserscheinungen berichteten SUPINA und Mitarbeiter[20].

Bis-phenetidyl-terephthalaldehyd[21,22] (6)

Die Versuche mit Bis-phenetidyl-terephthalaldehyd (s. Tabelle IV) sind noch nicht abgeschlossen. Es zeigte sich, dass diese Substanz bei einer Arbeitstemperatur von etwa 210° stabil ist und fast in jeder Hinsicht eine ähnlich gute Selektivität gegenüber "kritischen" Isomerenpaaren, insbesondere auch gegenüber α- und β-Naphthol, aufweist, wie sie bei den bislang untersuchten Substanzen gefunden wurde. Zumal die Substanz bequemer herstellbar als die anderen ist (aus Terephthalaldehyd und Phenetidin), sei darauf hingewiesen, dass sie in der Praxis, besonders im Dauerbetrieb, bemerkenswerte Vorteile gegenüber den anderen Substanzen haben dürfte. Ihr Schmelzpunkt liegt bei[21,22] 198°, der Klärpunkt bei 323°. Die angegebene Arbeitstemperatur von etwa 210° dürfte optimal sein; eine zu 15% beladene Säule kann nach bisherigen Erfahrungen mindestens 4 Wochen lang im Dauerbetrieb eingesetzt werden.

ZUSAMMENFASSUNG

Mit dem Ziel, geeignete flüssig-kristalline Phasen sowohl für niedrige (< 100°)

als auch für relativ hohe Arbeitstemperaturen (>200°) zur Verfügung zu haben, wurde eine Reihe nematogener Substanzen synthetisiert und auf ihre Beständigkeit sowie hinsichtlich ihrer Lösungsmitteleigenschaften unter den Arbeitsbedingungen der Gaschromatographie überprüft. Substanzen mit möglichst weitem Persistenzbereich der flüssig-kristallinen Phase erwiesen sich als besonders günstig. Hierfür wurden folgende Substanzen synthetisiert und auf ihre Selektivität untersucht: 1) das eutektische Gemisch aus 4,4'-Azoxyanisol und -phenetol, 2) 4-Methoxybenzyliden-4'-cyananilin, 3) 4-Methoxybenzyliden-4'-acetoxyanilin. Für diese stationären Phasen werden einige für die Isomerentrennung charakteristische Retentionsvolumina mitgeteilt.

Aus dem Kreis der verwendeten Substanzen mit Schmelzpunkten oberhalb 200° erwiesen sich als für die Praxis ausreichend bis gut geeignet: 4) 4,4'-Bis-benzyliden-benzidin, 5) 4,4'-Bis-(*p*-methoxy-benzyliden)-4,4'-diaminostilben (*trans*), 6) Bisphenetidyl-terephthalaldehyd. Für diese Substanzen werden spezifische Retentionsvolumina substituierter Aromaten bei einer im flüssig-kristallinen Bereich gelegenen, jeweils optimalen Arbeitstemperatur mitgeteilt. Besonders die unter 6) genannte Substanz ist für verschiedene Trennprobleme aus der Analytik industrieller Zwischenprodukte gut geeignet. Die Substanz hat ausserdem den Vorteil synthetisch leicht zugänglich zu sein. Trennung von α- und β-Naphthol, Benzoldicarbonsäureestern, kondensierten Aromaten, isomeren Benzylpyridinen und Chlortoluolen, werden typische Anwendungsmöglichkeiten. Die Herstellung der Substanzen und technische Details zur Gaschromatographie mit flüssig-kristallinen Phasen werden mitgeteilt.

SUMMARY

Nematic melts can be very efficient phases for the separation of positional isomers. In order to develop liquid-crystalline phases for working temperatures below 100° and above 200°, various nematic substances were synthesized and tested for stability and solvent properties under gas-chromatographic conditions. Substances with liquid-crystalline phases persisting over wide temperature ranges proved especially suitable for separation work. Retention volumes for various isomers are reported for stationary phases consisting of a eutectic mixture of 4,4'-azoxyanisole and -phenetole, 4-methoxybenzylidine-4'-cyanoaniline and -4'-acetoxyaniline.

Of the several substances with melting points above 200° examined, the most suitable for gas chromatography were 4,4'-bis-benzylidinebenzidine, 4,4'-bis(*p*-methoxybenzylidine)-4,4'-diaminostilbene, and bis-phenetidineterephthalaldehyde. Specific retention volumes for substituted aromatics and optimal working temperatures are reported. The bisphenetidine derivative, which is easily synthesized, is suitable for various industrial analytical separations. Separations of α- and β-naphthols, benzenedicarboxylic acid esters, condensed aromatics, isomeric benzylpyridines and chlorotoluenes, *etc.* are readily done.

ANHANG. DARSTELLUNG UND EIGENSCHAFTEN DER ALS STATIONÄRE PHASEN BENUTZTEN SUBSTANZEN

4-Methoxy-benzyliden-4'-cyananilin (2). (Schmelzpunkt 106°; Klärpunkt 117–

118°). Analyse: C, 76.3% (ber. 76.2%); H, 5.3% (ber. 5.1%); N, 12.1% (ber. 11.9%); O, 7.1% (ber. 6.8%).

18 g *p*-Methoxybenzaldehyd und 15 g *p*-Cyananilin werden 3 Stunden lang auf 90–95° erhitzt, das kristalline Produkt mit Äther verrieben, abgenutscht, mit Äther gründlich ausgewaschen und aus Hexan umkristallisiert.

4-Methoxybenzyliden-4'-acetoxyanilin (3). (Schmelzpunkt 81–82°; Klärpunkt 108–109°*). Analyse: C, 71.5–71.3% (ber. 71.4%); H, 5.6–5.8% (ber. 5.6%); N, 5.2–5.4% (ber. 5.2%); O, 17.7–17.9% (ber. 17.8%).

Die Darstellung erfolgte durch Acetylierung von 4-Methoxybenzal-4'-oxyanilin.

a) Herstellung von 4-Methoxybenzal-4'-oxyanilin. Versuche, *p*-Aminophenol in essigsaurer Lösung mit *p*-Methoxybenzaldehyd umzusetzen, ergaben schlechte Resultate. Die besten Ausbeuten wurden bei der Umsetzung von *p*-Aminophenol in methanolischer Lösung erhalten.

21.8 g *p*-Aminophenol in 200 ml Methanol p. a. durch Kochen am Rückflusskühler lösen und die Lösung nach Zusatz von 27.2 g Anisaldehyd 30 Min lang zum Sieden erhitzen. Nach dem Erkalten einige Stunden stehen lassen und unter Rühren und Einleiten von Stickstoff 100–110 ml Methanol abdestillieren, dann 200 ml dest. Wasser zutropfen lassen und mit Eiswasser kühlen. Den ausgefallenen, kristallinischen gelben Niederschlag von 4-Methoxy-benzal-4'-oxyanilin abfiltrieren und gründlich mit Wasser auswaschen. Dann über P_2O_5 im Vakuumexsikkator trocknen. Man erhält das Rohprodukt in fast theoretischer Ausbeute (ca. 45 g rohes 4-Methoxybenzal-4'-oxyanilin), das ohne Umkristallisation zum *p*-Acetoxyderivat weiterverarbeitet wurde.

b) Acetylierung von 4-Methoxybenzal-4'-oxyanilin zum 4-Methoxybenzal-4'-acetoxyanilin. Ca. 46 g (1/5 Mol) nichtumkristallisiertes 4-Methoxybenzal-4'-oxyanilin in 100 ml 5 *N* NaOH lösen, die gelbe Lösung in einem 1-l-Scheidetrichter mit der gleichen Menge Eiswasser versetzen und unter Umschütteln langsam eine Mischung von Essigsäureanhydrid und Benzol (1:10) bis zum Verschwinden der intensiv gelben Farbe zugeben. Dazu sind 240 bis 250 ml Anhydrid–Benzol-Lösung (= ca. 24 ml Anhydrid) erforderlich. Noch 100 ml Benzol zugeben, filtrieren und die beiden Schichten trennen. Die Benzolschicht mit 10%iger Natronlauge waschen, damit noch vorhandenes Ausgangsmaterial entfernt wird, anschliessend mehrmals mit Wasser waschen und die Benzollösung mit Chlorcalcium trocknen. Dann 250 bis 270 ml Benzol abdestillieren und unter Rühren und Kühlung 400 ml einer Mischung von Petroläther und Cyclohexan (1:1) zugeben, dabei fällt das Acetylierungsprodukt kristallinisch aus. Man erhält nach Umkristallisieren aus Petroläther ca. 10 g reines *p*-Methoxybenzal-*p'*-acetoxyanilin in fast farblosen Kristallen. Die Verbindung zeigt unter dem Polarisationsmikroskop die typische nematische Textur.

4,4'-Bis-benzyliden-benzidin (4). (Schmelzpunkt 239°; Klärpunkt 265° (zweimal umkristallisiert). Nach Literatur[27]: Schmelzpunkt 234°; Klärpunkt 260°). Analyse: C, 86.9% (ber. 86.7%); H, 5.7% (ber. 5.6%); N, 8.0% (ber. 7.8%).

20 g Benzidin p. a. in 800 ml Äthanol in der Siedehitze lösen, 24 g Benzaldehyd

* Nach HANSEN[26]: Schmelzpunkt 81.5°; Klärpunkt 108°.

zugeben und 2 Stunden unter Rückfluss und Rühren erhitzen. Nach dem Erkalten die Schiff'sche Base abfiltrieren und mit Methanol und Äther auswaschen, dann aus Toluol und ein zweites Mal aus Benzol umkristallisieren. Ausbeute ca. 60%.

Bis-(p-methoxy-benzyliden)-4,4'-diaminostilben (trans)[25] (5). (Schmelzpunkt 273–274°; Klärpunkt >340°). Herstellung über das reine 4,4'-Dinitrostilben (*trans*) aus reinem 4,4'-Diaminostilben (*trans*) durch Kondensation mit 2 Mol 4-Methoxybenzaldehyd.

4,4'-Dinitrostilben (trans) (*Fp. 292–294°*). Aus technischem Dinitrostilben nach mehrmaligem Umkristallisieren aus Nitrobenzol.

4,4'-Diaminostilben (trans) (*Fp. 232–233°*). Durch Reduktion von reinem 4,4'-Dinitrostilben (*trans*) in Diäthylenglykol mit Hydrazinhydrat (bei 180–200°) und Umkristallisieren des Diaminostilbens aus 2-Butanol; hellgelbe Kristalle.

Bis-(p-methoxy-benzyliden)-4,4'-diaminostilben (Fp. 273–274°). 8 g reines 4,4'-Diaminostilben (*trans*) in 900 ml Methanol lösen, 12 g 4-Methoxy-benzaldehyd zusetzen und 15–20 Minuten am Rückflusskühler erhitzen; nach dem Erkalten abfiltrieren, mit Methanol und Äther waschen und das getrocknete Kondensationsprodukt aus Xylol oder Dimethylformamid umkristallisieren; Ausbeute 11.1 g = ca. 66% der Theorie (bezogen auf 4,4'-Diaminostilben). Analyse: C, 80.7–80.8% (ber. 80.7%); H, 6.0–6.2% (ber. 5.9%); N, 6.2–6.3% (ber. 6.3%); O, 7.1–7.3% (ber. 7.1%).

Bis-phenetidyl-terephthalaldehyd[26,22] (6). (Schmelzpunkt 198–200°; Klärpunkt 320°). Analyse: C, 77.3–77.5% (ber. 77.4%); H, 6.7–6.8% (ber. 6.5%); N, 7.4–7.6% (ber. 7.5%); O, 8.2–8.3% (ber. 8.6%). 12 g Terephthalaldehyd in ca. 850 ml Methanol lösen, in die siedende Lösung 33 g *p*-Phenetidin eintragen, 15–20 Min unter Rückfluss erhitzen, nach dem Erkalten filtrieren, mit Methanol und Äther auswaschen, aus Toluol umkristallisieren und trocknen; Ausbeute ca. 25 g = 78% der Theorie.

LITERATUR

1 H. KELKER, *Ber. Bunsenges.*, 67 (1963) 698.
2 H. KELKER, *Z. Anal. Chem.*, 198 (1963) 254.
3 H. KELKER, *Gas-Chromatographie 1965*, Deutsche Akademie der Wissenschaften zu Berlin, Berlin, S. 271.
4 M. J. S. DEWAR UND J. P. SCHRÖDER, *J. Am. Chem. Soc.*, 86 (1964) 5235.
5 M. J. S. DEWAR UND J. P. SCHRÖDER, *ibid.*, (1965) 3485.
6 E. M. BARRALL II, R. S. PORTER UND J. F. JOHNSON, *J. Chromatog.*, 21 (1966) 392.
7 L. S. ORNSTEIN, *Z. Krist.*, 79 (1931) 90.
8 G. W. GRAY, *Molecular Structure and the Properties of Liquid Crystals*, Academic Press, New York, 1962.
9 D. VORLÄNDER, *Z. Krist.*, 79 (1931) 61.
10 L. WEYGAND UND R. GABLER, *J. Prakt. Chem.*, 155 (1940) 332.
11 H. ARNOLD UND H. SACKMANN, *Z. Phys. Chem.*, 213 (1959) 145.
12 F. M. ZADO UND R. S. JUVET, *VIth International Gas Chromatography Symposium Rome*, Preprints, Paper No. 19.
13 J. S. DAVE UND M. J. S. DEWAR, *J. Chem. Soc.*, (1954) 4616; (1955) 4305.
14 H. ARNOLD UND H. SACKMANN, *Z. Phys. Chem.*, 213 (1959) 137.
15 J. BILLARD UND R. CERNE, *Liquid Crystals Conference, Kent (Ohio), 1965*, Preprints, Paper No. 14.
16 E. FRÖHLICH, *Dissertation*, Halle, 1910.
17 H. KELKER, *Z. Anal. Chem.*, 220 (1966) 1.
18 H. D. SAUERLAND, *Brennstoff-Chem.*, 45 (1964) 33.
19 L. A. DU PLESSIS UND A. H. SPONG, *J. Chem. Soc.*, (1959) 2027.
20 W. R. SUPINA, R. S. HENLEY UND R. F. KRUPPA, *J. Am. Oil Chem. Soc.*, 43 (1966) 202 A.
21 M. E. HUTH, *Dissertation*, Halle, 1909.

22 CH. WIEGAND, *Z. Naturforsch.*, 12 b (1957) 512.
23 G. W. GRAY, J. B. HARTLEY, A. IBBOTSON UND B. JONES, *J. Chem. Soc.*, (1955) 4359.
24 A. SENIER UND R. B. FORSTER, *J. Chem. Soc.*, 107 II (1915) 1168.
25 F. JANECKE, *Dissertation*, Halle, 1910.
26 P. HANSEN, *Dissertation*, Halle, 1907.
27 L. GATTERMANN, *Ann. Chem.*, 347 (1906) 347.
28 HOUBEN-WEYL, *Die Methoden der organischen Chemie*, 7/1, Thieme, Stuttgart, 1960, 5458.
29 A. PRINS, *Z. Phys. Chem.*, 67 A (1909) 689.
30 D. VORLÄNDER, *Z. Phys. Chem.*, 126 (1927) 449.

Analytica Chimica Acta
Elsevier Publishing Company, Amsterdam
Printed in the Netherlands.

CHROMATOGRAPHY WITH SUPERCRITICAL FLUIDS

S. T. SIE AND G. W. A. RIJNDERS
Koninklijke-Shell-Laboratorium Amsterdam (Shell Research N.V.), (The Netherlands)

(Received November 1st, 1966)

The application of gas chromatography is restricted to substances which are reasonably volatile at the temperature of separation. Too often the required volatility cannot be reached at temperatures still permitted by the thermal stability of the system. In order to overcome this limitation, we studied the possibility of enhancing solute volatility by means of molecular interactions in the gas phase at pressures higher than usual.

It will be shown that pressure has a pronounced effect on equilibria. By using supercritical fluids instead of low-pressure gases the applicability of gas chromatography can be extended to substances of very high boiling points. This form of chromatography may be called fluid–liquid or fluid–solid chromatography, depending on whether a liquid or a solid adsorbent serves as the stationary phase. For the sake of brevity, we will denote these separation techniques by the initials FLC and FSC.

THE EFFECT OF PRESSURE IN GAS–LIQUID CHROMATOGRAPHY

For a better understanding of fluid chromatography it is of interest to examine more closely the role of pressure in GLC. We will discuss two aspects of importance for the separation, *viz.*, partition equilibria and column efficiency.

Effect of pressure on partition coefficients

If the carrier gas pressure in GLC is raised, equilibria may be affected in three ways,

1. by increasing molecular interactions in the non-perfect gas phase,
2. by the effect of pressure on the free energy of the solute in the liquid phase,
3. by solution of carrier gas into the stationary liquid.

The last effect is easy to visualize but the most difficult to describe quantitatively. Fortunately, for many systems of interest it proved to be of less importance than the two other effects which allow of a thermodynamic approach, at least at moderate pressures. Such an approach[1] leads to the equation

$$\ln k_P = \ln k_{P+} + \frac{P - P^+}{RT}(2B_{1,2} - v_2)$$

where k is the partition coefficient, P the pressure, P^+ a reference pressure (*e.g.*, one so low that the gas can be regarded as perfect), R the gas constant and T the absolute temperature. v_2 is the partial molar volume of solute in the liquid and $B_{1,2}$ the second virial cross coefficient of the system carrier gas–solute.

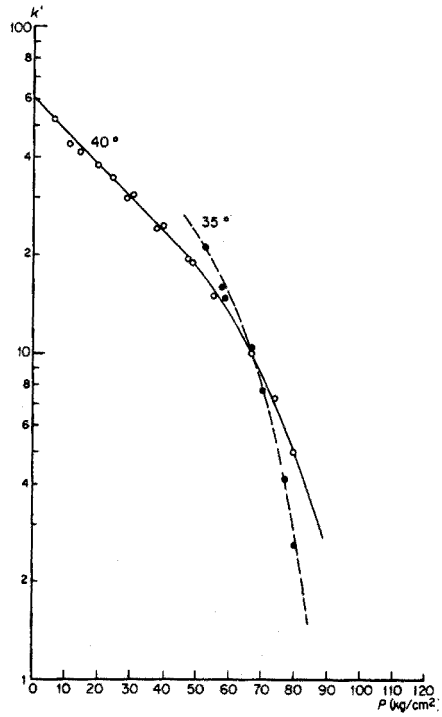

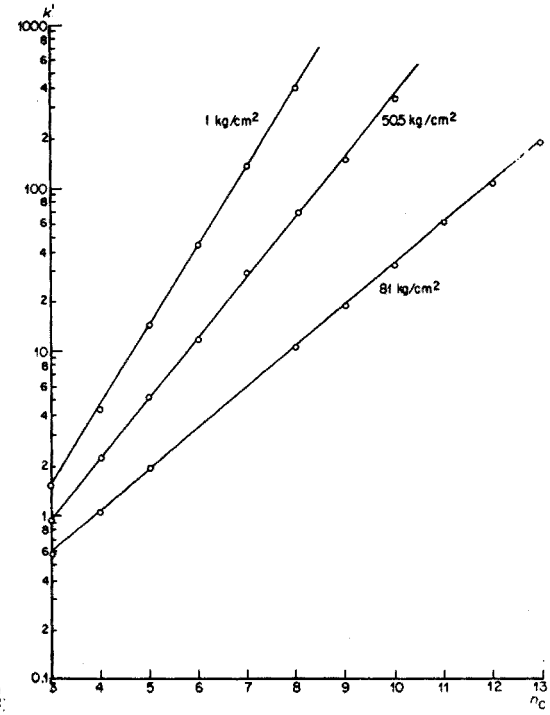

Fig. 1. Effect of pressure on retention of benzene. Carrier gas, CO_2. Column, 1 m × 6 mm ID with 23%-wt squalane on 50/70 mesh Sil-O-Cel.

Fig. 2. Retention of n-paraffins as a function of carbon atom number at different pressures. T, 40°. For other conditions see Fig. 1.

At temperatures below the Boyle point $B_{1,2}$ is negative while v_2 is generally positive. This means that the effects of an increase in pressure in the gas phase and in the liquid phase reinforce each other in shifting the equilibrium in a sense which may be looked upon as an enhancement of volatility.

A comparison of the theory with experiments with carbon dioxide as a carrier gas has been made elsewhere[1]. As a typical example, Fig. 1 shows the influence of pressure on k' (the capacity ratio, *i.e.* k multiplied by the phase ratio) for benzene as a solute. From this figure it can be inferred that at the critical pressure of CO_2 (73 atm) the "volatility" of benzene is higher than normal by a factor of 10. This enhancement roughly corresponds with a temperature increment of 100°. As appears from the steep drop of k' at near-critical pressures much more is to be gained by operating at considerably higher pressures.

The effect of temperature is of special interest: in the low-pressure region volatility decreases at lower temperatures and correspondingly k' is higher. At high pressures, however, the reverse is true. "Volatility" increases here with decreasing temperature because molecular interactions in the gas phase are more pronounced at the greater density accompanying the lower temperature. Hence, avoiding liquefaction of carrier gas, one can best use pressure at temperatures very near the critical point (31.1° for CO_2).

Figure 2 shows the relation between log k' and carbon number for the homologous series of n-paraffins. This relation is approximately linear both at low pressures (as usually observed in GLC) and at high ones. The slope of the lines becomes less steep at higher pressures, which has some important implications. Firstly, the enhancement of volatility is more pronounced for heavier substances, and it is just for these compounds that such an enhancement is desired. Secondly, the possibilities of separating neighbouring members of the series are reduced at higher pressures. In other words, light–heavy selectivity decreases. Thirdly, the decreased light–heavy selectivity promotes separations according to type in wide-boiling mixtures.

Effect of pressure on column efficiency

Figure 3 shows some plate height versus velocity curves for a typical GLC column with carbon dioxide as a carrier gas at various pressures. Axial molecular

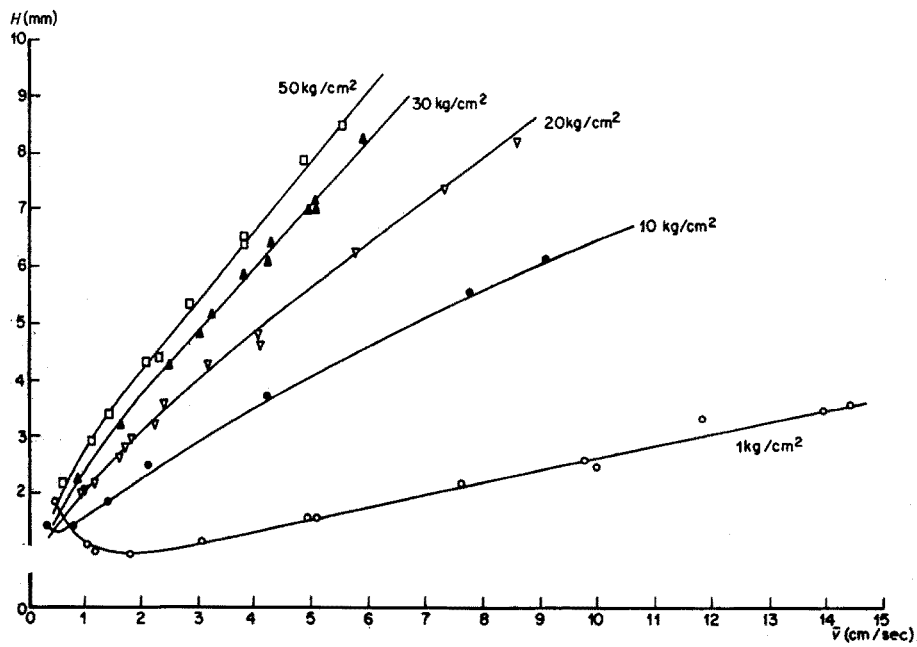

Fig. 3. Relation between plate height and mean carrier gas velocity at different outlet pressures. Solute, n-pentane. T, 40°. For other conditions see Fig. 1.

diffusion in the mobile phase is reduced with increasing pressure. This is reflected in a shift of the minimum in the HETP curve towards lower velocities. Above 10 kg cm^{-2} such a minimum is no longer discernible in the velocity range examined.

A factor of far greater importance to high-pressure GLC is the non-equilibrium contribution. As may be seen from Fig. 3 it increases with increasing pressure, rapidly at first and more slowly at high pressures. This increase cannot be explained by the classical van Deemter equation.

The observed facts may be understood if we consider the role of macroscopic flow profiles. As discussed elsewhere[2], these profiles are an important cause of

band-broadening, giving rise to an additive contribution to plate height (h) given by

$$h = \frac{2\kappa R^2}{\lambda_R d_p \bar{v} + \gamma_R D_g} \bar{v}.$$

Here κ is a dimensionless constant depending upon the profile, R the tube radius, d_p the mean particle diameter and $\bar{v}$ the mean velocity. λ_R and γ_R are dimensionless constants depending upon packing geometry and related with convective and diffusional mechanisms of lateral transport, respectively. D_g is the molecular diffusivity in the gas phase.

With λ_R approx. 1/30 and γ_R about 0.7 (*cf.* ref. 2) it follows that at low pressure (normal GLC conditions), $\gamma_R D_g$ is much larger than $\lambda_R d_p \bar{v}$ in the velocity range considered. Hence, the profile contribution is approximately first order in velocity and responsible for an appreciable part of the non-equilibrium term. With higher pressures D_g decreases in nearly inverse ratio to pressure and accordingly the profile contribution increases roughly in direct proportion to pressure, at least as long as $\lambda_R d_p \bar{v}$ remains small compared to $\gamma_R D_g$. The latter condition is no longer fulfilled at very high velocities and pressures (*cf.* Table I). When convective diffusivity ($\lambda_R d_p \bar{v}$) becomes the more important mechanism of lateral transport the profile contribution tends to become independent of velocity. This explains why in Fig. 3 the curves for pressures above 10 kg cm^{-2} are concave relative to the velocity axis, while the region of maximum curvature (where $\lambda_R d_p \bar{v}$ and $\gamma_R D_g$ are of the same magnitude) shifts to lower velocities according as the pressure is higher (*cf.* Table I).

In the region that is of most interest for fluid chromatography, *i.e.* at high pressures and high velocities (for CO_2, $P > 50$ kg cm^{-2} and $\bar{v} > 2$ cm sec^{-1}), the slope of the plate height curve no longer contains a significant contribution from flow profiles. It is important to know what other factors are responsible for this slope, since the latter is the main obstacle to rapid and efficient separations. The effect of flow profiles, reflected in a constant contribution to plate height, can in principle be diminished by a suitable technique of packing or by reduction of column diameter.

The slope of the plate height curve at high pressures and velocities proved to be mainly determined by the gas-phase mass transfer resistance in the intraparticle

TABLE I

VELOCITIES AT WHICH LATERAL CONVECTIVE DIFFUSIVITY EQUALS MOLECULAR DIFFUSIVITY, AS A FUNCTION OF PRESSURE

Carrier gas, CO_2; solute, n-pentane; temperature, 40°; mean particle diameter, 250 μ (50/70 mesh). λ_R, 1/30. γ_R, 0.7.

P (kg cm^{-2})	D_g[a] (cm^2 sec^{-1})	$\bar{v}$ (cm sec^{-1})
1	$7.7 \cdot 10^{-2}$	65
5	$1.5 \cdot 10^{-2}$	13
10	$7.7 \cdot 10^{-3}$	6.5
20	$3.9 \cdot 10^{-3}$	3.2
30	$2.6 \cdot 10^{-3}$	2.2
40	$1.9 \cdot 10^{-3}$	1.6
50	$1.5 \cdot 10^{-3}$	1.3

[a] Diffusivities calculated by means of the correlation formula of GILLILAND[3].

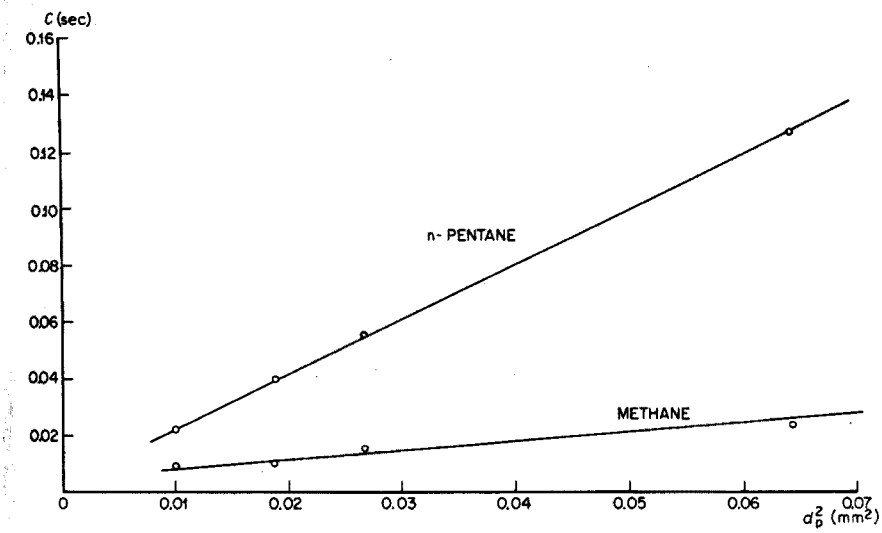

Fig. 4. Effect of particle size on coefficient of non-equilibrium contribution in high-pressure GLC. Carrier gas, CO_2; T, 40°; P, 57 kg cm^{-2}. Columns: 1 m × 3 mm ID (120/200 mesh Sil-O-Cel) and 1 m × 6 mm ID (100/120, 80/100 and 50/70 mesh Sil-O-Cel). Stationary liquid, squalane (23%-wt). Velocity range: 2–12 cm sec^{-1}.

pores. As Fig. 4 shows, the theoretically expected quadratic relationship between this slope and particle diameter exists and, moreover, the agreement is not only qualitative (*cf.* Table II).

Obviously, improvement can be obtained by reducing particle size. From Fig. 4 it can be inferred that with particles somewhat smaller than 100 μ the slope is reduced to about 10^{-2} sec, which is of the same order as the corresponding value for the same columns operated under normal GLC conditions. The use of such and even finer particles is quite feasible since high-pressure gases and supercritical fluids have low

TABLE II

RELATIONSHIP BETWEEN THE COEFFICIENT OF THE GAS CONTRIBUTION TO THE NON-EQUILIBRIUM TERM AND PARTICLE DIAMETER. COMPARISON BETWEEN THEORY AND EXPERIMENT

Carrier gas, CO_2; P, 57 kg cm^{-2}; T, 40°. d_p in cm.

Solute	C_g *(sec)*	
	Experimental[a]	*Theory*[b]
n-Pentane	$172\ d_p^2$	$170\ d_p^2$
Methane	$26\ d_p^2$	$23\ d_p^2$

[a] From the slope of the lines in Fig. 4.

[b] Intragranular gas-phase mass transfer contribution, calculated from

$$C_g = \frac{1}{30} \frac{(1 + k' - \Phi)^2}{(1 + k')^2 (1 - \Phi)} \frac{q}{\varepsilon_p} \frac{d_p^2}{D_g},$$

where Φ is the fraction of gas occupying interparticle space, ε_p the porosity of the particle and q a tortuosity factor (see ref. 4).

Numerical values are: $\Phi = 0.5$, $\varepsilon_p = 0.5$, $q = 1.3$, $D_g = 8.4 \cdot 10^{-4}$ cm^2 sec^{-1} (n-pentane), $D_g = 1.9 \cdot 10^{-3}$ cm^2 sec^{-1} (methane), $k' = 4.5$ (n-pentane), $k' \simeq 0$ (methane).

viscosities (compared with liquids) and since, moreover, a large pressure drop does not entail additional experimental inconvenience. Accordingly, we may expect fluid chromatography to be a fast and efficient separation technique, more or less comparable to gas chromatography and superior to liquid chromatography. For the latter technique, the possibilities of reducing the effect of intragranular diffusion by diminishing particle size are limited. The higher viscosities of liquids make it difficult to attain high eluant rates through the very fine packings necessitated by the small liquid diffusivities.

FLUID CHROMATOGRAPHY

Apparatus and technique

The studies with carbon dioxide as a carrier gas set forth above were made to provide a link between gas chromatography and fluid chromatography. In the follow-

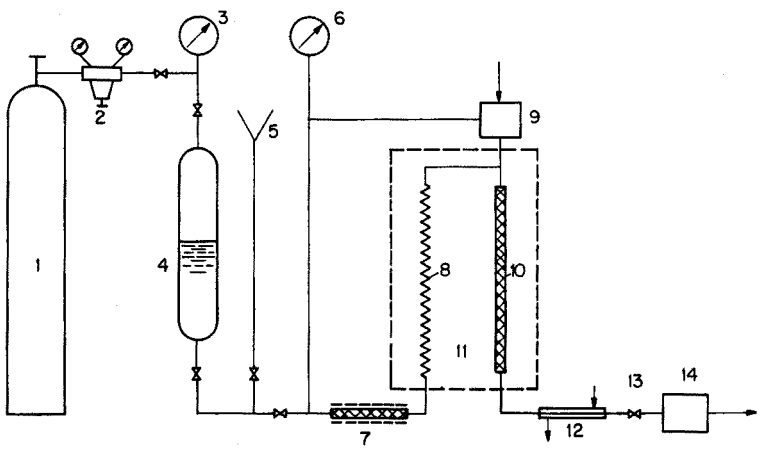

Fig. 5. Schematic diagram of apparatus for fluid chromatography. (1) cylinder with nitrogen; (2) reducing valve; (3) precision manometer; (4) high-pressure vessel with liquid; (5) filling funnel; (6) precision manometer; (7) heater; (8) temperature conditioning tube; (9) pneumatic injection device; (10) column; (11) air thermostat; (12) cooler; (13) needle valve; (14) UV monitor.

ing experiments we used other substances whose critical points render them more convenient for the handling of heavy substances. n-Pentane ($P_{crit} = 33.3$ atm, $T_{crit} = 196.6°$) and isopropanol ($P_{crit} = 47.0$ atm, $T_{crit} = 235.3°$) were chosen to represent a non-polar and a polar mobile fluid.

A schematic diagram of the apparatus is shown in Fig. 5. Liquid pentane or isopropanol is stored in a high-pressure vessel under adjustable nitrogen pressure. The liquid flows to the column via a heated tube (where it is brought to supercritical conditions) and a temperature-conditioning tube (kept in the column thermostat). By means of a pneumatically operated injection device* small samples (about 15 μl of a dilute solution) can be introduced into the system. Packed columns of 6 mm ID were employed in our experiments.

* To be described in another publication.

The column effluent is cooled in a capillary cooler before the pressure is released by means of a small needle valve also used to set the flow. Eluted substances are detected in the liquid phase by means of an UV absorption monitor. In view of this detection principle only aromatic substances were examined.

Fluid–liquid systems

An example of the effect of pressure is provided by Fig. 6, showing a log k'–P plot for two alkylnaphthalenes differing in alkyl chain length. We used a polar stationary liquid combined with a non-polar mobile fluid in these experiments.

In accordance with the results given before in Fig. 1 a drop of k' with pressure can be noted, which, however, is much sharper in the present case.

Figure 6 also illustrates the intermediate character of fluid chromatography: at low pressures light–heavy selectivity dominates and the elution order is the same as in GLC. At high pressures type selectivity appears to be more important and the elution order is as would be expected for LLC.

Temperature also exerts a strong influence on the separation pattern. This is particularly true in the neighbourhood of the critical point, where a difference of a few degrees centigrade can affect partition equilibria considerably (Fig. 7). In this region,

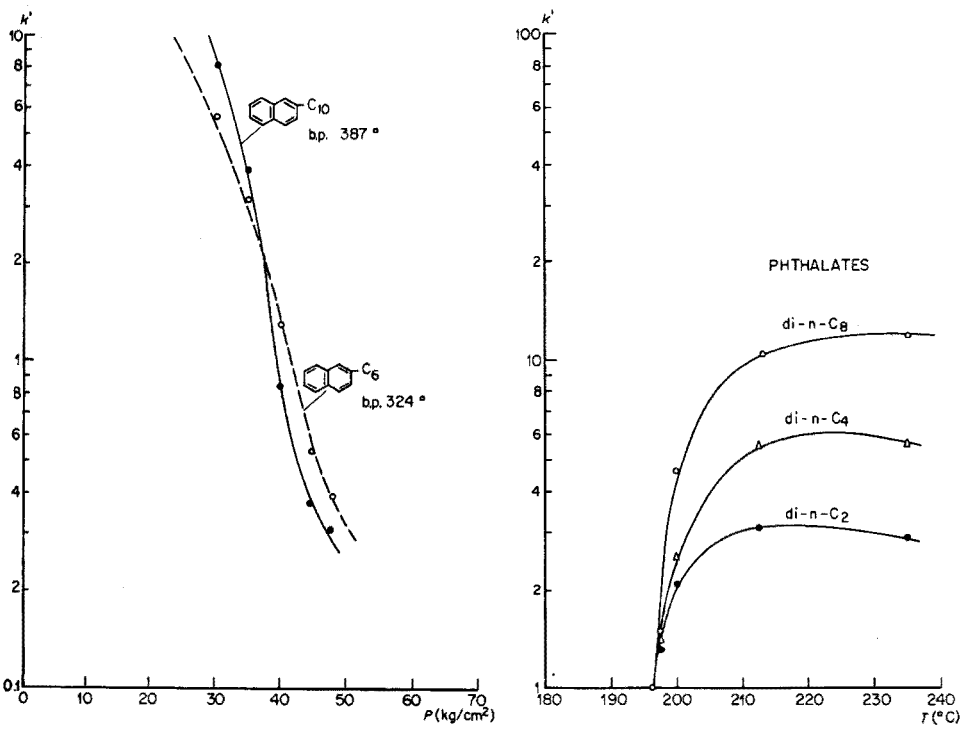

Fig. 6. Effect of pressure on retention in FLC. Mobile fluid, n-pentane; T, 210°, Column 2 m × 6 mm ID with 23%-wt PEG 6000 on 50/70 mesh Sil-O-Cel.

Fig. 7. Effect of temperature on retention in FLC. Mobile fluid, n-pentane; P, 35.0 kg cm^{-2}. Column: 2 m × 6 mm ID with 23%-wt PEG 6000 on 120/140 mesh Sil-O-Cel.

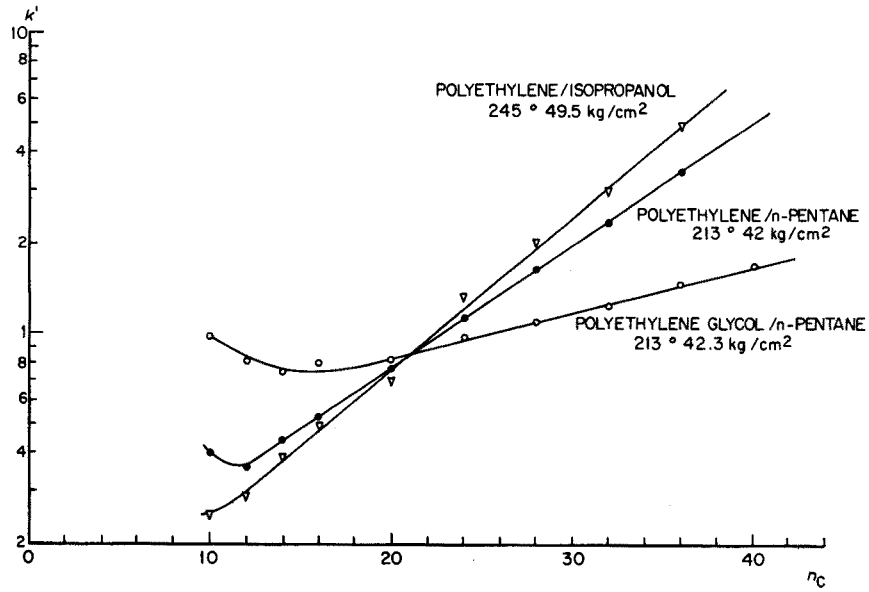

Fig. 8. Retention of di-n-alkylphthalates as a function of carbon atom number for different phase systems. Columns: 2 m × 6 mm ID with 23%-wt PEG 6000 on Sil-O-Cel 120/140 mesh and 10%-wt polyethylene on Sil-O-Cel 50/70 mesh.

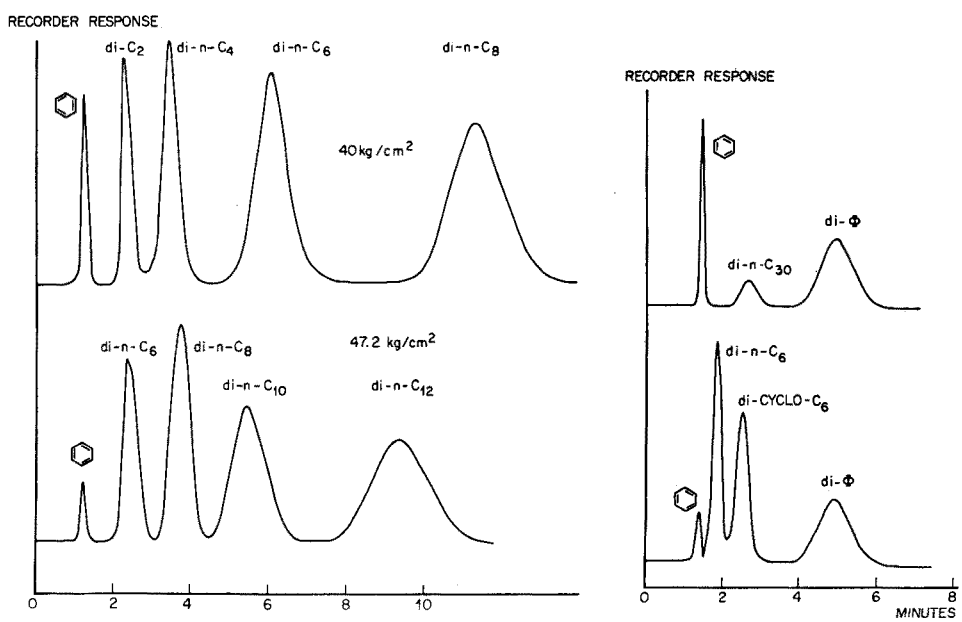

Fig. 9. Separation of di-n-alkylphthalates according to number of C atoms. Mobile fluid, isopropanol; T, 245°. Column: 2 m × 6 mm ID with 10%-wt polyethylene on 50/70 mesh Sil-O-Cel.

Fig. 10. Separation of phthalates according to type. Mobile fluid, n-pentane; T, 213°; P, 44.9 kg cm^{-2}. Column: 2 m × 6 mm ID with 23%-wt PEG 6000 on 120/140 mesh Sil-O-Cel.

lowering the temperature reduces k' (hence speeds up elution), in contrast to what happens in normal GLC.

The large effects of pressure and temperature as operational variables render FLC very flexible. Another contributing factor to this versatility is the possibility of varying the phase system. The freedom in choosing the phases appears to be greater here than in LLC and GLC. In GLC at high temperatures the choice of stationary liquids is limited to only a few relatively non-polar ones. In LLC the phases should be immiscible, which generally means that they must differ widely in polarity. In FLC, however, phases of the same or different polarity can be combined, provided that the stationary liquid has a sufficiently high molecular weight so as to be involatile under the conditions used.

Figure 8 illustrates how the variation of phase system can be turned to advantage. In this figure log k' is plotted against carbon number for the homologous series of di-n-alkylphthalates. With the exception of the first few members the plots are approximately linear. If the line for the completely non-polar system is taken as a reference, it is evident that the replacement of the stationary liquid by a polar one results in a shorter retention time of higher members of the phthalate series, in which

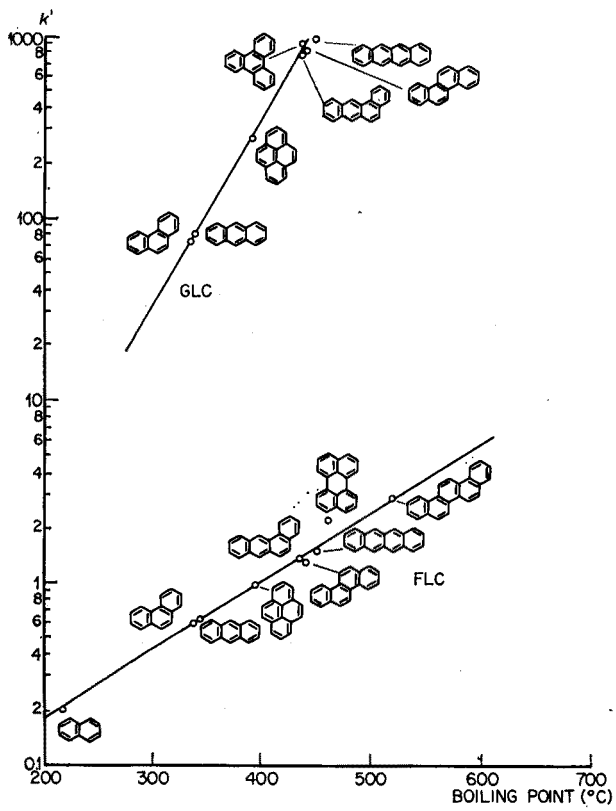

Fig. 11. Retention of polynuclear aromatic hydrocarbons as a function of boiling point. Comparison of GLC with FLC. GLC conditions: Carrier gas, argon; T, 213°; P $\simeq$ 1 kg cm^{-2}. Stationary phase, 5%-wt Apiezon-L on Sil-O-Cel. FLC conditions: Mobile fluid, n-pentane; T, 213°; P = 40 kg cm^{-2}. Stationary phase, 5%-wt polyethylene on Sil-O-Cel.

the paraffinic character of the alkyl groups is more pronounced. Thus, with a polar stationary liquid and a non-polar mobile fluid the effects of solute volatility and polarity tend to cancel each other, resulting in a flat slope of the log k'–n_c plot. These conditions are favourable for separating the alkylphthalates as one group from other types of compounds.

Conversely, if n-pentane is replaced by a polar mobile fluid the effects of solute volatility and polarity reinforce each other. Under such conditions the phthalates are easily separated according to alkyl chain length. An example of such a separation is given in Fig. 9.

Figure 10 shows some separations of phthalate esters according to alcohol type. Dimyricyl phthalate is eluted before diphenyl phthalate even though the former ester is appreciably heavier.

The ready elution of dimyricyl phthalate (mol.wt. 1006) may serve to prove the applicability of FLC for heavy substances. Further evidence is provided by Fig. 11 where FLC is compared with GLC at the same temperature. From this figure it can be inferred that the "volatility gain" by FLC amounts to nearly 10^3 for substances boiling at about 450°. Extrapolating, we may predict with some assurance that the volatility enhancement for a substance boiling at 600° is of the order of 10^4, while it should be possible to apply FLC to substances having a boiling point of about 1000°.

Fluid–solid systems

The limited application of GSC to substances appreciably heavier than permanent gases can be traced back to two shortcomings of commonly used adsorbents, *viz.*, a high adsorption affinity and a non-linear isotherm at reasonably low working temper-

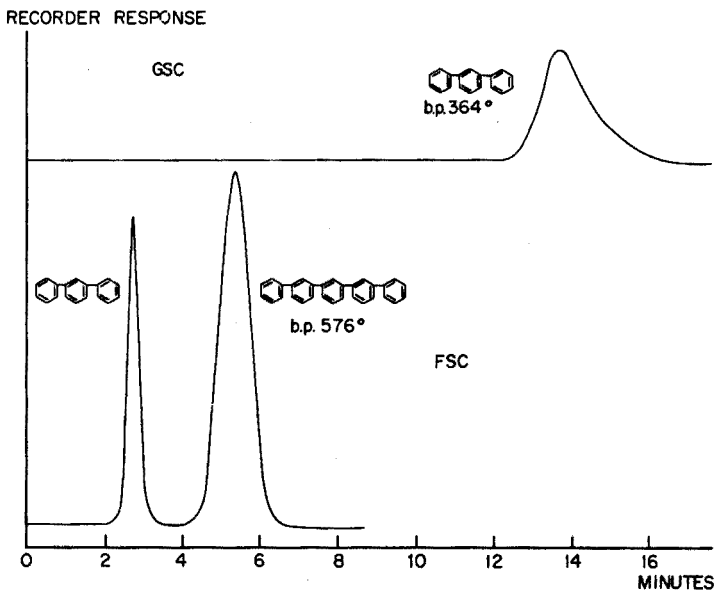

Fig. 12. Peak shape of polyphenyls in high-temperature GSC and FSC. GSC conditions: Carrier gas, helium; T, 350°; $P \simeq 1.5$ kg cm^{-2}. Stationary phase, treated alumina. FSC conditions: Mobile fluid, isopropanol; T, 245°; $P = 50$ kg cm^{-2}. Stationary phase, untreated alumina.

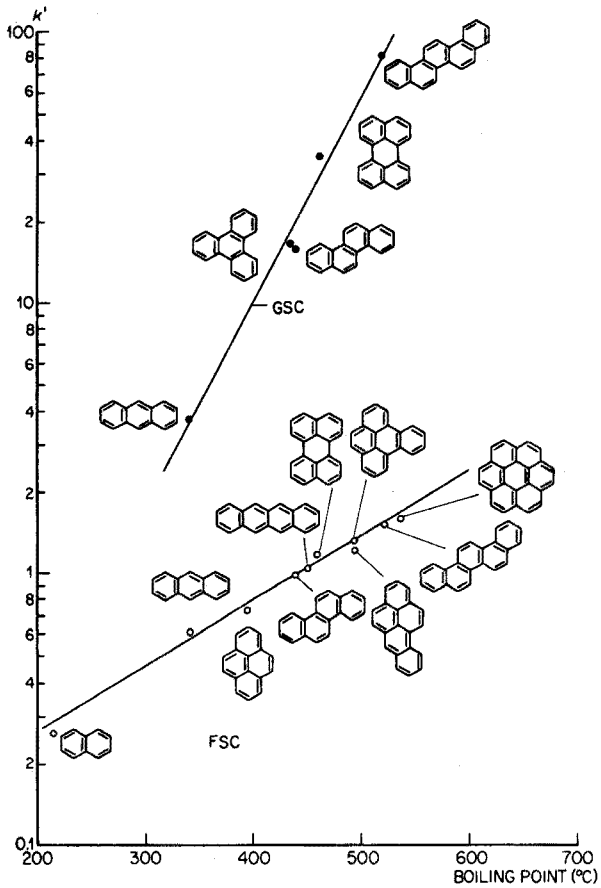

Fig. 13. Retention of polynuclear hydrocarbons as a function of boiling point. Comparison of high-temperature GSC with FSC. GSC conditions: T, 460°; for other conditions see Fig. 12. FSC conditions: see Fig. 12.

atures. As is well known, adsorbents may be improved by a modification consisting of, *e.g.*, calcining and treatment with a strongly adsorbing liquid. Despite such measures, however, GSC is still limited to substances boiling below or at most about 100° above the temperature of separation. Viewed against this background, FSC offers considerably greater scope. The application of high pressures not only promotes molecular interactions in the gas phase as in FLC, but the adsorption of carrier molecules onto the solid surface lowers the solute adsorption and improves the linearity of the isotherms. Thus, the adsorbent is "modified" *in situ* to an extent which can be easily varied with pressure and temperature.

In Fig. 12 high-temperature GSC is compared with FSC. In the GSC experiment the adsorbent (alumina basic type, activity grade I. M. Woelm, Eschwege, Germany) was modified by calcining at 1000° and by coating with 1%-wt of sodium hydroxide. Despite the very considerable improvement effected by this treatment the peak for *m*-terphenyl is still far from ideal. By contrast, the untreated adsorbent performs much better in FSC. As is seen in Fig. 12, even *m*-quinquephenyl (boiling

more than 300° above the operating temperature) elutes in a short time and gives a nearly symmetrical peak.

High-temperature GSC and FSC are compared in Fig. 13, where k' has been plotted on a logarithmic scale against boiling point for a number of polynuclear aromatic hydrocarbons. Taking a value of 100 for k' as a practical limit for an analysis* it can be inferred that even with the modified alumina at 460° the possibilities of GSC do not go beyond an adsorbate boiling point of about 550°. The possibilities of FSC, however, are far from exhausted at this level and should at least extend to an adsorbate boiling point of 800–1000°.

Just as in FLC, pressure and temperature have pronounced effects on elution speed and elution order in FSC, imparting a great deal of flexibility to the technique. It is possible also to vary the nature of the phases to suit a particular separation. An example of the effect of the mobile phase on the elution order is shown in Fig. 14.

Operational aspects of fluid chromatography

In discussing the effect of carrier gas pressure on column efficiency we antici-

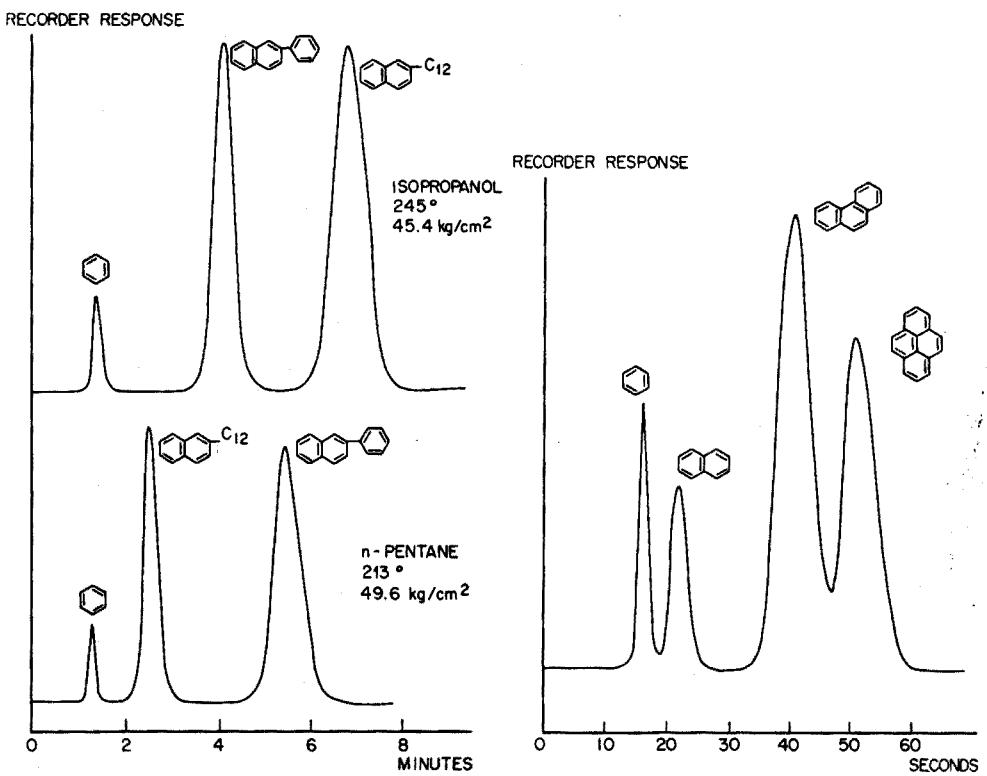

Fig. 14. Effect of mobile fluid on separation pattern in FSC. Column: 1 m × 6 mm ID; untreated alumina 120/140 mesh.

Fig. 15. Example of a fast separation by FSC. Mobile fluid, n-pentane; T, 213°; P, 50 kg cm^{-2}. Same column as in Fig. 14.

* This corresponds to an analysis time of a few hours, for a column of several metres length at a carrier gas velocity of a few cm sec^{-1}.

pated the possibility of rapid separations by fluid chromatography. As evidence of this possibility Fig. 15 shows the separation of a four-component mixture by FSC completed within 60 sec.

Besides speed, however, there are other aspects which fluid chromatography and gas chromatography have in common. With the set-up used, analyses by FLC and FSC were carried out in a comparable fashion to GLC. An important feature of both FLC and FSC is the possibility of using a programming technique. This is made attractive by the strong influence of pressure and temperature on elution speed. For samples containing components of widely different elution behaviour programmed-pressure FSC, for instance, may have advantages comparable to those of programmed-temperature GLC. In a pressure-programming technique the chromatographic system can easily be returned to starting conditions after each run, which is usually difficult in gradient-elution liquid chromatography techniques.

CONCLUSIONS

This study has shown that chromatography with supercritical fluids offers many interesting possibilities, being a very flexible technique applicable to heavy substances. It may be regarded as a cross between gas chromatography and liquid chromatography, combining features of both. By a suitable choice of operating parameters either boiling-point or molecular-type separations may be obtained.

Fluid chromatography enables rapid separations to be carried out. In this respect the technique is superior to liquid chromatography and more or less comparable to gas chromatography.

The authors wish to thank Mr. W. VAN BEERSUM who carried out most of the experimental work.

SUMMARY

Molecular interactions in the gas phase may be utilized for enhancing the volatility of substances in gas chromatography. A study of the effect of pressure on equilibria in GLC revealed that at higher pressures these interactions are quite appreciable, especially near the critical point. Measurements of plate heights show that with suitable adaptation of columns to the specific properties of high-pressure, dense fluids, the separating efficiency can be high and the speed of analysis fast. Experiments conducted with n-pentane and isopropanol as mobile fluids under supercritical conditions demonstrate that the volatility of heavy compounds may be enhanced by a factor of as much as 10^4. With either a liquid or a solid adsorbent as a stationary phase, chromatography with supercritical fluids proves to be very suitable for the rapid analysis of heavy compounds. The effect of various operational parameters on the separation is discussed. Certain features of the technique are illustrated with several examples.

REFERENCES

1 S. T. SIE, W. VAN BEERSUM AND G. W. A. RIJNDERS, *Separation Science*, in the press.
2 S. T. SIE AND G. W. A. RIJNDERS, *Anal. Chim. Acta*, 38 (1967) 1.
3 E. R. GILLILAND, *Ind. Eng. Chem.*, 26 (1934) 681.
4 J. C. GIDDINGS, *Anal. Chem.*, 33 (1961) 962.

Analytica Chimica Acta
Elsevier Publishing Company, Amsterdam
Printed in the Netherlands.

STRUKTUR UND RETENTIONSVERHALTEN VON OFFENKETTIGEN UND CYCLISCHEN KOHLENWASSERSTOFFEN UND DEREN EINFACHER SUBSTITUTIONSPRODUKTE*

GERHARD SCHOMBURG
Max-Planck-Institut für Kohlenforschung, Mülheim-Ruhr (Deutschland)

(Eingegangen den 1. November 1966)

Gaschromatographische Methoden werden vorzugsweise zur quantitativen Analyse von Mischungen bekannter qualitativer Zusammensetzung und zur Gewinnung kleinster bis grösserer Mengen reiner Verbindungen zur Anwendung chemischer oder physikalischer, insbesondere spektroskopischer Identifizierungsverfahren eingesetzt.

Steigende Trennleistung gaschromatographischer Systeme als Folge verbesserter Säulentechnik verleiht aber den Retentionsdaten ein grosses Gewicht für die Charakterisierung chemischer Verbindungen über strukturelle Einflüsse auf die intermolekulare Wechselwirkung.

Natürliche Voraussetzung für die Anwendung von Retentionsdaten zur Zuordnung gaschromatographisch getrennter Spezies zu chemischen Verbindungen mit bestimmter Struktur ist deren Standardisierung und die Reproduzierbarkeit ihrer Messung. Für logarithmische Retentionsgrössen, die in einem linear-proportionalen Zusammenhang mit Lösungsenthalpien stehen, ist — wie für die letzteren — additiver Einfluss struktureller Merkmale zu erwarten, vgl. hierzu PURNELL[1] und DUNKEL[2].

Im KOVATS'schen Retentionsindexsystem[3] erscheinen Retentionsdaten in Form von Lösungsenthalpien, die auf diejenigen der homologen n-Paraffine relativiert sind. Durch die Verwendung eines binären Systems von stationären Phasen mit verschiedener Polarität, von denen aber eine möglichst apolar ist, lässt sich in den sogenannten ΔI-Werten die Dipol–Dipol-Wechselwirkung in erster Näherung isoliert von der Dispersionswechselwirkung diskutieren. Aus den Retentionsindices in apolaren Phasen lassen sich wie für die ΔI-Werte Inkremente für strukturelle Merkmale (H^A-Werte) ableiten, die eine Abschätzung und gelegentlich auch Vorausberechnung der Dispersionswechselwirkung und damit des Retentionsverhaltens unbekannter Substanzen in apolaren und stationären Phasen ermöglichen, vgl. hierzu SWOBODA[4] und SCHOMBURG[5–9].

Die Zuordnung gaschromatographisch trennbarer Verbindungen über deren Retentionsdaten wird durch den Einsatz moderner Kombinationen mit Infrarot- oder Massenspektrometern nicht überflüssig, sie stellt vielmehr eine wertvolle Ergänzung für diese Kombinationstechniken dar, da es—wie z.B. in der Kohlenwasserstoffchemie — viele Fälle gibt, in denen die erhaltenen Massen- oder Infrarotspektren keinerlei charakterisierende Informationen geben. Schliesslich sind die mit Trenn-

* Zugleich Mitteilung V in der Reihe: Retentionsdaten und Struktur chemischer Verbindungen.

säulen hoher Trennleistung erhältlichen Substanzmengen vorläufig nur für eine Kombination mit der Massenspektrometrie ausreichend. Der Informationsgehalt eines Massenspektrums reicht auch in anderen Fällen allein nicht zur Identifizierung aus.

Andererseits ist natürlich die Identifizierung aus Retentionsdaten allein bei Mischungen, über die geringe oder keine Vorkenntnisse vorhanden sind, ausgeschlossen. Ist aber aus der Herkunft der Mischung oder deren chemisch-präparativer Vorgeschichte bekannt, mit welchen Verbindungsklassen gerechnet werden muss, so können Retentionsdaten über strukturelle Inkremente oder wenigstens Regeln zu sog. *relativen* Identifizierungen verwendet werden. Bei solchen Identifizierungen ist es nämlich weniger wichtig, eine Retentionsgrösse absolut zu messen oder zu berechnen als die relative Änderung einer Retentionsgrösse bei mehr oder weniger grossen Änderungen in Struktur und chemischer Zusammensetzung zu ermitteln.

Für die Anwendung von Retentionsgrössen zur Identifizierung im dargelegten Sinne ist es nun erforderlich, aus einem grossen Datenmaterial Inkremente zu bestimmen oder Regeln abzuleiten, die für die Berechnung oder Schätzung von Retentionsdaten unbekannter, aber verwandter Verbindungen geeignet sind. Dieses Datenmaterial ist nicht einfach zu gewinnen, da Modell- oder Vergleichssubstanzen von Verbindungen, die in gaschromatographisch noch trennbaren Mischungen vorkommen, meistens nur in langwieriger und mühevoller Arbeit oder garnicht rein dargestellt werden können. Natürlich hat die Gaschromatographie den Vorteil, dass keine wirklich reinen Substanzen zur Identifizierung benötigt werden. Geeignet sind hierzu durchaus auch Mischungen, in denen die gesuchte Komponente mit Sicherheit in überwiegender Menge vorhanden ist. Der Vergleich von Kapillar-Gaschromatogrammen isomerer Gemische verschiedener, aber definierter chemischer Herkunft führt häufig zur Identifizierung einzelner Isomerentypen, vgl. z.B. SCHOMBURG[8]. Es ist ein wesentlicher Vorzug der Gaschromatographie, dass natürlich auch die Retentionsdaten an Mischungen gewonnen werden können. Jedoch ist hierzu die sichere Zuordnung der einzelnen Spezies über die kombinierte Verwendung aller vorhandenen Informationen aus gaschromatographischen und anderen Quellen absolute Voraussetzung.

Im Kovatsschen Retentionsindexsystem, das binären Charakter hat, wird für polare Substanzen ein doppelter Satz von Retentionsgrössen erhalten; nur gesättigte offenkettige Kohlenwasserstoffe sind im Kovats-System apolar. Die Anwendung weiterer stationärer Phasen mit veränderter Polarität bedeutet nicht unbedingt auch, dass weitere neue, charakterisierende Retentionsgrössen erhalten werden.

Im folgenden soll gezeigt werden, wie man über eine systematische Bearbeitung der Retentionsdaten einfacher Substanzklassen zu sicheren Zuordnungen auch bei komplizierteren kommen kann. Für solche Arbeiten ist die Verwendung von Kapillarsäulen unbedingte Voraussetzung, da nur bei hohen Trennleistungen sich geringfügige strukturelle Variationen in messbaren Unterschieden der Retentionsdaten niederschlagen. Mit guten Kapillarsäulen (100 m Stahl 0.25 mm iD) kann noch bei Indexunterschieden von etwa 0.3 Indexeinheiten erkannt werden, ob es sich bei einem gaschromatographischen Peak um ein Dublett handelt oder nicht. Neben der Standardisierung der Retentionsgrössen (im Kovatsschen System auf die homologe Reihe der n-Paraffine) muss die Reproduzierbarkeit der Indexmessungen durch Verwendung von Apparaturen mit verlässlichen Regelvorrichtungen für Trägergasstrom und

Temperatur des Säulenofens gewährleistet sein. Mit kommerziellen Geräten ist eine Reproduzierbarkeit auf 0.5 I.E. möglich. Schliesslich muss auch die Polarität der verwendeten stationären Phasen durch Angabe von Kenngrössen (z.B. Indexwerte eines Satzes von Verbindungen mit wechselnder Polarität) charakterisiert werden, vgl. hierzu SCHOMBURG[9]. Im folgenden werden überwiegend die Indexwerte einer Auswahl von methylverzweigten gesättigten wie ungesättigten, cyclischen und offenkettigen Kohlenwasserstoffen diskutiert, die teilweise aus den petrochemischen Arbeiten des Max-Planck-Instituts für Kohlenforschung in Mülheim-Ruhr stammen, zum grösseren Teil aber durch Anwendung der methylene insertion reaction (MIR), vgl. hierzu VON DOERING[10], RICHARDSON, DURETT u.a.[11,12] aus anderen Kohlenwasserstoffen hergestellt wurden. Die Arbeiten wurden begonnen mit der gaschromatographischen Trennung und Zuordnung der MIR-Produkte der n-Alkane und einiger Monomethylalkane, für die ein inkrementeller Beitrag einer Methylverzweigung zum I^S-Wert ermittelt werden konnte. Analog wurden aus den Cyclanen die Methylcyclane hergestellt. Bei ihnen zeigt eine Methylverzweigung den gleichen Einfluss auf den Retentionsindexwert nach KOVÁTS an Squalan, I^S, wie in offenkettigen, in der Kettenmitte methylverzweigten Kohlenwasserstoffen. Durch Einführung einer Methylverzweigung in α- und β-Olefine sowie einige α-Diolefine wurden neue Kohlenwasserstofftypen erhalten, die mehrere verschiedene funktionelle Gruppen (Methylverzweigungen und Doppelbindungen) in einem Molekül enthielten. Die Gültigkeit der an den einfachen Verbindungen ermittelten Indexinkremente in Abhängigkeit vom Abstand der funktionellen Gruppen in der Kohlenstoffkette wurde geprüft. Die abgeleiteten Regeln über das Retentionsverhalten methylverzweigter Alkene und Cyclane wurden benutzt, um die Zuordnung der isomeren Methylcyclene bzw. Cyclodiene und -triene durchzuführen. Die Zuordnung der einzelnen Isomeren wurde geprüft mit Hilfe der Statistik der methylene insertion reaction und mit Hilfe einiger Modellsubstanzen aus definierten chemischen Synthesen.

Bei den Verbindungen 12 und 26 (3,4-Dimethylheptan bzw. -octan) gelang die Trennung der erythro- von der threo-Verbindung, bei den Verbindungen 13 und 27 (3,5-Dimethylheptan bzw. -octan) die Trennung der meso- von der racem-Form, die bis jetzt beim 3,6-Dimethyloctan noch nicht gelungen ist. Grössere I-Differenzen werden für die m- und r-Form des 3,5-DM-Heptans in der Phase Siliconöl DC 200 beobachtet. Die Absicherung der in diesem Zusammenhang durchgeführten Zuordnungen geschah gemeinsam mit HENNEBERG[13] in einer Kombination Kapillar-GC-MS. Hierüber wird an anderer Stelle zu berichten sein.

METHYLVERZWEIGTE PARAFFINE

Je nach Stellung der Methylgruppe in der Paraffinkette werden charakteristische I^S-Inkremente ($H^S = I^S$(n-Paraffin)$-I^S$(Methylparaffin)) für die einzelnen Methylalkane beobachtet, die zu kleinen C-Zahlen hin von der Kettenlänge abhängig sind und um so geringere Unterschiede für benachbarte Isomere zeigen, je weiter die Methylgruppe in der Mitte der Kohlenstoffkette steht, z.B. I^S: 5-Methyldodecan 1553, 6-Methyldodecan 1250. Vgl. hierzu Tabelle I.

Die I^S-Werte der Methylalkane nehmen in der Reihenfolge: 1, 3, 2, 4, 5 ... n-Methylalkan ab, vgl. hierzu auch MATSUKUMA[14]. Wegen der höheren Symmetrie (2 Methylgruppen am C-Atom) wird das 2-Methylalkan vor dem 3-Methylalkan eluiert.

Ist R nicht Methyl, sondern irgendeine funktionelle Gruppe, so wird immer die Reihenfolge: 1, 2, 3, 4, 5, . . . R-Alkan beobachtet.

Tabelle I enthält die I^S-Werte der Methyloctane und -nonane sowie die gemessenen und geschätzten I^S-Werte der Dimethylheptane und Dimethyloctane. Die Dimethylalkane wurden durch MIR mit 2-Methyl- und 3-Methylheptan bzw. -octan erhalten. Die Abweichungen von der Additivität der Verzweigungsinkremente verringern sich umsomehr, je weiter die Verzweigungsstellen auseinanderstehen. Schon

TABELLE I

EINFACH- UND ZWEIFACHVERZWEIGTE C_9- UND C_{10}-PARAFFINE

Nr.			I^S_{80}*			*Nr.*			I^S_{80}		
			g[a]	*b*[a]	*D*[a]				*g*	*b*	*D*
1	2-Me-Octan		865			15	2-Me-Nonan		964		
2	3-Me-Octan		871			16	3-Me-Nonan		970		
3	4-Me-Octan		863			17	4-Me-Nonan		961		
						18	5-Me-Nonan		958		
4	3-Ae-Heptan		868								
5	4-Ae-Heptan		861			19	4-Ae-Octan		952		
6	2,2-DM-Heptan		817	830	−13	20	2,2-DM-Octan		916	928	−12
7	2,3-DM-Heptan		857	836	+21	21	2,3-DM-Octan		953	934	+19
8	2,4-DM-Heptan		822	828	− 6	22	2,4-DM-Octan		915.5	925	− 9
9	2,5-DM-Heptan		834	835	− 1	23	2,5-DM-Octan		922	925	− 3
10	2,6-DM-Heptan		827	830	− 3	24	2,6-DM-Octan		932	934	− 2
11	3,3-DM-Heptan		839	842	− 3	25	2,7-DM-Octan		929	928	+ 1
12	3,4-DM-Heptan	E[b]	860	841	+19	26	3,4-DM-Octan	E	953	931	+22
		T	860.5	841	+20			T	954	931	+23
13	3,5-DM-Heptan	m[c]	833.5	842	− 9	27	3,5-DM-Octan	E	921	931	−10
		r	835	842	− 7			T	922	931	− 9
14	4,4-DM-Heptan		827	826	+ 1	28	3,6-DM-Octan		938	940	− 2
						29	4,4-DM-Octan		921	922	− 1
						30	4,5-DM-Octan	m	944.5	922	+23
								r	946.5	922	+25

[a] g = gefunden; b = berechnet; D = Differenz.
[b] E = Erythro-Form; T = Threo-Form.
[c] m = meso-Form; r = racem-Form.
* I^S_{80} = Retentionsindex nach KOVATS[3] an Squalan bei 80°.

wenn ein C-Atom zwischen den beiden Verzweigungsstellen steht, wird eine gewisse Additivität beobachtet. Für Kohlenwasserstoffe mit benachbarter Methylverzweigung werden aussergewöhnlich hohe I^S-Werte unabhängig von der Stellung in der Kohlenstoffkette beobachtet. Die Indexwerte der Verbindungen 7, 12, 21 und 26 zeigen, dass durch Einführung eines Inkrements von etwa 21 Indexeinheiten auch die I^S-Werte dieser Dimethylalkane ausgezeichnet berechnet werden können. Stehen zwei Methylgruppen an einem C-Atom, so ist nur für die 2,2-Dimethylalkantypen die Einführung eines zusätzlichen Inkrements von etwa +12 I.E. erforderlich, während sich für die 3,3- und 4,4-Dimethyltypen die richtigen Indexwerte ergeben, wenn das Inkrement für die einfache Methylverzweigung definierter Stellung verdoppelt wird.

EINFACH METHYLVERZWEIGTE CYCLANE

Sieht man von dem Indexunterschied von 100 I.E. ab, der sich aus der verschiedenen C-Zahl ergibt, so zeigt der I^S-Vergleich von Methylcyclanen und Cyclanen gleicher Ringgrösse, dass eine Methylverzweigung an einem Acht-, Elf- oder Zwölfring die I^S-Werte um die gleichen inkrementellen Beträge wie bei den entsprechenden mittelständig methylverzweigten n-Alkanen erniedrigt (Tab. II). Für die offenketti-

TABELLE II

METHYLVERZWEIGUNGEN IN CYCLANEN

Nr.		H^S [a]	*Nr.*		H^S [b]
1	Cyclooctan Methylcyclooctan	−41	4	n-Nonan 4-Methyloctan	−38
2	Cycloundecan Methylcycloundecan	−47	5	n-Dodecan 5-Methylundecan	−46
3	Cyclododecan Methylcyclododecan	−53	6	n-Tridecan 6-Methyldodecan	−50

[a] $H^S = I^S$ (Cyclan) + 100 − I^S (Methylcyclan).
[b] $H^S = I^S$ (n-Alkan) − I^S (Methylalkan).

gen gesättigten Kohlenwasserstoffe werden in einem binären System stationärer Phasen mit einer apolaren und einer polaren Phase keine ΔI-Werte beobachtet, wohl aber für die Cyclane und deren Derivate. Da die ΔI-Werte sich bei Einführung von Doppelbindungen in Cyclangerüste noch weiter erhöhen, sind sie für die Identifizierung ungesättigter Ringverbindungen von grossem Nutzen. Die ΔI-Werte der Methylcyclane liegen immer etwas niedriger als diejenigen der unsubstituierten Cyclane.

METHYLVERZWEIGTE OCTANCARBONSÄURE-METHYLESTER

Verbindungen, die polare funktionelle Gruppen wie z.B. die $COOCH_3$-Gruppe enthalten, zeigen bei Einführung einer Methylverzweigung in der Nähe der funktionellen Gruppe stark erniedrigte und wegen der verschiedenen Abschirmung charakteristische ΔI-Werte, während die ΔI-Werte aller anderen methylverzweigten Typen sich nicht wesentlich von dem des unverzweigten Octancarbonsäuremethylesters unterscheiden (Tab. III). Sie enthält die I- und ΔI-Werte der MIR-Produkte des Heptan-1-carbonsäure-methylesters. Ein Chromatogramm der MIR-Mischung ist auf dem Bild 1 für die stationäre Phase Squalan wiedergegeben. Zur Zuordnung der an dem von der funktionellen Gruppe abgewandten Ende der C-Kette methylsubstituierten Typen (Verbindungen 5, 6 und 7 der Tab. III) wurden die H^S-Werte ermittelt und mit denjenigen der entsprechenden methylverzweigten n-Paraffine verglichen. Das Beispiel zeigt, dass mit Hilfe der H^S-Werte (für methylverzweigte Typen), der ΔI-Werte und durch Extrapolation um eine C-Zahl dem Octan-1-carbonsäuremethylester alle Isomere der MIR-Mischung zugeordnet werden können. Die Zuordnung war ausserdem in Einklang mit der erwarteten Statistik der methylene insertion für die einzelnen Isomeren (vgl. hierzu SCHOMBURG[8]). Zur Identifizierung des Heptan-1-

TABELLE III

METHYLVERZWEIGTE OCTANCARBONSÄUREMETHYLESTER

Nr.		I^{S}_{100}*	I^{CW}_{100}†	ΔI	HS_{100}[a]	HS_{100}[b]
	Methylester der					
1	Heptan-1-carbonsäure	1062	1421	359		
2	1-Me-Heptan-1-carbonsäure	1097	1421	324		
3	2-Me-Heptan-1-carbonsäure	1105	1437	332		
4	3-Me-Heptan-1-carbonsäure	1120	1463	343		
5	4-Me-Heptan-1-carbonsäure	1120	1467	347	−41	−41
6	5-Me-Heptan-1-carbonsäure	1130	1482	352	−31	−29
7	6-Me-Heptan-1-carbonsäure	1126	1470	344	−35	−36
8	Octan-1-carbonsäure	1161	1516	355		
9	Heptan-1-carbonsäure-ae-ester	1133	1458	325		

* I^{CW}_{100} = Retentionsindex an Carbowachs bei 100°.
† $\Delta I = I^{S}_{100} - I^{CW}_{100}$.
[a] $HS = I^{S}$ (Octan-1-carbonsäure-me-ester) − I^{S} (Me-Heptan-1-carbonsäure-me-ester).
[b] $HS = I^{S}$ (n-Octan) − I^{S} (Me-Heptan).

carbonsäureäthylesters war einerseits das Inkrement für den Übergang von Methyl- zu Äthylestern bekannt, zum anderen lag der Ester als Modellsubstanz in reiner Form vor.

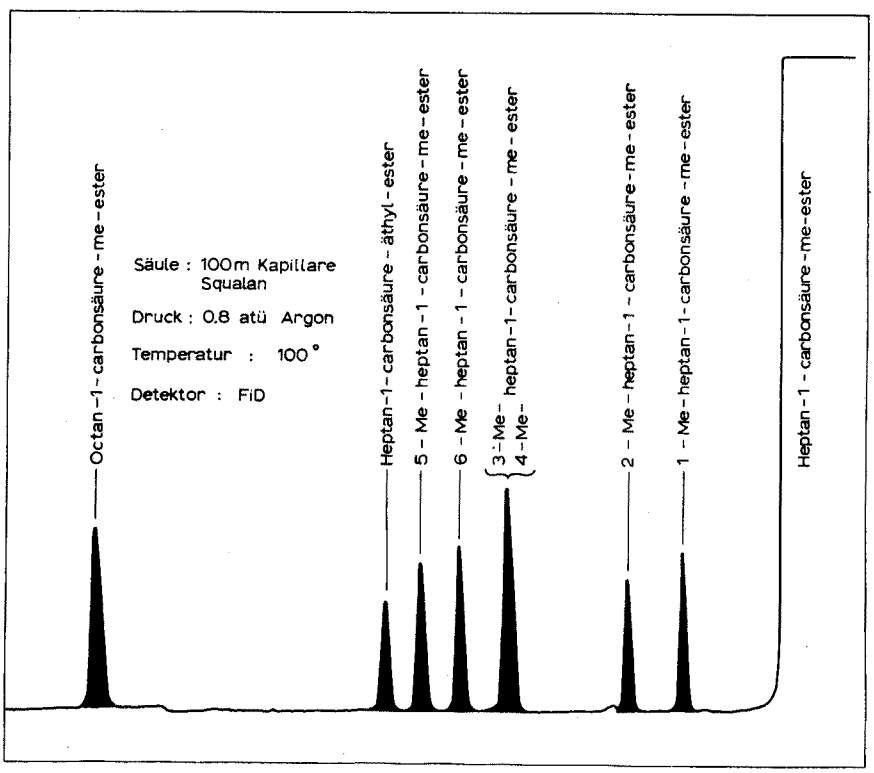

Fig. 1. "Methylen-insertion" Produkte des Heptan-1-carbonsäure-me-ester.

METHYLVERZWEIGTE OLEFINE MIT DOPPELBINDUNG IN 1-, 2- ODER 3-STELLUNG

Nach ihrem Retentionsverhalten, müssen diese Olefine in drei Klassen eingeteilt werden[6]:

a) an der Doppelbindung
b) in Allylstellung (γ-Stellung)
c) in δ- bis ω-Position methylsubstituierte Alkene

Die Tab. IV zeigt eine Auswahl von Werten, aus denen zu entnehmen ist, dass die 1-methylverzweigten Isomeren um 30 I.E. höhere und die 3-methylverzweigten Typen

ELLE IV

HYLVERZWEIGUNGEN IN α-OLEFINEN (C_7, C_8)

	I^S_{70}	H^S_{70}[a]	D[b]	*Nr.*		I^S_{80}	H^S_{80}[a]	D[b]
Hepten-1	682	−18		9	2-Me-Octen-1	874	+10	+28
Octen-1	782	−18		10	3-Me-Octen-1	839	−32	−14
Nonen-1	883	−18		11	4-Me-Octen-1	846	−13	+ 5
				12	5-Me-Octen-1	845	−14	+ 4
2-Me-Hepten-1	776	+12	+30	13	6-Me-Octen-1	853	−18	0
3-Me-Hepten-1	742	−30	−12	14	7-Me-Octen-1	847	−17	+ 1
4-Me-Hepten-1	748	−18	0					
5-Me-Hepten-1	757	−15	+ 3	15	2-Me-1,7-Octadien	857	− 7	+29
6-Me-Hepten-1	750	−14	+ 4	16	3-Me-1,7-Octadien	823	−48	−12
				17	4-Me-1,7-Octadien	830	−29	+ 7

= I^S (Methylalken) − I^S (Methylalkan).
= Differenz zu H^S-Wert von Nr. 1, 2, 3.

um 12–14 I.E. erniedrigte H^S-Werte haben. Diese H^S-Werte kommen zustande durch Indexvergleich mit den entsprechenden gesättigten Kohlenwasserstoffen des gleichen Verzweigungstyps, also unter Eliminierung des Verzweigungseinflusses. Bei den drei Dienen 15, 16 und 17, deren Doppelbindungen weit voneinander isoliert stehen, wird sehr gute Additivität der Inkremente beobachtet. Aus den H^S-Werten von 3 und 9 ergibts ich für 15 ein H^S-Wert von −8 statt −7, aus denjenigen von 3 und 10 für 16 von −50 statt −48 und aus denen von 3 und 11 für 17 ein H^S-Wert von −31 statt −29.

Methylverzweigte mittelständige Olefine

Da in den später zu untersuchenden ungesättigten Ringverbindungen nur mittelständige Doppelbindungen vorkommen, wurden auch von diesen die Retentionsdaten einer Reihe von Isomerentypen gemessen. Sie entstammten teilweise wieder aus MIR, überwiegend aber aus den Arbeiten von PAULING[15] und wurden durch Ylid-Reaktionen nach WITTIG[16] aus den entsprechenden Ketonen hergestellt. Ihre Identität wurde durch IR und NMR geprüft und durchweg bestätigt. Einige Isomerentypen wurden auf beiden Wegen dargestellt und ergaben die gleichen Retentionsindices. Um zu zeigen, dass die für die α- bzw. 1-Olefine abgeleiteten H^S-Werte auch als Indexinkremente für die methylverzweigten 2- und 3-Olefine geeignet sind, wurden deren H^S-Werte — ausgehend von den unverzweigten mittelständigen Olefinen — berechnet. Die berechneten Werte stimmen mit den tatsächlich gemessenen leidlich überein, wie die Tab. V zeigt. Mit den für die 1-Olefine abgeleite-

TABELLE V

METHYLVERZWEIGUNGEN IN MITTELSTÄNDIGEN OLEFINEN (C_6, C_7)

Nr.		*Temp.*	I^S	H^S [a]	*Berechnet*
1	2-Penten-*trans*	70°	503	+ 3	
2	2-Penten-*cis*	70°	507	+ 7	
3	2-Me-2-Penten	RT	599	+29	+31
4	3-Me-2-Penten-*trans*	RT	603	+18	+31
5	3-Me-2-Penten-*cis*	RT	613	+28	+31
6	4-Me-2-Penten-*trans*	RT	563	− 7	−13
7	4-Me-2-Penten-*cis*	RT	556	−14	
8	2,3-DM-Buten-2	RT	625	+56	
9	2-Hexen-*trans*	70°	598	− 2	
10	2-Hexen-*cis*	70°	603	+ 3	
11	2-Me-2-Hexen	60°	692	+25	+31
12	3-Me-2-Hexen-*trans*	60°	694	+17	+26
13	3-Me-2-Hexen-*cis*	60°	701	+24	+31
14	4-Me-2-Hexen-*trans*	60°	658	−19	−13
15	4-Me-2-Hexen-*cis*	60°	657	−20	
16	5-Me-2-Hexen-*trans*	60°	661	− 6	+ 1
17	5-Me-2-Hexen-*cis*	60°	670	+ 3	
18	2,3-DM-Penten-2	60°	705	+32	+30
19	2,4-DM-Penten-2	60°	641	+10	+17
20	3,4-DM-Penten-2-*trans*	60°	678	+ 5	
21	3,4-DM-Penten-2-*cis*	60°	670	− 3	
22	3-Hexen-*trans*	70°	593	− 7	
23	3-Hexen-*cis*	70°	593	− 7	
24	2-Me-Hexen-3-*trans*	60°	647	−23	−21
25	2-Me-Hexen-3-*cis*	60°	642	−28	
26	3-Me-Hexen-3-*trans*	70°	685	+ 8	+22
27	3-Me-Hexen-3-*cis*	70°	692	+15	

[a] $H^S = I^S$ (Methylalken) − I^S (Methylalkan).

ten Inkrementen werden H^S-Werte gefunden, die ein wenig zu hoch sind, und zwar im Mittel um etwa 5 I.E. Es genügt aber in unserem Fall nachzuweisen, dass der Einfluss von Methylverzweigungen auf die H^S-Werte auch bei mittelständigen Olefinen die gleiche Tendenz aufweist: Starke Erhöhung der H^S-Werte bei Substitution an der Doppelbindung, beträchtliche Erniedrigung bei Substitution in Allylstellung. In der Tab. V sind übrigens alle methylverzweigten mittelständigen C_6- und C_7-Olefine mit ihren Indexwerten in Squalan und Emulphor O aufgeführt. Bei den unverzweigten Olefinen führt die Verschiebung einer Doppelbindung in die Kettenmitte gegenüber dem zwei- und dreiständigen Olefin wieder zu einer Erniedrigung der H^S-Werte, so dass die gleichen Werte wie bei den 1-Olefinen gefunden werden[6].

METHYLCYCLANE MIT 1, 2 UND 3 DOPPELBINDUNGEN

Alle untersuchten Isomeren wurden durch Anwendung der methylene insertion-Reaktion auf ungesättigte Cyclane dargestellt. Dabei fallen auch die entsprechenden

bicyclischen Dreiringverbindungen mit an, so dass eine erhebliche Anzahl von Peaks in den Chromatogrammen zu erwarten war. Eine Reihe von diesen Isomeren war aber aus den Arbeiten von HEIMBACH[17] in reiner oder angereicherter Form zugänglich.

Bei den höheren Ringen mit unsymmetrischer Verteilung der Doppelbindungen ist die Zahl der insgesamt möglichen Isomeren so gross, dass eine vollständige Bearbeitung vorläufig zu schwierig erschien. Aus diesem Grunde wurde bei den Achtringen nur das *cis,cis*-Cyclooctadien-(1,5)-, bei den Zehnringen nur das *trans,trans*-Cyclodecadien-(1,6) und das *cis,cis*-Cyclodecadien-(1,6) der MIR unterworfen. Bei diesen Dienen wie auch bei den *cis,trans*-Isomeren des 1,5,9-Cyclododecatriens (im folgenden CDT genannt) sind die Doppelbindungen symmetrisch über den Ring verteilt, so dass die Zahl der möglichen Isomeren stark vermindert ist. Das *trans,cis*-Cyclodecadien-(1,6) ist nicht sehr beständig und war auch aus den Arbeiten des Mülheimer Instituts nicht zugänglich. Vom Cyclododecatrien-(1,5,9) sind vier Isomere möglich, von denen 3 aus den Arbeiten von WILKE und Mitarbeitern[18] gut bekannt sind und dem Autor in reiner Form zur Verfügung standen. Das vierte Isomere, das *cis,cis,cis*-CDT, wurde nach UNTCH UND MARTIN[19] rein dargestellt. Durch Anwendung der MIR werden aus den vier Isomeren insgesamt 22 neue Verbindungen gebildet, die mit Ausnahme eines Dubletts gaschromatographisch auch in Mischung alle getrennt werden konnten und deren Identität unter Zuhilfenahme der voranstehenden abgeleiteten Regeln und der bei der methylene insertion beobachteten Statistik festgestellt werden konnte. Die Retentionsindices aller gaschromatographisch getrennten und identifizierten Acht-, Zehn- und Zwölfringverbindungen sind in den Tab. VI, VII und VIII aufgeführt.

METHYLSUBSTITUIERTE CYCLOOCTENE UND CYCLOOCTADIENE

Durch Methylierung des Cycloocten-*cis* werden 4 Methylcyclooctene und der *cis*-Bicyclus erhalten, während aus dem *cis,cis*-Cyclooctadien-(1,5) zwei Isomere und eine bicyclische Verbindung erhalten werden. Die Zuordnung der MIR-Produkte des Cycloocten-*cis* ergab sich wie folgt:

1. Die 4 Methylcyclooctene 4, 5, 6 und 7 in Tab. VI werden entsprechend der erwarteten Statistik der MIR im Verhältnis 1:2:2:2 gebildet.
2. Die Dreiringverbindung 8 entsteht bevorzugt.
3. Wie bei den offenkettigen Olefinen muss die Verbindung 4 wegen ihrer Methylsubstitution an der Doppelbindung den höchsten Retentionsindex bzw. H^S-Wert und die Verbindung 5 wegen ihrer Methylsubstitution in Allylstellung den niedrigsten Retentionsindex haben. Das 1-Methyl-cycloocten lag auch in reiner Form vor, vgl. auch 10, 11, Spalte 6.
4. 1-methylsubstituierte Olefine haben immer höhere ΔI-Werte als 3-methylsubstituierte Olefine, vgl. ΔI von 4,5 und 10,11.

Die Zuordnung der Verbindungen 6 und 7 ist nicht ganz gesichert. Die Zuordnung der MIR-Produkte des *cis,cis*-Cyclooctadien-(1,5) ist dagegen sehr einfach:

1. Die Dreiringverbindung wird in grösster Menge gebildet.
2. Die Verbindungen 10 und 11 werden im Verhältnis 1:2 gebildet.
3. Die Verbindung 10 hat den höheren Retentionsindex als die Verbindung 11, weil sie an der Doppelbindung substituiert ist. Aus dem gleichen Grunde hat sie auch den höheren ΔI-Wert.

Zu den H^S- und ΔI-Werten der Tab. VI ist allgemein folgendes festzustellen:

TABELLE VI

METHYLSUBSTITUIERTE CYCLOOCTENE UND -OCTADIENE-(1,5)

Nr.		I^{S}_{100}	I^{EME}_{100}	ΔI_{100}†	H^{S}_{100}[a]	H^{S}_{100}[b]	$\delta(\Delta I)$[c]
1	Cyclooctan	934	1000	66	0		
2	Cycloocten-*cis*	905	1006	102	−29		
3	Me-Cyclooctan	995	1053	58	0		
4	1-Me-Cycloocten-*cis*	978	1069	91	−17		+33
5	3-Me-Cycloocten-*cis*	958	1043	85	−37		+27
6	4-Me-Cycloocten-*cis*	964	1053	89	−31		+29
7	5-Me-Cycloocten-*cis*	974	1066	92	−21		+34
8	*cis*-(6,1,0)-Bicyclononan	1003	1096	93	0		
9	*cis, cis*-Cyclooctadien-1,5	923	1086	163	−11	+18	
10	1-Me-*cis, cis*-Cyclooctadien-1,5	998	1150	152	+ 3	+20	+61
11	3-Me-*cis, cis*-Cyclooctadien-1,5	978	1124	146	−17	+20	+61
12	*cis*-(6,1,0)-*cis*-Bicyclononen-5	1012	1154	142	+ 9		+49

* I^{EMO}_{100} = Retentionsindex an Emulphor O bei 100°.
† $\Delta I = I^{S}_{100} - I^{EMO}_{100}$.
[a] $H^{S} = I^{S}$ (Cyclen) $- I^{S}$ (Cyclan).
[b] $H^{S} = I^{S}$ (Cyclodien) $- I^{S}$ (Cyclen).
[c] $\delta(\Delta I) = I$ (Cyclen) $- I$ (Cyclan).

1. Die Einführung einer zweiten *cis*-Doppelbindung in den Achtring führt zu keiner weiteren Erniedrigung des H^{S}-Wertes. Vielmehr werden die H^{S}-Werte um etwa 10–20 I.E. erhöht, Spalte 6.
2. Die 1-Methylverbindungen 4 und 10 haben die höchsten H^{S}-, die 3-methylsubstituierten Verbindungen 5 und 11 die niedrigsten H^{S}-Werte.
3. Die Einführung einer Doppelbindung verursacht einen $\delta(\Delta I)$-Wert von etwa 30 I.E., während die Einführung einer zweiten Doppelbindung einen $\delta(\Delta I)$-Wert von etwa 60 I.E. verursacht. Der ΔI-Wert für offenkettige Olefine beträgt zum Vergleich etwa 40–45 I.E., liegt also etwa in der Mitte zwischen beiden.

Durch die Einführung insbesondere der zweiten Doppelbindung wird offenbar die Geometrie bzw. die Beweglichkeit des gesättigten Achtrings so verändert, dass die daraus resultierenden Einflüsse auf die intermolekulare Wechselwirkung und damit auf die H^{S}- bzw. ΔI-Werte die bei den offenkettigen Olefinen gefundenen Effekte überlagern.

Methylsubstitutionsprodukte des Cyclodecen-trans und des Cyclodecen-cis sowie des trans, trans-Cyclodecadien-(1,6) und des cis,cis-Cyclodecadien-(1,6)

Mit den Dreiringverbindungen werden aus dem Cyclodecen-*trans* und dem Cyclodecen-*cis* jeweils fünf neue Verbindungen bei der MIR gebildet. Auch in diesem Falle ist die Zuordnung der 1- und der 3-Methylcyclodecen-Verbindungen allein vollständig gesichert. Sie erfolgte im Falle der 1-Methylverbindungen über vorhandene Vergleichssubstanzen mit Hilfe der bei den offenkettigen Olefinen abgeleiteten Regeln und über die Statistik der MIR. Für die Zuordnung der 3-Methyl-cyclodecene gilt das gleiche wie für die entsprechenden Achtringverbindungen. Die 4-, 5- und 6-Methylcyclodecene konnten vorläufig nicht sicher zugeordnet werden. Aus diesem Grunde

sind die Verbindungen 7 und 16 mit einem Fragezeichen versehen, die 5- und 6-Methylcyclodecene sind in der Tab. VII gar nicht aufgeführt. Die Zuordnung der

TABELLE VII

METHYLSUBSTITUIERTE CYCLODECENE UND CYCLODECADIENE-(1,6)

Nr.		I^{S}_{100}	I^{EMO}_{100}	ΔI_{100}	H^{S}_{100} [a]	H^{S}_{100} [b]	$\delta(\Delta I)$ [*]
1	Cyclodecan	1141	1217	76	0		0
2	Cyclodecen-*trans*	1115	1221	106	−26		+30
3	Cyclodecen-*cis*	1123	1233	110	−18		+34
4	Me-Cyclodecan	1195	1263	68	0		0
5	1-Me-Cyclodecen-*trans*	1197	1303	106	+ 2		+38
6	3-Me-Cyclodecen-*trans*	1166	1260	94	−29		+26
7	4-Me-Cyclodecen-*trans*	1168	1262	94	−27		+26
8	*trans*-(8,1,0)-Bicycloundecan	1200	1296	96	0		0
9	*trans, trans*-Cyclodecadien-1,6	1084	1217	133	−57	−31	+27
10	1-Me-*trans, trans*-Cyclodecadien-1,6	1178	1313	135	−17	−19	+29
11	3-Me-*trans, trans*-Cyclodecadien-1,6	1135	1253	118	−60	−31	+24
12	4-Me-*trans, trans*-Cyclodecadien-1,6	1150	1273	123	−45	−18	+29
13	*trans*-(8,1,0)-*trans*-Bicycloundecen-6	1169	1285	116	−31		+20
14	1-Me-Cyclodecen-*cis*	1193	1296	103	− 2		+35
15	3-Me-Cyclodecen-*cis*	1159	1249	90	−36		+22
16	4-Me-Cyclodecen-*cis*	1174	1272	98	−21		+32
17	*cis*-(8,1,0)-Bicycloundecan	1221	1323	102	0		0
18	*cis, cis*-Cyclodecadien-1,6	1103	1238	135	−38	−20	+25
19	1-Me-*cis, cis*-Cyclodecadien-1,6	1176	1306	131	−19	−17	+28
20	3-Me-*cis, cis*-Cyclodecadien-1,6	1135	1251	116	−60	−24	+26
21	4-Me-*cis, cis*-Cyclodecadien-1,6	1176	1306	130	−19	+ 2	+32
22	*cis*-(8,1,0)-*cis*-Bicycloundecen-6	1204	1333	129	−17		+27

[a] $H^{S}_{100} = I^{S}_{100}$ (Cyclen) − I^{S}_{100} (Cyclan).
[b] $H^{S}_{100} = I^{S}_{100}$ (Cyclodien) − I^{S}_{100} (Cyclen).
[*] $\delta(\Delta I) = \Delta I$ (Cyclen) − ΔI (Cyclen) bzw. ΔI (Cyclodien) − ΔI (Cyclen).

Dreiringverbindungen 8 und 17 ist aus statistischen Gründen sehr leicht möglich. Wesentlich einfacher ist die Zuordnung der MIR-Produkte der beiden Cyclodecadien-(1,6)-Verbindungen:

1. Die Verbindungen 10, 11 und 12 sowie 19, 20 und 21 werden wiederum so eluiert, dass die 1-Methylverbindung den höchsten und die 3-Methylverbindung den niedrigsten Retentionsindex — unabhängig von der Polarität der stationären Phase — besitzt.
2. Wie erwartet, werden die drei Verbindungen im Verhältnis 1:2:1 gebildet. Die Zuordnung der Dreiringverbindungen bereitete aus der Statistik jedenfalls keine Schwierigkeiten.

Zu den H^S-Werten der Spalte 5, die auf die entsprechenden gesättigten Zehnringverbindungen bezogen sind, ist folgendes zu sagen:

1. Die Einführung einer unsubstituierten *trans*-Doppelbindung in den Zehnring erniedrigt den H^S-Wert um 25–30 I.E., vgl. 2,1; 13,8.
2. Methylsubstitution der Doppelbindung erhöht den H^S-Wert erheblich, vgl. 5, 10, 14 und 19 mit 2, 9, 3 und 18.
3. Methylsubstitution in Allylstellung erniedrigt den H^S-Wert der *trans*-Doppelbindung ein wenig, denjenigen der *cis*-Doppelbindung stärker (vgl. 6,2; 11,9 sowie 15,3 und 20,18).

TABELLE VIII

METHYLSUBSTITUIERTE CYCLODODECENE UND CYCLODODECATRIENE-(1,5,9)

Nr.		I^S_{120}	I^{EMO}_{120}	ΔI_{120}	H^S_{120}*	$\delta(\Delta I)$†
1	Cyclododecan	1330	1417	87		
2	Cyclododecen-*trans*	1306	1421	115	−24	+ 28
3	Cyclododecen-*cis*	1315	1440	125	−15	+ 38
	Cyclododecatrien-1,5,9					
4	*trans, trans, trans*	1260	1424	164	−70	+ 77
5	*trans, trans, cis*	1284	1462	178	−46	+ 91
6	*trans, cis, cis*	1298	1488	190	−32	+103
7	*cis, cis, cis*	1294	1491	197	−36	+110
8	1-Me-Cyclododecan	1386	1463	77	0	0
9	1-Me-Cyclododecen-*trans*	1382	1500	118	− 4	+ 41
10	1-Me-Cyclododecen-*cis*	1392	1513	121	+ 6	+ 44
	1-Me-Cyclododetrien-1,5,9					
11	*trans, trans, trans*	1345	1507	162	−41	+ 85
12	*trans, trans, cis*	1364	1539	175	−22	+ 98
13	*trans, cis, trans*	1364	1539	175	−22	+ 98
14	*cis, trans, trans*	1353	1525	172	−33	+ 95
15	*trans, cis, cis*	1374	1557	183	−12	+106
16	*cis, trans, cis*	1370	1553	183	−16	+106
17	*cis, cis, trans*	1370	1554	184	−16	+107
18	*cis, cis, cis*	1366	1557	191	−20	+114
	3-Me-Cyclododecatrien-1,5,9					
19	*trans, trans, trans*	1308	1455	147	−78	+ 70
20	*trans, trans, cis*	1337	1502	165	−49	+ 88
21	*trans, cis, trans*	1331	1493	162	−55	+ 85
22	*cis, trans, trans*	1315	1474	159	−71	+ 82
23	*trans, cis, cis*	1348	1523	175	−38	+ 98
24	*cis, trans, cis*	1337	1507	170	−49	+ 93
25	*cis, cis, trans*	1331	1502	171	−55	+ 94
26	*cis, cis, cis*	1328	1507	179	−58	+102
	(10,1,0)-Bicyclotridecadien-(4,8)					
27	*trans*	1398	1507	109	0	0
28	*trans-trans, trans*	1357	1515	158	−41	+ 49
29	*trans-trans, cis*	1372	1541	169	−26	+ 60
30	*trans-cis, cis*	1382	1557	175	−16	+ 66
31	*cis-trans, trans*	1391	1564	173	−30	+ 54
32	*cis-trans, cis*	1405	1590	185	−16	+ 66
33	*cis-cis, cis*	1391	1587	196	−30	+ 77
34	*cis*	1421	1540	119	0	0

* $H^S_{120} = I^S_{120}$ (Cyclen) − I^S_{120} (Cyclan).
† $\delta(\Delta I) = \Delta I$ (Cyclen) − ΔI (Cyclan).

4. Das 4-Methyl-*cis,cis*-cyclodecadien-(1,6) hat einen aussergewöhnlich hohen I^S- bzw. H^S-Wert im Verhältnis zu der entsprechenden *trans*-Verbindung. So beträgt der Unterschied in den H^S-Werten zwischen Cyclodecen-*trans* und Cyclodecen-*cis* etwa 8 I.E., während der Unterschied für die Verbindungen 12 und 21, 26 I.E statt wie erwartet etwa 15 I.E. beträgt. Auch hier können nur besondere sterische Verhältnisse zur Erklärung dieses Phänomens herangezogen werden. Für die Zuordnung der einzelnen Isomeren ist allerdings dieser Unterschied ohne Belang.

Während in den I-Werten der Spalte 3 der Ring und die verschiedenen Doppelbindungen sich gemeinsam auswirken, sind die $\delta(\Delta I)$-Werte so gebildet worden, dass der Einfluss einer einzigen Doppelbindung auf den ΔI-Wert isoliert ist. So wird der $\delta(\Delta I)$-Wert des Cyclodecen-*cis* durch Subtraktion der ΔI-Werte des Cyclodecen-*cis* und des Cyclodecans erhalten, während der $\delta(\Delta I)$-Wert der Verbindung 21 sich aus der Subtraktion des ΔI-Wertes der Verbindung 16 von dem ΔI-Wert der Verbindung 21 ergibt.

1. Die Einführung einer einfachen *trans*-Doppelbindung ergibt einen $\delta(\Delta I)$-Wert von etwa 30, die Einführung einer unsubstituierten *cis*-Doppelbindung einen $\delta(\Delta I)$-Wert von 34 I.E., vgl. 2, 10, 11, 12, 13 sowie 3, 14, 15, 16, 22. Abweichungen von dieser Regel treten bei der Einführung einer weiteren Doppelbindung in die 3-Methyl-cyclodecene sowie in die Bicyclen auf.
2. Methylsubstituierte Doppelbindungen ergeben einen $\delta(\Delta I)$-Wert von etwa 35, in Allylstellung substituierte Doppelbindungen einen $\delta(\Delta I)$-Wert von etwa 25 I.E., vgl. 5 und 14.
3. Bei den Methyl-cyclodecadienen ist kein unterschiedlicher Einfluss einer *trans*- bzw. einer *cis*-Doppelbindung auf die $\delta(\Delta I)$-Werte zu beobachten. Er wird durch sterische Einflüsse verdeckt.

Es kann festgestellt werden, dass für die Identifizierung der Zehnringverbindungen der Tab. VII die Unterschiede in den H^S-Werten von grösserer Bedeutung sind als die in den ΔI-Werten.

Die Methylsubstitutionsprodukte der Cyclodeca-(1,5,9)-triene

Von den vier Isomeren mit den Doppelbindungskonfigurationen

ttt ttc tcc ccc

bilden sich die ersten drei bei der stereospezifischen Trimerisation von Butadien nach WILKE und Mitarbeitern[18] mit bestimmten Ziegler-Katalysatoren. Das vierte Isomere lässt sich auf völlig anderem Wege nach UNTCH UND MARTIN[19] darstellen. Die MIR-Mischungen, die aus den vier reinen Isomeren erhalten werden, müssen wegen der verschiedenartigen Symmetrie der Ausgangsverbindungen folgende Zahlen von Isomerentypen ergeben: (Die arabischen Zahlen beziehen sich auf die fortlaufende Numerierung der Tab. VIII, die alle an den Cyclododecatrienen, Methylcyclododecatrienen und den Dreiringbicyclen gemessenen Indexwerte enthält).

Nr.	*Isomeres CDT*	*Zahl der Methyl-CDT*	*Dreiringe*	*Nummer in Tabelle VIII*
4	*trans, trans, trans*	2	1	11, 19, 29
5	*trans, trans, cis*	6	2	12, 13, 14, 20, 21, 22, 30, 32
6	*trans, cis, cis*	6	2	15, 16, 17, 23, 24, 25, 31, 33
7	*cis, cis, cis*	2	1	18, 27, 34

TABELLE IX

STATISTIK DER "METHYLENE INSERTION"-REAKTION MIT HEXEN-1 (Gew.-%)

Nr.		*Gemessen*	*Gemessen (Normiert ohne Dreiring)*	*Berechnet (Normiert ohne Dreiring)*
1	2-Me-Hexen-1	2.9	5.2	8.3
2	3-Me-Hexen-1	8.8	15.7	16.7
3	4-Me-Hexen-1	10.3	18.4	16.7
4	5-Me-Hexen-1	10.9	19.5	16.7
5	Hepten-1	16.3	29.2	25.0
6	*trans*-Hepten-2	4.3	7.7	8.3
7	*cis*-Hepten-2	2.6	6.4	8.3
8	n-Butylcyclopropan	38.3		

ZUR STATISTIK DER METHYLENE INSERTION-REAKTION MIT OFFENKETTIGEN UND CYCLISCHEN OLEFINEN

VON DOERING u.a.[10] haben gefunden, dass die methylene insertion in primäre, sekundäre und tertiäre CH-Bindungen gleich schnell verläuft. Wird die Bildung von Sekundärprodukten durch Verwendung eines starken Unterschusses von CH_2-

TABELLE X

STATISTIK DER "METHYLENE INSERTION"-REAKTION MIT CYCLODODECATRIEN-(1,5,9)

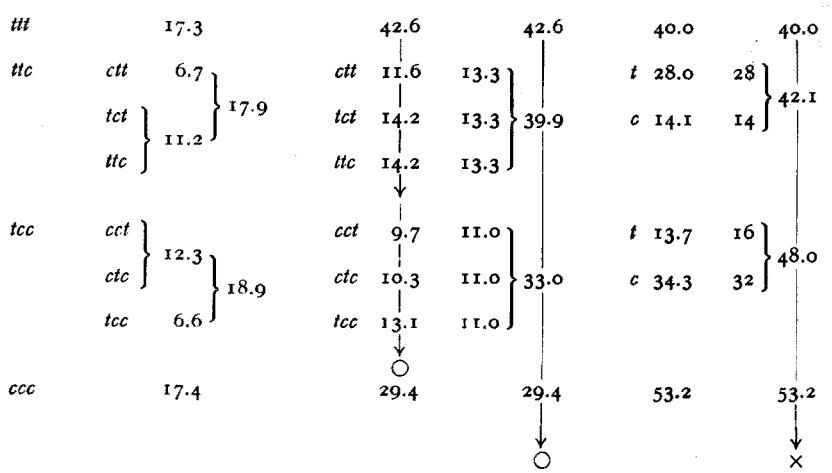

× = Dreiringbildung an der *cis*-Doppelbindung bevorzugt.
○ = Methylierung in 3-Stellung bevorzugt bei *trans*-Doppelbindung.

Radikalen vermieden, so werden die insertion-Produkte in Mengenverhältnissen gebildet, die durch den Gehalt der betreffenden CH-Bindungen im Gesamtmolekül gegeben sind. SIMMONS u.a.[11] haben die methylene insertion aus diesem Grunde mit Erfolg zur Identifizierung von gesättigten Kohlenwasserstoffen über die *Zahl* der Isomeren, die durch methylene insertion-Reaktionen entstehen, einsetzen können. Später haben DVORETZKY u.a.[12] die methylene insertion-Reaktion auch auf cyclische und ungesättigte Kohlenwasserstoffe angewandt. Sie stellten fest, dass z.B. bei der MIR mit 2-Methyl-buten-1 wie bei den gesättigten Kohlenwasserstoffen nur geringfügige Abweichungen von der erwarteten Statistik zu beobachten sind, wenn man den ebenfalls gebildeten Dreiring ausser Acht lässt. Wir konnten diese Beobachtung in etwa bestätigen. Tab. IX enthält die Statistik der MIR mit Hexen-1. Alle gemessenen Werte wurden mit einer Datenspeicherungs- und Integrations-Anlage der Firma Infotronics, Houston, Texas, Modell 11 HSB/42 (Integrator), CRS-40 TS (Rückspieleinheit), CRS 41 RSI (Bandgerät) ermittelt. Die berechneten und die gefundenen Werte zeigen allerdings eine Übereinstimmung, die nicht ganz so gut ist wie die von DVORETZKY und Mitarbeitern gefundene. Die Unsymmetrie, die durch die Doppelbindung in das Kohlenstoffgerüst des Hexans hineinkommt, ist offenbar die Ursache dafür,

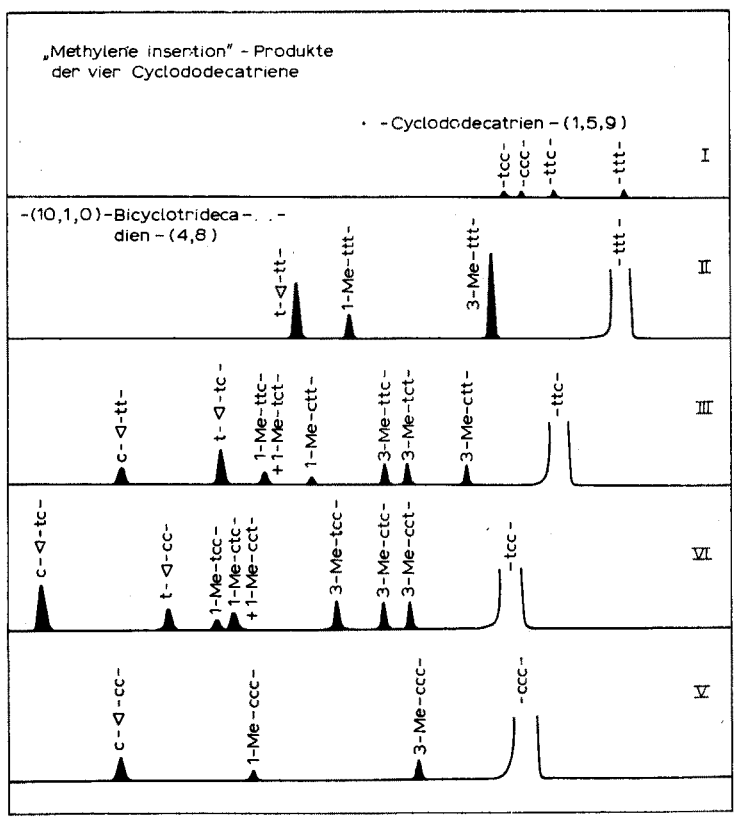

Fig. 2. "Methylen insertion"-Produkte von Cyclododecatrienen.

dass alle Isomere, die ihre Entstehung einer Einschiebungsreaktion in der Nähe der Doppelbindung verdanken, in geringen Mengen gebildet werden, während sich das 4- und das 5-Methyl-hexen-1 sowie das Hepten-1 in grösserer Menge als erwartet bilden. Ausserdem ist das *cis-trans*-Verhältnis beim Hepten-2 nicht, wie man für eine rein kinetisch kontrollierte Reaktion erwarten sollte, 1:1. Ein wenig anders liegen die Verhältnisse bei den MIR-Produkten der "symmetrischen" Ringolefine, wie Cyclodecadien-(1,6) und Cyclododecatrien-(1,5,9). Die Tab. X zeigt, dass nur die Bildung der 3-Methyl-cyclododecatriene an *cis*-Doppelbindungen gegenüber der Bildung von 3-Methyl-cyclododecatrienen an *trans*-Doppelbindungen benachteiligt ist (11.6% *cis, trans,trans* gegen 14.2% *trans,cis,trans* und *trans,trans,cis*), während für die Bildung der 1-Methyl-cyclododecatriene keine unterschiedliche Reaktionsfähigkeit zwischen *trans*- und *cis*-Doppelbindung beobachtet wird. Die Dreiringbildung ist an *cis*-Doppelbindungen (im Ring) gegenüber der an *trans*-Doppelbindungen stark bevorzugt, wie aus der Tabelle leicht zu entnehmen ist. Trotz dieser geringfügigen Abweichungen von der erwarteten Statistik der MIR waren die statistisch erwarteten Mengenverhältnisse der einzelnen Isomeren ein wertvolles Hilfsmittel für die Zuordnung der gaschromatographischen Peaks.

Die Substanzen 1, 2, 3, 8, 9 und 10 lagen als reine oder sehr stark angereicherte Verbindungen vor, 28 und 29 wurden durch MIR mit 2 und 3 dargestellt. Sie werden ebenfalls im Verhältnis 2:1 gebildet, wenn Verbindung 5 oder 6 der MIR unterworfen werden und das Reaktionsprodukt hydriert wird. Die Chromatogramme der MIR-Produkte der Verbindungen 4, 5, 6 und 7, also der vier Cyclododecatriene, in einer Kapillarsäule mit Squalan als stationärer Phase zeigt das Bild 2.

Zuordnung der Isomeren

Chromatogramm I: Die vier Cyclododecatriene lagen als reine Vergleichssubstanzen vor, deren Struktur vielfältig, insbesondere aber durch IR- und NMR-Spektroskopie gesichert war.

Chromatogramm II: *1.* An der Doppelbindung methylsubstituierte Isomere haben wesentlich höhere Retentionszeiten als die in Allylstellung substituierten Typen. *2.* 1-Methyl- und 3-Methyl-Verbindungen wurden wie erwartet im Verhältnis 1:2 gebildet. Bezüglich der Statistik der MIR der Cyclododecatriene vgl. die Tab. X, aus der alles Weitere zu entnehmen ist. *3.* Der Dreiring wird in grosser Menge gebildet und hat den höchsten I^S-Wert, vgl. SCHOMBURG[6].

Chromatogramm III: *1.* Es wird die richtige Isomerenzahl von 8 gefunden, wenn berücksichtigt wird, dass es sich bei Peak 5 um ein Dublett handelt, wie aus der grösseren Halbwertsbreite dieses Peaks ersichtlich ist, vgl. Punkt 4. *2.* Wegen der niedrigen Retentionszeiten muss es sich bei den ersten drei Peaks um allylsubstituierte, bei den drie folgenden um an der Doppelbindung substituierte Typen handeln. *3.* Die Zuordnung der Peaks 1, 2 und 3 ergibt sich daraus, dass die beiden Verbindungen 3-Methyl-*trans,trans,cis* und 3-Methyl-*trans,cis,trans* bezüglich ihres Retentionsverhaltens sehr ähnlich sein müssen, während sich die Verbindung 3-Methyl-*cis,trans,trans* von den beiden zuerst genannten stärker unterscheiden muss. Wie später gefunden wurde, führt die Methylsubstitution in der Allylstellung einer *cis*-Doppelbindung generell zu besonders niedrigen Retentionszeiten. *4.* Die Peaks 4, 5 und 6 sind wegen ihrer hohen Retentionszeiten die drei an der Doppelbindung substituierten Typen. Die beiden Verbindungen 1-Methyl-*trans,trans,cis* und 1-Methyl-*trans,cis,trans*

dürfen sich erwartungsgemäss nicht sehr stark unterscheiden, sie müssen darum dem Dublett Peak 5 und 6 zugeordnet werden. Mit dieser Zuordnung ist verträglich, dass die Fläche dieses Peaks doppelt so gross ist wie diejenige des Peaks 4, vgl. hierzu Tab. X mit den quantitativen Ergebnissen der MIR der vier Cyclododecatriene. Die Trennung dieser beiden sehr ähnlichen Isomeren ist auch mit stationären Phasen hoher Polarität nicht möglich. 5. Es werden wie erwartet zwei Dreiringverbindungen im Verhältnis 2:1 gebildet. Daraus ergibt sich die Zuordnung der *trans*- und *cis*-Konfiguration am Dreiring. Für die *cis*-Verbindung ist ausserdem ein höherer Retentionsindex zu erwarten als für die *trans*-Verbindung.

Chromatogramm IV: 1. Die Zuordnung der Peaks 1 bis 6 erfolgte wie bei Chromatogramm III, nur dass das Dublett von Peak 4 und 5 in der stationären Phase Emulphor O eindeutig in zwei Peaks aufgespalten werden kann. Peak 1 bis 3 müssen wiederum den in Allylstellung substituierten 3-Methyl-cyclododecatrienen zugeordnet werden. Peak 1 und 2 liegen näher beieinander und müssen darum den beiden sehr ähnlichen Isomeren 3-Methyl-*cis,trans,cis* und 3-Methyl-*cis,cis,trans* zugeordnet werden. Das gleiche gilt für den Peak 4, 5, der den beiden Verbindungen 1-Methyl-*cis,trans,cis* und 1-Methyl-*cis,cis,trans* zugeordnet werden muss. 2. Peak 6 und 7 sind die beiden Dreiringverbindungen, von denen der Ring mit *cis*-Konfiguration den höheren I^S-Wert haben und in doppelter Menge auftreten muss.

Chromatogramm V: Die Zuordnung erfolgte analog wie bei dem Chromatogramm II und bietet keine Schwierigkeiten.

Auf diese Weise war es möglich, die 22 Isomeren, die bei den MIR mit den vier Cyclododecatrienen gebildet werden, zuzuordnen, ohne dass Widersprüche auftreten zwischen den aus der Retentionsdaten-interpretation erhaltenen Ergebnissen und den aus der Statistik der MIR gezogenen Schlüssen.

Die an anderen Verbindungsklassen — nämlich offenkettigen Olefinen — abgeleiteten Regeln über Struktur und Retentionsverhalten ungesättigter Kohlenwasserstoffe waren ein wertvoller Beitrag für die "relative" Identifizierung der gaschromatographisch getrennten Isomere.

Die Retentionsdaten der Tab. VIII zeigen, dass innerhalb gewisser Grenzen, die durch die sterischen Besonderheiten der mittleren Ringe gezogen sind, der Einfluss struktureller Merkmale auf das Retentionsverhalten isomerer Verbindungen in etwa auch quantitativ erfasst werden kann. Es ist unmöglich, alle aufgeführten Retentionsdaten vollständig zu diskutieren. Im folgenden werden nur die für die Zuordnung solcher Isomerer wichtigen Regeln und einige Besonderheiten des Retentionsverhaltens dieser Verbindungen diskutiert.

H^S-Werte

Auch bei den Cyclododecatrienen und ihren Methylsubstitutionsderivaten ist offenbar, dass sich Änderungen der geometrischen Struktur durch Methylsubstitution oder Einführung von Doppelbindungen mit *trans*- oder *cis*-Konfiguration viel stärker in den H^S-Werten niederschlagen als in den ΔI-Werten.

Die Einführung einer *trans*-Doppelbindung in den Zwölfring führt zu einem H^S-Wert von -24, die Einführung einer *cis*-Doppelbindung zu einem Wert von -15 (Vgl. 2, 3 in Tab. VIII). Sind mehrere Doppelbindungen im Zwölfring enthalten, so kann kaum mit einer guten Additivität der Inkremente gerechnet werden, da die sterischen Verhältnisse im Ring durch zwei oder drei starre Doppelbindungen grund-

legend verändert werden. Für das *ttt*-CDT findet man aber einen H^S-Wert von −70 statt $3 \times -24 = -72$ I.E. und für das *ccc*-CDT einen H^S-Wert von −36 statt $3 \times -15 = -45$ I.E. Beim Übergang von 4 nach 5 wird wegen der Symmetrieverminderung und der Veränderung der sterischen Verhältnisse eine grössere Abnahme von 24 I.E. statt — wie erwartet — von −9 gefunden. Das gleiche gilt für die H^S-Differenzen der Übergänge 11, 12 und 19, 20. Beim Übergang von *ttc*- nach *tcc*-CDT (5, 6) wird eine H^S-Differenz von 14 I.E. gefunden, die sich bei den Übergängen 12, 15; 20, 23; 30, 31 in etwa wiederholt. Geht man vom *ccc*-CDT zum *cct*-CDT, so wird eine Zunahme von 4 I.E. gefunden, die wiederkehrt bei den analogen Übergängen 18, 17; 27, 26, nicht jedoch bei 34, 33. Methylsubstitution an der Doppelbindung erhöht die H^S-Werte unabhängig von der Konfiguration im Mittel um etwa 20 I.E. (2, 9; 3, 10; 7, 18; 11, 4; 5, 12 und 6, 15). Während Methylsubstitution in Allylstellung die H^S-Werte bei *trans*-Doppelbindungen nur geringfügig erniedrigt, im Mittel um etwa 10 I.E. (19, 4; 23, 6), beträgt die Erniedrigung der H^S-Werte bei *cis*-Doppelbindungen etwa 22 I.E. (27, 7; 26, 6; 22, 5). Hieraus erklärt sich auch, warum in den Chromatogrammen III und IV des Bildes 2 die 3-Methyl-cyclododecatriene mit Methylsubstitution in der Allylstellung zur *cis*-Doppelbindung dem Peak mit den kleinsten Retentionswerten zugeordnet wurden.

ΔI-Werte

In den ΔI-Werten der Spalte 3 der Tab. VIII sind sowohl die Beiträge des unsubstituierten bzw. substituierten Zwölfrings wie auch die der in dem Isomeren vorhandenen Doppelbindungen enthalten. Sie zeigen eine wesentlich bessere Additivität der Inkremente. Dafür sind aber charakteristische Änderungen selten. Bei den $\delta(\Delta I)$-Werten ist dagegen der Beitrag des Ringsystems eliminiert. Der $\delta(\Delta I)$-Wert einer unsubstituierten *trans*-Doppelbindung (vgl. SCHOMBURG[7]) beträgt etwa 25 I.E. (2, 4; 29, 32), der einer unsubstituierten *cis*-Doppelbindung 35 I.E. (3, 7; 31, 34). Methylsubstitution an der Doppelbindung mit *trans*- oder *cis*-Konfiguration erhöht die $\delta(\Delta I)$-Werte um etwa 5–10 I.E. pro Doppelbindung gegenüber den unsubstituierten Doppelbindungen (4, 11; 5, 12; 2, 9). Methylsubstitution in Allylstellung führt zu iner Erniedrigung der $\delta(\Delta I)$-Werte pro Doppelbindung um etwa 8–10 I.E. (7, 27; 6, 26).

Die vorgetragenen Ergebnisse über Struktur und Retentionsverhalten olefinischer Kohlenwasserstoffe können für die Aufklärung der Mechanismen katalytischer Reaktionen in der Chemie olefinischer Kohlenwasserstoffe grosse Bedeutung erlangen. Die Stereospezifität solcher Reaktionen durch richtige Auswahl oder Modifizierung der verwandten Katalysatorsysteme steuern zu können, ist das erklärte Ziel der Forschung. Hierzu ist es unbedingt erforderlich, die Struktur aller Reaktionsprodukte genau zu kennen. So konnten z.B. mit Hilfe der Retentionsdaten der isomeren Methylcyclododecatriene Gemische qualitativ und quantitativ analysiert werden, wie sie bei der Mischoligomerisation von Butadien mit *trans*- bzw. *cis*-Piperylen sowie Isopren nach WILKE UND HEIMBACH[20] mit speziellen Ziegler-Katalysatoren erhalten werden. Die Zahl und Art der ermittelten Isomerentypen erlaubt Rückschlüsse auf die sterische Anordnung der Oligomerisationspartner in den intermediär gebildeten metallorganischen Katalysatorsystemen, vgl. hierzu WILKE[21], die Einblick in den Ablauf stereospezifischer Oligomerisationen vermitteln.

ZUSAMMENFASSUNG

Stereospezifische katalytische Reaktionen spielen in der modernen Kohlenwasserstoff- und insbesondere der Olefin-Chemie eine grosse Roll. Die Analyse der dabei anfallenden Isomeren-Mischungen stellt eine besonders schwierige Aufgabe dar. Nur mit Hilfe der Gaschromatographie und bei Verwendung hochauflösender Säulen können die Isomeren der ungesättigten Kohlenwasserstoffe getrennt werden. Die Kombination Kapillargaschromatograph–Massenspektrometer liefert Spektren der einzelnen Komponenten, die oft nicht genügend charakteristisch sind, um eine Identifizierung zu ermöglichen. Hier kann die Auswertung der Retentionsdaten weiterhelfen, da selbst kleine strukturelle Unterschiede messbare Unterschiede der Retentionswerte zu Folge haben. Die Kenntnis der chemischen Vorgeschichte der zu analysierenden Mischung und, im Falle der Methylsubstituierten Isomeren, die Ergebnisse der "methylen insertion" Reaktion machen eine Zuordnung möglich.

SUMMARY

Modern hydrocarbon and especially olefin chemistry is concerned with the stereospecificity of catalytic reactions. Mixtures resulting from these reactions must be analyzed for all possible isomers. Only gas chromatography with high resolution and mainly open tubular columns is able to separate the different isomers of unsaturated hydrocarbons present in such mixtures. The identification of the separated species is difficult, as the modern combination of mass spectroscopy with capillary columns supplies spectra which are not characteristic enough for identification of such unsaturated hydrocarbons. However, the interpretation of retention data of hydrocarbons may be successful, because small structural variations correspond to definite differences of retention data. The chemical history of the analyzed products and, in the case of methyl-substituted isomers, data on the methylene insertion reaction, make it possible to obtain a relative correlation of separated species.

LITERATUR

1 H. PURNELL, *Gas Chromatography*, John Wiley and Sons, New York, 1962, S. 205.
2 M. DUNKEL, *Z. Phys. Chem.*, 138 (1928) 42.
3 E. KOVATS, *Helv. Chim. Acta*, 41 (1958) 1915; A. WEHRLI UND E. KOVATS, *ibid.*, 42 (1959) 2709.
4 P. A. SWOBODA, in M. VAN SWAAY (ed.), *Gas Chromatography 1962*, Butterworth, London, 1963, S. 279.
5 G. SCHOMBURG, *J. Chromatog.*, 14 (1964) 157.
6 G. SCHOMBURG, *J. Chromatog.*, 23 (1966) 1.
7 G. SCHOMBURG, *J. Chromatog.*, 23 (1966) 18.
8 G. SCHOMBURG, *Separation Science*, in Druck.
9 G. SCHOMBURG, in J. C. GIDDINGS (ed.), *Advances in Gas Chromatography*, Marcel Dekker, New York, in Druck.
10 W. E. VON DOERING, R. G. BUTTERY, R. G. LAUGHLIN UND N. CHAUDHURY, *J. Am. Chem. Soc.*, 78 (1956) 3224.
11 M. C. SIMMONS, D. B. RICHARDSON UND C. R. DURETT, in R. P. W. SCOTT (ed.), *Gas Chromatography, 1960*, Butterworths, London, 1960, S. 211.
12 T. DVORETZKY, D. B. RICHARDSON UND C. R. DURETT, *Anal. Chem.*, 35 (1963) 545.
13 D. HENNEBERG UND G. SCHOMBURG, unveröffentlicht.
14 I. MATSUKUMA, *J. Chem. Soc. Japan*, 84 (1963) 770.
15 H. PAULING, unveröffentlicht.

16 G. WITTIG, *Chem. Ber.*, 87 (1954) 13; 88 (1955) 1654.
17 P. HEIMBACH, unveröffentlicht.
18 H. BREIL, P. HEIMBACH, M. KRÖNER, H. MÜLLER UND G. WILKE, *Makromol. Chem.*, 69 (1963) 18.
19 K. G. UNTCH UND D. J. MARTIN, *J. Am. Chem. Soc.*, 87 (1965) 3518.
20 G. WILKE UND P. HEIMBACH, unveröffentlicht.
21 G. WILKE, *Angew. Chem.*, 75 (1963) 10.

Analytica Chimica Acta
Elsevier Publishing Company, Amsterdam
Printed in the Netherlands.

TWO-STAGE CAPILLARY GAS CHROMATOGRAPHY

P. A. SCHENCK* AND C. H. HALL
Shell Development Company—E. and P. Research Division, Houston, Texas (U.S.A.)

(Received November 1st, 1966)

As more is learned about the composition of complex mixtures, the demand for still more precise knowledge of these mixtures increases. This certainly holds for crude oils, for, although far more is now known about their structure than, say, 10 years ago, many questions still remain unanswered.

Capillary gas chromatography of saturated hydrocarbons has given much information: all existing isomers boiling below 120° can be separated on one capillary column[1]. Extension of the technique to higher-boiling fractions of saturated hydrocarbons from petroleums has shown a great number of peaks in the gas chromatograms. It is a reasonable guess that most of these peaks represent groups of compounds rather than one. In comparative studies of crude-oil composition, it is of interest to discover the structure of at least some of the compounds causing these peaks.

Although some information can be obtained by gas chromatography, the ultimate identification of the compounds must be made by other auxiliary techniques, mainly by mass spectrometry. The best mass-spectrometric results can be expected, however, when only a few molecular species are present at the same time. In the analysis of complex mixtures this requires a separation technique with high resolving power. Trapping of peaks as they emerge from capillary gas-chromatographic columns and re-injection into a column of different type would thus seem to be a good way of preparing samples for mass-spectrometric analysis. The small sample sizes then involved, however, make freezing of single peaks—that may still consist of several compounds—highly impracticable or even impossible.

A method was therefore sought by which information on the composition of the mixture causing a peak might be obtained without trapping the peak. In the method finally selected, two capillary gas-chromatographic columns are connected by a valve that enables the compound(s) emerging as a single peak from the first column to be injected directly into the second column. The use of columns of different type allows some conjectures to be made with regard to the composition of the compounds causing a peak. The combination of such a two-stage capillary gas chromatograph with a mass spectrometer for the study of the constitution of petroleum has given most encouraging results.

DISCUSSION OF THE METHOD

Three main types of gas-chromatographic column can be used for the separa-

* Present address: Koninklijke/Shell Exploratie en Produktie Laboratorium, Rijswijk, The Netherlands.

tion of saturated hydrocarbons. Roughly speaking, separation can be based on:

1. boiling point (*e.g.* SF 96 and SE 30 silicones from General Electric)
2. molecular type (*e.g.* EPON(R) 1001)
3. molecular weight (silica)[2].

Modifications can be made by using columns of mixed substrates, whereby one coating material is modified by the addition of another (*e.g.* a mixture of liquid phases of different polarity (SCHWARTZ AND BRASSEAUX[1])).

SIMMONS AND SNYDER[3] connected two packed columns of different type in series and obtained better separations in the C_5–C_7 range of petroleum. A valve between the columns allowed a portion of the sample to be taken from the first column and subsequently separated on the second one.

MCEWEN[4] connected two capillary columns by a valve that allowed separation through the first column only or through both columns in series. He also connected a packed column with a capillary column. After a portion of the sample had been analysed on both columns in series, the valve was turned and the remainder of the sample was backflushed off the first column on to the cooled second column, which was then heated to effect the separation. Only one detector was used in his work on the analysis of C_5–C_7 saturates and C_5–C_8 aromatics and olefins.

In the present work these approaches were modified and the high resolving power of two capillary columns of different type was utilized. Figure 1 shows a schematic diagram illustrating the principle of this arrangement.

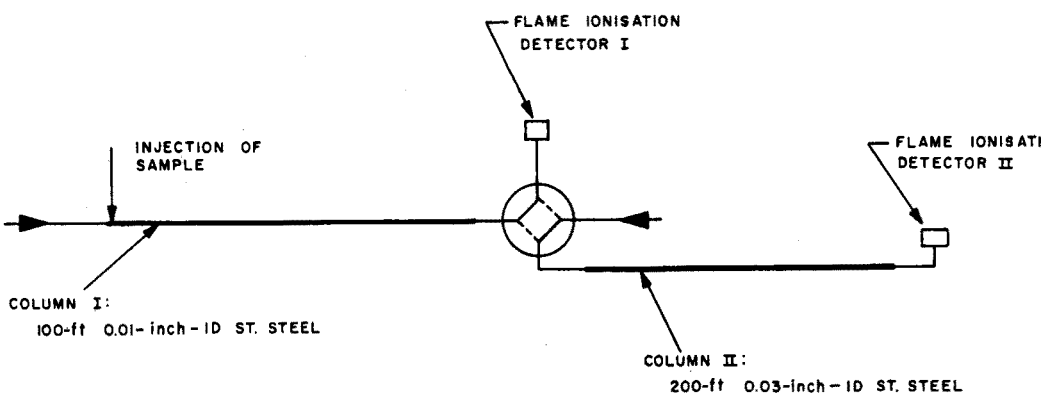

Fig. 1. Schematic diagram of chromatographic system. All connecting tubes 0.01-inch ID; lengths as short as possible; temp. ~ 200°. Tube between valve and flame I "filled" with wire of 0.008 inch diameter. Valve at ~ 150°. Column I: Coating, SE 30; carrier gas, H_2; inlet pressure, 10 p.s.i. Temperature programmed from 90° at 2°/min to 250°. Column II: Coating, silica; carrier gas, H_2; inlet pressure, 8 p.s.i.; temp., 233°.

A four-way valve with the smallest possible dead volume was placed after column I and before flame detector I. All connecting tubes were 0.01-inch-I.D. stainless steel capillaries. This valve makes it possible to force a peak from the first column immediately into the second one. The use of two flame detectors allows operation of the columns either independently or in series.

The method was applied to the analysis of the saturated hydrocarbons from

the C_{10}–C_{18} range of petroleum, but a wider application seems possible. Experimental details of the examples to be discussed are given elsewhere in this paper.

The time chosen for the valve to remain open can be either the elution time of a well-defined peak or a more or less arbitrarily fixed time. In this work the second alternative was chosen in order to obtain closely comparable "boiling-point fractions" from crude oils of various types. In other cases, a choice based on peak elution time might be preferable. The 35-sec period chosen, however, is the average width of a peak on the SE 30 column under the condition used.

Turning the valve to open causes a pressure change at the end of column I. This is partly because the inlet pressure of column II is higher than the outlet pressure of column I just before the flame. To reduce this effect, the "resistance" between the valve and flame detector I was increased by putting a 0.008″ wire into the 0.01″-I.D. capillary and the inlet pressure of column II was reduced from 8 p.s.i. to about 2 p.s.i. one minute before turning the valve. A change in flow rate remained unavoidable under these experimental conditions, however.

In later experiments—with a mass spectrometer connected to the outlet of the second column instead of a second flame-ionisation detector—this difficulty did not arise. Since the inlet pressure of the mass spectrometer (*i.e.* the end of the second column) is very low, the conditions can be adjusted in such a way that the inlet pressure of the second column is at atmospheric pressure or only slightly higher.

INTERPRETATION OF RESULTS

Although the method is applicable to mixtures of other types of compound, the use that will be illustrated here is that of separating saturated hydrocarbons in the C_{10}–C_{18} molecular weight range.

The following combination of columns was used: column I separated according to boiling point (SE 30 gum rubber) and column II according to molecular weight (silica; see Appendix).

Figures 2 and 3 show parts of the chromatograms obtained from the first capillary column along with the results of the second separation for each selected peak. The part of the sample that was removed from the chromatogram of the stream emerging from column I is represented by the shaded peaks in Figs. 2 and 3. It can be seen that this experimental arrangement provides further separation of the components forming the peaks distinguished by the first column; certain peaks which on the first column have the same retention times, though referring to different types of crude, can be seen in the more detailed separation to have a very comparable composition (peak 2), while others have a different one (peaks 4, 5).

The analyses of saturated hydrocarbons, first on a "boiling-point" column and subsequently on a "molecular-weight" column, provide a certain amount of structural information. Isoalkanes of a particular carbon number boil at a lower temperature than normal alkanes of the same carbon number. Cycloalkanes, on the other hand, may boil at either higher or lower temperatures than the normal alkane of the same carbon number, depending on the substituents on the ring. Thus, when a peak under investigation has emerged after a normal alkane with n C atoms from column I (boiling-point separation), this peak cannot contain isoalkanes with n C atoms. Therefore, if analysis of this peak on column II (molecular-weight separation) indi-

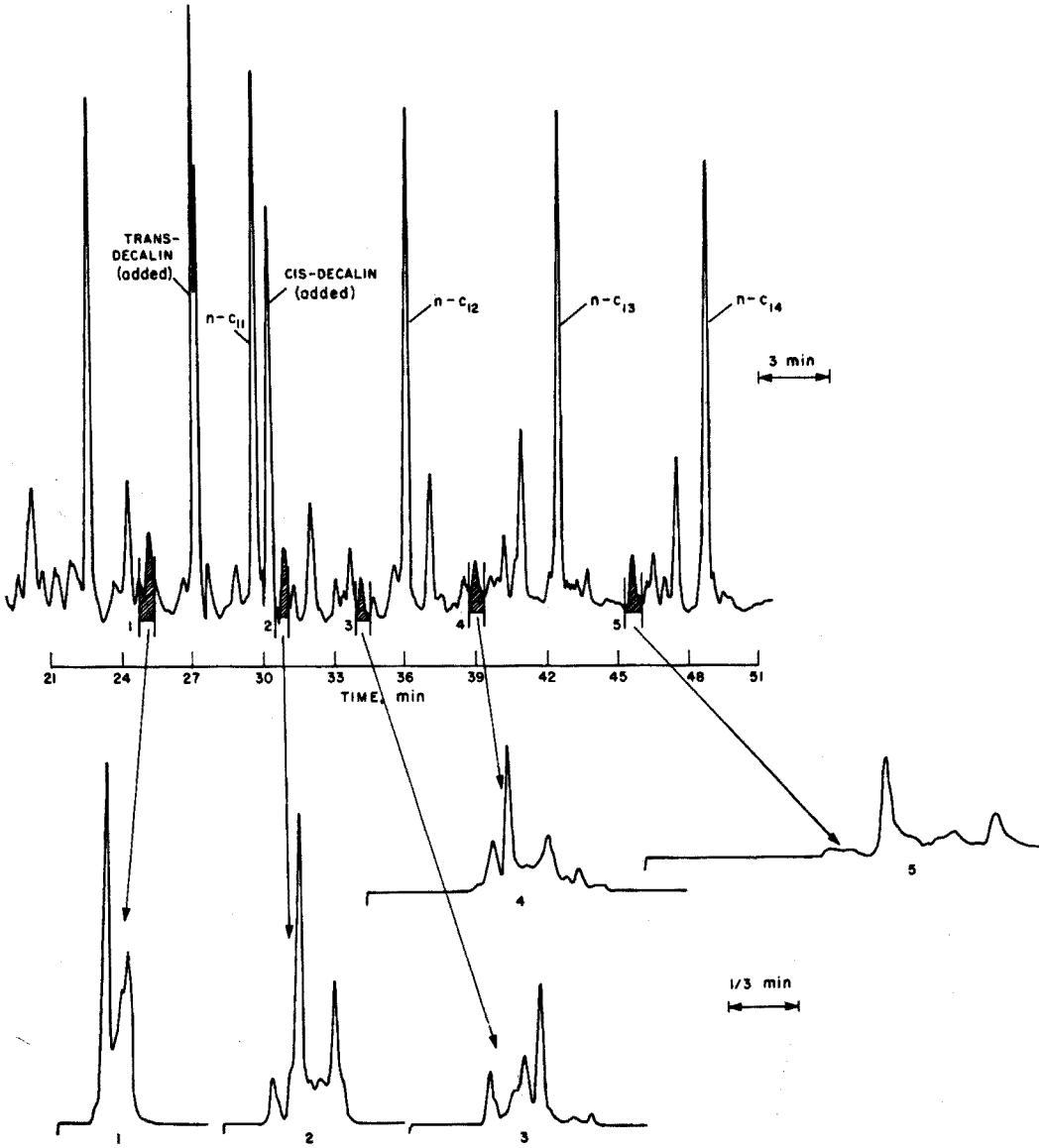

Fig. 2. Further separation of certain peaks from a boiling-point column (SE-30) on a molecular-weight column (silica gel) for a paraffinic crude.

cates the presence of molecules with n C atoms, such molecules must be ring compounds.

To extend this work still further, one might even consider coupling three columns together, *e.g.* first for separation according to boiling point, then according to molecular weight, and finally according to molecular type. A great deal of information on the structure of the compound could thus be obtained, since the number of possible compounds would be greatly reduced. If this multistage capillary gas-

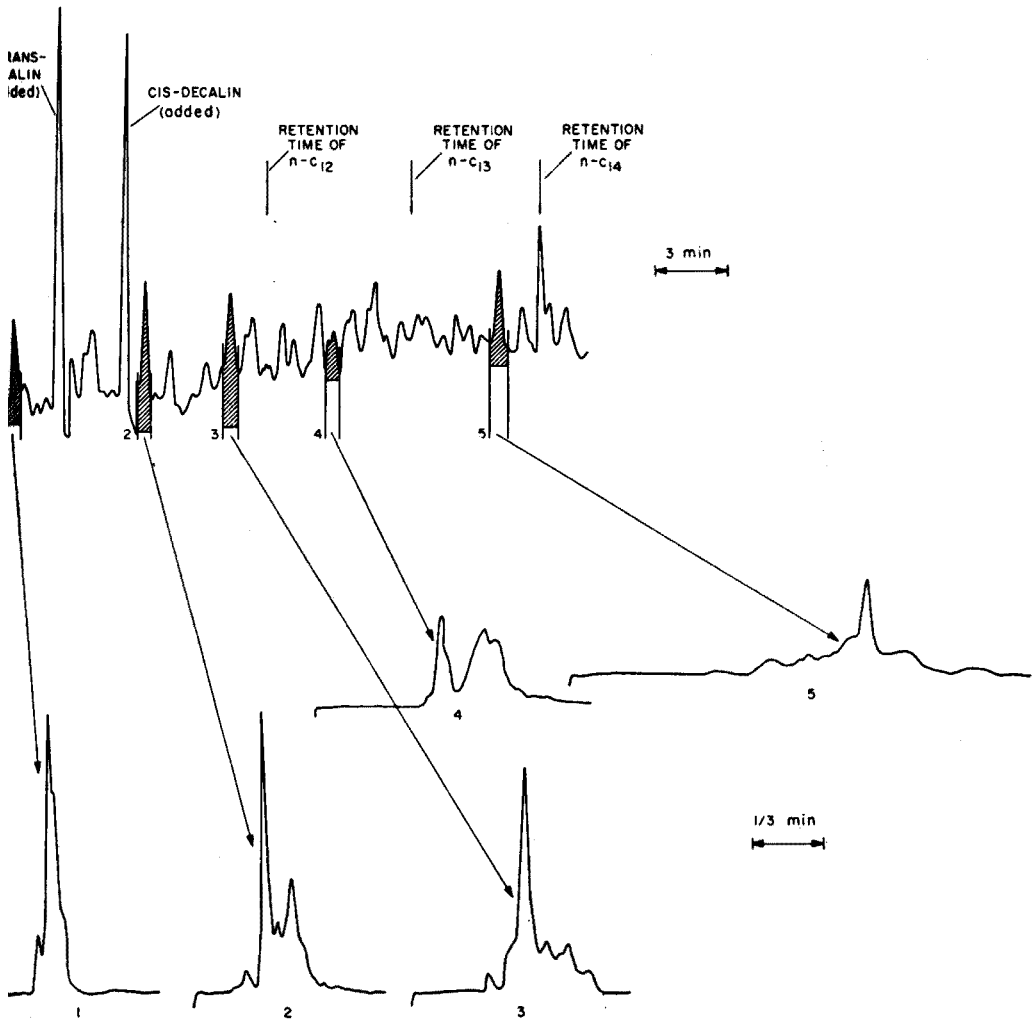

Fig. 3. Further separation of certain peaks from a boiling-point column (SE-30) on a molecular-weight column (silica gel) for a naphthenic crude.

chromatographic separation is followed by mass-spectrometric analysis, the interpretation of the mass spectra will be greatly facilitated by the additional information obtained from the gas-chromatographic data.

EXPERIMENTAL

For the examples given in this paper two stainless steel capillary columns were used*. All connecting tubes were 0.01″-I.D. stainless steel capillaries kept at 200°. The first column was a 100-foot 0.01″-I.D. stainless steel capillary coated with SE 30

* Handy and Harman Tube Company, Inc., Norristown, Pa.-type 316, 15 microfinish on inside, for gas chromatography.

TABLE I

EXPERIMENTAL CONDITIONS

	Column I	*Column II*
Coating	SE 30	Colloidal silica
Carrier gas	Hydrogen	Hydrogen
Detector	Barber–Colman Flame Detectors	
Inlet pressure (p.s.i.)	10	8
Air (ml min^{-1})	330	330
Flame H_2 (ml min^{-1})	15	15
Starting temperature (°C)	90°	233°
Programming rate	2 deg/min to 250°	Constant
Sample split	100/1	—
Chart speed (min^{-1})	1/8″	3″
Valve temperature (°C)	150°	

silicone gum rubber (General Electric). The second column was a 200-foot 0.03″-I.D. stainless steel capillary coated with colloidal silica (colloidal silica; Matheson, Coleman and Bell). Before they were coated, the capillary columns were cleaned by successive washings with acetone, benzene, chloroform and pentane. A 5% solution of SE 30 in normal pentane was slowly forced through the first column under nitrogen pressure. The excess SE 30 and pentane solvent were removed at room temperature, and the column was then slowly heated to 250° for bleeding overnight.

For the coating of the second column, the 35% colloidal-silica solution was used without further dilution.

The operating conditions for the analyses are listed in Table I.

APPENDIX

Separation of saturated hydrocarbons on silica-coated capillary columns

Separation of saturated hydrocarbons on silica-coated capillary columns has been previously described by SCHWARTZ *et al.*[2] for the lower molecular weight range. In order to determine whether the molecular weight is still the prevailing factor in the

TABLE II

RETENTION TIMES OF SATURATED HYDROCARBONS ON SILICA-COATED CAPILLARY

Column, 200-ft stainless steel capillary, 0.062″ OD by 0.030″ ID. Coating, silica. Carrier gas, hydrogen, 8-p.s.i. inlet pressure. Temperature: 222°.

Compound	*n*	*bp (°C)*	t_r *(mm)*
trans-decalin	10	187.3	101
n-C_{10}	10	174.1	101
cis-decalin	10	195.7	102
2-methyldecane	11	188.6	110
n-C_{11}	11	195.9	112
2,2,4,6,6-pentamethylheptane	12	175.5	113
n-C_{12}	12	216.3	127

separation on silica at higher molecular weights, some experiments were made with a few C_{10}–C_{12} saturated hydrocarbons.

The results given in Table II indicate that molecular weight is still the prevailing factor in the separation. For instance, the highly branched C_{12} compound, 2,2,4,6,6-pentamethylheptane, is eluted just after n-C_{11}, although the boiling point is twenty degrees lower.

On the SE 30 column the compounds mentioned in the Table are eluted according to boiling points. A possible exception is cis-decalin and n-C_{11}, although the boiling point of *cis*-decalin is given variously as[5,6,7] 193.3, 195 and 195.7°.

SUMMARY

A two-stage capillary gas-chromatographic method has been developed with the aim of obtaining a better separation of the saturated hydrocarbons from petroleum in the C_{10}–C_{18} molecular weight range. The method should also be applicable to other hydrocarbon fractions and to compounds other than hydrocarbons. Two capillary gas-chromatographic columns of different kinds and two flame-ionisation detectors were used. A four-way valve after the first column and before the first flame detector made it possible to force a fraction indicated by one peak of the chromatogram from the first column directly into the second one. Application of an immobile phase of different kind in the second column makes separations possible on this column that cannot be obtained by use of a single capillary column. The use of a second column which separates, say, according to molecular weight allows resolution of a mixture of compounds that have identical retention times when analysed over a "boiling-point" column.

REFERENCES

1 R. D. SCHWARTZ AND D. J. BRASSEAUX, *Anal. Chem.*, 35 (1963) 1374.
2 R. D. SCHWARTZ, D. J. BRASSEAUX AND G. R. SHOEMAKE, *Anal. Chem.*, 35 (1963) 496.
3 M. C. SIMMONS AND L. R. SNYDER, *Anal. Chem.*, 30 (1958) 32.
4 D. J. MCEWEN, *Anal. Chem.*, 36 (1964) 279.
5 N. A. LANGE, *Handbook of Chemistry*, Handbook Publishers, Sandusky, Ohio, 1946, p. 417.
6 R. C. WEAST (ed.), *Handbook of Chemistry and Physics*, The Chemical Rubber Co., Cleveland, Ohio, 1964, p. C-281.
7 S. W. FERRIS, *Handbook of hydrocarbons*, Academic Press, New York, 1955, p. 171.

Analytica Chimica Acta
Elsevier Publishing Company, Amsterdam
Printed in the Netherlands.

ETUDES THEORIQUES ET PRATIQUES SUR LA REALISATION ET LE FONCTIONNEMENT DE COLONNES PREPARATIVES DE DIAMETRE MOYEN. MODIFICATION DE LA STRUCTURE INTERNE DE CES COLONNES

MARIE-BLANCHE DIXMIER, BERNARD ROZ ET GEORGES GUIOCHON*
Société E.R.S.I., 92/Montrouge (France)

(Reçu le 1 novembre 1966)

L'emploi de la chromatographie préparative à la séparation de quantités importantes de produits est limité par deux difficultés essentielles: le volume de l'échantillon que l'on peut introduire dans la colonne, la chute d'efficacité intrinsèque des colonnes lorsque l'on cherche à augmenter leur diamètre. Cette chute entraîne la nécessité d'employer des colonnes préparatives plus longues que les colonnes analytiques correspondantes, si l'on désire obtenir le même degré de résolution. Quoique la capacité des colonnes augmente avec leur longueur, cet accroissement n'est pas proportionnel, et il en résulte une perte de rendement.

Il est important en effet de souligner qu'en chromatographie analytique, la résolution est le facteur prédominant tandis qu'en chromatographie préparative, c'est la production qui justifie l'utilisation de cette technique de séparation. La production sera caractérisée dans ce travail par la quantité d'échantillon injectée par unité de temps. Ceci suppose qu' il n'y a pas de pertes dans la colonne, ce qui est souvent le cas, et que le rendement de piégeage est total, ce qui n'est jamais réalisé. En tenant compte de ces réserves, on admet que la production réelle est proportionnelle à la quantité d'échantillon injectée.

DONNÉES EXPÉRIMENTALES

L'appareil que nous avons construit est de conception classique. Il comprend un four vertical permettant d'utiliser des colonnes de 1.50 m de long dont la température peut être maintenue constante sans que les écarts extrêmes dépassent 5° dans les points les plus proches des parois, grâce à un système de circulation d'air rapide en circuit fermé.

Le catharomètre utilisé est une cellule GowMac à filaments qui peut fonctionner avec un débit de gaz vecteur atteignant 2 l/min. Il est maintenu à température constante dans un four séparé. Les pièges sont à commande manuelle. Chacun d'eux peut être maintenu à la température la plus convenable grâce à une circulation de fluide. Le rendement de piégeage varie en effet sensiblement avec la température de piégeage.

---

* Laboratoire du Professeur L. JACQUÉ, Ecole Polytechnique, Paris, France.

La chambre de vaporisation a un volume qui dépend du diamètre des colonnes utilisées: un volume trop important de l'injecteur est une source de perte d'efficacité supplémentaire pour les colonnes de petit diamètre dans lesquelles on ne peut pas injecter de gros échantillons. Pour les colonnes de fort diamètre, il faut un injecteur adapté au volume des échantillons utilisés. Les injecteurs utilisés ont des volumes utiles respectifs de 10, 20 et 40 ml. Pour les produits fragiles, incapables de supporter les températures élevées de l'injecteur nécessaires pour une vaporisation rapide de l'échantillon, il est préférable d'utiliser une chambre de vaporisation placée en parallèle avec le circuit normal du gaz vecteur et pouvant être introduite dans ce circuit grâce à deux vannes pneumatiques pouvant fonctionner à 300°. On peut ainsi obtenir une volatilisation complète de l'échantillon à une température voisine de celle de la colonne sans le surchauffer, mais le volume qu'il occupe à l'injection est égal à celui de la chambre qui ne doit donc pas être trop grande.

Un clapet anti-retour placé en amont de l'injecteur empêche tout écoulement vers l'amont des vapeurs d'échantillon au moment de l'injection.

Les colonnes utilisées sont des éléments droits de 100 cm de long, fermés à chaque extrémité par un disque en métal fritté de grande perméabilité, serti dans le tube. Les colonnes sont réunies entre elles et avec l'appareil par des tubes de diamètre intérieur plus faible (4 mm pour les colonnes de 20 mm, 8 mm pour celles de 40 mm) reliés aux colonnes par des éléments coniques afin d'éviter les ruptures brutales de section provoquant des tourbillons, sources de perte d'efficacité.

Les colonnes étudiées sont remplies de poudre de Chromosorb P 250–315 μ ou 315–400 μ imprégnée à 20% de caoutchouc silicone SE 30. La méthode de remplissage utilisée est celle décrite par BAYER[1]. Elle donne d'excellents résultats bien reproductibles. On a étudié essentiellement les conditions de séparation du mélange de *cis*- et *trans*-décaline entre 150 et 210°. Ce problème constitue un bon exemple des séparations nécessaires dans la pratique.

EFFICACITÉ ET PRODUCTION

L'efficacité intrinsèque d'une colonne est par définition le nombre de plateaux théoriques mesuré sur le pic du composé intéressant, lorsque l'on injecte une très

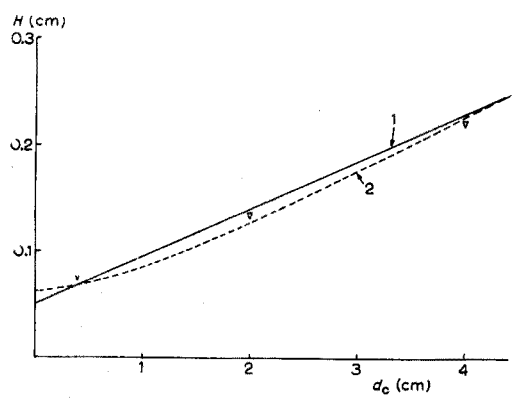

Fig. 1. Variation de l'efficacité intrinsèque avec le diamètre. (1) éqn. 1; (2) éqn. 2bis.

faible quantité de produit, le débit du gaz vecteur étant à sa valeur optimale. Cette efficacité décroît quand le diamètre de la colonne augmente, ainsi qu'on peut le voir sur la Fig. 1. Les différentes colonnes sont faites avec la même phase stationnaire et des tubes de diamètre croissant, remplis de la même façon. La relation linéaire entre H (HEPT) pour une charge nulle et d_c (diamètre de la colonne) est approximativement dans le domaine de diamètres étudié:

$$H = H_0 (1 + \beta d_c) = 0.05 (1 + 0.90 d_c) \quad (1)$$

Cette relation ne saurait être extrapolée vers les forts diamètres. Certains résultats expérimentaux[2] tendent en effet à montrer qu'au-delà d'un diamètre d'environ 5 cm, l'efficacité ne varie plus que très faiblement avec d_c.

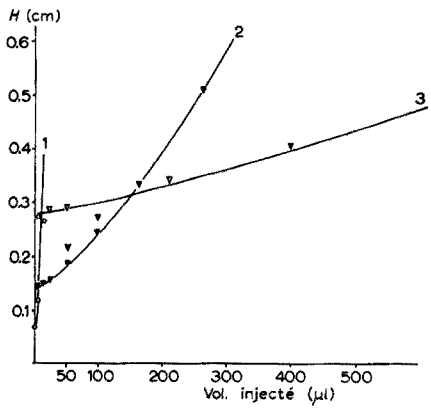

Fig. 2. Variation de $\mathcal{H}$ avec la quantité d'échantillon injecté pour trois colonnes de différents diamètres: (1), ∅ 4 mm; (2), ∅ 20 mm; (3), ∅ 40 mm.*

Mais l'efficacité nominale n'est qu'une des caractéristiques d'une colonne préparative. Son aptitude à se laisser surcharger est sa qualité la plus importante. La Fig. 2 montre la variation d'efficacité avec le volume de l'échantillon injecté. L'efficacité est caractérisée par le facteur:

$$\mathcal{H} = W_L^2/16L$$

dans lequel W_L représente la largeur de la bande d'élution du soluté dans la veine gazeuse sortant de la colonne de longueur L. W_L est relié à la largeur du pic W_t mesurée en unité de temps sur le chromatogramme par la relation:

$$W_L/L = W_t/t \quad \text{ou} \quad W_L = W_t\bar{u}$$

($\bar{u}$: vitesse linéaire moyenne du gaz vecteur, t_R: temps de rétention).

Le facteur $\mathcal{H}$ est égal à la hauteur équivalente à un plateau théorique H lorsque le pic est symétrique. Aux fortes charges, toutefois, le pic cesse d'être symétrique en raison de la trainée apparaissant à l'injection et surtout de la courbure de l'isotherme

* Pour la colonne de 4 cm de diamètre, la différence entre H (Fig. 1) et $\mathcal{H}_0$ (Fig. 2) vient de ce que les courbes d'efficacité et de charge ont été effectuées sur 2 chromatographes différents (contribution d'appareillage).

de dissolution. Dans ce cas, le pic n'étant plus gaussien, il n'est plus possible de parler ni d'écart-type ni de HETP, d'où la définition donnée ci-dessus. $\mathcal{H}$ permet de suivre la perte de performances des colonnes lorsqu'elles sont surchargées (Fig. 2). Il ne permet toutefois pas, comme le fait H pour les pics symétriques, de résoudre les problèmes de résolution et de calculer les instants où doivent se faire les commutations de piégeage. Des expressions plus complexes, telle l'impureté de bande[3] le permettent mais elles sont si complexes qu'elles ne se prêtent qu'à des calculs numériques sur des cas expérimentaux précis et non à des calculs théoriques.

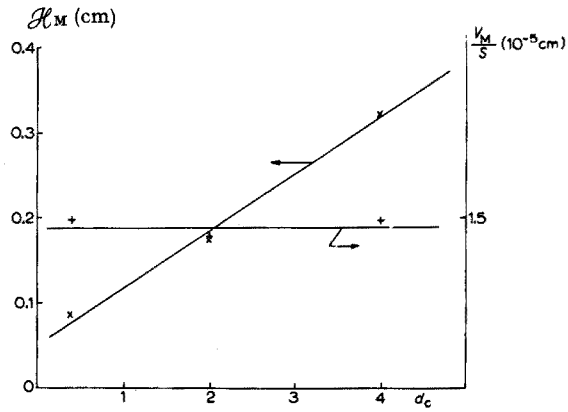

Fig. 3. Variation de la charge maximale admissible V_M par unité de section de la colonne et de l'efficacité correspondante, avec le diamètre de la colonne.

On peut définir avec BAYER[1,4] la charge maximale admissible V_M comme celle pour laquelle l'efficacité a diminué de 20%. Quoique cette définition soit arbitraire, elle peut être utile pour comparer entre elles des colonnes faites avec des phases différentes. La comparaison de 3 colonnes de même phase et de diamètres croissants montre (Fig. 3) que la charge admissible est proportionnelle à la section de la colonne, c'est-à-dire que la charge admissible par unité de section est constante, d'autre part que la valeur corerspondante de $\mathcal{H}(\mathcal{H}_M)$ croît linéairement avec le diamètre de la colonne, comme H (Fig. 1).

Parallèlement, la vitesse optimale du gaz vecteur décroît lorsqu'on augmente le diamètre des colonnes, ce qui traduit l'existence d'une contribution aux termes de résistance au transfert de masse en phase gazeuse par diffusion radiale qui est proportionnelle au carré du diamètre de la colonne. En négligeant les termes correctifs de décompression du gaz vecteur et le terme de couplage éventuel[5,6], l'équation donnant la valeur de H peut s'écrire:

$$H = B/u_0 + (C_g + C_l + \lambda d_c^2)u_0 \qquad (2)$$

La valeur minimum de H est alors donnée par:

$$H_{min} = 2\sqrt{B(C_g + C_l + \lambda d_c^2)}$$

D'après cette équation, H_{min} n'augmente pas linéairement avec d_c sauf aux très grandes valeurs. Si toutefois on prend pour C_g et C_l la valeur très plausible de 1 msec.,

pour D_g la valeur de 0.4 cm²/sec et pour γ ($B = 2\gamma D_g$) la valeur de 0.7*, les résults de la Fig. 1 conduisent à la valeur $\lambda = 1.32 \cdot 10^{-3}$. L'équation:

$$H_{min} = 2\sqrt{5.6\,(2 + 1.32\,d_c^2) \cdot 10^{-2}} \qquad (2 \text{ bis})$$

est celle de la courbe tracée en pointillé sur la Fig. 1. Compte tenu de leur précision (l'écart-type de la mesure de H est 3–4%), les résultats expérimentaux sont donc en accord aussi bien avec l'éqn. (1) qu'avec les éqns. (2) et (2 bis). Nous utiliserons par la suite l'éqn. (1).

Le terme supplémentaire λd_c^2 étant du à la résistance aux transferts de masse par diffusion radiale au travers de la colonne, λ est inversement proportionnel à D_g. Il en résulte et il faut le souligner que *la contribution C_1 étant négligeable dans les colonnes préparatives, H_{min} est indépendant du coefficient de diffusion, donc de la nature du gaz vecteur. Par contre, la vitesse optimale du gaz vecteur est proportionnelle à D_g.* (Les résultats expérimentaux sont en accord avec l'expérience). L'emploi de l'hydrogène ou de l'hélium à la place de l'azote permet donc, tous autres paramètres restant constants par ailleurs, de tripler environ la productivité d'une unité. Ce résultat justifie, c'est-à-dire permet d'amortir, une unité de recyclage des gaz ou les dispositifs de sécurité nécessaires à l'emploi de l'hydrogène.

La vitesse optimale est donnée par:

$$u_0 = \sqrt{B/C} = \sqrt{560/(2 + 1.32\,d_c^2)}$$

et pratiquement pour des diamètres supérieurs à 2 cm, on aura:

$$u_0 = C_1/(1 + \beta d_c) \qquad (3)$$

C_1 étant une constante.

Ce qui est également en bon accord avec les rêsultats expérimentaux.

La baisse de productivité relative des colonnes préparatives conduit à utiliser des colonnes plus étroites et plus longues que ne le voudrait l'extrapolation à partir de colonnes analytiques compte tenu des quantités à séparer. On doit donc accepter des durées accrues d'analyse. Ceci ne doit cependant pas être poussé à l'extrême: des durées d'analyse longues pouvant conduire à des taux de décomposition importants des produits thermolabiles. De plus, la charge n'augmente pas proportionellement à la longueur de la colonne; la durée d'analyse augmente plus vite que la longueur de la colonne dès que la perte de charge devient appréciable (t_R augmente proportionnellement à $L^{3/2}$ si la perte de charge dépasse 2.5 kg/cm² environ). Enfin, si pour diminuer la perte de charge on utilise des particules trop grosses, on observe une diminution sensible correspondante de la vitesse optimale même si la contribution à l'accroissement de H est négligeable pour des colonnes surchargées.

On conçoit donc intuitivement l'existence d'un compromis que des considérations théoriques simples peuvent aider à chercher. On peut se poser trois problèmes intéressants: comment la productivité d'une installation varie-t-elle lorsque le diamètre de la colonne augmente? étant donné une masse de phase stationnaire, comment construire la colonne ayant la plus grande production? et enfin comment séparer le plus vite possible une masse donnée de mélange? Ces trois problèmes sont liés, mais le problème fondamental du coût d'une séparation par chromatographie préparative

* Valeurs également très proches de la réalité.

peut difficilement être traité d'une façon générale. Il dépendra à la fois du diamètre de la colonne et de sa longueur (investissements), des paramètres déterminant les frais de fonctionnement et de la production. L'étude des trois problèmes posés permet néanmoins d'apporter des éléments importants et de caractère général à la solution du problème économique.

Nous supposerons qu'il s'agit de séparer un mélange donné sur une phase et à une température qui resteront les mêmes pour toutes les colonnes. D'après la formule donnant la résolution:

$$R = \frac{\sqrt{N}}{4} \frac{\alpha - 1}{\alpha} \frac{k'}{1 + k'} \tag{4}$$

α: rétention relative $= t'_{R_1}/t'_{R_2}$; k': facteur de capacité de la colonne $= (t_R - t_{R_0})/t_{R_0}$.

Il faudra donc obtenir sur chaque colonne une même efficacité pour obtenir la même résolution. Nous supposerons que la production maximale est obtenue sur chaque colonne pour une même valeur de la résolution (nettement inférieure à 1.0) qui peut être calculée lorsque les deux pics sont gaussiens. Le pourcentage de la fraction à recycler dépend des concentrations relatives des produits dans le mélange et du degré de pureté recherché.

Cette résolution étant choisie, N résulte de l'éqn. (4) et la longueur de la colonne est donnée par:

$$L = NH \tag{5}$$

La durée d'une analyse est alors:

$$t_R = \frac{(1 + k')\, L}{\bar{u}} = \frac{(1 + k')\, NH}{\bar{u}} \tag{6}$$

Nous supposerons, ce qui est vérifié en chromatographie préparative où l'on emploie des colonnes relativement courtes (2–5 m) et des particules de granulométrie assez grande (250–315 μ par exemple), que la perte de charge est assez faible pour que l'on puisse écrire:

$$\bar{u} \simeq u_0 \tag{7}$$

H étant donné par l'éqn. (1), on aura:

$$t_R = (1 + k')\, N\, (H_0/C_1)\, (1 + \beta d_c)^2 \tag{8}$$

D'autre part, la quantité de mélange à séparer que l'on peut injecter dans la colonne est proportionnelle à la section de la colonne et à une certaine puissance de la longueur, comprise entre 1/2 et 1 et généralement voisine de la première valeur:

$$V_M = C_2 \cdot d_c^2 \cdot [NH]^\omega \tag{9}$$

$$V_M = C_2 \cdot d_c^2\, [NH_0\, (1 + \beta d_c)]^\omega \tag{9 bis}$$

La productivité est donc donnée par l'expression:

$$P = \frac{V_M}{t_R} = \frac{C_3 d_c^2\, [NH_0\, (1 + \beta d_c)]^\omega}{(1 + k')\, NH_0\, (1 + \beta d_c)^2}$$

$$P = \frac{C_3\, (NH_0)^{\omega - 1}}{1 + k'} \cdot d_c^2\, (1 + \beta d_c)^{\omega - 2} = P_1 \cdot P_2 \tag{10}$$

La productivité est le produit de deux termes dont l'un est indépendant de d_c et dont les variations de l'autre (P_2) avec d_c sont données Fig. 4 pour différentes valeurs de ω et en prenant pour β la valeur numérique obtenue ci-dessus, soit 0.90. On voit que la productivité augmente indéfiniment comme d_c^{ω} lorsque le diamètre de la colonne augmente. Dans le cas le plus favorable où $\omega = 1$, on est encore loin de l'accroissement proportionnel à d_c^2, que l'on aurait pu escompter de colonnes préparatives dont l'efficacité serait indépendante du diamètre ($\beta = 0$).

Ce résultat nous permet de résoudre le troisième problème posé plus haut: la séparation la plus rapide d'une masse donnée d'échantillon sera effectuée en un cycle avec la colonne ayant un diamètre tel que la masse à séparer représente le volume maximal admissible. D'un point de vue économique, cette installation serait trop importante, les investissements n'étant pas justifiés par une telle production. D'où l'intérêt du second problème posé: étant donné une certaine quantité de phase stationnaire, quel diamètre et quelle longueur choisir pour la colonne préparative permettant la meilleure productivité?

Soit W le volume de phase dont on dispose:

$$W = (\pi d_c^2/4)\, L \qquad (11)$$

En raison de la nécessité d'obtenir une résolution minimale, la colonne doit

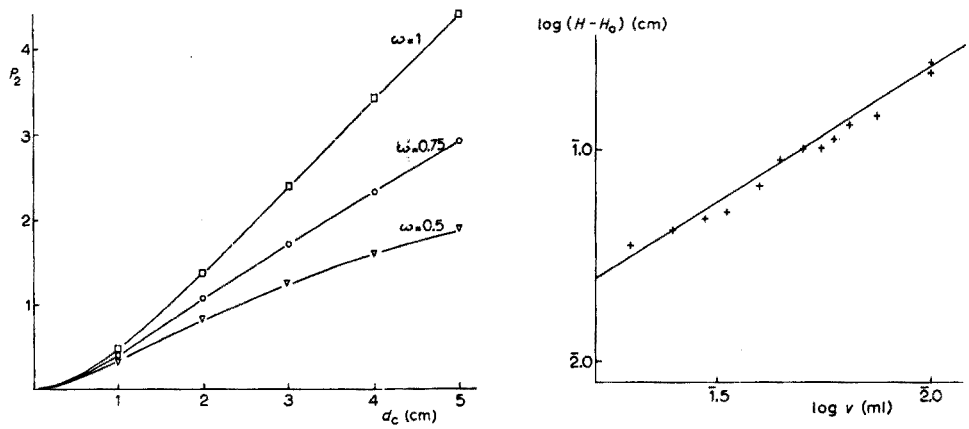

Fig. 4. Variation de la productivité avec le diamètre de la colonne pour différentes valeurs de ω.

Fig. 5. Variation de l'efficacité avec la charge de la colonne (colonne de 4 cm de diamètre, 2 m de long, *cis*-décaline à 150°, 1380 ml/min H_0).

avoir un nombre de plateaux au moins égal à une certaine valeur N' pour une charge nulle. Sa longueur doit donc dépasser un seuil critique:

$$L \geqslant L' \qquad L' = N'H' = N'H_0\,(1 + \beta d_c') \qquad (12)$$

La colonne ayant cette longueur permet d'obtenir juste la résolution nécessaire, avec une charge très faible. Il faudra donc toujours utiliser une colonne plus efficace, donc plus longue et plus étroite, pour pouvoir la surcharger. Le diamètre critique maximal est obtenu en combinant les éqns. (11) et (12):

$$W = \tfrac{1}{4}\pi/4\ d_c'^2\ N' H_0\ (1 + \beta d_c') \tag{13}$$

Etant donné la valeur de β, pour des valeurs de d_c supérieures à 1 cm, le diamètre critique n'augmente guère que proportionnellement à $W^{1/3}$.

Lorsque l'on prépare des colonnes de diamètre plus étroit, on peut injecter des quantités d'échantillon plus importantes, de façon à ramener l'efficacité de la colonne à une valeur voisine de N'. Ainsi que le montre la Fig. 5, l'efficacité d'une colonne diminue lorsque le volume injecté augmente, la relation étant:

$$H = H_1 + \alpha(V)^\delta \tag{14}$$

H_1 étant l'efficacité obtenue pour une charge nulle.

Pour des colonnes de 4 cm de diamètre, il a été vérifié expérimentalement que: $\alpha \simeq 0.2$; $\delta \simeq 1.2$. Pour des colonnes de 2 cm de diamètre, on trouve également $\delta \simeq 1.2$ (cf. Fig. 7).

En tenant compte, comme nous l'avons vu, que la charge est admissible proportionnelle au carré du diamètre de la colonne (éqn. 9), l'expression générale sera donc:

$$H = H_1 + a(V/d_c^2)^{1.2}$$

Par identification avec l'expression (14), H_1 étant donné par (1), on obtient l'expression suivante:

$$H = H_0\ (1 + \beta d_c) + 5.6\ (V/d_c^2)^{1.2} \tag{15}$$

La charge V doit être telle que l'efficacité de la colonne soit juste égale à N' eqn. (12), H éqn. (15) étant la nouvelle valeur de H'.

Le diamètre d_c est donc donné par l'équation:

$$4\ W/\pi d_c^2 = N'\ [H^0(1 + \beta d_c) + 5.6(V/d_c^2)]^{1.2}$$

ou:

$$4\ W/\pi N' = H_0\ d_c^2(1 + \beta d_c) + 5.6\ V^{1.2}/d_c^{0.4} \tag{16}$$

On a tracé sur la Fig. 6 le faisceau de courbes:

$$y = H_0\ d_c^2\ (1 + \beta d_c) + 5.6\ V^{1.2}/d_c^{0.4} \tag{16 bis}$$

soit ici:

$$y = 0.05\ d_c^2\ (1 + 0.90 d_c) + 5.6\ V^{1.2}/d_c^{0.4}$$

d_c étant la variable et V un paramètre.

Si la droite horizontale $y = 4\ W/\pi N'$, déterminée par le volume de phase disponible et le nombre de plateaux théoriques nécessaires coupe une de ces courbes en deux points A et B, cela veut dire qu'avec la charge V correspondante, toute colonne de diamètre compris entre d_c (A) et d_c(B) donne une efficacité supérieure à N'. Les colonnes de diamètre inférieur à d_c(A) ou supérieur à d_c(B) ne sont pas utilisables, les premières parce que trop surchargées, les secondes parce que de trop grand diamètre pour être assez efficaces.

Les meilleures conditions correspondront au point de contact de l'horizontale avec celle des courbes du faisceau qui lui est tangente. La colonne de diamètre correspondant admettra la charge maximale. Par exemple, si l'on dispose de 20 l de phase et que l'on veut effectuer une séparation nécessitant 2500 plateaux, on a $y = 4\ W/\pi N' = 10.2$.

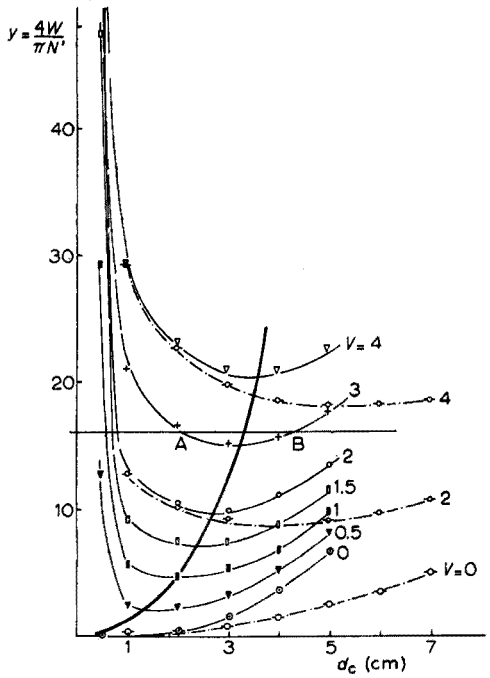

Fig. 6. Détermination du diamètre optimal lorsque le volume de phase disponible est fixé: W et V sont exprimés en cm³. (—) le lieu géométrique des minima des courbes du faisceau; (—·—) correspondent à des colonnes hypothétiques pour lesquelles H_1 (éqn. 14) ne dépendrait pas du diamètre mais resterait égal à 0.1 cm.

Le diamètre optimal sera 2.8 cm et la charge correspondante de 2.2 cm³. La longueur de la colonne sera de 32.5 m et la valeur de $\mathcal{H}$ de 1.3 cm. Avec un volume de phase de 5 l et pour une séparation ne demandant que 1000 plateaux, on obtient un diamètre de 2.3 cm et une charge d'environ 1.3 cm³. Ces valeurs correspondent à des colonnes relativement longues et étroites et résultent de la chute rapide de l'efficacité quand augmentent le diamètre de la colonne et surtout la charge introduite.

A titre indicatif, on a représenté Fig. 6 les courbes:

$$y = H_0\, d_c^2 + 5.6\, V^{1.2}/d_c^{0.4}$$

que l'on obtiendrait avec des colonnes préparatives ayant une efficacité indépendante du diamètre et en prenant pour H_0 la valeur réaliste de 0.1 cm. Dans le cas traité ci-dessus (20 l de phase, $N' = 2500$), on trouve un diamètre de 4.5 cm et un échantillon de 2.3 cm³.

Le résultat obtenu est qualitativement le même et n'est quantitativement guère modifié si l'on fait intervenir la productivité et non plus la seule charge introduite, mais les calculs sont compliqués par la nécessité de tenir compte de la compressibilité du gaz vecteur.

En conclusion, on remarquera que ce qui limite la productivité des colonnes préparatives, plus encore que l'augmentation de H avec leur diametre, c'est la perte tres rapide de l'efficacité des colonnes lorsque le volume d'échantillon introduit augmente.

Il convient donc d'étudier cette cause de perte de productivité et de chercher à l'éliminer.

FACTEURS INFLUENCANT LA PERTE D'EFFICACITÉ DES COLONNES PRÉPARATIVES

a) Pertes dues à l'augmentation du diamétre

La perte d'efficacité observée pour les colonnes de diamètre moyen (1–4 cm) est communément attribuée aux hétérogénéités du remplissage conduisant à des variations systématiques de la vitesse locale du gaz vecteur dans l'ensemble de la section droite de la colonne. Des fluctuations à plus faible échelle ou des variations de perméabilité sur la longueur de la colonne auraient un effet trop faible. GIDDINGS[7] a étudié théoriquement les effets d'une fluctuation systématique de la vitesse du gaz vecteur due à une ségrégation des particules du remplissage, les plus lourdes, c'est-à-dire pratiquement les plus grosses ayant tendance à s'accumuler près des parois, et provoquant ainsi un gradient radial de perméabilité. Aucun autre phénomène physique n'ayant pu être suggéré pour expliquer l'augmentation de H avec d_c, cette explication est communément admise et les bons résultats obtenus avec la méthode de remplissage décrite par BAYER[1] sont attribués au fait que les vibrations axiales appliquées à la colonne tendraient à provoquer une ségrégation telle que les grains lourds se déplacent vers les extrémités de la colonne, la variation longitudinale de perméabilité qui en résulte étant beaucoup moins nocive.

Il faut reconnaître que peu d'évidences expérimentales sont venues confirmer cette hypothèse pourtant généralement admise. GIDDINGS[7] suggérait que les effets de la ségrégation sur le profil de vitesse pourraient être compensés par l'emploi d'une phase mixte, composée de petites et de grosses particules, les secondes étant plus imprégnées de phase que les autres et l'écart entre les granulométries moyennes étant bien sûr réduit. Cette expérience, quoique simple et intéressante, ne semble pas avoir été faite[8]. Il est vrai que les difficultés expérimentales sont considérables, l'expérience ayant prouvé que, même pour des phases peu volatiles, les transferts de phase liquide dans une colonne sont assez grands pour provoquer une homogénéisation rapide. Les arguments tirés de l'augmentation de l'efficacité des colonnes obtenues, lorsqu'on resserre la granulométrie des supports utilisés, ne sont pas convaincants. La variation de H avec le diamètre (éqn. 1) est un argument plus fort mais non décisif.

Le seul travail expérimental comportant de mesures de vitesse du gaz vecteur est celui de HUYTEN, VAN BEERSUM ET RIJNDERS[9] qui ont mesuré la vitesse moyenne du gaz dans les 4 secteurs concentriques (un circulaire, 3 annulaires) de même aire découpés dans la section de sortie d'une colonne de 7.5 cm. Il résulte curieusement que les colonnes donnant le plus grand nombre de plateaux théoriques sont celles pour lesquelles l'écart de vitesse est le plus grand (il atteint 50% entre les vitesses moyennes des sections centrales et périphériques) et les transferts de masse par diffusion radiale les plus lents, sans qu'il y ait une corrélation nette entre efficacité et vitesse de transfert radial.

Ces résultats seraient en assez bon accord avec des résultats récents[2] montrant qu'aux diamètres supérieurs de 5 ou 6 cm, H n'augmente plus guère avec d_c: l'équilibre par échange radial entre les différentes fractions d'une section droite ne se faisant pratiquement plus, la colonne fonctionnerait en fait comme un faisceau parallèle de colonnes plus étroites.

On voit la complexité du phénomène et que l'existence d'un profil de vitesse dans la colonne pourrait n'être plus très dommageable si la diffusion n'en vient plus corriger les effets. L'extrapolation vers les grands diamètres est certainement beaucoup plus intéressante que ne le laisserait prévoir la discussion ci-dessus, valable seulement pour les colonnes de diamètre inférieur à 5 cm environ; dans l'état actuel de la technique, il est plausible que les colonnes de diamètre moyen constitueraient un domaine intermédiaire où les performances seraient nettement moins bonnes que dans les domaines des faibles ou des très forts diamètres, en raison de la forme de l'équation régissant la diffusion ($t_{dif} = d_c^2/8D_g$).

b) Pertes dues a l'augmentation de la charge

Ces pertes sont dues à la superposition de quatre phénomènes principaux et l'interprétation de l'effet résultant est très complexe:

1) si le volume occupé par la masse d'échantillon vaporisée n'est plus négligeable devant le volume gazeux intrinsèque de la colonne, le pic s'élargit. Ce phénomène est assez bien connu à présent[10].

2) L'augmentation de la pression partielle de l'échantillon dans le gaz vecteur. Cette pression partielle est limitée par la pression de vapeur saturante, mais bien avant que cette valeur ne soit atteinte, l'isotherme de solubilité cesse d'être linéaire et par conséquent les pics se déforment d'une façon de plus en plus prononcée. *Il est donc d'importance primordiale de choisir*, dans la mesure du possible, *des phases stationnaires pour lesquelles le domaine de concentration dans lequel l'isotherme de solubilité est linéaire soit le plus grand possible.*

Les différences de charges maximales admissibles ou de productivité trouvées dans la littérature pour divers couples soluté–phase stationnaire peuvent le plus souvent être attribuées à la différence de forme des isothermes: l'isotherme de solubilité du n-pentane ou du benzène dans le phtalate de didécyle reste linéaire pour des valeurs du rapport de la pression partielle à la pression de vapeur saturante (P/P_0) bien plus grande que l'isotherme de solubilité de la cis-décaline dans le SE 30.

L'étude détaillée de ce problème fera l'objet d'une publication ultérieure.

3) La volatilisation d'échantillons liquides importants est loin d'être instantanée en raison de la lenteur des transferts thermiques. Même avec une chambre de vaporisation chauffée à une température supérieure de plusieurs dizaines de degrés au-dessus de la température de la colonne, ce qui est préjudiciable à la stabilité thermique de l'échantillon, on obtient des profils de concentration à l'injection qui trainent fortement, ce qui provoque des trainées plus ou moins importantes des pics.

L'injection sous forme d'un signal carré, pendant laquelle la pression partielle du soluté est constante et forcément inférieure à sa pression de vapeur saturante, donne des résultats satisfaisants[11].

4) Un signal de pression et un signal thermique accompagnent l'élution d'un pic. Ces signaux sont d'autant plus intenses que la concentration est plus grande. Le signal thermique proportionnel à la dérivé du signal de concentration tend à provoquer l'élargissement des pics. Ce signal devient important dans les colonnes préparatives qui tendent à fonctionner en adiabatique, l'équilibre thermique radial étant très lent puisque le remplissage usuel est un excellent réfractaire.

Pour préparer des colonnes préparatives efficaces en charge, il faut d'abord préparer des colonnes ayant une efficacité aussi grande que possible à charge nulle.

La Fig. 7 montre que, contrairement à ce qu'on pourrait croire, les colonnes les plus efficaces aux fortes charges sont aussi les plus efficaces à charge nulle, l'écart ayant même tendance à s'accroître lorsque la charge augmente. Après leur remplissage, les cinq colonnes décrites ont subi les trois premières un conditionnement de 36 h à 225°, les deux dernières un conditionnement de 60 h à 300°. Elles diffèrent en outre par leur remplissage. On voit que toute amélioration des méthodes de remplissage se traduit par un accroissement sensible de productivité.

L'effet de la courbure de l'isotherme aux fortes pressions partielles peut être limité en utilisant de très fortes teneurs en phase stationnaire au début de la colonne: une grande partie de l'échantillon peut se dissoudre et la fraction restant en phase gazeuse est d'autant plus faible. Ceci conduit cependant à augmenter le temps de

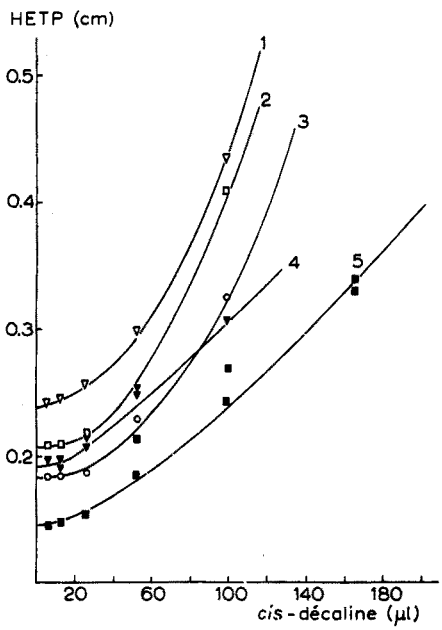

Fig. 7. Variation de H (cm) avec le volume de *cis*-décaline injecté (μl). Colonnes 2 cm de diamètre, 1 m de long, 20% SE30 sur Chrom. P. $T = 150°$. Valeur de H_1 et la valeur de δ dans l'équation $H = H_1 + \alpha V^{\delta}$: (1), $H_1 = 0.24$ cm; $\delta = 1.7$; (2), $H_1 = 0.21$ cm; $\delta = 2.2$; (3), $H_1 = 0.18$ cm; $\delta = 2.2$; (4), $H_1 = 0.19$ cm; $\delta = 1.2$; (5), $H_1 = 0.14$ cm; $\delta = 1.5$.

rétention. Pour limiter cet accroissement, on peut réduire ensuite la teneur en phase stationnaire puisque l'élution d'un pic s'accompagne d'une dilution progressive dans le gaz vecteur. Il est malaisé de conserver des trains de colonnes où un gradient important de concentration existe, car il se produit une homogénéisation progressive de la phase résultant des transferts par le gaz vecteur et des migrations provoquées par les gros échantillons[12]. Toutefois, un train constitué d'une colonne de 1 m remplie de phase imprégnée à 35%, d'une colonne de 1 m remplie de phase imprégnée à 20% et d'une ou plusieurs colonnes de 1 m remplie de phase imprégnée à 10% doit donner des résultats satisfaisants.

MODIFICATION DE LA STRUCTURE INTERNE DES COLONNES

Pour limiter les sources de pertes d'efficacité attribuées aux hétérogénéités du remplissage, on a cherché à utiliser des colonnes de section non circulaire (colonnes à secteur, en trèfle, colonnes annulaires). Ces dispositifs donnent de bons résultats mais ne sont pas extrapolables pour être utilisés avec des colonnes de grands diamètres. Le dispositif que nous avons utilisé peut être adapté à des colonnes de n'importe quel diamètre[13].

Nous avons introduit dans les colonnes un faisceau coaxial de tiges régulièrement espacées (cf. Fig. 8). Pour une colonne de 4 cm de diamètre, nous avons utilisé 13 tiges de 0.3 cm de diamètre. La nécessité de maintenir les tiges bien parallèles à l'axe empêche d'utiliser des tiges plus fines. 4 tiges suffiraient pour une colonne de 2 cm de diamètre; il en faudrait à peu près 80 pour une colonne de 10 cm. Les colonnes sont remplies de la même façon que les colonnes classiques.

La surface de contact du remplissage est doublée dans le dispositif adopté tandis que la section utile est diminuée de 8%. L'écart maximum d'un point du remplissage avec une paroi est de 0.4 cm environ. Si l'on admet l'hypothèse expliquant la perte d'efficacité des colonnes préparatives par l'apparition d'un gradient radial de perméabilité dû à la ségrégation des particules lors du remplissage, on devrait de la sorte améliorer sensiblement l'efficacité des colonnes; sans être considérable, le gain est

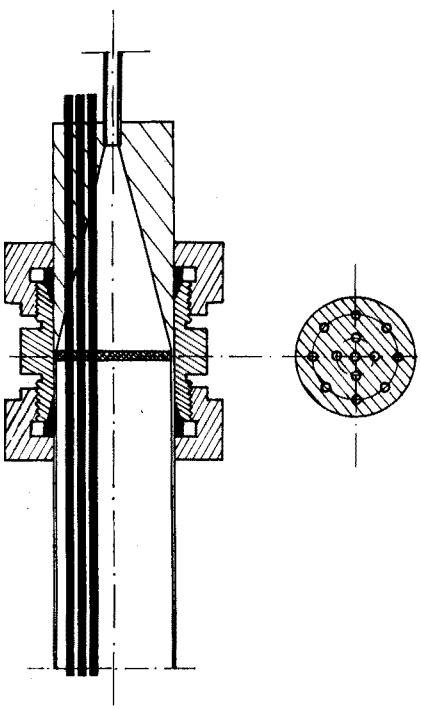

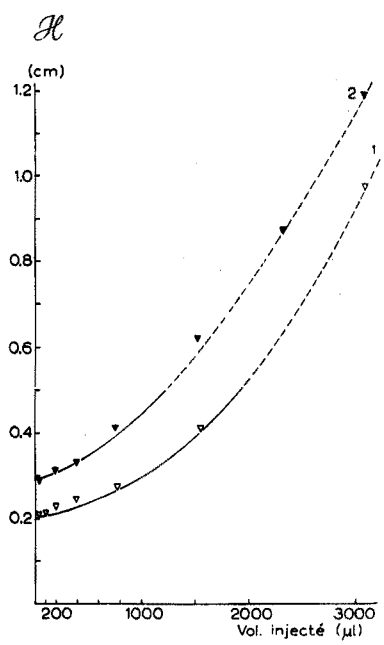

Fig. 8. Coupe à l'extrémité d'une colonne modifiée.

Fig. 9. Variation de $\mathscr{H}$ avec la quantité injectée pour deux colonnes de 2 m de long, l'une modifiée (1), l'autre classique (2), identiques par ailleurs, Chrom. P. à 20% SE 30, *cis*-décaline, $T = 192°$.

sensible puisque l'on obtient d'une façon très reproductible une valeur de H égale à 0.19 cm pour un échantillon de 40 μl de *cis*-décaline à 150° (moyenne de 3 colonnes).

Ce résultat expérimental semble apporter une réponse partielle à la contribution des effets de paroi dans l'élargissement des pics à l'échelle préparative: l'augmentation de 100% de la surface des parois n'améliore que de 20% au maximum l'efficacité intrinsèque des colonnes de 4 cm de diamètre.

Or, l'écart maximal entre un point du remplissage et une paroi est dans les colonnes que nous avons utilisées de l'ordre de grandeur de celui que l'on obtient dans les colonnes analytiques (environ 0.8 cm). Si la non-uniformité du régime gazeux dans les colonnes préparatives était, comme il est couramment admis, la cause essentielle de perte d'efficacité, on aurait dû observer, pour la colonne modifiée, une efficacité environ double, ce qui n'est pas le cas. Ceci tendrait donc à confirmer les hypothèses ci-dessus: dans les colonnes de grands diamètres, les conséquences de l'effet de paroi et du gradient de vitesse résultant sont d'autant moins importantes que le diamètre est plus grand; dans les colonnes de moyen diamètre, l'élargissement du pic est notablement accentué par la transition entre un équilibre par diffusion radiale quasi instantanée (colonnes analytiques) et un déséquilibre complet entre les éléments les plus éloignés d'une section droite dans les colonnes de très grands diamètres (10 cm et plus).

La Fig. 9 montre la variation de H avec la quantité de *cis*-décaline injectée pour deux colonnes de 2 m de long, à 192°, l'une modifiée, l'autre classique. Les courbes en pointillé correspondent à des pics plus ou moins déformés. Tant que la courbe reste en trait plein, les pics sont assez symétriques pour que l'on puisse parler de HETP. Pour obtenir une bonne séparation d'un mélange à 50–50% de *cis*- et *trans*-décaline, il faut environ 500 plateaux (SE 30 à 192°) soit pour 2 m de colonnes $H = 0.4$ cm. La quantité injectée en *cis*-décaline sera de 0.8 cm^3 sur la colonne classique, de 1.55 cm^3 sur la colonne modifiée pour laquelle le temps de rétention est 8% plus faible: la production est donc plus que doublée, ce qui montre l'intérêt des résultats obtenus.

Les courbes de charge obtenues (Fig. 9) sont parallèles. Ceci montre que dans le cas étudié les effets dus au volume de l'échantillon et à la courbure de l'isotherme de solubilité sont prédominants. Le remplacement de tiges de cuivre de conductibilité thermique élevée par rapport à celle du remplissage, par des tubes de laiton ou de quartz, ne modifie pas l'allure des courbes de charge. Ceci montre que le signal thermique accompagnant la bande d'élution est peu atténué par la présence de conducteurs thermiques parallèles à l'axe, ou que son effet dans les conditions décrites est négligeable.

La présence de tiges parallèles à l'axe offre l'avantage de permettre le chauffage interne de la colonne. On peut ainsi éventuellement programmer la température de colonnes de grand diamètre sans voir apparaître de gradients thermiques radiaux importants. On peut également, et c'est beaucoup plus important pour les applications industrielles, chauffer rapidement à la température de fonctionnement une grande masse de réfractaire dans laquelle les échanges de température sont normalement très lents. La présence de conducteurs thermiques axiaux modère également les gradients thermiques possibles.

On peut envisager plusieurs moyens d'utiliser les tiges axiales pour chauffer la colonne (chauffage par induction, utilisation de ces tiges comme conducteur ou emploi de tiges contenant des résistances incorporées) mais il est beaucoup plus facile et

moins dangereux pour le remplissage d'utiliser des tubes connectés à l'extérieur, à chaque raccord entre colonnes, et d'y faire circuler une fluide maintenu à température constante.

CONCLUSION

La réalisation de colonnes préparatives ayant des capacités de quelques centimètres cubes, si utiles pour les laboratoires de chimie organique et de biochimie, a fait ces dernières années des progrès lents et peu spectaculaires comparés à ceux obtenus en chromatographie analytique, mais qui en font cependant, dès à présent, ou outil souple et pratique, utilisable sans poser trop de problèmes technologiques complexes. Une unité de chromatographie préparative doit cependant faire l'objet d'une étude préalable en chromatographie analytique afin de calculer les paramètres permettant d'obtenir la productivité maximales.

Les auteurs remercient MM. GUY PREAU et LOUIS GOUNOT pour leur collaboration dans la réalisation de l'appareil.

RÉSUMÉ

Les auteurs discutent l'influence de différents paramètres sur l'efficacité et la productivité des colonnes préparatives utilisées en chromatographie en phase gazeuse. L'expérience montre que la hauteur équivalente à un plateau théorique (HEPT) augmente presque proportionnellement au diamètre de la colonne de 1–5 cm. La HEPT augmente aussi avec une certaine puissance du volume de l'échantillon injecté, puissance qui dépend de la qualité du remplissage et peut n'être que de 1.2. On souligne l'intérêt d'employer un gaz vecteur donnant de forts coefficients de diffusion (He, H_2) car on triple alors la productivité.

La productivité, quantité d'échantillon séparée par unité de temps, augmente malgré tout avec le diamètre de la colonne. Des considérations théoriques simples permettent, si l'on dispose d'un volume donné de phase stationnaire pour effectuer une certaine séparation, de calculer le diamètre de la colonne qui admettra l'échantillon le plus important. Les performances d'un système de chromatographie préparative sont limitées davantage par la capacité des colonnes que par leur perte d'efficacité quand le diamètre augmente.

On peut améliorer la capacité et la productivité des colonnes en introduisant dans le remplissage des tiges parallèles à l'axe de la colonne, régulièrement espacées. Ceci permet de chauffer la colonne par l'intérieur soit pour travailler en température programmée, soit pour porter rapidement les colonnes à la température d'emploi.

SUMMARY

The dependence of the efficiency and productivity of preparative-scale gas-chromatographic columns on various parameters is discussed. The minimum HETP is experimentally shown to increase almost proportionally to the column diameter in the range 1–5 cm. The HETP also increases with a power of the sample amount which depends on the quality of the column packing and can be as low as 1.2. High-

diffusivity carrier gases (H_2 and He) are shown to allow a three-fold increase of columns productivity.

The productivity (amount of sample separated/unit time) increases with the column diameter. Given a fixed volume of stationary phase and a known mixture, the column diameter which will accept the largest sample can be calculated. The performance of a preparative unit is limited more by the loadability of columns than by loss of efficiency with increasing diameters. The performances of preparative columns can be improved by putting rods parallel to the column axis regularly spaced in the packing. The column can be heated internally either for programmed temperature separations or to allow thermal equilibrium to be reached rapidly.

REFERENCES

1 E. BAYER, K. P. HUPE ET H. MACK, *Anal. Chem.*, 35 (1963) 492.
2 F. ET M., Scientific Note, 7, 4 (1966) 8.
3 A. S. SAID, *J. Gas Chromatog.*, 2 (1964) 60.
4 E. BAYER, Journées d'Etude du GAMS (19–21 Mai 1964).
5 J. C. GIDDINGS, *Nature*, 184 (1959) 357.
6 A. B. LITTLEWOOD, *Anal. Chem.*, 38 (1966) 2.
7 J. C. GIDDINGS, *J. Gas Chromatog.*, (1963) 12.
8 S. T. PRESTON, private communication.
9 F. H. HUYTEN, W. VAN BEERSUM *et* A. W. G. RIJNDERS, dans R. P. W. SCOTT, (red.), *Gas Chromatography 1960*, Butterworths, London ,1960, p. 224.
10 A. B. LITTLEWOOD, *Gas Chromatography, Principles, Techniques and Aplpications*, Acad. Press, 1962, p. 141.
11 G. M. C. HIGGINS ET J. F. SMITH, dans A. GOLDUP (red.), *Gas Chromatography 1964*, Inst. of Petroleum, Londres, 1965, p. 110.
12 L. MIKKELSEN, F. J. DEBBRECHT ET A. J. MARTIN, *J. Gas Chromatog.*, 4 (1966) 263.
13 M. B. DIXMIER, B. ROZ ET G. GUIOCHON, Brevet français no. 1 451 420.

Analytica Chimica Acta
Elsevier Publishing Company, Amsterdam
Printed in the Netherlands.

MOLECULAR SIEVE EFFECTS IN CHROMATOGRAPHY

PER FLODIN
Perstorp AB, Perstorp (Sweden)

(Received November 1st, 1966)

The ability of swollen three-dimensional networks, gels, to differentiate between solutes of different sizes is the basis for a group of separation methods developed during the last ten years. The possibility of predicting a separation from a knowledge of the molecular weights, the simple equipment necessary, and the speed of separation are probably the main factors behind the rapid increase in the number of applications. Before 1960 there were less than ten, while today over 800 publications dealing with these phenomena are available. In this rapid development, considerable confusion in terminology has arisen. Thus what is called gel filtration, exclusion chromatography, molecular sieve chromatography, gel chromatography, and gel permeation chromatography is basically the same phenomenon. For the sake of clarity, the most widely used term, gel filtration, will be used for all these methods throughout this text.

The gel filtration methods have been developed empirically beginning with LATHE AND RUTHVEN[1], who carried out molecular weight estimations on swollen starch grains. The availability of suitable gel materials gave impetus to further studies on the application of the method and this phase of the development continues today. First water-swollen gels were studied[2], and later organic solvent-swollen gels[3] and macroreticular gels[4]. As is so often the case, the theoretical treatment has lagged behind and the fundamentals of the method are still only vaguely known. Many excellent review articles are available on the applications of the method[5,6].

APPLICATIONS

Biochemical systems

In biochemical studies, the preparative isolation of a chemical individual is generally the prime object as contrasted to polymeric systems where molecular weight distributions are determined. Biochemical separations are generally performed in water which limits the choice of gel materials to those with hydrophilic backbones. Crosslinked dextran (Sephadex) or polyacrylamide (Biogel) are available in many different porosity grades suitable for different applications. The least porous ones have their separation range in the low molecular weight region and all large molecules are excluded and emerge in the effluent with the void volume. With increasing porosity, the separation range is displaced upwards, and solutes with molecular weight of several hundred thousand can be separated from larger ones, using extremely porous gels.

Simplest from the experimental point of view are separations of species differing widely in size and in which one of the components is of low molecular weight. Very simple apparatus can be used and the experiments are performed rapidly and

with excellent reproducibility. A few studies of experimental conditions have been published[7,8]. To improve resolution, small and uniform gel particle size, low flow rate and a low sample viscosity should be employed. Uniform packing of the column is of prime importance as was emphasized by ANDREWS[9].

A number of applications of this type of separation have been reported in the literature and a few typical ones will be cited in order to show the versatility. These are the removal of cofactors from enzymes[10], the separation of free ^{131}I from ^{131}I-labelled human growth hormone[11], and the isolation of vitamin B_{12} from sea water[12]. The separation of unbound dye from dye-protein conjugates has become a routine procedure in the labelling of antibodies for biological studies[13].

These separations can be performed with other techniques, *e.g.*, dialysis, and gel filtration should be regarded as an improvement of existing techniques. Fractionation of biological macromolecules, on the other hand, opened new areas for investigation. Typical examples are the separations of blood plasma proteins on passage through a column packed with a porous gel. The separation peaks were revealed by UV-analysis[14] (Fig. 1). Examination of the fractions in the ultracentrifuge showed a decrease in the sedimentation constant with an increase in the elution volume. Further separation of the fractions by electrophoresis and ion-exchange chromatography facilitated the isolation of several components[15]. By performing this type of separation by the thin-layer technique, small samples can be used and the chromatograms developed in a short time. The thin-layer technique also allows identification of specific components, thus increasing the usefulness of the method for clinical analy-

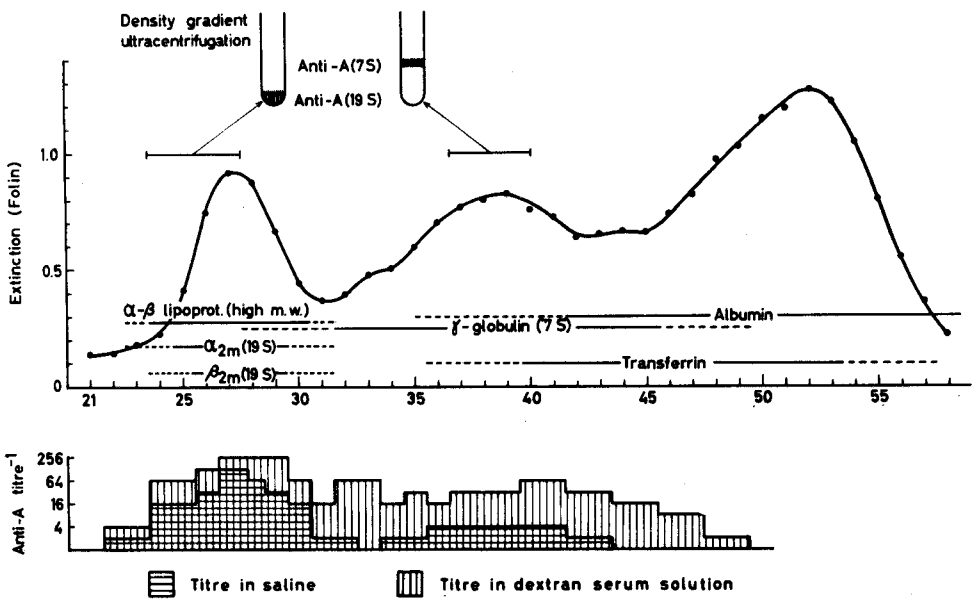

Fig. 1. Elution pattern of plasma proteins on Sephadex G-200. (—) UV-analysis of fractions. Test tubes indicate the positions of 19S and 7S antibodies as obtained by preparative ultracentrifugation. On X-axis distribution of some serum proteins as determined by immunodiffusion. Lower diagram, result of serological titration for the presence of anti-blood group A substance (from ref. 14). Gel filtration on Sephadex G-200, 10 ml serum (A.M.O.) in 0.2 *M* NaCl + 0.1 *M* tris at pH 8.

sis[16]. Gel filtration in combination with subsequent paper electrophoresis or immunoelectrophoresis of the fractions obtained has proven a valuable tool for the diagnosis of various diseases[17].

In the study of the structure of biological macromolecules, gel filtration has been used for the separation of products of partial degradation of macromolecules[18]. An advantage in these separations, is the possibility of choosing the eluant composition within wide limits. To avoid association phenomena 8 *M* urea solutions have been used for peptides. Another example of the importance of the eluant composition is illustrated in the separation of oligomers derived from chondroitin sulfuric acid[19]. The addition of 0.5 *M* sodium chloride to the eluant increased the zone sharpness to such an extent that complete separation of the components was obtained.

The separation of low molecular weight species has been studied much less than that of macromolecular ones, probably because many other methods are available for this range. However, some sharp separations have been reported, *e.g.* the separation of individual oligosaccharides of the cellobiose series up to hexose[20]. Perhaps this field will gain further interest now that new gel types with very high degrees of cross-linking and thus very small pores have become available.

In Fig. 2 is shown the separation of oligomers of ethylene glycol. The difference in molecular weight between the components is only 44 but still almost complete separation is possible. Very interesting, although not surprising in view of probable molecular sieve mechanism, is the fact that the conformation of the molecule influences its position in the chromatogram. Thus, glucose and its isomers fructose and mannose, are eluted at different volumes.

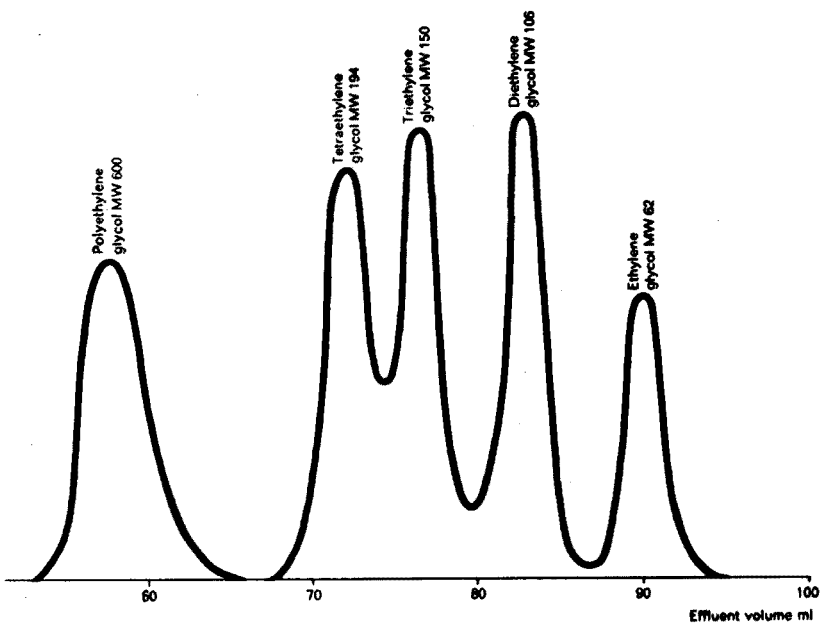

Fig. 2. Separation of oligomers of polyethylene glycol on Sephadex G-10. A 1 ml sample was applied to a 1.2 × 102 cm column and eluted at a rate of 6 ml/h (By permission of AB Pharmacia, Uppsala, Sweden).

A closer study of the elution behaviour of small solutes often shows anomalous behaviour under certain conditions. Thus, urea and thiourea are much more retarded on highly cross-linked gels than expected and this is appearingly little affected by changes in pH and ionic strength.

Molecular weight

The characterization of polymers is one of the most rapidly growing applications for gel filtration. The fractionation of dextrans on Sephadex gels was the first study in which the fractions obtained were characterized by number average and weight average molecular weight determinations[21]. The possibilities of the method were immediately apparent since very favorable heterogeneity ratios were obtained. In fact, the fractions were more homogeneous than those obtained by careful precipitation fractionation. The method has been perfected to a degree that 2 mg of dextran is sufficient to obtain a complete molecular weight distribution analysis[22] (Fig. 3). This has made possible the study of the fate of dextran as blood plasma in patients under normal and pathological conditions.

Cross-linked polystyrene beads swollen in benzene were used by VAUGHAN[23] to fractionate polystyrene. This method was later perfected by MOORE[4] using macromolecular polystyrene beads as screening agents. The wide distribution of pore sizes

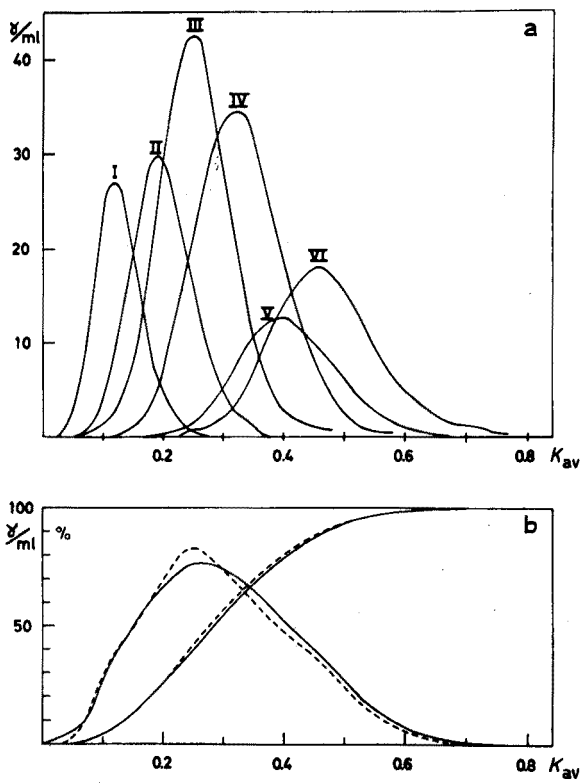

Fig. 3a. Elution profiles of six dextran fractions (Mw = 15 000–65 000) on Sephadex G-200. From these curves summation curves (— — —) were calculated and compared with elution profiles (—) for a mixture of the fractions (b) (By permission of Dr. K. GRANATH).

allows fractionation of molecular weights up to several millions. These macroreticular gels are commercially available under the name of Styragel.

A large number of polymers has been successfully fractionated and the method is becoming a standard tool for polymer characterization. Examples of polymers studied on macroreticular styrene gels are polyethylene[24], polystyrene[4], polymethylmethacrylate[25], and epichlorohydrin–bisphenol A condensates[26]. Gels made by polymerization of methyl methacrylate and ethylene glycol–bismethacrylate were used for the fractionation of polystyrene[27]. Polystyrene could also be fractionated on silica gels with controlled porosity[28]. In comparison with precipitation fractionation methods which are tedious, molecular sieve procedures offer the advantage of rapidity and reproducibility. The fact that the molecules are in solution during the separation process minimizes artefacts due to crystallization which so often cause irregular distribution of species between gel and supernate in precipitation fractionation.

Much work has been devoted to the study of correlations between sample molecular weight and elution volume from a gel. For a homologous series the relationship is rather simple and can be expressed as a straight line when the logarithm of the molecular weight is plotted against the elution volume or the distribution coefficient[21]. For a number of proteins this relationship has also been found to hold true[9]. Carbohydrate-free globular proteins ranging in molecular weight from 12,000 to 800,000 gave a straight line on Sephadex G-200. Thus, for proteins molecular weights can be estimated by a simple chromatographic experiment. The thin-layer technique can be used and is especially useful when only minute quantities of the substances are available[29].

For synthetic polymers, similar calibration can be made using narrow fractions with known molecular weights as standards[4]. The calibration from one polymer cannot be transferred to another. The relationship between molecular dimensions and the pore size of porous glass particles has been investigated[31]. By plotting the ratio of pore diameter to gyration radius of the polymer molecule against penetration, for a number of polystyrene fractions, it was found that the 50% penetration point was not far from the average maximum diameter of the statistical polymer chain. The problem of obtaining the true molecular weight distribution from chromatographic experiments has been discussed by TUNG[30]. When standard samples with known molecular weight and distribution are used, the true molecular weight distributions of a sample can be calculated from a chromatogram using only a few assumptions.

Non-ideal behaviour

Often departure from ideal molecular sieve behaviour is observed. Adsorption to the gel backbone gives elution volumes higher than expected. With hydrophilic gels, aromatic and heterocyclic substances are often adsorbed. Sometimes this may be turned into an advantage for the isolation of particular compounds such as flavoring substances in coffee extracts[32]. With organophilic gels the choice of solvent is also very important. Cross-linked polystyrene has thus been found to adsorb many solutes from benzene[33]. In tetrahydrofuran, rather small adsorption effects are observed and this is one of the reasons why this solvent is preferred for polymer fractionations[34].

Ion-exchange effects can sometimes be observed in work with Sephadex gels. When the eluant has a very low electrolyte content, basic substances may adsorb to the gel backbone. Also in other respects the electrolyte content can be important,

e.g., when solute–solute interactions may occur. An example is the very poor separations obtained with oligosaccharides from chondroitin sulfuric acid with distilled water as eluant; only when 0.5 *M* sodium chloride was added to the eluant, did the peaks separate efficiently[19]. The detection and study of rapidly associating systems can be carried out by means of gel filtration[35]. The migration rate of the complex-containing zone was lower the lower the solute concentration.

THE GELS

Any three-dimensional network expanded by an imbibed solvent gives a molecular sieve effect on solutes dissolved in the solvent. However, to be useful in chromatographic work, the gel must fulfil certain requirements. The network must not break down under the experimental conditions. If it is built up entirely of C–C-bonds as in styrene gels or of C–O–C-bonds as in dextran it is stable under most practical conditions. The N-acetal cross-linkages in polyacrylamide gels make these more sensitive especially to acids, but they are still very useful. Some gels used for special separations have hydrogen or van der Waals bonds as crosslinkages. An example is the agarose gels used by HJERTÉN for separation of cellular particles such as mitochondria and ribosomes[36].

To be used in a chromatographic column, the swollen gel should have sufficient mechanical strength to support the column. The rigidity is especially critical for gels separating in the high molecular weight ranges where the number of cross-linkages is low. The high rigidity of the macroreticular polystyrene gels is an advantage in this respect.

The dextran gels (Sephadex) are made by the cross-linking of dextran with epichlorohydrin in alkaline solutin[37]. Ether linkages are formed and the gel contains a high proportion of hydroxyl groups making it hydrophilic. The porosity can easily be changed by changing the proportion of reactants. In order to obtain spherical beads, the reaction is often carried out in suspension. Many other hydrophilic polymers can be crosslinked in a similar manner[37]. By free radical polymerization, excellent gels can be obtained from many monomer pairs. Thus acrylamide copolymerized with methylene–bisacrylamide (Biogel), methylmethacrylate with ethyleneglycol–diacrylate and styrene with divinyl benzene give excellent gels, which have a relatively narrow pore-size distribution. By performing the styrene–divinylbenzene copolymerization in the presence of a non-solvent for the polymer, a wide pore size distribution is obtained[4]. Furthermore, a relatively high mechanical stability is retained making separations in the very high molecular weight range possible.

The interaction between solvent and gel network is of utmost importance. Generally the solvent should be "good" causing expansion of the polymer chains until the cross-linkages prevent them from going into solution. With this requirement only a few combinations are suitable. For Sephadex, water and dimethylsulfoxide are good solvents which are useful for separation. For cross-linked polystyrene, tetrahydrofuran is the preferred solvent due to little adsorption and good swelling. Chemical modification of the network is sometimes effective to make possible the change from one solvent to another. As an example, esterification or etherification of the hydroxyl groups of a dextran gel makes it loose its hydrophilic character to become swellable in organic solvents.

THEORETICAL ASPECTS

The elution volume of a solute is given by the formula

$$V_e = V_o + K_d V_i$$

where V_o is the void volume, V_i the volume of solvent imbibed by the gel bed and K_d a constant characteristic for the solute and gel type. When only molecular sieve effects are operating the K_d cannot exceed unity. The volume in which the separation shall take place is thus smaller than the total volume of the column. This is different from other chromatographic methods in which much higher retentions are generally encountered. Consequently gel filtration requires very careful preparation of the column.

As shown above, V_e and thus K_d is related to the molecular size of the solute. For some groups of substances a linear relationship between the logarithm of the molecular weight and the distribution coefficient K_d is obtained. The significance of this value is thought to be the fraction of the imbibed solvent volume that is available to the solute. The larger the solute the smaller the fraction of the inner volume that can be penetrated. To test this hypothesis, LAURENT AND KILLANDER[38] studied a simple network model assuming the polymer chains to be straight rigid rods distributed at random. The volume available for spherical particles with the radius r_s is then

$$K_d = \exp\,[-\pi L(r_s + r_r)^2]$$

where L is the concentration and r_r the radius of the rods. In spite of the crude model relatively good agreement with experimental values was obtained.

Theories based on the assumption of restriction of diffusion in the gels have been less successful and experimental data strongly suggest an equilibrium process. In fact, zone widening depends on the same factors as in other chromatographic methods[7], *e.g.*, small particles and low flow rate give narrow zones. A theory of zone spreading in gel filtration has been given by GIDDINGS[39]. Contributions to the plate height by factors such as longitudinal diffusion, flow pattern, and non-equilibrium conditions are taken into consideration. It is concluded that the excess plate height observed is not due to stationary phase non-equilibrium.

SUMMARY

The utilization of molecular sieve effects is reviewed. Applications to biochemical separations and the determination of molecular weights are discussed, as well as the properties of the different gels and the theory underlying their use.

REFERENCES

1 G. H. LATHE AND C. R. J. RUTHVEN, *Biochem. J.*, 62 (1956) 665.
2 J. PORATH AND P. FLODIN, *Nature*, 183 (1959) 1657.
3 M. F. VAUGHAN, *Nature*, 188 (1960) 55.
4 J. C. MOORE, *J. Polymer Sci.*, A 2 (1964) 835.
5 P. ANDREWS, *Brit. Med. Bull.*, 22 (1966) 109.
6 H. DETERMANN, *Angew. Chem. Int. Edn.*, 3 (1964) 608.
7 P. FLODIN, *J. Chromatog.*, 5 (1961) 103.
8 K. SELBY AND C. C. MAITLAND, *Biochem. J.*, 94 (1965) 578.

9 P. ANDREWS, *Biochem. J.*, 96 (1965) 595.
10 R. L. KISLIUK, *Biochem. Biophys. Acta*, 40 (1960) 531.
11 F. C. GREENWOOD, W. M. HUNTER AND J. S. GLOVER, *Biochem. J.*, 89 (1963) 114.
12 K. W. DAISLEY, *Nature*, 191 (1961) 868.
13 W. GEORGE AND K. W. WALTON, *Nature*, 192 (1961) 1188.
14 P. FLODIN AND J. KILLANDER, *Biochem. Biophys. Acta*, 63 (1962) 403.
15 B. GELOTTE, P. FLODIN AND J. KILLANDER, *Arch. Biochem., Suppl.*, 1 (1962) 319.
16 B. G. JOHANSSON AND L. RYMO, *Acta Chem. Scand.*, 18 (1964) 217.
17 K. WIRTH, U. ULLMAN AND K. BRAND, *Klin. Wochschr.*, 43 (1965) 528.
18 R. J. HILL, W. KONIGSBERG, *J. Biol. Chem.*, 235 (1960) pc 11.
19 P. FLODIN, J. D. GREGORY AND L. RODÉN, *Anal. Biochem.*, 8 (1964) 424.
20 P. FLODIN AND K. ASPBERG, *Biol. Struct. Function, Proc. IUB-IUBS Intern. Symp. 1st, Stockholm, 1960*, 1, 345.
21 K. GRANATH AND P. FLODIN, *Makromol. Chem.*, 48 (1961) 160.
22 K. GRANATH AND B. KVIST, to be published.
23 M. F. VAUGHAN, *Nature*, 188 (1960) 55.
24 N. NAKAJIMA, *J. Polymer Sci.*, 5 (1966) 101.
25 G. MEYERHOFF, *Makromol. Chem.*, 89 (1965) 282.
26 G. D. EDWARDS, *J. Appl. Polymer Sci.*, 9 (1965) 3845.
27 H. DETERMANN, G. LÜBEN AND T. WIELAND, *Makromol. Chem.*, 73 (1964) 168.
28 H. W. KOHLSCHÜTTER, K. UNGER AND K. VOGEL, *Makromol. Chem.*, 93 (1966) 1.
29 C. J. O. R. MORRIS, *J. Chromatog.*, 16 (1964) 167.
30 L. H. TUNG, *J. Appl. Polymer Sci.*, 10 (1966) 375.
31 J. C. MOORE AND M. C. ARLINGTON, *I.U.P.A.C. Symposium on Macromolecular Chemistry, Tokyo–Kyoto, 1966*, Preprints Vol. 6, 109.
32 H. STREULI, *Chimia*, 16 (1962) 371.
33 B. CORTIS-JONES, *Nature*, 191 (1961) 272.
34 J. C. MOORE AND J. G. HENDRICKSON, *Polymer Sci.*, C, 8 (1965) 233.
35 D. J. WINZOR AND W. A. SCHERAGA, *Biochemistry*, 2 (1963) 1263.
36 S. HJERTÉN, *Arch. Biochem. Biophys.*, 99 (1962) 466.
37 P. FLODIN, *Dextran Gels and their Applications in Gel Filtration*, AB Pharmacia, Uppsala, Sweden, 1962.
38 T. C. LAURENT AND J. KILLANDER, *J. Chromatog.*, 14 (1964) 317.
39 J. C. GIDDINGS AND K. L. MALLIK, *Anal. Chem.*, 38 (1966) 997.

Analytica Chimica Acta
Elsevier Publishing Company, Amsterdam
Printed in the Netherlands.

CHROMATO–POLAROGRAPHIC ANALYSIS OF MONONITROETHYLBENZENE MIXTURES

WIKTOR KEMULA AND DANUTA SYBILSKA
Institute of Physical Chemistry, Polish Academy of Sciences, Warsaw (Poland)

(Received November 1st, 1966)

Various physicochemical techniques, *e.g.* colorimetric, radiochemical, refractometric, conductometric, potentiometric, *etc.*, have been used for analysis of eluates from chromatographic columns. The applicability of each technique is related to the type of the relationship between the quantity measured and the concentration of the substance determined in the eluate, on the sensitivity of determination and accuracy of measurement as well as on simplicity of the apparatus and possibility of automatic recording.

Polarographically active substances can be successfully determined by the chromato-polarographic method[1]. The straight-line current *vs.* concentration relationship, high sensitivity (10^{-8} g/ml), and automatic recording make the chromato–polarographic technique compare favorably in many cases with gas chromatography.

In the chromato–polarographic analysis of organic compound mixtures, the resolving power of the chromatographic system is of paramount importance. The scarcity of well-characterized chromatographic systems renders the choice of a suitable system somewhat difficult. It is evident from the basic principles of chromatography that the use of a mercury drop electrode for continuous analysis of the eluate restricts not only the number of measurable substances but also the range of applicable chromatographic resolving systems. The only suitable systems are those with relatively polar liquids as mobile phases, which are able to produce suitably conducting media; it is well known that the mobile phase must contain some of the supporting electrolyte and often a buffer solution, too. Therefore, investigations on the adaptation of the existing well-known resolving systems, and on the development of new ones, so that they meet the requirements of the chromato–polarographic method, have long been in progress in this Laboratory.

Partition chromatography systems are only slightly selective with respect to isomers. MARTIN's theoretical considerations[2] on separation of homologues have shown that isomers with the same number of identical functional groups should have the same partition coefficients and thus remain inseparable. Exceptions to this rule occur when the isomer molecules differ much in the degree of association or dissociation, in their ability to form intramolecular hydrogen bonds, or in polarity; the Martin equation takes no account of such factors. Therefore, with most mixtures investigated, *e.g.* isomeric mononitrotoluenes, nitroethylbenzenes, nitroxylenes, nitroalkanes, *etc.*, attempts to carry out resolution by partition chromatography were unsuccessful, whereas with nitroanilines and nitrophenols[3–6] and homologous nitroalkanes[7] a satisfactory resolution was obtained. Also, developing of chromatograms on ion-ex-

changer columns by the salting-out and salting-in techniques[8] has been found useful.

Chromatography lacks sorbents able to select compounds effectively with respect to shape. On porous sorbents, most suitable for shape segregation of molecules, sorption proceeds more or less irreversibly, thus ruling out their possible use for quantitative analysis.

Recently, we have introduced into chromatography a completely new type of column filler[9–13], which may span the existing gap to some extent. The new fillers, which are particularly efficacious for resolution of isomers, include the clathrates described by SCHAEFFER *et al.*[14].

There are many complexes of the Werner type able to form clathrates with organic molecules[14,15]. These include complexes of bivalent metals such as nickel, cobalt, iron, manganese and zinc. The metal ion coordinates neutral molecules having a basic nitrogen (*e.g.* methyl- and ethylpyridines) and two anions (thiocyanate, cyanate, bromide). The complexes are highly selective in caging of aromatic hydrocarbons. This selectivity is based on the shape rather than the volume of the caged molecules.

The above-mentioned complexes and their clathrates are of both theoretical and practical interest, because clathration by crystallization or by shaking has become an exceptionally successful method for resolution of aromatics, inseparable by other methods.

The results obtained show the Ni(γ-picoline)$_4$(CNS)$_2$ type clathrates to be effective as sorbents in chromatographic systems.

EXPERIMENTAL

Materials

The *o*-, *m*- and *p*-nitroethylbenzenes used had physical constants consistent with the literature data. All reactants and solvents used were of either analytical or reagent grade. All available γ-picoline preparations were contaminated with the β-isomer. The γ-picoline (γ-Pi) used contained 13% of β-picoline.

Preparation of Ni(γ-Pi)$_4$(CNS)$_2$, Co(γ-Pi)$_4$(CNS)$_2$, Fe(γ-Pi)$_4$(CNS)$_2$ and other clathrates was somewhat different from the original Schaeffer procedure. The clathrates were precipitated at a much slower rate and the aqueous picoline solutions used were more dilute. γ-Picoline was always used in excess over the stoichiometric amount.

Apparatus

A Radiometer PO4 polarograph was used. Commercial γ-picoline and β-picoline liberated from clathrates and complexes were analyzed on a Carlo Erba model R gas chromatograph. The chromato-polarographic examination was carried out along the usual lines[1]. Chromatographic columns were prepared as described earlier[12]. The elution technique of analysis was used invariably. Samples were run on to the column by means of a pipette. In quantitative analysis, this technique introduces errors of up to $\pm 2\%$.

Methods

The chromatographic resolution coefficients (C), partition coefficients (K) and selectivity coefficients (β) reported here were determined by the dynamic method and evaluated from V_{max} (eluate volume at peak maximum) and from known V_s (immobile

phase volume) and V_M (mobile phase volume) data. The number of theoretical plates (n) and HETP values were calculated from the width of the elution curves by the use of the Verzele and Alderweireldt formulae[16,17].

With isomeric nitroethylbenzenes, process isotherms were investigated mainly by the chromatographic, and in part by the static, method. A straight-line relationship was found to exist under the applied conditions between the content of the compound in the column and its concentration in the equilibrated mobile phase solution.

Polarographic investigations

The literature lacks data on the polarographic reduction of nitroethylbenzenes. With each mobile phase used, the potentials of the mercury drop electrode, ranging from −0.9 to −1.2 V (*vs.* SCE), were found to be suitable for polarographic detection of nitroethylbenzenes in the eluate from the chromatographic column; the polarograms obtained with one mobile phase, *viz.*, 0.2 *M* NH_4CNS–0.3 *M* γ-picoline–aq. 40% DMF, which is recommended for analytical purposes, have only a single reduction wave and the three nitroethylbenzene isomers were found to display approximately the same reduction behaviour. The half-wave potentials of polarographic reduction of the *o*-, *m*- and *p*-isomers are close to one another, being −0.43, −0.38 and −0.41 V (*vs.* SCE), respectively. The i_d *vs.* c curves within the concentration (c) range $2 \cdot 10^{-4}$—$2 \cdot 10^{-3}$ can be superimposed within the limits of experimental error (±3%). Thus, under the conditions described, the chromato-polarographic technique enables calibration curves to be constructed from measurements carried out with only a single isomer.

RESULTS

Chromatographic resolution of isomeric nitroethylbenzenes

The fundamental prerequisites to be met by a system suitable for chromatographic purposes include high selectivity and reversibility of the process occurring in the chromatographic column. Additional requirements are the solubility, stability and reproducibility. The new fillers meet these requirements satisfactorily.

Selectivity of resolution on clathrate columns

The new fillers are highly selective. Of the many complexes and clathrates investigated in this Laboratory, clathrates of the complexes with γ-picoline, $Ni(\gamma\text{-Pi})_4(CNS)_2$ and $Co(\gamma\text{-Pi})_4(CNS)_2$, were found to be most suitable for resolution of disubstituted benzene derivatives and monosubstituted naphthalene derivatives. However, much effort was required for establishment of the conditions under which partition of the aromatics occurs most selectively in the chromatographic column.

In the analysis of nitroethylbenzenes by elution in two systems (Figs. 1 and 2), resolution was complete and the elution curves were symmetrical.

According to SCHAEFFER *et al.*[14], the $Ni(\gamma\text{-Pi})_4(CNS)_2$ complex-forming clathrates with the disubstituted benzene derivatives select them always in the same manner according to the position of functional groups and irrespective of their nature. With the *p*-isomer, interactions are strongest and weakest, with the *o*-isomer. Therefore, in comparison with the starting mixture, the fraction contained in the clathrate

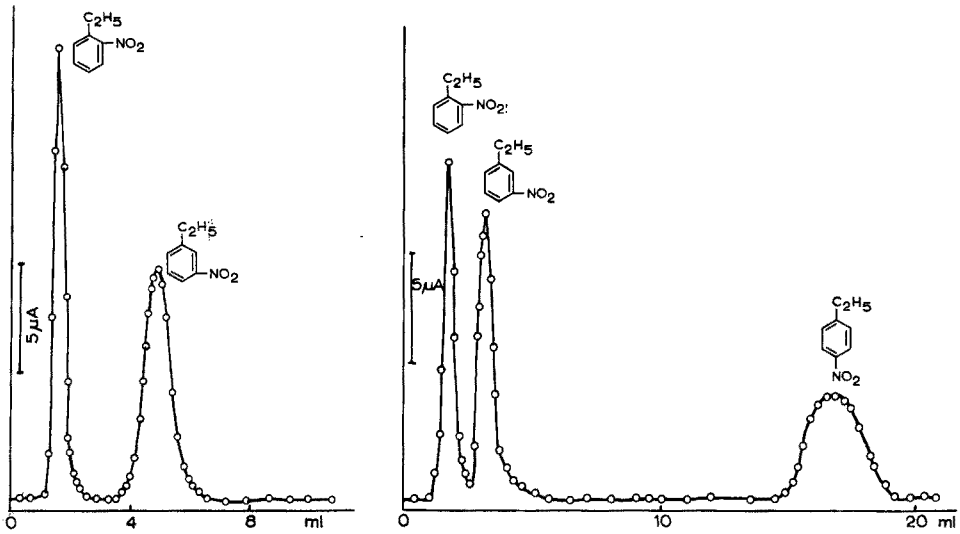

Fig. 1. Chromato–polarogram for the *o*-, *m*- and *p*-nitroethylbenzene eluate from a column (2.0 cm high, 0.5 cm in inner diam.) filled (70%) with 0.3 g of $Ni(\gamma\text{-Pi})_4(CNS)_2$; mobile phase: 2 *M* NH_4CNS—0.3 *M* γ-picoline—aq. 40% DMF; flow rate 5 ml/h.

Fig. 2. Chromato–polarogram for the *o*-, *m*- and *p*-nitroethylbenzene eluate from a column (3.2 cm high, 0.5 cm in inner diam.) filled (60%) with 0.5 g of $Co(\gamma\text{-Pi})_4(CNS)_2$; mobile phase: 0.2 *M* NH_4CNS—0.5 *M* γ-picoline—aq. 40% (v/v) EtOH; flow rate 5 ml/h.

column becomes enriched in the *p*-isomer. This regularity was found, on many examples with very few exceptions, to hold also in chromatographic systems. This corresponds to the course of resolution as recorded during the elution analysis of nitroethylbenzenes (Figs. 1 and 2), *i.e.* the *o*-isomer is the first, and the *p*-isomer the last to appear in the eluate; the *m*-isomer assumes an intermediate position. Its position in the elution curve (V_{max} of the *m*-isomer) is related to the composition of the mobile phase. The dipole moments of the isomers, which are known to be of consequence in partition chromatography, are here of minor importance. In the systems and under the conditions presented in Figs. 1 and 2, *p*-nitrotoluene (*p*-NO_2T) was found to interact with the filler much more weakly and it appeared in the eluate before *p*-nitroethylbenzene (*p*-NO_2EtB). For example, in the system shown in Fig. 1, $\beta = (K_{p\text{-}NO_2EtB}/K_{p\text{-}NO_2T}) \cong 9$, and all nitroxylenes ($NO_2X$) isomeric with nitroethylbenzenes left the column before *o*-nitroethylbenzene; $\beta = (K_{o\text{-}NO_2EtB}/K_{NO_2X}) > 1$ for each nitroxylene isomer.

Quantitative determination

The resolving power of clathrates as sorbents is highly related to the mobile phase composition. It was established beyond doubt that the mobile phase composition has a decisive effect on the composition and structure of the crystal surface as well as on the type of equilibrium, which occurs in the process of chromatographic resolution. In general, resolution in clathrate columns can be made reversible. The peaks then recorded are symmetrical and the elution of the individual species is quantitative.

With nitroethylbenzenes, studies were carried out on the resolution and recovery of the individual compounds in systems with the $Ni(\gamma\text{-Pi})_4(CNS)_2$ clathrate as the immobile phase and with various mobile phases. The following mobile phases: 2.0 *M* NH_4CNS–0.3 *M* γ-picoline–aq. 50% organic solvent (*e.g.* MeOH, EtOH, acetone, DMF, acetonitrile, and formamide) were found to be suitable for resolution of the isomers investigated and the compounds were recovered from the column quantitatively. The elution curves recorded in the continuous manner are symmetrical; this fact greatly simplifies the quantitative procedure. After suitable calibration curves have been obtained, a chromato–polarogram is recorded for the eluate and the peak areas bounded by the zero line are measured.

Table I summarizes a typical determination. The areas were measured plani-

TABLE I

QUANTITATIVE RESULTS OF EVALUATIONS OF *o*-, *m*- AND *p*-NITROETHYLBENZENE MIXTURES

No. of sample	*Compounds*	*No. of evaluation*	*Taken (μg)*	*Found (μg)*	*Average (μg)*	*Difference (μg)*	*Relative error (%)*
		1	70	73			
	o-nitroethylbenzene	2	70	71	71	+1	+1.5
		3	70	69			
		1	90	94			
1	*m*-nitroethylbenzene	2	90	94	92	+2	+2.2
		3	90	88			
		1	300	285			
	p-nitroethylbenzene	2	300	280	290	−10	−3.3
		3	300	305			

metrically. A column (4.0 cm high and 0.6 cm in internal diam.) filled with the $Ni(\gamma\text{-Pi})_4(CNS)_2$ clathrate was used; the mobile phase was 2 *M* NH_4CNS–0.3 *M* γ-picoline–aq. 40% DMF. Samples were dissolved in a supporting solution unsaturated with the complex. The error of such a determination is $\pm 5\%$. However, if necessary, it is possible to carry out chromato–polarographic determinations with a much higher precision by the use of a much more complicated apparatus.

Clathrate column efficiency

The resolving power of a given chromatographic column is related to the rate of establishment of equilibrium and is dependent on numerous factors. Its action is characterized in terms of the number (n) of theoretical plates or the HETP value.

The elution curves of *p*-nitroethylbenzene recorded for the eluate washed out from the $Ni(\gamma\text{-Pi})_4(CNS)_2$ column were used for calculations. The mobile phases used were 50% solutions of methanol, ethanol, acetone, acetonitrile, dimethylformamide, and formamide in aqueous 2.0 *M* NH_4CNS–0.3 *M* γ-picoline. The number of theoretical plates per 1 cm of the column was found to vary from 30 to 50, *i.e.* the HETP varied from 0.03 to 0.02 cm, with the composition of the mobile phase. With acetone, the column was least efficient, whereas with DMF and methanol in the mobile phase, the column was most efficient. Unlike the partition chromatography systems which were investigated earlier, the present fillers failed to reveal a simple relationship between

the viscosity of the solvent and the number of theoretical plates. The present HETP data are fractions of those found with reversed partition chromatography or ion-exchanger columns run by the salting-out or the salting-in technique. This fact shows that the resolution is presumably a surface process, diffusion into crystals as well as crystallization and recrystallization being less likely to occur.

Solubility, stability and reproducibility

Complexes of the $Ni(\gamma\text{-Pi})_4(CNS)_2$ type and their clathrates are slightly soluble in water and in aqueous solutions of organic solvents. The solubility can be controlled and highly depressed by addition of ligands or clathratable molecules to the solution. For example, the solubility of $Ni(\gamma\text{-Pi})_4(CNS)_2$ in water is $2 \cdot 10^{-3}$ mole/l and in aqueous 0.05 *M* NH_4CNS and 0.1 *M* γ-picoline it is as little as $2 \cdot 10^{-6}$ mole/l.

The addition of organic solvents to the aqueous mobile phase was aimed at enhancing the elution of the components investigated. With nitroethylbenzenes dissolved in solutions of the same volume percentages of various organic solvents, the partition coefficients (K) were considerably different, whereas the selectivity coefficients (β) were approximately ($\pm 10\%$) the same. The principal condition for maintenance of this regularity is to keep a constant composition and concentration of γ-picoline and of thiocyanate ions. For example, in the mobile phase 2 *M* NH_4CNS–0.3 *M* γ-picoline–aq. 50% (v/v) organic solvent, the coefficients were identical, *viz.*, $\beta_1 = (K_{meta}/K_{ortho}) = 2$; $\beta_2 = (K_{para}/K_{meta}) = 8$ and $\beta_3 = (K_{para}/K_{ortho}) = 14$ ($\pm 10\%$). Acetone solutions were an exception to this regularity.

The new column fillers are sufficiently stable and undergo no changes during operation of the column or during storage in suitable solutions. The columns keep their chromatographic properties for unlimited periods of time, and the results are reproducible. To achieve the reproducibility and stability of the composition of the clathrates employed, it is necessary to adhere to strictly constant conditions for the preparation of the complexes and filling and operation of the column. Of particular importance for preparation of the complexes with γ-picoline is the maintenance of a constant β-picoline proportion in the starting γ-picoline preparations. Investigations on the full standardization of clathrate preparation are in progress.

DISCUSSION AND CONCLUSIONS

On the basis of our extensive investigations on the analysis of nitroethylbenzene mixtures, we recommend the use of $Ni(\gamma\text{-Pi})_4(CNS)_2$ as the immobile phase. Under certain conditions, the $Co(\gamma\text{-Pi})_4(CNS)_2$ clathrate reveals a similar sorption and selectivity behaviour and also is likely to be useful; however, such clathrates have not yet been extensively investigated and experience has shown that even slight changes in the conditions or in mobile phase composition may have an essential effect on their chromatographic properties. The indications concerning the composition of the mobile phase in relation to the composition of the mixture of isomers examined are as follows.

The system with the mobile phase 2 *M* NH_4CNS–0.3 *M* γ-picoline–aq. 40% DMF (Fig. 1) is most suitable for analysis of mixtures containing the isomers in approximately the same proportions and for analysis of small amounts of the *o*- and *m*-isomers in the presence of an excess of the *p*-isomer.

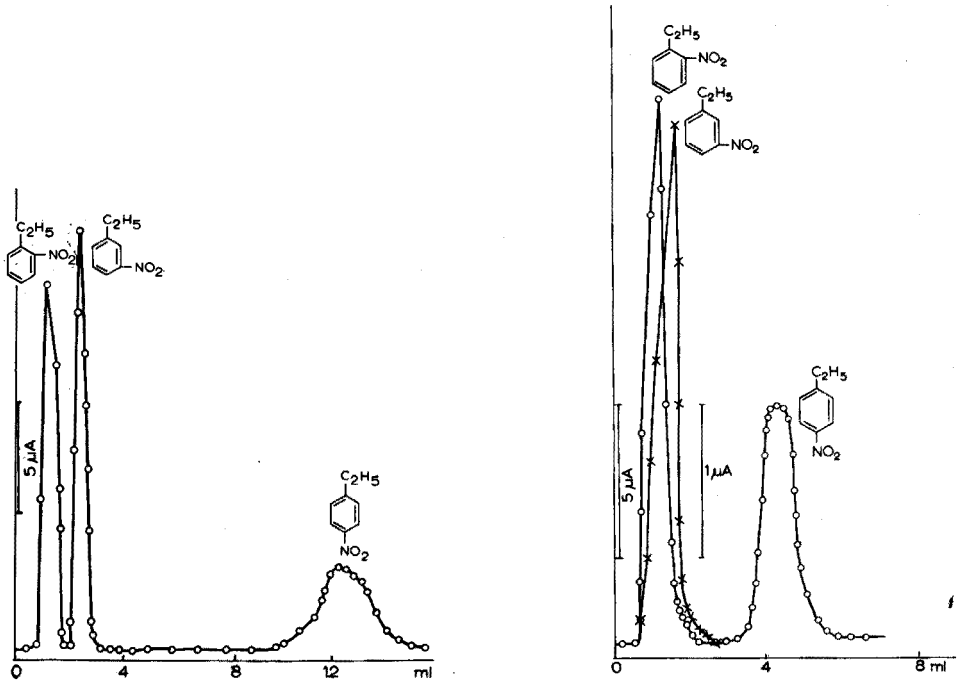

Fig. 3. Resolution of *o*-, *m*- and *p*-nitroethylbenzenes in a column (2.2 cm high, 0.5 cm inner diam.) filled with 0.3 g of $Ni(\gamma\text{-Pi})_4(CNS)_2$; mobile phase: 0.2 *M* NH_4CNS—0.3 *M* γ-picoline—aq. 40% DMF; flow rate 5 ml/h.

Fig. 4. Resolution of a (5:1) *o*-,*p*-isomer mixture in a column (2.1 cm high, 0.5 cm inner diam.) filled with 0.5 g of $Ni(\gamma\text{-Pi})_4(CNS)_2$: mobile phase; 2 *M* NH_4CNS—0.3 *M* γ-picoline—aq. 50% acetone; flow rate 6 ml/h. The *m*-isomer curve is designated by crosses.

If it is necessary to resolve the *o*- and *m*-isomers with particular accuracy, it is best to use mobile phases of weaker elution properties, like that used for elution in Fig. 3. Under these conditions, the *o*- and *m*-isomers can be determined and collected separately, but the peak of the *p*-isomer, which appears later and is much more diffuse, is unsuitable for quantitative analysis.

If the mixture contains little *p*-nitroethylbenzene, elution with acetone solutions is advisable (Fig. 4). Acetone is particularly effective in suppressing the interactions between the column filler and *p*-disubstituted benzene derivatives. Studies on reasons for such exceptional properties of acetone and on their practical use are in progress.

The other solvents investigated in solutions of the same vo ume percentages were found to have approximately the same effect on the selectivity of interactions between the immobile phase and the *o*-, *m*- and *p*-isomers.

Summarizing, the selectivity and reversibility of the chromatographic processes occurring on clathrates are related to the concentration of γ-picoline and to the content of β-picoline in the γ-picoline preparation, and to pH, temperature, and nature and concentration of the organic solvent. So far we have established some functional relationships in specified conditions. Investigations on the effect of eluant composition and operating conditions are continuing, mainly by the trial-and-error method.

SUMMARY

A method of partition and determination of *o*-, *m*- and *p*-nitroethylbenzenes with clathrates as fillers of the chromatographic column is described. The clathrate used was of composition Ni(γ-picoline)$_4$(SCN)$_2$·γ-picoline. The degree of filling of clathrate used was 0.4–0.7. The aqueous moving phase contained 2 *M* NH_4SCN, 0.3 *M* γ-picoline and 40–60 vol.% organic solvent. The applicability of the solvents: acetone, acetonitrile, ethanol, methanol, formamide and dimethylformamide, was checked; acetone and dimethylformamide were found best. Quantitative partition and evaluation of all three isomers was achieved on a 2.5-cm column. The recovery of the eluted individuals was complete. The samples used weighed only 0.05–0.3 mg. The relative error of evaluated components was not greater than $\pm 5\%$. The clathrate filler can be used many times.

REFERENCES

1 W. KEMULA, *Roczniki Chem.*, 26 (1952) 281; *Przemysl Chem.*, 33 (1954) 453; *Proc. Intern. Symp. Microchem., Birmingham, 1958*, Pergamon, London, 1959, p. 258; *Progress in Polarography*, Wiley, New York, p. 297.
2 A. J. P. MARTIN, *Biochem. Soc. Symp.*, 3 (1948) 4.
3 W. KEMULA, D. SYBILSKA AND J. GEISLER, *Roczniki Chem.*, 29 (1955) 645.
4 W. KEMULA, D. SYBILSKA AND J. GEISLER, *Chem. Anal. (Warsaw)*, 1 (1956) 36.
5 W. KEMULA, K. BUTKIEWICZ, J. GEISLER AND D. SYBILSKA, *Chem. Anal. (Warsaw)*, 1 (1956) 50.
6 W. KEMULA AND A. KRZEMIŃSKA, *Chem. Anal. (Warsaw)*, 1 (1956) 137.
7 W. KEMULA AND D. SYBILSKA, *Chem. Anal. (Warsaw)*, 4 (1959) 123.
8 W. KEMULA AND S. BRZOZOWSKI, *Roczniki Chem.*, 35 (1961) 711.
9 W. KEMULA AND D. SYBILSKA, *Nature*, 185 (1960) 237.
10 W. KEMULA AND D. SYBILSKA, *Acta Chim. Acid. Sci. Hung.*, 27 (1961) 237.
11 W. KEMULA, D. SYBILSKA AND K. CHLEBICKA, *Rev. Chim. Rep. Populaire Roumaine*, 7 (1962) 1003.
12 W. KEMULA, D. SYBILSKA AND A. KWIECIŃSKA, *Roczniki Chem.*, 39 (1965) 1101.
13 W. KEMULA, D. SYBILSKA AND K. DUSZCZYK, *Microchem. J.*, 11 (1966) 296.
14 W. D. SCHAEFFER, W. S. DORSEY, D. A. SKINNER AND C. G. CHRISTIAN, *J. Am. Chem. Soc.*, 71 (1957) 5870.
15 P. DE RADZITZKY AND J. HANOTIER, *Ind. Eng. Chem. Process Design Develop.*, 1 (1962) 10; *Ind. Chim. Belge*, 27 (1962) 125; *Erdoel Kohle*, 15 (1962) 892.
16 M. VERZELE AND F. ALDERWEIRELDT, *Bull. Soc. Chim. Belg.*, 64 (1955) 579.
17 M. VERZELE, F. ALDERWEIRELDT AND M. VANDEWALLE, *Bull. Soc. Chim. Belg.*, 66 (1957) 570.

Analytica Chimica Acta
Elsevier Publishing Company, Amsterdam
Printed in the Netherlands.

THE USE OF A MOVING WIRE DETECTOR SYSTEM FOR THE STUDY OF LIQUID CHROMATOGRAPHIC COLUMNS

T. E. YOUNG AND R. J. MAGGS
W. G. Pye & Co. Ltd., Cambridge (Great Britain)

(Received November 1st, 1966)

In gas–liquid chromatography the factors affecting column efficiency and resolving power have been thoroughly investigated, both practically and theoretically, and various column parameters have been optimised to produce the best column performance under given conditions[1,2]. These investigations have been made possible by the availability of small dead volume, high sensitivity detectors which continuously monitor the column eluate. Liquid–liquid chromatography, although the older of the two techniques, has not advanced at the same rate as gas chromatography. This has been due to the lack of suitable detection devices with small dead volumes and high sensitivity, which would enable column parameters such as particle size, column diameter, *etc.*, to be studied properly.

Practical examination of liquid column performance has been limited to a study of the adsorbent and solvent in relation to separation[3–5] and not the effect of experimental conditions on the efficiency of the column. However, the moving wire system devised by SCOTT[6] and JAMES *et al.*[7] provides a possible means of studying the column parameters which affect the efficiency and resolution of liquid–liquid chromatographic columns. This detection system has the properties of small dead volume, high sensitivity and continuous monitoring of the column eluate. To illustrate the potential of the moving wire detector as a means of investigating the performance of liquid columns, work has been done to study the effect of particle size, sample size and flow rate of the mobile phase on the efficiency of straight and coiled silicic acid columns using squalane as the sample material. The work has been extended to study the resolving power of these columns using the two partially resolved peaks of methyl oleate and olive oil.

EXPERIMENTAL

Apparatus

The Pye liquid chromatograph described in this paper enables the highly sensitive gas–liquid chromatographic detectors to be utilised for monitoring the liquid column eluant.

The detector system is shown schematically in Fig. 1. It consists of a moving stainless steel wire of 0.005″ diameter which passes through a cleaning oven where any contaminants, *e.g.* lubricants, are removed in a stream of argon which continuously flows through the oven. The wire then passes to the coating block at the column exit where it is coated with a film of the column eluate. To enable the solvent to be removed from the wire, a small oven is incorporated in the device and is maintained

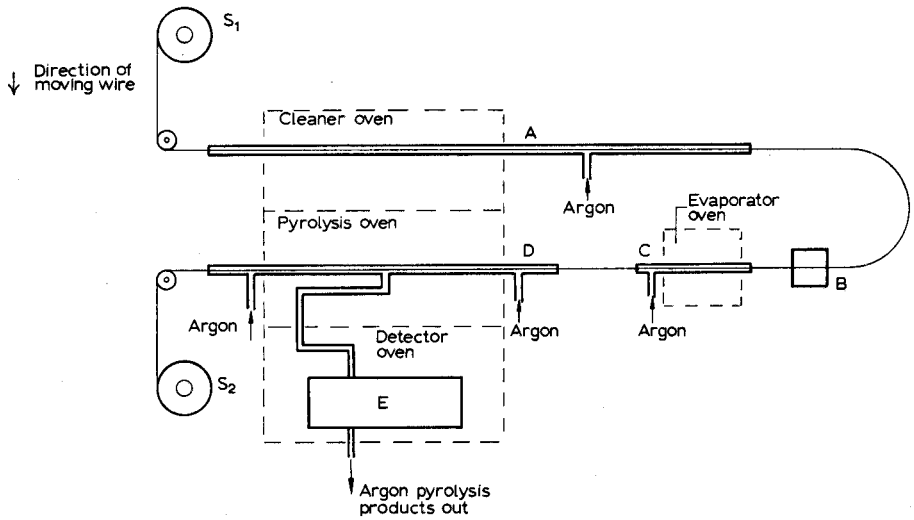

Fig. 1. Schematic diagram of the moving wire detection system. A, cleaner oven glassware; B, coating block; C, solvent evaporator glassware; D, pyrolysis oven glassware; E, macro-argon ionisation detector; S1 and S2, feed spool and collecting spool respectively.

at a suitable temperature for complete removal of the solvent in another argon stream. The wire, now coated with only the materials under investigation, passes through the pyrolysis oven which is maintained at a temperature 50° below that of the cleaning oven. The pyrolysis products of these materials are swept out of the oven by argon and into the gas chromatographic detector, which is contained in a separate oven operating between ambient temperature and 250°. The detector response is dependent upon the composition of the pyrolysis products and the signal is fed into a d.c. amplifier and hence to a 10-mV Honeywell Brown potentiometric recorder. The gas chromato-

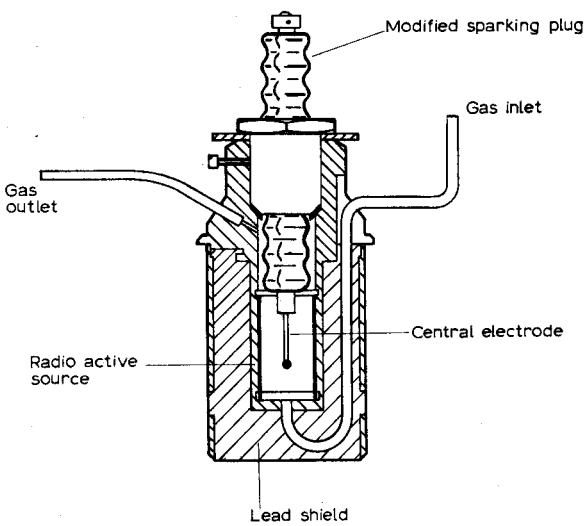

Fig. 2. The macro-argon ionisation detector.

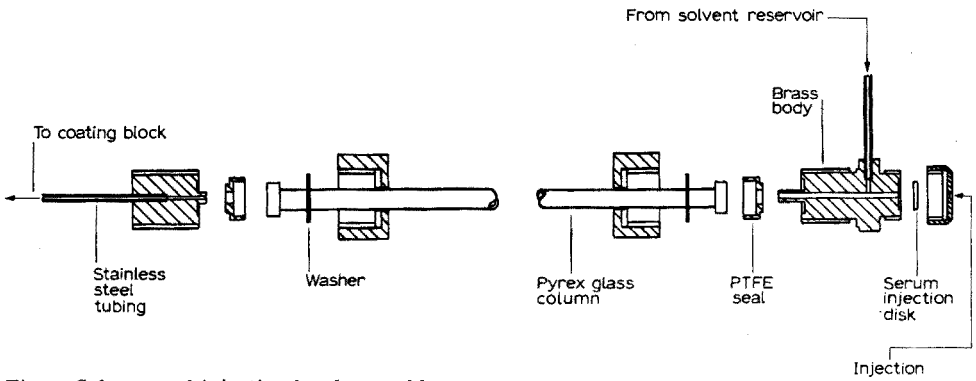

Fig. 3. Column and injection head assembly.

graphic detector employed (Fig. 2) is a macro-argon detector designed by LOVELOCK[8]. The detector is constructed of brass and contains a central cylindrical electrode that terminates in a small sphere. The electrode, which is a modified sparking plug, is insulated from the body of the detector by means of a ceramic sheet. The radioactive source (strontium-90) in the form of a foil is fitted concentric with the electrode.

The glassware in the three ovens is constructed of Supremax alumino–silicate glass. To prevent unnecessary waste of the carrier gas from the ovens, the glass tubing is constricted at both ends. In the case of the pyrolysis oven, these constrictions also minimise the loss of pyrolysis products which would result in a reduction of detector sensitivity.

Figure 3 shows the column assembly. The columns are made of Pyrex glass 4 mm I.D. × 24″ long, and packed with Mallinckrodt silicic acid. The column is connected to the coating block by means of a length of 1/32″ I.D. stainless steel tubing. The injection block consists of a solvent inlet and serum injection device

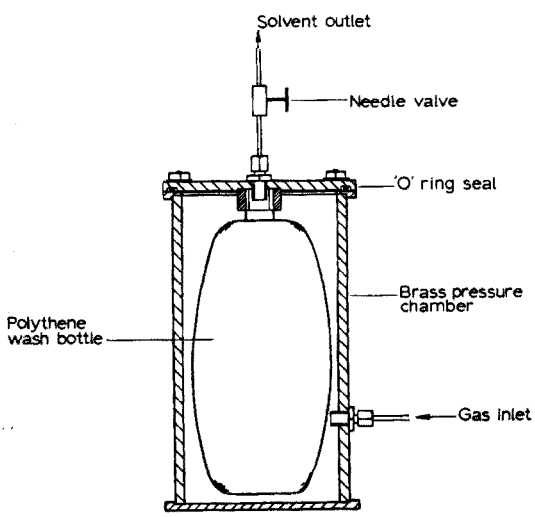

Fig. 4. Solvent reservoir and pump assembly.

which allows the introduction of samples onto the column by means of a syringe. The connections of the injection block to the column are made by means of pressure joints using PTFE seals. Figure 4 shows the solvent reservoir and pump system based on a design by SCOTT[6]. The reservoir consists of a 500-ml polythene wash bottle contained in a cylindrical brass chamber. The brass chamber can be pressurised by means of an argon gas supply which exerts a force on the solvent reservoir. The solvent flow caused by this external force on the wash bottle is controlled by means of a needle valve.

Throughout this work the solvents employed were mixtures of ether and n-hexane; both materials were obtained from May & Baker Ltd. in large enough quantities to eliminate batch variations. The squalane and methyl oleate samples were obtained from B.D.H. Ltd. and the olive oil from Boots Ltd. The sample injections were carried out with Hamilton syringes, *e.g.* 1.0, 10 and 100 μl.

Procedure

The silicic acid was obtained as a powder of particle size smaller than 100 mesh. Half the batch was sieved into suitable mesh ranges *e.g.* 100–120, 120–150, *etc.* The sieved fractions together with a quantity of the original batch were heated for 2 h at 110° and stored in stoppered bottles in a desiccator containing molecular sieve as a drying agent.

The straight column was packed by pouring silicic acid of the required mesh range into the empty column and subjecting it to mechanical vibration until no further movement of the support was observed. The coiled columns were packed by applying gas pressure to a glass vessel reservoir containing sufficient support material to fill the column. The column was connected to one end of the reservoir and the support material was blown into the column; the final packing down was done by mechanical vibration.

The columns were connected in turn to the solvent pump and a 5% v/v ether in hexane mixture was allowed to flow through them for a period of three hours before the columns were put in operation. The following experimental conditions were employed throughout this work.

Column	24″ × 4 mm I.D.
Column temperature	Ambient
Detector temperature	200°
Detector voltage	1250 V
Argon flow rate through detector	45 ml/min
Pyrolysis temperature	600°
Cleaner temperature	*ca.* 650°
Solvent evaporator	Ambient

The efficiency of squalane on silicic acid columns was investigated for various ranges of particle diameters, sample sizes and flow rates of the mobile phase on both coiled and straight columns. The resolving power of these columns was obtained for the partially resolved peaks of methyl oleate and olive oil. The efficiency (n) of the column was calculated from the relationship used in gas chromatographic calculations.

$$n = 16\,(R_v/\text{p.w.})^2 \qquad (1)$$

where n is the number of theoretical plates in the column; R_v is the retention time from the injection point to the peak maximum; and p.w. is the peak width at the base.

The height equivalent to a theoretical plate[9] was calculated from

$$\text{HETP} = \text{column length in cm}/n \qquad (2)$$

It was assumed that the plate theory employed in gas chromatography is also applicable to liquid columns. The resolving power (R)[9] for the separation of methyl oleate and olive oil was calculated from

$$R = \Delta R_v/\Sigma\text{p.w.} \qquad (3)$$

where ΔR_v is the difference in retention times of the two peaks, and Σp.w. is the sum of the peak widths at the base.

DISCUSSION OF RESULTS

Figure 5 shows a plot of HETP against the flow rate of the mobile phase for squalane on various ranges of particle size of silicic acid. The curves all follow a similar

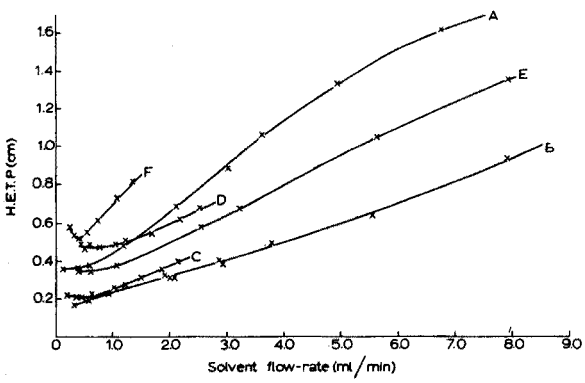

Fig. 5. The variation of HETP with solvent flow rate using different particle mesh ranges. Solvent 5% (v/v) ether in hexane; sample 0.5 μl squalane. Curve A, 100–120 mesh; B, 120–150 mesh; C, 150–170 mesh; D, 120–170 mesh; E, 100–150 mesh; F, 100 mesh powder.

pattern, passing through a minimum at flow rates between 0.5–1.0 ml/min. Assuming an effective column cross-section of 0.08 cm^2 for the mobile phase, the corresponding linear liquid velocities were 0.1–0.2 cm/sec. Curves A, B and C compare the effect of the particle mesh ranges 100–120, 120–150 and 150–170. It can be seen that the largest particle diameter gave a significantly poorer HETP than the other two. The curves B and C indicate that from a practical point of view the 120–150 mesh range can be employed over a wider range of flow rates before the column inlet pressure became excessively high, *e.g.* 120 p.s.i. Curves D and E compare the column HETP for relatively wide ranges of particle size. The column efficiency was found to be significantly lower for the smaller particles and the range of flow rates covered was restricted because of the practical limit of the pressure applied to the column inlet. The curve F shows the HETP for the range of particle size $>$100 mesh; it can be seen that the curve exhibits a very sharp minimum with a very steep gradient as the flow rate is increased, indicating a severe loss in column efficiency at the higher flow rates. Most of the curves exhibit linear regions at the higher flow rates but the curve obtained for 100–120 mesh

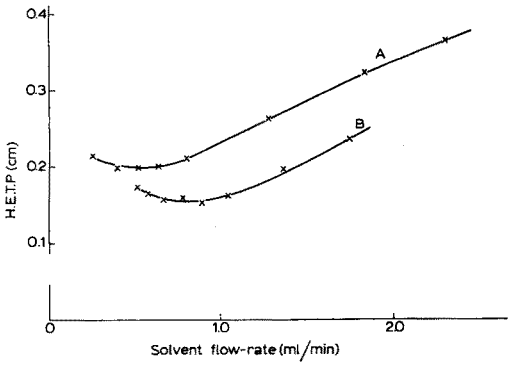

Fig. 6. The variation of HETP with solvent flow rate for coiled (A) and straight (B) columns. Solvent 5% (v/v) ether in hexane; sample 0.5 μl squalane; packing silicic acid 150–170 mesh.

shows a distinct curvature towards the flow rate axis at 5–7 ml/min. This has been predicted by KNOX[10] who has associated this phenomena with turbulence in the moving phase. It is possible that some of the other curves would have shown this effect if the flow rates could have been increased.

Figure 6 compares the HETP of coiled and straight columns of similar dimensions and under the same experimental conditions. Both curves pass through minima with linear regions at the higher flow rates. The difference between the two curves is not significant enough to assume that one is better than the other since the difference that does exist could be explained by the different packing procedures adopted. The effect of the amount of squalane on the column efficiency for a straight column is illustrated in Fig. 7; 3 curves were plotted and all passed through sharp maxima at 5–15 μl. Curves A and B show the effect of emptying and repacking the column using pure samples of squalane, i.e. variable sample size. These curves indicate the variation in column performance that can exist even when packing is done under similar conditions. Curve C was obtained by injecting constant sample sizes of solutions containing a known volume of squalane in the solvent and shows that the position of the maximum

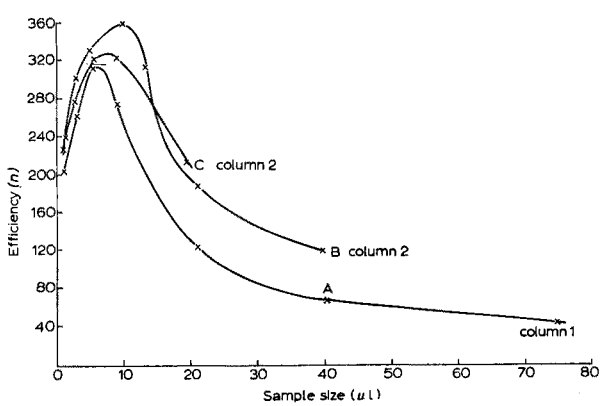

Fig. 7. The variation of efficiency with sample size of squalane. A and B injection with neat squalane; C injection with solutions of squalane.
Flow rate, 0.75 ml/min; column, silicic acid 150–170 mesh; solvent, 5% (v/v) ether in hexane.

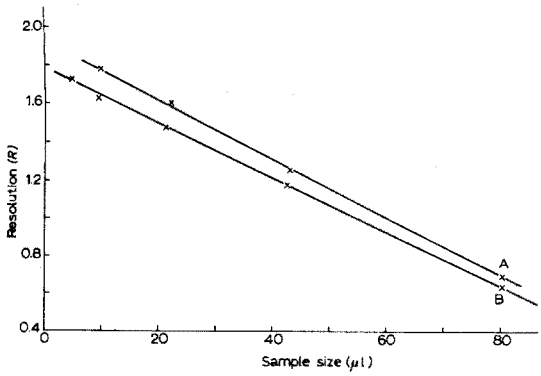

Fig. 8. The variation of resolution with sample size for straight (A) and coiled (B) columns. Sample, methyl oleate and olive oil (1:1, v/v); solvent, 7% ether in hexane; flow rate, 0.80 ml/min; column, silicic acid 150–170 mesh.

is not affected by the sample volume. Further work is being carried out to investigate the nature of these curves.

Figure 8 shows how the resolution of the partially resolved peak of methyl oleate and olive oil varies with sample size. Undiluted samples of equal volumes of the two materials were employed and it can be seen that there is a marked loss in resolution with increasing sample size for both coiled and straight columns. The curves exhibit a significant level of correlation between resolution and sample size but there is little indication of the practical advantage of one or the other.

CONCLUSION

The work described in this paper illustrates the potential of the moving wire system as a feasible method for studying the performance of liquid columns. It represents a very limited aspect of the valuable work that could be carried out with this detector. With the advent of detection devices which not only continuously monitor the column eluate but have inherent small dead volumes and high sensitivity, it is possible that liquid–liquid chromatography will soon be in a position to advance technically at the same rate as gas–liquid chromatography. The moving wire system is still in its infancy and a substantial amount of work is still needed to fully understand the detector characteristics. The results given in this paper are subjected to column and detector effects and work is in hand to evaluate quantitatively the detector effect on these results. It is hoped that the work described in this paper will stimulate interest in detector systems such as the moving wire device which will enable the optimum column performance in liquid chromatography to be realised.

The authors wish to thank Dr. R. P. W. SCOTT for his help and the directors of W. G. Pye and Co. for permission to publish this work.

SUMMARY

A detector system for liquid columns which employs a moving wire system and a gas–liquid chromatographic detector, is described. The performance of silicic

acid columns was studied by investigating the effect of particle size, sample size and flow rate of the mobile phase on the HETP of squalane for coiled and straight columns. The effect of sample size on the resolution of methyl oleate and olive oil on coiled and straight columns was also studied.

REFERENCES

1 R. P. W. SCOTT, in D. H. DESTY (ed.), *Gas Chromatography 1958*, Butterworths, London, 1958, p. 189.
2 A. I. M. KEULEMANS, *Gas Chromatography*, Reinhold, New York, 1957.
3 A. L. LEROSEN AND C. A. RIVET, JR., *Anal. Chem.*, 20 (1948) 1093.
4 H. M. STRAIN, *Anal. Chem.*, 18 (1946) 605.
5 A. L. LEROSEN, *Anal. Chem.*, 19 (1947) 189.
6 R. P. W. SCOTT, private communications.
7 A. T. JAMES, J. R. RAVENHILL AND R. P. W. SCOTT, in A. GOLDUP (ed.), *Gas Chromatography 1964*, Institute of Petroleum, London, 1964, p. 197.
8 J. E. LOVELOCK, *J. Chromatog.*, 1 (1958) 35.
9 R. P. W. SCOTT (ed.), *Gas Chromatography 1960*, Butterworths, London, 1960, p. 423.
10 J. H. KNOX, *Anal. Chem.*, 38 (1966) 253.

Analytica Chimica Acta
Elsevier Publishing Company, Amsterdam
Printed in the Netherlands.

HEATS OF PREFERENTIAL ADSORPTION OF CHELATES

M. P. T. BRADLEY AND D. A. PANTONY
Department of Metallurgy, Imperial College, London, S.W. 7 (Great Britain)

(Received November 1st, 1966)

A systematic investigation into the mechanism of adsorption of molecular organic chelates of metals on alumina and silica gel from organic solvents has been made with a view to applying results to the chromatographic separation of the metals. Among other properties, the heats of preferential adsorption have been measured and correlated with known chromatographic behaviour.

The main objectives of the work were: (a) to correlate the energetics (as heats) with the strength of the adsorption processes and with the ease of elution; (b) to correlate the heats of preferential adsorption with the two distinct stages of adsorption discovered during the course of rate studies; and (c) to provide a ready method of predicting orders of retention and possible elution of the chelates since, in general, visual inspection of the closely packed bands is inadequate for the purpose.

Theory

In an adsorption process there should be an overall heat change owing to the solute's changing its environment from the solvent to the adsorbent[1,2], provided that any displaced species does not provide an equal and opposite effect. Considering the adsorption of a chelate C from benzene solutions onto an adsorbent saturated with benzene, B, the changes in free energy caused by the adsorption of the chelate may be divided into three parts:

a) A change in free energy of the surface, ΔG_S, caused by the replacement of benzene by chelate.

b) A change in free energy associated with the decrease in concentration (activity) of the chelate in solution.

c) A change in free energy associated with the increase in concentration of benzene in solution.

If x is defined as the number of moles of chelate adsorbed, C_0 and B_0 as the original solution concentrations of chelate and benzene expressed as mole fractions respectively, C_f and B_f as the final concentrations, and A_C and A_B as the areas occupied by one mole of adsorbed chelate and benzene respectively, then the adsorption of x moles of chelate causes the displacement of $(A_C/A_B)\cdot x$ moles of benzene. Thus the change in free energy, ΔG, is given by:

$$\Delta G = \Delta G_S + xRT\ln\frac{C_f}{C_0} + \frac{A_C}{A_B}xRT\ln\frac{B_f}{B_0}$$

Therefore the heat evolved by the system, $-\Delta H$, is given by

$$-\Delta H = -\left[\Delta G_S + xRT\ln\frac{C_f}{C_0} + \frac{A_C}{A_B}\ln\frac{B_f}{B_0}\right] + T\Delta S$$

For the small volumes of very dilute solutions dealt with, the changes in free energy caused by concentration changes will be very small. Therefore:

$$-\Delta H \simeq -\Delta G_S + T\Delta S$$

Provided that the entropy changes on adsorption are small, or, more likely, for a series of compounds are of the same order[2], then the heat changes will be directly indicative of the change in free energy of the surface, and thus the order of elution of a series of similar compounds may be predicted from the order of the heats of preferential adsorption.

EXPERIMENTAL RESULTS

The experimental results are shown in Table I.

TABLE I

$-\Delta H$ (kcal mole^{-1})
S.D. $\pm$ 0.5 kcal mole^{-1}.

Cation	*2-Methyl-8-quinolinol chelates*			*8-Quinolinethiol chelates on alumina*
	On alumina	*On silica gel*	*On coated alumina*	
Fe(III)	−21.8	−31.7	−7.5	+2.4*
Ni(II)	−18.7	−31.2	−5	+3.4*
Cu(II)	−12.2	−14.6	−2.5	−2.6
Cr(III)	−10.4	− 8.6	−3.0	−5.8

A more detailed investigation of the adsorption of the iron and nickel 8-quinolinethiol chelates* indicates that the heat changes tabulated for them are for the *desorption* process. These chelates show an initial small evolution of heat, in both cases apparently amounting to approximately 1 kcal mole^{-1} which is discernible but too small for accurate measurement, followed immediately by an endothermic heat change presumably corresponding to their desorption. The desorption heat changes cannot be detected with the other chelates since they are sufficiently strongly adsorbed for the desorption step to be too slow for any heat evolution peak to be shown in the experimental conditions.

With the benzene solutions used it was established that complete retention on a chromatographic column occurred with all 2-methyl-8-quinolinol chelates. But it has been reported[3] that the chromium chelate is not adsorbed from 1+1 benzene–chloroform mixtures on an alumina column, while the chelates of iron, nickel, copper and most other elements are retained. Further investigation of the chromatographic behaviour of 2-methyl-8-quinolinol chelates has shown that the same phenomenon occurs on silica gel columns of several types[4]. With the benzene solutions of 8-quinolinethiol chelates, however, chromatographic elution of the chelates from alumina is possible in the order: Fe(III) (R_F=0.7), Ni(II) (0.6), Cu(II) (0.4), Cr(III) (0.1).

This suggests that with all these chelates a heat of preferential adsorption higher than about 6 kcal mole^{-1} corresponds to complete retention. Owing to the

unknown contribution from entropy changes, this particular value may be applicable to this type of system alone and somewhat different values could be expected when other structurally and dimensionally different molecules are investigated. Nevertheless, the method would still be applicable to these systems for internal comparisons.

During investigations of the kinetics of adsorption of these chelates it had been discovered[4] that the adsorption was a two-stage process with an abrupt change in rate characteristics at the completion of a "monolayer". Although this change corresponded to the saturation of the surface it was possible to adsorb at least a further five-fold quantity of chelate. The "coated" alumina samples were prepared by treating the alumina with a solution of chelate of such concentration that the equilibrium concentration was identical with the equilibrium concentration at a point of inflexion on the analogous adsorption isotherm corresponding to a complete monolayer of chelate. As can be seen from Table I, the heat of preferential adsorption on the coated surface is very much less than that on the clean surface.

From chromatographic studies it appears that the secondary layer is recoverable from the column, although it is a slow process and, generally, is impracticable for quantitative chromatographic elution. Clearly the whole adsorption process and its correlation with heats hinges on the first stage: here a high heat of adsorption indicates a chemical bonding during formation of a monolayer. The subsequent layers are probably retained by physical forces and the small values of their heats of adsorption are not then indicative of easy elution.

The behaviour of the copper 2-methyl-8-quinolinol chelate was investigated in further detail, since it was known that elution with solutions of 2-methyl-8-quinolinol in benzene caused selective elution of the chelate complex from alumina[5]. The heats of preferential adsorption of the copper chelate from 2-methyl-quinolinol in benzene solutions are shown graphically in Fig. 1. Quantitative recovery of the copper chelate can be achieved at reagent concentrations above approximately 0.2% when

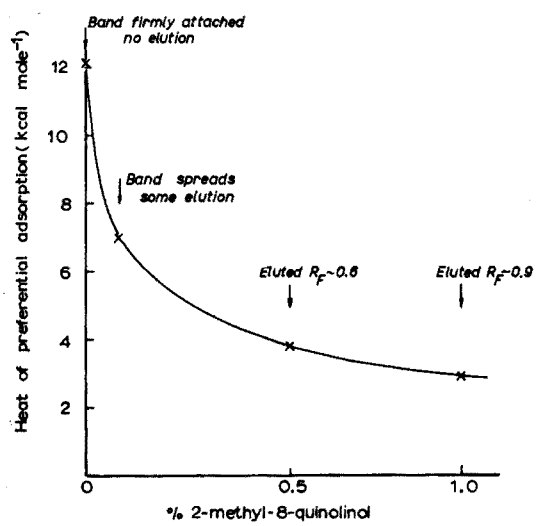

Fig. 1. Change of heats of preferential adsorption of the chelate of copper(II) and 2-methyl-8-quinolinol with changes of concentration of the reagent in chloroform–benzene.

the heat of adsorption falls below 6 kcal mole^{-1}. However, in order to render the elution practicably speedy, a concentration of 0.5% with an associated R_F value of 0.6, is chosen for analytical purposes. Higher concentrations cause spreading of certain other bands and high reagent blanks.

This tendency towards elution with reagent solutions is not shown to any marked degree by any other chelates; some spreading of the adsorbed bands is occasionally observed but the chelate is not completely removed from the column. Therefore, it is unlikely that the effect is purely the preferential adsorption of the reagent, which would be expected to affect all the chelates, especially that of chromium which exhibits a lower heat of preferential adsorption from benzene than does the copper chelate. Also, if this were the case, it would be expected that the effect of the reagent would be more marked if the adsorption took place from a dilute reagent solution, rather than from benzene with subsequent elution with dilute reagent solution. No such differences were noticeable chromatographically and it must be assumed that the reagent effect is more complicated.

The copper complex shows other interesting properties that may be relevant. For example, it forms a brown dihydrate readily losing water to give the green anhydrous compound $Cu(C_{10}H_8NO)_2$ on air-drying at 120°. Also, use of Job's method of continuous variations shows that a triligand complex $Cu(C_{10}H_8NO)_3$ is formed from copper(II) chloride and 8-quinolinol in ethanol solutions. Clearly the polar positions of the potentially octahedrally coordinated copper(II) ion must be active in these compounds and it may well be that intermediate formation of a triligand complex is involved in the elution of copper(II) 8-quinolinol chelate with organic solutions of the reagent.

EXPERIMENTAL

Apparatus

The calorimeter used for these studies was constructed according to GROSZEK's specification[6] and the whole apparatus and stock solutions, solvents, *etc.*, were kept in a room at a set temperature of 25±2°. The solvent system was controlled via a constant-delivery but adjustable peristaltic pump (H.R. Flow Inducer, Watson Marlow Air Pump Company, Marlow) and was so designed that the solvent flow passed through an annular jacket around the sample and thus allowed the sample to be in thermal equilibrium with the flowing solvent. Tests carried out by injecting benzene into a benzene flow showed that with this system, the heat effects caused by injecting a solvent sample into the solvent flow within the calorimeter were less than 2% of the heat effects observed during preferential adsorption of the metal chelates.

By using fused alumina, which has a negligible adsorption capacity for the metal chelates, it was also shown that the heat changes caused by injecting chelate samples were similar to those caused by injecting pure solvent into the solvent stream. This indicates that there were no significant dilution effects, as was to be expected since the chelate samples used were in the concentration range 10^{-2} to 10^{-3} *M*.

The change in resistance of the thermistors in the calorimeter was measured by means of a Wheatstone Bridge (Fig. 2) where the change in potential across the resistance R was measured and amplified such that 100 μV was equated to 2 mV, which was the full-scale deflection of the pen-potentiometric recorder (Leeds and

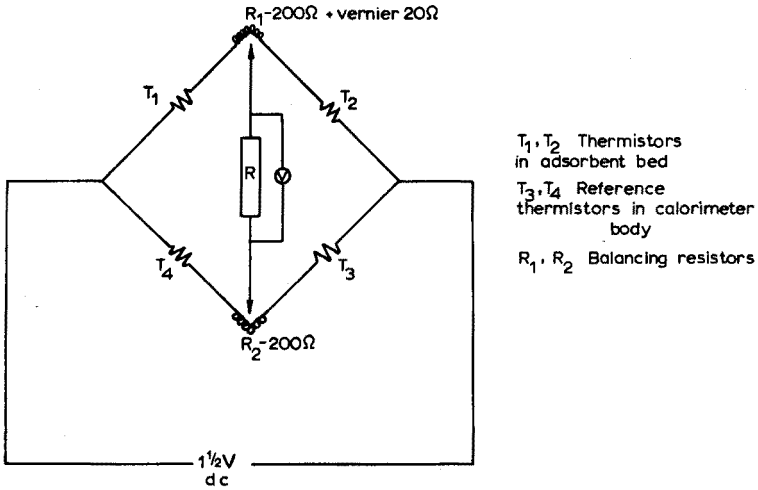

Fig. 2. Bridge circuit for measuring resistance changes in calorimeter.

Northrup model W with A.Z.A.R. attachment) used for presentation of resistance and, hence, thermal changes. The expedients used to equilibrate solutions and solvents also served to provide an excellently steady base line in the recorder. Since the base line was adjusted by means of the A.Z.A.R. to approximately centre scale, it was impossible to use the commercial Leeds & Northrup analogue integrator, which integrates from the mechanical zero of the pen. This meant that the heats of preferential adsorption were calculated from peak heights above the base line, but as the peaks were approximately isosceles triangles, and estimations of the heats of preferential adsorption calculated from manually integrated areas agreed, this method appeared to cause but slight loss of accuracy.

The calorimetric value of the observed heats of preferential adsorption were determined by reproducing the observed peaks with a 1 × 0.1 cm 2-Ω heater which was coiled into a flat spiral and inserted in the adsorbent bed. Known voltages could be supplied by means of a Solatron constant D.C. voltage source, type PSO AS 1412.

Preparation of metal chelates

The 2-methyl-8-quinolinol[7] and 8-quinolinethiol[8] chelates were prepared by standard methods. All the chelates were dried thoroughly, under vacuum in the case of those of 8-quinolinethiol. The chelates prepared in this manner were homogeneous and apparently quite stable: although aqueous dioxan solutions of the 8-quinolinethiol chelates are known to oxidise easily[9], benzene solutions of the dry chelates appear to be stable for at least 24 h.

CONCLUSION

In conclusion, heats of preferential adsorption are clearly closely correlated with strengths of adsorption of organic chelates of metals from organic solutions, so much so that it is possible to predict chromatographic behaviour from measurement of these heats.

The authors wish to express their thanks to Aerospace Research Laboratories for sponsorship of this research through the European Office of Aerospace Research (OAR) United States Air Force under Contract No. AF61(052)663, and for the maintenance grant to M.P.T.B.

SUMMARY

A method employing a flow calorimeter for determining heats of preferential adsorption of certain organic chelates of metals from organic solutions is described. Experimental heats of adsorption are correlated with the chromatographic behaviour of the chelates and it is shown that irreversible retention on a column occurs when the heat is greater than 6 kcal mole^{-1} for the first stage of the two-stage adsorption process. The special case of the 2-methyl-8-quinoline chelate of copper(II) and its elution with solutions of the reagent is examined in more detail: heats of preferential adsorption decrease with increasing concentrations of reagent and the optimum experimental concentration can be predicted from the heat results.

REFERENCES

1 F. E. Bartell and Fu Ying, *J. Phys. Chem.*, 33 (1929) 1758.
2 T. H. De Boer, *The Dynamical Character of Adsorption*, Oxford Univ. Press, London, 1953, p. 48, 100.
3 A. J. Blair and D. A. Pantony, *Anal. Chim. Acta*, 13 (1953) 1.
4 M. P. T. Bradley and D. A. Pantony, unpublished work.
5 A. J. Blair and D. A. Pantony, *Anal. Chim. Acta*, 16 (1957) 121.
6 A. J. Groszek, *Trans. Am. Soc. Lubrication Eng.*, 5 (1962) 105.
7 F. J. Welcher, *Organic Analytical Reagents, Vol. 1*, pp. 264 *et seq.*
8 J. H. W. Dalziel and D. Kealey, *Analyst*, 89 (1964) 411.
9 A. Corsini, Q. Fernando and H. Freiser, *Anal. Chem.*, 35 (1963) 1424.

Analtyica Chimica Acta
Elsevier Publishing Company, Amsterdam
Printed in the Netherlands.

THE DETERMINATION OF NORMAL PARAFFINS IN PETROLEUM PRODUCTS

J. V. MORTIMER AND L. A. LUKE
The British Petroleum Company Ltd., BP Research Centre, Sunbury-on-Thames, Middlesex (Great Britain)

(Received November 1st, 1966)

Gas chromatography is commonly used to obtain complete individual component analyses of light boiling distillates from crude oils[1-3] and the concentrations of normal paraffins up to normal octane are available from these analyses. However, chromatograms of distillates containing normal paraffins of higher carbon numbers are usually so complex that, at best, the normal paraffins elute together with other components in composite peaks whilst, in less favourable instances, the normal paraffins appear as prominent peaks above an envelope containing a multitude of unresolved components.

Methods involving a subtractive technique[4,5] have been developed for analysing these complex samples: the sample is eluted through a column to obtain a total chromatogram and then eluted again through the same column in series with a short precolumn packed with 5A-type molecular sieve. The sieve absorbs the normal paraffins in the gas stream and the second chromatogram represents only the non-linear hydrocarbons. Thus, provided that the operating conditions are identical for both chromatograms, and this is not difficult to achieve with isothermal operation, one chromatogram may be superimposed upon the other and the areas representing normal paraffins may be estimated by difference.

The subtractive technique is fairly satisfactory for the determination of normal paraffins of up to about 24 carbon atoms, but it does presuppose either that the detector responses to the normal paraffins and to the non-linear hydrocarbons are the same or that the relative responses may be easily established. In practice, calibration to allow for differences in responses is only undertaken when fractions from the same crude source are analysed frequently, as for example, when a gas oil is used as a process feedstock.

The subtractive technique is far less satisfactory for the analysis of distillates containing normal paraffins beyond tetracosane. If the boiling range is greater than about 150°, programmed-temperature gas chromatography must be used and it is then far more difficult to obtain pairs of chromatograms which correspond exactly when superimposed. Above triacontane the subtractive technique becomes unusable because, not only are the concentrations of the normal paraffins small, but the normal paraffins are close boiling and consequently less well resolved than in the lower boiling distillates. These two factors combine to make it impossible to attribute the small differences between the two chromatograms to individual components with any confidence.

A method for the estimation of the concentrations of normal paraffins in distillates boiling above 371° has recently been developed by BRUNNOCK[6]. The method consists in absorbing the normal paraffins by refluxing benzene solutions of the distillates with pelleted 5A-type molecular sieve. After refluxing, the sieve is washed free of unabsorbed material and the sieve structure is destroyed by treatment with hydrofluoric acid. This releases the normal paraffins which are recovered quantitatively and analysed using programmed-temperature gas chromatography. However, the disadvantage of this method is the elapsed time required which is normally about 4 days.

This present paper describes a modified version of Brunnock's method in which the normal paraffins are absorbed from a few milligrams of sample in the vapour phase. The new method can be completed in 2–4 h and is applicable to crude oil distillates boiling within the range 170–500°.

EXPERIMENTAL

The analytical procedure may be conveniently divided into two parts:

(a) the extraction of the normal paraffins from the sample and their subsequent recovery from the sieve;

(b) the gas chromatographic analysis of the recovered normal paraffins.

The first part of this procedure will be described and discussed in detail. The second part will only be covered briefly as it involves standard gas chromatographic practice.

The extraction and recovery of the normal paraffins

The normal paraffins are absorbed from the sample in the vapour phase by 5A-type molecular sieve in a microabsorber unit (Fig. 1). This consists of a Pyrex glass tube, length 15 cm, I.D. 3 mm, O.D. 6 mm, which is narrowed at one end to an

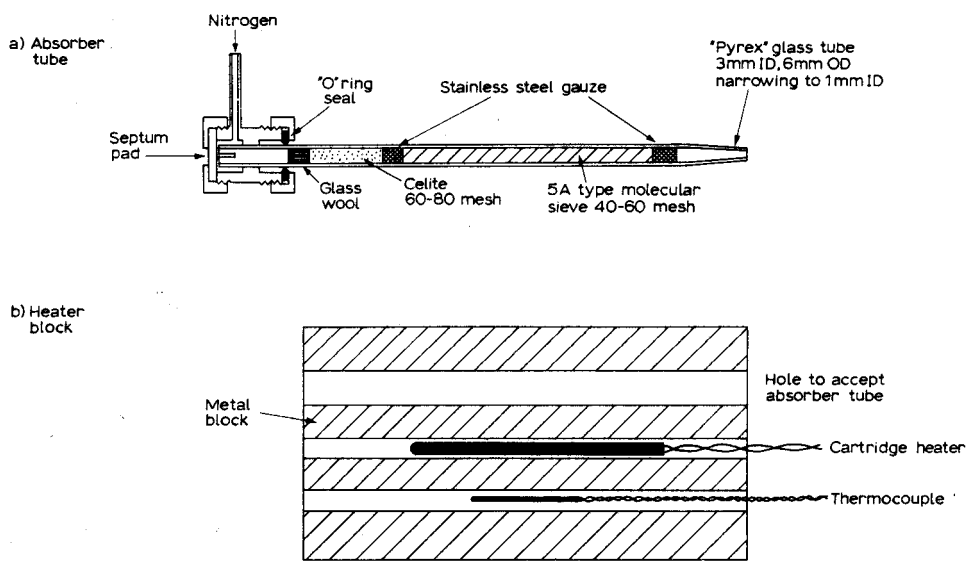

Fig. 1. Absorber unit.

I.D. of 1 mm. The other end is slotted to a depth of 3 mm. This tube is packed with a 2-cm length of 60–80 mesh celite and a 7-cm length of 40–60 mesh 5A-type molecular sieve (400 mg or 40 times the anticipated weight of normal paraffins), these materials being separated and held in position by small quantities of glass wool and stainless steel gauze.

A brass union with an "O" ring seal is used to hold a septum pad against the slotted end of the glass tube. This union is drilled to take the metal nitrogen inlet tube and the gas flows through the union, enters the glass tube via the slot, sweeps the face of the septum pad and passes through the celite and molecular sieve packings. Finally the gas leaves the tube at the narrowed end where the gas velocity is high and thus minimises condensation. The absorber tube fits into a lagged metal block drilled to accept a 175-W cartridge heater and a thermocouple. The power to the heater is controlled by a variac transformer and the thermocouple is connected to a pyrometer.

A normal paraffin, outside the range of the normal paraffins present in the sample, is blended quantitatively into the sample to serve as an internal standard. This presupposes some knowledge of the sample composition which, if necessary, must be gained from a chromatogram of the total sample. A high programming rate can normally be used for this exploratory analysis which need not add excessively to the overall analysis time.

If the blend of sample and internal standard is solid it is dissolved in iso-octane or cyclohexane and, with nitrogen passing through the absorber unit at 10 ml/min, a volume of sample, judged to contain *ca.* 10 mg of normal paraffins, is injected sufficiently deeply into the celite packing to ensure that it will be in the hot zone. The power to the heater is then switched on and the variac is set to give sufficient voltage to cause the block temperature to rise from ambient to 300° in 20 min and then to be maintained at that temperature.

When smoke stops issuing from the end of the absorber tube it is assumed that all the non-linear hydrocarbons have been eluted. The absorber tube is removed from the heater block and allowed to cool with nitrogen still passing through the sieve in order to prevent any water condensation. Then the molecular sieve is removed from the absorber tube and added to 1 ml of water in a 4-ml screw-capped glass vial which has been cooled in solid carbon dioxide so that the heat evolved is removed rapidly. The sieve sinks and the vial is left in the coolant until the water freezes. Hydrofluoric acid (1 ml of 40%) is added on top of the ice so that it can not react with the sieve before the screw-cap is replaced. By allowing the vial to warm just sufficiently to melt the ice and then gently agitating by hand with further cooling as necessary, most of the heat of reaction is dissipated. The vial is then shaken gently in a mechanical shaker for a further 30 min to ensure that the sieve structure is completely destroyed. (Excessively vigorous shaking should be avoided as this breaks the sieve into a fine powder which is difficult to separate from the hydrocarbon layer later.)

The normal paraffins are extracted from the acid treated sieve by adding 0.3 ml of iso-octane together with a pellet of potassium hydroxide which neutralizes the excess acid. This is followed by mechanical shaking for 15 min and centrifuging, when the iso-octane solution separates as a clear layer on top of the alkali/sieve slurry.

Gas chromatographic analysis of the recovered normal paraffins

The chromatograph used was a Microtek Model 2000R fitted with dual columns

and a dual flame ionisation detector. However, any programmed temperature instrument capable of operation up to 350° would be suitable. Several sets of operating conditions were tried but finally those detailed below were chosen as being suitable for separations of normal paraffins in the C_{10}–C_{40} range. Column: 3 ft × $^1/_8$ in. O.D. stainless steel; 2.5% (w/w) silicone gum on 60–100 mesh celite. Temperature programme: initial hold, 50° for 2 min (unless otherwise stated); programme, 6.5°/min. Carrier gas and inlet pressure: He at 110 p.s.i.g. Flow rate: constant at 140 ml/min. Hydrogen flow rate: 50 ml/min. Air flow rate: 500 ml/min. Sample: 1 μl of isooctane solution. However, the carrier gas, fuel gas and air flow rates required to ensure that the detector response to all the normal paraffins is equal throughout the range will differ from one instrument to another. The suitability of particular flow rates may be checked by analyzing synthetic blends of pure components.

A suitable volume of the isooctane solution (1 μl in the case of the chromatograph used) is analysed and the peak areas on the chromatogram are measured using

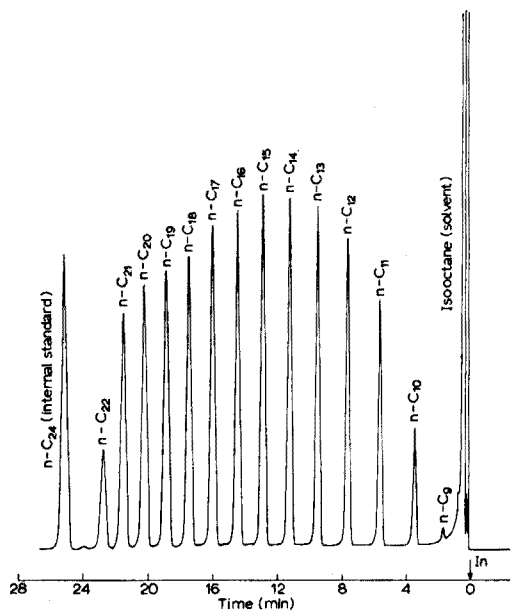

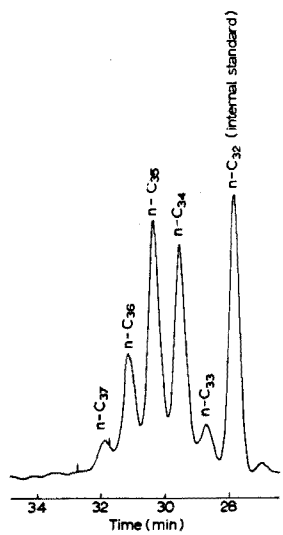

Fig. 2. Chromatogram of normal paraffins extracted from light gas oil (initial hold: 35° for 2 min).

Fig. 3. Chromatogram of normal paraffins extracted from 490°–510° fraction of Middle East crude oil.

an electronic integrator. The areas of the individual normal paraffin peaks are compared with the area obtained for the internal standard and, assuming the areas to be proportional to weight per cent, their concentrations in the original sample are calculated from the known blended concentration of the standard. The position of the standard in the chromatogram also serves as a marker for the identification of the other peaks.

Examples of the chromatograms obtained using this procedure are given in

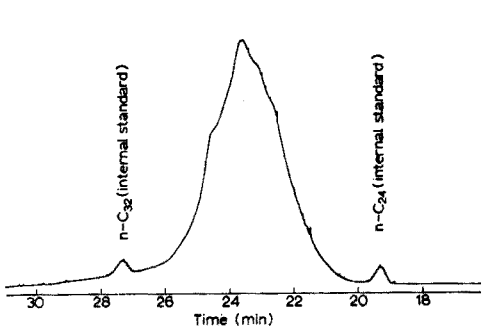

Fig. 4. Chromatogram of 430°–450° fraction of Middle East crude oil.

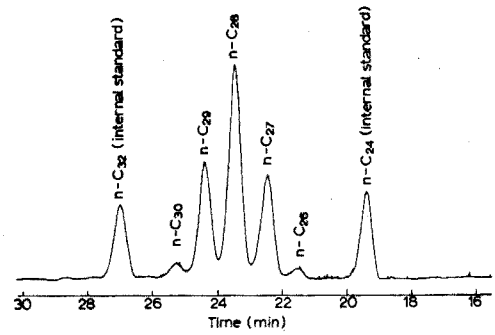

Fig. 5. Chromatogram of normal paraffins extracted from 430°–450° fraction of Middle East crude oil.

Figs. 2, 3 and 5. In Fig. 2 the sample was a light gas oil to which 6.8% (w/w) tetracosane had been added as internal standard while Fig. 5 shows the chromatogram obtained from the analysis of a 430–450° vacuum distillate to which had been added 1.2% and 1.1% (w/w) tetracosane and dotriacontane respectively. In Fig. 3 the sample was a 490–510° vacuum distillate to which 1.2% (w/w) dotriacontane had been added. Figure 4 is a chromatogram of the blend of internal standards and distillate corresponding to the chromatogram shown in Fig. 5.

ESTIMATE OF PRECISION

A mixture of normal paraffins in the C_{12}–C_{18} range was blended quantitatively into a denormalised gas oil at five concentration levels ranging from 12 to 36% (w/w) (Table I). Five samples of each blend were analysed in duplicate randomly over a

TABLE I

TOTAL NORMAL PARAFFIN CONTENTS OF GAS OIL BLENDS: SUMMARY OF RESULTS (%-wt)

Blend	*Blended concentration of normal paraffins*	*Mean value from 5 replicate analyses*	*Repeatability*[a]	*Long-term precision*[b]	*Reassessment of precision*[c]
A	12.10	12.28			
B	20.03	19.93			
C	24.83	25.00	1.3	2.6	1.6
D	30.73	30.71			
E	36.93	36.80			

[a] Repeatability: The difference between two results obtained in immediate succession (95% confidence limit).
[b] Long-term precision: The difference between two results obtained within a period similar to the duration of the programme (*i.e.* 25 days) with a 95% confidence limit.
[c] Reassessment of precision: An estimate of precision based on gas chromatographic analyses, performed within 2 days, of 10 of the solutions of normal paraffins extracted from blends B and C during the programme used to assess the repeatability and long-term precision. The analyses obtained on the 5 solutions from Blend C are given in Table II.

TABLE II

INDIVIDUAL NORMAL PARAFFIN CONTENTS OF GAS OIL BLEND C[a] (%-wt)

Analysis	*Normal paraffin*							*Total normal paraffin content*
	C_{12}	C_{13}	C_{14}	C_{15}	C_{16}	C_{17}	C_{18}	
1	0.02	0.63	3.61	7.22	6.68	5.17	0.54	23.87
2	0.08	0.73	3.91	7.73	7.05	5.28	0.55	25.43
3	0.04	0.67	3.81	7.58	6.91	5.22	0.54	24.77
4	0.06	0.65	3.63	7.38	6.77	5.08	0.55	24.12
5	0.03	0.72	3.68	7.39	6.76	5.08	0.60	24.26

[a] 24.83% (w/w) of mixture of normal paraffins blended into a denormalized gas oil.

period of 25 working days and the repeatability and long-term precision figures for the determination of the total normal paraffin concentrations were estimated.

In the statistical appraisal, one of the 25 pairs of results was rejected as being obviously in error. The overall repeatability obtained from the remainder was 1.3% (w/w) which was very satisfactory and the means of the determined total concentrations of the normal paraffins in the blends agreed well with the blended values (Table I). However, the value obtained for the long-term precision was 2.6% (w/w) which was surprisingly poor and warranted further investigation.

The variance in the long-term precision might have been associated with either the normal paraffin extraction stage or with the gas chromatographic analyses of the extracted normal paraffins. Consequently, one of each of the replicate pairs of solutions of extracted normal paraffins from blends B and C, *i.e.*, 10 solutions in all, was re-analysed chromatographically. This time all the chromatographic determinations were completed in two days and the precision figure obtained was 1.6% which was only a little in excess of that obtained previously for the repeatability. Thus, as the isooctane solutions represented extractions obtained over an 18-working day period, it was most likely that the variance in the long-term precision was associated mainly with the gas chromatographic analyses.

A blend of normal paraffins of carbon numbers 13, 17, 20 and 24 was then analysed on the gas chromatograph and it was found that the peak areas representing the normal paraffins were not proportional to the blended weight concentrations. Furthermore, repeat determinations indicated that the relative responses of the detector to the various normal paraffins were very sensitive to small changes in the flow rate of the carrier gas. The flow controllers for the carrier gas were checked and then various hydrogen and carrier gas flow rates were used to analyse the blend of normal paraffins until a set of conditions was established which gave equal response for all the normal paraffins. These conditions are now used for determinations of normal paraffins in gas oils and a blend is analysed periodically to ensure repeatable detector response at all times.

DISCUSSION

The procedure described overcomes the disadvantages of subtractive methods

based on the work of BRENNER AND COATES[4] and WHITTAM[5] and requires less time than the procedure used by BRUNNOCK[6]. It provides accurate estimates of the normal paraffins in light and heavy gas oils and distillates to 500°, being suitable for samples containing normal paraffins ranging from nonane to tetracontane. Lighter boiling normal paraffins tend to be lost by evaporation and quantitative recovery from the sieve depends on ensuring that hydrocarbon is not lost during the dissipation of the initial heat of reaction. The procedure has not been tested for samples containing normal paraffins above C_{40} because of a lack of high-purity, high-boiling normal paraffins.

Figures 2, 3 and 5 illustrate the simplicity of the chromatograms obtained using this procedure and the normal paraffins can be easily estimated. The chromatogram in Fig. 3 should be compared with that in Fig. 4 which clearly illustrates how impracticable it would have been to have attempted to estimate the normal paraffins from a chromatogram of the original sample.

The statistical programme on the gas oil blends was aimed at measuring the precision of the determined total normal paraffin contents. No effort was made to distinguish between the variances associated with the two parts of the analysis in the original statistical design. Thus, when the repeatability, based on the daily replicates, was half the long-term precision figure it was necessary to establish which stage of the procedure was causing the excessive error. From the results of the additional work it was obvious that the trouble was associated with the gas chromatographic analyses (attributed to a faulty flow controller) and that the precision of the absorption and recovery of the normal paraffins was acceptable. Although ideally the whole statistically designed programme should have been repeated using more carefully controlled chromatographic conditions, it was felt that the extra work required could not be justified.

This paper has concentrated on the novel aspects of the procedure and has largely neglected discussion of the gas chromatographic techniques involved. The application of programmed-temperature gas chromatography to high-boiling petroleum fractions is used for routine analysis in many laboratories where the pitfalls are well known. For those who have had little or no experience in this field it must suffice here to mention the three major causes of error.

1. It is not easy to introduce a small representative sample of a fraction of wide boiling range into a gas chromatograph fitted with a vaporization chamber, particularly if the sample is of a waxy nature and has been taken up in a low boiling solvent. This is because, in addition to the volume of sample delivered as the syringe plunger is depressed, the solvent and lighter components in the needle evaporate if the needle becomes hot leaving the heavier components which are removed with the syringe. It is far more satisfactory to use direct on-column injection where the sample is placed in the column packing and evaporation from the needle is negligible.

2. The hydrogen flame ionization detector can give responses which are close (but rarely equal) to weight per cent proportionality for most hydrocarbons but, under unfavourable operating conditions, the responses can vary considerably[2]. Even for homologous series, such as the normal paraffins, the responses can vary considerably during temperature programming of the column unless the flow rate of the carrier gas through the detector is maintained absolutely constant.

3. The presence of peak "ghosting" is the scourge of programmed-temperature

gas chromatography and is due to a portion of a sample being trapped or adsorbed in the system and subsequently released during later analyses. The trouble normally occurs in the injection system where the pressure increases and decreases with increase and decrease of column temperature if the flow rate is constant. Fortunately, "ghosting" is not usually serious if a vaporizing chamber is not used.

The best way to ensure that the gas chromatography is giving the correct answer in the procedure described is to analyse periodically a blend of normal paraffins and estimate the relative response factors for each component. If they are not all between 0.95 and 1.05 then the trouble is almost certainly due to one of the three sources of error discussed above.

The authors wish to acknowledge the value of discussions with Mr. J. V. BRUNNOCK. Permission to publish this paper has been given by The British Petroleum Company Limited.

SUMMARY

A normal paraffin, outside the carbon number range of the sample, is quantitatively added to the sample as an internal standard, and 10–100 μl of the mixture are injected into a small absorber unit which contains 400 mg of activated molecular sieve. The temperature of the absorber unit is raised from ambient to 300° at about 15°/min while nitrogen is passed. This elutes the non-linear hydrocarbons but leaves the normal paraffins absorbed. The sieve is removed from the absorber unit and the paraffins are released by destroying the sieve structure with hydrofluoric acid. A pellet of potassium hydroxide is then added to neutralise the excess acid and the released normal paraffins are extracted in 0.3 ml of isooctane. This isooctane solution is examined on a programmed-temperature chromatograph; the chromatogram obtained consists of a solvent peak followed by well-resolved peaks representing the normal paraffins. These are easily measured and the concentrations of the normal paraffins in the original sample are calculated against the internal standard.

REFERENCES

1 R. L. MARTIN AND J. C. WINTERS, *Anal. Chem.*, 31 (1959) 1954.
2 N. G. MCTAGGART AND J. V. MORTIMER, *J. Inst. Petrol.*, 50 (1964) 255.
3 A. G. POLGAR, J. J. HOLST AND S. GROENNINGS, *Anal. Chem.*, 34 (1962) 1226.
4 N. BRENNER AND V. J. COATES, *Nature*, 181 (1958) 1401.
5 B. T. WHITTAM, *Nature*, 182 (1958) 391.
6 J. V. BRUNNOCK, *Anal. Chem.*, 38 (1966) 1648.

Analytica Chimica Acta
Elsevier Publishing Company, Amsterdam
Printed in the Netherlands.

CORRELATIONS IN THE PARTITION THIN-LAYER CHROMATOGRAPHY OF ALKALI METALS

GILBERT E. JANAUER, ROBERT C. JOHNSTON, ANTHONY J. OLIVERI* AND JOHN CARRANO*
State University of New York at Binghamton, Binghamton, N.Y. 13901 (U.S.A.)

(Received November 1st, 1966)

Differential migration of inorganic ions on a thin layer of silica gel may be caused by differences in adsorption, partition, ion-exchange selectivity, tendency for complex formation, and in size[1,2] (mechanical exclusion). Often, several mechanisms may operate and it may be difficult to establish which prevails. The physical state, and the role in chromatographic separations of the stationary water adsorbed on silica gel have been the subject of numerous investigations[3–7]. Certain predictions are thus possible, but the properties of the stationary water phase are, at any given water content, not solely determined by the physical properties of the silica gel. Physical and chemical properties of solutes and eluants are both important and various possible interactions[8] can drastically change the state of the stationary phase (*e.g.*, by hydrogen bonding). Ion exchange and/or complex formation are probably of prime importance in the TLC separation of inorganic ions on silica gel[9]. However, other mechanisms must always be considered possible and only a detailed study may reveal the true physical picture for any particular case. Systematic studies of the chromatographic behavior of fairly simple homologous series of inorganic ions under carefully controlled and varied conditions might provide useful information. Among such series the alkali group seems to offer some advantages (in addition, this group presents a challenge to the separations chemist). Alkali ions have a single charge, increasing (and relatively large) ionic radii and little tendency for complex formation. Fundamental research work on the interaction of alkali ions with silica gels in aqueous systems has been carried out[10–12] and some analytical separations have been reported[13–16].

In the present paper an attempt is made to correlate some results obtained in the partition TLC of alkali polyiodides on silica gel with bulk extraction data and with general constants (ionic radii, free energy of hydration, dielectric constant of the solvent). Some unusual features of the polyiodide system are discussed.

EXPERIMENTAL

Equipment

Ribbed glass plates 2 × 8″ and 8 × 8″, plain glass plates 2 × 6″, Lang-Levy micropipettes of 2-μl and 5-μl capacity (Research Specialties Co.), filament tape 0.2-mm thick, modified Photovolt densitometer with sensing head positioned to accept

* Undergraduate research participants at State University of New York at Binghamton, 1966.

light transmitted through a plate from a collimated beam approximately 1 mm in diameter, a Perkin–Elmer Model 303 atomic absorption spectrophotometer with OSRAM arc discharge lamps (Na, K, Rb, Cs); Dipole meter DM-01 WTW with associated cells.

Materials

All chemicals used were of reagent grade. The adsorbent was Silica Gel Plain (Research Specialities Co.). Nitrobenzene and other solvents used were of reagent grade. A commercial grade of diethylene glycol was used.

Procedures

Thin-layer chromatography. Except in those experiments involving measurements of phase relations, all chromatographic determinations were performed with ribbed glass plates[13]. The runs in which phase volumes were determined were carried out on the 2 × 6″ plain glass plates as follows.

Two thicknesses of filament tape *ca.* 5 mm wide were fixed to each side of the plates which had been cleaned in chromic acid, rinsed in distilled water and dried. An aqueous slurry of silica gel (30 g in 105 ml water) was poured over the plate and the excess removed by drawing a glass rod over the plate. The plates were then air dried, the tape removed and the excess gel scraped off leaving an area *ca.* 3.2 × 13 cm. The plates were then dried for 60 min at 105°, cooled in a desiccator over concentrated sulfuric acid, and covered with a plate (2 × 6″ plate with a narrow thick strip of plastic insulating tape around three sides as a spacer to prevent contact with the gel). The covered plates were weighed, and equilibrated in a closed vessel over water–diethylene glycol for at least 12 h; the proportion of glycol to water was varied to give a range of relative humidities so that the resulting moisture in the gel varied from 0.015 g cm^{-2} (6–7% on the dried gel) to 0.2 g cm^{-2} (80% on the dried gel). Immediately after removal from the vessels, the plates were covered and reweighed. The cover glass was then moved to expose 2 cm of the gel and 2 μl of a 0.1 *M* solution of the alkali iodide in methanol/water (9:1, v/v) was spotted 2 cm from the bottom. This procedure resulted in no significant moisture change in the unexposed portion of the plate. The cover was positioned 1 cm from the bottom of the plate and clamped to the plate with a strong spring clip. The covered plate was then placed in a trough containing 0.1 *M* iodine in nitrobenzene to a depth of 3 mm. Development was continued until the solvent front had risen 10 cm. After weighing, the cover was removed and the solvent rapidly evaporated with the aid of heat and impinging air. The spot was revisualized by placing in an atmosphere of iodine vapor. The plate was again covered and the peak position determined with a densitometer.

The concentration at the peak was determined by scanning the area of the spot with the densitometer and recording the optical density readings at 0.1″ intervals. Background optical density readings were subtracted and the corrected values were summed. On the assumption that all the solute originally placed on the plate is in the spot after development, the concentration (in amount of solute per unit area) at the peak was given by the product of the corrected density at the peak (highest optical density value) and the amount of solute spotted, divided by the summation of all optical density values.

The weight of the silica gel was determined from an additional weighing after the silica gel was removed.

Bulk extractions. Bulk partition coefficients were determined[17] over a range of phase ratios and of concentration paralleling those on the chromatographic plate.

Transport water. Water present in 0.1 *M* iodine–nitrobenzene solution after contacting for 30 min with aqueous 0.1 *M* alkali iodide solution was determined by measuring the volume of hydrogen evolved by reaction with calcium hydride[18].

Dielectric constant measurements. Dielectric constants of the following solvents and mixtures of solvents were determined by means of the Dipolemeter: 20–80, 40–60, 60–40, 80–20, and 90–10% (v/v) mixtures of nitrobenzene–benzene, nitrobenzene–carbon tetrachloride, nitromethane–benzene, and nitromethane–carbon tetrachloride; acetone, benzaldehyde, benzonitrile, benzyl alcohol, dichlorobenzene, ethanol, n-amyl alcohol, nitrobenzene, nitroethane, nitromethane, and *m*-chloroaniline.

Iodine (0.1 *M*) was dissolved in each of the above solvents and used for the development of silica gel plates containing 5-μl spots of 0.04 *M* lithium iodide, sodium iodide, potassium iodide, rubidium iodide, and ammonium iodide. R_F values were determined in the usual manner.

RESULTS AND DISCUSSION

R_M values

Curve 1 of Fig. 1 shows R_M values (calculated from the average R_F of several repetitive runs) obtained in the polyiodide system (0.1 *M* iodine–nitrobenzene) on air-moist silica gel as a function of the crystallographic radii of the alkali ions. The

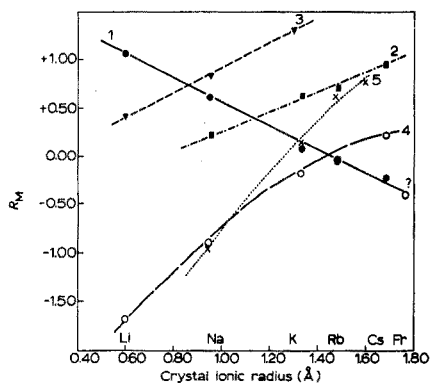

Fig. 1. Correlation of crystal ionic radii with experimental R_M values. (1) Results of present authors, using silica gel and nitrobenzene–iodine; (2) DRUDING[14], using silica gel and 5% 2 *M* HCl in tert-butanol; (3) SEILER AND ROTHWEILER[15], using 1% glacial acetic acid–absolute ethanol on silica gel; (4) DRUDING[14], using 5% glacial acetic acid–ethanol on silica gel; (5) LESIGANG[16] using ammonium phosphomolybdate–asbestos layer and 1 *M* NH_4NO_3 as the developer.

correlation seems good and a separation of francium from cesium in the same system is tentatively predicted.

Curves 2 to 5 connect R_M values calculated from R_F values reported by (or estimated from graphs of) other authors[14–16]. Any quantitative comparison of R_M values obtained under such widely different conditions would be meaningless, but some qualitative conclusions may be reached. It is obvious from Fig. 1 that our

experimental R_M values and those of other authors exhibit practically opposite trends, which indicates that a different separation mechanism is operative. However, when the R_M values of curves 2 to 5 are plotted against the *hydrated* ionic radii then R_M decreases linearly with the hydrated ionic radii just as curve 1 does with the crystallographic radii. Thus R_M for all conditions but ours follows the familiar Hofmeister lyotropic series. This is strong evidence for a cation-exchange mechanism[19]. Ammonium phosphomolybdate (curve 5) is widely used as an inorganic cation exchanger and there can be no doubt about the separation mechanism. TIEN[11] and MAATMAN[10] have shown that the natural order of alkali ion-exchange selectivities ($Cs^+ > Rb^+ > K^+ > Na^+ > Li^+$) is obtained on silica gels. Therefore, under our conditions (0.1 *M* iodine–nitrobenzene, slightly acidic conditions) an ion-exchange mechanism cannot account for the sequence of elution found. If TIEN's arguments are followed further it is also unlikely that a true adsorption on the (solid) silica surface would lead to the order of R_F values obtained. However, if certain extraction studies[20] are considered and if it is assumed that water structure-enforced ion pairs between alkali ions and bulky anions (polyiodide) are formed[21], the following crude picture of a partition mechanism may be formulated:

$$[M(H_2O)_n]^+_{SP} + PI^-_{SP} \rightleftharpoons [M(H_2O)^+_{(n-m)}PI^-]_{SP} + m\,HO_{SP} \qquad (1)$$

$$[M(H_2O)^+_{(n-m)}PI^-]_{SP} \rightleftharpoons [M(H_2O)^+_{(n-m)}PI^-]_{MP} \qquad \text{(phase transfer)} \qquad (2)$$

$$[M(H_2O)^+_{n-m}PI^-]_{MP} + x\,S \rightleftharpoons [M(H_2O)_{(n-m)}S_{x-y}]^+_{MP} + [PI^-S_y]^-_{MP} \qquad (3)$$

where SP = stationary phase; MP = mobile phase; M^+ = alkali metal ion; PI^- = (any) polyiodide ion, *e.g.*, I_3^-; S = organic solvent molecule; n = hydration number of metal ion in stationary phase; m = number of water molecules lost on ion pairing and phase transfer.

The stabilities of water structure-enforced ion pairs formed between a given bulky anion and the alkali group cations can be expected to increase with increasing size (structure-breaking effect) of the cation[21,22] (these are *not* Bjerrum-type ion pairs), which corresponds to increasing bulk extraction coefficients, and increasing R_F values from lithium to cesium in the present experiments. The most important contributions to the (overall) free energy of phase transfer may be [from (1) to (3)]

(a) the free energy of hydration of M^+ (partially or totally lost)
(b) the free energy of ion-pair formation (gained)
(c) the energy of reformation of hydrogen bonds (gained) when the cavity left by the ion pair collapses
(d) dissociation and solvation energies in the organic phase (these will depend on the dielectric constant and specific interactions).

The linearity of the R_M *vs.* $\Delta G_{hydration}$ plot (Fig. 2) suggests that the differences between the free energies of hydration of the various alkalies are a principal cause of the observed differences of transfer energies of the alkali ions from the stationary phase to the mobile phase. Thus step (1) seems to be the one where most of the differentiation arises, though energy contributions from the other steps may not be negligible. It may be tempting to look for a correlation between R_M and n (hydration number in the stationary phase) or $(n—m)$. Varying values for n under bulk conditions are given in the literature[23], but the order is roughly as expected (decreasing from lithium to cesium). Bulk extraction experiments by SLATER[24] show that in-

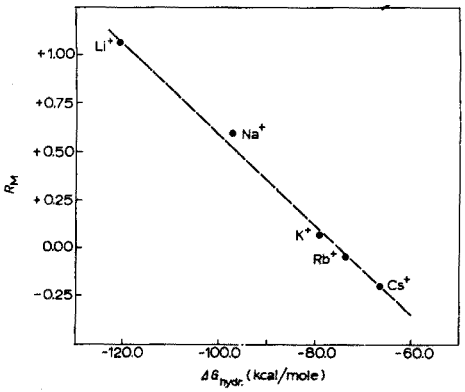

Fig. 2. Correlation of experimental R_M values with standard free energy of hydration of alkali metal ions.

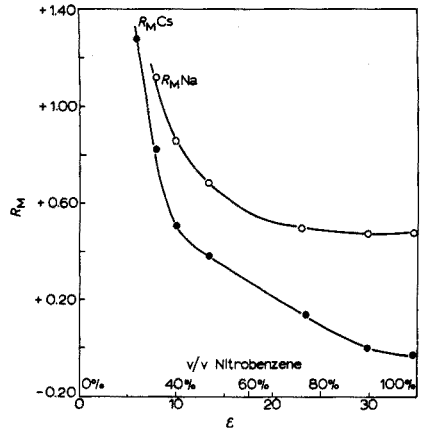

Fig. 3. Variation of R_M with variation of dielectric constant (ε) in mixtures of benzene with nitrobenzene.

creasing amounts of water per mole of sodium can be carried over into the organic phase as the iodine concentration in nitrobenzene is greatly increased. Our own bulk determinations showed that no water was transported into the organic phase with cesium at approximately the concentrations and phase ratio used in the TLC experiments yielding the reported R_M values. While transport water associated with the lower alkalies in the bulk organic phase may or may not be carried as water of hydration (the variation[24] of n from 4 to 8 may be remembered), the number of hydration of the alkali ions in a highly oriented water phase on silica gel may not be the same as in the bulk phase. The small amount of water present on the air-moist silica gel layer may be less available for hydration (and coextraction) and may cause changes in the net hydration energy differences. We can write (from Fig. 2):

$$R_M = k\Delta G_{\text{hydration}} + C_1 \tag{4}$$

$$\text{but also } R_M = \sum_{o}^{i} (\Delta\mu_i/2.3\ RT) + C_2 \tag{5}$$

$$\text{so that we may also write } R_M = \Delta\mu_o/2.3\ RT + k\Delta G_{\text{hydration}} + C_3 \tag{6}$$

where $\Delta\mu_o$ in analogy to homologous series of organic compounds might be taken as the free energy of transfer of the "parent compound" $[M^+PI^-]$.

Figure 3 shows R_M as a function of the dielectric constant (ε) of the mobile phase, when mixtures of nitrobenzene and benzene (all 0.1 M in iodine) are used for developing air-moist plates. It may be significant that the dielectric constant effect on R_M is stronger for cesium than it is for sodium. The widest spread of R_F values in this system corresponds to the highest dielectric constant (pure nitrobenzene). However, this does not mean that in other systems (*e.g.*, mixtures of nitroalkanes with benzene or carbon tetrachloride) the separation can be improved by just increasing the dielectric constant of the mixture, since this often moves everything up to the solvent front.

It can also be seen from Fig. 3 that R_M follows a smooth curve for sodium but

is almost linear over a considerable range ($\varepsilon = 13$ to 27) for cesium. The linear part of the curve may correspond to the increasing dissociation of cesium–polyiodide ion-pairs paralleling the increase of dielectric constant of the organic phase. Cesium–polyiodide is almost completely dissociated in pure nitrobenzene (DAWSON[20]). pK values of similar ion pairs (*e.g.*, alkali–picrate) have been found to exhibit a linear rise with $1/\varepsilon$ (ref. 25). The sharp rise of the R_M of cesium below $\varepsilon \cong 10$ may reflect a decrease in some specific interaction at mole ratios below 1:2 of nitrobenzene to benzene in the mixture. Various types of solvents and solvent mixtures having dielectric constants between 2 and 36 were tried as developers. However, as might be expected from Slater's bulk extraction data no relation between R_M (or R_F) and the dielectric constants of the elements could be established. It seemed the considerable movement of the alkalies on the plate could be obtained only when the dielectric constant of a solvent exceeded about 10, but several other factors are probably more important than the dielectric constant.

Specific interactions

When bulk extractants for the heavier alkali ions are compared, it is found that nitroaromatics and nitroalkanes are superior to other solvents[26]. In most of the systems studied where extraction occurred, a large bulky anion was available to the alkali ion. While a specificity of the (especially aromatic) nitro group for the heavier alkalies has been recognized, it still remains to be explained why the polyiodide anions are superior for extraction (at least under neutral or acidic conditions) as opposed to the perchlorate ion for instance. It seems likely that selective acceptor–donor interactions can play a major role in this system, *e.g.*, an interaction of the polyiodide anions with the π-acceptor nitrobenzene seems quite likely.

Recent research[27] has established the existence of well defined charge transfer complexes between (alkali) iodides and nitroaromatics and it is known that the triiodide ion (I_3^-) is *not* dissociated in nitrobenzene (DAWSON[20]) or acetonitrile[28]. Several runs with solutions in benzene of various nitroaromatics were made (using nitrobenzene, *m*-dinitrobenzene, *p*-nitrotoluene, trinitrobenzene, trinitrotoluene, *etc.*). The R_F values obtained decreased in an irregular way with the increasing number of nitro groups; these results cannot be easily interpreted, since all the higher aromatics apparently interact much more strongly with the silica surface[29], than nitrobenzene does. A further complication is the varying water content of such solvent systems, which seemed to play an important role.

Influence of the phase ratio

Figure 4 shows the variation of R_F values with phase ratio for cesium, rubidium, and sodium iodides. It is evident that at low values of the phase ratio (higher water content) the R_F values are higher than at lower (more normal) water contents. This implies that the larger the water phase, the lower the proportion of solute contained in it at any given time.

This effect is more clearly illustrated when the partition coefficient (α) obtained from the R_F data is plotted against phase ratio (Fig. 5). Also plotted in Fig. 5 are data for the (bulk) partition coefficients obtained by bulk extractions at overall concentrations approximating those at the spot peak on the plate. It is also seen that the chromatographic α values decline by almost two orders of magnitude as the stationary

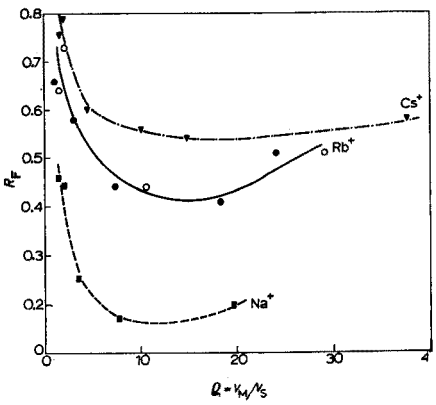

Fig. 4. Variation of R_F with the phase ratio S. (●) 1st run; (○) 2nd run.

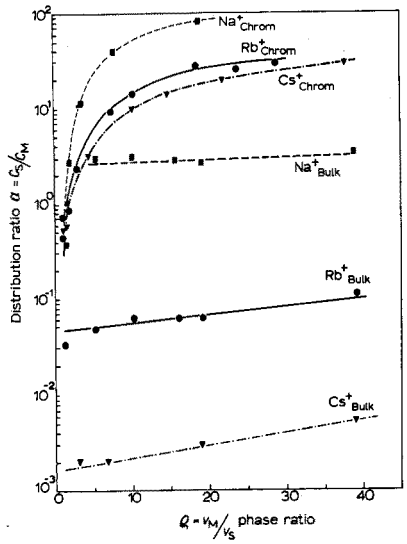

Fig. 5. Variation of chromatographic and bulk distribution ratios with the phase ratio.

phase volume approaches that of the mobile phase. This phenomenon may be understood from the fact that at phase ratios in the range 20–30, only about enough water is present for a monolayer in most silica gels[30]. Although a fairly high proportion of this water is probably present in the pores and not actually as a monolayer, it seems that at this level the water must be rather ordered and probably largely bound to the silica gel. Although the mechanism is not clear, it may well be related to this change in the state of the water.

It is interesting that the ratio of bulk α's to chromatographic α's varies from four orders of magnitude in the case of cesium to one order of magnitude in the case of sodium (see Table I). To explain this vast difference in the level of bulk and chromatographic partition coefficients, a reason must be sought for the vastly greater retention of the polyiodide ion pairs in the chromatographic water phase than in the bulk water phase.

A possible explanation for this high degree of polyiodide retention might lie in an abnormally high concentration of the ion pair at liquid–liquid interfaces[21]. On the silica gel the area of interfacial contact of mobile and stationary phases will be propor-

TABLE I

RATIO OF CHROMATOGRAPHIC α TO BULK α

$\varrho = 20$	α (Chrom) ($\times 10^{-2}$)	α (Bulk) ($\times 10^{-2}$)	$\frac{\alpha\ (Chrom)}{\alpha\ (bulk)}$
Na^+	8.0	28	2.9×10^1
Rb^+	2.4	60	4.0×10^2
Cs^+	1.7	0.30	6.0×10^4

tionately larger than in the bulk conditions, and much less of the solute would be expected in the mobile phase at any given time. With less solute in the mobile phase, substantially higher α values would be expected on the silica plates than in the bulk extractions.

It might also be inferrred that the much lower ratio of the chromatographic α to the bulk α of sodium, when compared to cesium, may be due to the size-exclusion effect noted by DALTON *et al.*[1]. The larger size of the hydrated sodium ion may lead to its exclusion from a part of the pores, whereas the smaller, unhydrated cesium ions are not excluded from the silica pores. This effect would thus oppose the interface effect in the case of sodium but would be relatively less important in the cesium case.

Further work will be needed to elucidate the various factors involved in this aspect of the described thin layer process.

The authors wish to thank Miss M. K. HARTMANN, science bibliographer, and the staff of State University of New York at Binghamton data processing center, for their kind assistance.

SUMMARY

The behavior of the alkali group in thin-layer chromatography on silica gel in the polyiodide–nitroaromatic system is described. R_M values are correlated with ionic radii, free energies of hydration, and the dielectric constant of solvent mixtures. The chromatographic distribution ratios on plates were measured as a function of the phase ratio and compared to bulk distribution ratios. Differences of orders of magnitudes between bulk and chromatographic distribution ratios are attributed to the peculiar nature of the water on the gel.

REFERENCES

1 R. W. DALTON, J. L. MCCLANAHAN AND R. W. MAATMAN, *J. Colloid Sci.*, 17 (1962) 207.
2 H. W. KOHLSCHÜTTER, A. RISCH, K. UNGER AND K. VOGEL, *Ber. Bunsenges. Phys. Chem.*, 69 (1965) 849.
3 J. PITRA AND J. REICHELT, *Coll. Czech. Chem. Commun.*, 31 (1966) 1392; J. PITRA, J. REICHELT AND Z. CEKAN, *Coll. Czech. Chem. Commun.*, 28 (1963) 3072.
4 H. J. CAHNMANN, *Anal. Chem.*, 29 (1957) 1307.
5 K. N. TRUEBLOOD AND E. W. MALMBERG, *Anal. Chem.*, 21 (1949) 1055; L. M. KAY AND K. N. TRUEBLOOD, *Anal. Chem.*, 26 (1954) 1566.
6 R. L. BURWELL, JR., R. G. PEARSON, G. L. HALLER, P. B. TJOK AND S. P. CHOCK, *Inorg. Chem.*, 4 (1965) 1123.
7 M. R. BASILA, *J. Chem. Phys.*, 35 (1961) 1151.
8 F. OEHME, *Chemiker-Ztg.*, 88 (1964) 657.
9 H. SEILER, in E. STAHL (ed.), *Thin Layer Chromatography*, Academic Press, New York, 1965, p. 472.
10 R. W. MAATMAN, *J. Phys. Chem.*, 69 (1965) 3196.
11 H. T. TIEN, *J. Phys. Chem.*, 69 (1965) 350.
12 D. L. DUGGER, J. H. STANTON, B. N. IRBY, B. L. MCCONNELL, W. W. CUMMINGS AND R. W. MAATMAN, *J. Phys. Chem.*, 68 (1964) 757; J. STANTON AND R. W. MAATMAN, *J. Colloid Sci.*, 18 (1963) 132.
13 G. E. JANAUER AND R. C. JOHNSTON, *Anal. Chem.*, 38 (1966) 786.
14 L. F. DRUDING, *Anal. Chem.*, 35 (1963) 1582.
15 H. SEILER AND W. ROTHWEILER, *Helv. Chim. Acta*, 44 (1961) 943.
16 M. LESIGANG, *Mikrochim. Acta*, (1964) 34.
17 K. RANDERATH, *Thin Layer Chromatography*, Academic Press, New York, 1964.
18 R. C. JOHNSTON, *M.A. Thesis*, State University of New York, at Binghamton, 1967.

19 J. O'M. BOCKRIS, *Modern Aspects of Electrochemistry*, No. 2, Butterworths, London, 1959, pp. 95–111.
20 H. M. DAWSON, *J. Chem. Soc.*, 99 (1911) 1609; R. BOCK AND T. HOPPE, *Anal. Chim. Acta*, 16 (1957) 406; L. M. SLATER, *Nucl. Sci. Eng.*, 17 (1963) 576.
21 R. M. DIAMOND, *J. Phys. Chem.*, 67 (1963) 2513.
22 D. R. ROSSEINSKY, *J. Chem. Soc.*, (1962) 785.
23 G. KORTUM, *Lehrbuch der Elektrochemie*, 2nd ed., Verlag Chemie, Weinheim, 1957, p. 121.
24 L. M. SLATER AND M. KUKK, International Conference on Solvent Extraction Chemistry at Göteborg, Sweden, August 27–September 1, 1966.
25 C. W. DAVIES, *Ion Association*, Butterworths, Washington, 1962, pp. 95–99.
26 L. A. BRAY AND F. P. ROBERTS, *U.S. At. Energy Comm. HW-76*, 222, 48 (1963).
27 A. B. TRONOV, *Zh. Obshch. Khim.*, 35 (1965) 1545.
28 A. I. POPOV, R. H. RYGG AND N. E. SKELLY, *J. Am. Chem. Soc.*, 78 (1956) 5740.
29 A. H. SPORER AND K. N. TRUEBLOOD, *J. Chromatog.*, 2 (1959) 499.
30 R. K. ILER, *The Colloid Chemistry of Silica and Silicates*, Cornell, 1955, pp. 247–248.

Analytica Chimica Acta
Elsevier Publishing Company, Amsterdam
Printed in the Netherlands.

PROCESSING ULTRACENTRIFUGE DATA WITH AN "ON-LINE" DIGITAL COMPUTER

S. P. SPRAGG
Department of Chemistry, The University, Birmingham 15 (Great Britain)

(Received November 1st, 1966)

The advent of the digital computer has, in general, induced new ways of processing analytical data, and, in the case of the analytical ultracentrifuge, various programs have been written which embrace both old and new concepts[1]. Many of these contain complete statistical analyses of the data and the results obtained so far show that often the errors in the computed parameters are larger than originally anticipated. These errors can be significantly reduced by replacing the photographic plate with a more precise recording method. This is now possible since in recent years various photoelectric scanners have been developed for recording the absorption profiles of the sedimenting substances; the results are then presented as pen recordings. However, this form of presentation, although desirable, is probably no more precise than the photographs.

A development of this procedure is to connect the photomultiplier directly to a digital computer and this results in a net gain in two directions: (1) the partially processed data, from which surplus information has been removed, is immediately available as the experiment proceeds, (2) the high-speed logic of the computer makes it possible to improve on the precision with which the coordinates are measured.

Since the electronic principles of this procedure are well known, they are omitted from this communication. Instead a discussion is presented of the problem and some of the proposed solutions.

EQUIPMENT

Ultracentrifuge

A Spinco Model E analytical ultracentrifuge fitted with a RTIC unit was used in the present work. The model has separate optical systems for the refractometric and light absorption detection methods. The recording medium for the former (*i.e.*, schlieren and Rayleigh interference systems) is film and a photoelectric scanner is used to detect and record the light absorption profile from the cell. This unit uses an oscillating mirror for moving the image of the cell across the stationary, masked photomultiplier[2]. Records are made with a high-speed pen recorder. A monochromator having a 250-W Xenon arc lamp provides light for the absorption system.

Digitising equipment

A PDP 8 processor (Digital Equipment Corp., Reading, England) fitted with an extended arithmetic unit and an a-d converter is the control unit. Connected to

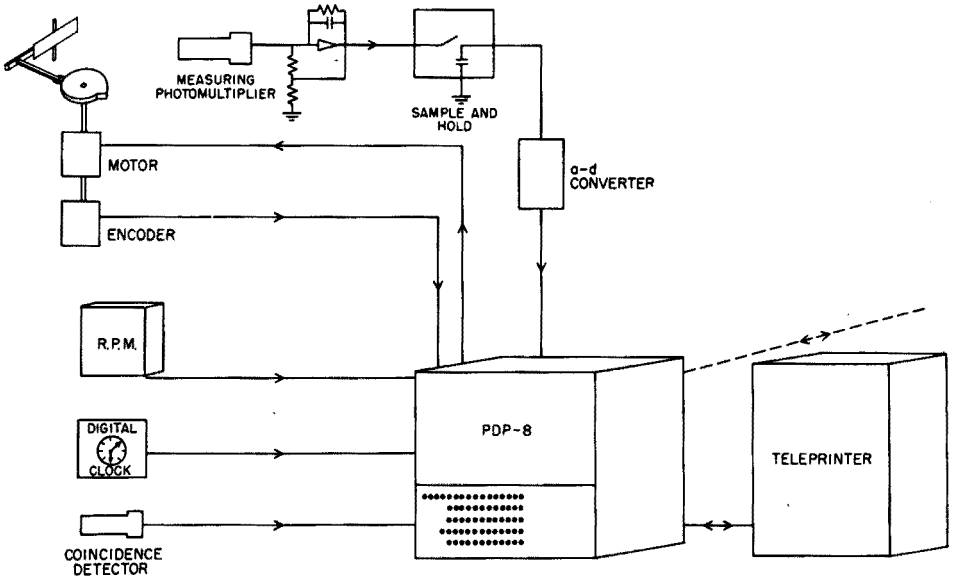

Fig. 1. Diagrammatic representation of the digitising equipment.

this, through the necessary electronic gates, are a frequency meter for measuring the rotor speed, digital clock, a unit for encoding the angular movement of the oscillating mirror, and finally, a second photomultiplier which has been called the coincidence detector (see p. 139). This arrangement is shown diagrammatically in Fig. 1 with arrows to indicate the flow of the information.

All the channels so far mentioned are from the centrifuge to the processor but the PDP 8 has the facility for controlling equipment based on program decisions and this is used to stop and start the scanning motor. Further channels can be added to the processor but this potential has not yet been exploited.

DEFINITION OF THE PROBLEM

Since the photoelectric scanner cannot resolve in the y axis, only the schlieren and absorption systems can be automated at present. However, these two are complementary both in principle and concentration range; hence, no attempt has been made to incorporate the interference system in the unit.

The pulses received from the photomultiplier can only carry information concerning the intensity of the detected light; thus the schlieren system must be modified to a form which gives light pulses having amplitude modulation. This can be achieved by using a knife edge as the schlieren diaphragm instead of the conventional phase plate, and by omitting the cylindrical lens in the optics. With this method the refracted light is blocked and the schlieren derivative curve is outlined as the envelope of many light pulses. The same detecting equipment can then be used for both the absorption and the refractometric method and the interpretation of the data is made by program changes in the processor.

At present the base line for both systems is formed by placing a second cell in

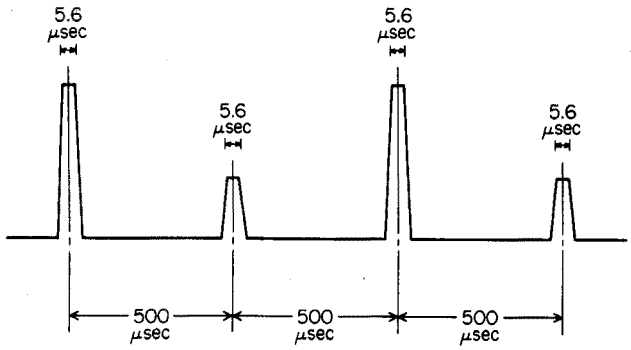

Fig. 2. Pattern of voltage pulses from photomultiplier.

the rotor; this contains the solvent and acts as the reference cell. The pattern of light from this combination, and hence the voltage pulses from the photomultiplier, is given in Fig. 2 together with the approximate time scale for 2° sector cells in a rotor travelling at 60 000 rot./min. The duration of the light pulse is approximately 5.6 μsec with an interval of 500 μsec between pulses. Assuming that the precision required is 0.1% for measuring the pulse amplitude, then the a–d converter requires approximately 29 μsec to carry out the conversion. To provide this time interval the pulse height is held steady for the interval between the pulses by a fast "peak detect and hold circuit". This will allow the processor 500 μsec for storing and editing the incoming data. The main processing can be carried out in the time interval between the exposures. Information must also be collected to calculate the radial dimensions of the pulses from the shaft encoder on the oscillating mirror, following an initial calibration. In addition to the pulse data from the measuring photomultiplier, records are collected of the rotor speed (frequency meter) and time of exposure.

Since the pulses from the cells and the reference holes may be similar both in amplitude and duration, additional information is required to indicate when the scan of the cell is complete. This can be detected with a second photomultiplier, the coincidence detector, connected via an "and" gate to the main photomultiplier. The gate is set to the "on" position when a pulse is seen by both photomultipliers at the same instance and the PDP 8 then reads the encoder and transfers control to a further part of the program.

For most normal runs much of the data is repetitive. For example, the pulse heights across the air space and in the plateau regions have only noise as a variation at any given instance in time; hence, only enough data need be recorded in these regions to give an analysis of the noise level. The essential information required for computing the molecular parameters is found in the meniscus and reference hole radial dimensions, and the x and y dimensions of the sedimenting boundaries. The processor has been programmed to search for these features and to treat them according to the method outlined below.

CALCULATION OF THE OPTIMUM SCANNING RATE

When a rotor travels at 60 000 rot./min, there occur 2,000 pulses per sec and since many of these are superfluous it is relevant to see if the optimum scanning speed

can be defined for the oscillating mirror and so reduce the information rate. It is easy to show that with a rotor travelling at w rot./sec and an image width of d cm, the scanning speed (s) can be calculated from eqn. (1), where l is the photomultiplier slit aperture and f is the overlap required for each sample.

$$s = d \cdot f / w \cdot l \tag{1}$$

The uncertain parameter in this equation is f and this represents the amount of information required to fully define the cell features. To evaluate f numerically at this stage is impossible, but information theory gives a clue to the minimum value. The Nyquist theorem states that if an event occurs with a frequency of α occasions per unit time then the number of samples required to define the event is $2\,\alpha$. In the present case one can put $f \geqslant 2$, and eqn. (1) can be rewritten in the inequality given in eqn. (2) (here t is the width of the narrowest boundary to be detected).

$$\frac{w \cdot t \cdot s}{d} - 2 \geqslant 0 \tag{2}$$

Assuming that the meniscus is the narrowest boundary to be detected and it measures 0.01 cm on an image of 2.54 cm wide, then for a rotor speed of 60 000 rot./min the maximum scanning speed should be 2 scans per sec. This would yield approximately 1000 pulses from the two cells for one complete scan of the image. Tests are being carried out to determine the optimum value for f.

IMPROVEMENT ON RANDOM ERRORS

The photomultiplier pulses have noise superimposed on the signal. This varies from a S/N ratio of approximately 4 db at low light intensities to greater than 10 db in the regions of high intensity. If one records the individual pulses with these S/N ratios then the precision will be much lower than that achieved with the pen recordings. However, it is possible to improve this ratio considerably and yet still examine a cell feature in detail.

Assuming that the noise is random and of finite narrow band width then the probability (P_n) that a single noise pulse will exceed a threshold level (E_t) is given by[3] eqn. (3).

$$P_n = \int_{E_t}^{\infty} E_n / v_0 \exp(-E_n^2/2v_0)\, dE_n \tag{3}$$
$$= \exp(-E_t^2/2\,v_0)$$

where v_0 is the variance of the noise voltage sometimes known as the noise power of the detector. This Rayleigh distribution changes to that shown in eqn. (4) when a signal occurs at the detector (*i.e.*, "sample and hold" circuit) in the presence of the narrow band noise[4].

$$P_d = \frac{1}{v_0} \int_{E_t}^{\infty} E_n \exp(-(E_n^2 + E_s^2)/2v_0)\, I_0(E_n E_s / v_0)\, dE_n \tag{4}$$
$$\simeq 1/2(1 + \operatorname{erf}((1/2 + S/N)^{1/2} - (\log(1/P_n))^{1/2})$$

The error function (erf) is defined as $\operatorname{erf}(x) = 1/\sqrt{\pi} \int_{-x}^{x} \exp(-y)^2\, dy$, and I_0 is a Bes

sel function of the first kind with imaginary argument, P_d is the probability that a single pulse will be a signal. Hence, in the present system P_n and P_d are put equal to the precision for each pulse. From this the required S/N can be either computed from eqn. (4) or found in tables[3]. Should the experimentally observed value for the S/N fall below this level, then it can be increased by integrating over a number of peaks, testing the resulting S/N after each summation and stopping when it reaches the preset value.

To put these concepts into operation the sequence for a single scan of the cell image is as follows. The mirror is allowed to traverse across the image until it reaches the start of a boundary. It is then stopped and the incoming pulses are summed together, checking the S/N after each pulse and testing against the previously determined value for the S/N from eqn. (4). When this is reached the mirror can be moved on by a preset increment and the procedure repeated.

CONCLUSIONS

Several benefits become apparent when designing a computerized system. The first is the immediate availability of the experimental parameters while the experiment is in progress. Since the PDP 8 has limited store (4096 words) this processing can only be regarded as a preliminary editing from which decisions can be made concerning the continuation of the experiment. Second is the ability to collect a lot of data over the important regions while rejecting repetitious data. This process can be operated while the data is being collected. This factor can only be used to advantage where two-way channels are incorporated into the system. Finally, the precision of the data can be predetermined within a set range without changes in the electronic equipment.

If these factors are employed it becomes obvious there are two reasons why a profile recorded by a pen recorder at the same time as the computer is operating would become unintelligible. The first is that data may be collected using a high-speed scan of the cell's image and the pen may not follow the profiles adequately. The second is that a pen recording of the scan is assumed to be linear with time in the x dimension. If the computer controls the scanner, this is untrue since it will dwell for uncertain periods on different regions of the image. In view of the need for a pictorial view of the cell features, a graph plotter guided by the PDP 8 is being incorporated into the system. Then after a complete scan of the cell, the computer can draw a full profile of the cell.

It should be stressed that the purpose of the PDP 8 is to edit, make decisions and control slave equipment; any determination of the parameters by the PDP 8 are secondary to this. The essential information can be printed out and processed by a large system after the experiment. It would obviously be an advantage if the PDP 8 could "talk" directly to the bigger machine, but this is a sophistication which is not essential for the aspects discussed above.

I wish to thank the Science Research Council (U.K.) for support through an equipment grant which has made it possible to construct and test the present system.

SUMMARY

A system is described for coupling the photoelectric scanner of an analytical

ultracentrifuge to a high-speed digital computer. Following from a definition of the problem, use is made of the theory of radar pulse reception to show how the uncertainty in the measured pulse amplitudes can be improved. A two-way information exchange between the ultracentrifuge and the processor is involved.

REFERENCES

1 R. TRAUTMAN, *Fractions*, Spinco Inc., Palo Alto, Calif., U.S.A., 1966, No. 2.
2 S. P. SPRAGG, S. TRAVERS AND T. SAXTON, *Anal. Biochem.*, 12 (1965) 259.
3 D. K. BARTON, *Radar system analysis*, Prentice–Hall, New Jersey, 1964.
4 D. O. NORTH, *R.C.A. Labs. Tech. Report, PTR-6C*, June 25, 1943.

Analytica Chimica Acta
Elsevier Publishing Company, Amsterdam
Printed in the Netherlands.

PARTICLE SIZE ANALYSIS OF INORGANIC PIGMENTS

M. H. JONES
Joyce, Loebl & Co. Ltd., Gateshead (Great Britain)
T. R. MANLEY
Rutherford College of Technology, Newcastle upon Tyne (Great Britain)

(Received November 11th, 1966)

Variations in the particle size distribution of pigments may cause differences in colour and hiding power amongst different batches of pigment. Until now there has been no rapid, reliable technique for the routine measurement of particles less than 10 μ. This size of particle is becoming of increasing importance because considerable economies in mixing processes are possible when these very fine or "micronized" pigments are used. Recently there has been a revival of interest in centrifugal techniques and a disc centrifuge has been introduced for work on dyestuffs by ATHERTON *et al.*[1].

A modification of this instrument has been used to determine the particle size of various inorganic pigments. In all instances the separation of the pigment into the various fractions was easily and rapidly achieved. Among the pigments investigated were titania, calcium carbonate (whiting), alumina, flake aluminium, iron oxide and carbon black. Results are given for three samples of a rutile titania and for two whiting dispersions. These show the utility of the centrifuge for particles below 10 μ and also below 1 μ.

EXPERIMENTAL

Disc centrifuge

A Joyce–I.C.I. particle size disc centrifuge (Joyce, Loebl & Co. Ltd., Gateshead) was used. Samples containing particles of different sizes are fractionated using a rotating probe which operates whilst the centrifuge rotor is in motion. This eliminates errors due to starting and stopping of the centrifuge. The range of particle size in each fraction is given by pre-computed (Elliott 803) tables. Analysis of each fraction then enables a cumulative distribution to be calculated.

The centrifuge rotor is made from glass or Perspex and spins about a horizontal axis. The rotor cavity measures 4" in diameter by $\frac{1}{4}$" wide and has a $1\frac{3}{4}$"-diameter entry port, through which the liquids and dispersions are introduced or extracted. The rotor is mounted on the shaft of a d.c. series motor and is rotated at seven fixed speeds, between 1,000 and 8,000 rot./min. The speed is stabilised to a very high degree using a phase lock servo system. The servo-control ensures constant speed and eliminates disturbances within the rotor cavity caused by hunting.

The contents of the centrifuge cell are illuminated by a synchronised stroboscope, which allows a close inspection of the sedimenting particles, to detect any in-

stabilities, such as "streaming", which consistently occur with two-layer centrifuge techniques.

Spin fluids are introduced into the spinning disc from a syringe or suitable dispenser. The dispersed particles are injected into the cusp from a calibrated syringe, which is mounted in the injection head and situated on the left-hand side of the disc. This cusp ensures good contact between the face of the disc and the injected particles, thus eliminating any turbulent mixing which would occur if droplets impinged directly onto the spin fluid surface.

After the particles have been in the centrifuge for the desired time, the probe (Fig. 1) automatically removes from the spinning disc the liquid and particles down to a pre-selected depth. The specially sharpened probe cuts the "undersize fraction"

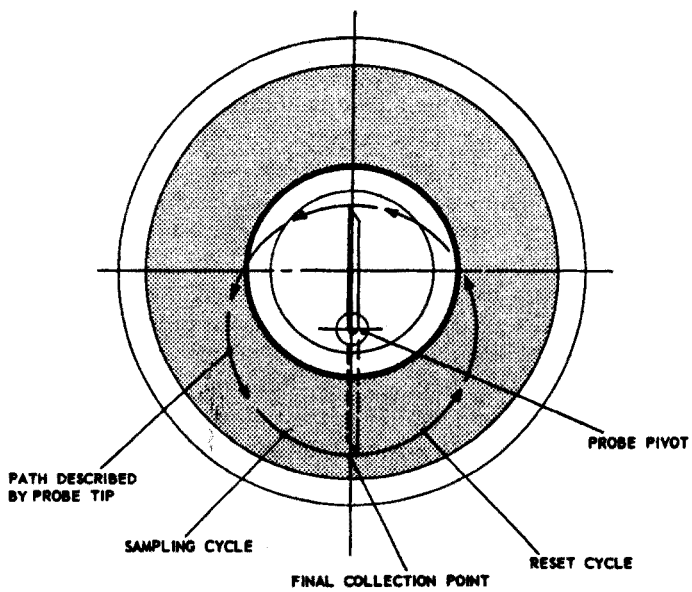

Fig. 1. Disc and probe relationship during sampling.

of particles from the disc during one revolution at 1 rot./min in the same way as "inside" turning on a lathe. The cut liquid is collected under reduced pressure. To ensure efficient collection, irrespective of the volume of spin fluid used, the rotating probe is panned axially across the rotor cavity to within 0.015" of each wall.

The computed tables give the following parameters: particle size (Stokes diameter); rotor speed; spin fluid volume and viscosity; centrifuging time for a particular density difference between the particles and the spin fluid.

The optimum spin fluid viscosity and density are obtained experimentally. These parameters plus the density of the particles enables a programme to be obtained for any given particle size. Each operation of the machine produces one point on the particle size distribution curve.

With such a discrete system the centrifuging speed and spin fluid volume can be selected for each particle size, to produce short spin times, thus making the overall

operating time quite short. Generally, particle size distributions can be obtained in under one hour, and production line checks made in minutes.

After centrifugation all the collected fractions are made up to 50 ml with spin fluid. A reference sample which contains the whole particle size range is obtained by diluting the normally injected volume of dispersion to 50 ml with spin fluid. The particle size distribution curve is obtained by analysing each fraction and equating the reference cumulative weight to 100%.

A distribution curve of percentage cumulative weight, undersize or oversize, (depending upon the fraction used) against particle size is obtained.

The two-layer or line-start system[2] is very easily interpreted but has serious streaming problems. It consists of floating a very thin layer of dispersed particles on the surface of an inert spin fluid, where the mean density of the particles and suspending medium is less than the spin fluid density. The particle density is, of course, greater than the spin fluid density and the sedimentation of particles from the sample layer is calculated from Stokes' equation.

Streaming is a complex phenomenon which is always encountered with two-layer techniques, and is stimulated by the movement of particles and the physical conditions existing at the interface between the spin fluid and the suspending medium of the injected dispersion.

A simple variation of the two-layer technique called the buffered-line start[3] was used; this is applicable to aqueous or non-aqueous systems, and consists of diffusing the troublesome interface. For aqueous systems, 1–2 ml of distilled water is introduced onto the surface of the spin fluid, and the disc is subjected to a transient acceleration or deceleration, which diffuses the interface and forms a very thin density gradient. The spin fluid is allowed to stabilise before the dispersion is introduced in the usual manner. Because the surface of the gradient is compatible with the injected suspending medium, this diffuses on contact and particles are allowed to settle without having to cross an interface where high surface tension forces exist.

The buffered-line start technique permits stable centrifugation of systems containing a very wide particle size range, including agglomerated materials. The figures obtained for a given size range are not swollen by particles broken down from larger aggregates. Closer agreement with the distribution encountered in practice is thereby obtained. Reproducibility of the conditions of dispersion is obviously critical.

Analysis of pigments

Titania. Three samples of a rutile titania were dispersed ultrasonically and centrifuged. The amount of titania in each fraction was obtained by fusion with potassium sulphate followed by a colorimetric determination with tiron (catechol-3,5-disulphonic acid, disodium salt)[4,5]. The original material contained 96% TiO_2, 2.1% Al_2O_3 and 1.6% SiO_2. The buffered-line start technique was used with 2 ml of distilled water as buffer. For each particle size determination 0.5 ml of a 0.5% (w/v) concentration of the sample in 1% sodium silicate plus a drop of wetting agent was used. The spin fluid was 20% (w/v) glycerol–distilled water. The results obtained are given in Table I.

Calcium carbonate (whiting). Two dispersions of one sample of calcium carbonate were centrifuged using the buffered-line start technique with 1 ml of distilled water as the buffer layer. For each particle size determination 0.5 ml of sample (1% (w/v))

TABLE I

PARTICLE SIZE DISTRIBUTION OF TITANIA AND CALCIUM CARBONATE

Particle size (μ)	*% Found*			*Particle size (μ)*	*% Found*	
	A	*B*	*C*		*A*	*B*
Titania				*Calcium carbonate*		
0.2	4.78	4.58	5.08	0.75	12.97	12.96
0.3	14.94	11.00	11.5	1	17.84	17.8
0.4	40.10	39.22	37.9	2	46.48	46.71
0.5	78.8	79.77	77.8	4	68.0	67.9
0.75	88.35	89.5	89.8	5	85.31	86.0
1	97.8	92.7	96.5	7.5	89.17	89.2
				10	95.26	95.46

was dispersed in a 0.1% solution of Dispersol T with Lissapol N as a wetting agent. The spin fluid was glycerol–distilled water. The calcium carbonate was determined by titration with 0.1 *N* hydrochloric acid using phenolphthalein as indicator. The results obtained are shown in Table I.

DISCUSSION

The reproducibility of the results is considered to be satisfactory. The variability of the titania results can be attributed to the non-uniformity of the dispersions between each operation. The calcium carbonate results are much more acceptable and show good repeatability; in this instance the dispersions were very closely controlled throughout the centrifuging period.

It is clear that the disc centrifuge gives good separation of particles, both in the 1–10 and the 0.1–1 μ ranges. A further advantage of the disc centrifuge is that the various fractions may be collected for use in research on the effects of variations in particle size on the properties of the final product in which the pigment is incorporated.

The experimental assistance of Mr. I. FRASER is gratefully acknowledged.

SUMMARY

A disc-type centrifuge has been found satisfactory for the fractionation of several inorganic pigments including titania and calcium carbonate. It is particularly useful for pigments of less than 10 μ.

REFERENCES

1 E. ATHERTON, A. C. COOPER AND M. R. FOX, *J. Soc. Dyers Colourists*, 80 (1964) 521.
2 C. E. MARSHALL, *J. Soc. Chem. Ind.*, 50 (1931) 444.
3 M. H. JONES, *Proc. Soc. Anal. Chem.*, 3 (1966) 116.
4 J. H. YOE AND A. R. ARMSTRONG, *Ind. Eng. Chem. (Anal. Ed.)*, 18 (1946) 255.
5 W. C. JOHNSON (Ed.), *Organic Reagents for Metals*, No. 28, p. 11, Hopkins and Williams, London, 1964.

Analytica Chimica Acta
Elsevier Publishing Company, Amsterdam
Printed in the Netherlands.

THE DETERMINATION OF MOLECULAR WEIGHTS, SEDIMENTATION COEFFICIENTS AND BUOYANT DENSITIES, USING THE ABSORPTION OPTICS OF AN ANALYTICAL ULTRACENTRIFUGE WITH AN ELECTRONIC SCANNING SYSTEM

W. S. BONT AND W. L. VAN ES

Departments of Biochemistry and Physics, Antoni van Leeuwenhoek-Huis: the Netherlands Cancer Institute, Amsterdam (The Netherlands)

(Received November 1st, 1966)

Absorption optics used in connection with the analytical ultracentrifuge have many advantages. In recent years various investigators have developed automatic scanning systems for the absorption optics in order to avoid the rather laborious procedure of measuring photographic plates with the aid of a densitometer[1–4].

This paper describes a system for a Spinco model E analytical ultracentrifuge, which can be used either as a single-beam or as a double-beam system. When the single beam is applied, two preparations can be placed in the two separate holes of the rotor and two experiments can be performed at the same time. A higher accuracy is obtained when one hole of the rotor is used for the solution and the other for the solvent.

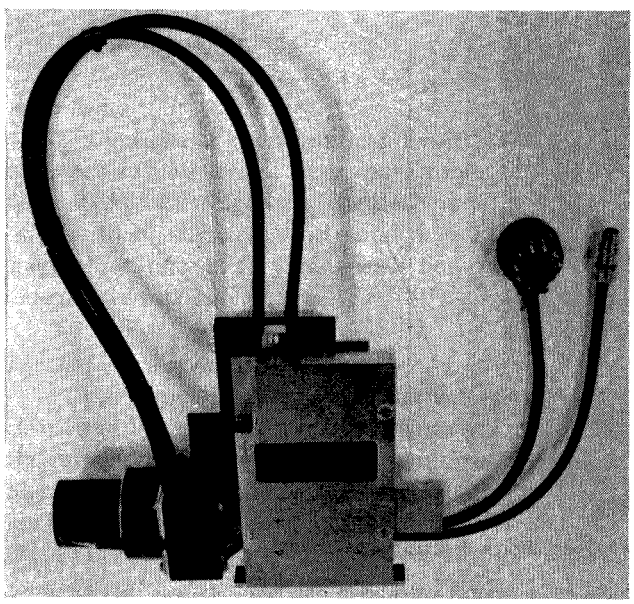

Fig. 1. Mechanical part of scanning system. In front the slit where the image is formed; at the right the synchronous motor.

In this case the double-beam system can be applied, which means that all influences due to solvent and impurities in the optics can be eliminated. In order to differentiate between pulses coming from the two holes, a light pulse from the small reference hole in the rotor was used.

The mechanical part (Fig. 1) of the scanning system can be placed in the holder for photographic plates, without any change in the optical system. The photomultiplier housing with the scanning unit is moved along the image by means of a spindle and a synchronous motor. Scan speed is 60 mm/min, with a slitwidth of 0.2 mm. It is, however, possible to change speed and/or slit.

The electronic cabinet (Fig. 2) contains four units. The upper unit is a servo recorder with a pen speed of 0.25 sec for full scale deflection. Below the recorder are the circuits for checking and controlling, the automatic interval timer, push buttons for manual control of the scanner and a meter for checking various currents and voltages, *e.g.* the high voltage on the photomultiplier. The third unit contains the ampli-

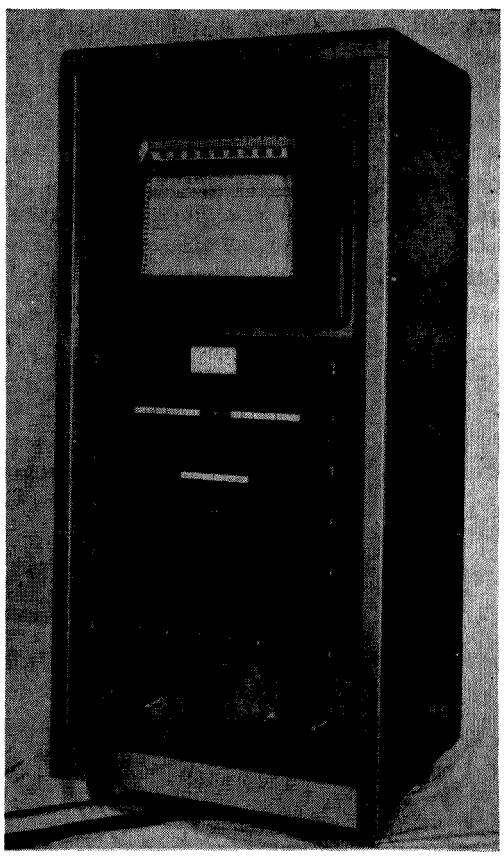

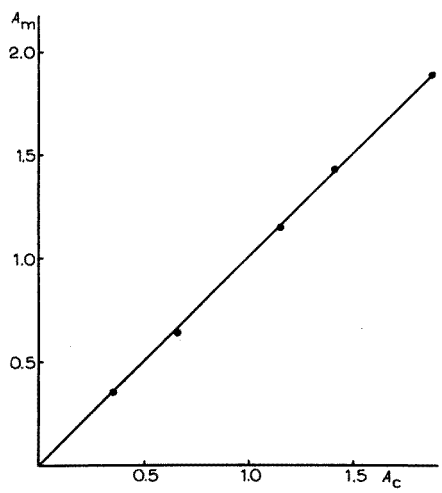

Fig. 2. Electronic part of scanning system. For a description see text.

Fig. 3. Curve of measured absorbance (A_m) against calculated one (A_c). A_c was calculated by measuring the absorbance in a Cary spectrophotometer at 277 mμ, taking into account the length (12 mm) of the centrifugal cell.

fiers, electronic switches, trigger generator log- and derivative circuits. With six push buttons, a choice can be made between the different modes of operation.

The fourth unit is the power unit which supplies the stabilized power to the electronic parts and the light source.

The signal from the photomultiplier is supplied on the following electronic circuits: 1. linear circuit for transmittance; 2. logarithmic circuit for absorbance; 3. derivative circuit; 4. an integrating circuit. Combinations of 1 and 2 with 3 and 4 are possible.

The transmittance is written down when the output of circuit 1 is connected to the recorder. The full scale corresponds to the range of 0–100% transmittance. With the logarithm circuit the range is 0–2 absorbance.

On account of the very high electronic stability of the instrument, no electronic calibrating unit is incorporated.

It is necessary to work with light of a well-defined wavelength; the wavelength to be used depends on the absorption characteristics of the solution. In order to meet all possible requirements the use of a monochromator seems to be the best solution. In practice, however, and particularly for the biochemist, the demands imposed on the range of wavelengths to be used is very limited since in biochemistry most of the measurements are carried out with proteins and nucleic acids with absorption maxima at 280 mμ and 260 mμ, respectively. Above 250 mμ, light filters with good optical properties are available, therefore the advantages of a monochromator are but few. In our apparatus light filters for 260 mμ and 280 mμ were used. These filters are described elsewhere[5].

The results obtained with the apparatus can be divided into two parts: one part comprises the calibration procedures, and the other presents centrifugation experiments.

CALIBRATION PROCEDURES

Absorbance

Solutions of known optical densities were used for the calibration. The absorbances were measured in a Cary spectrophotometer and corrected for the 12-mm light path of the centrifuge cell. The deflections of the recorder were a linear function of the absorbance between $A = 0$ and $A = 2$ (Fig. 3). They were not dependent on the speed of rotation; at very low speeds however (up to 3000 rev./min) no exact measurements were possible.

The derivative of the absorbance

For the calibration of the derivative circuit, two procedures were used. It is clear from Fig. 4 how, from absorbance gradients simulated by an electronic circuit, the curve in Fig. 5 can be constructed. From the latter curve it is evident that for very high absorbance gradients the derivative approaches a limit. Up to a derivative of about 10 cm on the recorder, the derivative changes linearly with the slope of the absorbance according to the relation:

$$\left(\frac{dA}{dr}\right)_m = \alpha \left(\frac{dA}{dr}\right)_c \qquad (1)$$

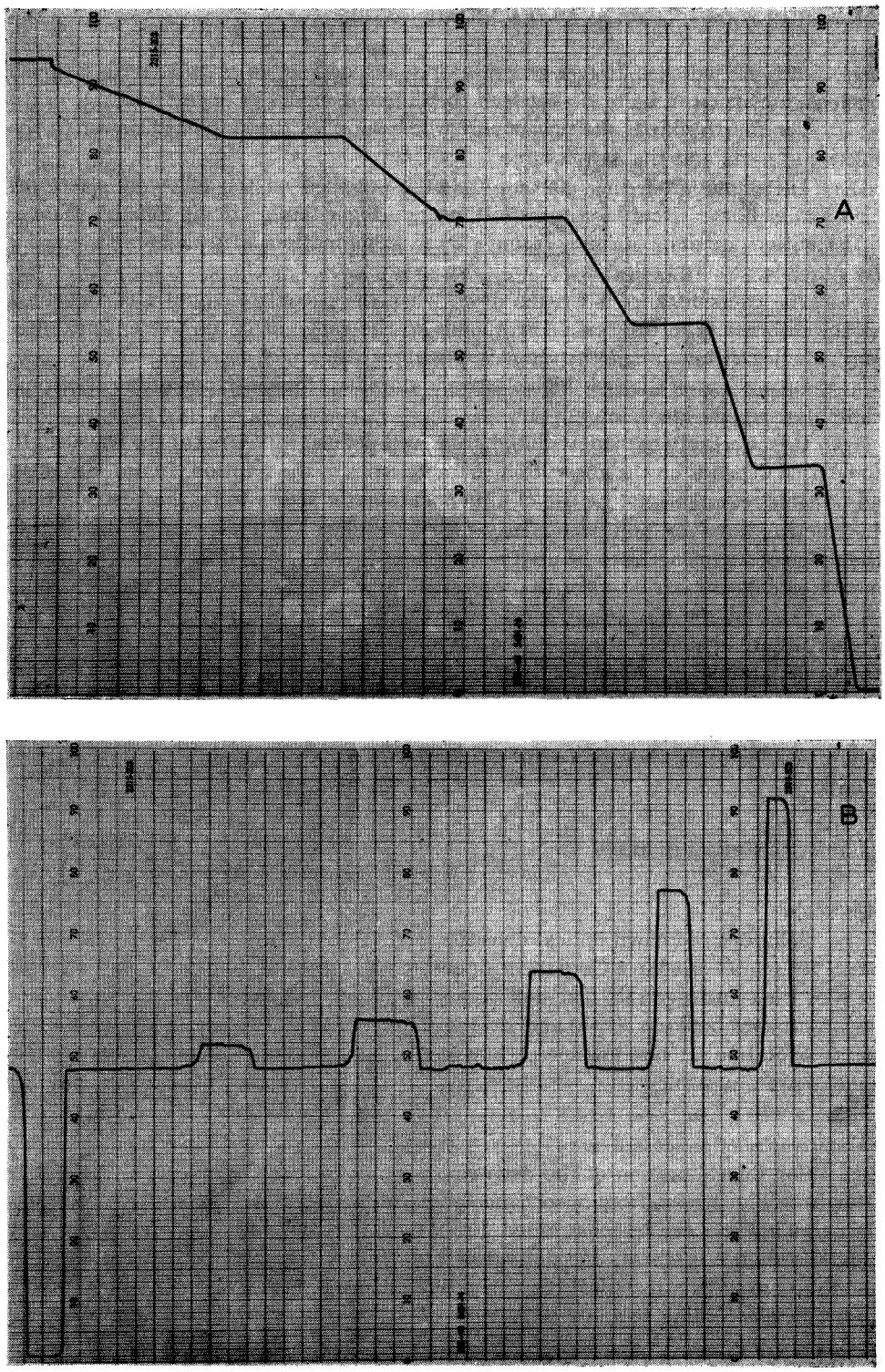

Fig. 4. Absorbance gradients were simulated electronically (A) and differentiated (B).

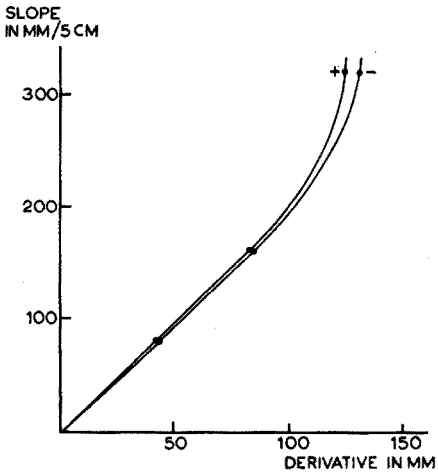

Fig. 5. Slopes in the upper curve (see Fig. 4) were plotted against the height of the plateau region in the lower curve. For very steep slopes the derivative approaches a limit. For positive (+) and negative (−) slopes, two separate derivative circuits are present; which of the two has to be used depends on the direction of the scanning.

where $\left(\frac{dA}{dr}\right)_m$ is the derivative as measured from the slope of the absorbance curve; $\left(\frac{dA}{dr}\right)_c$ is the derivative as calculated from the plateau region in the derivative curve; α is the constant of the apparatus.

When eqn. (1) is integrated, the following equation results:

$$\int\left(\frac{dA}{dr}\right)_m dr = \alpha \int\left(\frac{dA}{dr}\right)_c \qquad (2)$$

The difference in absorbance in a sedimenting boundary can be measured directly from the absorbance curve; the peak in the derivative curve (left side of eqn. (2)) was integrated with the aid of a planimeter. The constant α determined in this way was the same as that obtained electronically. When the slope in the absorbance is too steep, a deviation results, as explained above.

CENTRIFUGATION EXPERIMENTS

These experiments can be divided into three categories, depending on whether the analysis is based on measurements of (1) sedimentation coefficient, (2) buoyant densities, or (3) molecular weight.

Determination of the sedimentation coefficient. Band sedimentation velocity according to Vinograd

In this method[6], the separation is caused by a difference in the sedimentation coefficients of the components. When this method is applied, only small quantities of material are needed. Even for materials like DNA, the sedimentation coefficient of which is strongly dependent on the concentration, the solution may be regarded as infinitely diluted. For further details see the legend of Fig. 6.

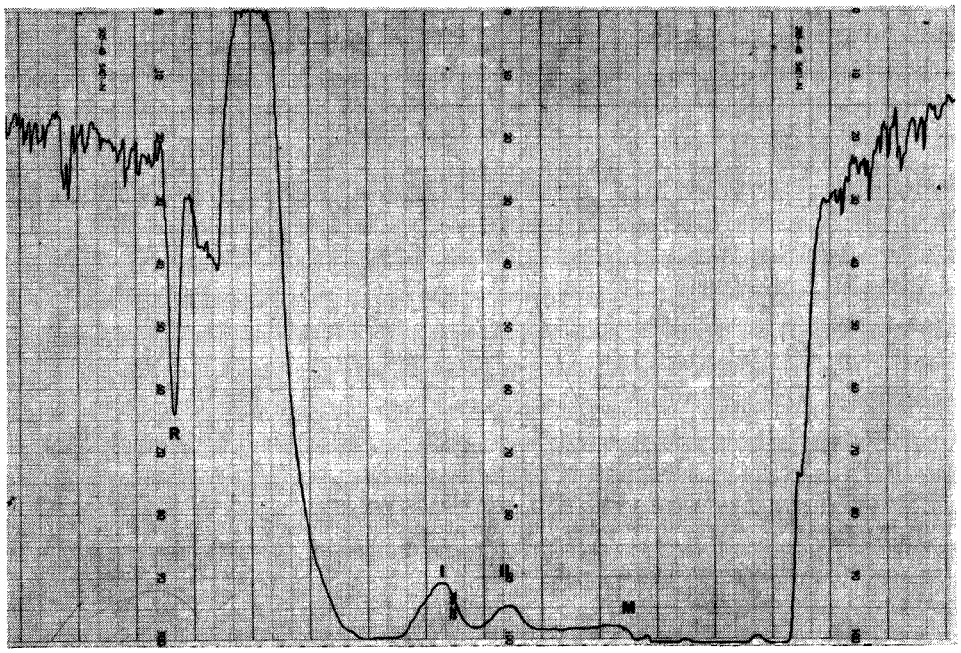

Fig. 6. Band centrifugation according to VINOGRAD *et al.*[6]. The composition of the bulk solvent consisted of caesium chloride, 3 *M*; sodium phosphate of pH 7.0, 10 m*M*; EDTA, 2 m*M*; sodium chloride, 30 m*M*; sodium citrate, 3 m*M*. A Kel-F cell, synthetic boundary type (12 mm), was used. 20 μl of a DNA solution, obtained from rat-liver mitochondria and corresponding to an amount of 0.7 μg, was layered on top of the caesium chloride solution, and centrifuged for 30 min at 5000 rev./min. Tracing was recorded 26 min after reaching maximum speed at 39,460 rev./min. Two components (I and II) and some slower sedimenting material could be detected. Measurements in all experiments were performed at 260 mμ.

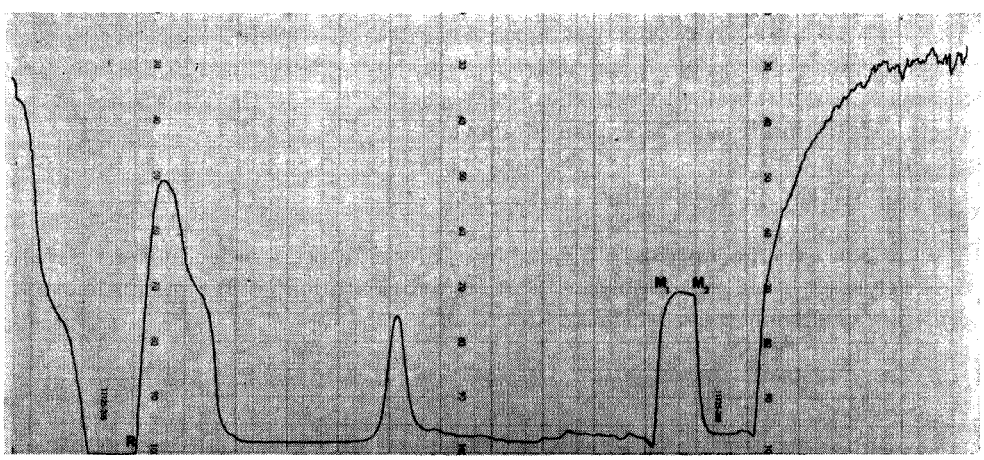

Fig. 7. Density gradient centrifugation in a CsCl gradient according to MESELSON *et al.*[8]. To the solution (as described in the legend to Fig. 6) 0.7 μg DNA from chicken-liver mitochondria was added. Density of the CsCl solution was 1.702 g/ml. Equilibrium was obtained after centrifugation for one night at 44,770 rev./min. R = reference point at a radial distance of 7,300 cm. M_1 = meniscus of the solution. M_2 = meniscus of the solvent.

Boundary sedimentation–velocity experiments with the absorption optics have been described earlier[7].

Determination of the buoyant density in a CsCl gradient

The separation of the components is due to a difference in their buoyant densities[8]. In a centrifugal cell, an equilibrium distribution of caesium chloride is obtained after centrifugation for one night at 44,770 rev./min. The DNA in our experiment (see Fig. 7) was concentrated at the position where the buoyant density of the material was the same as the density of the solution. Also with this technique only very small quantities are required.

Determination of the molecular weight. The sedimentation–diffusion equilibrium

At a certain speed of rotation, depending on the molecular weight of the substance, an equilibrium distribution of material is obtained; *i.e.* across any cross-section in the cell, no net flow of material occurs. From the distribution of material at equilibrium, the molecular weight can be determined. Analysis of the data is based on the equation of SVEDBERG AND PEDERSEN[9] for the molecular weight M:

$$M = \frac{2\,RT}{(1 - \bar{v}\varrho)\omega^2} \frac{\mathrm{d}\ln c}{\mathrm{d}\,r^2} \tag{3}$$

where R = gas constant; T = absolute temperature; $\bar{v}$ = partial specific volume; ϱ = density of the solution; ω = angular velocity; c = concentration at a radial distance r. $\mathrm{d}\ln c/\mathrm{d}\,r^2$ can be replaced by $\mathrm{d}\,mA/\mathrm{d}\,r^2$, *i.e.* the slope of ln A versus r^2, where A = absorbance. Equation (3) can be written in the form

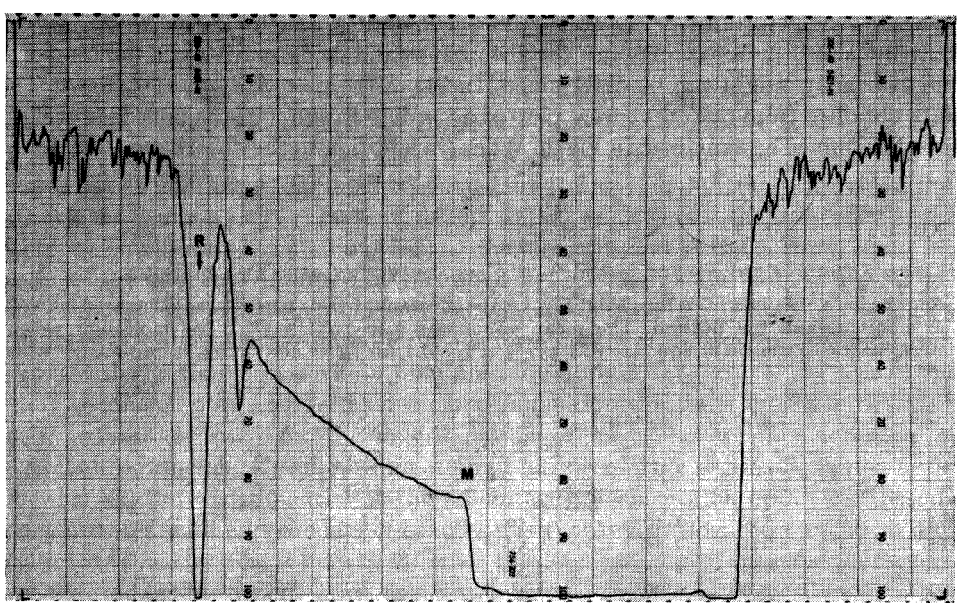

Fig. 8. Equilibrium of adenosine monophosphate in water after centrifugation for 1 night at 59,780 rev./min.

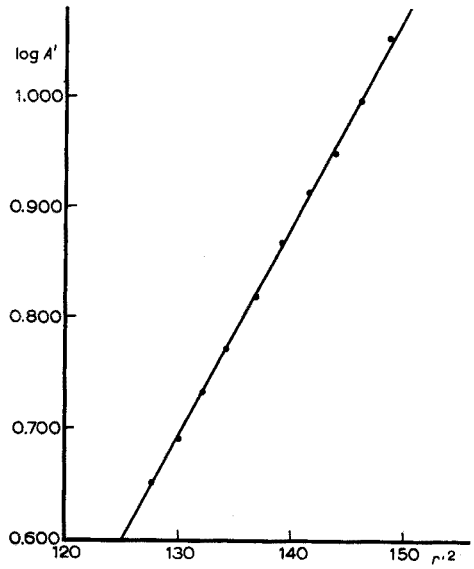

Fig. 9. Curve of log A' *vs.* r'^2. A' = absorbance in mm. r' = radial distance on the tracing of Fig. 8. From the slope of this curve a molecular weight of 326 was calculated. (theoretical value 347).

$$M = \frac{RT}{(1 - \bar{v}\varrho)\omega^2} \frac{\mathrm{d}A/\mathrm{d}r}{rA} \tag{4}$$

When equilibrium is obtained and the solution contains a single macromolecular species, the factor $(\mathrm{d}A/\mathrm{d}r)/rA$ must be a constant throughout the whole of the centrifugal cell[10]. By tracing both the absorbance and its derivative as a function of r, the molecular weight can be determined. In Fig. 8 the plot of A' *vs.* r' is shown. The data obtained from this curve were plotted according to eqn. (3); the molecular weight was determined as explained in Fig. 9. When, in addition to the absorbance, the deriv-

TABLE I

DETERMINATION OF THE FACTOR $(\mathrm{d}A'/\mathrm{d}r')_m/r'A'$ AS A FUNCTION OF RADIAL DISTANCE

From the data obtained from Fig. 8 and Fig. 10, the constant $(\mathrm{d}A'/\mathrm{d}r')_m/r'A'$ was calculated between the meniscus and the bottom. The mean value was $2.47 \cdot 10^{-3} \pm 3\%$. The molecular weight determined with the aid of eqn. (4) was $357 \pm 3\%$. $(\mathrm{d}A'/\mathrm{d}r')_m$ = derivative in cm, measured on the tracing.

r'	A'	$A'r'$	$(\mathrm{d}A'/\mathrm{d}r')_m$	$\frac{(\mathrm{d}A'/\mathrm{d}r')_m}{A'r'} \cdot 10^3$
114	4.9	559	1.40	2.50
115	5.4	621	1.55	2.50
116	5.9	684	1.75	2.56
117	6.6	772	1.90	2.46
118	7.4	873	2.10	2.41
119	8.2	976	2.30	2.36

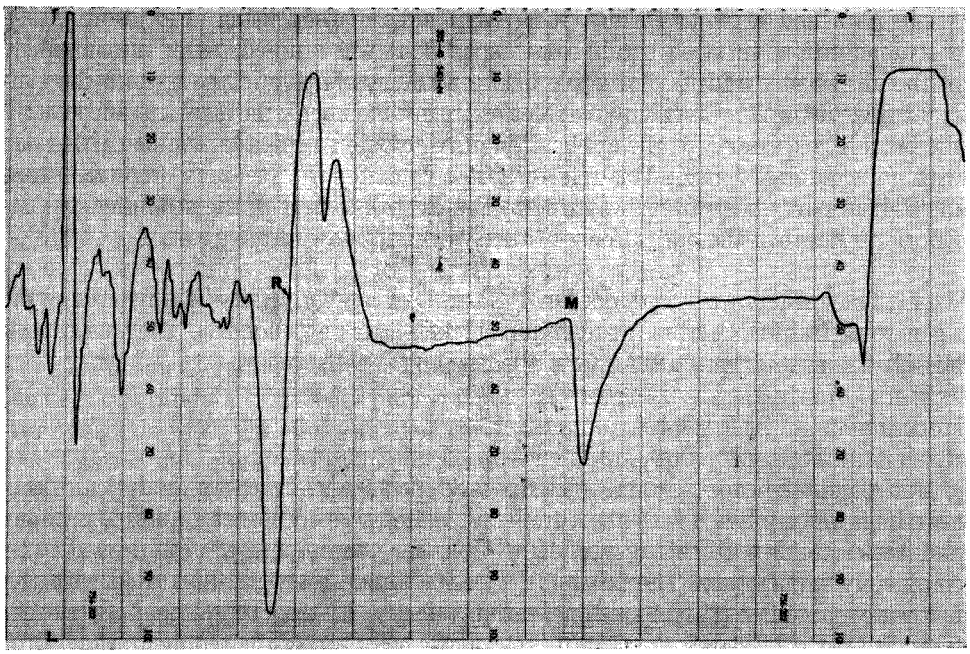

Fig. 10. The derivative curve of Fig. 8.

ative was also traced (Fig. 10), from the data of both Fig. 8 and Fig. 10 the molecular weight can be calculated according to eqn. (4) (Table I).

DISCUSSION

When equilibrium is obtained, *i.e.* when across any cross-section in the cell no net flow of material occurs, the distribution of the absorbance is easily traced. With the aid of eqn. (3) the molecular weight can be determined. At equilibrium the factor $(dA/dr)/rA$ in eqn. (4) must be a constant at any radial distance provided that a single molecular species is present. ARCHIBALD[10], who stressed the constancy of this factor at equilibrium, pointed out that at the meniscus and at the bottom, eqn. (4) is valid at any moment. As stated by this worker "..... no dissolved molecules can flow out of the cell through either end". The advantage of using Archibald's method lies in the relatively short time required for the determination of the molecular weight compared with the time necessary for obtaining equilibrium.

Schlieren optics, either alone or in combination with interference optics, have been extensively used for the determination of molecular weights according to Archibald's principle. Up till now no attempt has been made to use absorption optics for this kind of experiment. Yet the advantages of absorption optics can best be demonstrated with experiments of exactly this type, even though the practical difficulties are considerable. It may be said that the determination of the molecular weight with the aid of absorption optics, using Archibald's principle, is a crucial experiment; once this experiment is possible, all other experiments usually performed with the Schlieren or interference optics can be accomplished with the absorption optics.

As a first attempt to introduce Archibald's method using absorption optics, a sedimentation–diffusion equilibrium experiment was studied. After measurement of the absorbance and its derivative between the meniscus and the bottom the constant $(dA'/dr')/r'A'$ was calculated. Measurements at exactly the meniscus and exactly the bottom, necessary for the application of Archibald's principle, can be carried out with an accuracy of 30%. This relatively low value for the accuracy originates from the optical part and is in no way due to the electronic part of the scanning system. Efforts to improve the optical part of the system are now in progress.

The authors wish to thank Dr. P. BORST, of the University of Amsterdam, for a generous gift of DNA from rat-liver and chicken-liver mitochondria. They also thank Miss J. GEELS and Mr. C. SLEE for skilled technical assistance.

SUMMARY

A double-beam scanning system, developed for use with an analytical ultracentrifuge and equipped with absorption optics, is described. For the study of proteins and nucleic acids with this system, light filters for 260 mμ and 280 mμ proved to be completely satisfactory. The possibilities of the apparatus were illustrated with the following examples: (1) band sedimentation velocity; (2) density gradient centrifugation with CsCl; (3) determination of molecular weights from the sedimentation diffusion equilibrium. The possibility of applying Archibald's method with this system is discussed.

REFERENCES

1 J. B. T. ATEN AND A. SCHOUTEN, *J. Sci. Instr.*, 38 (1961) 325.
2 S. HANLON, K. LAMERS, G. LAUTERBACH, R. JOHNSON AND H. K. SCHACHMAN, *Arch. Biochem. Biophys.*, 99 (1962) 157.
3 H. K. SCHACHMAN, L. GROPPER, S. HANLON AND F. PUTNEY, *Arch. Biochem. Biophys.*, 103 (1963) 379.
4 S. P. SPRAGG, S. TRAVERS AND T. SAXTON, *Anal. Biochem.*, 12 (1965) 259.
5 W. L. VAN ES AND J. H. WISSE, *Anal. Biochem.*, 6 (1963) 135.
6 J. VINOGRAD, R. BRUNER, R. KENT AND J. WEIGLE, *Proc. Natl. Acad. Sci. U.S.*, 49 (1963) 902.
7 W. L. VAN ES AND W. S. BONT, *Anal. Biochem.*, 17 (No. 2) (1966).
8 M. MESELSON, F. W. STAHL AND J. VINOGRAD, *Proc. Natl. Acad. Sci. U.S.*, 43 (1957) 581.
9 T. SVEDBERG AND K. O. PEDERSEN, *The Ultracentrifuge*, Clarendon Press, Oxford, 1940, p. 349.
10 W. J. ARCHIBALD, *J. Phys. Chem.*, 51 (1947) 1204.

Analytica Chimica Acta
Elsevier Publishing Company, Amsterdam
Printed in the Netherlands.

CONTINUOUS PREPARATIVE THIN-LAYER CHROMATOGRAPHY

R. VISSER
Department of Chemical Technology, Technological University Twente, Enschede (The Netherlands)

(Received November 1st, 1966)

Chromatography has its main application in solving analytical problems, but since it can produce essentially pure compounds, preparative methods are of interest for synthetic work, for those identification techniques which need mg amounts and for isolation of minor constituents in mixtures. "Scaling-up" of the separation can be effected by enlargement of dimensions, by reiteration of a given cycle, if possible by automatic methods, and by continuous or semi-continuous procedures. Semi-continuous methods are regarded as consisting of a series of physically separated non-continuous systems following each other at constant time intervals.

For gas–liquid chromatography the first two methods, *i.e.* with large columns[1–4] and with a repeated cycle[5–7] are well-known. Recently, some continuous methods have been described[8–10], based on the counter-current principle, but their application seems to be limited. A semi-continuous method ("simultaneous multi-column analysis") has also been reported[11]. In paper chromatography both large-scale[12–16] and continuous[17,18] procedures are applied. For column chromatography large-scale techniques[19,20] and a semi-continuous method have been described[21]. Elegant methods for large-scale[22] and continuous[23,24] electrophoresis are well-known. Finally, large-scale preparative thin-layer chromatography has recently been developed[25].

Repetitive and continuous techniques are mainly based on the elution method, large-scale techniques both on the elution method (paper- and column chromatography) and on the fundamental procedure (paper-, column- and preparative-layer chromatography and block-electrophoresis).

The principal condition for a continuous method is movement of the complete system to be separated perpendicular to the direction in which the separation takes place. Thus, in continuous electrophoresis the separation is performed along a horizontal axis and the system as a whole is descending. In continuous cylindrical paper- and column chromatography the separation is realized parallel with a vertical axis, whilst the system is rotating around this axis, each point moving along a horizontal circle. In continuous circular paper chromatography the separation takes place along the radii, whilst each point of the system is moving along a circle.

Thin-layer chromatography has been widely used for analytical purposes, but no continuous preparative methods have so far been described. Both principles, cylindrical and circular, are at present being studied but in this paper only the analogue of a cylindrical system will be discussed.

DESCRIPTION OF THE APPARATUS

A diagram of the apparatus is shown in Fig. 1. Separations are performed on a belt of impermeable material (A) resistant to a temperature of 120° and to chemicals normally used in thin-layer chromatography. For this purpose PTFE on a glass-fibre base (thickness 0.35 mm) was chosen. As there were no endless belts commercially available, the ends of a rectangular sheet (width 0.25 m) were connected with cotton yarn and the seam covered with a strip of FEP (polyfluorethylenepropylene), heated under slight pressure to 275°. The belt passes around two horizontal cylinders (B and C) with a diameter of 74 mm, positioned in one horizontal plane, distance 0.60 m. The upper part is led over a flat plane, which is the upper surface of a series of compartments (D, E and F) between the upper and lower parts of the belt.

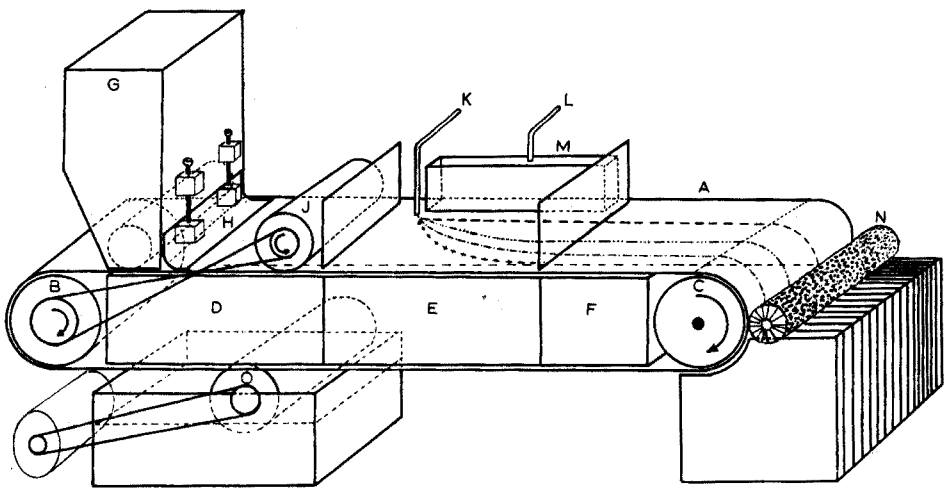

Fig. 1. Schematic view of the apparatus. The characters are explained in the text.

At the starting point on the upper surface of the belt a tank (G) is placed, containing dry silica gel, aluminium oxide or another adsorbent. Through an adjustable slit (H) a continuous layer of *e.g.* 1-mm thickness is spread on the moving belt.This layer is compressed by a cylinder (J) and, if desired, activated by heating by means of electric heaters mounted in the first compartment (D) (length about 0.20 m); moreover, the rest of the compartment can be heated by a circulating liquid.

At the beginning of the second part a continuous strip of the mixture to be separated is applied to the surface through a stainless steel capillary tubing (K), the distance to one edge being about 40 mm. In this part (length 0.23 m) the separation is also performed. To this end a continuous constant stream of eluant is fed through a tube (L) into a container (M) about 0.16 m long, placed along the edge at the same side as the point where the mixture to be separated is applied. This container is filled with cotton or glass wool and has a slit through which a strip of thick filter paper passes. This strip touches the border-line of the adsorbent layer to make contact for the solvent. Separation takes place perpendicular to the moving direction of the belt, the solvent going to the opposite edge. In order to perform the separation at a constant

temperature, the compartment under this part of the belt (E) can be connected with a circulating thermostat bath.

In order to obtain a reproducible separation dosage pumps were used for the application of both the mixture to be separated (Braun type Unita IIb) and the eluant (LKB, type 4900, all-teflon model).

In the third part the solvent is evaporated by heating and venting. The layer is removed by a rotating brush (N) with spindle in the same horizontal plane as the shaft of cylinder (C), and divided over a series of containers.

Finally the belt is cleaned by a rotating cylinder of foam plastic, partially immersed in a tank filled with running water (O).

The belt is driven by a synchronous motor equipped with a gearbox and a clutch. The normal speed is 0.125 m/h.

Most of the construction was done with stainless steel. The upper side is covered with glass plates. Since the distance between these plates and the upper surface of the belt is about 60 mm, a closed box of teflon and glass is positioned in the developing compartment. This reduces the volume to be saturated with the eluant vapour, leaving about 5 mm between the upper surface of the layer and the box.

RESULTS

As an example, the results of the separation of a mixture of three azo dyes are given. Some data are listed in Table I. The separation was performed by application of 0.678 ml of a solution containing 0.5% w/v of each of the three dyes in benzene during 1.5 h. Benzene was used as an eluant, and the flow rate was 51 ml/h. Kieselgel H (Merck) was used as an adsorbent; the thickness of the layer was 0.6 mm after compression. Longer runs were subject to some improvements in the apparatus.

The determinations were carried out by means of UV-spectrophotometry, after extraction of the fractions with ethanol in a soxhlet apparatus. The ethanol extract of one receiver between the front line and the first dye was used as a blank.

The separation was slightly better than separation performed with the same concentration on an analytical plate (ascending development). However, only receivers

TABLE I

AMOUNTS OF THREE AZO DYES FOUND IN A SERIES OF RECEIVERS AFTER SEPARATION

Number of receiver	*p-Amino-azobenzene (mg)*	*p-Phenyl-azoaniline-2-naphthol (mg)*	*p-Dimethyl-amino-azobenzene (mg)*
7	0.016	—	—
8	0.302	—	—
9	2.275	—	—
10	0.525	1.400	—
11	—	1.125	—
12	—	0.761	0.655
13	—	—	2.000
14	—	—	0.198
15	—	—	0.010
Total	3.118	3.286	2.863

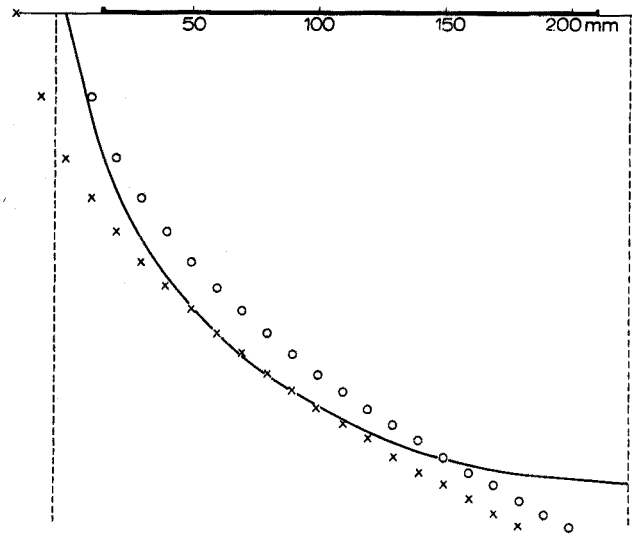

Fig. 2. Diagram of solvent front. The thick part of the y-axis indicates the length of the solvent contact strip.

with a width of 10 mm were available; as a result the border lines between two receivers did not coincide with the borders between two zones and overlap was found.

The shape of the front was studied (Fig. 2). If the y-axis is the edge of the layer (at the side of the eluant tank), the x-axis perpendicular to it and the origin of the coordinate system in the intersection of the front-line with the edge of the adsorbent layer, fair agreement could be found between the experimental curve (drawn line) and a parabola of the formula:

$$x^2 = a + c \cdot y$$

with $a = -1000$ mm^2 and $c = 210$ mm (circles). Since the speed along the y-axis is 125 mm/h this curve is identical with

$$x^2 = a + b \cdot t$$

(t in h) with $b = 26\,000$ mm^2/h. The values of a and b are equal to those found in the literature[26].

Improved agreement was reached by shifting the theoretical curve 20 mm to

TABLE II

R_F VALUES FOUND FOR A PREPARATIVE AND A STANDARD ANALYTICAL SEPARATION

Compound	R_F *found*	
	This experiment	*Analytical plate*
p-Aminoazobenzene	0.19	0.14
p-Phenylazoaniline-2-naphthol	0.29	0.23
p-Dimethylaminoazobenzene	0.41	0.41

the left (crosses). The discrepancies at both ends might be explained by slight evaporation close to the heated activation and drying compartments.

The results indicate that the elution pattern is essentially the same as with horizontal development of a standard analytical plate. This conclusion is supported by the R_F values obtained for this method and the standard ascending technique (Table II). Slight discrepancies may be explained by differences in the silica gel used (Kieselgel G for the standard plate) and in activation.

DISCUSSION

Continuous and semi-continuous preparative separations of non-volatile materials can be carried out with paper chromatography, thin-layer chromatography and column chromatography.

Comparison of continuous cylindrical and circular paper chromatography with continuous thin-layer chromatography leads to the conclusion that thin-layer chromatography has the following advantages. First, the stationary phase is continuously removed, so that no contamination with materials remaining from a former cycle can occur. Secondly, there is no need for long development times, *i.e.* it is not necessary to wait until the slowest compound has left the adsorbent; although this procedure leads fundamentally to a less efficient separation than elution analysis, the separation might come out better since shorter times and more homogeneous adsorbing materials lead to less diffusion (both longitudinal and "eddy" diffusion). Finally, the homogeneous adsorbent gives a more reproducible separation.

Column chromatography has, compared with thin-layer and paper chromatography, a great advantage in that the optimum plate number can be achieved by variation of the pressure upon the eluant[27]. However, semi-continuous column chromatography needs a series of identical columns. If this is not realized, the overall efficiency might be worse than that for each individual column. Furthermore, the total time of a cycle is again determined by the time the slowest compound needs to leave the column.

Finally, continuous thin-layer chromatography compared with preparative-layer chromatography demands a smaller amount of labour; ideally, it works without control. A major problem is that the speed of elution is determined by the rate of the viscous flow of the eluant liquid across the adsorbent. This means that the speed of the belt, the eluant flow and the thickness of the layer are closely related. As a result the supply of the eluant is critical and an additional regulating device should be designed in order to obtain the optimum flow.

Future developments

In principle it is possible to use the apparatus described above for continuous preparative thin-layer electrophoresis (or preferably electrochromatography). The simplest way to realize this is to mount two electrodes parallel to the edges of the adsorbent layer, to supply the buffer solution in a zone in the development compartment parallel with and directly behind the separation wall to the activation compartment, and the supply of the mixture to be separated at a point immediately behind the supply of the buffer solution.

It should be noted that the apparatus, though developed for preparative work,

could also be used for routine analytical separation of a series of samples, as a part of an "Auto-analyzer" type apparatus.

The author is indebted to prof. E. A. M. F. DAHMEN for his interest in this investigation, and to personnel of the Central Technical Service of this university for design and construction of the apparatus.

SUMMARY

A short survey of preparative chromatographic methods is given. An apparatus for general use in continuous preparative thin-layer chromatography is described, and its performance compared with some related preparative techniques.

REFERENCES

1 D. E. M. EVANS, W. E. MASSINGHAM, M. STACEY AND J. C. TATLOW, *Nature*, 182 (1958) 591.
2 J. J. KIRKLAND, in V. T. COATES, H. J. NOEBELS AND I. S. FAGERSON (eds.), *Gas Chromatography*, Academic Press, New York, 1957, p. 203.
3 F. H. HUYTEN, W. VAN BEERSUM AND G. W. A. RIJNDERS, in R. P. W. SCOTT (ed.), *Gas Chromatography 1960*, Butterworths, London, 1961, p. 224.
4 E. BAYER, in R. P. W. SCOTT (ed.), *Gas Chromatography 1960*, Butterworths, London, 1961, p. 236.
5 E. HEILBRONNER, E. KOVÁTS AND W. SIMON, *Helv. Chim. Acta*, 40 (1957) 2410.
6 H. BOER, *J. Sci. Instr.*, 40 (1963) 121.
7 H. BOER, *J. Sci. Instr.*, 41 (1964) 365.
8 D. GLASSER, *Proc. 6th Intern. Symposium on Gas Chromatography, Rome, 1966*, to be published (preprint no. 10).
9 P. E. BARKER AND D. H. HUNTINGTON, *ibid.* (preprint no. 11).
10 P. E. BARKER AND D. H. HUNTINGTON, *J. Gas Chromatog.*, 4 (1966) 59.
11 D. DINELLI, S. POLEZZO AND M. TARAMASSO, *J. Chromatog.*, 7 (1962) 477.
12 H. K. MITCHELL AND F. A. HASKINS, *Science*, 110 (1949) 278.
13 W. L. PORTER, *Anal. Chem.*, 23 (1951) 412.
14 E. VON ARX AND R. NEHER, *Helv. Chim. Acta*, 39 (1956) 1664.
15 L. HAGDAHL AND C. E. DANIELSON, *Nature*, 174 (1954) 1062.
16 L. HAGDAHL AND K. D. LERNER, *Sci. Tools*, 5 (1958) 23.
17 J. SOLMS, *Helv. Chim. Acta*, 38 (1955) 1127.
18 M. PAVLIČEK, J. ROSMUS AND Z. DEYL, *J. Chromatog.*, 10 (1963) 497.
19 R. J. HALL, *J. Chromatog.*, 5 (1961) 93.
20 R. TERANISHI AND T. R. MON, *J. Chromatog.*, 12 (1963) 410.
21 H. SVENSSON, C. AGRELL, S. DEHLÉN AND L. HAGDAHL, *Sci. Tools*, 2 (1955) 17.
22 H. BLOEMENDAL, *Zone Electrophoresis in Blocks and Columns*, Elsevier, Amsterdam, 1963.
23 H. SVENSSON AND I. BRATTSTEN, *Arkiv Kemi*, 1 (1949) 401.
24 W. GRASSMANN AND K. HANNIG, in HOUBEN-WEYL, *Methoden der organischen Chemie*, Georg Thieme Verlag, Stuttgart, 1958, Vol. I/1, p. 685.
25 H. HALPAAP, *Chem. Ing. Tech.*, 35 (1963) 488.
26 M. BRENNER, A. NIEDERWIESER, G. PATAKI AND R. WEBER, in E. STAHL (ed.), *Dünnschichtchromatographie*, Springer-Verlag, Berlin, 1962, p. 109.
27 J. F. K. HUBER AND J. A. R. HULSMAN, *Anal. Chim. Acta*, 38 (1967) 305.

Analytica Chimica Acta
Elsevier Publishing Company, Amsterdam
Printed in the Netherlands.

ION-EXCHANGE CHROMATOGRAPHY

OLOF SAMUELSON
Department of Engineering Chemistry, Chalmers Tekniska Högskola, Göteborg (Sweden)

(Received November 1st, 1966)

Column efficiency and differences in adsorbabilities at equilibrium determine the success of a chromatographic separation on a column. If the ratio between the equilibrium distribution coefficients, called the separation factor, is large, very primitive columns can give a quantitative separation. If, on the other hand, the distribution coefficients differ by only 10% or less, very efficient columns must be used to achieve a satisfactory separation.

In ion-exchange chromatography the distribution coefficients and separation factors can be varied within wide limits. Only in favorable cases can the influence of changes in working conditions be predicted theoretically. With examples from metal separations, separations of organic acids by ion exchange, and partition chromatography of sugars, the influence of some variables will be discussed.

METAL SEPARATIONS

In the first successful metal separations on cation-exchange resins the separation factors were increased to infinity by a transformation of one of the metal cations into a non-adsorbable anion. The first application of such a separation, published in 1939, was the determination of alkali metals in the presence of vanadium, converted before the separation into vanadate anions[1]. In other applications of the method complexing agents were used to convert metal ions such as cobalt and iron into non-adsorbable anions to effect a quantitative separation by selective sorption[2].

In separations of very similar species this technique cannot be used. Here the elution method is of predominant importance. The great potentialities of this technique became generally known in 1947 after the publication of the results of investigations, carried out as part of the Plutonium Project, on the separation of the fragments formed during fission of the heavy elements[3]. Striking results were the separations of rare earths and the first isolation of element 61 (Promethium). Again, advantage was taken of complexing agents such as citric acid to increase the separation factors of the elements to be separated.

Under certain conditions the order of elution is largely determined by the stability constants of the complexes. Simple theories, which account reasonably well for changes of complexing agent, eluant concentration, and pH during the elution, were presented by TOMPKINS AND MAYER[4] and by KETELLE AND BOYD[5]. These changes affect the fraction of the sorbable ions in the external solution and can be accounted for by the calculation methods used in classical solution chemistry.

Although the application of complexing agents is a most convenient way to

increase the separation factors, it must be stressed that many separations of importance in analytical chemistry, such as the separation of alkali metals[6], can be carried out in eluants which give no complex formation. The selectivity in such systems is dependent mainly upon the interaction forces inside the resin, interionic forces and hydration forces, and is also directly influenced by the size of the individual ions. Since the resin phase is a concentrated electrolyte solution a rigorous theoretical treatment is difficult. Practical calculations of the influence of eluant concentration and eluant composition can be made by approximate methods. Published selectivity coefficients determined in equilibrium experiments can be used to advantage.

Interaction forces with the resin matrix have often been neglected but can sometimes be of predominant importance. The uptake of negatively charged iron(III) complexes by cation-exchange resins from concentrated hydrochloric acid[7] is an example where the importance of such forces has been well established[8,9].

The availability of commercial anion-exchange resins with quaternary ammonium groups gave rise to new applications of both selective sorption and various elution techniques. Of great importance are the excellent metal separations in hydrochloric acid at high concentration first demonstrated by KRAUS AND MOORE[10], and similar separations in various other complexing agents. In separations by selective sorption with an anion-exchange resin in the EDTA-form, it was found that the separation factors could be increased by working with a water–ethanol solution instead of aqueous solutions[11]. The explanation given was that the chelates with certain metals (*e.g.* calcium) are more stable in the mixed solvent. Moreover, the separation factors in mixed solvents are affected by the difference in the solvent composition of the resin phase and the external solution[12,13]. This difference causes a kind of partition chromatography to be superimposed upon the ion-exchange chromatography. Systematic investigations by KORKISCH[14] and FRITZ AND RETTIG[15] published in recent years demonstrate the versatility of metal separations in aqueous–organic solvent mixtures. A rigorous theoretical treatment of such complex systems is extremely difficult.

SEPARATIONS OF ORGANIC ACIDS ON ANION-EXCHANGE RESINS

In separations of organic acids on anion-exchange resins, the separation factors are infinite or approach infinity in some important types of separations. One example of this, first demonstrated in experiments with sulfite waste liquor, is the separation of high-molecular-weight acids from low-molecular-weight acids[16]. This separation is based upon the fact that the "mesh size" in the network structure of the resin is smaller than the dimensions of the high-molecular-weight ions. These ions, therefore, are excluded from the resin phase and pass directly into the effluent. Sometimes a sorption on the surface of the resin particles interferes and this is one of the very few ion-exchange separations in which it is recommended that coarse resin particles be used.

Separation of strong acids from weak ones on a strongly basic resin in its sulfate form is another example where the separation factors approach infinity[17]. Other simple separations where large differences in sorbabilities occur are those of anions of different charges.

The tremendous progress made in gas chromatography during the last decade

is probably the main reason why comparatively little time has been devoted to ion-exchange chromatography of carboxylic acids (other than amino acids). With stable volatile acids and with samples containing only acids which are easily converted into derivatives of sufficient stability, gas chromatography is the method of choice. In analyses of complicated mixtures containing various types of hydroxy acids, together with large amounts of sugars and other non-electrolytes, it is believed that a combination of ion-exchange chromatography and gas chromatography gives better results. Such analyses are necessary in various branches of carbohydrate chemistry. The success of the Stein and Moore technique for ion-exchange chromatography of amino acids[18], and the development of monitors for analyzing protein hydrolyzates encouraged continued work in this laboratory on ion-exchange separations of interest in carbohydrate chemistry. Separations which 10 years ago required several weeks with tedious manual work are now effected overnight. The new technique with recorded chromatograms shows an improved reproducibility. Even separations of very similar acids can be accomplished within a few hours. The monitor was recently described in this journal[19].

In most of the work chromic acid oxidation was employed to determine the acids in the eluate. For this reason the eluants used in the runs must not contain compounds which are oxidized by chromic acid under the conditions used in the analyzing system. In the chromatogram reproduced in Fig. 1 the chromic acid oxidation

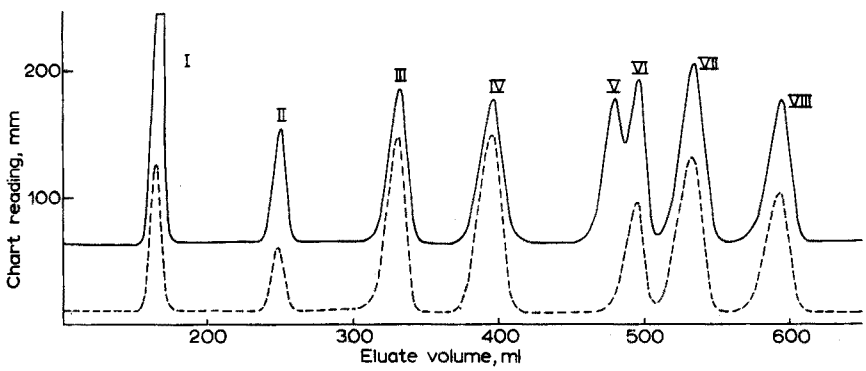

Fig. 1. Separation of 6-O-(β-D-glucopyranosyluronic acid)-D-galactose (I), cellobiouronic acid (II), 4-O-methyl-D-glucuronic acid (III), D-galacturonic acid (IV), erythronic acid (V), L-guluronic acid (VI), D-glucuronic acid (VII) and D-mannuronic acid (VIII). Carbazole method: broken line; dichromate method: full line. Column: 6 × 880 mm; Dowex 1 X-8, 13–17 μ. Eluant: 0.05 *M* sodium acetate. Flow rate: 1.1 ml/min.

as well as the carbazole reaction were recorded in different channels. It can be seen that all acids were recorded in the chromic acid channel whereas only uronic acids were recorded with carbazole.

Sodium acetate used as eluant in this run is suitable for separations of carboxylate ions corresponding to several monoprotic acids. As a rule saccharinic, aldonic, and uronic acids appear in order of decreasing molecular weight. Comparisons of the elution behavior of acids with the same number of carbon atoms but a different number of hydroxy groups, indicate that the interaction forces with the resin matrix increase

with a decreasing number of such groups. Many stereoisomers are well separated, a fact which is ascribed to differences in hydration and interionic forces. Some isomeric acids show almost identical distribution coefficients. No theory has been forwarded which permits a prediction of the elution position of various species, but some empirical rules can be traced.

For many purposes acetic acid gives more favorable separation factors than sodium acetate. Here the difference in acid strength of the acids to be separated is the most important factor. Expectedly, weak acids appear earlier on the chromatogram than stronger acids. The interaction forces with the resin matrix increase. On a resin with a polystyrene–divinylbenzene matrix these forces become very large with aromatic acids, and are of very great importance with aliphatic acids of low polarity also. These interaction forces are not taken into consideration in the simple theory (*cf.* ref. 20) which accounts for the fact that the agreement between calculated and observed peak positions is sometimes very poor. In elutions of hydroxy acids with mixtures of sodium acetate and acetic acid in varying proportions, the influence of changes in eluant composition can be predicted rather well from the fraction of anions in the external solution calculated by the mass action law.

A typical chromatogram showing a separation of carboxylic acids by elution with acetic acid is reproduced in Fig. 2.

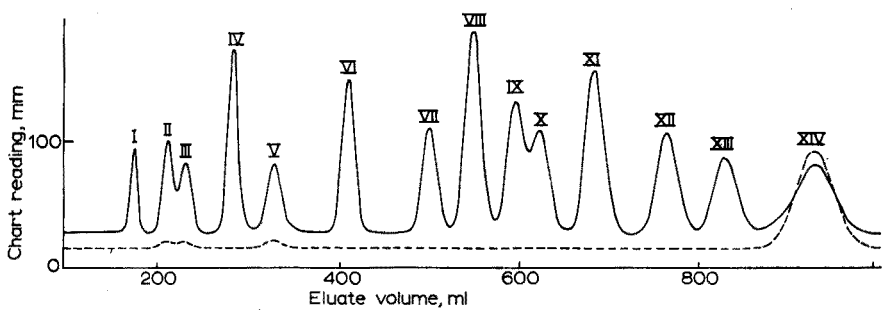

Fig. 2. Separation of levulinic (I), melibionic (II), lactobionic (III), talonic (IV), maltobionic (V), ribonic (VI), galactonic (VII), gluconic (VIII), gulonic (IX), arabinonic (X), xylonic (XI), mannonic (XII), erythronic (XIII) and galacturonic acid (XIV). Carbazole method: broken line; dichromate method: full line. Column: 6 × 1350 mm; Dowex 1 X-8, 26–32 μ. Eluant: 0.50 M acetic acid. Flow rate: 1.5 ml/min. (O. SAMUELSON AND L. THEDE: Unpublished work).

Attempts to speed up the separations by using eluants containing a cation which complexes with the anions to be separated have met with some success. Copper acetate and zinc acetate were used and theoretical expressions for the influence of the complex constants upon the elution behavior were derived[21]. The uncertainty of the stability constants reported in the literature for the actual systems where the central ion is present at large concentration and the ligands in only trace amounts is large and, therefore, only predictions of a qualitative kind can be made. Expectedly, species which give rise to non-sorbable complexes appear very early in the eluate. Aldonic acids belong to this group and are separated very easily from other acids such as the common uronic acids. Large individual differences exist between some adsorbable species. These eluants are valuable complements to sodium acetate and acetic acid.

The well-known formation of complex ions between borate and polyhydroxy

compounds was first applied by KHYM AND ZILL[22] to separations of sugars on anion-exchange resins. The anions of polyhydroxy acids obtain an increased charge in borate medium which explains why many polyhydroxy acids are held very strongly by a borate resin. Fortunately, the separation factors of many species which are difficult or impossible to separate in other eluants are improved. The application of this technique to the separation of the aldonic acids present in sulfite waste liquor (arabinonic, xylonic, mannonic, galactonic and gluconic acid) has met with success. Here, other methods have failed[23]. The relation between the structure of the acid and its elution position seems to be complicated, but from the theory of borate complexes with polyhydroxy compounds the order of elution in some systems can be predicted. The observations that aldonic acids appear in order of increasing molecular weight and that methylated uronic and biouronic acids appear much earlier than the corresponding non-methylated species are explained by existing theories, but these cannot explain the individual behavior of all stereoisomers.

Despite technical improvements and automation, separations in borate medium are in most cases more tedious than in other media. With many complicated systems, however, the method cannot be abandoned. In recent investigations on uronic acids, seven biouronic acids were studied. In sodium acetate (0.08 *M*) only three well separated bands were recorded. Acetic acid offered a separation into five bands while in sodium tetraborate all seven species were separated. In this medium one of the peaks had the same position as the most common monouronic acid in wood chemistry (4-O-methylglucuronic acid). In acetic acid the peak elution volumes of these two compounds differed by a factor of 3. Separations in various eluants are, therefore, necessary to obtain a complete resolution of complicated mixtures.

As in metal separations, the application of mixed solvents can greatly improve the separation factors of various organic acids. In mixtures of water and organic solvents the interaction forces with the resin matrix decrease[24], and activity coefficients, dissociation, and complex constants are altered. With the polyhydroxy acids partition effects become predominant. In aqueous ethanol, aldonic acids and uronic acids can be retained effectively by a resin in its sulfate form under conditions where less polar acids such as acetic acid pass directly into the effluent[25]. Very little work has been done on separations based upon partition effects of very similar acids.

PARTITION CHROMATOGRAPHY OF SUGARS

Among the 16 monosaccharides available from common commercial sources, 14 can be separated from one another on a column with a strongly basic anion exchanger in its sulfate form. Aqueous ethanol is used as eluant[26]. An early study of the sorption mechanism revealed that the sorption of strongly polar solutes is largely due to the higher water concentration inside the resin compared with that of the external solution. Interaction forces between the resin and the polar solutes cannot be neglected, however[27]. This was a hindrance to a simple thermodynamic treatment, but has recently been shown to be of practical importance. In this separation method the distribution coefficients of all sugars increase with an increased ethanol concentration within the interval of interest. The order of elution is unaffected, which facilitates a qualitative discussion of the influence of other variations upon the separations. Two examples are worth mentioning.

In experiments with a strongly basic resin with a matrix of cross-linked dextran, fructose and tagatose, which showed almost identical distribution coefficients on the styrene–divinylbenzene resin, were well separated. Rhamnose and 2-deoxyglucose were the only sugars which did not separate on either of the two resins. With the chloride form of the dextran resin, a mixture of the two sugars was resolved into two elution bands. In many other systems the chloride form is less satisfactory than the sulfate form.

These results, achieved by the trial and error method, demonstrate that interaction forces both with the resin matrix and the counter ions inside the resin are of great importance in separations based upon partition chromatography. More fundamental research is necessary before the influence of such variations upon the separation factors can be predicted.

SUMMARY

A review is given of variables which affect the separation factors in ion-exchange chromatography. In favorable cases the influence of complex formation, pH, and eluant concentration can be predicted by simple calculations, whereas the interaction forces inside the resin phase are still largely unexplored.

REFERENCES

1 O. SAMUELSON, *Svensk Kem. Tidskr.*, 51 (1939) 195.
2 O. SAMUELSON, *Svensk Kem. Tidskr.*, 57 (1945) 158.
3 C. W. JOHNSON, L. L. QUILL AND F. DANIELS, *Chem. Eng. News*, 25 (1947) 2494.
4 E. R. TOMPKINS AND S. W. MAYER, *J. Am. Chem. Soc.*, 69 (1947) 2859.
5 B. H. KETELLE AND G. E. BOYD, *J. Am. Chem. Soc.*, 69 (1947) 2800.
6 W. E. COHN AND H. W. KOHN, *J. Am. Chem. Soc.*, 70 (1948) 1986.
7 R. DJURFELDT AND O. SAMUELSON, *Acta Chem. Scand.*, 4 (1950) 165.
8 H. TITZE AND O. SAMUELSON, *Acta Chem. Scand.*, 16 (1962) 678.
9 G. E. BOYD, S. LINDENBAUM AND Q. V. LARSON, *Inorg. Chem.*, 3 (1964) 1437.
10 K. A. KRAUS AND G. E. MOORE, *J. Am. Chem. Soc.*, 71 (1949) 3263.
11 O. SAMUELSON AND E. SJÖSTRÖM, *Anal. Chem.*, 26 (1954) 1908.
12 H. P. GREGOR, D. NOBEL AND M. H. GOTTLIEB, *J. Phys. Chem.*, 59 (1955) 10.
13 C. W. DAVIES AND B. D. R. OWEN, *J. Chem. Soc.*, (1956) 1676.
14 J. KORKISCH, *Mikrochim. Acta*, (1964) 816.
15 J. S. FRITZ AND T. A. RETTIG, *Anal. Chem.*, 34 (1962) 1562.
16 O. SAMUELSON, *Svensk Papperstid.*, 46 (1943) 583.
17 F. NELSON AND K. A. KRAUS, *J. Am. Chem. Soc.*, 77 (1955) 329.
18 D. H. SPACKMAN, W. H. STEIN AND S. MOORE, *Anal. Chem.*, 30 (1958) 1190.
19 S. JOHNSON AND O. SAMUELSON, *Anal. Chim. Acta*, 36 (1966) 1.
20 O. SAMUELSON, *Ion Exchange Separations in Analytical Chemistry*, Wiley, Stockholm–New York, 1963.
21 O. SAMUELSON, *Svensk Kem. Tidskr.*, 76 (1964) 635.
22 J. X. KHYM AND L. P. ZILL, *J. Am. Chem. Soc.*, 73 (1951) 2399.
23 K. J. LJUNGQUIST, C. PARCK AND O. SAMUELSON, *Svensk Papperstid.*, 61 (1958) 1043.
24 K. K. CARROLL, *Nature*, 176 (1955) 398.
25 O. SAMUELSON AND R. SIMONSON, *Anal. Chim. Acta*, 26 (1962) 110.
26 P. JONSSON AND O. SAMUELSON, *Science Tools*, 36 (1996) 17.
27 H. RÜCKERT AND O. SAMUELSON, *Acta Chem. Scand.*, 11 (1957) 315.

Analytica Chimica Acta
Elsevier Publishing Company, Amsterdam
Printed in the Netherlands.

THE EFFECT OF THE MEDIUM ON ELECTROPHORETIC SEPARATIONS

H. BLOEMENDAL
Department of Biochemistry, University of Nijmegen (The Netherlands)

(Received November 1st, 1966)

Electrophoresis involves the migration of charged particles in solution under the influence of an electric field; this migration may occur either in free solution or in a buffer stabilized by an inert substance. It is now generally accepted that electrophoresis in a stabilizing medium is the more powerful tool both for analysis and isolation of charged components from complex mixtures. Although the designation ionophoresis, ionography or electrochromatography is sometimes used, most investigators prefer the name zone electrophoresis for cases when the medium in which the charged particles move is stabilized by paper, a powder, glass beads or gels. The classical method in free solution introduced by TISELIUS[1] is called moving boundary electrophoresis. This type of electrophoresis is performed in a thermostated U-shaped cell filled with an appropriate buffer.

In order to compare the merits and drawbacks of the various methods, the effect of various media on the electrophoretic behaviour of the same biological material was studied in the present work. The material considered was obtained from eye lenses.

The lens is a rather unique tissue, consisting mainly of protein and water. When an isolated lens is stirred in water or buffer, it gradually dissolves and, after a few hours, an opaque suspension is obtained which on centrifugation yields a sediment

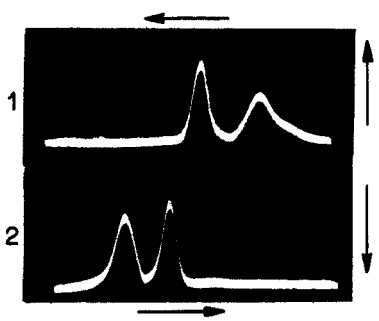

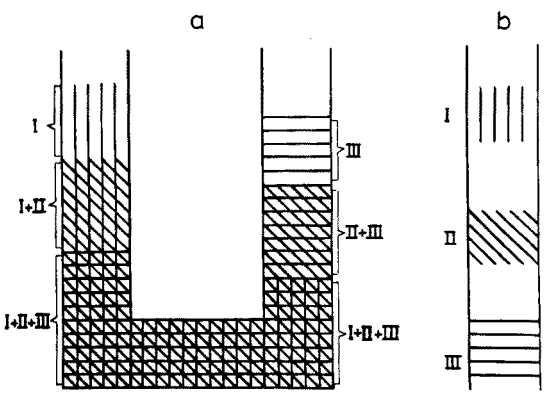

Fig. 1. Moving boundary electrophoresis of water-soluble lens protein (9 mA, 160 V; glycine–sodium acetate buffer ionic strength 0.1 at pH 7.7. (1) ascending, (2) descending. 1 h).

Fig. 2. Schematic representation of separation of 3 components with the aid of moving boundary (a) and zone (b) electrophoresis.

and a concentrated protein solution. The dissolved proteins are the so-called crystallins. In Fig. 1 is shown the pattern of the water-soluble bovine lens proteins observed in moving boundary electrophoresis. Two main fractions are visible. The peak with lower mobility (β) consists of two overlapping components; this overlapping indicates that quantitative separation is not feasible by this method. Figure 2 represents this disadvantage schematically. However, free electrophoresis can yield much useful information; *e.g.*, in the case of protein studies data are obtained on the charge, the degree of homogeneity, and the degree of interaction with other components etc. Especially for the calculation of mobilities, Tiselius' method is the most reliable technique.

The electrophoretic mobility, μ, is defined as the velocity of a charged particle under the influence of an electric field of unit strength:

$$\mu = \frac{\Delta x}{E\Delta t} = \frac{k\, q\Delta x}{i\Delta t} \qquad (1)$$

where Δx is the distance migrated by the particles, Δt the time of migration, E the field strength, k the specific conductance, i the current, and q the cross section of the electrophoresis cell.

The electrophoretic mobility depends on a number of parameters as follows: a) the charge, structure and molecular weight of the particle; and b) the electrolyte composition, ionic strength, pH and temperature of the solvent. Knowledge of the electrophoretic mobility of a protein at different pH values is necessary for the determination of the isoelectric point. The isoelectric point of a pure protein may be defined operationally as the pH at which the net charge over all protein molecules is zero. The isoelectric point is found by plotting the mobility versus pH. For α-crystallin,

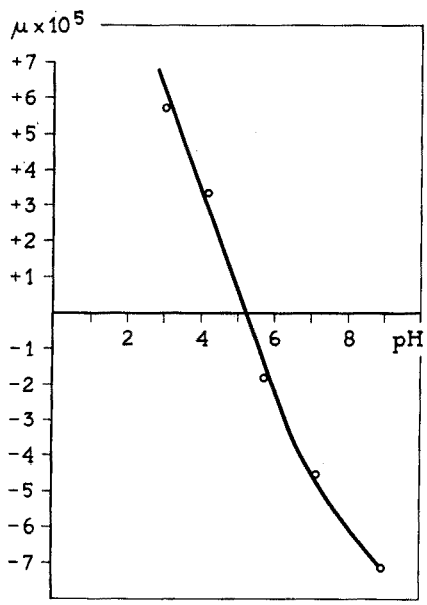

Fig. 3. Determination of the isoelectric point of α-crystallin with the aid of mobilities derived from moving boundary electrophoresis.

one of the lens proteins which has been studied most intensively, the isoelectric point is at pH 5.2 (Fig. 3).

From Fig. 1 it can be seen that the patterns in the ascending and the descending limbs of the U-shaped cell are not identical. Theoretically identical curves can be obtained at infinite dilution or at very high buffer-ion concentration. A second effect of non-ideality is the occurrence of the so-called δ and ε boundaries. For example, in the descending limb of an electrophoresis cell used in free electrophoresis, the protein boundary moves from the origin, the buffer concentration above the descending boundary changes and the so-called ε boundary, the mobility of which is low, appears. In the ascending limb analogous phenomena occur; the rising protein boundary displaces buffer ions, and again a false boundary is observed which is larger than the δ

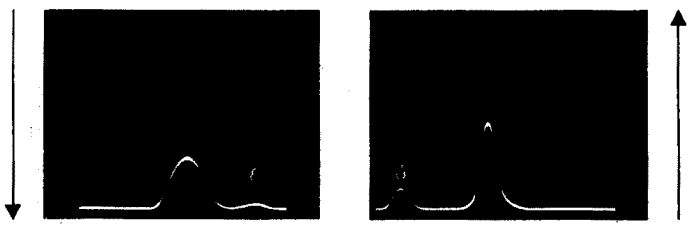

Fig. 4. "False" boundaries in the electrophoretic pattern of purified α-crystallin (conditions as in Fig. 1).

boundary since it is caused by a protein gradient. Figure 4 shows the δ and the ε boundary in the pattern of a purified α-crystallin preparation.

The application of moving boundary electrophoresis in the study of lens proteins in 1939 by HESSELVIK[2] provided evidence that at least one fraction exists in a homogeneous form. This fraction, α-crystallin, therefore was the component from the soluble lens proteins which appeared to be suitable for successful preparative electrophoresis.

The first widely applied stabilizer in zone electrophoresis was paper, which was introduced by KÖNIG[3] in 1937, and the merits of which have often been emphasized. This technique appeared to be very attractive because of its simplicity and cheapness.

A comparison of Fig. 1 with Fig. 5 clearly demonstrates that the resolution of the lens protein is better on paper than in moving boundary electrophoresis although careful thermostating was completely neglected. As in free solution α-crystallin moves

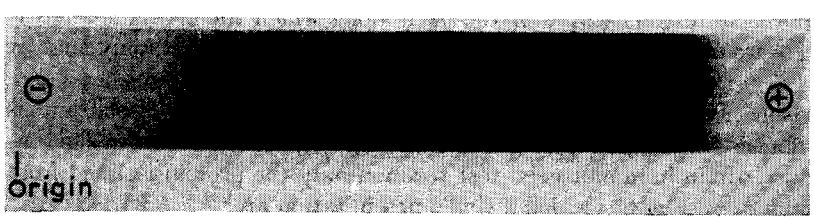

Fig. 5. Paper electrophoretic separation of soluble lens proteins (1.5 mA, 150 V; barbital buffer 0.025 ionic strength at pH 7.7; 4 h).

with the highest mobility. In some experiments the proteins of the β fraction were resolved into two components. Despite the vast number of publications on paper electrophoresis, very few deal with mobility studies because of complications. The theoretical treatment of electromigration in supporting media is generally difficult and the values obtained are in fact approximations. The equation for the electrophoretic mobility on paper μ_p is similar to eqn (1).

$$\mu_p = \frac{k\, q' \Delta x'}{i \Delta t} \tag{2}$$

where $\Delta x'$ is the distance migrated by the particle on paper, and q' is the cross sectional area of the paper strip.

In addition to the parameters which affect electrophoretic mobility in free electrophoresis (see p. 170), the mobility in a stabilizing medium is also affected by carrier effects (adsorption, liquid uptake of the support and sieving effects) and by electroosmosis and evaporation of the buffer. KUNKEL AND TISELIUS[4] reported that μ_p depends on the type of paper used. However, after multiplication by the factor l'/l (l = length of the path in the moving boundary electrophoresis cell; l' = path length on paper), values which differ only slightly for various filter papers are obtained. It has been recommended that constant current should be used in all cases of mobility studies[5,6]. In the present work, a value of 5.2 was derived for α-crystallin with the aid of free electrophoresis (Fig. 3). An analogous plotting of the data obtained by paper electrophoresis gave a value of 5. Paper has also been employed as stabilizer in continuous flow electrophoresis[7,8]. In this type of electrophoresis a buffer solution is transported in a direction perpendicular to the electric field, and the test substance is continuously admitted in the direction of the buffer flow. The individual charged components migrate at an angle to the direction of buffer flow and are collected separately at the bottom of the paper sheet. When efficient cooling is applied the potential gradient can be raised and the amount of protein to be separated can be increased. It is possible to handle quantities as large as 5 g of protein in 20 h.

The path of the migrating particle resulting from the electrical field and the gravitational forces becomes saturated after a certain time. Continuous flow electrophoresis has thus one clear advantage over many other zone electrophoretic methods: substances which are strongly adsorbed to the media in the discontinuous methods can be separated by this technique. WOOD *et al.*[9] separated the soluble proteins from rabbit lens into 5 distinct components.

In Fig. 6 the separation of bovine lens proteins by means of continuous flow electrophoresis is represented. It is clear that the track of the individual proteins in the paper depends on the field strength and the rate of buffer flow. Any change from constancy of both parameters will alter the path along which the crystallins move. MANSKI *et al.*[10] were able to show that the resolution patterns differed only slightly with time.

Comparison of the separations achieved by this method and by discontinuous paper electrophoresis reveals that stronger overlapping of fractions occurs in the continuous procedure. In an immunological test reaction only the protein isolated from drip points 2 and 3 (see Fig. 6) yielded a single precipitation arc.

For satisfactory preparative purposes, stabilizing media other than paper are more convenient. A survey of this subject was published a few years ago[11]. In Table I

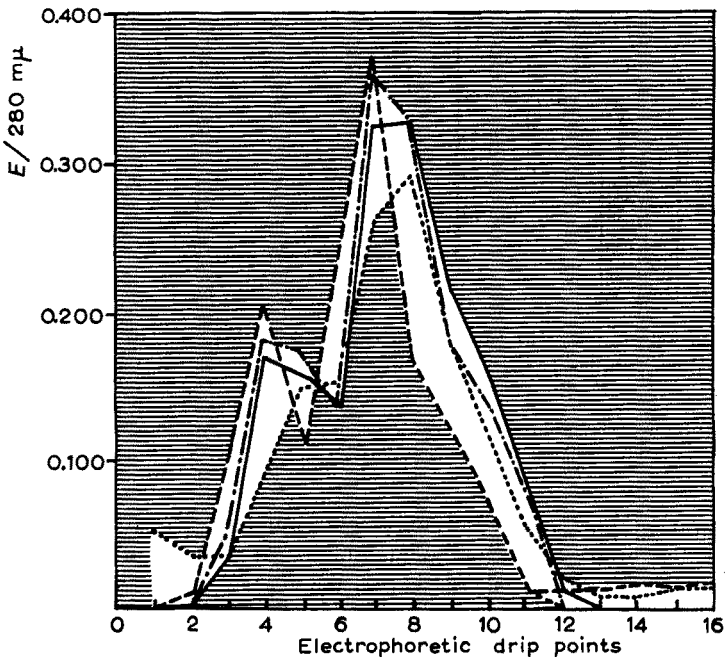

Fig. 6. Continuous flow electrophoresis of the soluble portion of bovine lens (32–36 mA, 450 V; phosphate buffer ionic strength 0.02 at pH 8.6). ———, 24 h; —·—·—·—·—, 48 h; — — — —, 72 h; - - - - -, 96 h. (Reproduced by courtesy of Dr. MANSKI.)

different zone electrophoretic techniques and the various media used are summarized. The apparatus required for most block- and gel electrophoresis methods is very simple. In Fig. 7 a scheme is represented for horizontal electrophoresis. Vertical arrangement of the trough gives improvement of separation in a number of cases, as electro-osmosis is counterbalanced by the hydrodynamic flow of the buffer. Of the media mentioned in the first column of Table I, starch granules and polyvinyl chloride powder have been used as support for the separation of lens proteins. Figure 8 shows the separation of the crystallins on a vertical starch block[12,13]; in this medium the β fraction is very complex (segments 6–16). Utilization of polyvinyl chloride as inert support

TABLE I

STABILIZING MEDIA FOR VARIOUS ZONE ELECTROPHORETIC TECHNIQUES

Block electrophoresis	*Column electrophoresis*	*Gel electrophoresis*
Starch granules	starch granules	starch (hydrolyzed)
Polyvinyl chloride	polyvinyl chloride	agar
Foam plastic	cellulose	agarose
Glass beads	glass beads (powder)	polyacrylamide
Silica (paste)	sucrose gradient	silica
Sephadex (cross-linked dextran)	Sephadex	
	agarose	

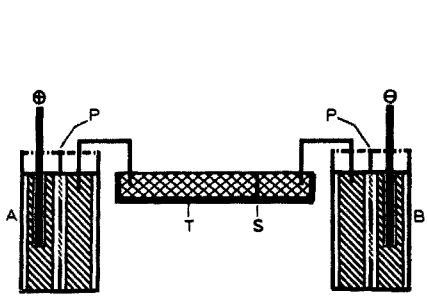

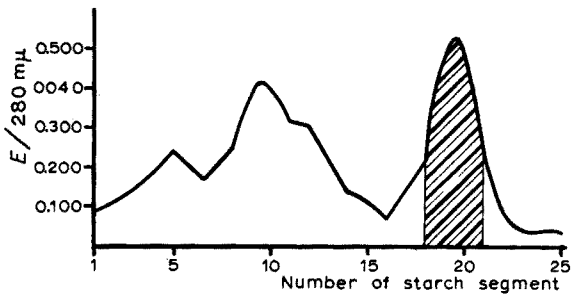

Fig. 7. Schematic representation of apparatus required for block electrophoresis. The trough (T) is connected with two electrode vessels (A, B) with semipermeable partitions (P). The sample is applied at (S).

Fig. 8. Starch block electrophoresis of soluble lens proteins (8 mA, 5 V/cm; phosphate buffer ionic strength 0.025 at pH 7.4, 16 h, starting zone at segment 2).

results in similar separation patterns[14]. Polyvinyl chloride has two advantages: 1) it is easier to prevent bacterial growth in this medium; and 2) some proteins are adsorbed less strongly than on starch. On the other hand, prewashing of starch is faster and easier. Electrophoresis on starch is more affected by the electro-osmotic flow than separations on filter paper. For the determination of the electrophoretic mobility on a stabilized medium, it is necessary to know the displacement of the charged particle due to electro-osmosis. The latter value (d_{el}) can be obtained by subjecting two known proteins to both moving boundary and zone electrophoresis. The following equations can then be applied:

$$\frac{\mu_1}{\mu_2} = \frac{\Delta x_1 - d_{el}}{\Delta x_2 - d_{el}} \tag{3}$$

where μ_1 is the mobility of protein 1 in free electrophoresis, μ_2 the mobility of protein 2 in free electrophoresis, Δx_1 the migration distance of protein 1 in zone electrophoresis, and Δx_2 the migration distance of protein 2 in zone electrophoresis.

The value d_{el} is necessary for the calculation of the electrophoretic mobility μ_s on starch (or polyvinyl chloride) blocks

$$\mu_s = d_{el} l / V \Delta t \tag{4}$$

where l is the length of the block (cm), V the average voltage across the ends of the block, and t the time (sec).

Of the material mentioned in Table I (second column) only cellulose has been utilized for the separation of lens proteins[15]. In Fig. 9, peak II representing the β-crystallin fraction has a symmetrical shape. The erroneous conclusion might be drawn that this component (at least at the pH of the experiment) is homogeneous. Starch block electrophoresis and other electrophoretic procedures however revealed that this assumption is not true.

Agar gels have often been applied for the separation of lens proteins. The electro-osmotic flow is considerably high in this medium[16–18].

A new type of electrophoresis was introduced by SMITHIES[19,20]. In gels prepared from starch hydrolyzed under standard conditions he obtained about 20 fractions

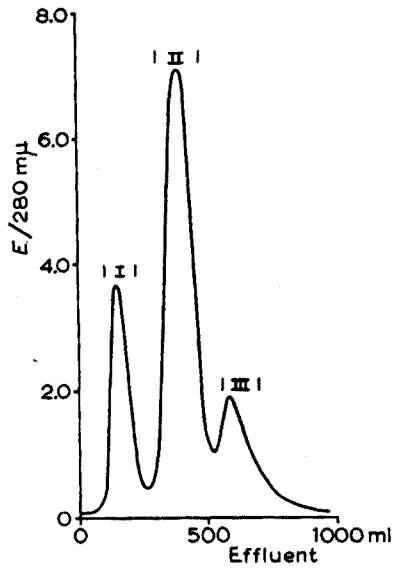

Fig. 9. Electrophoresis of calf lens proteins on a column packed with cellulose (5 V/cm; tris buffer 0.05 *M*, at pH 8, 46 h.) (Reproduced by courtesy of Dr. BJÖRK.)

from human serum. The enormous resolving power of starch gel is due to a molecular sieve effect. Whereas in paper, starch grains, agar or continuous flow electrophoresis, α-crystallin moves ahead of the other soluble lens proteins, a reversed pattern is observed in starch gel[21]. The conclusion that α-crystallin is a high-molecular-weight protein can easily be confirmed by sedimentation studies (19 S, mol.wt. 800,000). Gels of comparable or even higher resolving power can be prepared from polymerized acrylamide[22–25]. On this type of gel resolution of the total water-soluble lens protein into 5 fractions is achieved[26]. Again α-crystallin is retarded by the narrow pores of the gel (Fig. 10).

Initially it had been suggested that the cross-linking agent in the polymerisation mixture functioned only as a stabilizer without affecting the pore size of the gels[27,28]. JONGKIND *et al.*[29] however were able to show that lowering the amount of cross-linking agent resulted in an increase in pore size. The high-molecular-weight protein α-crystallin was used as test substance. The migration behaviour of α-crystallin in gels varies, depending on the amounts of N,N-methylenebisacrylamide; α-crystallin starts to migrate in gels containing 0.05% of this substance. Similar changes in migration rate have been observed in starch gels when the starch concentration is varied[30]. TOMBS[31] derived a semi-quantitative relationship between mobility and the distribution of pore size in polyacrylamide gels. In view of the insight which has recently been obtained in the mechanism of protein biosynthesis, the existence of protein molecules having a molecular weight of about 1,000,000 and consisting of one or two peptide chains can be excluded. Therefore, it was not surprising that α-crystallin split into a great number of bands when studied in starch gels containing high urea concentrations. Parallel experiments in buffered 7 *M* urea solutions with the ultracentrifuge revealed a decrease of the molecular weight from 800,000 to about 25,000.

Similar patterns were found in polyacrylamide gels polymerized in the presence

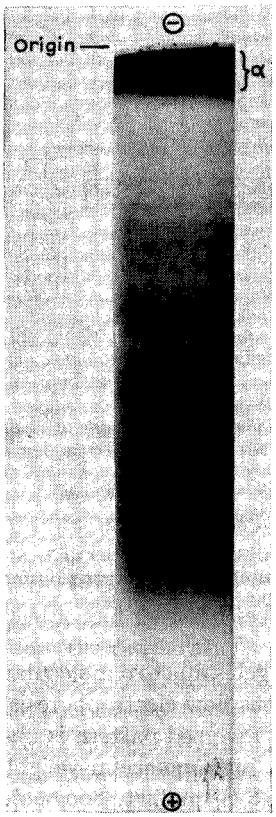

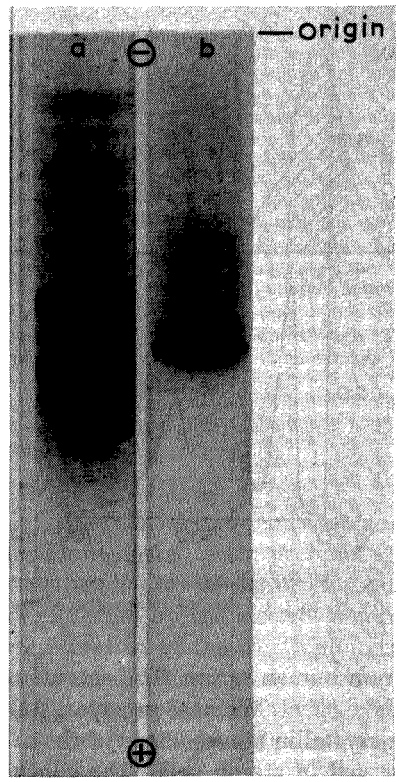

Fig. 10. Polyacrylamide gel electrophoresis of soluble lens proteins (5 mA, tris buffer 0.083 *M* at pH 8.9; 30 min).

Fig. 11. Electrophoretic pattern of α-crystallin in polyacrylamide gels. (2 mA; tris buffer 0.083 *M* at pH 8.6; 45 min). a) gels contain 7 *M* urea; b) gels contain 1 *M* β-mercaptoethanol and 7 *M* urea.

of urea (Fig. 11a). An interesting and important question is whether these subunits are identical or whether they differ in some way. The possible existence of monomers and polymers of the same subunit could be excluded by the ultracentrifugal data; but processes like isomerization, carbamoylation or disulfide interchange cannot completely be excluded. In such cases of doubt, substances other than urea or guanidine which disrupt non-covalent bands in proteins should be included in the electrophoretic studies. With polyacrylamide gels containing 1% sodium dodecylsulfate (SDS)[32], only 2–3 zones were observed. Parallel experiments in the analytical ultracentrifuge revealed that SDS treatment caused the same decrease in the sedimentation coefficient as 7 *M* urea. The large number of bands formed in the presence of 7 *M* urea was drastically reduced by addition of high concentrations of mercaptoethanol[33], a reagent which cleaves specifically disulfide bonds in proteins (compare Fig. 11b). It was also found that 2–3 zones occurred with acidic polyacrylamide gels. Again the ultracentrifuge revealed a drop in molecular weight from 800,000 to 25,000 at the acidic pH used in gel electrophoresis.

It may be concluded from these examples that application of various types of supporting media in electrophoretic procedures yields many fruitful results. Purification and isolation can be realized, mobility characteristics can be derived and, last but not least, data can be obtained which provide valuable information on the tertiary structure of high-molecular-weight proteins. It must be emphasized that additional verification with other physico-chemical techniques should never be neglected.

SUMMARY

Various electrophoretic techniques are discussed with bovine lens crystallins as test substance. Moving boundary, paper, starch-block, starch-gel and polyacrylamide gel procedures are compared.

REFERENCES

1 A. TISELIUS, *Nova Acta Reg. Soc. Scient. Uppsala*, Ser. IV, 7 (4) (1930).
2 L. HESSELVIK, *Skand. Arch. Physiol.*, 82 (1939) 151.
3 P. KÖNIG, *Actas Trabal. 3rd Congr. Sul. Am. Chem.*, 2 (1937) 334.
4 H. G. KUNKEL AND A. TISELIUS, *J. Gen. Physiol.*, 35 (1951) 89.
5 K. SCHILLING AND H. WALDMANN-MEYER, *Kem. Maanedsblad*, 39 (1958) 81.
6 K. SCHILLING AND H. WALDMANN-MEYER, *Acta Chem. Scand.*, 13 (1959) 1.
7 W. GRASSMAN AND K. HANNING, *Naturwissenschaften*, 37 (1950) 397.
8 E. L. DURRUM, *J. Am. Chem. Soc.*, 73 (1951) 4875.
9 D. C. WOOD, L. MASSI AND E. L. SALAMON, *J. Biol. Chem.*, 234 (1959) 329.
10 W. J. MANSKI, S. P. HALBERT AND T. P. AUERBACH, *Arch. Biochem. Biophys.*, 92 (1961) 512.
11 H. BLOEMENDAL, *Electrophoresis in Blocks and Columns*, Elsevier, Amsterdam, 1963.
12 H. BLOEMENDAL, *Koninkl. Ned. Akad. Wetenschap. Proc. Ser. C*, 59 (1956) 22.
13 H. BLOEMENDAL AND G. TEN CATE, *Arch. Biochem. Biophys.*, 84 (1959) 512.
14 J. H. WISSE, A. ZWEERS, J. F. JONGKIND, W. S. BONT AND H. BLOEMENDAL, *Biochem. J.*, 99 (1966) 179.
15 J. BJÖRK, *Biochim. Biophys. Acta*, 45 (1960) 1372.
16 R. J. WIEME AND M. KAMINSKI, *Bull. Soc. Chim. Biol.*, 37 (1955) 247.
17 W. F. BON AND P. C. NOBEL, *Rec. Trav. Chim.*, 77 (1958) 813.
18 J. FRANÇOIS AND M. RABAEY, *A. M. A. Arch. Ophthalmol.*, 61 (1959) 351.
19 O. SMITHIES, *Biochem. J.*, 61 (1955) 629.
20 O. SMITHIES, *Biochem. J.*, 71 (1959) 585.
21 H. BLOEMENDAL, W. S. BONT, J. F. JONGKIND AND J. H. WISSE, *Nature*, 193 (1962) 437.
22 S. RAYMOND AND L. S. WEINTRAUB, *Science*, 130 (1959) 711.
23 S. RAYMOND AND Y.-J. WANG, *Anal. Biochem.*, 1 (1960) 391.
24 P. E. HERMANS, W. F. MCGUCKIN, B. F. MCKENZIE AND E. D. BAYRD, *Proc. Staff Meetings Mayo Clinic*, 35 (1960) 792.
25 L. ORNSTEIN AND B. J. DAVIS, *Disc Electrophoresis* (preprint by Distillation Products Industries, Rochester 3, N.Y., 1962).
26 H. BLOEMENDAL, W. S. BONT, J. F. JONGKIND AND J. H. WISSE, *Exp. Eye Res.*, 1 (1962) 300.
27 B. J. DAVIS AND L. ORNSTEIN, *A New High Resolution Electrophoresis Method.*, Lecture for the Society for the Study of Blood, March 1959, New York Academy of Science.
28 S. RAYMOND AND M. NAKAMICHI, *Anal. Biochem.*, 3 (1962) 23.
29 J. F. JONGKIND, J. H. WISSE AND H. BLOEMENDAL, in *Protides Biol. Fluids, Proc. Xth Colloq., Brugge, 1962.*
30 O. SMITHIES, *Arch. Biochem. Biophys.*, suppl. 1 (1962) 125.
31 M. P. TOMBS, *Anal. Biochem.*, 13 (1965) 121.
32 H. BLOEMENDAL, W. S. BONT, E. L. BENEDETTI AND J. H. WISSE, *Exp. Eye Res.*, 4 (1965) 319.
33 H. BLOEMENDAL, H. J. HOENDERS, J. G. G. SCHOENMAKERS, A. ZWEERS AND J. J. T. GERDING, *Proc. Symp. Biochem. Eye, Tutzing, 1966*, in press.

Analytica Chimica Acta
Elsevier Publishing Company, Amsterdam
Printed in the Netherlands.

SEPARATION OF NOBLE METALS FROM BASE METALS BY MEANS OF A NEW CHELATING RESIN

G. KOSTER AND G. SCHMUCKLER
Department of Chemistry, Technion—Israel Institute of Technology (Israel)

(Received November 1st, 1966)

The noble metals dealt with in this work—platinum metals and gold—have an important property in common, namely, that in a certain environment they may be stabilized in a d^8 electronic configuration and form square-planar complexes with various ligands. NYHOLM AND TOBE[1] have given many examples of the possibilities of stabilizing the transition metals in various oxidation states by correctly chosen ligands.

In this work an attempt was made to stabilize the oxidation states of these metals (Pt^{2+}, Ir^{+}, Os^{0}, Pd^{2+}, Rh^{+}, Au^{3+}) by means of a chelating ion exchanger in which the active chelating agent contains two resonating amino groups attached to a carbon atom.

BAYER[2] was the first to stress the principle that if a ligand, which in an aqueous solution forms complexes with many different metal ions, is bound to a polymeric matrix, greater selectivity results, because the ligands have to assume a certain geometric arrangement in the resin.

Utilizing this principle, the authors succeeded in synthesizing a number of chelating ion exchangers of the general structure

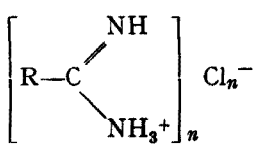

which very strongly bind the noble metals mentioned but do not bind the base metals at all. In order to determine the binding mechanism, some monomeric analogues of the polymeric system were investigated, among them benzylisothiouronium chloride (BTU) and sulphaguanidine (N'-amidinosulfanilamide) (SG). From their properties the processes in the polymer could be deduced.

It was found that the complexes formed by BTU with the noble metals enumerated are dimers with chlorine as the bridging atom, while the complexes formed with SG are monomers with a metal:ligand ratio of 1:2. Both complexes were found to be insoluble in water.

The tendency of these noble metals to form dimers with certain organic reagents is known from the literature, and examples may be found[3,4] in the carbonyl halides of Rh^{+}, in which chlorine serves as the bridging atom, or in the mercaptides[5], in which that function is filled by sulphur.

EXPERIMENTAL AND RESULTS

Reagents

S-Benzylisothiouronium chloride (Fluka AG, puriss) and *sulphaguanidine* (B.D.H., 99.0%) were used.

Chelating ion-exchange resin. The resonating amino groups were introduced into a styrene–divinylbenzene copolymer matrix by a method for which a patent has been applied[6]. The resin was rinsed with 0.1 *N* hydrochloric acid before use.

Preparation of the palladium–S-benzylisothiouronium complex (Pd–BTU)

To a palladium(II) solution (20 mg in 100 ml) at pH 1–2 was added 100 mg of solid S-benzylisothiouronium chloride (BTU) with constant stirring. A brown precipitate soon appeared and collected at the bottom of the vessel. Filtering the precipitate and washing and drying it at 100° produced the pure Pd–BTU. The BTU must be added as the solid and not in solution because of its relatively rapid hydrolysis in water.

Structural analysis of the palladium–BTU complex

Elemental analysis indicated that the complex corresponded to the formula $C_8H_9N_2SPdCl$, *i.e.* palladium(II) combined with one mole of BTU. For ignition of the organic complex at high temperature leaves the pure metal rather than its oxide.

The 1:1 reaction of palladium(II) with BTU was also proved by ordinary gravimetric methods; after the precipitate had been filtered and dried at 100°, its weight was determined, and then the palladium content was found after ignition at 1000°. From the formulae of the complex and of the reagent, it can be seen that two hydrogen atoms are liberated in the complex formation and this was proved by

TABLE I

pH CHANGES IN THE REACTION BETWEEN PALLADIUM AND BTU

No.	*Pd^{2+} concn. (moles)*	*Initial pH*	*Final pH*	*(H^+) evolved*
1	$3.16 \cdot 10^{-5}$	4.8	4.23	$5.9 \cdot 10^{-5}$
2	10^{-4}	4.71	3.65	$2.04 \cdot 10^{-4}$
3	$3.16 \cdot 10^{-4}$	4.45	3.12	$7.24 \cdot 10^{-4}$
4	10^{-3}	4.24	2.67	$2.08 \cdot 10^{-3}$
5	$3.16 \cdot 10^{-3}$	3.75	2.20	$6.13 \cdot 10^{-3}$
6	10^{-2}	3.79	1.77	$1.84 \cdot 10^{-2}$

potentiometric measurement of the pH before and after the addition of the ligand. Table I summarizes the experimental data obtained.

The amount of chlorine present in the palladium complex was determined by a semimicro modification of Schöniger's method, the chloride formed being determined by potentiometric titration with 0.05 *M* silver nitrate. The ratio of Pd to Cl was found to be 1:1.

Preparation of the palladium–sulphaguanidine complex

A solution containing 10 mg of palladium was diluted to 50 ml with distilled water, the pH was adjusted to 1.5–2.5 and the solution was heated to 70–80°. Sulphaguanidine (80–100 mg) was dissolved in 50 ml of hot distilled water and this solution was added slowly to the palladium solution with constant stirring. The precipitate did not form immediately; the solution had to be kept on a hot plate for 1½–2 h until the yellow precipitate settled. After the solution had cooled, it was filtered through a fine-pore Gooch crucible, washed with cold distilled water, dried at 100° for 1 h and weighed (gravimetric factor: 5.334).

Properties of the chelating resin

Maximum capacity of the resin. This was determined in 6 columns of 6-mm internal diameter and 15-cm length. Weighed samples of the dried (at 100°) resin were introduced into the columns. The concentration of the metal ions (in the form of their chlorides) flowing through the columns was invariably 1 mg/ml. The solutions were allowed to flow slowly through the columns until breakthrough was reached.

The columns were then flushed with water. The resin was taken out, weighed at 100° (in order to determine the weight of the bound metal), and ignited at 1000° in order to find the weight of the pure metals. To prevent the formation of oxides after the ignition the samples were allowed to cool in an atmosphere of carbon dioxide.

Table II summarizes the maximum capacities of the resin for the six noble metal ions.

TABLE II

MAXIMUM CAPACITY OF RESIN FOR NOBLE METALS

	Os^{3+}	Rh^{3+}	Ir^{4+}	Pd^{2+}	Pt^{4+}	Au^{3+}
Weight of dry polymer (mg)	537	532	537	521	600	524
Weight of polymer with bound metal ions at 110° (mg)	587	730.3	654.7	652.5	1067.1	1072.2
Weight of pure metal after ignition at 1000° (mg)		101.2	92.0	113.6	292.5	577.3
(mg) metal ion/(g) dry resin	93	190	158	218	488	1100
Millimoles metal ion/g dry resin	0.49	1.85	0.82	2.05	2.50	5.58
Volume changes during adsorption of metal ions	0.93	0.8	0.5	0.8	0.75	0.55

Influence of acidity. The noble metals must be adsorbed on the resin in an acidic medium, as in an alkaline environment hydrolysis of the metals as well as of the amine groups of the resin takes place. Increasing acidity, on the other hand, reduces the adsorptive capacity of the resin, since the binding of the metal ions is accompanied by the liberation of hydrogen ions: increasing the hydrogen ion concentration too far reverses the reaction. Figure 1 summarizes the experimental results for the metal ions Au^{3+}, Pt^{4+}, and Pd^{2+}. The experiments were conducted as follows: 100-mg batches of resin were placed in contact with the metal chloride solutions (containing 150 mg of Au^{3+}, 110 mg of Pt^{4+} or 106 mg of Pd^{2+} per 100 ml); to each batch a measured quantity of hydrochloric acid was added, and the solution was intensively stirred

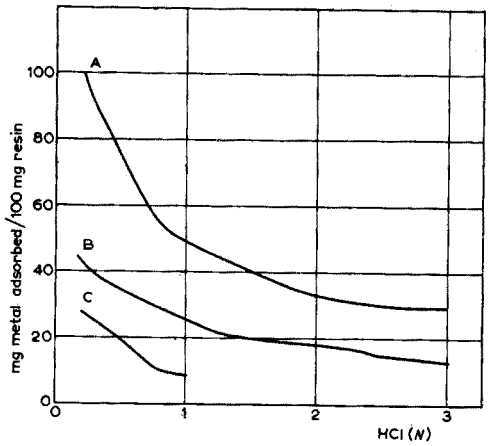

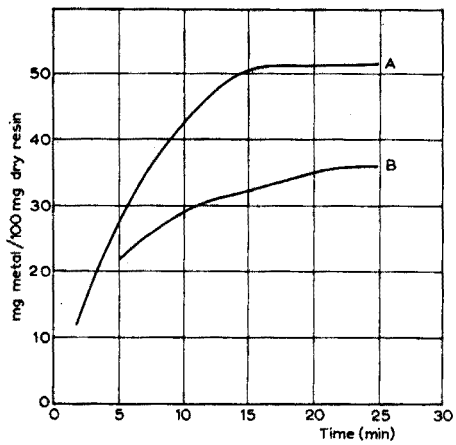

Fig. 1. Influence of acidity on the adsorption. For each batch of 100 mg resin: A, 1.50 g l^{-1} Au^{3+}; B, 1.10 g l^{-1} Pt^{4+}; C, 1.06 g l^{-1} Pd^{2+}.

Fig. 2. Rate of adsorption. A, 1.00 g l^{-1} Au^{3+}; B, 1.00 g l^{-1} Pt^{4+}.

for 24 h. After this the resin and the solution had been separated, and the amount of metal in the resin was determined.

Rate of adsorption. The rate of adsorption was determined for gold(III) and platinum(IV) in the following manner: 100-mg batches of resin were stirred with 100-ml batches of solution each containing 100 mg of the metal ion, and the resin was separated from the solution at fixed intervals. The amount of metal in the resin was found by ignition. Figure 2 summarizes the experimental results; it can be seen that adsorption is relatively rapid, the main portion of the metal ion being adsorbed within the first 15 min.

Adsorption in the presence of other metal ions. To illustrate the selectivity of the chelating resin, mixtures containing small quantities of platinum with large amounts of nickel(II), copper(II) or iron(III) were passed through columns containing 200 mg of resin. The results are summarized in Table III.

TABLE III

SELECTIVE ADSORPTION OF PLATINUM

Pt taken (mg)	*Base metal taken*	*Pt found by ignition of resin (mg)*
9.67	500 mg Ni^{2+}	9.65
9.67	500 mg Cu^{2+}	9.67
9.67	505 mg Fe^{3+}	9.56

DISCUSSION

For the determination of the reaction mechanism between a typical d^8 metal and the chelating reagents, the palladium(II) ion was selected. The reaction in an

acidic medium (pH 1–2) between palladium(II) and BTU gives a brown precipitate which, according to the analytical data, should be a dimer:

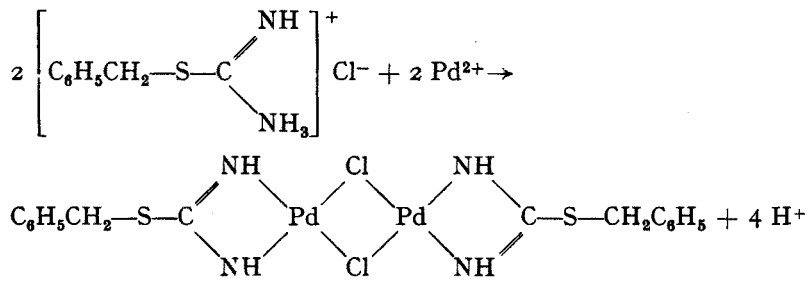

In the resin the reaction is entirely analogous, as regards the brown colour obtained, the amount of hydrogen liberated, and the ratio between palladium and chloride (1:1).

The reaction between palladium and SG produces a yellow precipitate in which the ratio of metal to ligand is 1:2 and coordination occurs through the resonating amino groups:

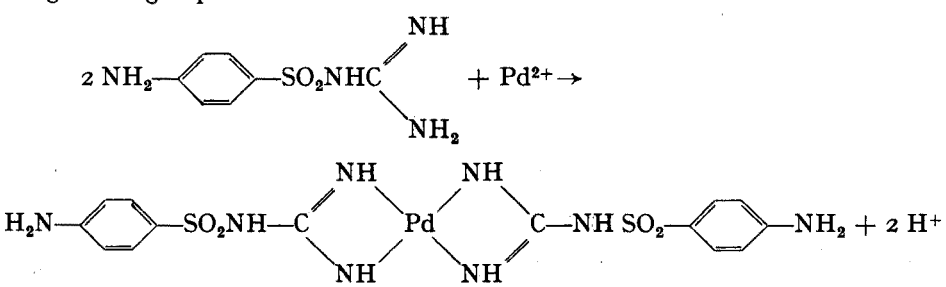

From Table II it can be seen that metal ions of different valencies were introduced into the columns. If the resin does indeed bind only ions with the d^8 electronic configuration forming square planar complexes, then only Pt^{2+} but not Pt^{4+} (in the case of platinum) ought to be adsorbed by the resin. In actual fact, however, the resin contains double bonds, so that it has redox properties. Some of the active groups in the resin are needed to reduce Pt^{4+} to Pt^{2+}, so that platinum(II) can be bound as a square planar complex. This may be proved by the diamagnetism of the compounds in the resin and by the fact that they can be eluted with oxidizing agents. The theoretical capacity of the resin according to the nitrogen analysis is 3.9 mmole/g, but the actual capacity is in most cases, except for gold, much smaller because of the redox reactions. The high capacity for gold is explained by the fact that the resin is able to reduce the gold to metallic gold. The formation of metallic gold on the resin is shown by the appearance of solid yellow spots. The reduction to metallic gold appears to take place in two stages, as suggested by LINGANE[7]; if a small quantity of metallic gold is present the reaction will be:

$$AuCl_4^- + 2\,Au + 2\,Cl^- \rightarrow 3\,AuCl_2^-$$

The univalent gold formed easily undergoes disproportionation to gold(III) and metallic gold, so that it is not surprising that the capacity for gold is very high indeed—5.58 mmole/g.

CONCLUSION

It is possible to stabilize oxidation states of metal ions which tend to form square planar complexes, by chelating in the solid phase in the presence of suitable ligands.

The following ions were examined: Os^{8+}, Rh^{3+}, Ir^{4+}, Pd^{2+}, Pt^{4+}, Au^{3+}.

When bound to the resin they assumed the valencies with which they have a d^8 electronic configuration, *viz.*: Os^0, Rh^+, Ir^+, Pd^{2+}, Pt^{2+}, Au^{3+}.

SUMMARY

A new type of chelating resin, which is highly selective for gold and the platinum metals, is described. Its properties and applications are indicated. The reaction mechanism between this resin and the noble metal ions was investigated with the aid of some monomer analogues.

REFERENCES

1 R. S. NYHOLM AND M. L. TOBE, (The Stabilization of Oxidation States of the Transition Metals), *Advan. Inorg. Chem. Radiochem.*, 5 (1963) 1.
2 E. BAYER, *Angew. Chem.*, 76 (1964) 76.
3 M. A. BENNETT AND P. A. LONGSTAFF, *Chem. Ind. (London)*, (1965) 846.
4 F. A. COTTON AND G. WILKINSON, *Advanced Inorganic Chemistry*, Interscience, New York, 1962, p. 843.
5 L. F. DAHL AND C. H. WEI, *Inorg. Chem.*, 2 (1963) 328.
6 *U.S. Patent*, Application No. 467,995.
7 J. J. LINGANE, *J. Electroanal. Chem.*, 4 (1962) 332.

Analytica Chimica Acta
Elsevier Publishing Company, Amsterdam
Printed in the Netherlands.

ADSORPTION OF THE RARE-EARTH ELEMENTS ON AN ANION-EXCHANGE RESIN FROM NITRIC ACID–ACETONE MIXTURES

J. ALSTAD
Department of Chemistry, University of Oslo (Norway)

A. O. BRUNFELT
Mineralogical-Geological Museum, University of Oslo (Norway)

(Received November 1st, 1966)

The effect of addition of miscible organic solvents to the aqueous phase on the ion-exchange adsorption behaviour of metallic ions has been given much attention during the last ten years. A paper, which mainly is concerned with thorium and uranium separation by KORKISCH AND JANAUER[1], gives extensive literature references on works in this field. A survey of organic solvents–nitric acid media specifically "designed" for anion-exchange separation of actinides and lanthanides has been given by STEWART *et al.*[2]. Concerning the rare-earth elements the latter authors concluded that solvent media providing a higher metal ion affinity for the resin than methanol, would yield possible systems for the separation of the individual heavier members of the series. In view of this it was considered worthwhile to investigate the acetone–nitric acid system as a medium for achieving rare-earth separation. Because of our research programmes on rare-earth distributions in rocks and minerals and their abundances in the biosphere measured by radioactivation analyses, fission yield determinations and nuclear property evaluations, it is of great importance to search for the optimum separation for application to the problems at hand. In addition, it was thought that the studies would contribute to a better understanding of the complex reactions involved in ion exchange from mixed-solvent systems.

EXPERIMENTAL

Reagents

Ion-exchange resin. Dowex 1-X8, 400 mesh, chloride form (Fluka AG), which is a strongly basic anion-exchanger, was employed. Before use the fine particles were removed by washing. The resin was purified by passing 6 *M* nitric acid and de-ionized water through a column until no trace of chloride was detectable in the effluent. The resin was further washed with acetone, air-dried, placed in an oven at 100° for 2–3 h and stored in a stoppered bottle.

Nitric acid–acetone solutions. The required volumes of analytical-grade (d. 1.42) nitric acid–acetone (E. Merck AG) mixtures were prepared just before use.

The hazard of an explosion with a nitric acid–ketone mixture has been emphasized earlier[3], and during this work the unstable character of nitric acid–acetone mixtures was confirmed. An increase in the relative amount of nitric acid in a mixture

increases the possibility that the mixture will undergo a violent reaction on standing. During the present work it was observed that mixtures of 40% nitric acid–60% acetone react violently after about one day. Before discarding, it is, therefore, recommended that the solutions should be diluted with large amounts of water.

Radionuclides. Oxides of elements of the lanthanum series and yttrium of 99.9% purity (Lindsay Chemical Co.) and scandium oxide (Johnson, Matthey and Co. Ltd.) were used. A few milligrams of each element were separately sealed in polyethylene vials and irradiated for 1–6 days in a neutron flux of 10^{12} n cm^{-2} sec^{-1} in the JEEP reactor, Institutt for Atomenergi, Kjeller. The following radioactive nuclides were used: 40-h ^{140}La, 32.5-d ^{141}Ce, 33-h ^{143}Ce, 19-h ^{142}Pr, 11.1-d ^{147}Nd, 2.6-y ^{147}Pm, 47-h ^{153}Sm, 9.3-h ^{152m}Eu, 12.4-y, 16-y ^{152,154}Eu, 18-h ^{159}Gd, 72.4-d ^{160}Tb, 2.35-h ^{165}Dy, 27.0-h ^{166}Ho, 7.5-h ^{171}Er, 127-d ^{170}Tm, 31-d ^{169}Yb, 4.2-d ^{175}Yb, 3.68-h ^{176}Lu, 6.7-d ^{177}Lu, 64.5-h ^{90}Y, and 84-d ^{46}Sc. The ^{147}Pm (chloride form) was supplied by the Radiochemical Centre, Amersham, England.

Stock solutions of these nuclides were prepared by dissolving the appropriate amounts of the irradiated oxides in nitric acid. (Ceric oxide was dissolved in nitric acid and hydrogen peroxide, the solution evaporated to dryness and the residue taken in nitric acid. The promethium chloride solution was evaporated to dryness and dissolved in nitric acid.)

Apparatus

Ion-exchange columns. Two columns were used, both 4 mm in internal diameter. The heights of the resin beds were 15 cm and 45 cm, respectively.

The automatic fraction collector was a Misco model 6722.

A well-type scintillation detector with a $1^7/_8 \times 2''$ thallium-activated sodium iodide crystal and a single channel γ-ray spectrometer (Nuclear Chicago Corporation model 1810) were used for the γ-activity measurements.

Determination of distribution coefficients

Approximately 0.5 g of resin samples was accurately weighed and transferred to 100-ml polyethylene screwcap bottles. An appropriate amount of the radionuclide solution of interest was added followed by the desired volumes of nitric acid and acetone, the sum of the volumes being 25 ml. The bottles were stoppered (at slightly less than the atmospheric pressure) and agitated in a mechanical shaker machine at approximately 25° for about 16 h. The resin was allowed to settle, and the activity, A_s, of an aliquot of the supernatant liquid was measured. By measurement of the activity, A_t, of an equal aliquot from a 25-ml blank sample, the activity adsorbed by the resin was determined. The distribution coefficient, D, was calculated as follows:

$$D = \frac{(A_t - A_s) \cdot \text{ml of solution}}{A_s \cdot \text{g of resin}} \qquad (1)$$

Studies of column elution behaviour

Before loading the column, the resin was preconditioned overnight in a solution of 10% 15.6 M nitric acid–90% acetone. A synthetic mixture of the irradiated rare-earth elements was taken up in 20 ml of the same mixed solvent and passed through the column. After the sorption step the elution was started with 20% nitric acid–80% acetone. As the concentration of the nitric acid was increased, a higher pressure was

needed to ensure a steady flow rate. The effluent leaving the column was collected in polyethylene vials in fractions of 1.25 ml and counted.

RESULTS AND DISCUSSION

Equilibrium studies

In Fig. 1 the variation of log D with vol.-% of conc. nitric acid in the acetone phase is shown for the rare-earth elements. At low per cent nitric acid it is seen that these elements are very strongly adsorbed, and that the distribution coefficients decrease smoothly with increasing acid content in the liquid phase. The cerium

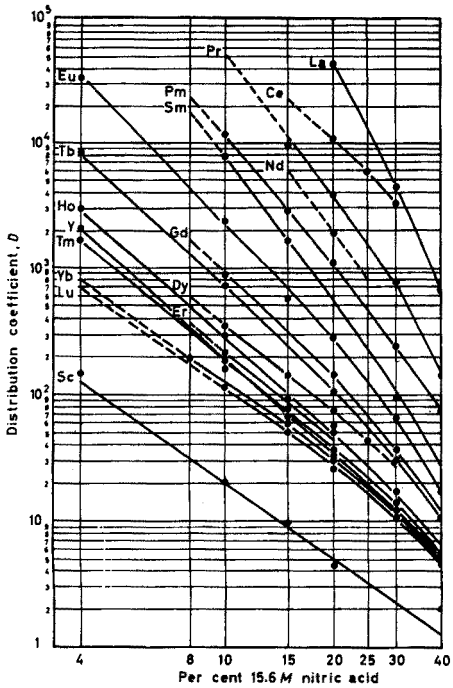

Fig. 1. Variation of distribution coefficient with volume per cent of nitric acid in acetone. Dowex 1-X8, 400-mesh resin.

distribution curve declines less than those of the neighbours and might indicate a partial oxidation of the cerium(III) to cerium(IV) at high acid concentrations. It is also apparent that the value of the distribution coefficients for yttrium is in the vicinity of that of thulium in the whole range of acid concentration studied. The trend for scandium looks approximately like the rare-earth elements, but the adsorption is much less.

The distribution coefficients decrease with increasing atomic number in the lanthanum series. This trend is in accordance with the results for aqueous lithium nitrate solutions determined by MARCUS AND NELSON[4]. The same trend is also found for the light rare-earth elements in 8 M nitric acid studied by ICHIKAWA[5]. The anion-

exchange behaviour in the nitrate medium is, however, the reverse of that found in chloride[6], thiocyanate[7] and carbonate[8] media.

The general effect of a mixed solvent compared to a pure aqueous system is a substantial increase in distribution coefficients. From the present work, the 90% acetone system increases the distribution coefficients of the rare earths by a factor of 10^3–10^5, as may be seen in Fig. 2. The increase in log D with increasing $1/\varepsilon$, where ε is the dielectric constant of the solvent, is shown qualitatively by comparison of ICHIKAWA's data on the aqueous ($\varepsilon = 80$) nitric acid[5], the results of FARIS AND

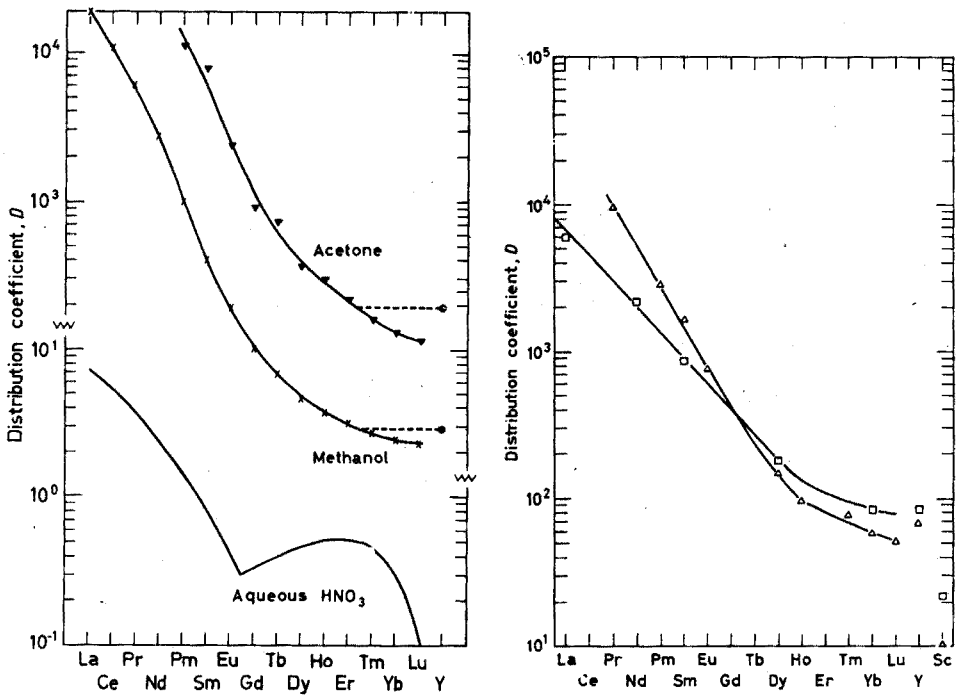

Figs. 2–3. Equilibrium adsorption on anion-exchange resin.
Fig. 2. ▼, present study, 10% nitric acid–90% acetone, Dowex 1-X8, 400 mesh resin. ×, FARIS AND WARTON[9], 10% nitric acid–90% methanol, Dowex 1-X4, 200–400 mesh resin. Line drawn without symbols, ICHIKAWA[5], 8 M nitric acid, Dowex 1-X8, 100–200 mesh resin.
Fig. 3. △, present study, 15% nitric acid–85% acetone, Dowex 1-X8, 400 mesh resin. □, FRITZ AND GREENE[10], 15% nitric acid–85% isopropanol, Amberlyst XN-1002, 60–100 mesh resin.

WARTON[9] on the 90% methanol ($\varepsilon = 32.6$) system, and the present work on the 90% acetone ($\varepsilon = 20.7$) system. The slope of the distribution coefficient as a function of atomic number gives a measure of the separation factors, and a comparison of the systems shows a general increase of the separability by mixed solvents.

The pattern of the distribution coefficients for the acetone and the methanol systems is very similar, but the acetone system seems slightly favorable in the heavy region of the lanthanides. This small effect may be due partly to the difference in the cross-linking of the Dowex 1 used in the two studies (acetone system–Dowex 1-X8 and methanol system–Dowex 1-X4).

A further comparison of mixed solvents is shown in Fig. 3 where the work of FRITZ AND GREENE[10] on the nitric acid–85% isopropanol system with Amberlyst XN-1002 is related to the present data for 85% acetone. A pure dielectric coefficient effect should result in slightly higher distribution coefficients of rare earths in the isopropanol ($\varepsilon = 18.3$) system. This is observed only in the heavy lanthanides, yttrium and scandium, while the opposite situation is found for the light lanthanides. This results in a significantly higher separation ability of the acetone–Dowex 1-X8 system compared to the isopropanol–Amberlyst XN-1002 one. This difference in behaviour may be due to two effects. The first is the usual decrease in selectivity with decrease in cross-linking which is similar to the effect discussed for the acetone and methanol systems above. The second effect to be considered is the influence of the type of exchange groups on the magnitude of the ion-exchange adsorption and the selectivity. Both Dowex 1 and Amberlyst XN-1002 contain exchange groups of the quaternary ammonium type, but there is a difference in the organic radicals attached to the nitrogen atom. The Dowex 1 exchange group is trimethylbenzylammonium while the Amberlyst one is a dimethylethanolammonium. If we assume that the mechanism of anion-exchange adsorption from mixed solvent is an extraction of the metallic salt, Dowex 1 should have a higher metal acceptor power than Amberlyst owing to the difference in the polarizability of their nitrogen atoms. This effect of metal acceptor power is observed for the light elements, but gradually disappears for the heavy lanthanides, yttrium and scandium. This trend follows the decrease of the basicity in the series from lanthanum through lutetium to scandium.

In order to study the influence of the different organic solvents only, the distribution of scandium between Dowex 1-X8 and acetone, ethanol and methanol was investigated at different amounts of concentrated nitric acid in the liquid phase. The log D *vs.* log per cent nitric acid functions, as shown in Fig. 4, indicate that the log D increases with $1/\varepsilon$ at low acid concentrations for these solvents. With about 10% nitric acid in the liquid phase, however, the distribution coefficients become equal in the acetone and ethanol systems, and on further increase in the concentration of nitric acid, the distribution coefficient in the ethanol solvent becomes the higher one. At all concentrations of nitric acid used the methanol system attains the lowest distribution coefficient values. In order to explain this puzzling behaviour of the distributions for various organic solvents in the mixed liquid phase, it may be necessary to consider the dependence of the activity coefficients on ion association[11–13]. In the present systems one has to take into consideration especially the different states of the nitric acid in the various mixed liquid phases.

A plot of the log D in the acetone system *vs.* the inverse value of the ionic radii for the lanthanum series is shown in Fig. 5 at different nitric acid proportions. The slope of these functions, which represents the influence of a pure electrostatic force influence on the separation power, divides the lanthanides into two groups with a distinct break at gadolinium. The smaller slope in the heavy region indicates the generally known greater difficulty in separating this group of the elements. By decreasing the nitric acid portion the slopes increase in both the light and the heavy elements indicating an optimum separation of all these ions by a pure acetone liquid phase. It is not likely that a change in concentration of the nitric acid itself influences the observed effect on the separability. The content of water in the liquid phase, however, varies proportionally with the acid portion and, consequently, the amount

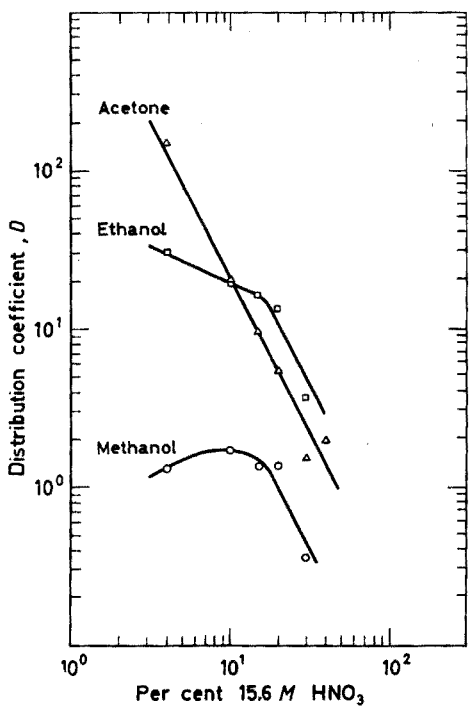

Fig. 4. Variation of distribution coefficient for scandium with vol.-% of nitric acid in organic solvent. Dowex 1-X8, 400-mesh resin.

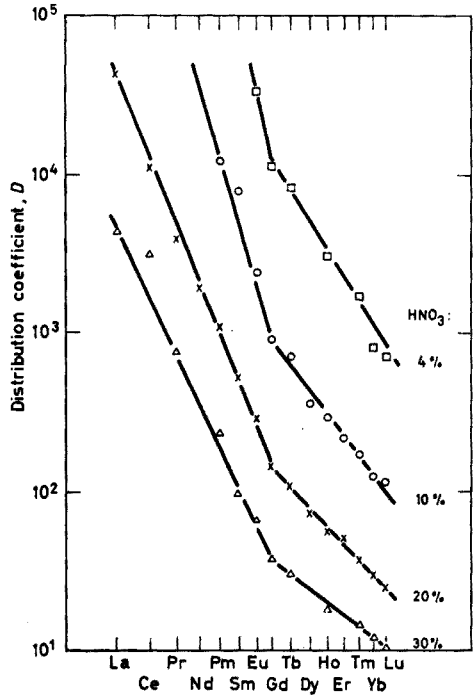

Fig. 5. Variation of distribution coefficient with the reciprocal of the ionic radius of the rare-earth ion. Nitric acid–acetone system. Dowex 1-X8, 400-mesh resin.

of water available for hydration of the metallic ions decreases with decreasing nitric acid content. In a non-aqueous acetone solution one should have an association of dehydrated ions with a maximum of difference in the adsorption of adjacent lanthanide ion salts.

The distribution coefficient for terbium was measured at different overall concentrations of nitric acid in 80% acetone mixed solvent. The results show that the log D increases linearly with the log HNO_3 concentration indicating a 1.4 power dependence of the acid concentration. This is approximately a factor of 2 higher than the dependence found by FARIS AND WARTON[9] in their 90% methanol system and by HINES *et al.*[14] who studied some actinides also in the 90% methanol system. Both these values show that from an extraction mechanism point of view the reaction equation involved is complex.

Column studies

The batch equilibrium studies indicated that, in order to obtain sufficiently high separation factors for the heavy lanthanides, it is necessary to perform the elution by a mixed solvent containing a high percentage of acetone. In this case, however, the D values are inconveniently high, resulting in large elution volumes and time-consuming separation. As an initial experiment it was therefore decided to start with

20% nitric acid in the eluting agent and to increase the percentage of acid successively in order to elute the lighter lanthanides from the column in reasonable time. As shown in Fig. 6 the peaks of the heavy elements overlap, whereas scandium, as the first element to be eluted (after the activity of the impurities), is well separated from these elements. Even with a column of 45 cm height the lutetium through holmium tracers are eluted in a bulk. The lighter elements are easily separated and their peaks are

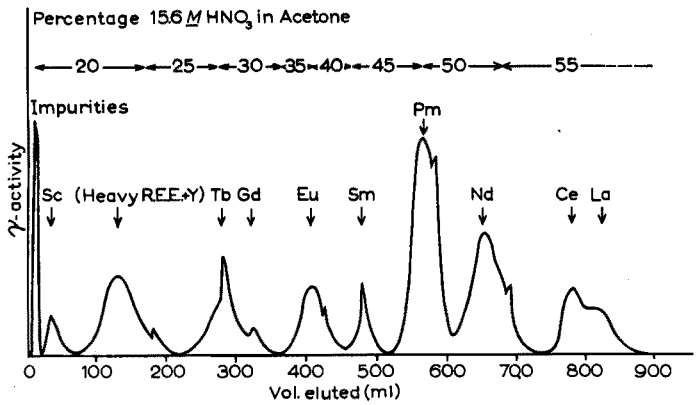

Fig. 6. Elution curve for the separation of a synthetic mixture of rare-earth elements, Dowex 1-X8, 400 mesh resin. Column dimensions 15 cm × 4 mm. Flow-rate 0.2 ml min^{-1} cm^{-2}.

apparently symmetrical except for the small extra peaks due to the changes in the composition of the eluting agent. The absence of tailing indicates an exchange rate of sufficient magnitude for effective column separations even at higher elution flow rates than the 0.2 ml cm^{-2} min^{-1} which was used in these experiments.

After the present study had been undertaken a work on separation of thorium from the rare-earth elements using Dowex 1-X8 and diluted nitric acid–acetone was published by KORKISCH AND AHLUWALIA[15]. Their results show a less than marginal separation power for the four elements of the lanthanum series (lanthanum, cerium, gadolinium and dysprosium) used and are consistent with the present more detailed work on the rare-earth elements, namely that the separation factors decrease with increasing water content in the mixed solvent.

CONCLUSION

The Dowex 1-X8 resin with a nitric acid–acetone medium is a powerful system for separating the rare-earth elements. Under the conditions for optimal separation of the heavy lanthanides, however, the distribution coefficients are too high for conventional column separation of all the rare earths, *i.e.* the ratio between the amount of ion exchanger and the solvent in a column is too high for a straight-forward application of the system.

The authors are indebted to Professor A. C. PAPPAS for his encouragement in this work. The financial support by the Royal Norwegian Council for Scientific and

Industrial Research and the Norwegian Research Council for Science and the Humanities is gratefully acknowledged.

SUMMARY

The distribution coefficients on Dowex 1-X8 anion-exchange resin were determined for all the rare earths at various proportions of concentrated nitric acid and acetone, using radioactive tracers of the metallic ions. In the range 4–40% nitric acid, the distribution coefficients decrease with increasing content of nitric acid, and at a given ratio of acid to acetone, they decrease with increasing atomic number in the lanthanum series. The value for yttrium is close to that of thulium; scandium is much less adsorbed. Literature data for aqueous systems and other mixed solvent systems are discussed. The distribution of scandium between Dowex 1-X8 and conc. nitric acid–methanol, ethanol or acetone systems is described. The separation power of the nitric acid–acetone system at different acid concentrations is analysed. Dowex 1-X8 resin with a nitric acid–acetone solvent is shown to be sufficient for separation of the rare-earth elements by ion-exchange chromatography.

REFERENCES

1 J. KORKISCH AND G. E. JANAUER, *Talanta*, 9 (1962) 957.
2 D. C. STEWART, C. A. A. BLOOMQUIST AND J. P. FARIS, *USAEC Report ANL-6999*, 1965.
3 L. E. GLENDENIN, K. F. FLYNN, R. F. BUCHANAN AND E. P. STEINBERG, *Anal. Chem.*, 27 (1959) 59.
4 Y. MARCUS AND F. NELSON, *J. Phys. Chem.*, 63 (1959) 77.
5 F. ICHIKAWA, *Bull. Chem. Soc. Japan*, 34 (1961) 183.
6 E. K. HULET, R. G. GUTMACHER AND M. S. COOPS, *J. Inorg. Nucl. Chem.*, 17 (1961) 350.
7 J. P. SURLS, JR. AND G. R. CHOPPIN, *J. Inorg. Nucl. Chem.*, 4 (1957) 62.
8 T. TAKETATSU, *Bull. Chem. Soc. Japan*, 37 (1964) 906.
9 J. P. FARIS AND J. W. WARTON, *Anal. Chem.*, 34 (1962) 1077.
10 J. S. FRITZ AND R. GREENE, *Anal. Chem.*, 36 (1964) 1095.
11 J. S. FRITZ AND H. WAKI, *J. Inorg. Nucl. Chem.*, 26 (1964) 865.
12 A. T. DAVYDOV AND R. F. SKOBLIONOK, *Zh. Fiz. Khim.*, 32 (1958) 1703.
13 G. POPA, C. LUCA AND V. MAGEARU, *J. Chim. Phys.*, 62 (1965) 449.
14 J. HINES, M. A. WAHLGREN AND F. LAWLESS, *Proc. 6th Conf. on Anal. Chem. in Nucl. Reactor Technology, Gatlinburg, Tenn., October 1962*, USAEC Report TID-7655, 1963, p. 247.
15 J. KORKISCH AND S. S. AHLUWALIA, *J. Inorg. Nucl. Chem.*, 28 (1966) 264.

Analytica Chimica Acta
Elsevier Publishing Company, Amsterdam
Printed in the Netherlands.

MACRORETICULAR ION-EXCHANGE RESINS: SOME ANALYTICAL APPLICATIONS TO PETROLEUM PRODUCTS

P. V. WEBSTER, J. N. WILSON AND M. C. FRANKS
The British Petroleum Company Ltd., BP Research Centre, Sunbury-on-Thames, Middlesex (Great Britain)

(Received November 9th, 1966)

The profound effect which trace components can have upon the behaviour of a material is well known. For example, certain properties of petroleum products can be considerably affected by the presence of naturally occurring non-hydrocarbons such as alkylphenols, naphthenic (carboxylic) acids, nitrogen bases and pyrrollic compounds. There is also a formidable number of additives which, even when used in trace amounts, can greatly modify specific properties of a product. If these trace components, naturally occurring or additive, can be separated according to their chemical characteristics and concentrated into fractions, then the subsequent analysis of the constituent compounds will usually be simpler and more effective.

This paper describes the use of macroreticular strong ion-exchange resins for the separation from both model solutions and petroleum products of certain polar non-hydrocarbons. Use is made of the facility shown by these resins under non-aqueous conditions for the physical adsorption of polar molecules, and also of the ability of cation-exchange resins in transition metal form to adsorb many ligand-forming materials from hydrocarbon solution.

MACRORETICULAR ION-EXCHANGE RESINS

MUNDAY AND EAVES[1] showed that orthodox ion-exchange resins can be used to adsorb certain basic and non-basic nitrogen compounds, alkylphenols and naphthenic acids from both model solutions and petroleum products. Their work was limited, however, by the fact that the ion-exchange resins they used were designed for use under aqueous conditions and were relatively inefficient in reacting with bulky organic molecules in non-aqueous media. Since their work was published, macroreticular ion-exchange resins, designed for use in non-aqueous media, have become commercially available. They differ from orthodox resins in possessing a spongelike structure with large pores of up to 1000 Å diameter, which are relatively unaffected by the solvent medium. Thus large organic molecules in hydrocarbon solution may diffuse freely within the resin phase. In addition the resin matrix possesses great mechanical strength, and unlike orthodox resins shows no marked deterioration when subjected to repeated changes from an aqueous to a non-aqueous environment. The resins used in the present work were Amberlyst 29, a quaternary ammonium anion exchanger, and Amberlyst 15, a sulphonic acid cation exchanger, both manufactured

by Rohm and Haas; and Deacidite K, a macroporous anion-exchange resin, manufactured by the Permutit Company Limited.

SEPARATION OF NATURALLY OCCURRING TRACE COMPONENTS

TABLE I

ADSORPTIONS FROM TOLUENE SOLUTION USING A MACRORETICULAR STRONG ANION-EXCHANGE RESIN

Resin form (Counter ion)	*Mode of adsorption*		
	Naphthenic acids	*Alkylphenols*	*Pyrrollic compounds*[a]
Chloride	Physical	Physical	Physical
Carbonate	Chemical	Physical	Physical
Hydroxide	Chemical	Chemical	Physical

[a] Pyrrole itself polymerises on the resin and is strongly adsorbed.

As with conventional ion-exchange procedures, separation in a non-aqueous medium is effected by two operations, those of adsorption and desorption. However, in addition to ion-exchange reactions, physical adsorption becomes a major factor when polar compounds are applied to resins in non-polar solvents, such as hydrocarbons. This is illustrated in Table I, which shows the mode of adsorption of pyrrollic compounds, alkylphenols and naphthenic acids when applied in toluene solution to strong anion exchangers with various counter ions.

The physically adsorbed materials may be readily eluted with polar solvents

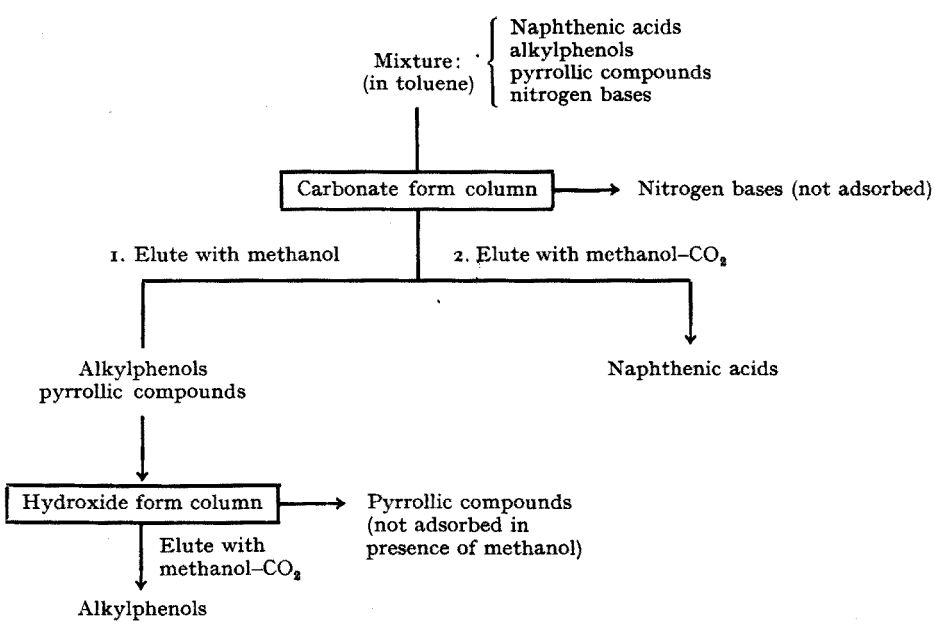

Fig. 1. Separations using macroreticular anion-exchange resin.

such as the lower aliphatic alcohols. This treatment with lower aliphatic alcohols does not remove chemically bound materials which may however be desorbed with polar solvents saturated with carbon dioxide. Thus a physically adsorbed material may be separated from one which is chemically adsorbed by a two-stage desorption process. If two resin columns are used, one in the carbonate, the other in the hydroxide form, it is possible to separate the four classes of compounds from a model solution containing naphthenic acids, alkylphenols, pyrrollic compounds and nitrogen bases. This separation is shown schematically in Fig. 1. The nitrogen bases, which are not adsorbed by anion-exchange resins, may be extracted by percolation through a strong cation-exchange resin in the free acid form, and recovered by elution with solutions of ammonia.

The technique illustrated has been applied to solutions of model compounds, and to a range of petroleum products.

EXPERIMENTAL

Preparation of resin columns

The beds of resin, contained in glass columns, were washed alternately with 10% hydrochloric acid and 10% sodium hydroxide solution to remove trace impurities. Deacidite K and Amberlyst 29 were left in the hydroxide form, and Amberlyst 15 in the acid form. Excess alkalinity or acidity was removed by water washing. Water was removed with dry methanol. Carbonate columns were generated by percolating methanol saturated with carbon dioxide through the hydroxide form of the anion exchanger. Finally the columns were washed with toluene to remove the methanol. After this treatment the carbonate and hydroxide forms of the anion-exchange resins and the free acid form of the cation-exchange resin were shown to have about 80% of the manufacturers specified exchange capacity at 10% breakthrough, *i.e.*, when the concentration of unadsorbed material in the effluent is 10% of the concentration in the influent solution. The total capacity of the resins from the combined effects of both physical and chemical adsorption could be as much as double this figure of 80%.

Experiments with anion-exchange resins

With model compounds. To establish a method for the separation of alkylphenols from carboxylic acids, experiments were conducted with solutions in toluene of *p*-cresol and naphthenic acids, using both hydroxide- and carbonate-form columns of Amberlyst 29 and Deacidite K. No satisfactory two-stage desorptions were obtained using hydroxide columns, since both species were chemically adsorbed, but a number of separations were obtained using carbonate-form columns. These results are shown in Table II. With carbonate columns, methanol was a very efficient desorbent for the physically bound *p*-cresol, but possessed one disadvantage in that it was not possible to determine the phenol content of the effluent by potentiometric titration. As desorbents, pyridine in toluene (1:4 by volume) was as effective as methanol, and *tert*-butanol rather less so, but neither possessed the disadvantage mentioned. Methanol, being relatively volatile, was the best desorbent where recovery of the phenols was required. Methanol saturated with carbon dioxide was an ideal desorbent for naphthenic acids, although other desorbents were also employed. The use of desorbing solvents in which dissolved carbon dioxide gas is the active reagent was an innovation

TABLE II

ELUTION OF *p*-CRESOL AND NAPHTHENIC ACIDS FROM CARBONATE-FORM COLUMNS OF ANION-EXCHANGE RESINS

Resin	*Charge of each species in meq*	*Two-stage elution system*	*Recovery (%)*	
			p-Cresol	*Naphthenic acids*
Deacidite K	1.0	1) Pyridine in toluene 1:4 (v/v)	97	3
		2) Methanol–CO_2	not detected	93
Deacidite K	5.0	1) Pyridine in toluene 1:4 (v/v)	95	3
		2) *N* HCl in 1:1 isopropanol–water	not detected	95
Amberlyst 29	0.5	1) tert-butanol	95	not detected
		2) Methanol–CO_2	2	103
Amberlyst 29	0.5	1) Methanol	98	1
		2) Methanol–CO_2	not detected	92

as far as the authors are aware. Used in conjunction with carbonate-form columns, it not only achieved the desired desorption but improved an already clean and simple procedure as the initial and final forms of the column were the same. Thus there was no specific step of regeneration.

Model solutions of nitrogen compounds were also examined. For a limited range of compounds it was established that nitrogen bases are not adsorbed on anion-exchange resins, whilst non-basic materials are held physically, provided that polar solvents are absent. This was true of both hydroxide- and carbonate-form columns. The compounds used were typical of the classes of nitrogen compound found in the lower boiling petroleum fractions, up to and including the heavy gas oil cut. For example, it proved possible to separate indole and carbazole from pyridine and quinoline, and carbazole from acridine. Table III shows the results of a typical experiment in which four components in a mixture were separated by the method illustrated in Fig. 1.

TABLE III

SEPARATION OF FOUR COMPONENTS FROM SOLUTION, USING CARBONATE AND HYDROXIDE FORMS OF AMBERLYST 29

Component	*Amount present (meq.)*	*Eluant*	*Recovery (%)*
Acridine	1.25	Toluene	100
Carbazole	0.625	Methanol	100
p-tert-butylphenol	1.25	Isopropanol–CO_2	95
Naphthenic acid	1.25	Methanol–CO_2	98

Acridine, *p-tert.*-butylphenol, and naphthenic acid recoveries were determined by titration, and carbazole recovery was determined by weighing.

With petroleum products. The techniques established with model compounds were applied to petroleum fractions. Typical separations of alkylphenols and naphthenic acids from kerosine and heavy gas oil are shown in Table IV. Some of the heavy gas oil phenols passed through a carbonate column, and the additional use of a hydroxide column was required to complete the separation.

A fraction containing pyrrollic compounds was also isolated from heavy gas

TABLE IV

ADSORPTION AND DIFFERENTIAL DESORPTION OF ALKYLPHENOLS (AP) AND NAPHTHENIC ACIDS (NA) FROM PETROLEUM PRODUCTS USING DEACIDITE K ANION-EXCHANGE RESIN

Product	*Total meq. present*		*Resin form*	*Eluting system*	*Recovery (%)*	
	AP	*NA*			*AP*	*NA*
Kerosine	0.17	0.28	CO_3	(i) methanol	102	
				(ii) methanol–CO_2		93
Kerosine	0.17	0.28	CO_3	(i) pyridine–toluene 1:4 (v/v)	96	
				(ii) methanol–CO_2		97
Kerosine	0.17	0.28	CO_3	(i) tert-butanol	93	
				(ii) methanol–CO_2		96
Heavy gas oil	2.1	1.4	CO_3	tert-butanol	90	
			OH	isopropanol–CO_2		
			CO_3	methanol–CO_2		92
Heavy gas oil	2.1	1.4	CO_3	pyridine–toluene 1:4 (v/v)	94.5	
			OH	isopropanol–CO_2		
			CO_3	methanol–CO_2		97

oil which, together with the nitrogen bases subsequently separated from the sample, accounted for approximately two-thirds of the total nitrogen present. It is possible that nitrogenous material not recovered was insufficiently polar to be adsorbed. This low recovery however still represents an improvement on separation techniques hitherto employed.

Amongst trace components isolated from other materials were phenolic additives and naturally occurring acids from bitumen, pentachlorophenol from a kerosine contaminated with a gas oil based wood preservative, and minute traces of fatty acids from paraffin wax.

Experiments with cation-exchange resins in the free acid form

The experiments with cation-exchange resins were designed to establish that nitrogen bases could be removed and recovered from model solutions and petroleum products. It was established that Amberlyst 15 in the free acid form effectively adsorbed a wide range of nitrogen bases from hydrocarbon solution including pyridines, quinolines, acridines and anilines. There was a slight falling off in resin capacity with the higher molecular weight compounds, especially acridine. Despite this, however, a complete recovery of basic material from heavy gas oil was obtained. The eluant in

all the experiments was a solution of ammonia in methanol, or methanol and ether. Excess ammonia was readily removed from effluent solutions, leaving the desorbed bases uncontaminated.

Experiments with cation-exchange resins in the transition metal form

The observations of HELFFERICH on ligand exchange[2] suggested that some useful separations might be possible on the basis of comparative ligand-forming properties using cation-exchange resins in the transition metal form. A limited series of experiments was undertaken, using Amberlyst 15 resins in the nickel, copper and iron form. These metals were chosen as showing a range of co-ordination numbers and ligand affinities. The immediate object was to investigate the potential of the resins as ligand adsorbers from non-aqueous solutions, in order to remove, concentrate and determine potential ligands in hydrocarbons.

Columns were prepared in the metal form by application of aqueous solutions

TABLE V

ELUTION OF LIGAND-FORMING MATERIALS WITH METHANOL FROM AMBERLYST 15 RESIN IN THE COPPER, NICKEL OR IRON FORM

(+) Desorbed by methanol; (−) not desorbed by methanol.

Compound	*Resin form*		
	Copper	*Nickel*	*Iron*
Naphthenic acid	+	+	+
Substituted succinic acid[a]	+	+	+
Salicylic acid	+	+	+
Stearic acid derivative of sarcosine[a]	+	+	
Dimer of linoleic acid[a]	+	+	+
Long-chain aliphatic diamine[a]	+	+	+
Bis-salicylideneethylenediimine[a,b]	+	+	−
Ammonia	−	−	
Primary aliphatic amines	−	−	
Ethylenediamine	−	−	
Glycine		−	
Benzotriazole	−	−	−
Acetylacetone	+	+	−
Oxine	−	−	−
Catechol	−		−
Dimethylglyoxime		−	
Ethylenediaminetetraacetic acid[b]	+	+	+

[a] commercially available additives.
[b] elution with methanol removed metal complex.

of copper, iron and nickel salts to the free acid form of the resin. Excess salts were removed with water, and non-aqueous conditions established as previously described. A series of compounds capable of forming unidentate, bidentate and multidentate ligand bonds, including a number of commercially available additives were applied in toluene solution to the resins. Compounds naturally occurring in petroleum fractions, for example naphthenic acids were also examined. The materials were all adsorbed, and complex formation was indicated in some instances by the appearance of a coloured band in the resin. The materials were classified into those desorbed and those not

TABLE VI

DETERMINATION OF BIS-SALICYLIDENEETHYLENEDIIMINE IN KEROSINE NICKEL COMPLEX MEASURED AT 405 mμ (p.p.m.)

Added	0.0	2.4	4.8	9.6	12.0	24.0
Found	0.3	3.0	4.8	9.9	11.1	24.6

desorbed by methanol, as shown in Table V. The materials not desorbed by methanol could be removed by either ligand exchange or acid elution. The five commercially available petroleum additives were all desorbed with methanol, and one of these, bis-salicylideneethylenediimine, removed nickel or copper from the column in the form of a coloured complex. This behaviour proved of considerable interest since it showed that the additive, a copper deactivator, could be determined colorimetrically as the nickel complex. Table VI shows results of the analysis of a sample of kerosine containing various added amounts of the additive.

DISCUSSION

This paper is not intended to be an exhaustive study of the application of non-aqueous ion exchange to petroleum analysis, but rather to indicate that this is a fruitful field for the use of the technique. In view of the wide use of aqueous ion-exchange procedures and of the clear lead given by MUNDAY AND EAVES eight years ago, the authors were surprised to find so few recently published papers concerning non-aqueous applications.

The techniques which have been outlined find regular application in the laboratories of the British Petroleum Company's Research Centre at Sunbury, where they have eliminated the need for certain laborious separation processes and in some cases led to the solution of analytical problems which might otherwise have remained unsolved.

The ligand-exchange experiments were limited by choosing one resin, one solvent system and three metals. Clearly the potentialities of this technique require further investigation in which these factors are varied, for example by using resins with carboxylic or phenolic exchange groupings, and other metal forms. Their potential application in organic preparations is extremely interesting.

The advent of macroreticular resins is of great significance and it is hoped that commercially produced resins with oleophilic rather than hydrophilic exchange groups will become available. Recently, a base exchanger of this type was produced with a satisfactory exchange capacity for organic bases up to a molecular weight of[3] 800.

The authors wish to thank the Directors of The British Petroleum Company Ltd. for permission to publish this paper.

SUMMARY

Extraction and subsequent recovery, in four separate fractions, of naphthenic acids, alkylphenols, pyrrollic compounds and nitrogen bases can be made from

petroleum products using macroporous ion-exchange resins. Distinctive features of the technique are the use of dissolved gases in polar solvents as eluants and the application of the carbonate form of anion-exchange resins. The transition metal form of a macroreticular cation exchanger is shown to extract ligands from non-aqueous systems and a specific application to petroleum analysis is given.

REFERENCES

1 W. A. MUNDAY AND A. EAVES, *World Petroleum Congr. Proc. 5th N.Y. 1959*, Sect. V, Paper 9.
2 F. HELFFERICH, *Nature*, 189 (1961) 1001.
3 H. P. GREGOR, P. TEYSSIE, G. K. HOESCHELE, R. FEINLAND, M. SHIDA AND A. TSUK, Am. Chem. Soc. Division of Polymer Chemistry, September 1964, pp. 873–876.

Analytica Chimica Acta
Elsevier Publishing Company, Amsterdam
Printed in the Netherlands.

DIE ANWENDUNG DER IONEXEIGENSCHAFTEN DES SILIKAGELS ZUR TRENNUNG VON METALLEN

FRANTIŠEK VYDRA
Analytisches Laboratorium, J. Heyrovský Polarographisches Institut, Tschechoslowakische Akademie der Wissenschaften, Prag, Jilská 16 (Tschechoslowakei)

(Eingegangen den 1. November, 1966)

In den letzten Jahren wurden die günstigen Oberflächeneigenschaften des Silikagels immer öfter auch in der anorganischen Analyse ausgenützt. Hauptsächlich in der analytischen Chemie von radioaktiven Isotopen wurde es wegen seiner Widerstandskraft gegenüber der radioaktiven Strahlung verwendet. In dieser Arbeit sind vorwiegend Erkenntnisse unseres Laboratoriums über die Sorptionseigenschaften des Silikagels gegenüber Metallkomplexen und ihre analytische Anwendung zusammengefasst.

DER MECHANISMUS DER SORPTION VON METALLVERBINDUNGEN AN SILIKAGEL

Die Metallverbindungen werden an Silikagel in der Form von verschiedenen komplexen Kationen, oder in der Form von Kolloidpartikeln von Verbindungen (die im Wasser nur beschränkt löslich sind) gebunden.

Der Mechanismus der Sorption von Metallionen an Silikagel kann am günstigsten unter statischen Bedingungen studiert werden. Es ist möglich das Verhältniss der Menge der am Silikagel sorbierten Metallverbindung zu der Menge der frei gewordenen Wasserstoffionen zu bestimmen. Die bei der Sorption der Metallverbindung an der Silikageloberfläche freigewordenen H^+ beweisen den Ionenaustauschmechanismus. Soweit bei der Sorption des Metallsalzes an Silikagel keine Freimachung von H^+ erfolgt, kann man annehmen, dass hier eine Adsorption stattfindet, die durch die physikalische Eigenschaften der adsorbierten Metallverbindung ermöglicht wird. Die Sorption der Metallionen und ihrer kationischen Komplexe an Silikagel verläuft nach folgender Gleichung:

$$m\,(\equiv SiOH) + Me^{n+} \rightleftarrows [(\equiv SiO)_m Me^{m-n}] + m\,H^+ \qquad (1)$$

Der Sorptionsmechanismus von Metallhydraten an Silikagel nach (1) wurde durch das Studium der Sorption der Metallkationen festgestellt. Bei allen studierten Metallen wurde $m = n$ [Gleichgewicht (1)] gefunden, d.h. bei der Sorption eines Gramions des Metalles wird ein Gramion H^+ freigemacht, entsprechend der positiven Ladung des adsorbierten Ions[1]. Ein entsprechender Mechanismus ($m = n$ bei Gleichgewicht (1)) wurde beim Studium der Sorption von Äthylendiamin[2] und Tris-Phenanthrolin-Komplexen einiger Metalle gefunden[3].

Etwas komplizierter ist die Erklärung der Adsorption von hydrolytischen Produkten der mehrwertigen Metalle am Silikagel. Komplizierte hydrolytische Gleich-

gewichte zwischen einige Hydroxokomplexen und kolloiden Hydroxide ermöglichen nur selten und in einem beschränkten Bereich der pH-Werte eine eindeutige Erklärung des Mechanismus der Bindung der Metallverbindung. Sehr oft erfolgt nämlich gleichzeitig eine Ionex-Sorption von Hydroxokomplexen und eine physikalische Adsorption von kolloiden Hydroxiden, die in der Lösung gleichzeitig anwesend sind. Im Fall von Fe(III) z.B. erfolgt schon aus Lösungen mit pH~3 gleichzeitig mit der Sorption der Hydroxokomplexe (Freimachung von H^+) auch die Adsorption der kolloiden Hydroxide (H^+ werden nicht freigemacht). Unter diesen Bedingungen ist es unmöglich die Struktur der sorbierten Hydroxokomplexe festzustellen. Im Fall der Sorption von hydrolytischen Produkten des Al besteht die Möglichkeit aus dem molaren Verhältniss des sorbierten Metalls und der freigesetzten H^+ (wenn gleichzeitig auch die zugehörigen hydrolytischen Gleichgewichte bekannt sind) auf den wahrscheinlichen Sorptionsmechanismus zu schliessen. Im Interval pH 3.5–5.0 wurde bei der Sorption ein konstantes Verhältnis $Al:H^+ = 1:2$ gefunden; unter Voraussetzung, dass das Gleichgewicht (1) gültig ist, wird Al unter gegebenen Bedingungen als $AlOH^{2+}$ sorbiert. Im Fall von Cr(III) wurde festgestellt, dass im pH Bereich 4–6 bei der Sorption der Cr-Verbindungen kein H^+ frei wird, was ein Zeichen dafür ist, dass es sich hier um eine Adsorption von Kolloidpartikeln von wenig lösbaren hydrolytischen Produkten des Cr handelt[9].

Wenn Me^{n+} [im Gleichgewicht (1)] ein kationischer Komplex (einfach oder gemischt) ist, der nicht genug stark ist, kann die Konkurrenz der –OH Gruppen des Silikagel eine Rolle spielen, wobei es zu einer Verdrängung der Liganden kommt, die am Metall gebunden sind. Die Sorption verläuft dann laut Gleichgewicht (1), aber mit $m \neq n$.

DIE AUSNÜTZUNG DER IONEXEIGENSCHAFTEN VON SILIKAGEL ZUR TRENNUNG VON METALLEN

In unserem Laboratorium wurde zunächst die Möglichkeit der Ausnützung der Sorption der kationischen Metallkomplexe am Silikagel verfolgt. Mit Rücksicht auf die verhältnismässig niedrige Kapazität des Silikagel bei der Sorption von kationischen Komplexen (10^{-5}–10^{-3} mol/g), die Qualität des sorbierten Ions, und die spez. Oberfläche des Silikagels, kann man nur verhältnismässig kleine, also vom analytischen Standpunkt nur Spurenmengen der Metalle feststellen.

Für die Analytik ist wichtig, dass die Sorption der kationischen Komplexe sehr wenig durch die Ionenstärke beeinflusst wird (die Adsorption der Kolloidpartikeln von wenig lösbaren Metallverbindungen wird wohl durch die Ionenstärke beeinflusst) und dass die Metallkomplexe des anionischen Typs (ÄDTA, Zitronensäure udgl.) am Silikagel nicht sorbiert werden. Durch eine geeignete Wahl des kationischen Komplexes des zu bestimmenden Metalls und der komplexbildenden Substanz zum Maskieren der begleitenden Metalle kann man eine äusserst selektive Trennung von Spurenkonzentrationen von einem grossen Überschuss der begleitenden Metalle durchführen.

Silikagel kann also in der Spurenanalyse prinzipiell zweierlei ausgenützt werden.

(1) Trennung von Spurenelementen von einem grossen Überschuss der begleitenden Metalle,

(2) Konzentrierung des Metalls aus einem grossen Volumen einer sehr verdünnten Lösung.

Die beiden Möglichkeiten können selbstverständlich gleichzeitig ausgenutzt werden.

Silikagel

Zur analytischen Verwendung ist jedes Silikagel mit einer spezifischen Oberfläche von wenigstens 300 m^2/g geeignet. Silikagele mit einer kleineren spez. Oberfläche haben eine zu niedrige Kapazität. Zur Konzentrierung sehr kleiner Mengen von Metallen darf das verwendete Silikagel keine schweren Metalle enthalten. In dieser Hinsicht eignen sich Silikagele, die durch Hydrolyse organischer Si-Verbindungen dargestellt wurden, z.B. aus $Si(OC_2H_5)_4$, sehr gut.

Allgemeines Arbeitsverfahren

Weil die Sorption am Silikagel schnell abläuft, und weil man in der Spurenanalyse meistens sehr kleine Mengen von Metallen verwendet, kann eine relativ kurze Silikagelsäule benutzt werden, und die Sorption kann bei einer ziemlich grossen Durchflussgeschwindigkeit stattfinden. In unserem Laboratorium wurden mit Erfolg Silikagelsäulen von 50 mm Höhe, Durchmesser 12 mm, verwendet. Wenn man Silikagel von der Korngrösse 0.1–0.2 mm benutzt, kann man mit einer Durchflussgeschwindigkeit von einigen ml/min arbeiten.

Vor jeder Analyse muss die H^+-Form des Silikagels durch Waschen mit *ca.* 25 ml 0.1 *M* Puffer (nach vorhergehendem gründlichen Durchwaschen mit Wasser) bereitet werden. Nach der Sorption wird die Säule nochmals gründlich mit Puffer von gleichem pH wie er bei der Sorption benutzt wurde, durchgewaschen. Das Auswaschen der sorbierten Komplexe erfolgt im allgemeinen mit 10–20 ml verdünnter Säure (Amokomplexe, Hydrokomplexe, Äthylendiaminkomplexe udgl.). Im Fall der Tris-phenanthrolinkomplexe müssen zum Auswaschen elektroneutrale Ionenpaaren dieser Komplexe mit einigen Anionen schwacher Säuren gebildet und eventuell ein wasser-alkoholisches Milieu verwendet werden. In diesem Fall eignen sich die Säuren nicht, denn das Auswaschen erfolgt nicht quantitativ. Die Metallbestimmung wird mittels einer geeigneten analytischen Methode durchgeführt.

Die Ausnutzung der Selektivsorption von Ag als $Ag(NH_3)_2^+$

Zur Trennung von Spurenkonzentrationen Ag und grossen Überschüssen einiger Metalle ist die Hochselektivsorption von $Ag(NH_3)_2^+$ an Silikagel in Anwesenheit von ÄDTA, mit dem eine Reihe von Metallen maskiert werden können, ausgenützt worden. Es wurde festgestellt, dass Ag quantitativ aus 10^{-4} molaren Lösungen von pH 8.5 und höher sorbiert wird.

So konnte man z.B. 50 μg Ag neben 1–2 g Cu, Hg, Cd, Zn, Ni, Fe(III) und Bi mit relativen Fehler von 1–5% bestimmen. Praktisch wurde die ausgearbeitete Methode zur Bestimmung von Ag in elektrolytischem Kupfer ausgenützt[4].

Die Ausnutzung der Selektivsorption des Fe und Co als Tris-phenanthrolinkomplexe

Tris-phenanthrolinkomplexe von Fe(II) und Co(II) werden am Silikagel auch in Anwesenheit von ÄDTA und Zitronensäure sorbiert. Die Sorption von Fe(II) als Tris-phenanthrolinkomplex erfolgt bei einem Überschuss von ÄDTA im pH-Interval

von 1.5–8 quantitativ. Bei einem ÄDTA-Überschuss wird Co(II) am Silikagel bei pH 6.5–8 in Anwesenheit eines Überschusses von Zitrationen im Interval pH 2–7.5 quantitativ sorbiert. Durch ÄDTA und Zitronensäure konnten selbst hohe Konzentrationen einer Reihe von Metallen maskiert werden. Insbesondere ist die Bestimmung von Fe-Spuren durch die ausgearbeitete Methode fast spezifisch (höhere Co-Konzentrationen, sowie Ag und Hg stören die Bestimmung).

Die ausgearbeitete Methode ermöglicht die Bestimmung von Fe–Co-Spuren in den verschiedensten Materialien. Besonders vorteilhaft ist sie für die Bestimmung beider Metalle neben einer hohen Konzentration der "Farbmetalle"[5,6].

Die Ausnutzung der Selektivsorption von Co als $Co(en)_3^{3+}$

Zur Bestimmung von Co-Spuren in Ni und dessen Salzen kann das oben beschriebene Prinzip verwendet werden. Mit Rücksicht auf den verhältnissmässig hohen Preis des 1,10-Phenanthrolins kann in diesem Fall dieser Komplexbildner durch Äthylendiamin ersetzt werden. Es bildet mit Co(III) einen sehr festen Komplex, dessen Bildung durch die Anwesenheit von ÄDTA nicht gestört wird. Dank seines kationischen Charakters wird dieser Komplex von Co(III) mit Äthylendiamin am Silikagel bei pH 8 und höher sorbiert. ÄDTA erhöht auch in diesem Fall die Selektivität der Sorption bedeutend[7]. Bei der Bestimmung von Co in Ni und Ni-Salzen konnten noch 10^{-3}% Co bestimmt werden[8].

Die Ausnutzung der Selektivsorption von Al als $Al(OH)^{2+}$

Die Sorption von Al^{3+} am Silikagel als $Al(OH)^{2+}$ erfolgt quantitativ im pH-Bereich 4–6. Die Sorption wird praktisch durch keine zweiwertigen Metalle gestört, Cr^{3+} stört bloss in höheren Konzentrationen. Fe^{3+} wird — wenn auch nicht quantitativ — zusammen mit Al^{3+} sorbiert. Die Fe^{3+}-Sorption kann durch die Maskierung mit Thioglykolsäure unterdrückt werden. Diese Methode wurde zur Bestimmung von Al im Messing und einer Reihe von Reinchemikalien verwendet[9].

Die Bestimmung von Zn in elektrolytischem Cu

Zur Bestimmung von Zn in Cu wurde die Selektivsorption von Zn, wahrscheinlich als ZnO^+ (aus NH_3-freier Lösung) benützt. Diese Sorption wird in Anwesenheit von Zitrat bei pH 8.5–10 selbst nicht von Gramm-Mengen Cu gestört. Die Bestimmung von Zn nach der Trennung wurde polarographisch durchgeführt. Durch die vorgeschlagene Methode konnten z.B. 0.0024% Zn im Kupfer bei einem gegebenen Gehalt von 0.002% Zn gefunden werden[10].

ZUSAMMENFASSUNG

Der Mechanismus der Sorption von kationischen Metallkomplexen an Silikagel und die Anwendung diesses Prozesses zur Trennung von Metall-Spuren wird diskutiert. Einige praktische Beispiele wurden gegeben.

SUMMARY

The mechanism of sorption of cationic metal complexes on silica gel and the utilization of this process for separation of trace concentrations of metals are discussed. Some practical examples are given.

LITERATUR

1 D. L. DUGGER, J. H. STANTON, B. N. IRBY, B. L. MCDONNELL, W. W. CUMMINGS UND R. W. MAATMAN, *J. Phys. Chem.*, 68 (1964) 457.
2 F. VYDRA UND V. MARKOVÁ, *J. Inorg. Nucl. Chem.*, 26 (1964) 1319.
3 F. VYDRA UND V. MARKOVÁ, *Collection Czech. Chem. Commun.*, im Druck.
4 F. VYDRA, *Talanta*, 10 (1963) 753.
5 F. VYDRA UND V. MARKOVÁ, *Talanta*, 10 (1963) 339.
6 F. VYDRA, *Talanta*, 11 (1964) 433.
7 F. VYDRA UND V. MARKOVÁ, *Collection Czech. Chem. Commun.*, 30 (1965) 2382.
8 F. VYDRA UND V. MARKOVÁ, *Chemist–Analyst*, 54 (1965) 69.
9 F. VYDRA UND J. GALBA, *Collection Czech. Chem. Commun.*, im Druck.
10 F. VYDRA UND V. MARKOVÁ, *Collection Czech. Chem. Commun.*, 31 (1966) 1398.

Analytica Chimica Acta
Elsevier Publishing Company, Amsterdam
Printed in the Netherlands.

ANWENDUNG DER IONENAUSTAUSCHCHROMATOGRAPHIE ZUR AKTIVIERUNGSANALYTISCHEN BESTIMMUNG VON NATRIUM UND KALIUM IN MOLYBDÄN UND WOLFRAM

H.-G. DÖGE
Institut für Metallphysik und Reinstmetalle der Deutschen Akademie der Wissenschaften zu Berlin, Dresden (Deutschland)

(Eingegangen den 1. November, 1966)

Die aktivierungsanalytische Bestimmung sehr geringer Natrium- und Kaliumgehalte in Molybdän und Wolfram erfordert wegen der ausserordentlich hohen Matrixaktivitäten eine sorgfältige Abtrennung der Grundmaterialien von den zu bestimmenden Spuren. Andernfalls werden, wie ohne Trennung ausgeführte aktivierungsanalytische Natriumbestimmungen in Wolfram[1,2] zeigten, nur 10^{-3}% als kleinste nachweisbare Konzentration erreicht. Ausserdem müssen auch Natrium und Kalium getrennt werden, weil die durch (n,γ)-Reaktion entstehenden radioaktiven Nuklide der beiden Elemente sich in ihren Strahlungseigenschaften sehr ähneln. Für beide Trennungen sind Ionenaustauschverfahren geeignet, weil mit ihrer Hilfe sowohl Natrium und Kalium vollständig von Molybdän und Wolfram isoliert als auch voneinander getrennt werden können.

TABELLE I

KERNPHYSIKALISCHE DATEN DER INTERESSIERENDEN NUKLIDE

Target-nuklid	*Häufigkeit (%)*	*Aktivierungsquerschnitt (b)*	*Gebildetes Nuklid*	*Halbwertszeit (h)*	*Energie der β-Strahlung (MeV)*	*Energie der γ-Strahlung (MeV)*	*Zerfallsprodukt (HWZ)*
^{23}Na	100	0.56	^{24}Na	15	1.39	1.37; 2.75	^{24}Mg (stabil)
^{41}K	6.8	1	^{42}K	12.46	3.5	1.53	^{42}Ca (stabil)
^{98}Mo	23.75	0.51	^{99}Mo	67	0.41; 1.18	0.14; 0.74	^{99m}Tc (6 h)
^{186}W	28.4	34	^{187}W	24	0.64; 1.33	0.48; 0.69	^{187}Re (stabil)

Einen Überblick über die wichtigsten der bei der Bestrahlung von Natrium, Kalium, Molybdän und Wolfram mit thermischen Neutronen entstehenden Nuklide, sowie deren kernphysikalische Eigenschaften gibt Tab. I. Aus ihr ist zu entnehmen, dass bei der Untersuchung von Molybdän ausserdem mit einer der Molybdänaktivität etwa entsprechenden gleich grossen Technetiumaktivität gerechnet werden muss.

METHODISCHES

Durch geeignete Wahl der Reaktionsbedingungen (Ionenaustauscher, Elutionsmittel, Komplexbildner) kann man in günstigen Fällen entweder das Grundelement oder die zu bestimmenden Spuren an dem Austauscherharz adsorbieren, während jeweils der andere Partner nahezu ungehindert die Austauschersäule passiert. Für die vollständige Abtrennung hat es sich nach unseren bisherigen Erfahrungen bei Molybdän und Wolfram fast immer als zweckmässig erwiesen, die Hauptkomponente an dem Ionenaustauscher zu adsorbieren und die zu bestimmenden Elemente im Eluat aufzufangen.

Bei Untersuchungen über das Verteilungsverhalten von Molybdän und Wolfram zwischen dem stark basischen Ionenaustauscher Wofatit SBW und Lösungen der beiden Elemente zeigte sich, dass für Molybdän und Wolfram im Salzsäure–Oxalsäure–Wasserstoffperoxid-Gemisch auch bei verhältnismässig hohen Konzentrationen der beiden Elemente Verteilungskoeffizienten $>100\,000$ erreicht werden, während die Verteilungskoeffizienten für Natrium und Kalium <1 sind. Ausserdem hat das Salzsäure–Oxalsäure–Wasserstoffperoxid-Gemisch die vorteilhafte Eigenschaft, dass es Molybdän- und Wolframoxid, sofern sie nicht bei zu hohen Temperaturen geglüht wurden, gut löst, ohne dass neben Wasserstoffionen andere Kationen oder Fluoridionen im Lösegemisch vorhanden sind.

Einen Überblick über das Elutionsverhalten von Natrium und Kalium geben Modelluntersuchungen an einer mit Natrium-24 und Kalium-42 indizierten Molybdänprobe (Abb. 1). Während Natrium und Kalium innerhalb der Schwankungsbreite der Aktivitätsmessungen vollständig im Eluat wiedergefunden werden, sind Molybdän bzw. Wolfram im Eluat nicht nachweisbar.

Für die nachfolgende Natrium- und Kalium-Trennung benötigt man zum Beladen der Austauschersäule eine rein wässrige Lösung der Metallsalze. Die dazu notwendige Entfernung von Salzsäure, Oxalsäure und Wasserstoffperoxid erreicht man durch Eindampfen des Eluats zur Trockne nach Zusatz von konzentrierter

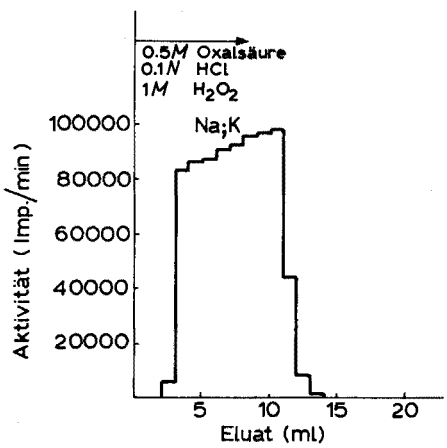

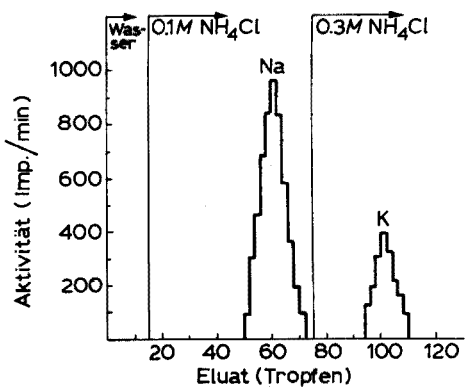

Abb. 1. Elutionsdiagramm der Natrium- und Kaliumabtrennung von Molybdän und Wolfram.

Abb. 2. Elutionsdiagramm von Natrium und Kalium nach Isolierung aus einer Molybdänprobe.

Schwefelsäure. Ausserdem verflüchtigt sich bis auf geringe Reste beim Abrauchen der Schwefelsäure das aus Molybdänproben miteluierte Technetium als Technetiumheptoxid.

Unter der Voraussetzung, dass die Masse der beiden Elemente nicht zu gross ist, lässt sich eine Natrium–Kalium-Trennung ausserordentlich schnell mit einer mit Ammoniumwolframatozirkonat-Austauscher gefüllten Mikrosäule ausführen.

Untersuchungen über das Verteilungsverhalten von Natrium und Kalium zwischen einem nach ZASUCHIN und Mitarbeiter[3] hergestellten Ammoniumwolframatozirkonat-Austauscher und Ammoniumchloridlösungen verschiedener Konzentration ergaben die in Tab. II zusammengestellten Verteilungskoeffizienten, die gut mit

TABELLE II

VERTEILUNGSKOEFFIZIENTEN VON NATRIUM UND KALIUM ZWISCHEN AMMONIUMCHLORIDLÖSUNGEN UND AMMONIUMWOLFRAMATOZIRKONAT-AUSTAUSCHER

In Klammern Literaturwerte[3].

Element	*Verteilungskoeffizient*	
	0.1 M NH_4Cl	*0.3 M* NH_4Cl
Na	3.7 (5)	0.8 (1)
K	9 (12.5)	2.5 (4)

den von den genannten Autoren ermittelten Werten übereinstimmen. Für Natrium und Kalium ergibt sich bei Anwendung von 0.1 *M* Ammoniumchloridlösung ein Trennfaktor 2.4.

Abbildung 2 zeigt das Elutionsdiagramm von Natrium- und Kaliumspuren, die aus einer aktivierten Molybdänprobe isoliert wurden. Eine gegenseitige Verunreinigung der beiden Fraktionen konnte weder durch γ-Spektrometrie noch bei Halbwertszeitmessungen festgestellt werden. Ebenso waren in den beiden Fraktionen keine anderen Radionuklide nachweisbar. Modellversuche mit Natrium-24 und Kalium-42 ergaben, dass die Ausbeuten nach vollständiger Durchführung der Analyse stets $>95\%$ sind. Die Analyse kann deshalb ohne Ausbeutebestimmung ausgeführt werden.

Die γ-spektrometrische Überprüfung der Natrium- und Kalium-Abtrennung von aktivierten Molybdän- bzw. Wolframproben zeigte, dass ausser diesen beiden Elementen auch radioaktive Kupfer- und Kobaltnuklide aus der Anionenaustauschersäule ausgewaschen werden. Störungen bei der Natrium- und Kaliumbestimmung treten jedoch nicht ein, weil beide Elemente weder mit 0.1 noch mit 0.3 *M* Ammoniumchloridlösung aus der Ammoniumwolframatozirkonataustauschersäule eluiert werden. Ebenso stören die geringen Technetiumreste, die nach dem Abrauchen der Schwefelsäure in der Probe verbleiben, die Bestimmung nicht, da das Pertechnetation auf dem Kationenaustauscher nicht adsorbiert wird und unmittelbar nach dem freien Kolonnenvolumen aus der Säule ausgewaschen wird.

Arbeitsvorschrift

Nicht mehr als 100 mg der zu analysierenden Probe und je 1 mg Natrium- bzw.

Kaliumnitrat werden im Reaktor 10 h mit einem Fluss von 10^{13} n sec^{-1} cm^{-2} bestrahlt.

Die bestrahlte Probe wird nach Zusatz von je 100 μg Natrium- und Kaliumchlorid als Träger in 5 ml eines Flusssäure–Salpetersäure-Gemisches (Volumenverhältnis 3:1) gelöst und die Lösung zur Trockne gedampft. Unter Erwärmen löst man das Oxid in 10 ml eines Gemisches, das 0.1 *N* an Salzsäure, 0.5 *M* an Oxalsäure und 1 *M* an Wasserstoffperoxid ist und gibt die Lösung auf eine mit dem Anionenaustauscher Wofatit SBW (Korngrösse 0.09–0.06 mm) gefüllte Säule von 100 mm Länge und 7 mm Durchmesser, wobei die Fliessgeschwindigkeit der Lösung 10 Tropfen/min beträgt. Die Elution von Natrium und Kalium wird mit 10 ml des Aufgabegemisches vervollständigt. Wegen der hohen Aktivität der Grundmaterialien werden Lösen und Ionenaustauschtrennung hinter einer Bleiabschirmung vorgenommen.

Das Eluat wird nach Zusatz von 0.5 ml konzentrierter Schwefelsäure zur Trockne gedampft. Den Rückstand bringt man in wenigen Tropfen Wasser gelöst auf die mit Ammoniumwolframatozirkonat-Austauscher (Korngrösse 0.03–0.06 mm) gefüllte Säule von 100 mm Länge und 2 mm Durchmesser. Nachdem mit einigen weiteren Tropfen Wasser alles Natrium und Kalium am Kolonnenkopf gesammelt ist, wird Natrium mit 0.1 *M* und Kalium mit 0.3 *M* Ammoniumchloridlösung eluiert. Jedes der beiden Elemente ist in ca. 1 ml Eluat enthalten. Die Aktivität wird in einem Bohrlochkristall-Szintillationszähler gemessen.

Die beiden Standards werden in je 100 ml Wasser gelöst. Zur Aktivitätsmessungen verwendet man, gegebenenfalls nach Verdünnen, aliquote Teile dieser Lösungen.

Bewertung des Verfahrens

In Tab. III sind auf diese Weise ermittelte Natrium- und Kaliumgehalte den Variationskoeffizienten für die genannten Bestimmungen gegenübergestellt. Den Werten liegen je 12 Einzelbestimmungen zugrunde.

TABELLE III

ERGEBNISSE UND REPRODUZIERBARKEIT DER NATRIUM- UND KALIUMBESTIMMUNGEN; ZAHL DER STATISTISCHEN FREIHEITSGRADE 11

Element	*Mo*		*W*	
	Gehalt (p.p.m.)	*Variations-koeffizient (%)*	*Gehalt (p.p.m.)*	*Variations-koeffizient (%)*
Na	13	3	1.8	5
K	9	5	2.5	7

Unter den angegebenen Arbeitsbedingungen liegt die Nachweisgrenze für Natrium bei $5 \cdot 10^{-10}$ und für Kalium bei $5 \cdot 10^{-9}$ g. Bei Einwaagen von 100 mg Probenmaterial entspricht dies 5 p.p.b. Natrium bzw. 50 p.p.b. Kalium.

Zur Durchführung einer Analyse werden etwa 3 Stunden benötigt; es lassen sich aber mehrere Proben gleichzeitig bearbeiten. Das vorgeschlagene Trennverfahren ist mit geringen Änderungen ausserdem zur aktivierungsanalytischen Bestimmung von Rubidium- und Cäsiumspuren in Molybdän und Wolfram geeignet.

ZUSAMMENFASSUNG

Es wird ein Verfahren zur aktivierungsanalytischen Bestimmung von Natrium- und Kaliumspuren in Molybdän und Wolfram beschrieben, bei dem Natrium-24 und Kalium-42 radiochemisch rein von anderen Radionukliden durch Anionen- und Kationenaustauschchromatographie abgetrennt werden. Die Nachweisgrenzen liegen bei 5 p.p.b. Natrium bzw. 50 p.p.b. Kalium.

SUMMARY

A method for the determination of traces of sodium and potassium in molybdenum or tungsten by activation analysis is described. Radiochemically pure sodium-24 and potassium-42 are separated from other radionuclides by anion- and cation-exchange chromatography. The limits of detection are 5 p.p.b. of sodium and 50 p.p.b. of potassium.

LITERATUR

1 R. J. REULAND UND A. F. VOIGT, *Anal. Chem.*, 35 (1963) 1263.
2 V. I. SPITSYN, M. P. GLAZUNOV, P. N. KODOCHIGOV UND V. P. IONOV, *Zh. Analit. Khim.*, 18 (1963) 1272.
3 E. N. ZASUKHIN, A. I. KALININ, R. A. KUZNETSOV UND V. V. MOISEEV, *Radiokhim. Metody Opred. Mikroelementov, Akad. Nauk SSSR, Sb. Statei*, (1965) 168.

Analytica Chimica Acta
Elsevier Publishing Company, Amsterdam
Printed in the Netherlands.

APPLICATION OF RADIOISOTOPES IN COLUMN CHROMATOGRAPHY ON SUBSTITUTED CELLULOSES. PART V.

THE SEPARATION OF ARSENIC FROM COPPER AND OTHER METALS

R. A. A. MUZZARELLI AND G. MARCOTRIGIANO*
Department of Chemistry, Faculty of Sciences, University of Sherbrooke, Sherbrooke, P.Q. (Canada)

(Received November 1st, 1966)

In the literature on inorganic chromatography on celluloses, there is only one indication concerning the chromatographic behaviour of arsenic: this element, as well as uranium, was not adsorbed on natural cellulose from a solution of uranyl nitrate in ethyl ether–nitric acid mixture[1]. The behaviour of arsenic has not been otherwise studied because the applications of celluloses have been mainly concerned with the purification of uranium, although SCHULEK *et al.*[2] have examined them for pre-concentration purposes in qualitative work. No data have been published about the adsorption of arsenic on substituted celluloses, but copper has been found to be adsorbed on natural cellulose from ethyl ether and from a solution of uranyl nitrate in ethyl ether–nitric acid mixture and to be eluted with a solution of thiocyanate[3].

A discussion on the separation of traces of copper from high-purity arsenic has been recently published, and an analytical method presented[4] based on six different operations including ion-exchange chromatography and electrolysis. From the analytical point of view, the separation of arsenic from copper is of importance in neutron activation analysis and in radiochemistry, because of the similarity of the γ-ray spectra of ^{76}As and ^{64}Cu. For preparative purposes and in technology, the purification of arsenic from traces of copper is of interest in electronics.

Numerous elements at the nanogram level have been studied on natural and substituted celluloses and several separations at the trace or macro level have been performed[5]. It appears that if arsenic is not adsorbed on celluloses, it would be separable from many elements, including antimony[6], which has not only similar chemical properties but also in neutron activation analysis, gives ^{122}Sb whose γ-ray spectrum strictly corresponds to that of ^{76}As.

The following elements are adsorbed on cellulose under the same standard conditions as those adopted in the present work: Cs, Sr, Ba, Sc, Y, the lanthanides, Cr, Mn, Fe, Co, Ag, Zn, Cd, In and Sb. These metals should therefore be collected on cellulose from the solutions containing arsenic, and would be eluted as already described[3–5]. To verify the feasibility of these separations, the adsorption of traces of arsenic was studied for each cellulose, so that the cellulose with the lowest adsorption capacity for arsenic and the highest for other metals could be chosen. Further, the chromatographic behaviour of traces of copper on substituted celluloses was stu-

* Permanent address: Istituto di Chimica Generale e Inorganica, Università di Modena, Modena, Italy.

died, in order to confirm the previously established trend that metals are more strongly adsorbed on substituted celluloses than on natural cellulose, and to establish the optimum conditions for separation and the quantitative elution.

EXPERIMENTAL

Solutions

Reagent-grade chemicals and solvents were used for the preparation of all solutions, without any further treatment.

(a) anhydrous ethyl ether
(b) 2 ml 90% nitric acid dissolved in 98 ml of ethyl ether
(c) 40 mg of NH_4SCN dissolved in 20 ml of methanol plus 80 ml of ethyl ether
(d) 5 g of NH_4SCN dissolved in 20 ml of methanol plus 80 ml of ethyl ether

Celluloses

The following cellulose powders were examined: Whatman CF 11, natural; Whatman DE 11, diethylaminoethyl; Whatman AE 11, aminoethyl; Whatman CM 11, carboxymethyl; Whatman P 11, phosphate; Whatman ET 11, epichlorohydrin triethanolamine Ecteola; Cellobiose Sigma CB, (glucose-β-glucoside); Bio-Rad SE, sulfoethyl; Bio-Rad PAB, *p*-aminobenzyl.

Radioisotopes

Copper–64, arsenic–77 and bismuth–207 were supplied by Nuclear Science Engineering Corp., Pittsburg, Pa., U.S.A.; the other radioisotopes were the same as used previously. The concentration of ^{77}As was 0.67 mg As/ml and 10 μl were diluted to 10 ml with 90% nitric acid; aliquots of 50–250 μl of this solution corresponding to 33.5–167.5 ng As were used for each experiment. Carrier-free ^{207}Bi was diluted in the same way. The concentration of ^{64}Cu was 0.64 mg Cu/ml and amounts varying between 10–200 ng Cu were used.

Radioactivity measurements

The eluted aliquots and the cellulose powders were collected in plastic bottles of uniform shape and capacity. Their radioactivity was measured by a 128-channel γ-ray spectrometer ND-110 electronically coupled to a NaI(Tl) crystal, and compared with a standard. The mean dispersion of results of quantitative determinations was 8%.

Preparation of the columns of celluloses

The columns (I.D. 10 mm; reservoir 200 ml; Teflon stopcock) were prepared as described earlier[5], and operated under pressure to obtain a flow of about 20 ml/min. The bed of cellulose was 15 cm high. The time for preparing two columns, and running two complete chromatograms was 1 h.

Preparation of high-concentration solution of arsenic

Arsenic trioxide (1 g) was warmed gently with 1 ml of 90% nitric acid and 0.6 ml of 5 *N* hydrochloric acid in methanol; the solutions were selected to avoid excess of water. This solution was diluted with 20 ml of anhydrous ethyl ether and,

if necessary, a few drops of 90% nitric acid were added to avoid phase separation.

The indicated quantities of 90% nitric acid containing ^{77}As and other radioisotopes were added to the solution containing the macro amount of arsenic and the solution was poured into the column.

For the preliminary determinations of arsenic, the samples of effluent from the chromatographic columns were concentrated and their radioactivity measured in low geometry to increase the sensitivity.

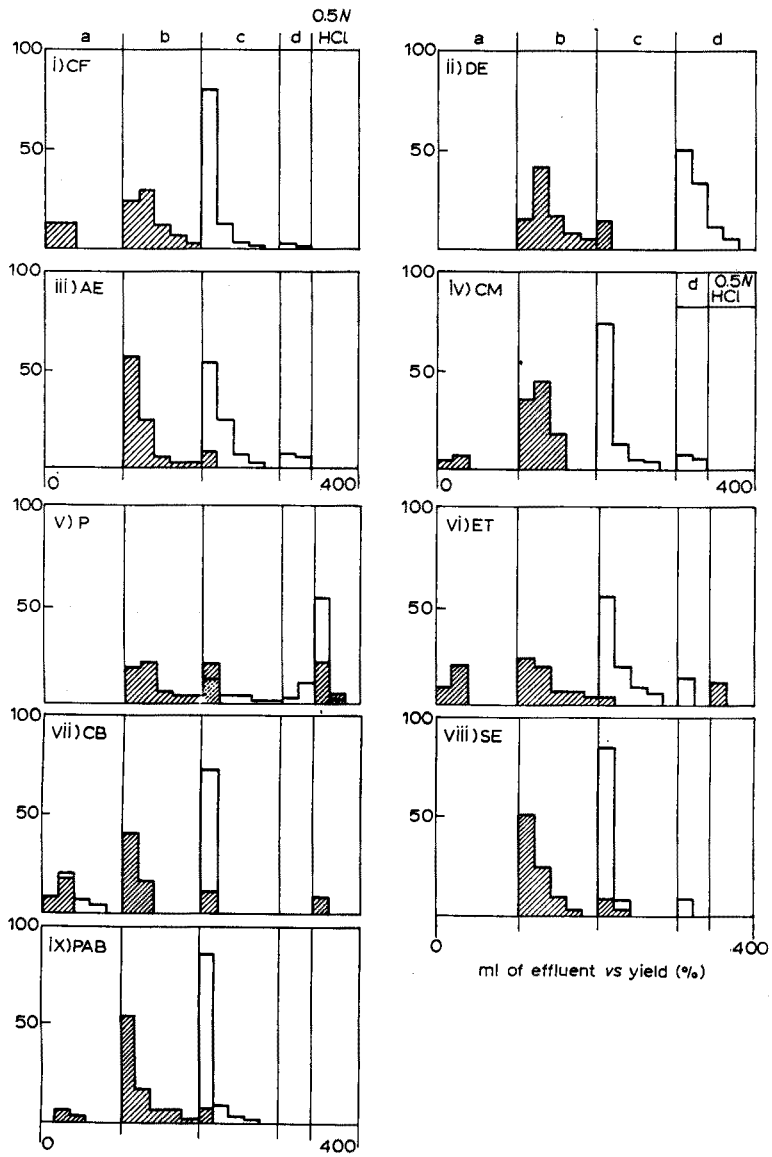

Fig. 1. The elution curves of traces of arsenic (shaded area) and traces of copper from 9 substituted celluloses with 5 eluants (solns. a, b, c, d, see Experimental, and 0.5 *N* hydrochloric acid in methanol).

RESULTS AND DISCUSSION

The elution curves presented in Fig. 1 show the chromatographic behaviour of traces of arsenic and copper. The curves confirmed that arsenic is practically not adsorbed on natural cellulose from ethyl ether or ethyl ether–nitric acid mixture. With the substituted celluloses, as well as cellobiose, a little arsenic was adsorbed and was generally eluted with the first fraction of diluted thiocyanate solution (c). This behaviour was the same on anionic and cationic celluloses, showing that neither adsorption nor chemical retention of arsenic occurs to any great extent. The chromatography on cellobiose (Fig. 1, vii) followed the general trend, which indicates that the interaction of arsenic with the macromolecule is comparable to that with the dimer.

Copper was quantitatively adsorbed from ethyl ether and from ethyl ether–nitric acid mixture, and was generally eluted with thiocyanate solution (c) except from diethylaminoethylcellulose (DE) where it was eluted only by the concentrated

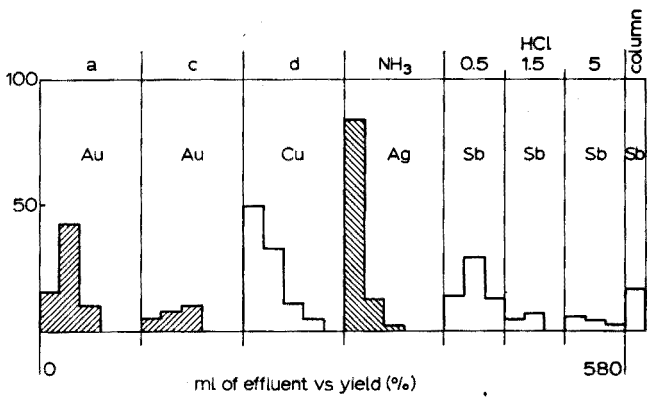

Fig. 2. The purification of gold from copper, silver and antimony on diethylaminoethyl cellulose. a. c, and d, see Experimental; 3 *N* NH_4OH and HCl in methanol.

thiocyanate selution (d) (Fig. 1, ii). From cellulose phosphate (Fig. 1, v) a little copper is eluted with solutions (c) and (d) and 0.5 *N* hydrochloric acid in methanol can elute the remaining copper.

Since the declared capacities of DE and AE celluloses are the same (*ca.* 0.8 meq/g), the difference of adsorption of copper on these two celluloses indicates the formation of different copper complexes with the amino groups. It has been supposed that the formation of complexes plays an important role in the retention of transition metals on substituted celluloses[7].

From the preceding description it appeared that traces of arsenic are separated from traces of copper on both natural (CF) and diethylaminoethyl (DE) celluloses; the difference in behaviour of these two elements is clearer on the DE cellulose. For the separation of traces of copper from macro amounts of arsenic, natural and diethylaminoethyl cellulose were therefore examined. The concentrated solution of arsenic in ethyl ether was used with traces of copper, and it was found that both elements gave elution curves exactly corresponding to those reported in Fig. 1, i and ii, showing

TABLE I

ELEMENTS SEPARATED FROM ARSENIC ON SUBSTITUTED CELLULOSES AT THE NANOGRAM LEVEL

(+), quantitative separation; (−), incomplete separation; blank, no data available.

Element tested	*DE*	*AE*	*CM*	*P*	*ET*	*SE*	*PAB*
Cu	+	−	−	−	−	−	−
Fe	+	−	−	−	+		
Sb	+	+	+	−	−	+	+
Co	+	−	−	−			
Mn	+	−	−	−	+		
Ag	+	−	−	−	−		
Zn	+	+	−	−	−		
Cd	+	+	−	−	−		

that the retention of nanograms of copper was not affected by the presence of gram amounts of arsenic, and that the elements were recovered quantitatively.

On the basis of data obtained previously[5,6], it is possible to plan separations of traces of arsenic from traces of numerous elements; Table I is a partial survey of the possibilities offered.

The results for copper can also be extended to other separations; for instance, copper can be separated from mercury on all celluloses where mercury was studied, and also from gold on CF and DE celluloses[5]. The separation of traces of copper, silver and antimony from gold and the selective elution of each impurity is presented in Fig. 2.

CONCLUSIONS

Among the elements so far studied on natural and substituted celluloses, arsenic shows a peculiar behaviour corresponding to that of mercury[5]. The two elements are not adsorbed on natural or substituted celluloses from ether–nitric acid mixture, and can thus be separated from many impurities. Gold and uranium are not retained on natural cellulose; on substituted celluloses, gold is retained to a limited extent[5], and uranium has not yet been studied.

The four elements mentioned are essentially unrelated and it is impossible to explain why they are not adsorbed on the celluloses whilst other elements which strictly resemble them in ordinary ion-exchange chromatography on resins, are so strongly retained on celluloses.

In any case, the results presented are of interest in chromatography and should have important applications in analytical and preparative chemistry. The separation of traces of copper from arsenic is possible by a method which includes only two operations (dissolution and chromatography); the separated elements are present in organic solutions which are convenient for rapid concentration and further chemical treatment, and should also be suitable for neutron activation analysis, because they contain only ammonium thiocyanate. Chromatography on celluloses makes it possible to treat >1 g As_2O_3 containing only 10 ng of copper, instead of 140 mg of arsenic containing 10–100 ng of copper, as in the most recent method[4]. The same considerations about rapidity, simplicity and convenience can be repeated for the separation

of copper from gold (Fig. 2) and for the separation of copper from mercury. The results of these studies show that celluloses allow separations of not only the metals of Groups II-A and II-B from each other[5,8] but also the metals of Group I-B and those of Group V-A.

This research was conducted under Grant No. 422-20, National Research Council of Canada, which is gratefully acknowledged.

SUMMARY

The chromatographic behaviour of arsenic and copper was studied with radioisotopes on natural cellulose, cellobiose and seven substituted celluloses in ethyl ether. Arsenic was not adsorbed; copper was retained and eluted quantitatively. For preparative purposes, one gram of arsenic trioxide was purified from nanograms of copper on natural and diethylaminoethyl celluloses. The possibility of purifying arsenic from several other metals, and gold and mercury from copper is indicated.

REFERENCES

1 *The determination of uranium and thorium*, Her Majesty's Stationery Office, London, 1963.
2 See, *e.g.* E. SCHULEK, Z. REMPORT-HORVÁTH, A. LÁSZTITY, E. KÖRÖS AND L. PATAKI, *Analytical Chemistry, 1962*, Elsevier, Amsterdam, 1963, p. 21.
3 R. A. A. MUZZARELLI AND L. C. BATE, *Talanta*, 12 (1965) 823.
4 G. NIZET, J. FOUARGE AND G. DUYCKAERTS, *Anal. Chim. Acta*, 35 (1966) 370.
5 R. A. A. MUZZARELLI, *Talanta*, 13 (1966) 193, 809 (Also in press).
6 R. A. A. MUZZARELLI AND G. MARCOTRIGIANO, *Talanta*, in press.
7 R. A. A. MUZZARELLI, Inorganic chromatography on columns of natural and substituted celluloses, in J. C. GIDDINGS AND R. A. KELLER (eds.), *Advances in Chromatography, Vol. VI*, Marcel Dekker Inc., New York, N.Y., U.S.A., to be published.
8 J. FOUARGE, *Anal. Chim. Acta*, 18 (1958) 225.

Analytica Chimica Acta
Elsevier Publishing Company, Amsterdam
Printed in the Netherlands.

CRITERIA FOR SUCCESSFUL SEPARATION BY CONTINUOUS ELECTROPHORESIS AND ELECTROCHROMATOGRAPHY IN BLOCKS AND COLUMNS

E. RAVOO* AND P. J. GELLINGS
Afdeling Chemische Technologie, Technische Hogeschool Twente, Enschede (The Netherlands)

TH. VERMEULEN
Department of Chemical Engineering, University of California, Berkeley, Calif. (U.S.A.)

(Received November 1st, 1966)

Continuous electrophoresis and electrochromatography have found analytical as well as preparative application in recent years. The principles and development of these techniques have been reviewed by PUČAR[1]. Most of the work has related to specific biochemical and clinical problems and little attention has been paid to the physics of the method. The object of this paper is to report an analysis of some important process variables and to derive criteria for successful separation. In connection with the theory, some experimental results obtained by VERMEULEN and coworkers at the University of California, Berkeley will be presented.

The principle of continuous electrophoresis may be described as the separation of electrically charged species of different mobility from a continuous feedstream by application of direct current perpendicular to the direction of flow. Here only packed-bed systems will be considered. The feed is admitted continuously from a line-source into a column or rectangular block filled with either an inert or an adsorptive packing or support. This material is bathed continuously and uniformly by a suitable carrier electrolyte or eluant. In the bed (see Fig. 1) the ionic components from the feed will move in zones (bands), vectorially determined by (a) convective transport in the direction of bulk flow, possibly retarded by adsorptive action of the packing, (b) electromigration in the direction of the field.

In steady-state operation each feed component can be collected continuously from the respective position of its zone at the downstream end of the bed.

The process is termed continuous electrophoresis in the absence of adsorption or migration in the adsorbed state. If on the other hand adsorption plays a role, the process is known as continuous electrochromatography. Adsorptive action of the packing need not necessarily have a favourable effect on the separation. However, CAPLAN[2] has demonstrated that the use of ion-exchange resins, particularly in combination with complexing agents, will generally improve the separation.

The major fundamental difficulties in packed-bed continuous electrophoresis and electrochromatography fall into four categories.

(1) Prediction of electrophoretic mobilities in moderately concentrated, multi-

* 1961–1963, Department of Chemical Engineering, University of California, Berkeley.

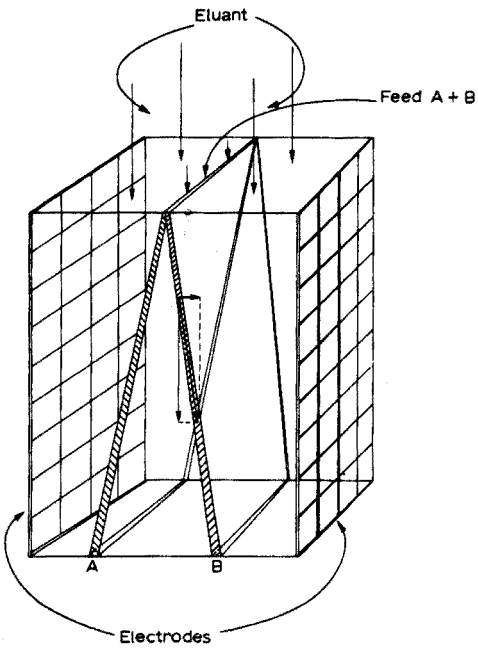

Fig. 1. Schematic representation of continuous electrophoretic separation.

component, temperature-dependent systems. In spite of considerable theoretical progress by various authors, *e.g.* OVERBEEK[3] and more recently WIERSEMA[4], the practical worker is still confronted with a general lack of data or at best finds a poor collection of semi-empirical correlations at his disposal.

(2) Problems associated with the nature of the supporting medium. Intended to minimize convection due to local density gradients, the supporting medium may introduce serious complications. The packing will generally affect mobilities and other transport properties, and may in some cases promote electroosmotic flow. The complexity of the transport phenomena will be aggravated by the heterogeneity of the bed. An interesting discussion on the role of supporting media in electrophoresis has been written by KUNKEL AND TRAUTMAN[5].

(3) The rise of temperature due to the passage of current represents a serious limitation in continuous electrophoresis. This is especially important for the separation of heat-labile substances, with high voltages, in apparatus with a high volume to cooling surface ratio. Part of this paper will be devoted to a general theory correlating power input, residence time and temperature rise for rectangular and cylindrical geometries.

(4) The occurrence of transverse dispersion by molecular and eddy-diffusion may impose another limiting factor. One of the following sections will describe how and to what extent the separating capacity can be maximized without undue overlap of the bands.

Along with these fundamental problems many constructional and operational difficulties arise. Since most of these aspects are well covered, *e.g.* by BLOEMENDAL[6], BIER[7] and FINN[8] (the latter with emphasis on large-scale techniques), further discus-

sion is unnecessary. This paper is restricted to an analysis of heat dissipation and transverse spreading, and a discussion of the implications for the limitations and optimization of continuous electrophoresis.

ANALYSIS OF HEAT DISSIPATION

The first analysis of temperature distributions in electrophoresis columns was published by PORATH[9].

His work, however, centered on batch processes in cylindrical beds with the electrodes at the ends of the column. Here a more general theory will be presented for continuous separation in rectangular as well as cylindrical (annular) beds. The symbols used are defined in Table I. In all cases the following assumptions are made:

(a) The bulk process-stream (feed + eluant) moves with uniform velocity $v_z = L/\tau$ in the longitudinal direction of the bed.

TABLE I

SYMBOLS AND DEFINITIONS USED

A, B	Typical feed components
C	Concentration of feed component (moles/cm^3)
c_p	Specific heat of process stream (J/g °C)
D_y	Total transverse diffusion coefficient (cm^2/sec)
D_m	Molecular diffusion coefficient (cm^2/sec)
D_e	Transverse eddy diffusion coefficient (cm^2/sec)
d_p	Packing diameter (cm)
E	Voltage across the bed; E_y, voltage across rectangular bed; E_{ab}, voltage across cylindrical bed (V)
L	Length of the bed (cm)
Pé	Péclet-number for transverse eddy diffusion
q	Strength of feed line-source (moles/cm sec)
r	Radial coordinate; r_a, outer radius of annular bed; r_b, inner radius of annular bed (cm)
r_F	Feed position in annular bed; r_L, take-off position in annular bed (cm)
R	Ratio of lateral dimensions for rectangular bed
Re	Reynolds number for flow in packed bed
S	Bandwidth (cm)
T	Local bed temperature; T_{max}, maximum bed temperature (°C)
T_0	Temperature of coolant and entering process stream (°C)
ϑ_c	Dimensionless residence time in cylindrical bed
ϑ_r	Dimensionless residence time in rectangular bed
u	Effective electrophoretic mobility of feed component in the bed (cm^2/Vsec)
v_z	Plug flow velocity in longitudinal bed direction (cm/sec)
x	Lateral coordinate in rectangular bed (perpendicular to electric field) (cm)
X	Lateral bedwidth in x-direction (cm)
y	Lateral coordinate in rectangular bed (in direction of electric field) (cm)
y_b	Transverse coordinate measured from the centre of the band (cm)
y_F	Feed position in rectangular bed; y_L, take-off position in rectangular bed (cm)
Y	Lateral bedwidth in y-direction (cm)
z	Longitudinal coordinate (cm)
ε	Porosity of the bed
Θ	Dimensionless temperature rise; Θ_{max}, maximum dimensionless temperature rise
κ	Effective electrical conductivity of the bed (Ω^{-1} cm^{-1})
λ	Effective thermal conductivity of the bed (W/cm °C)
ϱ	Density of process stream (g/cm^3)
τ	Residence time (sec)
$\Phi_{m,k}$	Algebraic function, see definitions to eqn. (2)

(b) A constant voltage drop E in transverse direction is maintained over the entire length of the bed.
(c) The bed is cooled by keeping two or more of its lateral faces at a constant temperature equal to the inlet temperature of the process-stream T_0.
(d) Longitudinal convection of heat is large compared to longitudinal conduction.
(e) Transverse convection (*e.g.* by electro-osmosis) is negligible.
(f) Physical properties of the fluid and the packing are constant throughout the bed.
(g) End effects are neglected.
(h) The separation proceeds at steady state.

Rectangular geometry

Three cases will be considered (see Fig. 2): (1) cooling at the electrode-faces

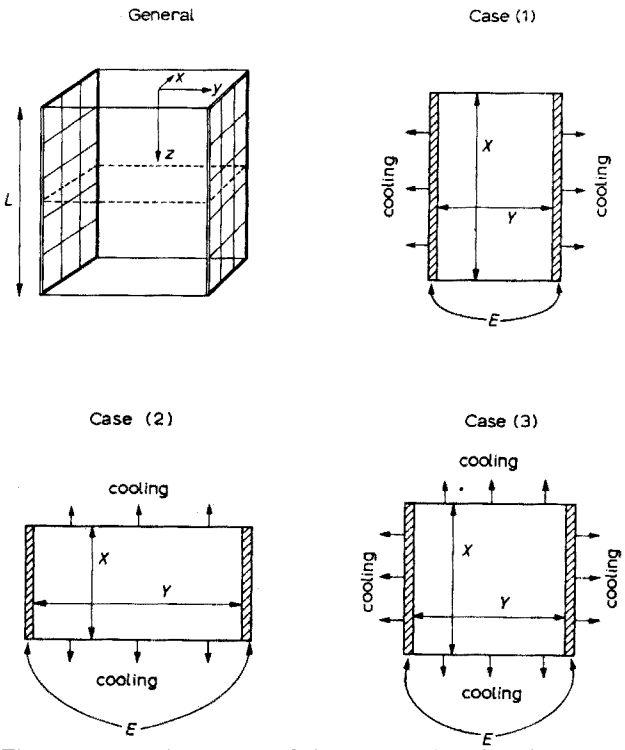

Fig. 2. Rectangular models of electrophoresis units with lateral cooling.

of the bed only; (2) cooling at the two lateral faces perpendicular to the electrode-faces; (3) cooling at all four faces.

The analysis of model (3), although considerably more tedious, is certainly most rewarding. Not only does it generate special solutions for the first two cases as a by-product, it also allows an evaluation of their usefulness for approximation purposes.

Under the assumptions mentioned above, the heat balance for an infinitesimal volume element $dx \cdot dy \cdot dz$ in the bed takes the form:

$$\lambda\left(\frac{\partial^2 T}{\partial x^2}+\frac{\partial^2 T}{\partial y^2}\right)-\varrho c_p\frac{\partial T}{\partial \tau}+\kappa\left(\frac{E}{Y}\right)^2=0 \qquad (1)$$

with the boundary and initial conditions: $T = T_0$ at $x = \pm X/2$, at $y = \pm Y/2$, and at $\tau = 0$. The respective terms in eqn. (1) represent thermal conduction in the two lateral directions, longitudinal convection and ohmic heat generation.

A full analytical solution of the problem is available, from which the maximum temperature—which is of course of most concern—can be derived. In dimensionless form, the following expression for the maximum temperature rise (located at the center of the bed) is obtained:

$$\Theta_{max}=\frac{16}{\pi^4}\sum_{k=0}^{\infty}\sum_{m=0}^{\infty}\frac{(-1)^{k+m}}{(2k+1)(2m+1)}\cdot\frac{1-\exp(-\pi^2\Phi_{m,k}\mathcal{T}_r)}{\Phi_{m,k}} \qquad (2)$$

where $\Theta = \{\lambda(T-T_0)\}/\kappa E^2$; $\mathcal{T}_r = \lambda\tau/\varrho c_p Y^2$; $\Phi_{m,k} = \{(2m+1)/R\}^2 + (2k+1)^2$; $R = X/Y$.

Calculated values of the dimensionless maximum temperature rise versus dimensionless residence time with varying ratio of the lateral bed dimensions are summarized in Fig. 3.

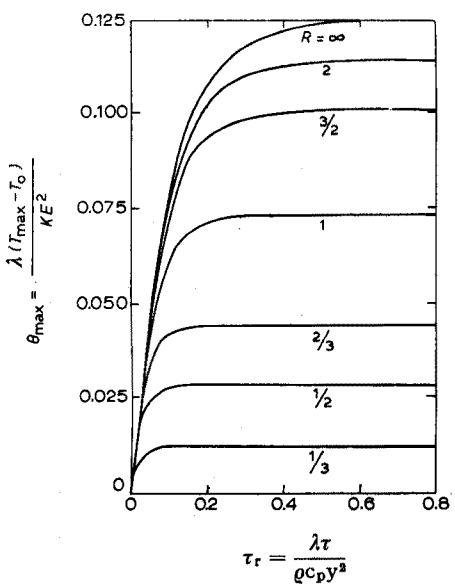

Fig. 3. Maximum temperature in rectangular beds, in terms of (lateral) dimension ratio and residence time (in dimensionless units).

As can be seen from the curves, Θ_{max} rapidly approaches an asymptotic value*, depending upon the dimension ratio R. Since in most practical separations the dimensionless residence time $\mathcal{T}_r$ will be of the order 0.3 to 30, the asymptotic maxima provide a safe and sufficiently exact guide for successful operation.

Figure 4 depicts the asymptotic temperature rise as a function of R. It is

* Physically this means that all ohmic heat is dissipated by conduction in a lateral direction.

interesting to note that the behaviour of beds with cooling at the electrode faces only is reflected by the upper end of the curve, and the case of cooling perpendicular to the direction of current by the lower part. Apparently, the cross-section of the bed need not be very oblong in order to approximate quasi-two-sided cooling.

In that event the following approximate criteria can easily be derived from eqn. (2)

$$R > 4 \qquad \Theta_{max} = \tfrac{1}{8} \quad \text{or} \quad T_{max} - T_0 = \frac{\kappa}{\lambda}\frac{E^2}{8}$$

$$R < \tfrac{1}{4} \qquad \Theta_{max} = \frac{R^2}{8} \quad \text{or} \quad T_{max} - T_0 = \frac{\kappa}{\lambda}\frac{E^2X^2}{8Y^2}$$

For $\frac{1}{4} < R < 4$ the use of Fig. 4 is recommended. From these considerations it may be concluded that the best dissipation of heat during continuous separation in rectangular systems can be attained in relatively thin slabs, with narrow electrode

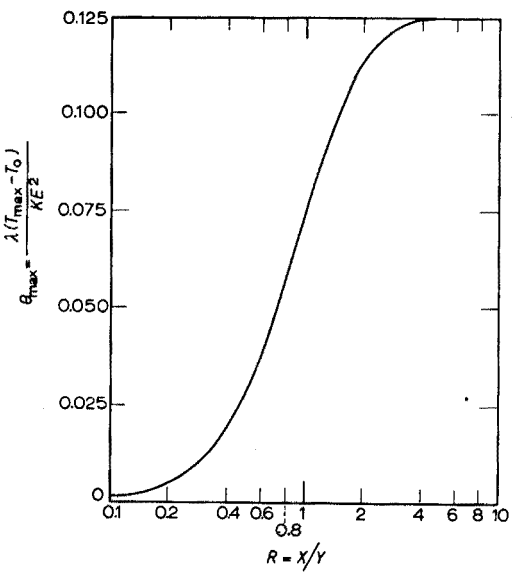

Fig. 4. Asymptotic behaviour of the maximum bed temperature as a function of dimension ratio.

faces and sidewise cooling, perpendicular to the passage of current. A high ratio of thermal to electrical conductivity in the bed is desirable, and the voltage should be kept as low as possible. Even in less favourable geometries θ_{max} will never exceed 1/8.

Cylindrical geometry

A diagram of a cylindrical electrophoresis unit, with electrodes situated at the center and at the periphery of the column, and cooled via the electrode compartments, is shown in Fig. 5.

With the same assumptions as before, the balance between radial conduction, axial convection and ohmic production of heat in an annular element $2\pi r \cdot dr \cdot dz$ can be formulated:

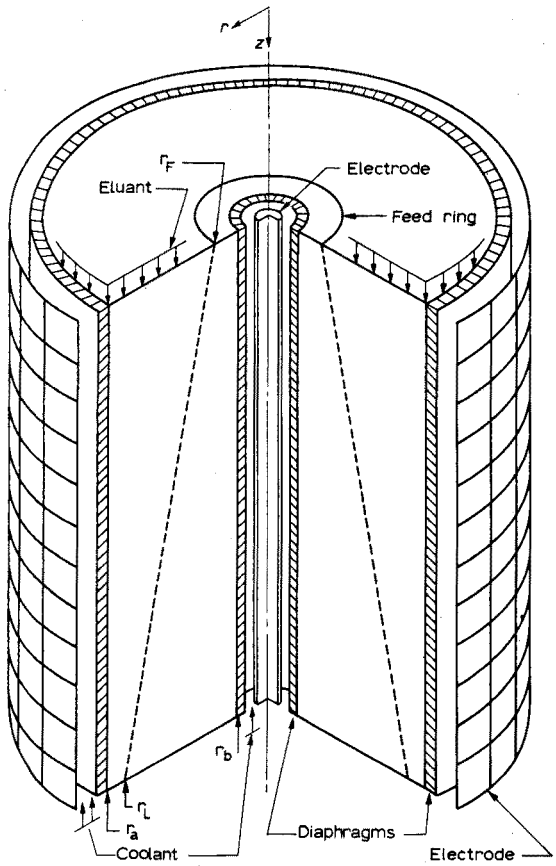

Fig. 5. Exploded view of cylindrical electrophoresis column with annular bed.

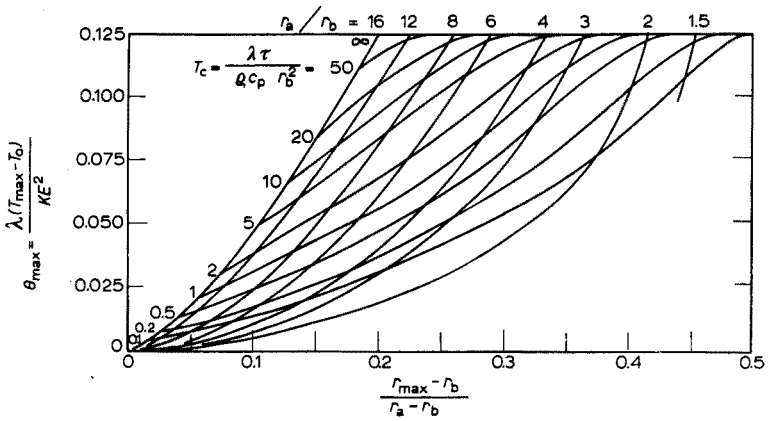

Fig. 6. Maximum temperature and its radial location in annular beds, in terms of radius ratio and residence time (in dimensionless units).

$$\frac{\lambda}{r}\frac{\partial}{\partial r}\left(r\frac{\partial T}{\partial r}\right) - \varrho c_p \frac{\partial T}{\partial \tau} + \kappa\left[\frac{E}{r\ln(r_a/r_b)}\right]^2 = 0 \qquad (3)$$

The boundary and initial conditions are: $T = T_0$ at $r = r_a$, at $r = r_b$ and at $\tau = 0$.

The analytical solution of eqn. (3) has been reported by HYBARGER *et al.*[10] and results in an expression for the temperature rise as a function of voltage, residence

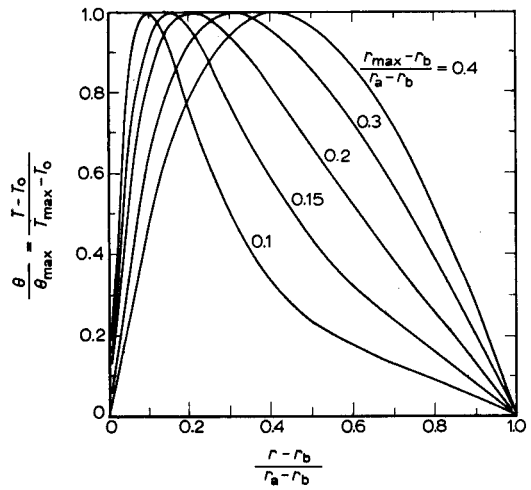

Fig. 7. Temperature distribution in annular beds as a function of maximum temperature location.

time and geometry, in the form of a series of Bessel-functions. The maxima in the temperature profiles, though not accessible analytically, were determined by a combination of graphical and computer techniques by RAVOO *et al.*[11,12]. The results for a wide range of radius ratio r_a/r_b and dimensionless residence time $\mathcal{T}_c = \lambda\tau/\varrho c_p r_b^2$, are summarized in Fig. 6. The graphs show that θ_{max} will approach 1/8 for sufficiently long residence times, particularly in thin annuli. Naturally this behaviour is similar

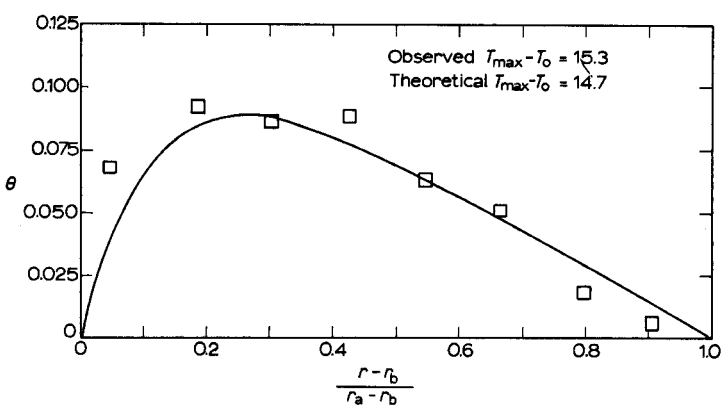

Fig. 8. Comparison of theoretical (solid line) and measured temperature profiles (based on data by NADY *et al.*[13]). Configuration as in Fig. 5; r_a = 9.7 cm, r_b = 1.73 cm, r_a/r_b = 5.6; voltage drop E_{ab} = 13.7 V; residence time 2 h; eluant composition 0.05 *M* $NaNO_3$; packing 80–150 mesh polystyrene beads.

to that in a rectangular bed cooled at its electrode faces. The asymptotic value of θ_{max} for $\mathcal{T}_c \to \infty$ is located at a radius $r_{max,as} = \sqrt{r_a r_b}$. In most cases, however, θ_{max} will remain well below 1/8 at realistic residence times. Starting from known geometry and conditions of separation, the maximum temperature and its location can rapidly be estimated with Fig. 6. If desired, complete temperature profiles can then be constructed using Fig. 7.

A typical profile, based on actual conditions in a cylindrical column in operation at Berkeley, is shown in Fig. 8. The experimental points coïncide fairly well with the theoretical curve. The differences may be accounted for by errors in the measurements and deviations from the assumptions made earlier.

TRANSVERSE DISPERSION

Spreading of the bands of different components by transverse dispersion represents a problem, since the actual distance over which separation can take place is limited in a practical unit. To a large extent undue overlap of the bands can be prevented by using a suitable combination of packing and separation length, as will be shown in a simplified analysis for rectangular geometry. Since the zones are assumed to be narrow compared to the electrode distance—which is the desirable situation in practice—the same reasoning may be applied to cylindrical columns with few modifications.

If longitudinal mixing is ignored and the packing is homogeneous, with diameters small compared to the bed dimensions, the diffusion of the bands obeys the differential equation

$$D_y \frac{\partial^2 C}{\partial y_b^2} - \frac{v_z}{\varepsilon} \frac{\partial C}{\partial z} = 0 \tag{4}$$

For a line-source of infinitesimal width and strength q the solution has the Gaussian form

$$C(y_b, z) = \frac{q}{2\sqrt{\pi \varepsilon v_z D_y z}} \exp\left(-\frac{v_z y_b^2}{4\varepsilon D_y z}\right) \tag{5}$$

With the band-width S defined as the horizontal range containing a specified percentage of the total solute at any depth, it follows that after passage through the bed

$$S^2 = 16 \frac{\varepsilon D_y L}{v_z} \ln\left[\frac{C_{max}}{C(S/2, L)}\right] \tag{6}$$

with $C_{max} = q/2\sqrt{\pi \varepsilon v_x D_y L}$.

The relation between total solute recovery and local concentration (Fig. 9) then allows the prediction of band spreading for given conditions at any arbitrarily chosen recovery value, *e.g.* 98% for $C_{max} = 10\, C(S/2, L)$.

Transverse mixing is the result of true molecular diffusion and microscopic fluctuations of the flow around the particles in the bed, "eddy" diffusion*. Since the eddy diffusivity is related to the Péclet-number for mass transfer, D_y can be expressed

$$D_y = D_m + D_e = D_m + v_z d_p/\varepsilon \text{ Pé} \tag{7}$$

* In fact a misnomer, since there may not be any eddies in laminar flow.

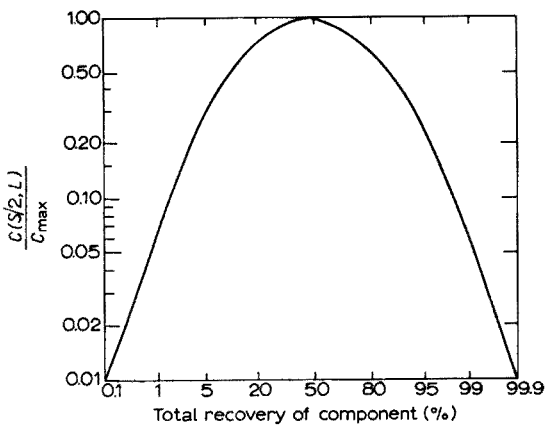

Fig. 9. Gaussian concentration profile in terms of total solute recovery.

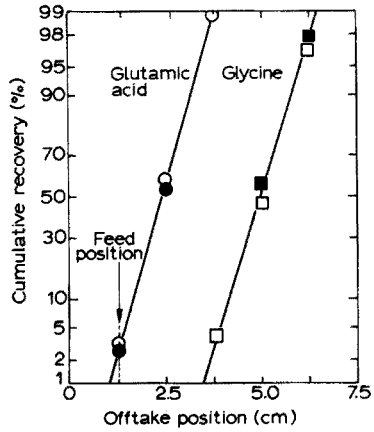

Fig. 10. Behaviour of two amino acids in rectangular column, with acids fed separately and combined (data from ref. 13). (L = 50 cm; Y = 7.5 cm; τ = 0.5; E_y = 25 V; packing 60–90 μ glass-beads; eluant 0.003 M Na_2HPO_4–0.003 M NaH_2PO_4). Filled in points indicate combined feed.

In the range of interest (Re< 10) the Péclet-number is found to be a constant, depending on the nature of the packing, as shown in Table II. From these data it can easily be seen that, even at low flow-rates and with small particle dimensions, the eddy diffusion will usually be predominant. Hence, from eqns. (6) and (7), neglecting D_m,

$$S^2 = 16 \frac{d_p L}{Pé} \ln \left[\frac{C_{max}}{C(S/2, L)} \right] \tag{8}$$

Thus a simple relationship exists between bandwidth, particle size, bed length and percentage of recovery, which, with Fig. 9 and Table II, allows rapid estimation of suitable separation conditions.

TABLE II

PÉCLET NUMBERS FOR TRANSVERSE EDDY DIFFUSION IN LAMINAR FLOW (Re < 10)

Pé = $v_z d_p/\varepsilon D_e$	*Packing used*	*Reference*
12	polystyrene pellets	14
12	random packing of mixed spheres	15
43	random packing of uniform spheres	16
17	Ottawa sand	14

The Gaussian solution of the band-profile will correspond to a straight line if the cumulative sums of the recovered fractions are plotted on a probability scale, against linear offtake position. As illustrated by Fig. 10, a reproducible Gaussian distribution is indeed observed during actual separation, so that, even with the simplifying assumptions made, the developed model appears to be quite satisfactory.

OPTIMIZATION OF TWO-COMPONENT SEPARATION

As an example of the applicability of the combined operational criteria, the optimization of a two-component separation will be discussed. Since the resolution of multicomponent systems is determined by the smallest difference in mobility between two of the components, the example is representative for more involved separations as well. All conditions and dimensions used are typical for the large-scale rectangular and cylindrical electrophoresis units developed by VERMEULEN and coworkers. Originally designed to study scaling-up of preparative electrophoresis, the apparatus is quite suitable for demonstration of the separation criteria. Details on construction and accessory equipment have been described elsewhere[13,17,18]. For a full understanding of the separation it is necessary to consider the equations of electrophoretic motion of the two components A and B in the bed. For rectangular bed electrophoresis as shown in Fig. 11, the separation distance Δy_L of the two components is found to be

$$\Delta y_L = \frac{(u_A - u_B)\tau E_y}{Y} \tag{9}$$

Optimal use of the bedwidth requires that A and B each occupy half of it at the downstream end. (All physical properties given, this can always be realized by using a

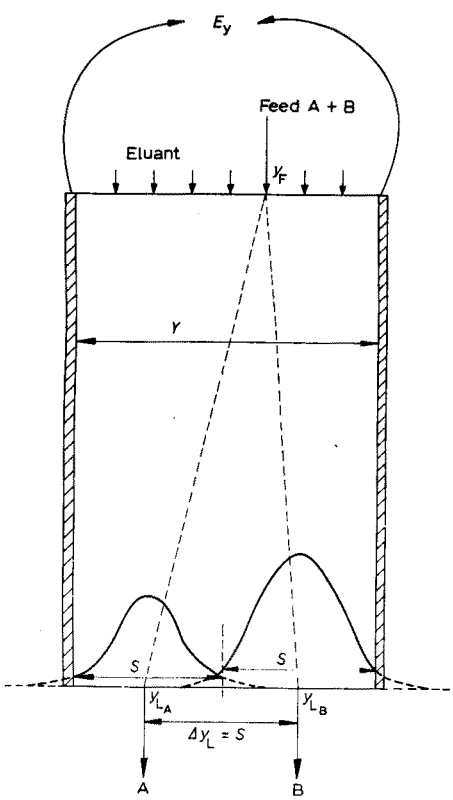

Fig. 11. Schematic representation of optimal resolution of a binary mixture in a rectangular bed.

suitable injection point y_F.) Therefore, with the same bandwidth for the two components (molecular diffusion ignored), it follows that

$$S = \Delta y_L = Y/2 \tag{10}$$

Since S is related to packing size, bedlength and degree of recovery by eqn. (8) and Fig. 9, any of these quantities can precisely be adjusted to specified values of the other. Combining eqns. (9) and (10) results in:

$$E_v\tau = \frac{Y^2}{2(u_A - u_B)} = \frac{2\,S^2}{u_A - u_B} \tag{11}$$

This implies that for the optimal *resolution* of a given system in a given apparatus, it is immaterial what combination of residence time and voltage is used, as long as the total power input (V h/mole separated) is adequate.

For the annular configuration similar conclusions apply. The equations corresponding to eqns. (10) and (11) are

$$S = \Delta r_L = \frac{r_a - r_b}{2} \tag{12}$$

and

$$E_{ab}\tau = \frac{(r_a - r_b)^2}{(u_A - u_B)} \frac{\ln(r_a/r_b)}{4} = \frac{S^2 \ln(r_a/r_b)}{u_A - u_B} \tag{13}$$

In order to find the optimal combination of E and τ for the *separation* as a whole, the other process limitations need to be considered. The combination of short residence time and high voltage ($\sim 1/\tau$) is attractive because it allows a high throughput ($\sim 1/\tau$) with a low energy consumption ($\sim E\tau^2$). However, in practice serious limitations are encountered, like pressure loss in the bed, expensive high-voltage equipment, and above all the temperature lability of the feed components (temperature rise proportional with E^2 and less than proportional with τ).

Thus the allowable maximum voltage and minimum residence time depend on the maximum permissible temperature rise and can be predicted by means of eqn. (11) or (13) and Fig. 4 or 6.

For the rectangular unit at Berkeley, with cooling at the electrode faces and the other lateral faces insulated, the approximate equation, $T_{max} - T_0 = \kappa E^2/8\lambda$, applies, so that

$$E_{y\,max} = \sqrt{8\lambda(T_{max} - T_0)/\kappa} \tag{14}$$

and with eqn. (11),

$$\tau_{min} = \frac{Y^2}{4(u_A - u_B)} \sqrt{\frac{\kappa}{2\lambda(T_{max} - T_0)}} = \frac{S^2}{u_A - u_B} \sqrt{\frac{\kappa}{2\lambda(T_{max} - T_0)}} \tag{15}$$

The optimization procedure is illustrated in Table III. For a known system, geometry and bed conditions, the optimal recovery, voltage and residence time are calculated. From the results it is obvious that the rectangular column would allow a slow but very sharp separation, whereas in the cylindrical column a rapid separation in relatively impure fractions would take place.

In sum, the results indicate that the derived criteria may be helpful to the analytical chemist, and contribute to a better insight into optimization and limitations

TABLE III

OPTIMIZATION OF TWO COMPONENT SEPARATION

Rectangular bed, $L = 50$ cm, $Y = 7.5$ cm. Cylindrical column, $L = 120$ cm, $r_a = 9.7$ cm, $r_b = 1.73$ cm. General data: $u_A = +2 \cdot 10^{-4}$ cm²/Vsec, $u_B = -1 \cdot 10^{-4}$ cm²/Vsec, $0.04 < d_p < 0.06$ cm, $c_p = 4.2$ J/g °C, $\varrho = 1$ g/cm³, $\lambda = 5 \cdot 10^{-3}$ W/cm °C, $\kappa = 1 \cdot 10^{-3}\ \Omega^{-1}\text{cm}^{-1}$, $T_{max} = 50°$, $T_0 = 25°$.

Bed	*Rectangular*		*Cylindrical*	
S	Eqn. (10)	3.75 cm	Eqn. (12)	1.98 cm
Pé	(Table II)	12	(Table I)	12
$C_{(S/2,L)}/C_{max}$	Eqn. (8)	0.015	Eqn. (8)	0.61
Recovery	(Fig. 9)	99.7%	(Fig. 9)	82%
$E\tau$	Eqn. (11)	26.0 V h	Eqn. (13)	6.3 V h
E_{max}	Eqn. (14)	31.6 V	(Fig. 6)	~ 110 V
τ_{min}		50 min		~3.5 min

of continuous electrophoresis and electrochromatography. The theory may also be applied for the scaling-up and design of preparative apparatus. Deviations from the theory are to be expected when the assumptions made are not realistic. In particular, electroosmotic flow and variation of the physical properties with temperature might lead to errors. However, further work at Berkeley[13] indicates that electroosmosis can be suppressed by using suitable materials for bed packing and diaphragms. Computer calculations revealed[19,20] that temperature effects can adequately be accounted for by taking all properties at an average bed temperature $(T_{max}-T_0)/2$.

This work was sponsored in part by the National Institute of General Medical Sciences, United States Public Health Service, Research Grant GM-08042.

SUMMARY

By analysis of some important process variables, criteria for successful separation by continuous electrophoresis and electrochromatography in packed beds are derived. A general theory correlating power input, residence time and temperature rise in cylindrical and rectangular geometries is presented. The limitation of the separating capacity by transverse diffusion effects is shown to be predictable in terms of other operational conditions. These separation criteria appear to be in agreement with experimental evidence, and may find analytical as well as preparative application.

REFERENCES

1 Z. PUČAR, in M. LEDERER (ed.), *Chromatographic Reviews*, Vol. 3, Elsevier, Amsterdam, 1961, p. 38.
2 S. R. CAPLAN, *J. Electrochem. Soc.*, 108 (1961) 577.
3 J. T. G. OVERBEEK, *Thesis*, Utrecht, 1941.
4 P. H. WIERSEMA, *Thesis*, Utrecht, 1964.
5 H. G. KUNKEL AND R. TRAUTMAN, in M. BIER (ed.), *Electrophoresis*, Chap. 6, Academic Press, New York, 1959.
6 H. BLOEMENDAL, *Zone electrophoresis in blocks and columns*, Elsevier, Amsterdam, 1963.
7 M. BIER (ed.), *Electrophoresis*, Academic Press, New York, 1959.
8 R. K. FINN, in H. M. SCHOEN (ed.), *New chemical engineering separation techniques*, Interscience, New York, 1962.

9 J. PORATH, *Arkiv Kemi*, 11 (1957) 161.
10 R. M. HYBARGER, C. W. TOBIAS AND T. VERMEULEN, *Ind. Eng. Chem. Process Design Develop.*, 2 (1963) 65.
11 E. RAVOO, R. M. HYBARGER, C. W. TOBIAS AND T. VERMEULEN, paper presented for the Am. Chem. Soc. 30th Ind. Eng. Chem. Div. Symp. on Fluid–Solid Separations, University of Maryland, 1963.
12 E. RAVOO. C. W. TOBIAS AND T. VERMEULEN, *Annular-bed electrochromatography**, *Report 2*, 1963.
13 L. NADY, V. N. GUPTA AND D. G. HOWERY, *Annular-bed electrochromatography**, *Report 4,1*, 1965.
14 G. L. JAQUES AND T. VERMEULEN, *Univ. California Radiation Lab. Report 8029*, 1957.
15 A. CHAMPION, unpublished work, University of California, 1963.
16 J. W. HIBY, *Proc. Symp. Interaction Fluids Particles*, Inst. Chem. Eng., London 1962, p. 312.
17 V. S. ENGLEMAN, *Annular-bed electrochromatography**, *Report 3,2*, 1963.
18 D. G. HOWERY AND T. VERMEULEN, *Birmingham Univ. Chem. Eng.*, 15,3 (1964) 72.
19 M. C. KAVANAUGH, *Annular-bed electrochromatography,** *Report 3,4*, 1963.
20 M. MASSON AND T. VERMEULEN, *Annular-bed electrochromatography**, *Report 5B*, 1965.

---

* These Reports are available at the Department of Chemical Engineering, University of California, Berkeley, Calif.

Analytica Chimica Acta
Elsevier Publishing Company, Amsterdam
Printed in the Netherlands.

DISPLACEMENT ELECTROPHORESIS

A. J. P. MARTIN AND F. M. EVERAERTS
Technische Hogeschool Eindhoven (The Netherlands)

(Received November 1st, 1966)

The three methods of running chromatograms, *viz.* by elution, frontal analysis and displacement have been made generally familiar by TISELIUS. There are also three similar methods of conducting electrophoresis. Only two of these methods are currently in use. The classical Tiselius moving boundary method for proteins is, of course, analogous to frontal analysis. The many variants of zone electrophoresis are analogous to elution chromatography. But there appears to be only a single publication on the displacement method. This was a separation of chlorate, bromate and iodate by LONGSWORTH[1], performed in a Tiselius-type apparatus. It was the result of a discussion of the early results of MARTIN and was a specially chosen example suitable for existing apparatus. MARTIN first conceived the method in 1942 and demonstrated a separation of sodium and potassium[2] then. In 1946 in a more sophisticated apparatus he separated chloride, acetate, aspartate and glutamate[2]. This work has recently been resumed at the Technische Hogeschool in Eindhoven. The method is at present capable of analysing mixtures of strong ions, requiring around 10^{-7} moles of each component. The behaviour of weak ions has not yet been fully worked out, but the method should be feasible in many cases at least.

EXPERIMENTAL

Apparatus

The apparatus consists essentially of a thin glass capillary (length about 1 m,

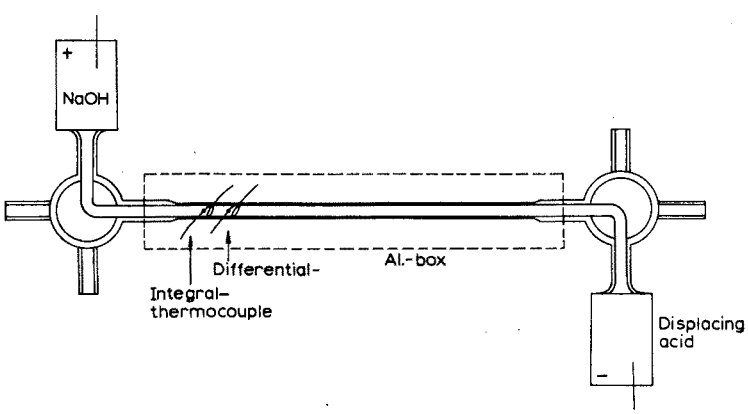

Fig. 1. Apparatus.

outside diameter 0.7 mm, inside 0.4 mm). Each end of the capillary is connected with its own four-way tap to its own reservoir. The reservoirs, of infinite volume compared to the tube, contain respectively an anode and a cathode (Fig. 1).

If separation of anions is required, the cathode reservoir is filled with a solution of acid whose ions are less mobile than any in the mixture to be investigated. The anode reservoir contains sodium hydroxide. The capillary is filled with a solution of sodium chloride with a few percent of a soluble polymer (hydroxyethylcellulose). The polymer contains no ionisable groups, is linear and of high molecular weight and serves to increase the viscosity of the tube filling. It reduces the electroendosmotic flow to a few percent of what it would be in its absence, without appreciably affecting the mobility of the ions.

Description of method

The ions to be separated are introduced into the bore of the plug of the four-way tap joining the capillary tube to the cathode. A constant current is started between the electrodes. From the anode, there are, in succession, a solution of sodium hydroxide, a solution of sodium chloride, the sample and the displacing acid. Thus the only cations in the anode reservoir and capillary tube are sodium ions which move towards the cathode. The anions in the various parts all move towards the anode. The different anions have of course different mobilities. Where several are present in the same solution the more mobile gradually move ahead of the less mobile. The anions will thus arrange themselves in order of mobility, a more or less sharp front occurring between the chloride and the most mobile anion in the sample, and between every other successive pair of ion species. The sharpness of the front will be greater, the greater the difference in mobility of the two anions composing the front. Once the separation is complete all the anions move at the same speed, the original speed of the chloride ions in the tube, without further change.

The potential gradient of each zone will be such as to compel each anion to move at the same speed, *i.e.*, will be inversely proportional to the mobility of the anion. The cations (Na^+) will accelerate as they move from one zone to another of a higher potential gradient, and this will result in each successive zone being more dilute than the previous.

The passage of the current produces heat, and the rate of production of heat is proportional to the potential gradient; since the heat capacity of the tube is small, the temperature of the tube is proportional to the rate of generation of heat. Thus the temperature of the tube forms a step function when plotted along the length of the tube, a step in the temperature occurring wherever a front between ions exists within the tube.

Thus if the temperature at a point on the tube be measured by a thermocouple fixed to it, a recorder connected to the thermocouple will plot a series of steps as the fronts run, at a constant rate, beneath the couple. The height of the step will measure the temperature and hence the mobility of the ion. The distance between the steps will measure the length of tube occupied by one species of ion, and after allowing for the dilution mentioned above, the amount of that ion present.

It is, however, more convenient to measure the position of the step by means of a differential thermocouple, measuring the difference in temperature along a short length of the tube. This produces a curve which is the first differential of the step

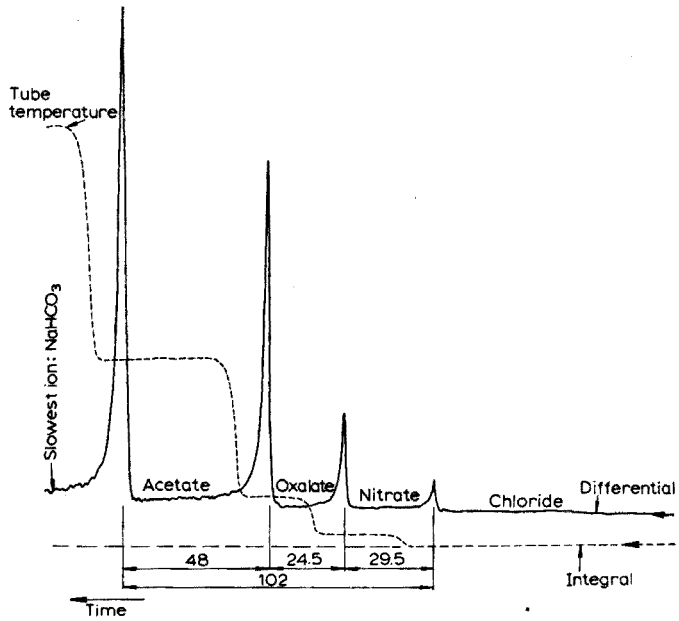

Fig. 2. Integral and differential measurement. Current: 80 μA. Sample: $^1/_{60}$ N $NaNO_3$, $^1/_{60}$ N Na-oxalate, $^1/_{30}$ N Na-acetate. Displacing acid: HCO_3^-. Quickest ion: Cl^-.

function; the peaks indicate the passage of fronts, and the area under the peaks the difference in mobility between the anions on either side of the front.

Either method of presentation contains all the information necessary for an analysis, but for investigation of the method it is very valuable to have both working simultaneously (Fig. 2).

DISCUSSION

The simple theory works well for the separation of strong ions. But so far no attempt at highly accurate work has been undertaken. For instance, no attempt at accurate temperature control of the environment has been made. It is impossible to say, therefore, how important are a number of second-order effects that disturb the simple theory. The next stage will require consideration of the following effects.

(*a*) The heat output and, therefore, temperature difference is inversely proportional to the mobility of the anion. But in that the temperature of each zone is different, mobilities are compared at different temperatures. To obtain mobilities at the same temperature, a correction of about 2% has to be applied and it may be difficult to estimate the correction with much accuracy.

(*b*) A change in temperature from any cause will cause a small alteration in the ratio of the mobility of the anions and cations. This will cause a small change in concentration and may lead to slowly moving concentration fronts.

(*c*) A change in concentration from any cause which alters the ratio of mobility of anions and cations may also lead to slowly moving fronts. (It causes also, of course, a change in temperature.)

(*d*) The electroendosmotic flow throughout the tube will not be constant during the course of the experiment. As the potential gradient rises, so, other things being equal, does the local electroendosmosis. Changes of concentration and temperature will also affect the rate of endosmosis. Change of ions will result in change of adsorbed ions on the glass resulting in changes of the zeta potential. So the rate and pattern of electroendosmotic flow will be complicated. By the use of the high polymer, these effects are thought to be small, but there are, as yet, no figures for their present magnitude.

(*e*) The most difficult problems concern weak ions. A weak ion zone between two strong ion zones gives off hydroxyl ions to the anode and hydrogen ions to the cathode, the pK and concentration of the ion determining the pH on either side of the weak acid zone.

A succession of weak ion zones will form a complicated interacting system difficult to interpret. Multiple-charged ions may give rise to several steps or only one depending, perhaps, on the other substances present. The use of a buffering cation is possible and simplifies the picture but has not yet been fully investigated. The theory of these second-order effects is not yet fully understood.

Relation between mobility and concentration

Consider a front between two salts of the same cation. Let us neglect diffusion or bulk movement of fluid within the tube.

Let the more mobile cation be at the positive end of the tube and the concentration of this ion be constant along the tube. Then if the current be I and the area of cross-section of the tube be a and the velocities of the anions A_1,A_2 and the cation B are U_1,U_2 and U_B with concentrations C_1,C_2 and C_B, we find:

$$I/a = K(C_1U_1 + C_1U_{B1}) = K(C_2U_2 + C_2U_{B2})$$

where $K = 1/96.5$, C_1C_2 *etc.* are concentrations in moles/l, velocities in cm sec^{-1}, a is in cm^2 and I is in amperes.

When m_1,m_2 and m_B are the mobilities of the ions in cm^2 V^{-1} sec^{-1} we find:

$$I/a = K\{C_1U_1 + C_1(m_B/m_1)U_1\} = K\{C_2U_1 + C_2(m_B/m_2)U_1\},$$

when we have a steady state.
Or:

$$C_1/C_2 = m_1/m_2\ \{(m_2+m_B)/(m_1+m_B)\}$$

Theory suggests that allowing for diffusion, for a potential gradient of 100 V cm^{-1} and a mobility difference of 1%, a change in the ratio of the concentration of the two anions at a front will occur over a distance of the order of 0.1 cm.

On passing through a front, the concentration of an ion species decreases exponentially with distance, and for small mobility differences the front is almost symmetrical. But the temperature change showing the existence of the front is steeper on the advancing side than on the receding side since the source of extra heat moves with the front.

Usefulness of the method

It seems probable that the method can be developed into a satisfactory method

for the separation and analysis of microgram quantities of strong ions differing in mobility by one or two percent.

It has been found convenient to use 0.01 N sodium chloride to fill the tube, and a zone 1-mm long can be detected without difficulty, representing $7.3 \cdot 10^{-8}$ g. A current of about 80 μA is used. The voltage rises during the experiment from 1 or 2 to 6 or 7 kV, according to length of tube and the nature of the ions.

Since the system is ideally arranged to remove heat the potential gradient can be high. Potential gradients up to 100 V cm^{-1} are suitable. This gives the method great resolving power and makes for quick separations.

The time required for a separation depends on the length of the tube. The length of the tube for a given separation depends on the length of tube occupied by the most difficultly separable pair of ions divided by (1 — the ratio of the mobilities of this pair of ions).

As with all displacement methods, a substance in the sample is concentrated to an approximately constant concentration. Substances present in small amount are thus much less likely to be overlooked.

Many methods are now available for the analysis of most strong ions. Only if it is possible to extend the use of the method to weak ions, particularly large molecules such as proteins, can a very wide use be foreseen for it. If it can be extended to such molecules it can be confidently expected to be of great value in clinical analyses and biochemistry in general.

SUMMARY

The displacement method of electrophoresis has been studied for strong anions, electropherograms being given as integral and/or differential temperature recordings. The theory and utility of the method are discussed.

REFERENCES

1 G. LONGSWORTH, Natl. Bur. Std. (U.S.) Circ., 524 (1953) 59–68.
2 A. J. P. MARTIN, unpublished work.

Analytica Chimica Acta
Elsevier Publishing Company, Amsterdam
Printed in the Netherlands.

MOBILITÄTSBESTIMMUNGEN BEI DER ELEKTROPHORESE IN AGARGELEN

H. J. HOENDERS, W. DE BOER UND P. A. J. DE BOER
Universiteit van Nijmegen, Laboratorium voor Biochemie, Nijmegen;
Universiteit van Amsterdam, Anthropobiologisch Laboratorium, Amsterdam (Nederland)

(Eingegangen den 1. November, 1966)

Die Bestimmung der relativen elektrophoretischen Beweglichkeit (μ_{rel}) von Proteinen kann auf schnelle und gut reproduzierbare Weise mittels Mikro-Agargelelektrophorese durchgeführt werden[1,2]. Es ist üblich Humanserumalbumin als Bezugssubstanz ($\mu_{rel}=1$) und Dextran als Nullpunktsindikator ($\mu_{rel}=0$) zu verwenden.

Eigene Untersuchungen[3,4] ergaben, dass mehrere methodische Faktoren hierbei genau zu beachten sind, u.a.:

(*1*) Probe und Bezugsgemisch (Dextran + Albumin) müssen unbedingt im gleichen Gel (d.h. auf der gleichen Trägerplatte) wandern. Unterschiede von 10 und mehr Prozent zwischen den von einer bestimmten Komponente auf verschiedenen Platten des gleichen Ansatzes zurückgelegten Strecken stellten keine Ausnahme dar.

(*2*) Eine chemische Markierung der Dextranfront[4,5] (örtliche Anfärbung mit $KMnO_4$) ist der mechanischen Markierung (Einritzen des Gels an der Stelle, wo das Dextran nach Acetonbehandlung sichtbar wird) vorzuziehen; aus einer statistischen Prüfung ging hervor, dass die Streuungen der Wanderungsabstände dann signifikant kleiner sind. Die Möglichkeit zur Proteinanfärbung bzw. zur Bestimmung der relativen Anteile der aufgetrennten Komponenten bleibt bei dieser $KMnO_4$-Markierung voll und ganz erhalten.

Nachdem auf diese Weise das Markierungsproblem befriedigend gelöst war, wurde der Einfluss der Dextrankonzentration im Referenzgemisch auf die Mobilitätsbestimmung systematisch untersucht. Es hatte sich nämlich herausgestellt, dass die Dextranzonen bei ansteigender Konzentration asymmetrische und sogar aufgetrennte Gipfel auf den Densitogrammen ergaben. Es war daher erforderlich, eine optimale Konzentration für diesen Nullpunktsindikator zu ermitteln. Als Versuchssubstanz wurde bei der vorliegenden Untersuchung das Serumprotein Transferrin (Siderophilin), das im elektrischen Feld bei pH 8–9 etwa halb so schnell wie das Serumalbumin wandert, verwendet.

Zusätzlich mussten und konnten im Rahmen dieser Ermittlung des Einflusses der Dextrankonzentration wichtig erscheinende neue Fragestellungen untersucht werden, so z.B. ob eine Alterung der aus Agargel bestehenden Kontaktkissens und der Ort der Agarplatten im Trenngerät bei der Mobilitätsbestimmung zu berücksichtigen sind.

Weiterhin wurde untersucht, ob die Flexibilität der Mikro-Agargelelektrophorese (namentlich schnelles Umwechseln auf Pufferlösungen anderer Art und Ionenstärke oder anderen pH-Wertes) durch Anwendung von Kontaktkissen aus Schaum-

kunststoff an Stelle der Agargelkissen vergrössert werden konnte. Diese Modifikation führte unter im übrigen identischen Bedingungen zu einem niedrigeren Beweglichkeitswert für das als Standardprotein eingesetzte Transferrin. Für die beiden Kontaktkissenmaterialien wurden systematische Vergleiche angestellt bezüglich des Zahlenwertes und der Reproduzierbarkeit der direkten Messgrössen der relativen Beweglichkeit, sowie in Bezug auf den Einfluss der Laufzeit und des Ortes der Agarplatten im Elektrophoresegerät.

METHODIK

Im wesentlichen wurde entsprechend den Angaben von WIEME[2] verfahren. Das aus Polymethylmethacrylat hergestellte Elektrophoresegerät war für die Aufnahme von 10 Objektträgern (25 mm × 76 mm) geeignet. Diese Glasplättchen wurden mit der Agarschicht nach unten auf die Kontaktkissen (1%-iges Agargel oder Schaumkunststoff) gelegt und besorgten so den Stromdurchgang. Durch die Kontaktkissen aus Agargel wurde direkt unter den Kontaktstellen mit den Agarplatten Platindrähte verlegt, sodass der Spannungsabfall in den Platten mit guter Annäherung gemessen werden konnte.

Als Trägerschicht wurde 1%-iges Agargel ("Special Agar Noble", Difco, Detroit, U.S.A.) in Veronal–Acetat-Puffer, pH 8.6, Ionenstärke 0.05, verwendet (3 ml/Platte). Vor dem Gebrauch verblieben die Platten 48–60 h in einer feuchten Kammer. Für die Elektroden- und Kontaktkissenräume wurde von der gleichen Pufferlösung, die nach jedem Ansatz erneuert wurde, Gebrauch gemacht.

Zur Probenaufgabe wurden mittels einer "Guillotine" auf jeder Platte 2 Schlitze zu je 7 mm Breite und mit 4 mm Zwischenraum in die Agarschicht gestanzt. Die Schlitze wurden jeweils mit 2 μl Probelösung folgender Zusammensetzung beschickt:

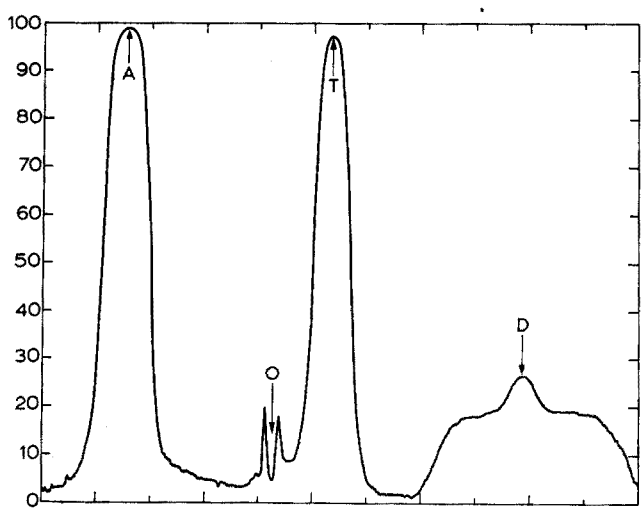

Abb. 1. Densitogramm eines mittels Agargelelektrophorese aufgetrennten Gemisches von Dextran (20 mg/ml), Transferrin (9 mg/ml) und Humanserumalbumin (11 mg/ml). D = Dextran, T = Transferrin, O = Aufgabestelle, A = Albumin.

Dextran mit mittlerem MG 75 000 ("Macrodex", Poviet NV, Amsterdam, Niederl.) in variierter Konzentration;
Transferrin (Behringwerke, Marburg/Lahn), 0.9%;
Humanserumalbumin, trocken, "reinst" (Behringwerke), 1.1%.

Die Elektrophorese erfolgte im kalten Raum (2°) mit konstant gehaltener Stromstärke von 9 mA pro Platte. Der Spannungsabfall in den Platten betrug 50–55 V, derjenige zwischen den Anschlussklemmen der Elektroden 65–73 V (Agarkissen) bzw. 76–85 V (Schaumkissen).

Die Anfärbung der Protein- und Dextranzonen erfolgte nach der in einer früheren Mitteilung[4] genau beschriebenen Arbeitsweise. Die Auswertung wurde an Hand der mit einer Photovolt-Ausrüstung (Photovolt Corp., New York) erhaltenen Densitogramme vorgenommen (Abb. 1).

ERGEBNISSE

Einfluss der Dextrankonzentration

Zur Untersuchung des Einflusses der Dextrankonzentration im Referenzgemisch auf die Bestimmung der relativen Beweglichkeit und die Form des Dextrangipfels im Densitogramm wurden 10 Versuchsreihen zu je 8 Platten mit Proben zu-

TABELLE I

MITTLERE RELATIVE BEWEGLICHKEIT VON TRANSFERRIN BEI VARIIERTER KONZENTRATION DES DEXTRANS

(n = Zahl der Ansätze, s^2 = Varianz, s = Standardabweichung, s_{rel} = relative Standardabweichung)

Dextrankonz. (%)	n	$\bar{\mu}_{rel}$	$s^2 \cdot 10^6$	$s \cdot 10^3$	s_{rel} *(%)*
0.5	9	0.486	34.75	5.89	1.21
1	10	0.478	31.30	5.59	1.16
2	10	0.476	30.44	5.42	1.12
3	8	0.474	18.63	4.32	0.91
4	9	0.472	46.88	6.85	1.44
5	9	0.475	46.63	6.83	1.41
7.5	10	0.476	55.00	7.42	1.54
10	9	0.474	38.13	6.18	1.32

nehmender Dextrankonzentration angesetzt. Die Laufzeit betrug stets 75 Minuten. Auf jeder Platte befand sich neben dem Dextran–Transferrin–Albumin-(DTA-)-Gemisch mit variierter Dextrankonzentration das entsprechende Gemisch mit 2% Dextran. Die aus 8 bis 10 Ansätzen pro Dextrankonzentration errechneten Mittel für die relative Beweglichkeit des Transferrins sind aus Tabelle I zu ersehen.

Einfluss der Art der Kontaktkissen

Zur Klärung der Frage, ob der Ersatz von Agarkissen im Elektrophoresegerät durch solche aus Schaumkunststoff unbedenklich sei, wurden Versuchsreihen mit je 10 Agarplatten und mit 5 verschiedenen Laufzeiten für beide Kissenmateralien angesetzt. Auf jeder Platte wurde neben einem DTA-Gemisch mit 2% Dextran ein

TABELLE II

MITTELWERTE DER RELATIVEN BEWEGLICHKEIT VON TRANSFERRIN IN ABHÄNGIGKEIT VON DER LAUFZEIT FÜR DIE KISSENMATERIALIEN AGARGEL BZW. SCHAUMKUNSTSTOFF

(Dextrankonzentration 2%; n = Zahl der Agarplatten, s = Standardabweichung, s_{rel} = relative Standardabweichung)

Kissen-material	*Lauf-zeit (')*	n	$\overline{\mu_{rel}}$	s	s_{rel} *(%)*
Agargel	55	10	0.476	0.006	1.3
Agargel	65	10	0.475	0.004	0.9
Agargel	75	10	0.472	0.008	1.7
Agargel	85	9	0.475	0.009	1.9
Agargel	95	10	0.474	0.011	2.3
Schaumk.	55	10	0.472	0.008	1.7
Schaumk.	55	10	0.471	0.005	1.2
Schaumk.	65	9	0.467	0.005	1.1
Schaumk.	75	10	0.461	0.007	1.6
Schaumk.	75	10	0.465	0.009	1.8
Schaumk.	85	10	0.463	0.006	1.3
Schaumk.	95	9	0.466	0.008	1.8
Schaumk.	95	10	0.453	0.005	1.2

solches mit 1% Dextran aufgebracht. Letzteres geschah mit dem Ziel, endgültigen Aufschluss über die Frage zu erhalten, ob der Dextrangehalt nicht von 2% auf 1% herabgesetzt werden könne (vergl. dazu auch die Diskussion auf S. 244). Es stellte sich heraus, dass fast ausnahmslos 3 bis 5 von jeweils 10 DTA-Gemischen mit 1% Dextran zweifelhaft bis unbrauchbar in Bezug auf die Lagebestimmung des Dextrangipfels waren. Die mit den 2% Dextran enthaltenden DTA-Gemischen gefundenen und pro Ansatz gemittelten Werte für die relative Beweglichkeit des Transferrins sind in Tabelle II zusammengefasst.

DISKUSSION UND STATISTISCHE AUSWERTUNG

Einfluss der Dextrankonzentration

Die Untersuchung der Frage, welche Dextrankonzentration als optimal zu betrachten ist, führte zu folgenden Problemstellungen:

(1) Verursacht Alterung der Agar-Kontaktkissen im Elektrophoresegerät eine Änderung der μ_{rel}-Werte des Transferrins?

(2) Spielt der Ort der Agarplatten im Trenngerät eine Rolle bei der μ_{rel}-Bestimmung?

(3) Bei welcher möglichst niedrigen Dextrankonzentration tritt die chemisch markierte Dextranzone im Densitogramm noch als gut ausmessbarer Gipfel in Erscheinung?

(4) Wird die Reproduzierbarkeit der Mobilitätsbestimmungen durch die Dextrankonzentration beeinflusst?

(5) Führt Erhöhung der Dextrankonzentration zu einer Asymmetrie und schliesslich zur Aufspaltung des Dextrangipfels im Densitogramm?

(6) Ist die für Transferrin ermittelte relative Beweglichkeit abhängig von der Dextrankonzentration im Bezugsgemisch?

Ad 1: *Alterung der Kontaktkissen.* Es wurden die 2% Dextran enthaltenden DTA-Gemische von 10 Ansätzen zu je 8 Platten zur Klärung dieser Frage herangezogen. Die Elektrophoreseläufe erfolgten im gleichen Gerät in einem Zeitraum von 8 Tagen und ohne Erneuerung der Agar-Kontaktkissen.

Die Fragestellung wurde an Hand der gefundenen μ_{rel}-Werte für Transferrin statistisch verteilungsfrei geprüft (Test auf Trend[6]) und es ergab sich, dass der fragliche Einfluss der Alterung äusserst unwahrscheinlich war ($49.20\% > P_R > 48.80\%$).

Ad 2: *Ortsabhängigkeit.* Auch diese Frage konnte mit Hilfe der Ergebnisse der eben erwähnten 10 Versuchsreihen beantwortet werden, da der Ort der einzelnen Agarplatten im Trenngerät bekannt war.

Die statistische Analyse (Test auf Trend[6]) ergab einen signifikanten Trend ($\alpha = 0.10$; $P_R = 8.85\%$), überwiegend im Sinne einer Zunahme der μ_{rel}-Werte, je weiter die entsprechenden Agarplatten von den Anschlussklemmen des Trenngerätes entfernt gewesen waren.

Eine nähere Analyse wurde mit den Grössen $\overline{DT}$, $\overline{DA}$ und $\overline{DO}$ vorgenommen. Sie zeigten alle drei ebenfalls einen signifikanten Trend (Rang-Korrelationstest nach SPEARMAN[6]; $\alpha = 0.10$) und zwar vorwiegend eine Abnahme der Werte mit zunehmender Entfernung von den Anschlussklemmen.

Obwohl es sich bei obigen Befunden um relativ geringe Trends ohne wesentliche praktische Bedeutung handelte, erschien es doch angebracht, die Frage zu stellen, ob nicht auch innerhalb einer Agarplatte derartige Ortsabhängigkeiten zu verzeichnen seien. Zu diesem Zwecke wurden die μ_{rel}-Werte für Transferrin, die bei 10 verschiedenen Ansätzen jeweils auf einer Platte mit 2 identischen DTA-Gemischen (2% Dextran) erhalten wurden, mit einander verglichen. Es konnte aber innerhalb der Platten keineswegs eine Ortsabhängigkeit wahrscheinlich gemacht werden (Rangzeichentest oder Symmetrietest nach WILCOXON[6]; $\alpha = 0.10$; $48\% > P_R > 47\%$).

Die Erklärung für die hier gefundenen Trends ist u.E. darin zu suchen, dass eine Abhängigkeit von der Feldstärke vorgelegen hat. Als Beleg hierfür möge die Tatsache gelten, dass der Abstand $\overline{DO}$, der als Masstab für die Endosmose und damit auch für die Feldstärke betrachtet werden kann, ebenfalls einen Trend aufwies. Dies würde bedeuten, dass die Agar-Kontaktkissen nicht homogen gewesen sind und am einen Ende des Geräts einen anderen Spannungsabfall innerhalb der Kissen als am anderen Ende ergaben. Dieser Effekt war manchmal auch im gegenläufigen Sinne und in anderen Fällen nicht vorhanden. Auf jeden Fall handelt es sich hier um eine wohl kaum eliminierbare Variable in den Versuchsbedingungen (vgl. dazu auch S. 247).

Ad 3: *Noch gerade gut ausmessbare Gipfel im Densitogramm.* Die Anfärbemethode mit $KMnO_4$ ergibt um die Dextranzone herum einen braunen Untergrund von MnO_2. Im Densitogramm stellt dieser sich als Plateaugebiet dar, auf welchem der Dextrangipfel superponiert ist (Abb. 1).

Bei einer Dextrankonzentration von 0.5% war in 10 untersuchten Fällen der Dextrangipfel des Densitogramms nur mühsam zu erkennen. Bei den 1% Dextran enthaltenden Proben war in 5 von 10 Fällen nicht die Rede von einem gut wahrnehmbaren, spitzen Gipfel. Proben mit 2% Dextran gaben nur in einem von 10 Fällen einen ungenügend scharfen Dextranpeak. Der Unterschied in Gipfelqualität — ausgedrückt als die Anzahl gut bzw. schlecht ausmessbarer Gipfel — wurde für die Gruppen von Proben mit 1% bzw. 2% Dextran statistisch geprüft (Vierfeldertest[7]; $\alpha = 0.05$): 2%

TABELLE III

BEURTEILUNG DER GIPFELFORM DES DEXTRANS

Dextran-konz. (%)	*n*	*Symmetrisch*	*Asymmetrisch*	*Doppelgipflig*
0.5	9	(9)[a]	(0)[a]	0
1	10	10 (100%)	0 (0%)	0
2	10	8 (80%)	2 (20%)	0
3	8	6 (75%)	2 (25%)	0
4	9	3 (33%)	6 (67%)	0
5	9	2 (22%)	7 (78%)	0
7.5	10	—	—	10 (100%)
10	9	—	—	9 (100%)

[a] Die Gipfel waren zu klein für eine gute Beurteilung der Symmetrie.

Dextran lieferte eine signifikant grössere Anzahl brauchbarer Gipfel als 1% Dextran.

Ad 4: Reproduzierbarkeit der Mobilitätsbestimmungen. An Hand der erhaltenen Varianzwerte (s^2; Tabelle I) konnte durch statistische Prüfung (BARTLETT-Test; P_R=99.99%) festgestellt werden, dass für die verschiedenen Dextrankonzentrationen keine Unterschiede in der Reproduzierbarkeit vorlagen.

Ad 5: Asymmetrie und Aufspaltung des Dextrangipfels. Auf Grund visueller Beurteilung der Densitogramme wurde bezüglich der Form der Dextrangipfel die in Tabelle III gegebene Übersicht erhalten.

Man ersieht aus den Daten dieser Tabelle, dass bereits bei 2% Dextran die Tendenz zur Ausbildung asymmetrischer Gipfel auftritt. Oberhalb 5% Dextran waren ausnahmslos 2 mehr oder weniger gut von einander getrennte Peaks wahrzunehmen; nur der von der Aufgabestelle am weitesten entfernte Gipfel ergab vernünftige Beweglichkeitswerte für das in den Proben enthaltene Transferrin. Zur Frage, ob die Aufspaltung der Dextranzone durch das Vorhandensein geladener Anteile bedingt ist oder ob es sich um Artefakte handelt, die durch Inhomogenität des elektrischen Feldes (infolge der hohen Dextrankonzentration) verursacht werden, ist bisher keine Antwort möglich.

Durch statistische Analyse (Vierfeldertest; α=0.05) wurde bestätigt, dass bei den Proben mit 4 und 5% Dextran signifikant grössere Anzahlen asymmetrischer Gipfel auftraten als bei denen mit 2 bzw. 3% Dextran.

Ad 6: Abhängigkeit der Transferrin-Mobilität von der Dextrankonzentration. Es musste bei der Behandlung dieser Frage der Tatsache Rechnung getragen werden, dass die μ_{rel}-Werte eine Abhängigkeit vom Ort der entsprechenden Agarplatten im Trenngerät aufwiesen (vgl. Ad 2). Da auf jeder Platte neben der Probe mit variierter Dextrankonzentration eine solche mit 2% Dextran aufgegeben worden war und da innerhalb der Platten keine Ortsabhängigkeit nachgewiesen werden konnte (vgl. Ad 2), war es möglich, die Ortsabhängigkeit zu eliminieren. Zu diesem Zwecke wurde pro Platte der Unterschied zwischen den beiden μ_{rel}-Werten für Transferrin ($\Delta\mu_{rel}$) ermittelt. Bei den Proben mit 7.5 und 10% Dextran wurde nur der Dextrangipfel berücksichtigt, der zu vernünftigen Beweglichkeitswerten führte. Die relevanten Daten sind aus Tabelle IV zu ersehen.

Die Tabelle IV suggeriert eine Abnahme von μ_{rel} bei Zunahme der Dextran-

TABELLE IV

ZUR ABHÄNGIGKEIT DER RELATIVEN BEWEGLICHKEIT DES TRANSFERRINS VON DER DEXTRANKONZENTRATION

Dextrankonz. (%)	*n*	$\overline{\Delta\mu_{rel}}$[a]	$s^2 \cdot 10^6$	*s*
0.5	8	+0.0105	2238	0.0046
1	10	+0.0024	5961	0.0077
2	10	+0.0003	1684	0.0040
3	8	−0.0009	2743	0.0051
4	9	−0.0033	5008	0.0070
5	9	−0.0029	3260	0.0057
7.5	10	−0.0027	2273	0.0048
10	9	−0.0026	3282	0.0057

[a] Relative Mobilität, erhalten aus der Probe mit variierter Dextrankonzentration, minus jene, die aus der Probe mit 2% Dextran hervorging.

konzentration von 0.5 bis 4% und daran anschliessend eine schwache Zunahme (vgl. auch Tabelle I). Nur zwischen 0.5% und allen übrigen Dextrankonzentrationen, nicht dagegen bei allen anderen Kombinationen, konnte ein statistisch gesicherter Unterschied für $\overline{\Delta\mu_{rel}}$ nachgewiesen werden (einfache Varianzanalyse einschl. Test nach NEWMAN UND KEULS[6]; $\alpha=0.05$). Es sei allerdings auch erwähnt, dass die $\Delta\mu_{rel}$-Werte in der Folge 1%→5% Dextran einen Trend im Sinne einer überwiegenden Abnahme aufwiesen (Test auf Trend[6]; $\alpha=0.05$); daher kann nicht ausgeschlossen werden, dass bei grösserem Umfang des Zahlenmaterials $\overline{\Delta\mu_{rel}}$-Unterschiede innerhalb dieser Konzentrationsreihe doch noch signifikant würden. In der Folge 4%→10% Dextran konnte ein Trend nicht wahrscheinlich gemacht werden ($\alpha=0.05$; $P_R=33\%$).

Einfluss der Art der Kontaktkissen

Für die Planung der entsprechenden Versuche war zunächst die Wahl einer adäquaten Dextrankonzentration in den DTA-Gemischen erforderlich. Dem Bestreben, möglichst geringe Dextrankonzentrationen anzuwenden (geringere Wechselwirkung; bessere Symmetrie der Gipfel im Densitogramm), mussten Überlegungen technischer Art (Gipfellokalisierung) entgegengesetzt werden. Als Kompromiss wurde eine Dextrankonzentration von 2% gewählt. Der Vergleich zwischen den Kontaktkissen aus Agargel bzw. Schaumkunststoff wurde bei 5 Laufzeiten (55, 65, 75, 85 und 95 min) durchgeführt. Die Beurteilung der Brauchbarkeit des Schaumkunststoffs als Kontaktkissenmaterial[8] wurde mittels folgender Fragestellungen untersucht:

(1) Ist die Reproduzierbarkeit der Beweglichkeitsbestimmungen unterschiedlich für die beiden Kontaktkissenmaterialien?

(2) Sind die für Transferrin gefundenen μ_{rel}-Werte abhängig von der Art der Kontaktkissen?

(3) Beeinflusst die Dauer des Elektrophoreselaufs die μ_{rel}-Werte?

(4) Existiert ein linearer Zusammenhang zwischen den Messgrössen $\overline{DT}$ bzw. $\overline{DA}$ und der Laufzeit?

(5) Spielt der Ort der Agarplatten im Trenngerät eine Rolle in Bezug auf die erhaltenen μ_{rel}-Werte?

Ad 1: *Reproduzierbarkeit.* Die Varianzen (s^2) der μ_{rel}-Werte wurden pro Laufzeit für die beiden Kissenmaterialien verglichen. Die statistische Prüfung (F-Test; $\alpha=0.10$) ergab keine signifikanten Differenzen.

Ad 2: *Abhängigkeit der μ_{rel}-Werte von der Art der Kontaktkissen.* Die pro Ansatz gemittelten μ_{rel}-Werte waren für alle Laufzeiten bei Anwendung von Kontaktkissen aus Schaumkunststoff signifikant kleiner als bei Anwendung von Agarkissen (STUDENT-Test; $\alpha=0.10$). Die Zahlenwerte sind in Tabelle II aufgeführt.

Zur näheren Analyse dieser Erscheinung wurden die Grössen $\overline{DT}$, $\overline{DA}$ und $\overline{DO}$ (letztere als Mass für die Endosmose) verglichen. Global zusammengefasst lautete das Ergebnis, dass $\overline{DT}$ und $\overline{DO}$ bei Schaumkunststoffkissen im Mittel kleinere Werte aufwiesen als bei Agarkissen, während dieser Sachverhalt für $\overline{DA}$ nicht wahrscheinlich gemacht werden konnte.

Ad 3: *Einfluss der Laufzeit auf μ_{rel}.* Im Falle der Agarkontaktkissen konnten zwischen den bei den einzelnen Laufzeiten erhaltenen $\overline{\mu_{rel}}$-Werten für Transferrin keine signifikanten Unterschiede festgestellt werden (einfache Varianzanalyse[6]; $\alpha=0.10$; $P_R>25\%$). Ganz im Gegensatz hierzu standen die auf Schaumkunststoff erhaltenen Befunde: es wurden sehr eindeutige Differenzen konstatiert ($\alpha=0.05$;

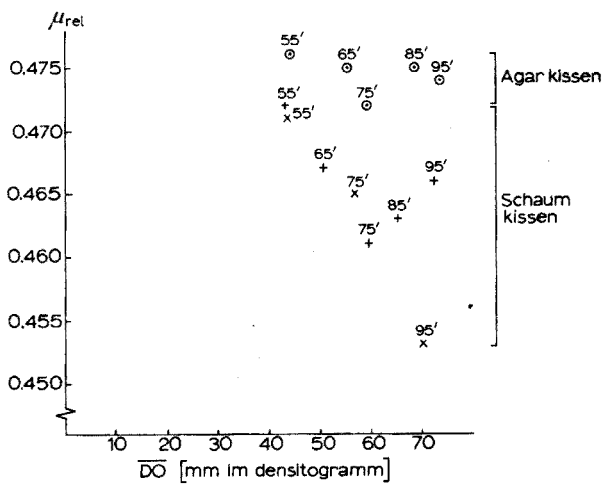

Abb. 2. Relative Beweglichkeit von Transferrin bei verschiedenen Laufzeiten unter Anwendung von Kontaktkissen aus Agargel (⊙) bzw. Schaumkunststof (×, +). Über den Messwerten sind die Laufzeiten angegeben; zur Wahl der Abszissenskala s. Text.

$5\%>P_R>2.5\%$). In Abb. 2 sind die Mittelwerte ($n=9$–10) der Beweglichkeiten graphisch dargestellt und zwar als Funktion von $\overline{DO}$, da diese Grösse als geeignetster Masstab für die Wirkung des elektrischen Feldes während gewisser Zeiten erkannt wurde (vgl. Ad 4). Die Betrachtung der Abb. 2 lehrt, dass die μ_{rel}-Mittelwerte bei den Agarkissen von 0.472 bis 0.476, bei den Schaumkissen von 0.453 bis 0.472 streuen. Die aus dem Diagramm abzulesende Tendenz einer Zunahme von μ_{rel} mit abnehmender Laufzeit bei Schaumkunststoff wurde statistisch geprüft (Test nach NEWMAN UND KEULS[6]; $\alpha=0.05$). Es stellte sich heraus, dass der bei 55 min Laufzeit erhaltene Wert signifikant grösser war als die bei 75 und 85 min erhaltenen Werte.

Ad 4: Linearer Zusammenhang zwischen $\overline{DT}$ bzw. $\overline{DA}$ und der Laufzeit. Beim Auftragen der Abstände $\overline{DT}$ und $\overline{DA}$ (Mittelwerte der einzelnen Ansätze, $n=9$–10) gegen die Zeit wurden nur angenähert Geraden erkennbar. Da die Stromstärke bei allen Läufen konstant (9 mA/Platte) gehalten wurde und die vorgesehenen Laufzeiten genau eingehalten worden waren, blieben als Erklärung für die Abweichungen von der Geraden Fluktuationen in der Feldstärke. Tatsächlich hatte die mittlere Spannung zwischen den Kontaktstellen der Agarplatten mit den Kissen bei den verschiedenen Ansätzen für beide Kissenarten von 49 bis 56 Volt gestreut. Bei den individuellen Ansätzen sank die Spannung in den ersten Minuten um einige V und blieb dann im weiteren Verlauf innerhalb eines Intervalls von 1–3 V konstant.

Um nun zu einer genaueren Darstellung der Abstände $\overline{DT}$ und $\overline{DA}$ als Funktion der sie beeinflussenden Grössen zu gelangen, müsste man sie gegen das Produkt Feldstärke · Zeit auftragen. Dies war jedoch nachträglich nicht möglich, da Spannungsmessungen nur alle 15 min und relativ grob erfolgt waren. Stattdessen wurde der Abstand $\overline{DO}$, ein Mass für den erfolgten endosmotischen Transport, gewählt. Lässt man nämlich gelten, dass die endosmotische Strömungsgeschwindigkeit der angelegten Spannung innerhalb kleinerer Bereiche proportional ist, so stellt $\overline{DO}$ ein Mass für das Produkt Feldstärke · Zeit dar.

Die graphische Darstellung von $\overline{DA}$ und $\overline{DT}$ gegen $\overline{DO}$ ergab ausgezeichnete Geraden, deren Extrapolation zwanglos durch den Koordinatenschnittpunkt führte. Die Regressionsanalyse (Test auf Linearität) bestätigte dies für die mit Agarkissen erhaltenen Werte, indem sogar für $\alpha=0.10$ noch ein linearer Trend erhalten wurde; für die Schaumkunststoff-Kissen konnte das Fehlen einer Abweichung von der Linearität nicht eindeutig wahrscheinlich gemacht werden.

Ad 5: Ortsabhängigkeit. Die bei den auf S. 243 beschriebenen Versuchen festgestellte Abhängigkeit des μ_{rel}-Wertes vom Ort der betreffenden Agarplatte im Elektrophoresegerät, wurde jetzt vergleichend für die beiden Kontaktkissenmaterialien untersucht. Pro Ansatz wurde geprüft, ob eine Signifikanz bezüglich dieser Ortsabhängigkeit vorhanden war (Rangkorrelationstest nach SPEARMAN; $\alpha=0.10$). Bei 15 Ansätzen mit Kontaktkissen aus Agar war dies neunmal der Fall (5 negative, 4 positive Korrelationen), von 8 Ansätzen mit Schaumkissen dagegen nur einmal. Die Anzahl der Läufe mit Ortsabhängigkeit des μ_{rel}-Wertes war damit für die Agarkissen signifikant grösser als für die Schaumkissen (Vierfeldertest; $\alpha=0.05$).

ZUSAMMENFASSUNG

Die Elektrophorese in Agargelen bietet die Möglichkeit, auf einfache und schnelle Weise die Beweglichkeit eines Proteins, bezogen auf die eines Referenzeiweisses (z.B. Humanserumalbumin), zu bestimmen. Der durch Elektro-Osmose bedingte Transport wird mit Hilfe einer ungeladenen Substanz, üblicherweise Dextran, ermittelt. Die Ortslokalisierung der Dextranzone erfolgt aus Genauigkeitsgründen besser chemisch als mechanisch. Die chemische Markierung erfordert einen Kompromiss für die Dextrankonzentration im Bezugsgemisch; entsprechende Versuche ergaben, dass 2% Dextran als optimale Konzentration anzusehen ist. Ferner stellte sich bei diesen Versuchen u.a. heraus, dass mit 0.5% Dextran eine signifikant höhere Mobilität des Transferrins erhalten wird als mit höheren Dextrankonzentrationen.

Zur Untersuchung der Frage, ob die Kontaktkissen aus Agargel im Trenngerät

unbedenklich durch solche aus Schaumkunststoff ersetzt werden können, wurden identische Ansätze bei 5 Laufzeiten (55–95 min) mit den beiden Kontaktkissenmaterialien durchgeführt. Die Agarkissen ergaben signifikant grössere Beweglichkeitswerte für Transferrin, die Streuungen der Mittelwerte bei den einzelnen Ansätzen waren wesentlich kleiner als bei den Schaumkissen und es wurde keine Abhängigkeit von der Laufzeit festgestellt, wie es bei letzteren der Fall war. Ein Vorteil der Schaumkissen war dass die bei der Anwendung von Agarkontaktkissen beobachtete schwache Abhängigkeit der relativen Mobilität vom Ort der betreffenden Agarplatte im Trenngerät praktisch nie bei ersteren auftrat. Die Reproduzierbarkeit der Beweglichkeitsbestimmungen zeigte keine signifikanten Unterschiede für die beiden Kissenmaterialien. Es erwies sich als empfehlenswert, ein "inneres Mass" für das Produkt Feldstärke · Zeit, nämlich den Abstand Dextranzone–Aufgabesort ($\overline{DO}$), einzuführen. Die Abstände Dextran–Transferrin bzw. Dextran–Albumin, aufgetragen gegen $\overline{DO}$, ergaben, zumindest bei Anwendung von Kontaktkissen aus Agargel, ausgezeichnete Geraden (Regressionsanalyse), die nach Extrapolation zwanglos durch den Koordinatenschnittpunkt führten.

SUMMARY

Agar-gel electrophoresis allows a simple rapid determination of the mobility of a protein in relation to a reference protein (*e.g.* human serum albumin). The electroosmotic transport is determined by means of an uncharged substance, usually dextran. The dextran zone can be located more exactly by chemical than mechanical means. However, chemical marking makes the correct choice of the dextran concentration important; 2% dextran seems to be optimal. The mobility of transferrin is significantly higher with 0.5% dextran than with higher concentrations.

Replacement of agar bridges with foam plastic was studied for 5 migration times of 55–95 min. With agar the mobilities for transferrin were significantly higher and their fluctuations lower. Also, a dependence on migration time was found with foam but not with agar. A more exact parameter for the product field-strength · time proved desirable: *viz.* the distance between the dextran zone and the point of application ($\overline{OD}$). The distances dextran–transferrin and dextran–albumin plotted against $\overline{OD}$ showed perfect straight lines, which could be extrapolated to the origin.

LITERATUR

1 M. RABAEY, *Over de eiwitsamenstelling der ooglens, Diss.*, Univ. Gent, 1959.
2 R. J. WIEME, *Clin. Chim. Acta*, 4 (1959) 317; *Diss.*, Univ. Gent, 1959; *Biochem. Taschenb.*, 2 (1964) 947; *Agar Gel Electrophoresis*, Elsevier, Amsterdam, 1965.
3 H. J. HOENDERS, *Über die Proteinzusammensetzung der Augenlinse des Huhns, Diss.*, Univ. Amsterdam, 1965.
4 W. DE BOER, H. J. HOENDERS, P. A. J. DE BOER UND H. A. TOOROP, *Clin. Chim. Acta*, im Druck.
5 J. P. BENNETT UND J. C, BOURSNELL, *Biochim. Biophys. Acta*, 63 (1962) 382.
6 H. DE JONGE, *Inleiding tot de Medische Statistiek*, Nederlands Instituut voor Praeventieve Geneeskunde, Leiden, 1964.
7 J. R. GEIGY AG (Hrsg.), *Documenta Geigy Wissenschaftliche Tabellen*, 6. Aufl., Basel, 1960.
8 R. MASSEYEFF, *Bull. Mem. Ecole Nat. Med. Pharm. Dakar*, 7 (1959) 248.

Analytica Chimica Acta
Elsevier Publishing Company, Amsterdam
Printed in the Netherlands.

ELECTROPHORETIC SEPARATION OF INORGANIC CATIONS ON CELLULOSE ACETATE

K. AITZETMÜLLER, K. BUCHTELA AND F. GRASS
Atominstitut der Österreichischen Hochschulen, Wien (Austria)

(Received November 1st, 1966)

During investigations of short-lived radioactive substances, various methods for separating small amounts of material in short intervals of time were tested. The separation of the rare-earth elements was of particular interest. Many reviews indicate the usefulness of electromigration as an analytical tool and the electrophoretic behaviour of the lanthanides was therefore examined. Numerous references to the separation of inorganic ions by paper electrophoresis show the usefulness of hydroxycarboxylic acids as electrolytes[1–7]. It is well known that α-hydroxyisobutyrate solution is one of the best eluants for the ion-exchange chromatography of rare earths[8–12]. A comparison of the complex constants of these elements in various hydroxycarboxylic acid media indicated that a good electrophoretic separation of the lanthanides could be achieved in solutions of α-hydroxyisobutyric acid.

EXPERIMENTS

Materials and apparatus

When acetylcellulose films were used as supporting material instead of filter paper strips, much better results were obtained with regard to the shape and size of the migrating spots. Acetylcellulose films have been previously used mainly in medical research and diagnosis. Usually gelatinized acetylcellulose films* are stored in vessels filled with methanol. Before use they were kept for some hours in an aqueous solution of the electrolyte which was employed for electrophoresis. The wet films were then taken out of their containers and placed on the glass plate of the cooling cell. The excess electrolyte solution was removed with blotting paper. In handling the strips it is essential to avoid any damage to the surface of the films.

Solutions of mixtures to be separated were added to the strip on the starting point either from micropipettes or from small paint brushes when quantitative analysis was not necessary.

For controlling the temperature of the moist film during the electric migration, a flat cell made of glass and plastic was provided with inlet and outlet tubes and was cooled with running water. The temperature of the cooling water was about 10°. The strip was in a chamber saturated with water vapor to avoid excessive evaporation of the aqueous solution from the supporting material.

Commercially available apparatus can be used for electrophoresis when the

* "Cellogel", Chemetron Chimica, Milano.

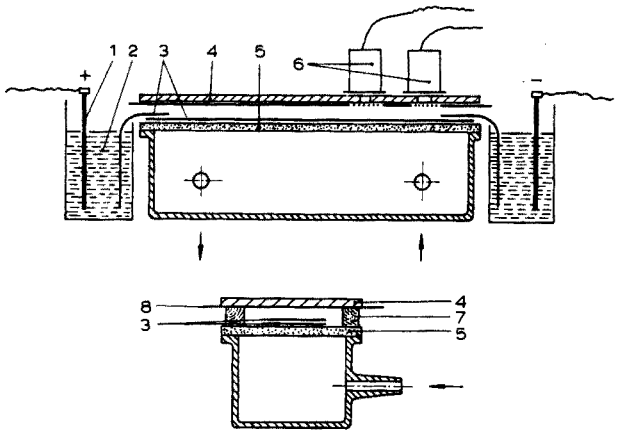

Fig. 1. Schematic picture of the electrophoresis apparatus used for radiochemical separations on acetylcellulose films. 1) Platinum electrode. 2) Solution. 3) Acetylcellulose strip. 4) Lead plate. 5) Glass plate of the cooling cell. 6) Geiger–Müller tubes. 7) Plastic material for the chamber saturated with water vapor. 8) Moist filter paper.

device for cooling the strip is provided. This is necessary because voltages up to 5000 V are applied. The electrophoresis apparatus used in these investigations was made of glass and plastic material[13]. Figure 1 shows a schematic picture.

When radioactive substances were used, the positions of the fastest migrating substances could be easily located during the separation by Geiger–Müller tubes. These detectors were placed on the holes of a lead plate on top of the apparatus near the end of the strip (Fig. 1). The detection of radioactivity near the end of the strip indicated that longer separation time would cause the substances to migrate into the electrolyte vessels. An alarm signal showed the end of the separation procedure and the current was switched off.

When the radioactive material had been separated, the strips were put on a glass plate after the electrophoresis and heated to 80–100° for 5–10 min. The strips became transparent and the radioactive substances were included in the film, so that there were no risks of contamination when the electropherogram was handled for autoradiography or scanning.

RESULTS

Figure 2 compares the separation of cerium and thulium in lactic acid and α-hydroxyisobutyric acid. The figure also shows the advantages of acetylcellulose because the spots are small and round and the results are much better than with filter paper. For these experiments gelatinized acetylcellulose strips were used. The migrated zones were easily detected by means of radioactive isotopes and autoradiographic techniques. It can be seen that the adsorption effects are very small because no contamination could be detected between the migrated zones.

Figure 3 shows another example of this separation procedure, using inactive mixtures and "Membranfolien"*. The detection of the zones was done by spraying the

* Membranfolien zur Elektrophorese; Schleicher und Schüll, DBR.

dried strips with a solution of alizarin S and ascorbic acid. Reddish spots appeared on a yellow background. The mixture of the rare earths contained radioactive promethium which could be detected by autoradiography. These separations took 14–17 min with a voltage gradient of about 140–170 V cm^{-1}. Usually the electrolyte consisted of an aqueous solution of 0.35–0.8 *M* α-hydroxyisobutyric acid. Lanthanum migrated fastest and the sequence of the rare earths corresponded to the sequence of the lanthanides in the periodic system of the elements[14].

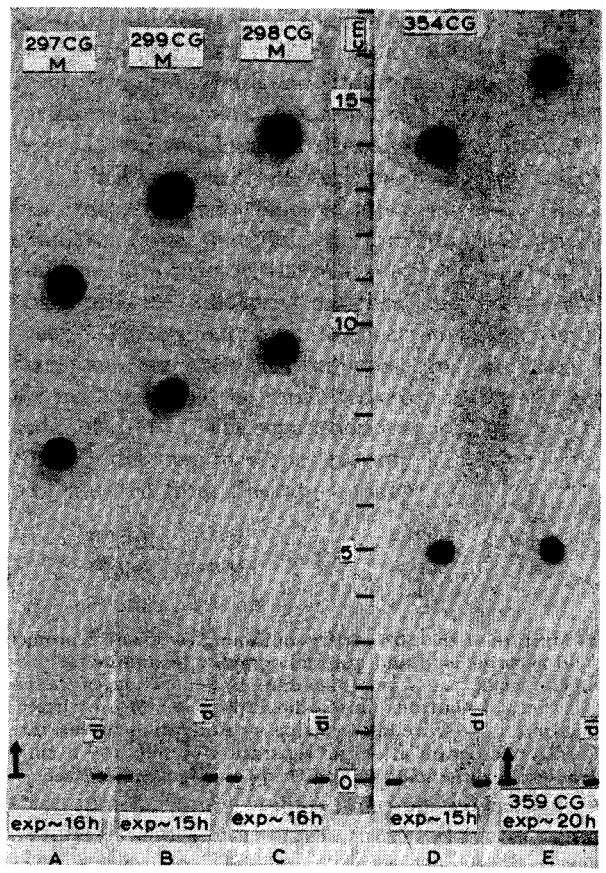

Fig. 2. Separation of cerium-144 and thulium-170 on acetylcellulose films (autoradiography). Cerium migrates faster than thulium. (A) 0.5 *M* lactic acid, 46 V cm^{-1}, 15 min; (B) 0.5 *M* lactic acid, 46 V cm^{-1}, 19 min; (C) 0.5 *M* lactic acid, 46 V cm^{-1}, 21 min; (D) 0.4 *M* α-hydroxyisobutyric acid, 46 V cm^{-1}, 24 min; (E) 0.4 *M* α-hydroxyisobutyric acid, 46 V cm^{-1}, 27 min.

It can be assumed that these good results are due to the homogeneous structure and the low adsorption of the supporting material. Several acetylcellulose products for electrophoresis had been tested and the material turned out to be very suitable especially for the separation of small amounts of substances such as carrier-free radioactive nuclides. On gelatinized acetylcellulose a complete separation of the radioactive lanthanides was achieved with a maximum migration distance of 13 cm from the start for lanthanum (Fig. 3b).

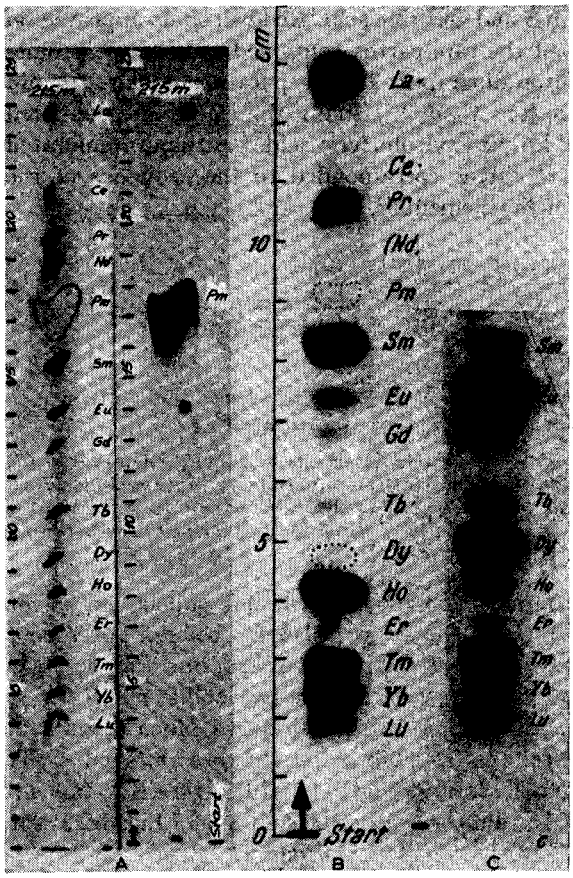

Fig. 3. Separation of the rare earths. a) Mixture of the rare earths containing radioactive promethium-147. Detection with alizarin S and ascorbic acid and autoradiographic technique for promethium-147. 0.35 *M* α-hydroxyisobutyric acid, 140 V cm^{-1}, 16 min. b) Separation of radioactive rare earths after irradiation with thermal neutrons (autoradiography). 0.8 *M* α-hydroxyisobutyric acid, 45 V cm^{-1}, 29 min; gelatinized acetylcellulose strips. c) Activation of the rare earths by neutron irradiation of the electropherogram after the separation (5 min, 10^{12} n cm^{-2} sec^{-1}, thermal neutrons). 0.8 *M* α-hydroxyisobutyric acid, 47 Vcm^{-1}, 33 min; gelatinized acetylcellulose strips.

The results of the experiments with the rare earths were so encouraging, that separations of some other inorganic cations were investigated. For the following investigations gelatinized acetylcellulose films were mainly used.

First, mixtures of neutron-irradiated lanthanides were analysed. The above-mentioned sequence of the migrating rare earths was verified by γ-spectrometric analysis of the radioactive spots on the electropherogram after autoradiographic localization. Test spectra of neutron-irradiated, spectroscopically pure substances were compared with the spectra of the rare-earth spots. Thus the various radioactive elements could easily be identified and no impurities could be detected.

When activation analysis is applied to the lanthanides, it may be of some interest that short-lived radioactive isotopes of these elements can be produced and measured after the separation by irradiating the electropherogram. The time of irra-

diation is only some minutes and the background activity of the impurities in the acetylcellulose film is low. The activity of the spots is high enough to be detected by autoradiography or scanning (Fig. 3c). For mounting radioactive samples for counting, acetylcellulose material offers some advantages because of its solubility in many organic solvents. By evaporation very thin films can be produced which include the radioactive material and are suitable for 4-π-counting and especially for the measurement of low-energy radiation without considerable self-absorption.

Some problems concerning the separation and analysis of small amounts of impurities in substances were investigated. Thus it was possible to analyse the impurities in rare earths which are available as spectroscopically-pure substances. In a spectroscopically-pure gadolinium sample, for instance, the impurities of other rare earths such as samarium, europium, terbium, thulium, ytterbium and lutetium, could be separated and detected after an irradiation time in the reactor of more than 500 h.

With the electrophoretic method, small amounts of substances can be separated from rather large excesses of other material. This is necessary when an analysis of irradiated target material is performed. By the irradiation of rare earths with thermal neutrons in a reactor, the heavy isotopes are transformed into radioactive elements which produce radioactive daughter nuclides of the neighbour elements in the periodic system. These small amounts of carrier-free material are difficult to separate from the target substance. By electrophoresis on acetylcellulose films, these radioactive daughter nuclides could be separated even when the quantitative proportion was of the order of 10^8 to 1. The separation was achieved in a few minutes and no contamination could be detected by γ-spectroscopy. The end-product of the following reactions could be separated from the target material.

$$^{150}\mathrm{Nd}(\mathrm{n},\gamma)^{151}\mathrm{Nd} \xrightarrow{-\beta^-} {}^{151}\mathrm{Pm}$$
$$^{148}\mathrm{Nd}(\mathrm{n},\gamma)^{149}\mathrm{Nd} \xrightarrow{-\beta^-} {}^{149}\mathrm{Pm}$$
$$^{154}\mathrm{Sm}(\mathrm{n},\gamma)^{155}\mathrm{Sm} \xrightarrow{-\beta^-} {}^{155}\mathrm{Eu}$$
$$^{160}\mathrm{Gd}(\mathrm{n},\gamma)^{161}\mathrm{Gd} \xrightarrow{-\beta^-} {}^{161}\mathrm{Tb}$$
$$^{170}\mathrm{Er}(\mathrm{n},\gamma)^{171}\mathrm{Er} \xrightarrow{-\beta^-} {}^{171}\mathrm{Tm}$$
$$^{176}\mathrm{Yb}(\mathrm{n},\gamma)^{177}\mathrm{Yb} \xrightarrow{-\beta^-} {}^{177}\mathrm{Lu}$$

From the other experiments only some examples are cited here: the separation of radioactive alkaline-earth metals and their decay products including calcium, strontium, barium, scandium, yttrium and lanthanum; the fission products of neutron-irradiated plutonium; the natural radioactive elements and their decay products; the transuranium elements; complex compounds of the platinum metals, *etc.* In other papers the application of the method for rapid analysis of commercial products has been discussed. The detection of decay products of radium-226 in commercial actinium-227 has been described[15].

The application of this method for the transuranium elements was tested. The results of ion-exchange chromatography and of electrophoretic separation (both methods with α-hydroxyisobutyric acid) showed some similarities. The distances of the spots on the electropherogram and the distances of the corresponding elution peaks of the ion-exchange chromatogram were rather small between praseodymium and neodymium, and large between europium and gadolinium. Plots of the distance from the start of the electropherogram under normalized conditions versus the logarithm of the drop number of the peak positions in ion-exchange chromatography

indicated that the electrophoretic behaviour of a lanthanide can be predicted if the ion-exchange data are known. The same should be valid for the transuranium elements. The electrophoretic behaviour of americium was examined and in all experiments the distance of migration from the start differed by only a few millimeters from the predicted value. The deviations were about $\pm 2\%$ from the predicted migration distance. The separation of curium from neutron-irradiated americium was performed. Unfortunately, the separation of other transuranium elements could not be carried out, since they were not available.

SUMMARY

The electrophoretic separation of mixtures of rare earths was investigated. All rare-earth elements could be separated using α-hydroxyisobutyric acid and acetylated cellulose films; the separation times were 14–20 min. This method is very suitable for the separation of small amounts of radioactive samples. Separation of radioactive rare earths, alkaline earths, fission products, transuranium elements, natural radioactive elements and their decay products, *etc.*, are feasible.

Small amounts of carrier-free radioactive daughter products produced by β-decay of neutron-irradiated rare-earth elements could be separated from a considerable excess of starting material. A method for using activation analysis for the detection of cations after the electrophoretic separation on acetylcellulose strips is discussed.

REFERENCES

1 Z. KONRAD-JAKOVAC AND Z. PUCAR, *J. Chromatog.*, 7 (1962) 380.
2 Z. PUCAR AND Z. KONRAD-JAKOVAC, *J. Chromatog.*, 9 (1962) 106.
3 T. R. SATO, H. DIAMOND, W. P. NORRIS AND H. H. STRAIN, *J. Am. Chem. Soc.*, 74 (1952) 6154.
4 D. IMRISOVA AND V. KNOBLOCH, *Collection Czech. Chem. Commun.*, 28 (1963) 331.
5 M. MAKI, *Japan Analyst*, 5 (1956) 571.
6 M. LEDERER, *Compt. Rend.*, 236 (1953) 209; *Anal. Chim. Acta*, 11 (1954) 145; *J. Chromatog.*, 1 (1958) 86; 5 (1961) 356.
7 V. P. SHVEDOV AND A. P. STEPANOV, *Radiokhim.*, 1 (1959) 112.
8 G. R. CHOPPIN, S. G. THOMPSON AND B. G. HARVEY, *U.S. Pat.* 2925431 (1960), ref.: *NSA*, 14 (1960) 15718.
9 M. VOBECKY AND A. MASTALKA, *Collection Czech. Chem. Commun.*, 28 (1963) 709, 743.
10 G. R. CHOPPIN AND R. J. SILVA, *J. Inorg. Nucl. Chem.*, 3 (1956) 153.
11 H. L. SMITH AND D. C. HOFFMANN, *J. Inorg. Nucl. Chem.*, 3 (1956) 243.
12 B. K. PREOBRAZHENSKII, *UCRL*-Trans-551-(L) (1960).
13 K. AITZETMÜLLER, K. BUCHTELA AND F. GRASS, *J. Chromatog.*, 22 (1966) 431.
14 K. AITZETMÜLLER, K. BUCHTELA AND F. GRASS, *Mikrochim. Ichnoanal. Acta*, (1964) 1089.
15 K. AITZETMÜLLER, K. BUCHTELA AND F. GRASS, *Atomkernenergie*, 10 (1965) 269.

Analytica Chimica Acta
Elsevier Publishing Company, Amsterdam
Printed in the Netherlands.

GEGENSTROMIONOPHORESE. III. NEUE APPARATIVE ANORDNUNG ZUR KONTINUIERLICHEN TRENNUNG NACH DEM GEGENSTROMPRINZIP

W. PREETZ UND H. L. PFEIFER
Institut für analytische Chemie und Radiochemie der Universität des Saarlandes, Saarbrücken (Deutschland)

(Eingegangen den 1. November 1966)

In früheren Mitteilungen wurde das Prinzip der sich selbststeuernden Gegenstromionophorese allgemein abgeleitet[1] und am Beispiel der Trennung farbiger Modellanionen in einem kapillaren Gegenstromtrennrohr[2] experimentell bestätigt. Hinsichtlich theoretischer und praktischer Einzelheiten wird auf diese Arbeiten verwiesen; nur die wesentlichen Grundtatsachen seien hier kurz erwähnt.

Bei geeigneten Versuchsbedingungen ordnen sich unter dem Einfluss eines elektrischen Feldes und einer kompensierenden Gegenströmung die zu trennenden Anionen bzw. Kationen nach fallenden Ionenbeweglichkeiten in gegen einander abgegrenzten Zonen stationär an. Dazu müssen am Gegenstromzulauf Ionen grosser, am Gegenstromablauf Ionen kleiner Beweglichkeit eingesetzt werden. Je höher der Beweglichkeitsunterschied dieser das Trenngemisch begrenzenden Ionen ist, um so grössere Schwankungen der Spannung bzw. der Gegenstromgeschwindigkeit werden durch die automatische Steuerung des Trennvorganges ausgeglichen. Der auftretende treppenförmige Feldstärkeverlauf längs des Trennweges bewirkt die Fokussierung der Ionen in Zonen gleichbleibender Grösse, entgegen ihrer Verbreiterung durch Diffusion und Konvektion und gewährleistet eine hohe Trennschärfe. Die Konzentration der Zonen nimmt in Richtung der Gegenströmung stufenweise ab und ist durch die Konzentration der Gegenstromlösung eindeutig festgelegt.

Übertragung des Gegenstromprinzips auf die Durchflussionophorese

Da bei der Gegenstromionophorese gleichmässige Flüssigkeitsbewegungen senkrecht zum elektrischen Feld und zur Gegenstromrichtung die Entmischung nicht stören, kann die „eindimensionale" Trennung in einer Kapillare entsprechend der trägerfreien Durchflussionophorese[3,4] auf eine laminar durchströmte Fläche erweitert werden. Der Trennvorgang wird so kontinuierlich gestaltet.

Für das Beispiel der Trennung der beiden Anionen A und B, von denen das erstere die grössere Ionenbeweglichkeit besitzt, gibt Abb. 1 ein schematisches Fliessbild.

Die wesentliche Veränderung gegenüber der trägerfreien Durchflussionophorese[3,4] besteht in der Erzeugung einer zusätzlichen Elektrolytströmung (Gegenstrom), die der Wanderung der zu trennenden Ionen im elektrischen Feld (Anionenstrom) entgegen gerichtet ist und diese kompensiert. Dadurch lassen sich beliebig grosse Wanderungsstrecken in einer kleinen Apparatur verwirklichen.

Die Durchflusszuleitungen fördern drei verschiedene mit gleicher Geschwindig-

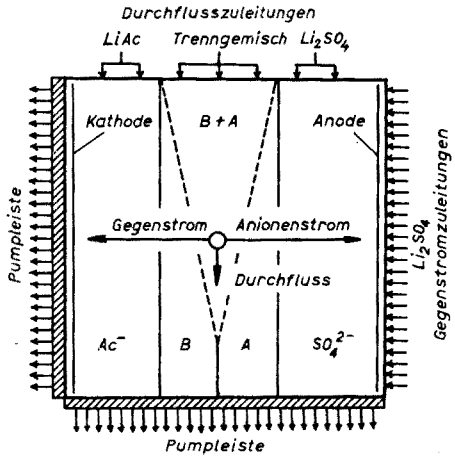

Abb. 1. Fliessschema zur kontinuierlichen Gegenstromionophorese.

keit fliessende Lösungen in die Trennfläche. Das im mittleren Bereich über eine gewisse Breite einfliessende Trenngemisch (A + B) wird auf der Seite des Gegenstromzulaufs durch eine Lösung mit Ionen grösserer Beweglichkeit (im Beispiel SO_4^{2-}-Ionen) auf der Abflusseite von Ionen kleinerer Beweglichkeit (Acetationen) abgegrenzt. Damit sind die Bedingungen für die Einstellung stationärer Verhältnisse erfüllt, sofern auch die Konzentrationen der eingesetzten Lösungen auf einander abgestimmt sind[1].

Beim Betrieb der Apparatur beobachtet man zunächst eine scharfe Abgrenzung der beiden Teilflächen mit den Acetat- bzw. SO_4^{2-}-Ionen. Je nach ihrem Beweglichkeitsunterschied und den herrschenden Feldstärken entmischen sich die Ionen A und B auf ihrem Weg durch die Trennkammer mehr oder weniger schnell, indem sie nach beiden Seiten hin zu reinen Zonen auswandern. Die Verweilzeit in der Apparatur ist so einzustellen, dass bei Erreichen der unteren Pumpleiste völlige Entmischung eingetreten ist, d.h. die keilförmige Mischzone (A + B) muss noch innerhalb der Trennfläche enden.

AUFBAU DER APPARATUR

Die neue Trennvorrichtung nach dem Gegenstromprinzip* wurde aus einer seit längerer Zeit bewährten Apparatur der trägerfreien Durchflussionophorese, dem Pheroplan[3,4], entwickelt.

Die Apparatur ist in Abb. 2 schematisch dargestellt. Die Abb. 3 und 4 geben als Schnittzeichnungen besonders die Einzelheiten des eigentlichen Trennsystems und der Pumpvorrichtungen wieder.

Zwei von Kühlsole (15) durchflossene Glasplatten (1, 2) in den Abmessungen von etwa 30 × 30 cm bilden, durch inkompressible Kunststoffscheibchen (24) der Dicke 0.03–0.05 cm in konstantem Abstand von einander gehalten, eine kapillare Trennfläche (14), die seitlich von Klebe- oder Gummistreifen (17) begrenzt wird. Die

* Zum D.B.P. angemeldet.

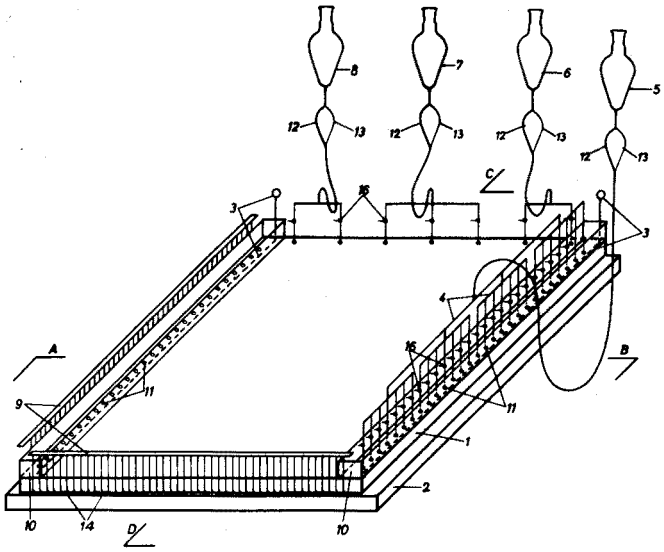

Abb. 2. Apparatur zur kontinuierlichen Trennung nach dem Gegenstromprinzip.

an den Seiten liegenden Elektrodentröge (10) mit den Platinelektroden (3) stehen über 28 Bohrungen (11) durch die obere Glasplatte, die mit Steinwolle oder Asbest als Diaphragmen gefüllt sind, mit der Trennfläche (14) in Verbindung. Auf der Seite des Zuflusses befindet sich eine Glasharfe (4), die die Gegenstromlösung (5) auf Glasröhren verteilt, die durch die Diaphragmen (11) bis in den Trennspalt führen. Zu ihrer Spülung tragen sie Dreiwegehähne (16). Das Trenngemisch (7) und die begrenzenden Elektrolytlösungen (6, 8) gelangen über kleine Glasharfen und Rohre mit Dreiwegehähnen (16) direkt in die Trennfläche.

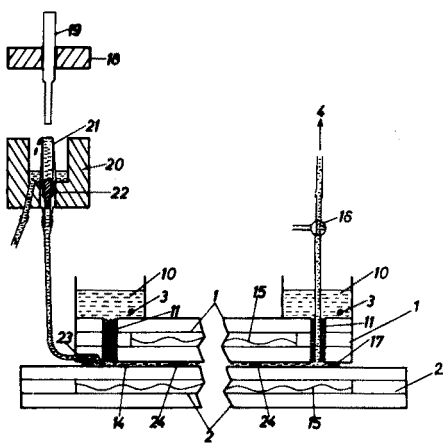

Abb. 3. Trennapparatur im Schnitt nach Linie A–B der Abb. 2.

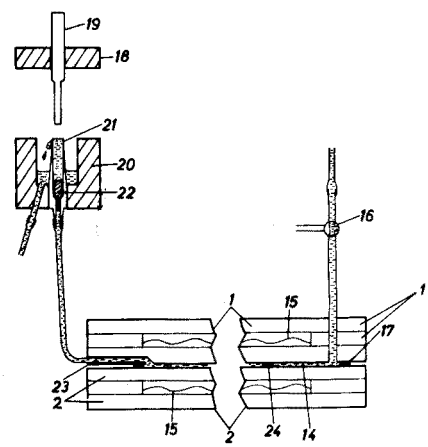

Abb. 4. Trennapparatur im Schnitt nach Linie C–D der Abb. 2.

Zur Erreichung einer hohen Trennschärfe muss die gleichmässige und laminare Bewegung der Lösungen in der Trennfläche sowohl in Richtung des Gegenstroms wie auch in Richtung des Durchflusses gewährleistet sein. Das wird durch dosiertes und regelbares Zu- und Abfliessen der Elektrolyten erreicht.

Der Zulauf aller Lösungen erfolgt aus Niveaugefässen (5–8), deren Leitungen verzweigt sind. Die Zweigleitungen (12) mit dem grösseren Durchmesser dienen ausschliesslich der Spülung und schnellen Füllung der Kammer. Sie sind während des Versuches geschlossen. In die Verbindungen (13) sind feine Kapillaren eingesetzt. Sie ermöglichen den konstanten und, durch Änderung der Niveauhöhe, in weiten Grenzen variablen Zufluss der Lösungen (5–8).

Den gleichmässigen Abfluss über die gesamte Breite der Trennfläche gewährleisten die Abnahmevorrichtungen (9). Ihr Aufbau ist aus den Schnittzeichnungen der Abb. 3 und 4 ersichtlich. Längs den beiden Abnahmeseiten sind im gleichen Abstand je 49 dünne Polyäthylenschläuche (23) in eingeschliffene Kerben der oberen Kühlplatte fest eingekittet. Sie stellen als kommunizierende Röhren die Verbindung zwischen der Trennfläche (14) und den beiden Abnahmeleisten (9) her. Jede Leiste enthält 49 horizontal und in gleicher Höhe angeordnete Abnahmestellen. Diese bestehen aus zwei in einander gesetzten Bechern (20, 21), von denen der innere ein Ventil (22) enthält, das ein Verwischen der Grenzen zwischen den Zonen durch zurückfliessende Lösung verhindern soll. Durch kurzzeitiges Absenken der Leisten (18) mit den Stiften (19) werden aus allen Bechern (21) gleiche kleine Flüssigkeitsvolumina verdrängt, die in Auffanggläschen abfliessen. So wird zwangsweise die gleichmässige laminare Flüssigkeitsbewegung erreicht. Der Rhythmus der Pumpvorgänge wird über zwei Schaltuhren gesteuert und ist der Zulaufgeschwindigkeit so anzupassen, dass erst bei annähernder Füllung der Becher (21) die Pumpleisten abgesenkt werden. Die Stifte (19) in den Leisten (18) sind auf Gleitsitz gearbeitet, d.h. sie können während des Versuches einzeln etwas auf- und abbewegt werden. Durch die variable Eintauchtiefe lassen sich gewisse Ungleichmässigkeiten in der Strömung, die durch Ausbuchtungen in den Zonen angezeigt werden, ausgleichen.

ARBEITSTECHNIK

In die blasenfrei mit destilliertem Wasser gefüllte Trennkammer lässt man, über die Dosierkapillaren (13) reguliert, aus den Niveaugefässen (6 und 8) die begrenzenden Elektrolytlösungen, z.B. bezogen auf die Ladung der Anionen 0.0075 *N* Li_2SO_4- und 0.005 *N* LiAc-Lösung, aus dem Gefäss (7) das Trenngemisch (etwa 0.006 *N*) einfliessen. Dabei ist nur die Durchflusspumpe in Betrieb. Nach Abgleich der Zulaufgeschwindigkeiten durch Änderung der Höhe der Niveaugefässe erreicht man die Besetzung des linken Teils der Trennfläche mit Acetat-Ionen, des rechten mit SO_4^{2-}-Ionen. Dazwischen liegt in Form eines breiten Stromfadens das Trenngemisch. Die scharfe Abgrenzung der drei Lösungen bei Eintritt in das Trennsystem begünstigt die Trennung[1].

Der Anodentrog wird mit 0.1 *M* LiOH gefüllt, die Kathodenlösung ist je 0.1 *M* an Essigsäure und Natriumacetat. Durch gelegentliche Erneuerung dieser Lösungen ist dafür zu sorgen, dass die Neutralisation der durch Elektrolyse entstehenden H^+- bzw. OH^--Ionen jederzeit gewährleistet ist.

Aus einem leistungsfähigen Kryomaten pumpt man Kühlsole (Glycerin–Wasser

Gemisch) von 0° durch die Kühlplatten. Gleichzeitig mit der Spannung (2000–3000 V) wird die Gegenströmung (0.0075 *N* Li_2SO_4-Lösung) eingeschaltet und die Pumpleiste auf der Kathodenseite in Betrieb genommen. Innerhalb weniger Minuten bildet das Trenngemisch scharfe Grenzen gegen den Ac^-- und den SO_4^{2-}-Bereich aus. Die Gegenstromgeschwindigkeit wird dann so eingeregelt, dass sich das Trenngemisch als breite Zone parallel zu den Elektroden im mittleren Bereich der Trennfläche stationär anordnet. Bei den herrschenden mittleren Feldstärken um 100 V/cm entspricht das etwa einer Gegenstromgeschwindigkeit von 1 cm/min.

Die Durchflussgeschwindigkeit richtet sich gemäss Abb. 1 nach der für die vollständige Trennung der Ionen erforderlichen Verweilzeit in der Trennfläche.

KONTINUIERLICHE TRENNUNGEN

Der Verlauf der kontinuierlichen Gegenstromionophorese in der beschriebenen neuen Apparatur wurde am Beispiel der Trennung farbiger Komplexanionen beobachtet.

Trennung von Ionen mit grossen Beweglichkeitsunterschieden

Entsprechend der allgemeinen Arbeitstechnik wird ein Gemisch von gelben $[IrCl_6]^{2-}$- und blauvioletten $[IrBr_6]^{2-}$-Ionen, deren Beweglichkeiten sich um etwa 12% unterscheiden, zwischen Zonen mit Acetat- und SO_4^{2-}-Ionen der Gegenstromionophorese unterworfen. Lässt man das Gemisch als etwa 10-cm breite Zone einfliessen, so genügt zur vollständigen Trennung eine Verweilzeit von ungefähr 30 bis 40 Min. Wie in Abb. 1 dargestellt, endet die keilförmige Mischzone kurz vor der Abnahmestelle.

Die aus der Apparatur abfliessenden Komplexzonen erweisen sich als reine wässrige $Li_2[IrBr_6]$- und $Li_2[IrCl_6]$-Lösungen. In ihnen sind weder Acetat- noch SO_4^{2-}-Ionen nachzuweisen.

Trennung sehr ähnlicher Ionen

Mit Hilfe der trägerfreien Durchflussionophorese lassen sich unter den günstigsten Bedingungen noch Ionen trennen, die einen Beweglichkeitsunterschied von mindestens 5% aufweisen.

Die Versuche mit der beschriebenen Gegenstromapparatur zeigen, dass bei Verweilzeiten von 3 bis 4 Stunden auch Gemischtligandkomplexionen des Typs $[MCl_xBr_{6-x}]^{2-}$ ($M = Ir, Os$; $x = 0,1,\ldots,6$) getrennt werden können. Der Beweglichkeitsunterschied beträgt für benachbarte Glieder dieser Komplexreihen weniger als 2%[4].

Bei ausreichend hohen Verweilzeiten dürfte auch die kontinuierliche Trennung bzw. Anreicherung von Isotopengemischen gelingen.

Wir danken dem Direktor des Instituts, Herrn Prof. E. BLASIUS, für häufige Beratung und Diskussion. Für finanzielle Unterstützung der Arbeit danken wir der Deutschen Forschungsgemeinschaft, dem Bundesministerium für Wissenschaftliche Forschung und der Wissenschaftlichen Gesellschaft des Saarlandes.

ZUSAMMENFASSUNG

Durch die Erzeugung einer zusätzlichen Strömung entgegen der Wanderung

der zu trennenden Ionen wird das Gegenstromprinzip auf die trägerfreie Durchflussionophorese übertragen. In der beschriebenen neuen Apparatur können chemisch sehr ähnliche Ionen wegen der frei wählbaren Verweilzeit beliebig lange dem Trennprozess unterworfen werden. Dadurch gelingt die kontinuierliche Trennung von Gemischtligandkomplexen des Typs $[MCl_xBr_{6-x}]^{2-}$ (M = Ir, Os; x = 0, 1, ... , 6), deren Beweglichkeitsunterschiede unter 2% liegen. Die abfliessenden getrennten Zonen sind reine wässrige Salzlösungen definierter Konzentration, die im Gegensatz zur Durchflussionophorese ohne Gegenstrom nicht durch einen Grundelektrolyten verunreinigt sind.

SUMMARY

A new apparatus is described for separation by countercurrent carrier-free electrophoresis. Chemically very similar ions can be separated because of the freely variable sojourn time. It is possible to separate continually mixed ligand complexes of the type $[MCl_xBr_{6-x}]^{2-}$ (M = Ir, Os; x = 0, 1 . . . ., 6); the differences in mobilities are below 2%. The separated zones are pure aqueous salt solutions of definite concentrations, which are not contaminated by base electrolyte.

LITERATUR

1 W. PREETZ, *Talanta*, 13 (1966) 164.
2 W. PREETZ UND H. L. PFEIFER, *Talanta*, im Druck.
3 J. BAROLLIER, E. WATZKE UND H. GIBIAN, *Z. Naturforsch.*, 13b (1958) 75.
4 E. BLASIUS UND W. PREETZ, *Z. Anorg. Allgem. Chem.*, 335 (1965) 1, 16.

Analytica Chimica Acta
Elsevier Publishing Company, Amsterdam
Printed in the Netherlands.

ZONE MELTING AND COLUMN CRYSTALLIZATION AS ANALYTICAL TOOLS

H. SCHILDKNECHT
Institute of Organic Chemistry, University of Heidelberg (Germany)

(Received November 1st, 1966)

Crystallization offers several advantages as a general method of separation and purification. The first, and perhaps most important, stems from the fact that the crystalline state is the most ordered one.

Normal freezing—one of the easiest applications of crystallization—can be used to concentrate very dilute solutions, without any loss by decomposition and solvent volatility, by freezing out the solvent, *i.e.* "normal freezing" or ice zone melting[1,2]. The solute tend to be excluded when crystals of pure solvent are formed and large separation factors result. Thus in the case of an ideal eutectic mixture, the crystal formed from a melt is pure solvent.

NORMAL FREEZING

When a dilute solution in a glass tube is slowly lowered into a freezing mixture, at a speed of 1 to 5 cm/h, pure solvent freezes out from the bottom and the solute, or its concentrated solution, is collected in the last droplets at the upper end of the tube. Even if the original concentrations are very low, only one step is necessary, whereby a stirrer is kept above the phase boundary with a stirring speed of about 2500 rpm. After the dilute solutions have been concentrated by this process, unknown substances therein can be characterised by spectroscopy or by thin-layer chromatography in conjunction with suitable colour reactions.

In connection with our phytochemical work, we were interested in the chemotropism of the pollen tubes of gymnosperms[3]. In higher flowering plants, germination begins at the stigma on the top end of the pistil. Starting from here, the pollen grain sends a pollen tube down through the centre of the pistil, its growth being directed through the style towards the ovary. However, the fertilization proper, that is fusion of the contents of the sperm and ovule, only occurs when the pollen tube grows in towards the embryo sac within the ovary in the lower part of the pistil. Since there is no mechanical device for directing its growth in the proper course, the pollen tube is led by a chemical attraction with the aid of gamete hormones which are secreted from the ovary. The nature of the effective agent was unknown. In order to identify the active principle involved, the ovules of oenothera were extracted with water; this extract exerted a strong attraction on growing pollen tubes of oenothera, which could be observed under the microscope.

The pollen tubes grew towards a channel into which the chemotropically active extract had been placed. Very surprisingly, the extracts apparently contained only a

few unessential compounds. It was only after the extract had been subjected to normal freezing that a concentrate was obtained in which fourteen compounds reacting with ninhydrin could be detected. Five of these were found to be peptides, one an amine, and seven others amino acids. The individual compounds identified were lysine, arginine, aspartic acid, proline, valine, phenylalanine, and leucine. Chromatography in several solvent systems and spraying of the chromatograms with various reagents made it possible to detect and identify various sugars in the extract concentrate. Sugars which were definitely detected in this way were saccharose, glucose, galactose, fructose, and arabinose. In general, the samples that gave the highest values in the affinity tests were those that contained, together in the eluates, both sugars and substances which reacted with ninhydrin.

The technique of normal freezing can be used to enrich and isolate small amounts of solute from dilute solutions only when the compounds concerned do not form mixed crystals, *i.e.* solid solutions, with the solvent. If this is the case, one must resort to a multi-stage crystallization procedure, *i.e.* zone melting[1,2].

The most important requirement for zone melting is a sharply bounded molten zone, which should be as narrow as possible, and flanked on both sides by crystalline solid. Such a molten zone is formed if a small cross-sectional part of a rod of crystalline material is melted with the aid of a furnace. It is not easy to confine the molten region within definite limits simply by regulating the temperature of a furnace. Small coolers are therefore fitted in front of and behind the furnaces; this is particularly necessary if it is desired to melt several closely-spaced regions of one and the same ingot.

ZONE MELTING

Figure 1 shows multi-stage zone-melting apparatus with several heaters and coolers. The glass tube containing 15–25 g of substance travels through the zone-melting apparatus from bottom to top at a speed of 1–10 mm/h. With this apparatus, it is possible to purify substances with a melting point within the range 0°–*ca.* 300°. It is presupposed that the compound freezes from the melt as crystals, is not decomposed in the melt and that the melt is not too viscous. Above all, zone melting serves for the purification of crystalline compounds without the use of other media, *e.g.* solvents, as can be illustrated by the following example.

The zone melting of the 2,4-dinitrophenylhydrazone of acetone provides a good example. Here the purification achieved is so good that it can even be detected by the strong colouration at the end of the frozen ingot. For recording purposes, however, it is preferable to divide the ingot up into sections and to determine the melting-points of the individual fractions and thus to construct a melting-point curve; it is important to record not so much the melting-point as the *melting-range*. The smaller the melting-range the purer the fraction; this can be seen from the melting-ranges shown in Fig. 2.

Frequently, no matter how many zones are passed through during the purification, the purity of the product in the end-zone cannot be improved. It is then expedient to take the portions of two ingots at which the steady state has been reached, and to subject them together to individual zone-melting processes. Figure 3 shows the distributions of the melting-ranges along the daughter ingots for acetanilide; quite similar results are obtained for diphenylamine.

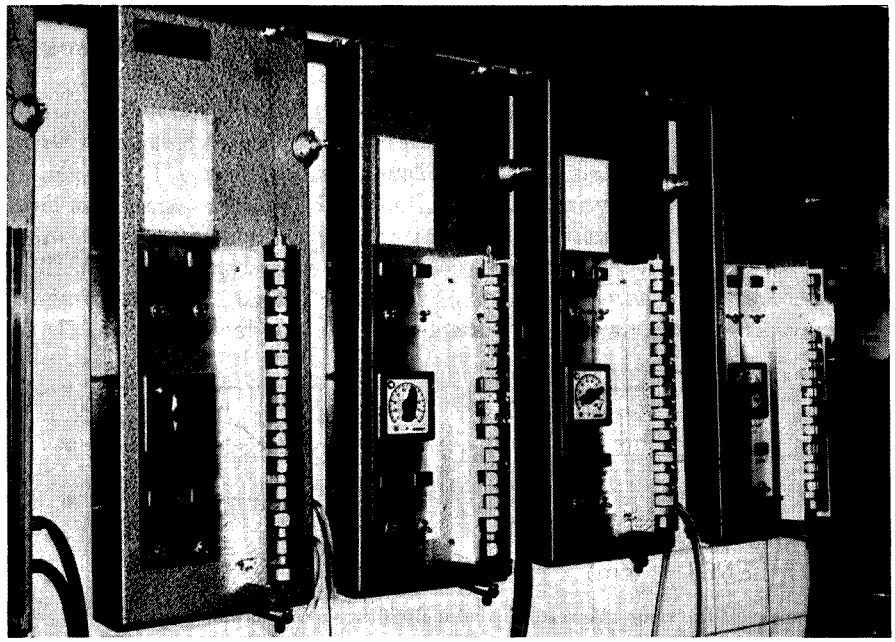

Fig. 1. Arrangement of multi-stage zone-melting apparatus (Fa. Desaga, Heidelberg).

Really pure substance has been obtained from this so-called zone-melting fractionation only when the melting-ranges of the fractions at the ends of the daughter ingots are very small.

In addition to the absolute purification of organic compounds, fractional zone melting can also serve to separate mixtures of compounds. This can be exemplified by the separation of an isomeric mixture of 3,4- and 3,5-dimethylphenol. In spite of the small difference in melting-points, it was assumed that a separation by zone melting would be more successful than by distillation since both substances are already considerably volatile far below their boiling points and thus the requisite reflux will be impeded by distillation. When the starting products were zone-purified, 3,4-dimethylphenol, m.p. 62.5° and 3,5-dimethylphenol, m.p. 65.5°, were obtained. It was

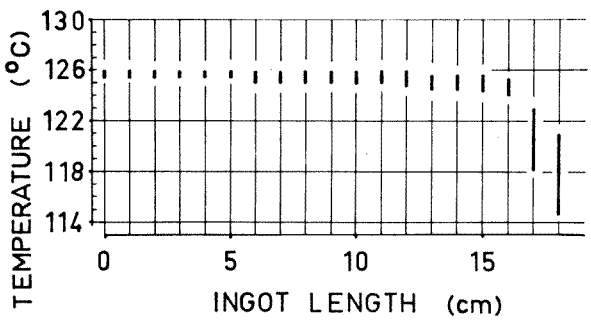

Fig. 2. Melting ranges determined from a zone melted ingot of 2,4-dinitrophenylhydrazone of acetone after 16 zone passes at a travelling speed of 5 mm/h.

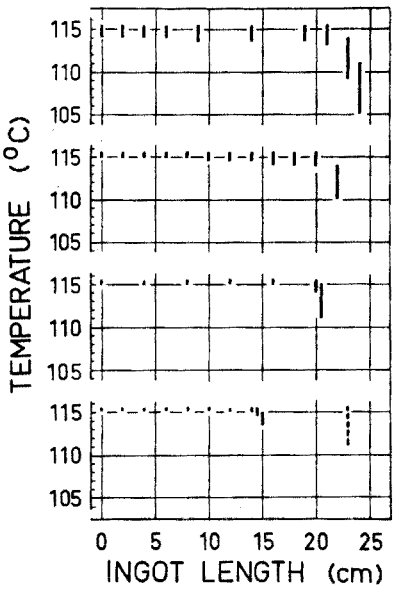

Fig. 3. Melting ranges of fractions taken from zone-melted ingots of acetanilide after 21 + 22 + 13 + 24 zone passes at a travelling speed of 2 mm/h.

concluded from a trial contact sample of the zone-purified samples that the phenols formed a eutectic mixture[4]. Whether complete or only partial immiscibility was present could only be determined with the help of a phase diagram. As is evident from the diagram (Fig. 4), the two phenols form in part mixed crystals and a eutectic. Thus, after a zone-melting process, the mixture of the two phenols should give pure material at the head, mixed crystals in the middle and a eutectic at the end of the zone-melted bar. The fractional zone melting should, as well as pure phenol, afford pure eutectic. It was demonstrated that this was in fact the case with a mixture of 88 mol% 3,5-dimethylphenol and 12 mol% 3,4-dimethylphenol; from 20.3 g of the mixture, 15.0 g of pure 3,5-dimethylphenol, *i.e.* 96% of the theoretical quantity, and

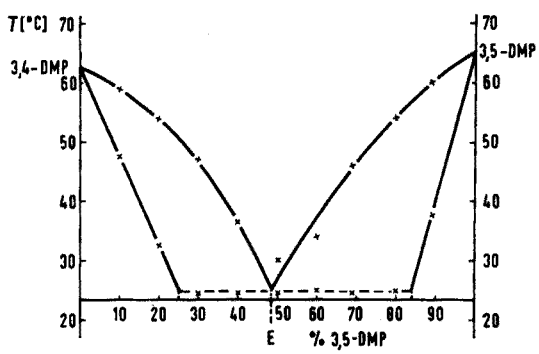

Fig. 4. Equilibrium diagram of binary mixtures of 3,4- and 3,5-dimethylphenol; eutectic mixture: 49% 3,5-dimethylphenol, eutectic temp. 24.5°.

4.8 g of impure eutectic were obtained. From transference and removal of substance for a melting-point determination, a loss of 0.5 g was incurred.

The two methylcrotonic acids can be separated by freezing out[5] or by fractional crystallization of the calcium salts[6]. The melting-point difference of the *cis*- and *trans*-isomers indicated that a good separation of the angelic acid from the tiglic acid should be possible. The zone-purified angelic acid (*cis*) melted at 45.2°; the zone-purified tiglic acid (*trans*) at 64.4°. Information about the system of the isomeric acids was again given by the contact preparation. At the contact zone of the two compounds, a eutectic was immediately formed whose congealing-point lay in the region of 15°. A mixture of 90.2% tiglic acid and 9.8% angelic acid was fractionated, by zone melting. The melting-point curve of two zone-melted bars and the distribution of the bars

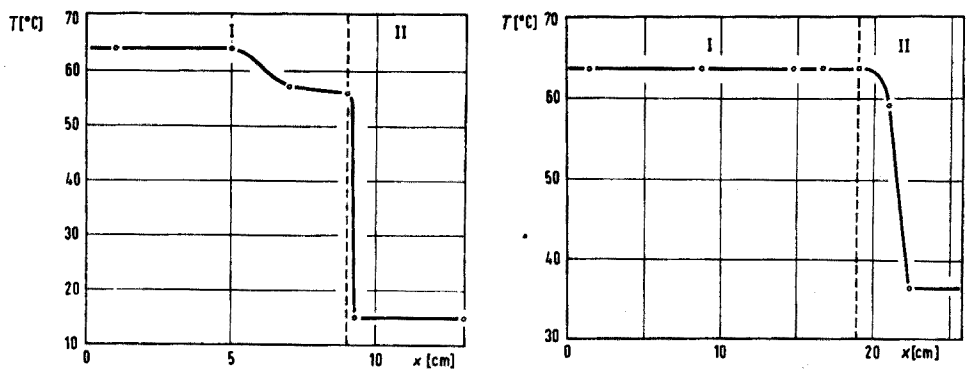

Fig. 5. Melting-point curve of an ingot of 90.2 mol% tiglic acid and 9.8 mol% angelic acid after 12 zone passes at a speed of 3 mm/h; length of melting zone 1–1.5 cm, ingot length 13 cm.

Fig. 6. Melting-point curve of an ingot formed from part I of the bar in Fig. 5 after 14 zone passes at a speed of 2 mm/h; length of melting zone 1 cm, ingot length 26 cm.

are shown in Figs. 5 and 6; it is clear that extensive separation was achieved. Portion A II contained 1.0 g of eutectic mixture and, on re-zoning melting portion A I, portion B I was found to contain 7.2 g of pure tiglic acid and portion B II to consist of unseparated material in an amount of only 0.6 g.

Micro zone melting

Using zone melting, traces of substances may also be isolated from solid solutions on a micro-preparative scale, and mixtures of substances, *e.g.* insect waxes and fatty alcohols, can even be separated. This procedure, which uses a moving liquid zone can also be used to fractionate low-melting substances. Even if only a few milligrams of a liquid, which solidifies in crystalline form, are available, it is possible to separate it, without loss, into pure and impure fractions, or to isolate traces of an unknown compound, using micro-zone melting techniques.

The main part of a micro-zone melting apparatus, the cooling and heating plates, is shown in Fig. 7. With this apparatus one can often isolate components from a few milligrams of a mixture without any loss. In the scope of our work, the genesis of petroleum and adipocere was of interest. Zone melting of adipocere gave the melting-point curve shown in Fig. 8; the highest melting fraction concentrated in the head

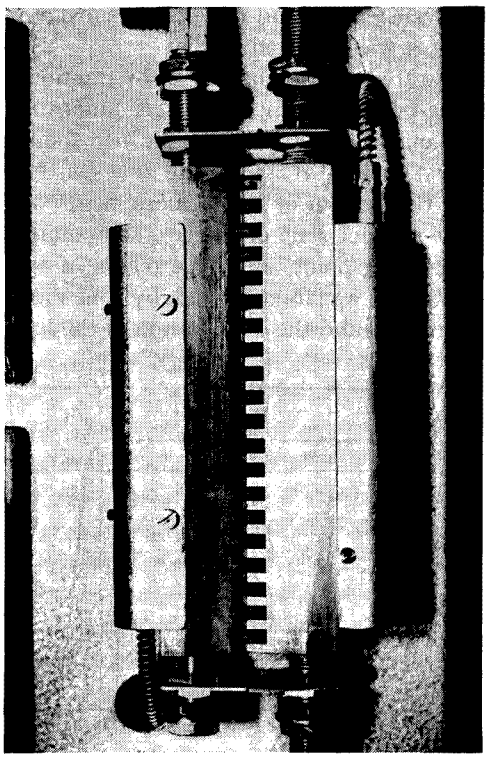

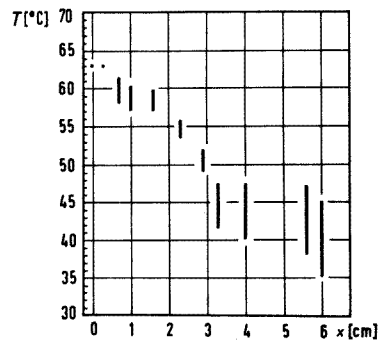

Fig. 7. Photograph of the heating and cooling plates of a micro-zone melting apparatus without a motor.

Fig. 8. Melting ranges determined from a zone-melted micro-ingot of adipocere after 45 zone passes at a travelling speed of 0.5 mm/h.

of the zone-melted bar was isolated and it was clearly shown, by a melting-point determination and infrared spectrum, that the substance was palmitic acid[7].

The importance of purifying "pure" compounds oneself before using them for analytical comparisons was proved from the melting-point curve of a zone-melted bar of "pure" palmitic acid. Only the front part (*ca.* 2 cm) of the zone-melted bar could be used for the determination of comparison data. The end of the bar (3–4.5 cm) was so strongly contaminated that a sample taken from it melted over a range of 49.5–58.5°.

It is also important, for the modern structural interpretation of natural products in small quantity using substance-sparing spectroscopic methods, that the research material should be available in its purest form. This can be exemplified by the case of mollugin[8]. This new crystalline component from *Galium mollugo* cannot be purified sufficiently by multiple recrystallizations for the NMR-spectrum to be satisfactorily interpreted. The spectrum taken of the sublimed compound showed bands, in the range of the aliphatic protons, which were not consistent with the empirical formula. The number of protons present, obtained by integration of the NMR-spectrum, of a zone-melted sample, *i.e.* 16.6 protons, agreed very well with the empirical formula, $C_{17}H_{16}O_4$. It was interesting that the compound was decomposed by

traces of oxygen, but remained stable in zone melting when it had previously been filled into the tube under nitrogen as shown schematically in Fig. 9.

It is also possible to isolate, by zone melting, the components from a few milligrams of a mixture of several natural products; this has been demonstrated by the clarification of the defence secretion of the water beetle[9]. Especially in the case of freshly caught water beetles, one finds glistening yellow bladders. Their content is not completely soluble in ethanol but gives a yellow solution and a colourless precipitate which was at first recognised only as a glycoprotein[10]. Chromatography on silica gel of the solution from one beetle gave about 3 mg of colourless crystals, which could be readily sublimed (m.p. 110°), and had a low molecular weight (115), but a very complex infra-red absorption spectrum, and were made up of a homogeneous substance.

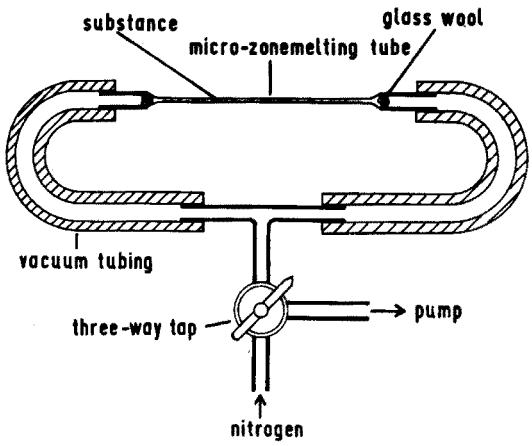

Fig. 9. Method of filling the micro-zone melting tube under nitrogen.

Since the mixture of substances could be separated by micropreparative zone melting, the bladder secretion of the great water beetle was subjected to micro-zone melting. After the passage of 20 zones through a micro-ingot, at first two fractions were obtained. A eutectic was separated from the low melting fraction by renewed zone melting. Figure 10 shows how chemical characterisation of the components of the secretion became possible by comprehensive analysis of the fractions obtained by zone melting. It was found that, as expected, benzoic acid was separated from the molten ingot faster than *p*-hydroxybenzaldehyde because of the higher melting-point of the former. The eutectic mixture which was not further separable by fractional melting, was subjected to thin-layer chromatography and yielded a substance, which after repeated zone melting, was pure enough to be identified as methyl *p*-hydroxybenzoate. All the species of the genus *Dytiscus* investigated by us defend themselves, presumably only against attack by micro-organisms, with a mixture of benzoic acid, methyl *p*-hydroxybenzoate, and *p*-hydroxybenzaldehyde. The first two compounds may also be used, according to German food laws, for stabilizing foodstuffs, especially canned fish.

Now an example is given from preparative organic chemistry where, in synthesis, one often obtains isomeric mixtures which are difficult to separate. This was

	Fraction		
	I	*II*	*E*
2,4-Dinitrophenyl-hydrazone	—	M.p. 279°	—
Ultraviolet absorption maxima (log ε)	in water 227 mμ (4,1) 273 mμ (3)	in ethanol 221 mμ (4.22) 285 mμ (4.35)	
Infrared absorption band for			
	γ_{CH} 708 cm^{-1}	—	—
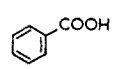	$\omega_{C=O}$ 1695 cm^{-1} Γ_{OH} 935 cm^{-1}	—	—
	—	γ_{CH} 832 cm^{-1}	
	—	ν_{OH} 3250 cm^{-1}	
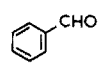	—	$\omega_{C=O}$ 1675 cm^{-1}	—
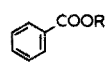	—	—	$\omega_{C=O}$ 1690 cm^{-1} ω_{C-O} 1292 cm^{-1}; 1119 cm^{-1}
Elemental analysis	$C_7H_6O_2$	$C_7H_6O_2$	—
Result		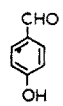	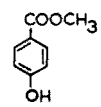

Fig. 10. Chemical characterization of the zone-melted fraction of the defensive substances of *Dytiscidae*.

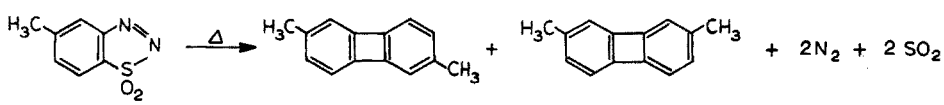

I II III

found by WITTIG AND VARGAS[11] in the thermolysis of 1,2,3-benzothiadiazol-1,1-dioxide (I) via the corresponding dehydrobenzene intermediate, which gave an isomeric mixture of 2,6- and 2,7-dimethylbiphenylene (II and III) with m.p. 93–128°. The components could not be isolated from the mixture either by column, thin-layer or gas-chromatography, or by fractional distillation, sublimation or complex-formation. However, it was possible by micro-zone melting to separate 2,6-dimethylbiphenylene (III) with m.p. 141–142°. This corroborated the hypothesis that the dehydro bond in the intermediate-formed dehydrobenzene of toluene is an extremely weakly polarized bond which is best depicted using mesomeric structures as suggested by WITTIG.

COLUMN CRYSTALLIZATION

The aim of the selective isolation of volatile compounds such as the defensive excreta from insects, is to secure samples of the substances that are as pure as possible in order to facilitate their identification. During the processes of selective isolation and generally afterwards as well, solvents are required for convenient manipulation of the minute amounts of materials being dealt with.

Because the amounts of the active principles available are so small, the solvents should also be extremely pure in order to avoid artefacts. However, the conventional methods of purification, such as distillation, are often unsatisfactory. Here too, better results are obtained by crystallization, especially when recourse may be taken to a genuine multi-stage or continuous countercurrent process analogous to fractional distillation. We have developed a suitable technique for fractional crystallization which we call *column crystallization.*

The column crystallizer consists basically of two concentric tubes with a metal spiral rotating in the annular space between them. Crystals are formed by removing heat from the top of the column. The crystals are scraped off and transported down the column by the action of the spiral. Re-melting of the crystals at the bottom of the

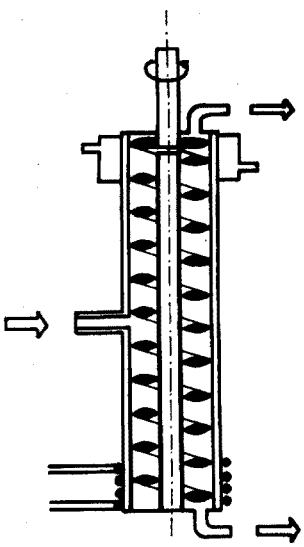

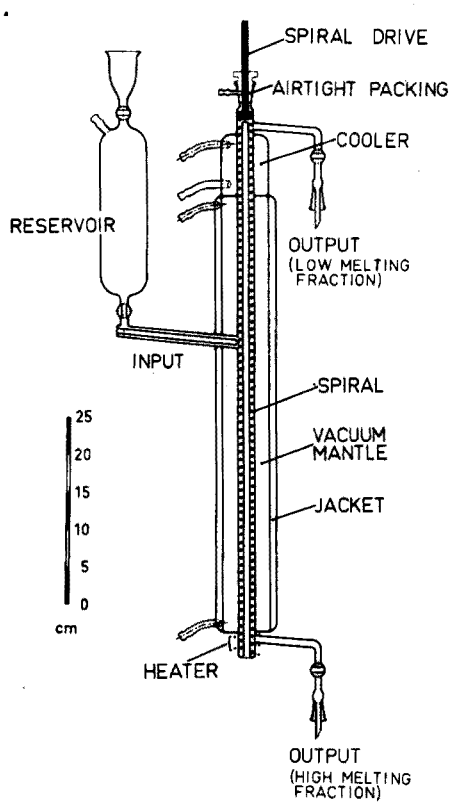

Fig. 11. Scheme of continuous-flow column crystallizer.

Fig. 12. Column crystallizer for liquids.

column provides liquid for counter-current contacting with the down-coming crystals. Significant purifications and separations are attained rapidly (Fig. 11).

In order to purify substances that are liquid at room temperature it was necessary to construct a special column crystallizer (Fig. 12) with a vacuum mantle placed around the tube between the heating and cooling zones in order to ensure adiabatic operation. If the column has to be run at very low temperatures, refrigerated fluid is circulated through a jacket surrounding the vacuum mantle. Relatively simple modifications of this basic apparatus permit one to produce large amounts of highly purified materials. Thus, a reservoir can be fitted at the middle of the column. Operation of the column crystallizer with continuous flow is in principle very simple.

Although the separation of isomers and other substances with low melting points was of interest, the primary purpose in constructing the columns was to obtain high-purity benzene. The absolutely pure solvent was necessary for extracting carbonaceous meteorites in order to extract any organic materials that they contained without introducing artefacts. The few grams of a meteorite must naturally be extracted with absolutely pure solvents that leave no residue on evaporation, in order to have the guarantee that any organic material found has really come from the meteorite.

The benzene used for these extractions was purified on a continuous basis. Starting with the purest benzene available, 200 ml of top-purity benzene were obtained after two runs through the column crystallizer. It is possible to produce about

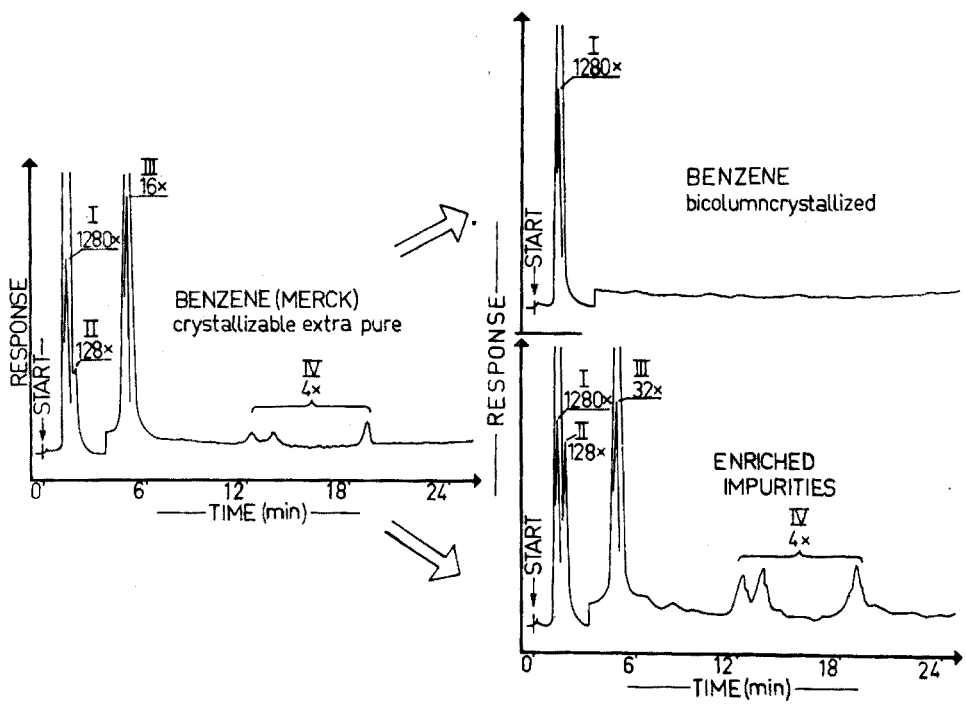

Fig. 13. Comparison of the gas chromatograms of purissimum-quality benzene and of benzene that has been column crystallized twice. (Aerograph 1520 (FID); column: 5% Apiezon L, 6'1/8"; temp. program 40–160° (4°/min). I, benzene; II, methylcyclopentane; III, thiophene; IV, aliphatic compounds.

30 ml of ultra-pure benzene per hour. This proves that gas chromatography is much less suitable than column crystallization for producing large amounts of best-quality solvents. However, gas chromatography is very suitable for making quality controls on the solvents; fig. 13 shows the gas chromatogram of purissimum-quality benzene compared with that of absolutely pure benzene and that of the concentrate of the impurities taken from the column crystallizer. It was only after no impurities could be detected in the top fraction following several runs through the column crystallizer, that the solvent was used for extracting the meteoritic material. It was found that there was then no residue after evaporation of the column-crystallized benzene. Spectra for "extra-pure", purissimum, gas-chromatographed and column-crystallized benzene over the range 4000–600 cm^{-1} showed very clearly that only column-crystallized benzene was free from aliphatic compounds; only in the residue spectrum

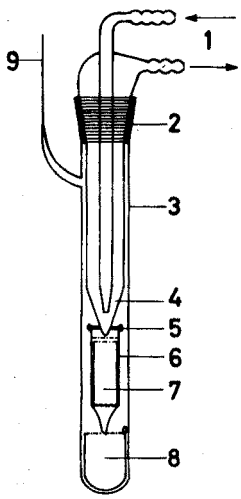

Fig. 14. Extracting apparatus for the meteorite samples. 1, cooling water; 2, teflon sleeve; 3, tube; 4, cold finger; 5, glass nail + hooks; 6, holder for filter; 7, sintered glass filter; 8, receiver; 9, capillary.

of the column-crystallized sample did no –CH– bands occur. In fact, the column-crystallized sample gave essentially the same spectrum as pure KBr. Benzene which was designated as "extra pure" was found to be completely unsuitable, and contained even larger amounts of impurities than the "purissimum" grade.

The extraction of the carbonaceous meteorite samples was carried out in an apparatus specially developed for this purpose (Fig. 14)[12]. Benzene, 6 ml in all, seeped continuously under reflux through the material contained in a beaker. It was extracted until the solvent, by a further extraction, no longer showed the presence of organic compounds. Despite the intensive extraction with little solvent and a relatively long extraction time—6 to 8 days—the solution of the required organic substances obtained may be too dilute for an exact chromatographic analysis. Usually such solutions are concentrated by evaporation of the solvent, but traces of the dissolved material may be lost by this method. A preliminary test should therefore always be carried out by attempting to freeze the solvent out, *i.e.* by normal freezing. Figure 15 shows

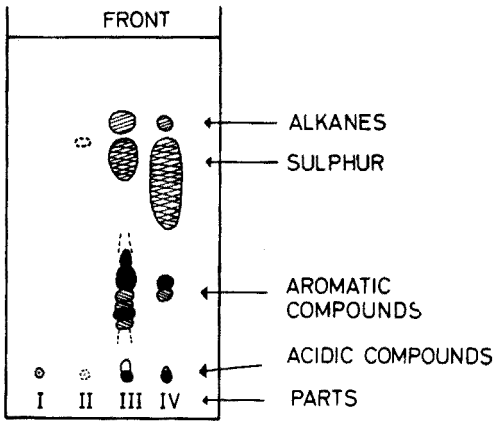

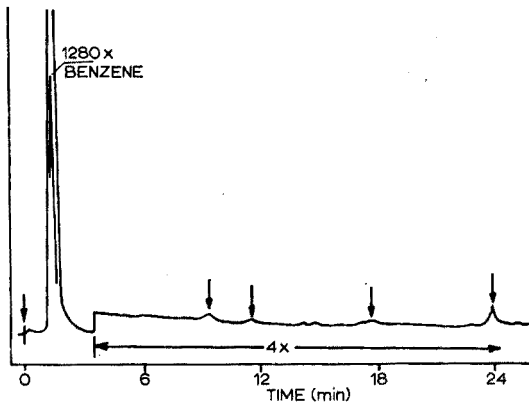

Fig. 15. Thin-layer chromatogram of the normal frozen extract from the Essebi meteorite. I, solvent; II, 2nd concentration; III, 1st concentration. Solvent: cyclohexane (traces of benzene); Silicagel G.

Fig. 16. Gas chromatogram of the benzene extract from the Essebi meteorite concentrated by normal freezing; Aerograph 1520 (FID); column: 5% Silicon SE 30; 12′, $^1/_8$″; temperature 150° (isothermal).

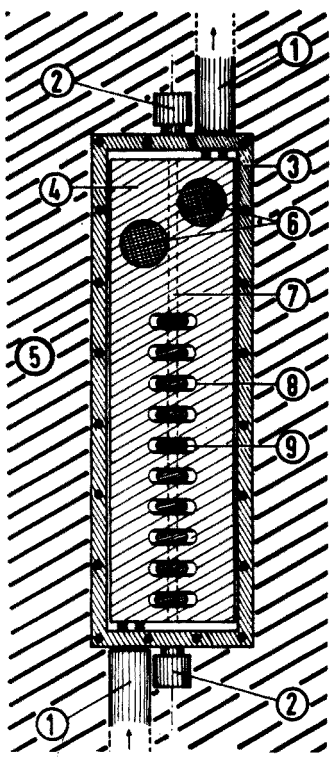

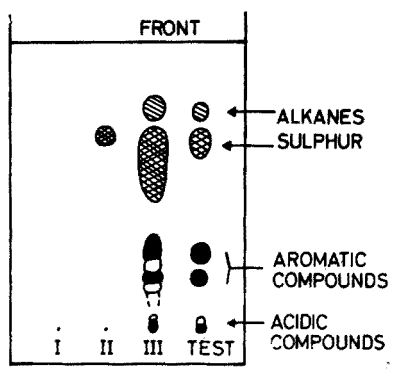

Fig. 17. Scheme of a micro ice zone-melting apparatus. 1, cooling liquid; 2, stopper; 3, insulating box; 4, cooling block; 5, insulation; 6, drying medium; 7, channel; 8, heater slot; 9, heating element.

Fig. 18. Thin-layer chromatogram of parts of normal frozen and zone-melted Essebi extract. Solvent: cyclohexane (traces of benzene); silica gel HF.

the enrichment effect on a thin-layer chromatogram in which the concentrated solution contains no more organic substances. Whereas in the unconcentrated extract scarcely any substances were identified by gas chromatography, after enrichment by normal freezing, more components could be found (Fig. 16), although the concentration was still too small to guarantee an incontestable analysis. The extract was therefore enriched by multi-stage zone melting, with the result that almost all the organic substances were concentrated in the last fractions to freeze. The micro ice zone-melting apparatus used for the enrichment of the meteorite extract is shown in Fig. 17. The zone-melted ingot finally obtained could be divided into pure benzene (part I), benzene with traces of sulphur (part II), organic material and sulphur (part III), and solid sulphur with traces of organic material (part IV). In the thin-layer chromatogram of this zone-melted concentrate, it was possible to perceive further aromatic spots (Fig. 18).

The eluate of the thin-layer chromatogram was also so rich, from a material standpoint, that it was possible to separate the alkanes by gas chromatography. It was also possible to identify the aromatic compounds by mass spectrometry after the removal of the aliphatic elements by chromatography.

SUMMARY

The techniques of normal freezing, zone melting and column crystallization are discussed; special attention is given to micro zone melting. The preparation of absolutely pure benzene by column crystallization is shown to be possible. Many examples of the utilization of these techniques are given, including work on isomeric compounds, plant and animal products and meteorite samples.

REFERENCES

1 W. G. PFANN, *Zone melting*, 2nd. ed., Wiley, New York, London, Sydney, 1966.
2 H. SCHILDKNECHT, *Zonenschmelzen*, Verlag Chemie, Weinheim/Bergstr., 1964; *Zone Melting*, Academic Press, New York and London, 1966.
3 H. SCHILDKNECHT AND H. BENONI, *Z. Naturforsch.*, 18b (1963) 45.
4 U. HOPF, *Dissertation*, University Erlangen, 1961.
5 F. BEILSTEIN AND E. WIEGAND, *Ber.*, 17 (1884) 2261.
6 R. FITTIG, *Ann.*, 283 (1894) 105.
7 H. SCHILDKNECHT AND S. SCHIMPEL, unpublished.
8 V. SCHEIDEL, *Diplomarbeit*, University Heidelberg, 1966.
9 H. SCHILDKNECHT AND K. H. WEIS, *Z. Naturforsch.*, 17b (1962) 448.
10 R. BÜHNER, *Diplomarbeit*, University Heidelberg, 1967.
11 G. E. VARGAS-NUÑEZ, *Dissertation*, University Heidelberg, 1963.
12 R. KELLER, *Dissertation*, University Heidelberg, 1967.

Analytica Chimica Acta
Elsevier Publishing Company, Amsterdam
Printed in the Netherlands.

EFFECT OF INTERACTION OF MACROMOLECULES IN GEL PERMEATION, ELECTROPHORESIS AND ULTRACENTRIFUGATION

G. A. GILBERT
Department of Chemistry, The University, Birmingham 15 (Great Britain)

(Received November 1st, 1966)

All the commonly used molecular transport methods (electrophoresis, sedimentation, chromatography or gel permeation, *etc.*) designed to resolve different types of macromolecule in solution tend to fail when the molecules undergo reversible interaction with each other. An obvious reason for studying the effect of interaction is to circumvent this inconvenience, but quite often further information about the interaction itself, rather than ways of eliminating its effect, becomes the aim of the experimenter. Of course, as far as biology is concerned, the central role of specific interaction between discrete components explains why this should be so. In practice both aspects, the elimination of the effect of interaction, and the evaluation of the stoichiometry and energetics underlying the interaction, turn out to be indispensable parts of a complete study.

The first step in any study, and often an inadvertent step, is the recognition of interaction. In a recent review[1] NICHOL, BETHUNE, KEGELES AND HESS describe in detail the various ways in which interaction is manifested in transport experiments, and therefore it will only be necessary to summarise them here. Foremost is the anomalous dependence on concentration of the sedimentation velocity or elution volume of a constituent. The extent of reversible reaction to form complexes or aggregates increases with the concentration of a constituent. Because of this, the constituent sedimentation velocity tends to increase, and the constituent elution volume to decrease with increase of concentration. Experience soon enables one to appreciate these indications of interaction even when they are opposed by changes in the opposite direction due to the various hydrodynamic effects, and geometrical and charge effects, which are present for all solutes whether interacting directly with each other or not.

Next in importance is boundary shape, displayed most distinctly in schlieren or derivative patterns. Any pattern which is not easily explicable in terms of independent components must lead to the suspicion of interaction, and this is especially so when the shape of the pattern changes in an unusual way with change of concentration.

Thirdly, interaction can sometimes be detected by a comparison of leading and trailing boundaries, since these may be non-enantiographic if reaction boundaries are present (LONGSWORTH[2]). Qualitatively, this is explained by the dissymmetry of the events taking place in the two boundaries. In one boundary, the relative motion of a complex may be towards solution in which it is stable, and in the other towards solvent in which it decomposes. Electrophoresis and gel permeation have an advantage over sedimentation in this respect by providing two boundaries for observation.

Given that interaction has been detected in one of these ways, how should it be studied further? The problem is a difficult one, and presumably each case will have to be treated individually until there is a much wider range of experience on which to draw than at present.

As an illustration of a useful method of approach, the investigation by gel permeation of the simplest type of interaction, the reversible formation of dimer from monomer, may be considered. In experiments of this kind it is essential to make sure that the leading and trailing boundaries displayed on the elution record are properly separated by a plateau region in which the concentration of solute is constant[3]. This is achieved by applying a broad band of solute to the gel column. If a narrow zone is used, the boundaries merge and progressive dilution occurs as the solute passes down the column, with a consequent change in extent of reaction and a wholly unnecessary complication of the situation.

The example given is not based on an actual experiment, but on data derived from a model; in other words on a simulated experiment. This device is proving very useful in this field for testing in advance whether a proposed experimental study could achieve its aim, which is here the determination of the parameters of a reversibly reacting system. For this purpose a model is set up with given parameters, the numerical consequences of the model are then calculated, and from these generated data, pseudo-experimental data are obtained by adding random errors appropriate to the experimental means available. These data are then analyzed by a least-squares procedure[4] in the way that actual data would be to see how accurately the original parameters can be recovered. If they cannot be found within reasonable limits of error, neither could they be from an actual experiment, and it would be a waste of time to carry out the experiment without modification. Pointers to the direction in which it is desirable to modify an experiment can also be obtained by this method. For instance the effect on the recovered values of the parameters of increasing the range or number of the data can be tested, or of refining the experiment to give greater reproducibility.

The example below illustrates the effect of increasing the concentration range over which measurements are made, and is relevant to investigations of a kind now being carried out in many laboratories.

Suppose that a monomer–dimer system is being studied by gel permeation, and that constituent elution volumes are being measured as a function of solute concentration. It is reasonable to assume that errors in concentration can be ignored in comparison with errors in elution volume, although of course this need not always be the case. It is also reasonable to assume a standard error of 0.1 ml in elution volume, which is not difficult to achieve in practice.

Elution volumes depend slightly upon the concentration of solute, even when chemical interaction between the solute molecules is absent[3]. As in the case of sedimentation, where an analogous dependence occurs, there is not much known quantitatively about the detailed mechanism of this dependence. It introduces a small correction factor, and will be allowed for in the model by assuming that the elution volume, V_i, of a dissolved molecular species, i, varies with total concentration, w, of solute in accordance with the equation

$$V_i = (V_i)_0 (1 - gw) \qquad (1)$$

where $(V_i)_0$ is the limiting value of the species elution volume at zero concentration

of solute. The value of g will be assumed to be the same for the monomer and dimer species, giving for the respective elution volumes of monomer and dimer the equations

$$V_1 = (V_1)_0 \, (1-gw) \tag{2}$$

and

$$V_2 = (V_2)_0 \, (1-gw) \tag{3}$$

If w_1 and w_2 are the concentrations (g/dl) of the monomer and dimer respectively, then

$$w = w_1 + w_2 \tag{4}$$

Also, if the law of mass action is assumed to apply, then

$$w_2 = L_{1,2} w_1^2 \tag{5}$$

where $L_{1,2}$ is the association constant for the reaction, expressed in dl/g. The constituent elution volume, $\bar{V}$, is found from the equation[5]

$$\bar{V} = (1/w) \, (V_1 w_1 + V_2 w_2) \tag{6}$$

i.e.

$$\bar{V} = \{(1-gw)/w\} \, (w_1 \, (V_1)_0 + L_{1,2} w_1^2 \, (V_2)_0) \tag{7}$$

where, by eqns. (4) and (5), w_1 is the positive root of the equation

$$L_{1,2} w_1^2 + w_1 - w = 0 \tag{8}$$

After numerical values for $L_{1,2}$, $(V_1)_0$, $(V_2)_0$ and g have been chosen, a curve can be constructed for $\bar{V}$ as a function of w using eqns. (7) and (8). The curve in Fig. 1 has been obtained in this way for $L_{1,2} = 40$ dl/g, $(V_1)_0 = 27$ ml, $(V_2)_0 = 23$ ml and $g = -0.02$ dl/g.

The question to be posed now is whether these parameters could be found by

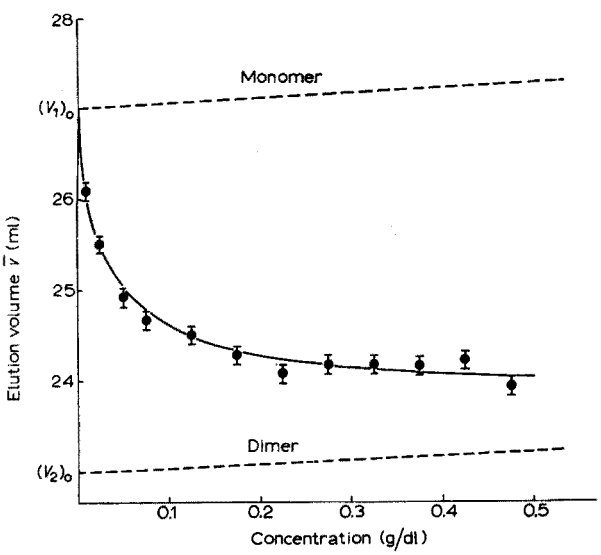

Fig. 1. Gel permeation of reversibly reacting systems. (—), theoretical curve for monomer–dimer system; (- - - -), elution volume of individual species; (⊕), simulated experimental points with standard deviation from curve of 0.1 ml.

analysing experimentally observed values of $\bar{V}$ at various values of w. To simulate an experiment random errors (taken from a table of random numbers with mean value equal to zero and standard deviation about zero of 0.1) have been added to $\bar{V}$ at twelve values of w ranging from 0.01 to 0.475 g/dl as shown in Fig. 1.

A published computer program[4] has been adapted to find the values of the parameters $L_{1,2}$, $(V_1)_0$ and $(V_2)_0$ which give the best fit, judged by the minimum value for the squares of the residuals of the curve of $\bar{V}$ *vs.* w to these points. With g taken as -0.02 dl/g, the values obtained for the parameters were $L_{1,2} = 74 \pm 38$ dl/g, $(V_1)_0 = 27.6 \pm 0.6$ ml and $(V_2)_0 = 23.2 \pm 0.1$ ml respectively. It can be seen that even though g has been fixed at its correct value, which would not be possible in practice, because g would also have to be found, the experiment has failed to provide a useful value of $L_{1,2}$. The points as plotted in Fig. 1 would give an experimenter little hint without such an analysis that an interaction constant could not be evaluated without more data or better precision.

The lowest concentration in the set of twelve points was 0.01 g/dl, and the highest 0.475 g/dl. By reducing the lowest concentration to 0.005 g/dl, raising the highest to 1 g/dl and increasing the number of points to nineteen in all, still with a standard error of 0.1 ml in elution volume, the situation becomes completely changed. It is now possible to find g as well as the other three parameters, and a least-squares fit gives $L_{1,2} = 32.7 \pm 10.5$ dl/g, $(V_1)_0 = 26.8 \pm 0.19$ ml, $(V_2)_0 = 22.9 \pm 0.23$ ml and $g = -0.022 \pm 0.009$ dl/g.

The residual uncertainty in $L_{1,2}$, even for this very simple system, underlines the need to adopt differential methods when closely related systems are to be compared. Suitable experimental techniques have been described for sedimentation[6] and gel permeation[7] methods.

I thank my wife (LILO M. GILBERT) for collaborating in the preparation of this paper and for the computer programs used for the calculations. The approach described owes much to discussions with Dr. S. P. SPRAGG and Dr. RODES TRAUTMAN who suggested the use of the method of NELDER AND MEAD[4].

SUMMARY

The recognition of interaction in solution, when macromolecules are studied by transport methods, is usefully followed by model building and the comparison of model and experiments. An example is given to show how models can be used to improve the effectiveness of experiments.

REFERENCES

1 L. W. NICHOL, J. L. BETHUNE, G. KEGELES AND E. L. HESS, in H. NEURATH (ed.), *The Proteins*, 2nd ed., Academic Press, New York, 1964, p. 305.
2 L. G. LONGSWORTH, in M. BIER (ed.), *Electrophoresis: Theory, Methods and Applications*, Academic Press, New York, 1959, p. 91.
3 D. J. WINZOR AND H. A. SCHERAGA, *Biochemistry*, 2 (1963) 1263.
4 J. A. NELDER AND R. MEAD, *Computer J.*, 7 (1965) 308.
5 G. K. ACKERS AND T. E. THOMPSON, *Proc. Nat. Acad. Sci. U.S.*, 53 (1965) 342.
6 H. K. SCHACHMAN, *Ultracentrifugation in Biochemistry*, Academic Press, New York, 1959.
7 G. A. GILBERT, *Nature*, 212 (1966) 296.

Analytica Chimica Acta
Elsevier Publishing Company, Amsterdam
Printed in the Netherlands.

A FAST METHOD OF ZONE MELTING AS AN AID IN ANALYTICAL CHEMISTRY

N. J. G. BOLLEN, M. J. VAN ESSEN AND W. M. SMIT
Institute for Physical Chemistry, TNO, Utrecht (The Netherlands)

(Received November 1st, 1966)

Zone melting could be a powerful aid in analytical chemistry; it provides a means of preparing primary standards and of concentrating contaminants. Moreover, the (substance) distribution along a zone-melted column may give information concerning the components of the system dealt with. Zone melting operates without foreign chemicals or solvents, and it requires no unacceptable amounts of substance, no special skill and only a small amount of personal attendance.

In spite of these advantages zone melting has found only restricted application in analytical chemistry. There seems to be a tendency to prefer other methods to zone melting, unless other methods appear hopeless. This attitude is largely caused by the fact that zone melting of organic substances at zone travel rates down to 3 cm/h appeared to be almost completely ineffective. Even at somewhat lower zone travel rates, bad separations resulted and the relation between the actual and the theoretical distribution coefficient was severely obscured. As a consequence, effective zone melting of organic substances was an extremely time-consuming process, which was therefore already unattractive for analytical purposes. Moreover, many organic substances do not withstand very prolonged heating.

The causes of these drawbacks are relatively simple. During the liquid–solid transition some impurity must in most cases be expelled from the freezing part of the substance, and this amount will initially collect at the solid–liquid interface, before becoming dispersed throughout the bulk of the remaining liquid phase by means of diffusion and convection. If the speed of zoning is too high, the solid rejects

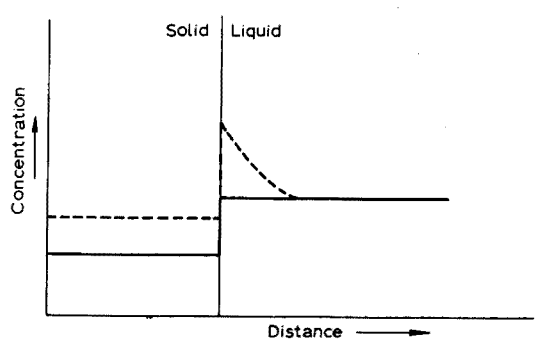

Fig. 1. Distribution of impurity near solid–liquid interface. (—) complete mixing; (--) restricted mixing.

impurities more rapidly than these can diffuse into the bulk of the liquid. Now the composition of the solid is determined by the composition of the liquid in the *boundary* layer. As soon as the concentration of the impurity in the boundary layer is higher than that in the bulk of the liquid, the amount of impurity contained in the solid to be formed will increase (see Fig. 1). As proven by experiments this increase may soon become so large that no purification is obtained at all. Thus the efficiency of a zone-melting operation depends on the effectiveness of mass transfer from the solid–liquid interface into the bulk of the zone.

The various mechanisms thus far devised for promoting this mass transfer appear to have had little effect on the stagnant boundary layer.

A FAST METHOD OF ZONE MELTING

In the Institute for Physical Chemistry TNO, an apparatus has been developed which is especially intended to reduce the effect of the stationary layer. The substance to be treated is contained in a tube and this tube is subjected to a high-speed rotation which is periodically reversed. In this way periodically shifting shearing forces are exerted at the boundary layer, resulting in an intensive mixing of the liquid by turbulence.

Another feature of this apparatus is the direction of zone travel. Zone-melting apparatus with vertical containers, usually operate with zones moving downwards. This direction of movement has several advantages; in the first place, zones are created at the open end of the container, so that the expansion of the melting substance does not lead to cracking of the tube. Secondly, the freezing occurs at the upper interface of the zone. At this upper interface the thickness of the stationary boundary layer is supposed to be somewhat reduced by thermal convection. Finally, recontamination of purified material due to seeping back of liquid is impossible when the zones move downwards. However, the downward movement of zones also includes a serious drawback. It is hardly possible to prevent the occurrence of voids or gas bubbles near the upper interface of the zone. When crystallization occurs at the upper interface, the voids or gas bubbles cause irregular crystallization which hampers the purification. Large voids or bubbles may even stop the purification by blocking the tube.

Because of the seriousness of this drawback, an attempt was made to design an apparatus with zones moving upwards. Zones moving from the bottom to the top guarantee a good contact of liquid and solid at the freezing interface. It was realized that the thermal convection at the freezing interface had to be sacrificed, but this loss could be more than compensated by the method of stirring applied. The good contact between solid and liquid combined with the fast flow of liquid along the interface satisfies the essential conditions for obtaining a smooth interface which favors the purification. Of course, the upward zone movement necessitates special precautions for preventing the breakage of containers during the formation of the zone; therefore, the lower side of the tube is closed by a PTFE stopper inserted into the tube. This stopper has a fixed position with respect to the apparatus. The expansion of the substance during the formation of a zone results in a temporary movement of the tube and its contents in an upward direction.

In the apparatus to be described no extremely careful control of factors such as ambient temperature, heater power and heater travel rate is necessary. Since the

zone travel rates are of the order of 60 cm/h a temporary increase in the crystallization speed, *e.g.* by 1 cm/h will not lead to entrapment of impurities. A special arrangement for preventing the breakage of containers due to a small increase in the amount of melted substance in a zone is described below.

In order to meet the different and somewhat contradictory demands of analytical chemists, it was deemed necessary to design 2 different apparatus: one to deal with 50–100 ml amounts of substance and another for quantities of about 4 ml. The 4-ml, or midget, apparatus is intended for the separation of multicomponent mixtures before analysis. Its dimensions were chosen so that the fractions obtained after the separation are large enough for further analysis, *e.g.* by means of the melting-curve method[1].

The 100-ml apparatus is primarily intended for preparative purposes (*e.g.* the preparation of high-purity standard substances), and possibly for the preconcentration of minor amounts of impurities contained in a large sample. Further concentration may then be done in the midget apparatus. Both apparatus are intended for substances with melting points between 50 and 250°; it is possible to extend this temperature range, especially to lower temperatures. Whereaes both apparatus operate on the same principle only the midget apparatus will be described.

EXPERIMENTAL

Description of the apparatus

A schematic diagram of the apparatus is shown in Fig. 2 and a photograph in Fig. 3. The container is a pyrex glass tube (4) placed vertically and closed at its lower end by a PTFE stopper (10) inserted to about 6 cm into the tube. This container is filled to a height of about 20 cm. The shaft (1) of a reversible electric motor protrudes into the lower end of the tube; the PTFE stopper rests on this shaft. The tube is connected to the shaft by a coupling device (2), permitting a simultaneous upward movement of the coupling device and the rotating tube. Thus the force on the stopper, due to expansion of the substance on melting, results in a small upward displacement of the tube. The maximum speed of rotation of the tube is 125 rev./sec and the direction of rotation is reversed twice per second. The time required for the reversal from 125 rev./sec in one direction to 125 rev./sec in the other direction is about 0.25 sec (see Fig. 4).

Five resistance heaters (5, 6, 7, 8 and 9) are placed around the tube at 4-cm intervals. Between the heaters the tube is cooled by compressed air streaming via a duct (3) through sets of small orifices, further indicated as coolers. Heaters and coolers gradually move 4 cm upwards and then fall rapidly, thus transferring each heater to the next zone; the lower heater starts forming a new zone. This reciprocating motion is repeated. The power of the 4 upper heaters (5, 6, 7 and 8) is somewhat less than that of the lower heater (9). Thus the amount of melted substance in a zone formed by the lower heater decreases when the zone is taken over by the next heater; this results in the formation of a void at the upper interface. This void does not hamper the separation but acts as a buffer capable of accounting for small changes in zone length due to changes in heat transfer or heater travel rate.

Each formation of a zone leads to a small upward displacement of the tube with respect to the stopper. As will be obvious this sets a limit to the total number

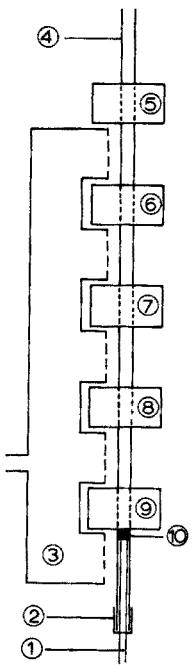

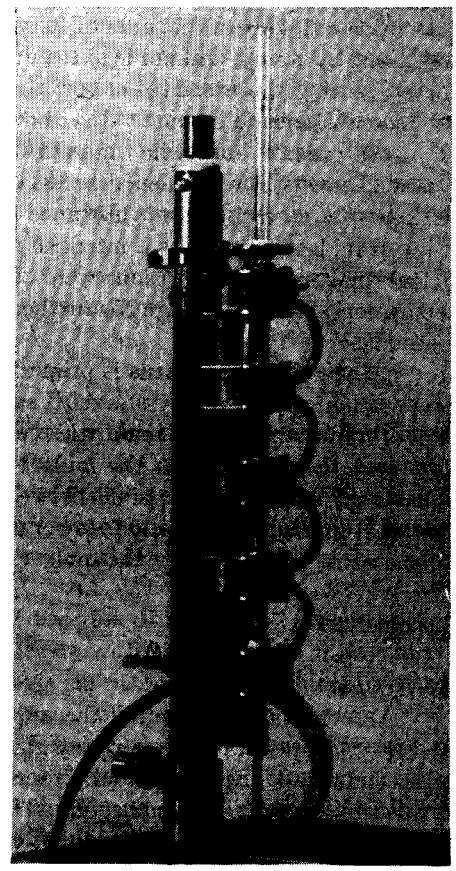

Fig. 2. F.C.I. zone-melting apparatus. Patents pending.

Fig. 3. Photograph of midget apparatus for zone melting (upper part).

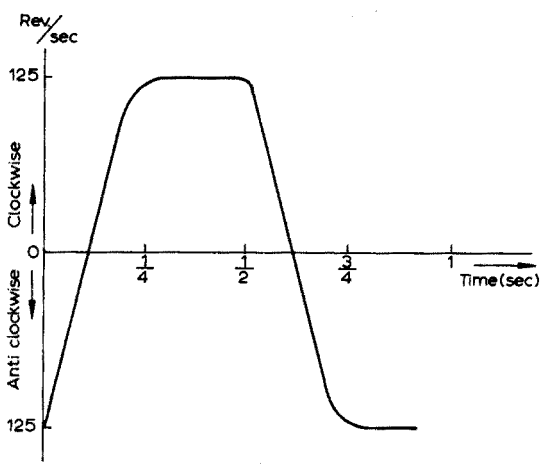

Fig. 4. Speed and direction of rotation of the container as a function of time.

of zones that can pass through the tube. The maximal number of zones is determined by the length of the tube under the stopper, the zone length and the percentage of volume increase on melting. As the zone length is about 1/10 of the length of the charge the maximal number of passes amounts to about 30 in most cases.

The efficiency of a zone refiner can be increased if the zone-melting operation is preceded by normal freezing. Therefore an automatic device enabling the contents of the zone-melting tube to freeze from the lower end is incorporated in the apparatus. The zone-melting operation starts immediately after normal freezing; the first zone follows 4 cm behind the freezing interface.

Applications

The following examples demonstrate the rapid and good operation of the apparatus.

(*1*) The system bismuth–antimony forms solid solutions. The theoretical distribution coefficient as determined from the phase diagram amounts to 2.1. A mixture of bismuth and antimony was submitted to normal freezing. The container was rotated as described above. The speed of crystallization was 80 cm/h. The effective distribution coefficient derived from the results appeared to be 1.9.

(*2*) The system naphthalene–sudan red is a simple eutectic system; 5g of naphthalene containing 0.01% of the dye was treated in the midget apparatus. The zone travel rate was 80 cm/h. It took 15 min to remove the dye completely from 80% of the sample.

(*3*) The system biphenyl–phenanthrene forms solid solutions. The theoretical distribution coefficient is 0.27. Biphenyl containing 1 mol% phenanthrene was submitted to normal freezing followed by zone melting. The rate of zone travel was 60 cm/h. The distribution coefficient after the treatment was determined from melting curves. The effective distribution coefficient derived from these results appeared to be 0.30!

DISCUSSION AND CONCLUSIONS

On the strength of the results obtained with the system naphthalene–sudan red, it may be concluded that even at zone travel rates of 60–80 cm/h the entrapment of impurities is prevented and the effect of seeping back which is inherent in zones moving upward is compensated to such an extent that this effect becomes almost negligible.

The small differences between the effective and theoretical distribution coefficients found in the two examples of mixed crystals show clearly that the mass transfer in the boundary layer, which is essential for obtaining good separations, has been improved to a large and satisfactory extent. The time required for a normal freezing operation followed by the passage of 20 zones has been reduced from several days to about 1.5 h for a charge of 4 ml of *organic* substance and from weeks to about 6 h for a charge of 100 ml in the 100-ml apparatus.

Cracking of containers due to changes in heat transfer is completely overcome.

SUMMARY

A new zone-melting apparatus is described which allows relatively high zone

speeds up to 100 cm/h. The time required for effective separations is only a few hours so that the apparatus can be used for analytical purposes. The difference between the theoretical and actual distribution coefficients obtained is small; the distribution coefficients of unknown substances in mixtures can thus be derived from the result of zone melting, which offers a means of identification. The apparatus is fully automated and normal freezing is incorporated as a first step. A means of preventing the breakage of the glass tube containers is described. The principles of operation and possible applications are discussed.

REFERENCE

1 H. F. VAN WIJK, P. J. VAN DER MOST AND W. M. SMIT, *Anal. Chim. Acta*, 38 (1967) 285.

Analytica Chimica Acta
Elsevier Publishing Company, Amsterdam
Printed in the Netherlands.

ZONE MELTING AS AN AID TO IMPURITY DETERMINATION BY THERMAL ANALYSIS

H. F. VAN WIJK, P. F. J. VAN DER MOST AND W. M. SMIT
Institute for Physical Chemistry, TNO, Utrecht (The Netherlands)

(Received November 1st, 1966)

When the temperature of a substance is plotted as a function of the amount of heat supplied to it, the resulting curve is indicated as a temperature–heat content curve. Such a curve comprising the melting range of the substance is called the melting curve. Almost every impurity soluble in the melt will influence the shape of the melting curve, and, in fact, the melting curve offers a very general sensitive and non-destructive criterion for purity. However, when attempts are made to state the data on purity in exact figures, difficulties are encountered. In other words, the quantitative interpretation of the melting curve so that the purity of a substance, or rather its impurity content, can be calculated, constitutes a problem that has not yet been completely solved.

In the interpretation of melting curves two categories of impurities must be distinguished, *viz.* solid insoluble impurities (impurities forming no mixed crystals with the main component), and solid soluble impurities (forming mixed crystals). When a substance contains only solid insoluble impurities, the determination of the melting curve and its quantitative interpretation presents no essential difficulties[1–5]. Unfortunately, this is of restricted importance in dealing with "pure" substances. Very often substances are purified by means of crystallization or extraction. Both processes are very effective in removing solid insoluble impurities but are far less effective on solid soluble impurities and may even enrich the solid soluble impurities in the desired substance. Thus purified substances will often contain solid soluble impurities.

In the past distinct progress has been made in the determination of these impurities by means of melting curves. It appears possible to solve the problem completely when only one solid soluble contaminant is present[6]. When more than one solid soluble contaminant is present, it is possible to show that the concentration does not exceed a distinct value.

In the present paper, further progress in the development of impurity determination by the melting curve is reported.

When a sample is to be investigated, it must first be ascertained whether solid soluble contaminants are present or only solid insoluble ones. The shape of the melting curve of the sample may already be conclusive in some cases. However, a better test on mixed crystals is possible (see below). When this test shows the presence of mixed crystals and the system appears to be a multicomponent system, one melting curve will seldom give sufficient information for a complete analysis[7].

It will be shown in this paper that the application of zone melting combined

with the measurement of several melting curves will often make it possible to obtain a complete analysis of all impurities with distribution coefficients different from 1. In the past, the application of zone melting for analytical purposes has been seriously hampered because zone melting was such a very time-consuming process. However, this difficulty has been overcome with the construction of a new apparatus which permits the passage of over 20 zones through a sample of 4 g within an hour[8].

Test on mixed crystals

No mixed crystals are present when a slowly frozen sample gives a melting curve obeying the equation of WHITE[1]:

$$Y^{-1}X = -\frac{Q}{RT_s^2}\Delta T \qquad (1)$$

where Y is the fraction that has melted; X the total amount of the contaminants in mol fraction; Q the heat of melting in cal/mol; T_s the melting point of the substance in °K; ΔT the depression in °K; and R the gas constant in cal/degree·mol. Uncertainties in the value of Y may obscure eqn. (1). Thus, when a melting curve is not in accordance with the equation of White the conclusion that mixed crystals must be present may be incorrect.

A better test on mixed crystals is based on the differences between the melting curves of a slowly and a quickly frozen sample. In two previous papers[6,9], it has been shown that if mixed crystals occur a slow solidification of a sample results in an inhomogeneous distribution of the impurities analogous to the distribution after normal freezing. A quick solidification results in a more homogeneous distribution of the impurities. As a consequence of these differences a slowly frozen sample containing mixed crystals will melt at a lower temperature level than the quickly frozen sample, particularly at small values of Y. Moreover, the temperature differences along the melting curve of a slowly frozen sample are larger than those of a quickly frozen sample. When no mixed crystals occur the melting curves of the quickly and the slowly frozen sample will be identical.

The application of this very reliable test on mixed crystals requires certain precautions. The quick-freezing procedure often results in very imperfect crystals and sometimes in metastable modifications. In order to obtain perfect and stable crystals an annealing procedure is advisable. After solidification the sample must be kept at a temperature 3–5° below the melting range of the substance for at least 1 h.

Operations like slow solidification and annealing can be easily performed when the melting curves are determined by the thin film method[5,10,11].

THE INTERPRETATION OF MELTING CURVES OF A SAMPLE CONTAINING n CONTAMINANTS

The multicomponent system

When n contaminants are present in a sample and the distribution coefficients k_n of these contaminants can be considered as constants, the general T,Y relation for the melting curve of a slowly frozen sample is[7]:

$$\sum_1^n (1 - k_n) Y^{k_n - 1} X_n = \frac{Q}{RT_s^2}(T_s - T) = -\frac{Q}{RT_s^2}\sum_1^n \Delta T_n \qquad (2)$$

where n is the number of contaminants; k_n the distribution coefficient of the contaminant n; Y the fraction that has melted; X_n the mol fraction of contaminant n; T the temperature in °K when Y has melted; and ΔT_n the depression of the temperature caused by contaminant n.

When nothing is known about the sample, the values of X_n, k_n, T_s and n are unknown. From one melting curve a number of relations between T and Y can be obtained but in general it is impossible to compute all unknown quantities accurately from one melting curve.

The problem may be simplified somewhat by substituting a distinct set of mean k_n-values covering the whole range of possible distribution coefficients. However, this approximation appears to be insufficient for adequate interpretation of a melting curve. The number of unknown quantities remains too large and moreover several combinations of X_n and k_n may exist giving approximately (within the accuracy of the measurement of Y and T) the same function of T. Only if the range of possible k_n-values is very restricted, can melting curves be interpreted accurately without making use of a computer.

It is therefore highly desirable to reduce the number of unknown quantities to a low figure. This can be done by subjecting the sample to zone melting. Before this subject is dealt with, some typical cases will be discussed.

The melting curve of a sample with apparently only one contaminant

When n can be reduced to 1 or when the sum of the depressions caused by all components but one is known, eqn. (2) can be reduced to:

$$(1 - k_1) Y^{k_1 - 1} X_1 = - \frac{Q}{R T_s^2} \Delta T_1$$

The value of k_1 and X_1 can be easily obtained by plotting $\log Y$ against $\log|\Delta T|$. The slope of the straight line obtained gives the value of $(k_1 - 1)$ and the intercept on the $\log|\Delta T|$ axis gives the value of $\log[(RT_s^2/Q)\,(1 - k_1)X_1]$ for $k_1 < 1$ and of $\log[(RT_s^2/Q)\,(k_1 - 1)X_1]$ for $k_1 > 1$. When T_s is unknown its value can be calculated from the melting curve as has been described in a previous paper[6].

A sample containing n contaminants with only slightly differing k_n-values, will often behave like a sample with only one contaminant with a mean distribution coefficient $\bar{k}$. This is clear from the following considerations. When

$$\sum_1^n (1 - k_n) Y^{k_n - 1} X_n = (1 - \bar{k}) Y^{\bar{k} - 1} \sum_1^n X_n,$$

$\bar{k}$ must be a function of Y. This function can be written:

$$(1 - \bar{k}) = \sum_1^n (1 - k_n) Y^{k_n - \bar{k}} X_n / \sum_1^n X_n$$

When, *e.g.*, $-0.1 < k_n - \bar{k} < 0.1$ and Y varies from 0.1 to 1, the value of $Y^{k_n - \bar{k}}$ will vary only from 1.25 to 0.8. Moreover, every $Y^{k_m - \bar{k}}$ value larger than 1 is opposed by a $Y^{k_p - \bar{k}}$ value smaller than 1. Thus the value of $\bar{k}$ will vary only slightly with Y and the mean distribution coefficient $\bar{k}$ will be close to:

$$\sum_1^n k_n X_n / \sum_1^n X_n.$$

The value of $\bar{k}$ is found experimentally by drawing a straight line through the plot of log$Y$ against log$|\Delta T|$. The total amount of impurity calculated according to this approximation will be close to the value of $\sum_1^n X_n$.

The melting curve of a sample containing impurities with $k<1$ and $k>1$

Suppose that the system may be considered as a main component with two contaminants. Eqn. (2) reduces to:

$$(1-k_1)Y^{k_1-1} + (1-k_2)Y^{k_2-1} = \frac{Q}{RT_s^2}(T_s - T) = -\frac{Q}{RT_s^2}(\Delta T_1 + \Delta T_2) \qquad (2b)$$

In this equation $k_1<1$ and $k_2>1$ may be the real distribution coefficients of the contaminants or the mean distribution coefficients of two sets of impurities having only slightly differing distribution coefficients within each set. At small values of Y the value of ΔT_2 may dominate over ΔT_1

When log$Y$ is plotted against log$|\Delta T_1 + \Delta T_2|$ a strongly curved line or a function in two portions is obtained (see Fig. 1). One or both ends of this line may be approximately straight.

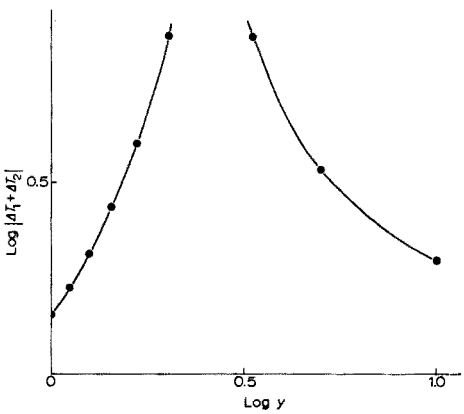

Fig. 1. Plot of log$|\Delta T_1 + \Delta T_2|$ against log$Y$ for two impurities with $k = 0.7$ and $k = 2$ present in equal concentrations (the scale of ΔT-values is arbitrarily chosen).

The following method of successive approximation can now be followed. The tangents at one or both ends of the line (*e.g.* $Y = 0.1$ and $Y = 0.9$) are drawn. It is assumed that these lines represent as a first approximation the functions

$$\log(-\Delta T_1) = (k_1-1)\log Y + \log[(RT_s^2/Q)(1-k_1)X_1] \qquad (2c)$$

and

$$\log(\Delta T_2) = (k_2-1)\log Y + \log[(RT_s^2/Q)(k_2-1)X_2] \qquad (2d)$$

From the first tangent the depressions ΔT_1 are calculated in the range $Y = 0.5$–1 and from the second tangent the elevations ΔT_2 in the range $Y = 0.1$–0.5. Now the ΔT_1-values are corrected with the calculated ΔT_2-values and the ΔT_2-values are corrected with the calculated ΔT_1-values. The logarithms of these corrected values are

plotted again against $\log Y$. The graphs through these plots will show a much smaller curvature than the original curve. The correction of ΔT_1 and ΔT_2 may be repeated using the new corrected graphs until the obtained lines are perfectly straight. These lines will represent the functions (2c) and (2d) from which k_1, k_2, X_1 and X_2 can be calculated.

ZONE MELTING AS AN AID IN THE DETERMINATION OF IMPURITY CONTENT BY MEANS OF MELTING CURVES

When a substance is subjected to zone melting the impurities are redistributed along the ingot depending on the distribution coefficients of the impurities. To a certain extent a classification of the impurities according to their distribution coefficients will be obtained. In some parts of the ingot the concentration of several impurities may be reduced beyond a detectable value while other impurities are less reduced or enriched. After a sufficient number of zone passes the first part of the ingot will only contain impurities with k close to 1 or >1. In most cases the first part of the ingot will give interpretable melting curves.

The actual determination of the impurity content of a sample can thus be performed in the following way. The substance is subjected to zone melting and after an arbitrarily chosen number of zone passes, the melting curves of several parts of the ingot are determined. From the set of melting curves obtained, those melting curves are selected that can be interpreted as described in the previous section of this paper. When the concentration and the distribution coefficient of a contaminant (or a group of contaminants) can be determined in a part of the ingot, the concentration in every part of the ingot and the mean concentration can be computed. This means that for every melting curve the ΔT_n-values caused by this contaminant can be calculated.

The melting curves are corrected for these ΔT_n-values; and from these corrected melting curves again those melting curves are selected that can be interpreted. The remaining curves are corrected again and the whole process is repeated until all impurities and the distribution coefficients are determined. In general, every determination of the impurity content of a sample is a new problem and rules concerning the number of zone passes and the parts of ingot that will give interpretable melting curves cannot be given. Much depends on the number, kind and concentration of the contaminants.

Often the number of impurities giving mixed crystals with the main component is restricted and in most cases the value of n is only 3 or less. In these cases the rather cumbersome procedure described above is not necessary. From the melting curves of several parts of the ingot, the distribution coefficients of the impurities can be easily determined. The obtained set of distribution coefficients is used in the interpretation of the melting curve of the original sample.

An important value in the interpretation of melting curves when impurities with $k>1$ and $k<1$ are present is the melting point of the pure main component. By zone melting a relatively pure main component can be obtained from which the value of T_s can be determined more accurately.

SUMMARY

The determination of the impurity content of a sample by means of the melting-

curve method (calorimetric analysis) is often seriously hampered when solid soluble contaminants are present. Solid solutions often occur in substances purified by crystallization or extraction. A simple test on mixed crystals is described. When three or more impurities are present the relations obtainable from a melting curve are insufficiently accurate for computing the unknown concentrations and distribution coefficients to an acceptable extent. Only melting curves obtained from samples containing one or two impurities permit an exact, simple interpretation. A complex of impurities may be analysed when the sample is subjected to zone melting and a set of melting curves is obtained for parts of the ingot.

REFERENCES

1 W. P. WHITE, *J. Phys. Chem.*, 24 (1920) 393.
2 R. N. M. A. MALOTAUX AND J. STRAUB, *Rec. Trav. Chim.*, 52 (1933) 275.
3 F. W. SCHWAB AND E. WICHERS, *Temperature, its Measurement and its Control in Science and Industry*, Reinhold, New York, 1941, p. 256–264.
4 B. J. MAIR, A. G. GLASGOW AND F. D. ROSSINI, *J. Res. Natl. Bur. Std.*, 26 (1941) 591.
5 W. M. SMIT, *Thesis*, Vrije Universiteit, Amsterdam, 1946.
6 H. F. VAN WIJK AND W. M. SMIT, *Anal. Chim. Acta*, 23 (1960) 545.
7 W. M. SMIT, *Z. Elektrochem.*, 66 (1962) 779.
8 N. J. G. BOLLEN, M. J. VAN ESSEN AND W. M. SMIT, *Anal. Chim. Acta*, 38 (1967) 279.
9 H. F. VAN WIJK AND W. M. SMIT, *Anal. Chim. Acta*, 24 (1961) 45.
10 W. M. SMIT, *Rec. Trav. Chim.*, 75 (1956) 1309.
11 W. M. SMIT, *Anal. Chim. Acta*, 17 (1957) 23.

Analytica Chimica Acta
Elsevier Publishing Company, Amsterdam
Printed in the Netherlands.

COMPARAISON DE LA PURIFICATION PAR FUSION DE ZONE ET PAR CRISTALLISATION EN COLONNE DANS LE CAS D'AMINES AROMATIQUES LIQUIDES A TEMPERATURE ORDINAIRE

BERNARD POUYET
Faculté des Sciences de l'Université de Lyon (France)

(Reçu le 1 novembre, 1966)

La purification par la méthode de la zone fondue conduit à des résultats en général excellents et cette technique est probablement une de celles qui permettent d'obtenir les produits les plus purs[1,2]. Toutefois lorsqu'on désire travailler sur des substances liquides à température ordinaire ou dont le point de fusion est inférieur à 0°, l'appareillage devient assez compliqué. De plus toute opération continue par cette méthode est pratiquement impossible, ou tout au moins conduit à de moins bons résultats comme l'ont montré quelques études sur ce sujet[3].

Afin d'éliminer ces deux restrictions, des méthodes voisines de celle de la zone fondue ont été proposées. En particulier celle qui nous a paru la mieux adaptée à nos conditions de travail est la méthode de cristallisation en colonne, méthode déjà décrite par SCHILDKNECHT et ses collaborateurs[4,5]. Ce procédé dont nous donnons sommairement le principe plus loin permet en effet de travailler en régime continu. De plus, les produits que nous désirions purifier sont relativement visqueux au voisinage du point de solidification. De plus ils présentent la plupart du temps une surfusion très importante et dans certains cas, il est même impossible d'obtenir la cristallisation si l'on n'amorce pas à l'aide d'un petit cristal. (Celui-ci est obtenu par une méthode archaïque mais efficace, qui consiste à frotter une baguette de verre dans le liquide surfondu).

Comme nous le verrons, avec de tels produits la méthode de la zone fondue est difficile à mettre en oeuvre et les résultats de purification sont longs à obtenir. Par contre, la cristallisation en colonne, nécessite un seul amorçage pour une quantité très importante de substance, et elle conduit à des résultats satisfaisants dans un temps relativement court.

Notre but est d'obtenir des substances très pures en vue d'études photochimiques. Les techniques dont nous parlons sont donc pour nous seulement des outils. C'est pour cette raison que nous n'avons pas fait d'étude systématique sur la variation de tous les paramètres.

Nous nous contentons de donner les caractéristiques des appareils employés, caractéristiques qui nous ont permis d'obtenir des produits satisfaisants pour notre travail photochimique; les constantes physiques de ces produits sont également données.

PURIFICATION PAR ZONE FONDUE

Dans un premier travail nous avons purifié nos substances par la méthode de

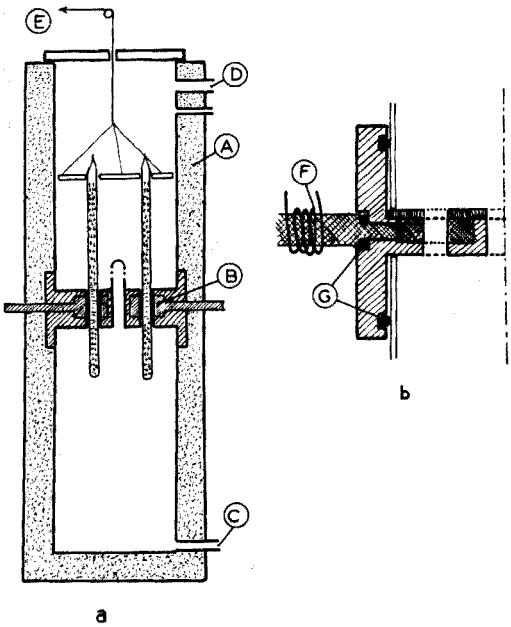

Fig. 1. Appareil pour purification par fusion de zone. (a) Disposition générale, (b) Détail d'un four. (A) Isolation par laine de verre. (B) Fours. (C) Circulation de fluide froid. (D) Trop-plein. (E) Entraînement. (F) Chauffage par cordon. (G) Joints toriques.

la zone fondue. La plupart d'entre elles étant liquides à température ordinaire nous avons été amené à construire un appareil relativement simple, permettant de travailler jusqu'à des températures voisines de −40°.

Le schéma de cet appareil est donné Fig. 1: une circulation de fluide froid dans une colonne de diamètre 80 mm et hauteur 2 m permet la solidification dans les tubes contenant les échantillons. Une série de six fours cylindriques crée dans chacun des tubes, une zone fondue. Le mouvement d'ascension du tube est commandé simplement par un moteur avec démultiplication suffisante.

La température du fluide froid est réglable ainsi que celle des fours. Ces derniers peuvent être commandés séparément car chacun d'eux est équipé d'un cordon chauffant extérieur.

Les tubes contenant les échantillons sont scellés sous vide. Pour la plupart d'entre eux la solidification se fait soit par simple immersion dans le fluide réfrigérant, soit par amorçage du liquide surfondu, en créant un point froid (azote liquide) sur la paroi du tube. Toutefois certaines substances (en particulier la diméthyl-2,4-aniline ou xylidine-2,4) se refusent à cristalliser de cette façon et donnent naissance à un verre. Nous avons alors procédé de la façon suivante: avant de sceller le tube nous le refroidissons très légèrement au-dessous du point de solidification. Nous amorçons avec un petit cristal, comme nous l'avons précisé précédemment.

Lorsque la cristallisation est faite nous ne conservons qu'un petit volume solide au fond du tube, le reste étant fondu. Le scellement peut alors se faire sous vide, le dégazage étant pratiquement complet dans le liquide. Il suffit ensuite de procéder comme pour les autres échantillons.

La capacité moyenne des tubes est environ 70 g, ce qui permet donc au total de travailler sur 400 g. La vitesse de passage de la zone a été prise dans tous les cas de 15 mm/h. La largeur de cette zone est environ 2 cm c'est à dire sensiblement 1/30 de la longueur totale du barreau solide à purifier. La température du fluide réfrigérant est maintenue à environ une dizaine de degrés au-dessous du point de fusion du produit étudié. Le nombre de passages de la zone à travers le barreau a varié entre 15 et 20 selon les échantillons.

Ces conditions de travail étant données, nous considérerons maintenant les divers produits que nous avons utilisés. Nos travaux portent actuellement sur l'oxydation photochimique par l'oxygène moléculaire, d'amines simples aromatiques. Au cours de cette oxydation apparaissent de nouveaux produits plus ou moins colorés et la cinétique de cette coloration dépend d'une façon très importante des impuretés présentes dans les produits de départ.

Nous avons montré que la mesure du point de fusion et de la densité optique dans le proche ultraviolet[6,7] étaient nécessaires pour le contrôle de l'élimination de produits organiques tandis que la conductivité électrique nous renseignait sur l'élimination de substances ioniques généralement minérales (H_2O en particulier).

Les produits avant purification nous sont fournis commercialement; ils sont généralement colorés en jaune ou rouge-brun. Bien que les garanties concernant ces produits, données par le fournisseur soient quelquefois excellentes, au cours du stockage l'action de l'air et de la lumière a dégradé de façon assez sensible la qualité de ces produits. Par exemple dans le cas de l'aniline, le point de fusion varie entre −6.35 et −6.65° et le liquide est rouge-orangé, alors que le produit pur a un point de fusion de −6.0° et est parfaitement incolore[7].

TABLEAU I

POINTS DE FUSION ET ABSORPTION DANS LE PROCHE ULTRAVIOLET DES AMINES, AVANT ET APRÈS PURIFICATION PAR FUSION DE ZONE

Amine	*Point de fusion*		*log I_0/I[a] (cm)*		*Température du fluide réfrigérant*
	Avant	*Après*	*Avant*	*Après*	
Aniline	− 6.10°	− 6.00°	0.215	0.195 (λ = 3400Å)	−15°
o-Toluidine	−23.80°	−23.70°	0.080	0.030 (λ = 3650Å)	−30°
m-Toluidine	−30.10°	−30.05°	0.150	0.100 (λ = 3400Å)	−40°
Diméthyl-2,3-aniline	3.40°	3.80°	0.320	0.300 (λ = 3400Å)	−15°
Diméthyl-2,4-aniline	−15.10°	−14.90°	0.230	0.215 (λ = 3900Å)	−25°
Diméthyl-2,5-aniline	15.30°	15.75°	0.290	0.250 (λ = 3600Å)	0
Diméthyl-2,6-aniline	10.80°	11.25°	0.210	0.180 (λ = 3640Å)	0°

[a] log I_0/I est la densité optique de l'amine correspondante, sous 1 cm d'épaisseur à la longueur d'onde figurant entre parenthèses.

Nous donnerons ici les résultats concernant les amines suivantes: aniline, *o*-toluidine, *m*-toluidine, diméthyl-2,3-aniline, diméthyl-2,4-aniline, diméthyl-2,5-aniline et diméthyl-2,6-aniline.

Tous les échantillons ont subi successivement une distillation à la pression atmosphérique, une distillation sous pression réduite, une cristallisation simple. Ce n'est qu'après tous ces traitements que la méthode de la zone fondue est appliquée. Nous savons en effet que c'est une méthode de purification ultime et que l'efficacité est alors importante.

Les fractions recueillies après purification sont celles qui sont situées entre le premier et le dernier quart du tube: on récupère donc ainsi sensiblement la moitié du produit de départ.

Les critères de pureté employés sont ici le point de fusion et le coefficient d'extinction moléculaire dans le proche ultraviolet.

Les résultats obtenus sont réunis dans le Tableau I. Nous constatons que les améliorations concernant le point de fusion sont d'autant plus importantes que le point de fusion de l'amine est plus élevé. Quant à la diminution de la densité optique elle n'est généralement pas très importante, car rappelons le, les produits de départ ont subi déjà plusieurs distillations et une cristallisation. Toutefois les produits colorés qui s'éliminent ici, sont la plupart du temps quasiment impossibles à extraire par une méthode physique courante.

Cette méthode est donc extrêmement intéressante pour le photochimiste car la présence d'impuretés, même à l'état de traces, peut permettre certaines réactions par sensibilisation, ce qui fausse évidemment l'étude photochimique proprement dite.

PURIFICATION PAR CRISTALLISATION EN COLONNE

La méthode de purification par zone fondue nous le voyons est très satisfaisante du point de vue résultats. Toutefois nous l'avons dit sa mise en oeuvre nécessite des opérations relativement compliquées (amorçage de la cristallisation, récupération des produits, répétition des opérations pour obtenir des quantités importantes). De plus, étant donné la viscosité des amines au voisinage du point de fusion, la vitesse de purification n'est pas très rapide et il faut donc un temps relativement long pour obtenir des échantillons purs (trois semaines environ par opération).

La deuxième technique que nous avons utilisée repose également sur les propriétés de l'équilibre liquide–solide: elle a été proposée pour la première fois par SCHILDKNECHT ET VETTER[5].

L'appareil schématisé (Fig. 2) consiste essentiellement en deux tubes concentriques et une spirale métallique qui tourne dans l'espace annulaire entre les deux tubes. Les cristaux sont formés par refroidissement à la partie supérieure de la colonne. Ces cristaux sont captés et transportés vers le bas par la spirale, leur fusion a lieu à la partie inférieure de la colonne après qu'il y ait eu brassage par contre courant entre le liquide et les cristaux.

Trois tubulures ont été placées sur cette colonne ce qui permet un fonctionnement de façon continue[8].

La purification obtenue est rapide puisqu'il nous a suffi de faire fonctionner la colonne pendant quatre heures pour avoir un résultat appréciable. Les autres caractéristiques de fonctionnement sont les suivantes:

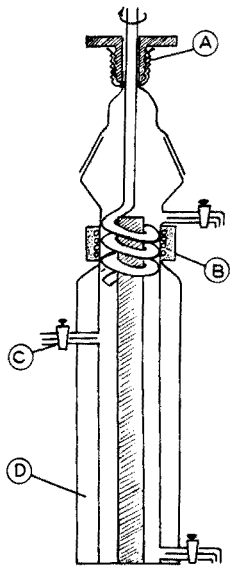

Fig. 2. Dispositif de cristallisation en colonne. (A) Passage étanche en téflon avec joint torique. (B) Circulation de fluide froid. (C) Robinet d'alimentation. (D) Isolation par gaine de vide.

vitesse de rotation de la spirale: 70 tours/min,
diamètre extérieur de la spirale: 35 mm,
diamètre intérieur de la spirale: 15 mm,
longueur totale de la colonne: 60 cm.

A l'aide de cet appareil nous avons purifié les mêmes échantillons que ceux utilisés pour la méthode de la zone fondue. Les résultats (Tableau II) montrent que l'efficacité est légèrement inférieure à celle de la précédente expérience, mais en reprenant à nouveau les produits ainsi purifiés on obtient une limite très voisine de celle de la zone fondue. Les différences sont surtout indiquées par la valeur de l'absorption dans le proche ultraviolet du fait de l'imprécision de nos appareillages concernant la mesure du point de fusion.

TABLEAU II

RÉSULTATS DE LA PURIFICATION DES AMINES PAR CRISTALLISATION EN COLONNE

Amine	*Après un passage dans la colonne*		*Après trois passages dans la colonne*	
	Point de fusion	*log I_0/I*	*Point de fusion*	*log I_0/I*
Aniline	− 6.00°	0.210	− 6.00°	0.200
o-Toluidine	−23.70°	0.050	−23.70°	0.035
m-Toluidine	−30.05°	0.120	−30.05°	0.110
Diméthyl-2,3-aniline	+ 3.80°	0.310	+ 3.80°	0.300
Diméthyl-2,4-aniline	−14.90°	0.225	−14.90°	0.220
Diméthyl-2,5-aniline	15.70°	0.275	+15.70°	0.255
Diméthyl-2,6-aniline	11.25°	0.200	+11.25°	0.185

TABLEAU III

PURIFICATION D'AMINES TRÈS IMPURES, PAR CRISTALLISATION EN COLONNE

Amine	*Départ*		*Arrivée*	
	Point de fusion	*log I_0/I*	*Point de fusion*	*log I_0/I*
Aniline	− 6.4°	>2	− 6.10°	0.220
o-Toluidine	−24.7°	1.90	−23.85°	0.090
m-Toluidine	−33.1°	>2	−30.20°	0.155
Diméthyl-2,3-aniline	− 1.2°	~2	+ 3.30°	0.340
Diméthyl-2,4-aniline	−15.7°	1.80	−15.10°	0.240
Diméthyl-2,5-aniline	13.2°	~2	+15.70°	0.300
Diméthyl-2,6-aniline	+18.7°	>2	+11.10°	0.210

Nous avons également travaillé sur des produits relativement impurs et nous avons constaté comme le montrent les résultats du Tableau III que la purification est très importante dès le premier passage dans la colonne. Il est probable que la limite est provoquée par l'entraînement de produit non purifié lors de la prise. Il est à prévoir que la fréquence et l'importance des soutirages sont importantes. A cet effet nous avons essayé de voir l'influence du débit lorsqu'on travaille de façon continue.

Pour ceci une réserve de produit à purifier est ajoutée de façon à introduire du produit brut au niveau du tiers supérieur de la colonne. Le soutirage se fait par deux tubulures, l'une au sommet de la colonne pour le produit enrichi en impuretés l'autre au bas de la colonne pour le produit purifié. Le liquide brut est refroidi dans le récipient réserve de façon à ne pas perturber l'équilibre thermique au sein de la colonne. Les débits sont réglés au moyen de robinets montés sur des tubes capillaires.

On constate que la densité optique reste sensiblement constante jusqu'à une valeur limite du débit voisine de 0.4 cm³/min pour augmenter ensuite de façon rapide. La Fig. 3 montre les résultats obtenus avec le diméthyl-2,3-aniline.

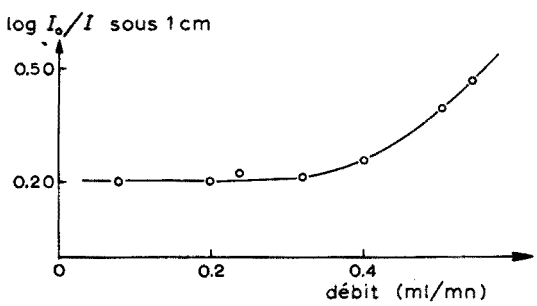

Fig. 3. Variation de la densité optique de la diméthyl-2,3-aniline suivant le débit de la colonne de cristallisation.

CONCLUSION

Nous pouvons donc penser que dans le cas de la purification d'amines aromatiques, les appareils que nous avons utilisés sont satisfaisants. Toutefois la méthode de

purification par cristallisation en colonne s'avère très intéressante car elle conduit à des limites de pureté voisines de celles obtenues par la méthode de la zone fondue mais elle est beaucoup plus rapide que cette dernière.

Son efficacité en temps limité et le fait de pouvoir travailler de façon continue rendent cette méthode très intéressante tant au stade du laboratoire qu'au stade industriel. Il est possible de monter ces colonnes en cascades comme l'ont indiqué MAAS ET SCHILDKNECHT[8].

Signalons que dans la région lyonnaise une telle colonne est à l'étude au stade semi-industriel pour la purification de dérivés aromatiques.

RÉSUMÉ

Dans la première partie les résultats concernant la purification par la méthode de la zone fondue de sept amines aromatiques sont donnés. L'appareil utilisé permet de purifier 400 g de substance par opération, à des températures variant entre $+15°$ et $-35°$. Les critères de pureté employés et quelques constantes physiques concernant les amines purifiées sont donnés. Dans une deuxième partie, une méthode voisine de celle de la zone fondue est exposée: la cristallisation en colonne. Cette technique est appliquée aux mêmes produits que précédemment et les résultats sont comparés. Cette étude montre que les deux méthodes de purification sont assez comparables quant aux résultats. Cependant la cristallisation en colonne, tout en ne permettant pas une purification ultime aussi bonne, présente néanmoins les avantages suivants: possibilité de travailler de façon continue, purification satisfaisante en un temps relativement court, et possibilité d'utiliser des produits de départ assez impurs ce qui n'est pas le cas avec la fusion de zone.

SUMMARY

Purification by zone melting of seven aromatic amines was studied; 400 g of substance could be purified at one time between $+15°$ and $-35°$. Criteria of purity and some physical constants of purified amines are given. A related method—column crystallisation—was also studied for the same starting materials and the results are compared. The two methods of purification give comparable results. Column crystallisation does not give such good purification as zone melting, but has the advantages that it can be operated with continuous throughput, much less time is needed, and rather impure starting materials can be employed.

BIBLIOGRAPHIE

1 W. G. PFANN, *Trans. Am. Inst. Min. Engs.*, 194 (1952) 747.
2 E. F. G. HERINGTON, *Zone melting of organic compounds*, 1st edn., Blackwell, London, 1963.
3 J. MAIRE, J. C. MORITZ ET R. KIEFFER, *Symposium über Zonenschmelzen, Karlsruhe, 1963.*
4 H. SCHILDKNECHT ET K. MAAS, *Wärme*, 69 (1963) 121.
5 H. SCHILDKNECHT ET H. VETTER, *Angew. Chem.*, 73 (1961) 121.
6 G. ARMANET, P. MEALLIER ET B. POUYET, *Communication aux Journées de Chimie*, Orsay, 1965.
7 G. ARMANET ET B. POUYET, *Bull. Soc. Chim. France*, (1966) 1931.
8 K. MAAS ET H. SCHILDKNECHT, *Symposium über Zonenschmelzen, Karlsruhe, 1963.*

Analytica Chimica Acta
Elsevier Publishing Company, Amsterdam
Printed in the Netherlands.

ULTRAMICRO ZONE MELTING

KLAUS MAAS AND HERMANN SCHILDKNECHT
Organisch-Chemisches Institut der Universität Heidelberg (Germany)

(Received December 1st, 1966)

In the last 15 years, more than 1000 articles and patents have been published dealing with the different techniques and apparatus used for zone melting as a method of high purification and enrichment of inorganic and organic substances. The temperature scales range from $-100°$ to 4000°, and the starting quantities from several kilograms in the factory to a few milligrams in analytical work. There is no single classification for the order of magnitude of the substances treated; the appropriate subdivisions in literature usage, as shown in Fig. 1, are therefore open to discussion.

$< 5 \cdot 10^{-4}$ cm³ = < 500 μg	ultra-micro scale
$> 5 \cdot 10^{-4}$–$5 \cdot 10^{-1}$ cm³ = > 500 μg–500 mg	micro scale
$> 5 \cdot 10^{-1}$–$5 \cdot 10^{0}$ cm³ = > 500 mg–5 g	semi-micro scale
$> 5 \cdot 10^{0}$–$5 \cdot 10^{1}$ cm³ = > 5 g–50 g	macro scale
$> 5 \cdot 10^{1}$–$5 \cdot 10^{2}$ cm³ = > 50 g–500 g	semi-technical scale
$> 5 \cdot 10^{2}$ cm³ = > 500 g	technical scale

Fig. 1. Subdivision of zone melting methods with respect to volume, i.e. for $d = 1$, to weight.

The basis of the system is a unit of five, which is modified by powers of ten. The longitudinal sections of single ingots possess the frequently used diameter/length relationship of 1:20, and for a density of 1, the volume data are expressed in g. A standardisation of apparatus could best be achieved by use of a cubic centimetre system. The micro zone-melting region comprises three powers of ten. Above $5 \cdot 10^{2}$ cm³ (= 500 g) is the technical zone-melting region and below $5 \cdot 10^{-4}$ cm³ (= 500 μg) begins the ultra-micro zone-melting region. Until now, the limit for micro zone melting was around a few milligrams. For the completion of the designated regions of differing dimensions, and particularly with regard to the chemistry of natural products and radiochemistry, further diminution appeared interesting.

EXPERIMENTAL

Apparatus

The transition into the microgram range required thin capillary tubes as sample holders; Fig. 2 shows graphically the relationship between the sample diameter (corresponding to the inner capillary diameter), length, and volume, *i.e.* the weight of sample when $d = 1$. The points—partially surrounded by circles—indicate a diameter/length relationship of 1:20.

A zone-melting apparatus of this order of magnitude can be prepared most simply on the "comb principle", whereby the plates of the heating block and those of the cooling block fit into each other like two combs. If one calculates to the 0.5 mm of the largest sample diameter shown in Fig. 2, the thickness of the capillary walls and also a small clearance space, the plates must contain a through passage of about 0.6 mm diameter. Long concentrical bores of this precision are practically impossible. A

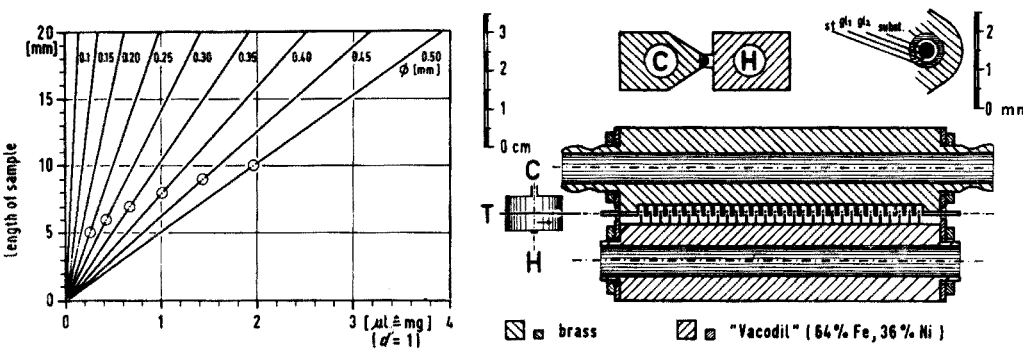

Fig. 2. Relationship between sample diameter, length, and volume, i.e. weight.

Fig. 3. Technical design of an ultra-micro zone-melting apparatus; C cooling block, H heating block, T transport device; st steel capillary, gl_1 guiding capillary, gl_2 sample capillary, subst. substance.

steel capillary tube (*e.g.* a hypodermic needle) is therefore firmly soldered into a lateral groove of the two blocks. After subsequent milling, only the plates depicted in Fig. 3 remain. The plates of the liquid cooled block (C) are 1.0-mm thick and those of the electrically heated or better still thermostatically-controlled liquid heated block (H) are 0.5-mm thick. The clearance of the plates from one another amounts to 0.5 mm, so that a complete "zone melting unit" (1 heater, 1 cooler, and 2 clearances) measures only 2.5 mm. The limit of a further realisable diminution may be about 1.7 mm, *i.e.* 0.4 mm for the heater, 0.7 mm for the cooler and twice 0.3 mm for the clearances. Thinner plates, which are difficult to mill, require very high heating to result in a definite heat content. Small clearances can be only obtained from materials with a low coefficient of expansion. The expansion of the heating block as opposed to the temperature constant cooling block must be fully calculated in the clearance space since an expansion in only one direction often results. Whilst an increase of about 0.4 mm per 10 cm of brass is usual for a temperature increase from 20° to 200°, the increase of the iron–nickel alloy used for the apparatus described ("Vacodil"—Fe, 64%; Ni, 36%; Vakuumschmelze Co., Hanau/Germany) is only about 0.04 mm. Apparatus

for "ice zone melting" (i.e. for low melting substances) should also have cooling blocks made from this alloy, as it is then possible to make a further reduction in the clearance space. The heating and cooling blocks are joined together with strips of "Vacodil" and adjusted to one another. The strips have a hole in the middle for the passage of the capillary tube and slits on both sides in order to minimize the transition of heat.

The ultramicro sample should not be subjected to temperature variation during the zone melting since this may bring about substance displacement and thus formation of bubbles. The 28 heating and 29 cooling elements arranged one after another have a total length of only 7.5 cm (about 5 cm using a unit length of 1.7 mm instead of 2.5 mm) and render the dangerous displacement of the sample unnecessary.

The sample is moved forward by a steel wire of about 0.4 mm thickness which is driven forward between two rubber rollers (transport mechanism T in Fig. 3). By changing the driving roller or altering the speed of the motor, one can alter the travelling speed of the sample. The axis of the enclosed synchronized motor revolves once every 24 h and the feed rate of the sample is usually 2 mm/h. The second roller may be removed so that the steel wire, which is guided through a capillary, can be placed exactly.

Sample capillaries of less than 0.4-mm outer diameter are—like the transporting wire—best carried in a glass capillary which fits the 0.6 mm passage exactly. Any loss of heat is thereby reduced to a tolerable level. Figure 3 shows, above the main diagram, the concentrical interlocking arrangement of steel capillary, guide capillary, sample capillary and sample, magnified (×10). If the sample capillary breaks, it is possible to recover the valuable material from the guide capillary.

When work is carried out with liquids at low temperatures ("ice zone melting"), the apparatus must not be allowed to come into contact with atmospheric moisture. It is therefore placed in a transparent plastic cylinder sealed with a flange. The cooling liquid lead and electrical leads to a fluorescent lamp, driving motor and rheostat-heater are passed through air-tight fittings. A three-way tap permits rapid drying of the inner space by alternate evacuation and filling with dry gas. Using a balloon, a small excess pressure may then be maintained within the space. With extremely air-sensitive substances, an inert gas is recommended so that the sample remains undamaged even if the capillary breaks.

Capillary preparation

The preparation of the diminutive sample-capillaries requires a special technique. On sealing the capillary, the sample must not be overheated; the sample thread must not break since the resulting pieces each act as separate ingots. The technique for non-air-sensitive samples is illustrated in stages in Fig. 4.

Stage 1: A capillary of suitable diameter for the amount of substance it must contain is drawn out. Depending on the thickness of the wall, between 0.05 and 0.2 mm is added to the value taken from the graph in Fig. 2. A small metal block in which steel capillaries of known inner diameter are fixed, serves as a gauge. After some practice, one is able to judge the outer diameter and wall thickness of the requisite capillary of definite dimensions.

Stage 2: The selected capillary is heated over a hot plate or in a pierced cylinder. The melted sample is immediately sucked into the tube by capillary action.

Stage 3: The melt is easily brought into the middle of the capillary since within the tube only the force of gravity is effective.

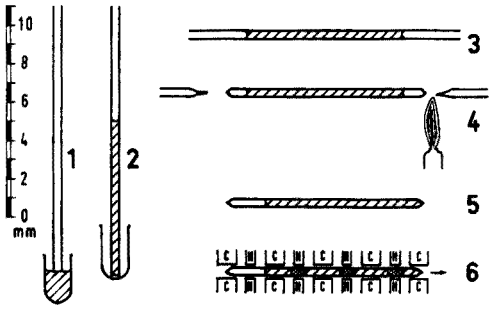

Fig. 4. Technique of ultra-micro zone melting.

Stage 4: Both ends of the capillary are sealed using a 2–3 mm high micro-flame.

Stage 5: The substance is centrifuged at several thousand r.p.m. into one end of the capillary. To prevent decomposition products formed in the sealing of the capillary impairing the purification the clean end of stage 2 is preferable.

Stage 6: The prepared sample is placed into the cold apparatus and the heating is so controlled that a melting zone of under 1 mm is produced. For this purpose it is best to use a microscope.

In the case of air-sensitive substances, the starting tube in stage 1 is filled with nitrogen and in this way a capillary filled with protective gas is obtained. This is separated from the parent tube in a nitrogen-filled dry-box and filled with the melt. The ends, in this case, must be electrically sealed.

Many compounds contract very strongly on solidifying and form cavities in the sample thread. On zone melting, this can cause the formation of bubbles. The cavity formation is avoided by slowly removing the capillary from a heated tube (in the case of "ice zone melting" by slowly inserting into a correspondingly cooled tube).

DISCUSSION

Ultramicro zone melting affords results in a very short time. Since the number of the passing zones in a fixed time and at constant speed is a function of the length of the heater, cooler and clearance, the ultramicro apparatus with its closely packed plates already operates—on a purely mechanical basis—several times faster than the previously favoured micro zone-melting apparatus. Compared with the macro-scale apparatus this can amount to a factor of 10, 20 or more. The theoretically expected thermodynamic improvement through the melting zones which are less than 1-mm wide and the steep temperature gradient have not been taken into consideration here. The favoured travelling speed of 2 mm/h in micro zone melting is certainly very slow in ultramicro zone melting. An exact investigation of favourable feed rates is possible, *e.g.* with high-melting alkanes and quantitative gas chromatography.

Eutectics can be purified in several hours. Stearic acid with about 1% azobenzene or azulene as coloured impurity serves as a useful test compound for demonstration purposes.

Since ultramicro zone melting requires only a fraction of a milligram of substance, it finds particular application in the chemistry of natural products and radiochemistry. For example, small amounts of marked compounds, which have decom-

posed by auto-radiation, can easily be separated from the decomposition products formed. The low time requirement for 10–20 zone passes (12–25 h) protects heat-sensitive substances and enables quick preliminary tests to be carried out before one submits large amounts to zone melting; this time, calculated on a travelling speed of 2 mm/h, can be certainly diminished by higher speeds. The preparation of the sample capillary takes between 10 and 30 min, depending upon the circumstances.

SUMMARY

A systematic classification of zone melting is discussed with respect to the volume, *i.e.* weight, of the ingot. A new apparatus and technique of "ultra-micro zone melting" are described for amounts less than 500 μg. The plates of the heating and cooling blocks are placed into one another like two combs; an iron–nickel alloy with a very low coefficient of expansion permits "zone melting units" between 1.7 mm and 2.5 mm in size. Because of the close packing of the 30 "units" and a steep temperature gradient, separation effects can be achieved after a few hours. For work at low temperatures and under inert gas, the apparatus can be enclosed in an air-tight plastic cylinder. The sample capillaries are prepared by capillary action followed by centrifuging. Ultramicro zone melting finds application in natural product chemistry and radiochemistry.

Analytica Chimica Acta
Elsevier Publishing Company, Amsterdam
Printed in the Netherlands.

A STUDY OF LIQUID CHROMATOGRAPHY IN COLUMNS. THE TIME OF SEPARATION

J. F. K. HUBER AND J. A. R. J. HULSMAN
Institute of Analytical Chemistry, University of Amsterdam (The Netherlands)

(Received November 1st, 1966)

See Errata : Vol. 38, No. 4 Pages. 587, 1967

In order to describe a separation process, a quantity characterizing the degree of separation must first be defined; the term resolution is generally used in chromatography to measure the separation of two successive components[1]. A comparison between different chromatographic techniques makes sense only if the resolution is related to working conditions such as time of separation, sample feed, pressure, column dimensions, *etc.* In gas chromatography, these relations have been studied intensively. This paper on the time of separation is the second of a series describing such a study performed for liquid chromatography in columns. The first paper of the series dealt with the fundamentals[2]; a third devoted to the sample feed will be published in the near future.

THEORY

The basic equation which was introduced to describe time of separation in gas chromatography[3,4], can also be applied in liquid chromatography and is obtained from the expression for the resolution.

The resolution, R_{BA}, of two components, A and B, is defined as the ratio between the difference of the average residence times $t_{RB}-t_{RA}$ of the two components and the standard deviation σ_{tA} of the elution curve of the component, A, which elutes first from the column. The average residence time of a component is called retention time. The elution curve describes the concentration in the moving phase at the end of the column as function of time.

The resolution is caused by the counteraction of the migration and dispersion of the components and is related to a number of variables. For solution chromatography the following expression is obtained[2]

$$R_{BA} = \frac{t_{RB} - t_{RA}}{\sigma_{tA}} = \left(\frac{K_B}{K_A} - 1\right) \frac{\varepsilon_\beta K_A}{(\varepsilon_\alpha + \varepsilon_\beta K_A) H_A^{\frac{1}{2}}} L^{\frac{1}{2}} \qquad (1)$$

where K_A and K_B are the respective distribution coefficients which are the concentration ratios at equilibrium; ε_α and ε_β are the fractions of the column volume, which are occupied by the moving phase α and the stationary phase β; L is the length of the column and H_A is the length which characterizes the dispersion of the component A on the way through the column, *i.e.* the "height equivalent to a theoretical plate". In adsorption chromatography the volume ratio ε_β has to be replaced by the surface to volume ratio. If in eqn. (1), L is substituted by $t_{RA}\langle v\rangle\varepsilon_m/(\varepsilon_\alpha+\varepsilon_\beta K_A)$ an expression which relates the retention time t_{RA} to the resolution is obtained[2].

$$t_{RA} = \left\{\frac{R_{BA}}{(K_B/K_A) - 1}\right\}^2 \frac{(\varepsilon_\alpha + K_A\varepsilon_\beta)^3}{(K_A\varepsilon_\beta)^2\varepsilon_m} \frac{H_A}{\langle v\rangle} \quad (2)$$

where $\langle v\rangle$ is the average interstitial fluid velocity.

The H-value is composed of a number of additive terms[2]. These arise from mixing in the moving fluid by diffusion (H_{Md}) and convection (H_{Mc}), as well as from mass exchange between moving fluid and stationary bed contributing the terms H_{Em} and H_{Es} (referring to the moving fluid and stationary medium respectively).

$$\begin{aligned} H &= H_{Md} + H_{Mc} + H_{Em} + H_{Es} \quad (3)\\ H_{Md} &= (2\varepsilon_m/\tau_m)\ (D_\alpha/\langle v\rangle)\\ H_{Mc} &= 2\lambda_1 d_s/\{1 + \lambda_2\,(D_\alpha/\langle v\rangle d_p)^{1/2}\}\\ H_{Em} &= \{(\varepsilon_\alpha - \varepsilon_m + K\varepsilon_\beta)^2\,\varepsilon_m^{1/2}/3\,\psi(\varepsilon_\alpha + K\varepsilon_\beta)^2\,(1-\varepsilon_m)\}\\ &\quad (d_p^{3/2}\nu_\alpha^{1/6}\langle v\rangle^{1/2}/D_\alpha^{2/3})\\ H_{Es} &= \{(\varepsilon_\alpha - \varepsilon_m + K\varepsilon_\beta)\varepsilon_m(1-\varepsilon_m)\ \tau_s/30\,(\varepsilon_\alpha + K\varepsilon_\beta)^2\varepsilon_s]\ (d_s^2\langle v\rangle/D_s) \end{aligned}$$

ε_m is the volume fraction of the column in which a flow occurs; τ_m is the tortuosity factor of the corresponding pores; λ_1 and λ_2 are constants characterizing the geometry of the bed; ε_s is the volume fraction of the column which is occupied by stationary fluid; τ_s is the tortuosity factor of the corresponding pores; d_s is the effective diameter of the particles forming the stationary bed and Ψ is a factor related to the shape of the particles. D_α is the binary diffusion coefficient in the moving fluid α and ν_α is its kinematic viscosity. D_s is the effective diffusion coefficient in the stationary fluid system within the particles; it depends on the volume ratio of the fluid phases α and β, and their distribution in the pores of the particles. If the pores of the particles of the stationary bed are filled completely either with α or with β, the effective diffusion coefficient D_s becomes equal to the corresponding binary diffusion coefficient D_α and D_β.

The retention time in a column section of length H due to flow is $H/\langle v\rangle$ and approaches, according to eqn. (3), a minimum value at increasing fluid velocity.

The minimum value of the retention time in the column is therefore given by

$$\lim_{\langle v\rangle\to\infty} t_{RA} = \left\{\frac{R_{BA}}{(K_B/K_A) - 1}\right\}^2 \frac{(\varepsilon_\alpha + K_A\varepsilon_\beta)\,(\varepsilon_\alpha - \varepsilon_m + K_A\varepsilon_\beta)(1-\varepsilon_m)\tau_s d_p^2}{30\,\varepsilon_s\,(K_A\varepsilon_\beta)^2} \frac{}{D_s} \quad (4)$$

This equation holds for gas–liquid and liquid–liquid chromatography. If the particles of the stationary medium contain only the liquid phase β, ε_α becomes equal to ε_m, ε_β equal to ε_s and D_s equal to D_β. In this limiting case the minimum separation time is the same for given values of K_B, K_A, ε_α, ε_β, τ_s, d_s and D_s and is independent of whether a gas or liquid is used as eluant. If the pores of the particles of the stationary medium are partially filled with the liquid phase β and partially with the eluant α, D_s will be larger and lim t_{RA} smaller in gas chromatography.

In principle, the selectivity coefficient K_B/K_A depends on the nature of the eluant. If different gases are used as eluant the value of the selectivity coefficient is nearly the same, but for different liquids it can change greatly. In liquid–liquid chromatography special selectivity effects can therefore be obtained.

The minimum separation time based on eqn. (4) can be obtained only if the standard deviation of the elution curve is produced in the column. This means that the standard deviation of the conc.–time curve at the column inlet must be small compared to its increase during the migration to the outlet. Furthermore, the incre-

ment produced on the way from the column outlet to the inlet of the detector or fraction collector, must be negligible. The overall variance is the sum of the variances of the different contributions[5]:

$$\sigma_t^2 = \sigma_{ti}^2 + \Delta\sigma_{tf}^2 + \Delta\sigma_{tc}^2 \quad (5)$$

σ_{ti}^2 is the time variance which is produced at the injection point; $\Delta\sigma_{tf}^2$, and $\Delta\sigma_{tc}^2$ are the increments added in the flow lines and in the column.

The increase of the standard deviation of a sample distributed in a fluid flowing through a tube can be calculated[6,7] if $L \gg \Delta\sigma_t\, w/A$:

$$\Delta\sigma_t = (2A^3 D_a L/w^3 + A^2 L/75\, wD_a)^{1/2} \quad (6)$$

where A is the cross-sectional area of the tube, L the length and w the volume flow.

From eqn. (6) the requirements for the flow lines between sample injector and column inlet and column outlet and detector can be derived.

EXPERIMENTAL

Apparatus and procedure

The scheme of the chromatography apparatus is shown in Fig. 1. It can be considered to consist of two major systems, a separation system and a measurement system. The separation part consists of a pumping device, a sample injector, a thermostatted separation column, and possibly a fraction collector. The measurement group is built up by a detector and a registration unit.

The separation system. The pumping device must satisfy some limiting condi-

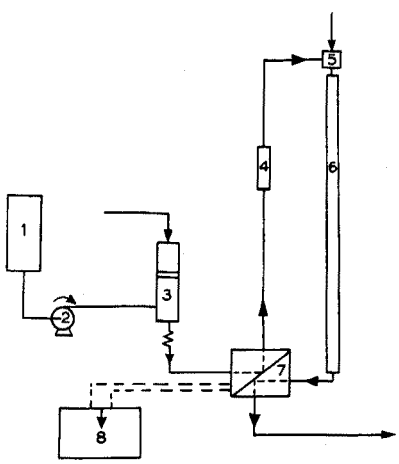

Fig. 1. Scheme of a chromatograph. (1) eluant stock; (2) pump; (3) damping device; (4) precolumn; (5) injector; (6) thermostatted column; (7) detector; (8) recorder.

tions. The flow rate must be constant, different flows must be available and the capacity must be large enough for supply during at least one separation period. These qualities are achieved with a pulsating pump (Milton Roy type 196-31) supplied with a damping system. The latter consists of a 1-m capillary tube (diameter 0.5 mm)

and an expansion vessel of 0.1 l. By applying nitrogen pressure the time needed to achieve stationary flow conditions is shortened to about 5 min. The pulses of the pump are eliminated satisfactorily in this way. With regard to the gas solubility in the moving phase, it is necessary to avoid any contact between gas and liquid. This is achieved by using a moving piston in the cylinder of the buffer vessel. The occurrence of gas bubbles at the lower pressure at the bottom of the column is prevented in this way. The flow rate is measured at the detector outlet by a flow meter.

An injector of the membrane type is used. It is constructed in such a way that the dead volume between the injection point and the column inlet amounts to only about 10 μl. The injection piece is inserted into the top of the column and sealed by an elastomer O-ring. The sample dissolved in the eluant, is introduced to the injection unit through the membrane by a precision injection syringe (Hamilton 701 N).

The columns are constructed from precision-bore straight glass tubes with an internal diameter of 2 mm and a length of 50 or 100 cm. The ends are sealed by the injector and a connector, which introduces only a very small dead volume. The connector can be joined to the detector inlet by a 3-cm teflon tube with an internal diameter of 0.5 mm. By the use of columns with connectors on both ends, column combination of any length can be constructed. The columns are filled in small portions with the dry packing. The packing is prepared by wetting an inert granular porous material (*e.g.* diatomaceous earth) of a certain particle size range with a solution of the stationary liquid in a volatile solvent. The solvent is removed by evaporation without boiling. After that the air is displaced from the column by the eluant. Before use the eluant has to be deaerated and saturated with stationary liquid. To assure equilibrium between eluant and stationary liquid a pre-column containing the same packing is arranged before the injector.

Detector unit. The detector connected to the outlet of the column is a differential refractometer (Waters type R4). The signal of the detector is fed to a 10-mV recorder (Servogor type RE 511). Because of the dependency of the refractive index on the temperature it is necessary to thermostat the detector cell and connecting tubings. In the original detector designed for high volume flows the effluent is led to the cell through a thermostatted tube 2-m long and 0.8-mm in diameter, to assure a highly constant temperature. The band broadening caused by this heat exchanger is of the magnitude of that of the column itself. For this reason the heat exchanger had to be shortened. A tube 10-cm long and 0.5 mm in diameter proved a good compromise. The increase of the peak broadening under the influence of this tube was small compared to that of the detector cell, which has a volume of 10 μl.

RESULTS

Mixing outside the column

If the behaviour of a chromatographic column is to be studied, the mixing outside the column must be evaluated to ensure correct results. The concentration profile entering the detector results from the initial profile produced at the injection point and the increase during the migration to the detector. According to eqn. (5) $(\sigma_{ti}^2 + \Delta\sigma_{tt}^2)$ must be small compared to $\Delta\sigma_{tc}^2$ if the residence time distribution of the column is to be measured.

Furthermore, the detector must have a response time which is small compared

to the width of the concentration profile at the detector inlet otherwise the response peak will not be a true representation of the concentration profile.

If the column is replaced by a short narrow tube (*e.g.* $d = 0.5$ mm, $L = 100$ mm) and a small sample volume is injected (*e.g.* 0.2 μl) the profile broadening in the flow line outside the column can be determined since $\Delta\sigma_{tc}^2$ becomes negligible and σ_{tl}^2 does not dominate.

Figure 2 shows the results obtained with the apparatus described in the preceding section. Although the conditions for the validity of eqn. (6) are only par-

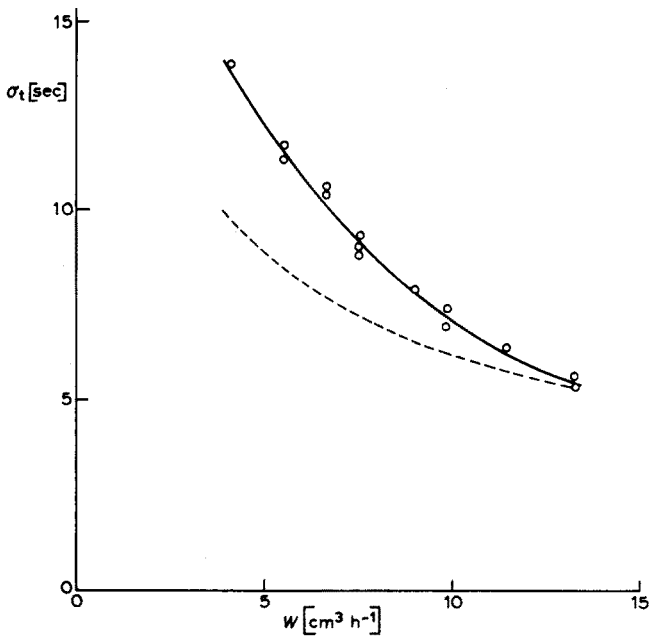

Fig. 2. Mixing in the apparatus outside the column. (—) overall value σ_t; (— —) partial value σ_{tt}^2.

tially fulfilled, it can be used to calculate the value $\Delta\sigma_{tt}^2$. The first term within the brackets of eqn. (6) can be neglected if the flow rate is not extremely low. Further, the product $\sigma_{tl}w$ can be assumed to be about constant. Under these conditions an approximate expression for the overall value σ_t can be given.

$$\sigma_t \approx ((\sigma_{tl}w)^2/w^2 + A^2L/75D_aw)^{1/2} \qquad (7)$$

A and L are effective values since the cross-section of the flow line is not constant. The standard deviation σ_{tl} produced at injection does not affect the overall value at high flow rate. Therefore the constant $A^2L/75D_a$ can be determined from measurements at high flow rates and the partial curves σ_{tl} and σ_{tt}^2 can be calculated (Fig. 2). The value of σ_t is small and it is proved that narrow concentration profiles can be measured by the apparatus. The limitations with respect to the minimum allowable profile width given by the apparatus will hardly be reached in practice.

Separation time

A sample peak disperses in the column due to mixing in the moving phase and mass exchange between the moving phase and the stationary bed. The dispersion is characterized by the length H which depends on the fluid velocity $\langle v \rangle$. The dependence of H on $\langle v \rangle$ can be expressed most conveniently by a graphical representation.

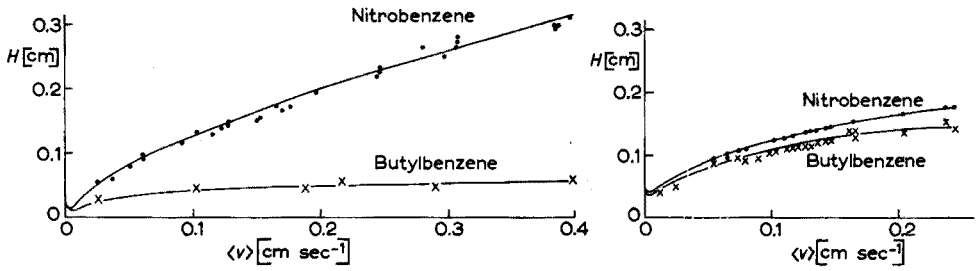

Fig. 3. Dependence of H on fluid velocity. Column: dimension 50 × 0.20 cm; particle size 63–80 μ; particle loading 1,2,3-tris-cyanoethoxypropane (ε_β = 0.07); eluant 2,2,4-trimethylpropane (ε_α = 0.82). Sample: 0.6 μl (0.5% w/w butylbenzene (×) + 1.5% nitrobenzene (●) + eluant).

Fig. 4. Dependence of H on fluid velocity. Column: dimension 100 × 0.20 cm; particle size < 25 μ (37% w/w), 25–56 μ (28%), 56–80 μ (35%); particle loading 1,2,3-tris-cyanoethoxypropane (ε_β = 0.11); eluant 2,2,4-trimethylpentane (ε_α = 0.60). Sample: 0.6 μl (0.5% w/w butylbenzene (×) + 1.5% nitrobenzene (●) + eluant).

Figures 3 and 4 show typical examples. All the curves have a minimum at very low fluid velocity and approach the ordinate asymptotically. The interpretation of these results is given by eqn. (3).

The partition coefficient of butylbenzene in the liquid–liquid system of 2,2,4-trimethylpentane–1,2,3-tris-cyanoethoxypropane at 25° is smaller than 0.1. Therefore and because the particles do not contain eluant, the mass transfer term in the expression for H of butylbenzene is negligible. The curves for butylbenzene in Figs. 3 and 4 are caused practically by the mixing terms alone. At higher fluid velocity the convective mixing dominates, at lower ones, the diffusion. On the column containing less uniform and smaller particles (Fig. 4), a considerably higher H curve is obtained for non-retarded compounds like butylbenzene owing to stronger convective mixing. This observation is found to be significant and it must be concluded that particles of greatly different or very small size tend to give a less regular packing.

Nitrobenzene has a partition coefficient of about 6.8 which causes a considerable mass transfer term. Since the diffusion coefficients of butylbenzene (D = 1.4 10^{-5} cm^2 sec^{-1}) and nitrobenzene (D = 1.8 10^{-5} cm^2 sec^{-1}) in 2,2,4-trimethylpentane differ only slightly, the mixing terms are also similar and the difference of the H curves of both substances gives an indication of the magnitude of the two mass transfer terms together. Figures 3 and 4 confirm that the mass transfer terms are much smaller with smaller particles.

In Fig. 3 the H curve at higher fluid velocity is determined mainly by the mass transfer term, in Fig. 4 by the convective mixing term. Fig. 5 demonstrates how the overall curve can be built up from the four partial curves which refer to the dif-

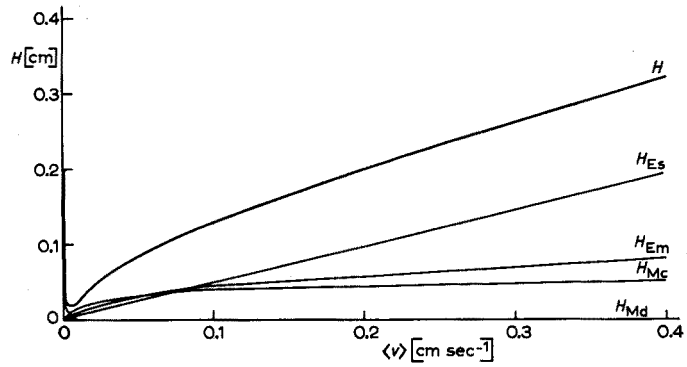

Fig. 5. Contributions to H; evaluated for the curve of nitrobenzene in Fig. 3.

ferent dispersion processes. The theoretical H curve obtained from the partial curves according to eqn. (3) fits the experimental results very well.

With respect to the particle size the aim must be to find the best compromise between the increasing non-regularity of the packing and the benefit of faster mass transfer using smaller particles. Another factor which has to be considered is that the specific pore volume of porous grains decreases on grinding.

According to eqn. (2), the time in which a given resolution is produced depends mainly on the dimensionless selectivity coefficient K_B/K_A and the time $H/\langle v \rangle$. Figure 6 confirms the prediction of eqn. (3) that $H/\langle v \rangle$ approaches a minimum value at increasing flow velocity. If the H–$\langle v \rangle$-curves are related to the pressure drop, another influence of the particle size becomes distinct. Only slightly different

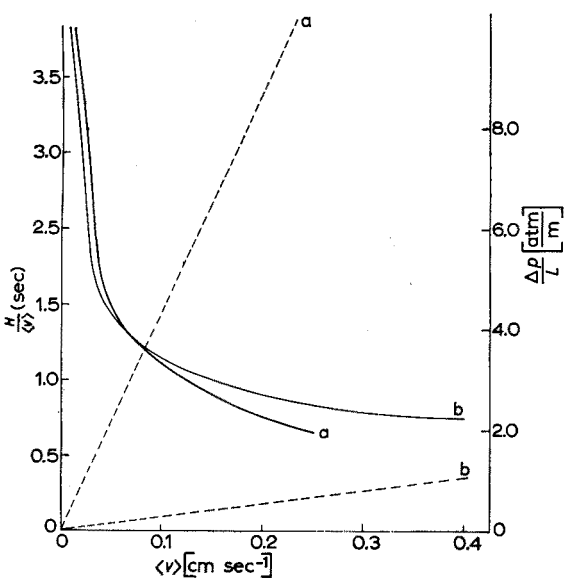

Fig. 6. Relation between the ratio $H/\langle v \rangle$ and the pressure drop. Sample: nitrobenzene. Column: a. the same as in Fig. 4; b. the same as in Fig. 3.

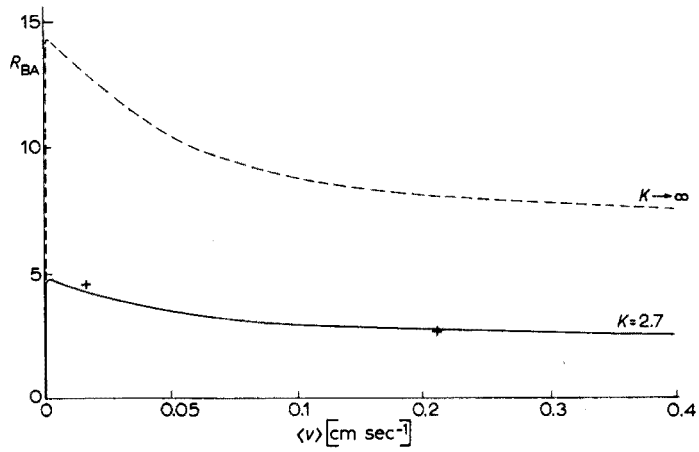

Fig. 7. Resolution as function of fluid velocity and partition coefficient. Column: the same as in Fig. 4. Sample: 0.6 μl (1.7% w/w *m*-nitrotoluene + 1.7% *p*-nitrotoluene + eluant). (Points marked on the curve agree with the results shown in Fig. 8.)

H–$\langle v \rangle$ curves are found for the same sample on two columns prepared from a narrow and a wide particle size range with the same upper limit (80 μ). The pressure drop, however, is much smaller for the column produced from the granular material which does not contain fines.

Fig. 7 shows an example of the dependence of the resolution on fluid velocity and demonstrates the influence of the distribution coefficient. The resolution changes with the value of the partition coefficient because of the change of the factor $(K_A\varepsilon_\beta)/(\varepsilon_a + K_A\varepsilon_\beta)H_A^{1/2}$ in eqn. (1). Together with eqn. (3), it can be concluded that R_{BA} approaches a maximum value for high values of the partition coefficient. The more dominating the mixing terms in the expression for H become, the more the resolution will diminish with partition coefficient.

To demonstrate this effect, a pair of compounds with low partition coefficients have to be separated on a column with relatively high mixing terms. From Fig. 7 it is clear that the maximum resolution value is obtained at very low fluid velocity. Further it can be confirmed that the resolution diminishes considerably with K on a

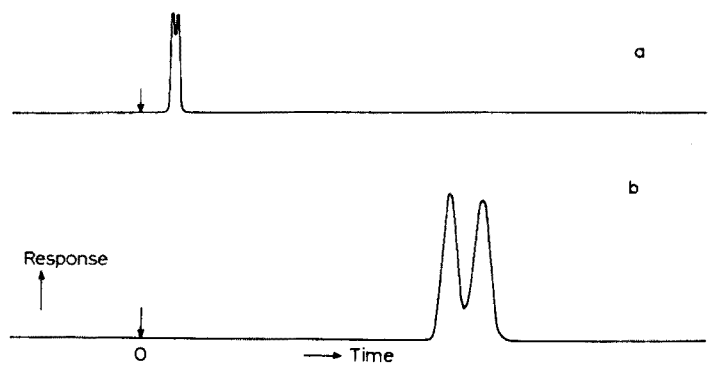

Fig. 8. Resolution and separation time on a given column. a. $R_{BA} = 2.5$, $t_{RA} = 1170$ sec; b. $R_{BA} = 4.4$, $t_{RA} = 10950$ sec. Column: the same as in Fig. 4.

column in which relatively strong mixing occurs. For gaussian peaks of equal size a practically complete separation is achieved if $R = 6$. At $R = 2$ both peaks overlap so strongly that only a single superimposed peak is observed. Figure 8 illustrates the meaning of the R–$\langle v \rangle$-diagram by the presentation of chromatograms. A two-fold increase of resolution on the same column requires a nine-fold increase in the separation time.

From the results described in this paper, it can be predicted that the separation time can be reduced at least by a factor of 10 if smaller particles (limited by the packing-effect), higher flow rate and longer columns are used. The benefit of a shorter separation time has to be compensated by a higher pressure drop. The problems involved in high pressure chromatography will be discussed in a later paper.

The authors are very grateful to Mr. E. E. CHALLA for his assistance with the measurements.

SUMMARY

The factors affecting the time in which a given resolution can be obtained are investigated. It is concluded that for columns of the same bed geometry, the minimum separation time is much longer in liquid chromatography than in gas chromatography. However, the separation time in liquid chromatography can be reduced considerably if a higher pressure drop is acceptable. The expected improvement is restricted by the difficulty of obtaining regular packings from very small particles.

REFERENCES

1 W. L. JONES AND R. KIESELBACH, *Anal. Chem.*, 30 (1958) 1590.
2 J. F. K. HUBER AND J. H. QUAADGRAS, *J. Chromatog.*, in press.
3 J. H. PURNELL AND C. P. QUINN, in R. P. W. SCOTT (ed.), *Gas Chromatography*, Butterworths, London, 1960, p. 184.
4 R. J. LLOYD, B. O. AYERS AND F. W. KARASEK, *Anal. Chem.*, 32 (1960) 698.
5 J. F. K. HUBER AND C. A. M. G. CRAMERS, *J. Chromatog.*, in press.
6 G. TAYLOR, *Proc. Roy. Soc. (London)*, A219 (1953) 186.
7 R. ARIS, *Proc. Roy. Soc. (London)*, A235 (1956) 67.

Anal. Chim. Acta, 38 (1967) 305–313

END OF THE SYMPOSIUM CONTRIBUTIONS

Since this broadening of the scope does not involve any change in the basic interests of the journal, the title has been only slightly modified. From January 1967 it has become:

JOURNAL OF ELECTROANALITICAL CHEMISTRY AND INTERFACIAL ELECTROCHEMISTRY

An International Journal Devoted to all aspects of Electroanalytical Chemistry, Double Layer Studies, Electrokinetics, Colloid Stability, and Electrode Kinetics.

Since the aim of a journal must be to publish papers rapidly, the number of volumes per year has at the same time been increased from two to three. The delay in publication has thereby been reduced to a minimum level.

Dr. R. H. Ottewill of the University of Bristol has agreed to join the board of Editors, and will have special responsibility for the papers which fall within his field of interest.

Papers for publication should be sent to one of the following addresses:

Professor J. O'M. Bockris, John Harrison Laboratory of Chemistry, University of Pennsylvania, Philadelphia 4, Pa. 10104, U.S.A.

Dr. R. H. Ottewil, Department of Chemistry, The University, Bristol 8, England

Dr. R. Parsons, Department of Chemistry, The University, Bristol 8, England (until July 1967: Gates and Crellin Laboratories of Chemistry, California Institute of Technology, Pasadena, Calif. 91109, U.S.A.)

Professor C. N. Reilley, Department of Chemistry, University of North Carolina, Chapel Hill, N.C. 27515, U.S.A.

A pamphlet "hints to authors" is available free of charge from the publishers, who will be glad to supply further information to intending authors.

Subscription price for 1967: £18.18.0, US$52.50 or Dfl. 189.00 plus postage 8s. 6d., US$1.25 or Dfl. 4.20. Subscription orders and requests for specimen copies may be sent to your usual supplier or directly to the publisher.

ELSEVIER PUBLISHING COMPANY

P. O. BOX 211 - AMSTERDAM - THE NETHERLANDS

ANNOUNCEMENT

JOURNAL OF

ELECTROANALYTICAL CHEMISTRY

AND INTERFACIAL ELECTROCHEMISTRY

International Journal devoted to all Aspects of Electroanalytical Chemistry, Double Layer Studies, Electrokinetics, Colloid Stability, and Electrode Kinetics.

The boundaries between what are regarded as electroanalytical chemistry, electrochemistry and colloid chemistry are becoming increasingly diffuse. This has for some time been reflected in the pages of the *Journal of Electroanalytical Chemistry* where many of the papers published are of interest to chemists who consider themselves as falling under any of these three broad divisions.

The linking phenomena are those associated with the electrical double layer, and it was felt that it would be both useful and appropriate to acknowledge these broader interests by extending the scope of the journal to include all phenomena in which the electrical double layer plays an essential role.

These extend from applications in analytical chemistry, through the fundamentals of electrode reactions, which have always been the staple part of the journal, to studies of the double layer around colloidal particles, the stability of dispersions and electrokinetic phenomena as well as other surface chemical problems such as monolayers and soap films.

CONTENTS

Proceedings of the International Symposium on Physical Separation Methods in Chemical Analysis, Amsterdam, April 10–14, 1967